PROCEEDINGS OF THE UNITED STATES - PEOPLE'S REPUBLIC OF CHINA BILATERAL SYMPOSIUM ON DROUGHTS AND ARID-REGION HYDROLOGY, SEPTEMBER 16-20, 1991, TUCSON, ARIZONA

Property of
Flood Control District of MC Library
Please Return to
2801 W. Durango
Phoenix, AZ 85009

FLOOD CONTROL DISTRICT
RECEIVED
DEC 12 1991

	CH ENG		P & PM
	DEP		HYDRO
	ADMIN		LMGT
	FINANCE		FILE
	C & O		JJT
	ENGR		

REMARKS

U.S. GEOLOGICAL SURVEY

Open-File Report 91-244

PROCEEDINGS OF THE UNITED STATES - PEOPLE'S REPUBLIC OF CHINA BILATERAL SYMPOSIUM ON DROUGHTS AND ARID-REGION HYDROLOGY

SEPTEMBER 16-20, 1991, TUCSON, ARIZONA

Compiled by W. H. Kirby and W. Y. Tan

U.S. GEOLOGICAL SURVEY

Open-File Report 91-244

Reston, Virginia

1991

U.S. DEPARTMENT OF THE INTERIOR

MANUEL LUJAN, JR., Secretary

U.S. GEOLOGICAL SURVEY

Dallas L. Peck, Director

For additional information
write to:

Chief, Office of Surface Water
U.S. Geological Survey
415 National Center
Reston, Virginia 22092

Copies of this report can
be purchased from:

U.S. Geological Survey, Books
and Open-File Reports Section
Box 25425, Federal Center
Denver, Colorado 80225

PREFACE

The United States - People's Republic of China Bilateral Symposium on Droughts and Arid-Region Hydrology was organized under the auspices of the Protocol for Scientific and Technical Cooperation in the Study of Surface-Water Hydrology, between the U.S. Geological Survey of the Department of the Interior of the United States of America and the Department of Hydrology of the Ministry of Water Resources of the People's Republic of China. The objective of the symposium is to provide a forum for exchange of scientific information on surface-water hydrologic aspects of droughts and arid regions. Large portions of both the United States and China have arid or semi-arid climates or are subject to recurrent droughts; thus the subject of the symposium is of practical importance as well as scientific interest. The contributions to the symposium show that hydrologists in both the United States and China have devoted much effort to the study of droughts and arid-region hydrology, but in many cases have approached their work from somewhat different points of view. This symposium provides an opportunity for hydrologists from the two countries to share these points of view and thus improve the breadth as well as the depth of their understanding.

The contributions to the symposium were organized into the following major categories:

- Characterization and Quantification of Droughts
- Characteristics of Arid-Region Hydrology
- Monitoring and Forecasting
- Frequency Analysis, Regionalization, and Stochastic Analysis
- Water-Resource Modeling and Management

We would like to acknowledge the contributions made by the Organizing Committee, consisting of M. E. Moss and R. D. Mac Nish (U.S. Geological Survey), D. A. Woolhiser (U.S. Agricultural Research Service), and B. Bartocha, M. Hughes, and R. A. Clark (University of Arizona), and the keynote speaker, D. R. Dawdy.

W. H. Kirby
U.S. Geological Survey

W. Y. Tan
Nanjing Institute of Hydrology
and Water Resources

DISCLAIMER

The U.S. Geological Survey agreed to publish the proceedings of the United States - People's Republic of China Bilateral Symposium on Droughts and Arid-Region Hydrology because the subject matter is related to the mission of the Geological Survey. These proceedings have been published in the Open-File series pending approval to publish them as a Water-Supply Paper. The usual standards for this series have been modified to accommodate the variety of styles used by the participants in this symposium. The opinions and conclusions expressed herein by non-Geological Survey authors do not necessarily represent those of the U.S. Geological Survey. Any use of trade, product, or firm names is for identification only and does not imply endorsement by the U.S. Geological Survey.

CONTENTS

Page

Chinese contributions to hydrologic drought studies: by W.Y. Tan and S.Y. Hu 1

U.S. contributions to studies of droughts and arid-region hydrology: by W.H. Kirby 9

TOPIC A--CHARACTERIZATION AND QUANTIFICATION OF DROUGHTS

A discussion on drought in arid regions of China: by S.K. Li 17

The 1988-89 National Water Summary--A summary of floods and droughts in the United States: by R.W. Paulson, E.B. Chase, J.S. Williams, and R.S. Roberts 23

Examination of dryness in agriculture with moisture balance indices: by Z.Y. Guan and Z.W. Feng 31

Transformation between hydrological drought and industrial and agricultural drought in semi-arid areas: by Z.Z Chen 39

A national drought atlas for the United States of America: by G.E. Willeke, Nathanial Guttman, and W.O. Thomas, Jr. 45

Prediction of regional soil water and drought: by B.G. Li 51

TOPIC B--CHARACTERISTICS OF ARID-REGION HYDROLOGY

Flood hydrology of arid basins in southwestern United States: by H.W. Hjalmarson 59

Hydrological characteristics of the semi-arid Haihe River basin, China: by Y. Feng 65

Preliminary investigation for characterization of drought and streamflow in the Western Great Basin--Distinguishing climate change from natural variability: by Alex Pupacko 73

Rainstorm characteristics in the arid area of China: by J.Q. Wang 79

Effects of global climate change on erosion stability in arid environments using WEPP: by R.H. Hawkins, V.L. Lopes, R.A. Parker, and M.A. Weltz 85

Hydrology of aquifer recharge in arid regions: by H. J. Morel-Seytoux, C.M. Zhang, C. Miracapillo, and H. Khadr 91

CONTENTS (continued) Page

Analysis and forecast of the water-quality state of main rivers in Xinjiang: by Y.L. Hao 97

Irrigation induced water-quality problems in the western United States: by H.R. Feltz 103

Surface-water chemical changes due to human activities in the Tarim Basin: by Z.Y. Wei 105

Concentration and distribution of selenium associated with irrigation drainage in the western United States: by R.A. Engberg 113

Impact of water-resources utilization on the ecological environment in the Xinjiang arid region, China: by T.X. Zhou and M.D. Tang 125

Measurements of vapor pressure over natural vegetation at a high desert site in southeastern Arizona: by A.M. Sturrock, Jr., and W.D. Nichols 131

Evaporation properties and estimates in the landlocked arid region in Xinjiang, China: by G.W. Zhang and Y.C. Zhou 139

Estimating evapotranspiration by phreatophytes in areas of shallow ground water in a high desert valley: by W.D. Nichols 145

TOPIC C--MONITORING AND FORECASTING

A simplified approach for evaluating evaporation using satellite-based remotely sensed data: by M.S. Moran and R.D. Jackson 155

Remote sensing and evapotranspiration estimates: Influence of ground-based meteorological data: by P.W. Brown and S.J. Owen-Joyce 161

Climatological analysis of seasonal snow resources in the Qilian Mountains of North China: by Q. Chen and T.Y. Chen 167

Developing an index of hydrologic drought for the Gunnison River basin, Colorado: by R.S. Parker 175

Forecasting dry-season drought and runoff in China: by F.Y. Zhang 183

CONTENTS (continued)

Page

Low streamflow forecast model for Longyangxia hydropower station on the Yellow River: by B.Y. Yang and H.X. Sun 189

TOPIC D--FREQUENCY ANALYSIS, REGIONALIZATION AND STOCHASTIC ANALYSIS

Estimating low-flow characteristics at gaging stations and through the use of base-flow measurements: by W.O. Thomas, Jr., and J.R. Stedinger 197

Frequency distribution for hydrologic samples with zero events: by S.X. Wang 207

Estimating low-flow characteristics of streams at ungaged sites: by G.D. Tasker 215

Stochastic analysis of drought properties of the main rivers in China: by R.F. Yang, J. Ding, and Y.R. Deng 221

Streamflow drought statistics by stochastic simulation: by J.D. Salas and M.W. Abdelmohsen 227

Synthetic streamflows for global climate change: by W.L. Lane 235

Preliminary analysis of streamflow drought characteristics in the middle reach of the Yellow River: by C.X. Li, J. Shen, and R.S. Fan 241

An event-based model of precipitation for analyzing occurrence and severity of summer droughts in southern Arizona and New Mexico: by V.L. Lopes, M.M. Fogel, L. Duckstein, and B.M. Imam 247

Droughts and floods in North and East China, 1380-1989 A.D.: by S.W. Wang, G.X. Wang, and Z.M. Zhang 255

Tree rings and the severity of hydrologic drought: by David Meko 261

Annual runoff series extension and runoff variations in Lanzhou-Sanmenxia reach of Yellow River, China: by X.F. Ma, Y.Z. Wang, and S.Q. Huo 267

Recurrence probability of 11-year continuous low water period (1922-1932 A.D.) in the Yellow River: by F.C. Shi, G.A. Wang, P. Mu, G.A. Ma, and Z.D. Gao 273

CONTENTS (continued) Page

Analysis of persistence of hydrological drought on the Upper Yellow River, China: by W.D. Wang, H.X. Sun, and J.B. Shi 281

TOPIC E--WATER-RESOURCE MODELING AND MANAGEMENT

Reservoir sizing criteria for Bureau of Reclamation projects: by E.L. Johns 289

Quantifying marketable hydropower at reclamation powerplants giving recognition to periods of drought: by C.R. Phillips 295

Application of a simulation model for water-supply planning in an arid region of China: by S.F. Zhang and J.P. Wang 301

Effects of drought on public-supplied water use--Three case studies from the central United States: by R.A. Herbert and D.W. Litke 309

Evaluating drought risks for large highly regulated basins using monthly water balance modeling: by G.D. Tasker 317

A model of water-resources transformation and its results in simulating the Urumqi River basin, China: by F.J. Liu and Y.G. Qu 323

Droughts in a stream-aquifer system, San Simeon Creek, California: by E.B. Yates 331

Water balance analysis in the mountain area of the Urumqi River basin: by Y.C. Zhou, G.W. Zhang, and E.S. Kang 337

CONVERSION FACTORS AND ABBREVIATIONS

Multiply	By	To obtain
	Length	
inch	2.54	centimeter (cm)
foot (ft)	0.3048	meter (m)
mile (mi)	1.609	kilometer (km)
	Area	
square foot (ft^2)	0.09290	square meter (m^2)
mu	1/6	acre (ac)
mu	667	square meter (m^2)
acre (ac)	4,047	square meter m^2)
acre (ac)	0.4047	hectare (ha)
square mile (mi^2)	2.590	square kilometer (km^2)
	Volume	
gallon (gal)	0.003785	cubic meter (m^3)
cubic foot (ft^3)	0.02832	cubic meter (m^3)
acre-foot (acre-ft)	1,233	cubic meter (m^3)
	Volume per unit time	
cubic foot per second (ft^3/s)	0.02832	cubic meter per second (m^3/s)
million gallon per day (mgd)	0.04381	cubic meter per second (m^3/s)

Temperature

degree Celsius = (degree Fahrenheit - 32)/1.8

Sea Level: In this report, in reference to locations in the United States, "sea level" refers to the National Geodetic Vertical Datum of 1929 (NGVD of 1929)--a geodetic datum derived from a general adjustment of the first-order level nets of both the United States and Canada, formerly called Sea Level Datum of 1929.

CHINESE CONTRIBUTIONS TO HYDROLOGIC DROUGHT STUDIES

Tan Weiyan and Hu Siyi

Nanjing Research Institute of Hydrology and Water Resources, Nanjing

ABSTRACT

This paper is a survey of the papers submitted to the PRC–US Bilateral Symposium on Droughts and Arid–Region Hydrology in Tucson, Arizona, in September, 1991. Firstly, it gives a brief description of basic features of hydrologic droughts in China, and the kinds of data used in their studies.Then, the Chinese papers are grouped according to the topics involved, including drought indices, stochastic models, hydrologic models, regional water–balance models, monitoring and forecasting of droughts and low flows,local intense storms in arid and semi–arid regions, water–quality problems, and impacts of human activities and strategies towards droughts.

GENERAL DESCRIPTION OF HYDROLOGIC DROUGHT IN CHINA

In China the area of arid and semi–arid regions amounts to about half the 9.6 million km^2area for the whole country. Areas with an annual mean precipitation less than 250 mm cover nearly three–fourths (about 3.6 million km^2) of the total area classified as arid. Among them, the Northwest–China arid region, situated in the hinterland of the Asia–Europe Continent and centered in eastern Xinjiang, is the largest one with an area of over 3 million $km^2$and mostly with an elevation of over 1000 m. It is surrounded by high mountains, and some also stand in its interior. The mountainous areas, with mean annual precipitation of over 600 mm, are classified as runoff–generation areas. Downstream of the mountain fronts are the runoff–diminishing areas, which have small patches of densely populated oases. The non–flow areas of the interrupted rivers form several huge basins where extensive deserts and gobis are distributed. As regards the semi–arid regions, farming, foresting and stockbreeding areas are scattered there, taking the 400–mm contour of mean annual rainfall as a transition between agricultural and pastoral areas. A distinctive semi–arid region is the famous Loess Plateau with an area of 620,000 km^2. Its basic topographic feature is that thick loess layers are deeply cut and separated by river networks, resulting in high water losses, soil erosion and very low groundwater elevation.

The chief features of drought in China are as follows:

(1) High frequency. In almost every year some areas of the country experience drought. Even in a humid region or in a wet year, the occurrence of drought in some places is still possible. Among the five chief meteorological calamities (drought, water–logging, freezing, typhoon, dry–hot wind), drought is most frequently encountered.

(2) Regional variability. Drought occurs more frequently in North China than in South China. The drainage basins of the Yellow River, the Huaihe River and the Haihe River suffer the most serious agricultural droughts, whereas Northwest China is the driest area with the poorest water resources.

(3) Seasonality. Due to the effect of monsoon in spring, drought often occurs in the North of China, while water–logging occurs in the South; in mid–summer the situation is re-

versed. In South and Southwest China, drought often lasts from autumn to winter or from winter to spring.

(4) Persistency. A serious drought often lasts from spring to summer in the northern provinces, or from summer to autumn in the southern provinces. A widespread multi–year drought is not a rarely encountered event, as ten–year drought–periods have been observed for some rivers. Of course, for a fixed location, dry and wet conditions may possibly occur alternately within the same year.

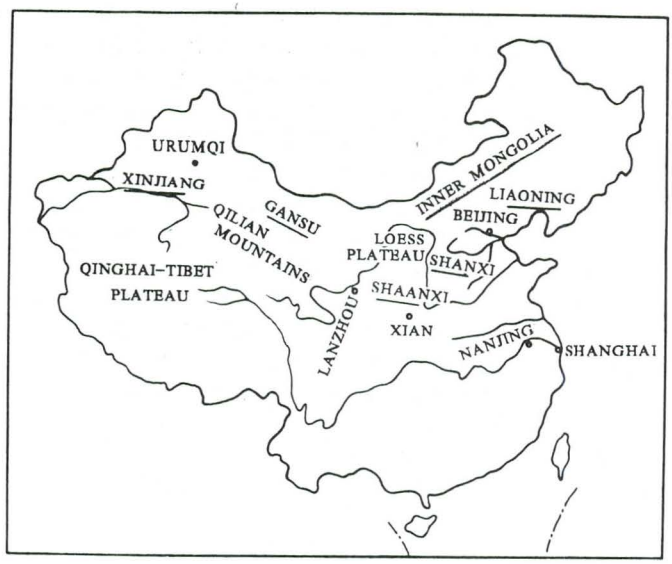

UTILIZATION OF ALL POTENTIAL AND USEFUL DATA

In China, a hydrologic drought analysis makes use of data from the following sources:

(1) Modern hydrologic–meteorologic observations. If available, such observations provide a sound basis for the drought analysis; however, they commonly play a limited role due to low density of gauging stations, nonuniformity of their distribution and shortage of long–term records. China has only a few discharge records longer than about one hundred years, and only a few rainfall records longer than about three hundred years. In regional analysis, the data available generally cover only 30 to 40 years.

(2) Field investigation. One aim is to collect small–scale, high–intensity storm data, covering an area usually smaller than 1000 km^2, sometimes even under 100 km^2. In addition, China also organized field investigations into historical droughts and low flows, similarly to the studies of historical floods.

(3) Historical literature and relics. Such information is used mainly for reconstructing time series composed of qualitative grades of drought and water–logging, in order to understand past fluctuations. The "Yearly Charts of Dryness / Wetness in China for the Last 500–Year Period" (Chinese Academy of Meteorological Science, 1981), has provided systematic and very useful data.

(4) Meteorologic satellite data. These data can be used for estimating the area extent and thickness of glaciers and accumulated snow, and yielding further equivalent water volumes. Satellite imagery can also be used to determine the distribution and variation of soil moisture, and provide an indirect basis for estimating evapotranspiration.

(5) Tree–ring data. Research into tree rings has been carried out intermittently in China since the 1930's (Gong and others, 1983). Past research has been focused on reconstruction of annual rainfall and runoff series, and on analysis of climatic variability and streamflow fluctuation. Recently, the technique of dendroclimatology has been extensively utilized, and the data obtained have been applied in the design of water projects and the prediction of long–term droughts.

DROUGHT INDICES

For distinguishing arid and semi–arid regions from humid and semi–humid ones,the fol-

lowing indices are commonly used in the Chinese hydrologic practice:(1) mean annual rainfall = 400 mm; (2) mean annual relative humidity = 60%; (3) degree of aridity (ratio of annual evapotranspiration capacity to annual rainfall) = 1.5; (4) aridity index (ratio of annual evaporation capacity from water surfaces to annual rainfall) = 3; (5) annual runoff coefficient (ratio of annual runoff to annual rainfall) = 0.1.

In order to describe the degree of drought severity at a location (or region) in a period, the chief indices used are: (1) the absolute (or relative) deviation of annual (or monthly) rainfall (or runoff) from its mean value, sometimes expressed as a ratio to its standard deviation; (2) its frequency of occurence. Moreover, many other indices appropriate for regional or agricultural drought analyses have been proposed. These indices are mainly based on the law of soil–moisture content variability and incorporate some other factors such as groundwater level and crop water demand. Experience shows that these kinds of indices are valuable for reflecting agricultural droughts in a region. One of them requires that the ratio of soil moisture to field moisture capacity should be smaller than 60%. An agricultural drought index which has been used widely in North China is used in a drought analysis for the Loess Plateau region in the Shanxi and Shaanxi provinces (Guan and others, 1991).

STOCHASTIC MODELS

At present, statistical methods are still the chief means of drought analysis and low–flow computation. To improve the accuracy of the results, a key lies in the acquisition of reliable data which is as long as possible. In a paper (Wang, S. W., and others, 1991), a time series taken from the aforementioned Atlas has been extended to about six hundred years.

To determine a return period for the successive droughts between 1922 and 1932 over the upper or middle Yellow River basin, Wang Weidi and others and Shi Fucheng and others constructed annual–runoff stochastic models and generated synthesized series with the Monte–Carlo method (Wang and others, 1991, and Shi and others, 1991), which are utilized for estimating the return period. The conclusion was also verified through a field investigation in 1964 into historical droughts and low flows, and by using an abundance of quotations from historical literature. Based on the relations between the natural runoff, dryness and wetness grades, and three groups of tree–ring indices, Ma Xiufeng and others reconstructed a runoff record for the middle reach of the Yellow River between Lanzhou and Sanmenxia dating back to 1749 (Ma and others, 1991).

To determine reliably the time–space variability of droughts and low streamflows, besides fully utilizing various information sources about droughts and low flows, it is also required to use random models correctly. The classical correlation analysis, and the modern time series analysis (including power spectrum analysis and various auto–regressive models), as well as the synthetic generation of hydrologic series with the Monte–Carlo method, etc.,have found applications in the above–mentioned papers and also in some others (Li and others, 1991, and Yang and others, 1991).

A special problem, peculiar to the low–flow frequency analysis, arises from the inclusion of several zero–values in the sample series, on which Wang Shanxu has made some discussions (Wang, S. X., 1991).

HYDROLOGIC MODELS

Several conceptual hydrologic models which are popular in the estimation of floods based on rainfall, have recently been used to simulate daily discharge processes in some rivers. To do this, some links in the procedure should be more or less modified and supplemented, so that they are applicable to arid regions. For instance, the replenishment of melted glaciers and snow, and the effect of frozen ground should be incorporated in the models.

REGIONAL WATER–BALANCE MODELS

These models express how rainfall can be transformed into water resources, and also describe the balance and interactions between surface water, groundwater and soil water. In China, models of transformations among "three types of water" have been widely established for various regions and subregions. Liu Fengjing and others constructed a general–purpose model for the simulation of the transformations between different components of water resources for the Northwest–China arid region (Liu and others, 1991).

The variation of soil moisture in an arid region plays an important role in transforming the rainfall into water resources. So it is necessary to strengthenthe research into non–gravity water in an unsaturated soil layer, especially for the Loess Plateau, where the groundwater level is very low, and where the soil layer within one meter from the ground surface is actually the most active zone for the storage and movement of soil moisture. Li Baoguo derived an equation for the balance of distributive soil moisture, in order to estimate its regional storage (Li, B. G., 1991).

The estimation of evapotranspiration for the three components of water is another key problem. In the central area of the Northwest–China arid region, mean annual rainfall is under 100 mm, the mean annual number of rainy days is less than 10, and mean relative humidity is only about 30%, whereas annual evaporation from water surfaces may be 2000 mm or more. Zhang Guowei and others modified the Penman evaporation formula so as to be applied to the Xinjiang arid region (Zhang, G. W., and others, 1991). Moreover, by an analysis of the observed data from several groundwater experimental stations, they obtained evaporation coefficients for groundwater at various depths and in different types of soil layers. But evaporation from the land surface has been only rather crudely estimated up to now.

In the runoff–diminishing regions of inland river basins, the runoff suffers from large losses due to infiltration into streambed and diversions for irrigation uses. Where the ground surface slope becomes gentler, the groundwater sometimes appears above the ground again in the form of springs. Such a process of transformation between surface water and groundwater may repeat itself several times. In the estimation of water resources, the overlapped amount should be subtracted. Zhou Yuchuo and others give a water–balance analysis for the Urumqi River, which is typical of that region (Zhou, Y. C., and others, 1991).

As regards the melting glaciers and accumulated snow over high mountains, Chen Qian and others estimated the seasonal amount of snow accumulated over the top of the Qilian Mountains using satellite remote–sensing data (Chen, Q., and others, 1991).

MONITORING AND FORECASTING OF DROUGHTS AND LOW FLOWS

Drought forecasts must be made on the basis of long–term weather forecasts. The chief methods used nowadays need to recognize precedent meteorologic factors and to establish correlations between them and the future rainfall (or runoff). Unfortunately, the accuracy is rather unsatisfactory. So Chinese hydrologic services often predict the variation of soil moisture with some hydrologic methods, according to the observed rainfall, soil moisture and its depletion curve, and then make drought forecasts by references to the weather forecast and field soil–moisture investigation. Li Baoguo established a storage model for forecasting regional soil–moisture storages by using GIS techniques, with which it is possible to draw regional drought maps according to the requirements of crops on the soil–moisture (Li, B. G., 1991).

Low–flow forecast is often based on the observed depletion process of river discharge, and has a sound physical basis. Yang Baiyin and others present several alternatives of low–flow forecasts for the Longyang–Creek Hydropower Station with success (Yang and

others, 1991). A brief introduction to various methods used in the drought and low–flow forecasts by the Hydrologic Water Resources Management Center can be found in Zhang Fuyi's paper (Zhang, F. Y., 1991).

A SPECIAL PROBLEM DUE TO LOCAL STORMS

In arid and semi–arid regions, it is possible that highly convective storms occur in summer, with the characteristics of low frequency, short duration and small coverage area. But these events often cannot be observed at sparsely distributed stations. Since the first field rainfall investigation was made in 1959, several storm events that exceed the highest records in the southern humid regions have been discovered, including a few short–duration point–rainfall estimates that are close to or even beyond the world records. Wang Jiaqi summarized an abundance of relevant data and some characteristics of this type of storm (Wang, J. Q., 1991).

WATER–QUALITY PROBLEMS FOR RIVERS AND LAKES

Water–quality problems make the shortage of water resources more sensitive in arid and semi–arid regions. Hao Yuling analyzed the water–quality conditions for the major rivers in the Xinjiang autonomous region (Hao, 1991), and pointed out that control of water quality in the dry season is crucial to improving the water–quality condition for the whole year. Wei Zhangyi analyzed both vertical and seasonal variations of the chemical characteristics of surface water in the Tarim Basin (Wei, 1991). Moreover, the salinization of Lake Bosteng (the largest inland fresh–water lake in China) during the past thirty years, has resulted first from the pollution due to large–scale drainages from cultivated areas, and second from the increase of irrigated water.

IMPACTS OF HUMAN ACTIVITIES AND STRATEGIES TOWARDS DROUGHTS

Since 1949 the problem of water shortage in arid and semi–arid regions has been becoming more pronounced due to large–scale economic development activities. In some papers (Li, S. K., 1991, Feng, 1991, Chen, Z. Z., 1991, and Zhou, T. X., and others, 1991), the authors describe the natural laws of drought and the effects of water resources utilization on water balances and the environment, for some of the northern provinces in China, respectively. They also suggested strategies to lessen the effects of droughts, which can be summarized as follows:

(1) cultivating grasses and trees and adjusting the compositions of crops, so as to improve the ecologic environment;

(2) reforming the farming systems and improving the soil so as to raise its water–holding capacity;

(3) drawing up unified planning and management for comprehensive water resources utilization over a whole river basin, so as to protect the ecologic environment;

(4) saving on irrigated water and decreasing infiltration losses, so as to increase its effective uses;

(5) regulating both surface and groundwater and promoting their transformations, so as to intensify the repeated uses of water;

(6) strengthening real–time monitoring of droughts and predicting their evolution;

(7) controlling pollution and remedying the water–quality problems in situ,so as to raise the availability of water resources.

Zhang Shifa emphasized that it is necessary to analyze the historical evolution of droughts, and pay great attention to the research of it (Zhang, S. F., and others, 1991). They

introduces the applications of simulation models as tools in water–supply planning.

CONCLUDING REMARKS

As reported in this symposium, we have made some valuable progress in the knowledge of cause and effect and of temporal–spatial variabilities of hydrologic droughts, and in the techniques of their prediction. However, much still remains unknown to be further explored and studied. Due to the rapid growth of the world population and economic developments, and the deterioration of natural environment caused by mankind himself, drought damages would become even more severe.

China and the US are two nations which are similar in many aspects of physiographic and hydrological conditions. Through scientific exchanges and cooperation between the hydrologists of the two countries, the upper hands both in a long–standing history of drought–fighting and in advanced sciences and technologies can be combined together, so that our understandings on hydrologic droughts can be deepened and raised to a new high level.

REFERENCES

1. Chinese Academy of Meteorological Science (ed.), 1981, Yearly Charts of Dryness / Wetness in China for the Last 500–Year Period (in Chinese), Cartography Press, Beijing.
2. Gong, G., Zhang, P., Wu, X., and Zhang, G., 1983, Methods for Analyzing Historical Climatic Variations (in Chinese), Science Press, Beijing, p.59.
3. Guan, Z. Y., and Feng, Z. W., 1991, Examination of Dryness in Agriculture with Moisture Balance Indices, Proc. this Symposium.
4. Wang, S. W., Wang, G. X., and Zhang, Z. M., 1991, Droughts and Floods in North and East China, 1380–1989 A.D., ibid.
5. Wang, W. D.,Sun, H. X., and Shi, J. B., Analysis of Persistence of Hydrological Drought on the Upper Yellow River, China, ibid.
6. Shi, F. C., Wang, G. A., Mu, P., Ma, G. A., and Gao, Z. D., 1991, Recurrence Probability of 11–Year Continuous Low Water Period (1922–1932 A.D.) in the Yellow River, ibid.
7. Ma, X. F., Wang, Y. Z., and Huo, S. Q., 1991, Annual Runoff Series Extension and Runoff Variations in Lanzhou–Sanmenxia Reach of Yellow River, ibid.
8. Li, C. X., Shen, J., and Fan, R. S., 1991, Preliminary Analysis of Streamflow Drought Characteristics in the Middle Reach of the Yellow River, ibid.
9. Yang, R. F., Ding, J., and Deng, Y. R., 1991, Stochastic Analysis of Drought Properties of the Main Rivers in China, ibid.
10. Wang, S. X., 1991, Frequency Analysis of Hydrologic Samples with Zero Events, ibid.
11. Liu, F. J., and Qu, Y. G., 1991, A Model of Water Resources Transformation and its Results in Simulating the Urumqi River Basin, ibid.
12. Li, B. G., 1991, Prediction of Regional Soil Water and Drought, ibid.
13. Zhang, G. W., and Zhou, Y. C., 1991, Evaporation Properties and Estimates in the Land–Locked Arid Region in Xinjiang, China, ibid.
14. Zhou, Y. C., and Zhang, G. W., 1991, Water Balance Analysis in the Mountain Area of the Urumqi River Basin, ibid.
15. Chen, Q., and Chen, T. Y., 1991, Climatological Analysis of Seasonal Snow Resources in the Qilian Mountains, China, ibid.
16. Yang, B. Y., and Sun, H. X., 1991, Low Streamflow Forecast Model for Longyangxia Hydropower Station on the Yellow River, ibid.
17. Zhang, F. Y., 1991, Forecasting Dry–Season Drought and Runoff in China, ibid.
18. Wang, J. Q., 1991, Rainstorm Characteristics in the Arid Regions of China, ibid.

19.Hao, Y. L., 1991, Analysis and Forecast of the Water Quality State of Main Rivers in Xinjiang, ibid.
20.Wei, Z. Y., 1991, Surface–Water Chemical Changes due to Human Activities in the Tarim Basin, ibid.
21.Li, S. K., 1991, A Discussion on Drought in Arid Regions of China, ibid.
22.Feng, Y., 1991, Hydrological Characteristics of the Semi–Arid Haihe River Basin, China, ibid.
23.Chen, Z. Z., 1991, Transformation Between Hydrological Drought and Industrial and Agricultural Drought in Semi–Arid Areas, ibid.
24.Zhou, T. X., and Tang, M. D., 1991, Impact of Water Resources Utilization on the Ecological Environment in the Xinjiang Arid Region, China, ibid.
25.Zhang, S. F., and Wang, J. P., 1991, Application of a Simulation Model for Water–Supply Planning in an Arid Region of China, ibid.

U.S. CONTRIBUTIONS TO STUDIES OF DROUGHTS AND ARID-REGION HYDROLOGY

W. Kirby

U.S. Geological Survey, Reston, Virginia

ABSTRACT

An overview is given of U.S. contributions to the study of droughts and arid-region hydrology. Twenty-four U.S. papers were presented at this symposium. The topics covered included characterization of drought magnitude and frequency, frequency analysis of low flows at gaged and ungaged sites, stochastic time-series and event-based analyses of low flows and droughts, hydrologic processes in arid regions, use of remotely-sensed and ground-based data in evapotranspiration measurement, reservoir design, water-use determinations, and hydrologic water-balance modeling. The symposium was a valuable forum for exchange of ideas, and will serve as a basis for further progress in the study of droughts and arid-region hydrology.

INTRODUCTION

In broad qualitative terms, drought and aridity both are commonly recognized as conditions of scarcity of water. Drought is generally recognized as an extended period during which the supply of water is significantly less than normal. Aridity is a relatively permanent condition of scarcity relative to an absolute or global average level of water availability.

For purposes of water management or administration, more specific definitions or criteria might be needed. The details of these definitions can depend on actual or planned normal modes of water use, and on community activities that might be affected by water shortage. Four broad categories of drought are generally recognized: meteorological, agricultural, hydrologic, and socioeconomic. Meteorological drought refers solely to shortage of precipitation, agricultural drought to shortage of soil moisture, and hydrologic drought to shortage of surface-water and ground-water supplies and storage levels. Socioeconomic drought refers to water shortages that have adverse effects on human affairs, without regard to their hydrometeorological nature.

Water has been called the elixir of life. Because of water's central role in human life and society, shortages in water supply have far-reaching social and economic repercussions. These range from interference with water-based recreation and river navigation to disruption of industrial and agricultural production, and, in extreme cases, even to forced migration and famine. Many of the most effective means for alleviating the socioeconomic effects of drought are technological, administrative, legal, and political measures to

improve the efficiency of use of the limited water supply that is available (National Research Council, 1986; Grigg and Vlachos, 1988).

Information on drought hydrology is important for drought mitigation planning even though the actual remedial measures might not deal with explicitly hydrologic issues. Drought magnitude and frequency information are needed for long-range planning. Monitoring and forecasts are needed for administration and operation of facilities. Fundamental studies also are needed to identify the relevant hydrologic variables for describing drought magnitude and for elucidating the hydrometeorological processes that control the onset, evolution, and cessation of drought. Finally, mathematical models and case studies are needed to provide techniques and guidance for practical application.

This paper presents a general overview of the U.S. contributions to this symposium, with emphasis on how the contributions relate to needs for drought information. For convenience of reference, the U.S. contributions are referred to by authors' names only; the contributions themselves are contained in this volume and can be found by reference to the table of contents.

CHARACTERIZATION OF DROUGHT MAGNITUDE

Quantification and statistical summarization of droughts is difficult because of their multidimensional character. To obtain a measure of drought magnitude, it is necessary to identify and integrate measures of water availability, water demand, temporal duration, and spatial extent. The frequency of recurrence of droughts of a particular magnitude is defined by the joint probability distribution of these variables.

A major challenge is the integration of time-series data at numerous gages in a region to obtain a coherent spatial representation of the data. R.W. Paulson and his colleagues describe how the U.S. Geological Survey (USGS), in its National Water Summary 1988-1989 (NWS88-89), has assembled, analyzed, and presented streamflow data to depict the magnitude and frequency of historical droughts (and floods) throughout the U.S. NWS88-89 is intended for use by the non-technical public, political leaders, and policy makers. G.E. Willeke and his colleagues describe an interagency effort led by the U.S. Army Corps of Engineers to develop a drought atlas showing regional variations of frequency distributions of several measures of drought magnitude, including precipitation and soil moisture (Palmer drought severity index) as well as stream flow. The atlas will contain more detailed statistical information than the NWS88-89 and is directed at a more technical audience of engineers, planners, and administrators.

CHARACTERISTICS OF ARID-REGION HYDROLOGY

A chief characteristic of arid-region hydrology is the extreme variability of rainfall and runoff in both time and space. Many arid-region streams are dry except when floods occur. The floods commonly disappear after flowing for a short distance because the water infiltrates into the alluvial stream beds;

this infiltration is a major mechanism for replenishment of the ground water. H.W. Hjalmarson describes the temporal and spatial patterns of flood occurrence in arid regions. He also shows that methods of flood frequency analysis developed in humid environments are not appropriate for use in arid regions. H.J. Morel-Seytoux and his colleagues analyze aquifer recharge processes that govern the exchange of water between surface runoff and ground water; this information is valuable for planning the conjunctive use of surface water and ground water. R.H. Hawkins and his colleagues describe rainfall and soil-erosion processes in arid regions and describe the use of an erosion-simulation model for estimating potential effects of changes in precipitation regimes on erosion.

A. Pupacko presents a case study of evaluating the variability of streamflows of the snowmelt-fed Carson River. The study illustrates the variety of streamflow characteristics that are subject to change, whether from possible climate changes or from normal statistical variability. R.S. Parker analyzes streamflow variability in the Gunnison River basin by correlating annual flow with the water content of the snow pack in order to evaluate the probability of drought in any year.

A continuing challenge to hydrologists and climatologists is the determination of evaporation from natural land surfaces and vegetation. Measurement of the relevant variables is difficult in the field and the heterogeneity of natural environment makes it difficult to integrate point measurements for determination of areal totals. Nonetheless, information on areal evaporation is important for defining water balances, assessing water resources, and modeling of ground water, surface water, and climate. A.M. Sturrock and W.D. Nichols compared three types of vapor-pressure sensors in field trials. They found close agreement among the sensors and concluded that low-cost units merited further evaluation for use at remote field sites. W.D. Nichols presents energy budget measurements of evapotranspiration (latent heat flux) and shows that they can be estimated by correlating them with measurements of net radiation, soil heat flux, and calendar date.

Evaporation measurement by energy budget methods offers the prospect of using remote sensing for operational monitoring of evaporation on an areal or regional basis. M.S. Moran and R.D. Jackson show how spectral data from satellite-based sensors can be used (in conjunction with calibrations developed from ground-based data) to evaluate all terms of the energy budget. P.W. Brown and S.J. Owen-Joyce investigate the effects of data acquisition rate and location of ground-based instruments on evaporation measurements made by conjunctive use of remotely-sensed and ground-based data.

Water-quality problems associated with irrigated agriculture have become a major focus of public concern and hydrologic study. H.R. Feltz presents an overview of a program of studies of irrigation-induced water-quality problems being conducted by the USGS and other agencies in the U.S. Department of the Interior. R.A. Engberg presents results from these studies for the concentration and distribution of selenium, which is one of the principal elements of concern, in the western United States.

FREQUENCY ANALYSIS OF LOW FLOWS

For many applications in engineering planning, design, and regulation, it is necessary to know frequency distributions of annual minimum flows. For example, the annual minimum 7-day-mean flow with 10 percent annual chance of non-exceedance is a widely-used basis for regulating the discharge of wastewaters to streams. Other low-flow characteristic discharges having different averaging periods and probabilities might be of interest for other applications.

Although it is straightforward to estimate low-flow characteristics from continuous records of streamflow, such records are not available at many sites where low-flow characteristics are needed. W.O. Thomas, Jr., and J.R. Stedinger describe procedures for estimating frequency distributions of low flows using correlations between base-flow measurements at ungaged sites and continuous records at index sites. G.D. Tasker describes procedures for correlating streamflow characteristics with drainage basin characteristics to obtain regional estimating equations for use at sites where no streamflow data are available.

STOCHASTIC ANALYSIS OF LOW FLOWS AND DROUGHTS

Annual low flows and droughts are extreme events in the continuous time series of streamflow. The intensity, duration, and spatial extent of these extremes are controlled by the nature and strength of serial and cross correlations in the streamflow stochastic process. J.D. Salas and M.W. Abdelmohsen present mathematical time-series models that not only reproduce monthly and annual streamflow statistics without use of disaggregation but also reproduce observed drought duration and magnitude statistics. W.L. Lane describes the application of a multi-site autoregressive disaggregation time series model to simulate streamflows in a major water storage and transbasin diversion project. V.L. Lopes and his colleagues present an event-based model of rain storm occurrence and use it to derive statistics of summer-season droughts in the U.S. southwestern desert.

The limited length of instrumental records of streamflow and precipitation is an impediment to statistical analysis of droughts, and especially of multi-year droughts. D.M. Meko explains how tree growth rings have been used to reconstruct regional drought history in the U.S. southwest for a period extending back to A.D. 1600 and shows that this long record is needed for proper understanding of drought variability.

MODELING AND MANAGEMENT

Measures for alleviating the effects of droughts include both the use of reservoirs to store water for use during droughts and the planning of water deliveries to avoid over-commitment of limited water supplies. E.L. Johns describes the procedures used by the U.S. Bureau of Reclamation to determine optimum reservoir storage capacity; this determination involves consideration

of the water-supply quantity and variability, water losses, and costs of water shortages, as well as construction costs. C.R. Phillips describes the Bureau of Reclamation's procedures for determining the quantities of water that can be reliably delivered from reservoirs of a given size. R.A. Herbert and D.W. Litke present water-use data that show how municipal and domestic water use varies in response to drought conditions and the imposition of water-use restrictions and conservation measures.

Hydrologic drought results from an interplay of factors including precipitation, evapotranspiration, and ground-water and surface-water flows and storages. Comprehensive hydrologic models provide a valuable framework for integrating all available information about the various factors affecting drought flows. G.D. Tasker presents a monthly water-balance model that uses precipitation and temperature data to estimate evapotranspiration, streamflow, and storage changes; effects of present or possible future regulation and diversion patterns can be simulated. E.B. Yates presents a comprehensive case study of droughts in a stream-aquifer system, using a ground-water flow model that included soil-moisture-accounting and streamflow-routing algorithms; tree-ring records were used to supplement rainfall and streamflow data for estimation of drought frequencies.

CONCLUSIONS

From the foregoing summary of U.S. contributions to this symposium, it is clear that considerable interest and effort is being directed at drought and arid-region hydrology in the U.S. Nonetheless, much remains to be done. The fundamental problems that remain include: representation of the multidimensional frequency distribution of drought intensity, duration, and spatial extent; identification and elucidation of the hydrometeorological processes that govern drought onset, evolution, and termination; estimation of low-flow characteristics at ungaged sites; and aggregation and disaggregation of data at point-measurement and various regional scales. A better understanding of the interconnections of all components of the hydrologic cycle still is needed.

This symposium provides a valuable opportunity for U.S. and Chinese hydrologists to share their unique perspectives on the study of droughts and arid-region hydrology. It is hoped that hydrologists in both countries will gain a broader and deeper understanding as the result of this exposure.

REFERENCES

Grigg, N.S., and Vlachos, E.C., eds., 1988, Drought Water Management, Proceedings of a National Workshop, Washington, DC, November 1-2, 1988: Colordo State University, International School for Water Resources, 265 p.

National Research Council, 1986, Drought Management and Its Impact on Public Water Systems, Report on a Colloquium Sponsored by the Water Science and Technology Board, September 5, 1985: Washington, DC, National Academy Press, 127 p.

TOPIC A

CHARACTERIZATION AND QUANTIFICATION OF DROUGHTS

A DISCUSSION ON DROUGHT IN ARID REGIONS OF CHINA

Li Shikui

Academy of Meteorological Science,
State Meteorological Administration, Beijing, China

ABSTRACT

Focusing on analyzing the generation law of drought in arid regions of China, the paper comprises the following parts: the influences of drought on agriculture in arid regions, the relations between the generation of drought climates and geographic positions, the classification and evaluation of humid climatic situations in the northern arid regions of China, and some suggestions on the strategy to lessen the effects of drought.

INTRODUCTION

Large arid and semi-arid regions make up half of the territory of China; the semi-arid regions make up approximately 20 percent and the arid regions, where annual precipitation is under 250 mm, approximately 30 percent. The northern semi-arid regions of China are used for agriculture, animal husbandry and forestry, and are significant construction base areas of the three Norths Shelter-Belt (in the western part of Northeast China, North China, and Northwest China). Rain-supplied agriculture is the most common practice in semi-arid regions. The ecosystems of grasslands in arid regions depend entirely on sparse precipitation, and are relatively unstable. The effects of droughts in the steppes of China's arid regions are intensified due to desertification as a result of overcropping, overpasturing, and overcutting trees; most of the steppe's grasslands have deteriorated seriously. Their grass output is low and grass quality is poor; stock capacity and animal productivity are lower than those of many other countries. During the last 30 years the average annual drought-ridden area of China covered 294 million mu(1 mu=1/15ha.), equal to 19.2 percent of its arable area, and the disaster-ridden area was 100 million mu. From 1950 to 1983, there were 8 cases when the drought-ridden area exceeded 400 million mu,and the relatively serious droughts occurred within a span of 12 years.

CAUSES OF ARID CLIMATE

Drought is a natural climatic phenomenon. The arid, semi-arid regions, and desert zones of most of the world are usually located in central areas and western seashores of the continents, lying in subtropical high pressure belts and trade-wind belts, where the existence of subtropical high pressure is an essential and direct cause of the drought and rare rainfall. But the arid regions and desert zones of China are different from the above cases. They are located in westerly belts of the middle latitudes. The influence of the Qing-Zang Plateau plays an important role in the causes of the extremely arid climate and the desert in the northern part of the Plateau.

Two different types of mechanism of short-term climatic variation exist in arid regions. The first is global, such as the influence of oceans' variation upon the atmosphere. In recent years, a large number of studies in China and other countries on the El-Nino phenomenon and the Southern Oscillation have shown that these

phenomena have an important influence on short-term climatic variation , although not all relevant phenomena can be explained yet. The second is a feedback mechanism. It mainly includes: (1) humidity and evapo-transpiration and (2) surface albedo. The studies, postulating that changes in surface characteristics may influence the climate, have shown that the feedback effects of soil moisture, evapo-transpiration and surface albedo cannot be ignored.

REGULARITIES OF THE OCCURENCE OF DROUGHT CALAMITIES

China is a country well known for its monsoon climate; thus its droughts not only occur frequently, but also cover vast areas. Drought is one of the main natural calamities affecting agricultural production of our country. According to the rainfall records found in many historial documents and measurements taken in Beijing over 256 years(1726-1981), the five-year average variation of precipitation had its dry and wet spells: there was a relatively dry spell from 1728 to 1778; yet 1779-1810 and 1868-1896 were relatively wet spells. The past 500 years in eastern China can be divided into three ages. From 1479 to 1691 the drought frequency was high, and the gravest droughts occurred 10 times. From 1692 to 1890 the droughts took place less often, the gravest droughts occurring only 4 times. Since 1891 droughts have occurred more frequently again. Within each age there were series of wet-dry variation with a time scale of 10-20 years. During these dry spells droughts occurred more frequently. According to relevant statistical data, droughts in China took place 1056 times from 206 B.C. to 1949 A.D.. According to the historical data of the last 500 years and the rainfall records of recent times, the scrious droughts in China took place 26 times in latitudes 25°-30°N, 34 times in 30°-35°N, 58 tines in 35°-40°N, and successive droughts were not rare. The drought situation of northern China in the last four centuries is shown in Table 1.

Table 1.-- Numbers of drought years in recent centuries in provinces of North China.

Year	Hebei	Henan	Shandong	Shanxi
1501-1600	72	63	74	47
1601-1700	89	84	67	67
1701-1800	70	63	74	52
1801-1900	79	60	91	69

Temporal and Spatial Distribution of Drought in Northern China

The water deficiency of the northern arid regions of the China has remarkable regional characteristics.According to the moisture status,the regions are divided into three types. The semihumid region is mainly distributed in the middle-south of North China and in the middle of the Songhua River and Nen River Plains of Northeast China; the semiarid region is mainly distributed in the north of North China and in the west of Northeast China; the arid region is mainly distributed in the inland of Northwest China. Agricultural management mode of the regions is mainly dependent upon the water deficiency level. Classification of the arid regions in accordance with the humidity condition is shown in table 2 and Figure 1.

Table 2.-- Classification and Assessment of Humidity Condition in Northern Arid Regions of China.

Aridity conditions	Arid	Semiarid
Humidity	<0.3	0.3-0.6
Annual precipitation (mm)	<250	250-400
Water deficiency (mm)	600-1200	300-600
Effects on agriculture	no irrigation means no agriculture	yield is unstable if no irrigation

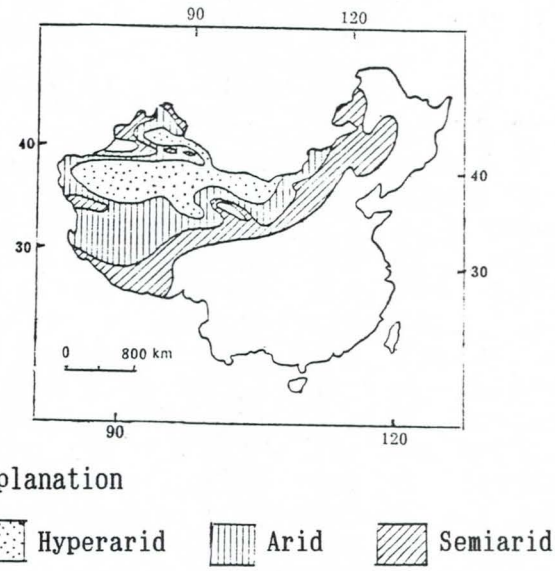

Explanation

Hyperarid Arid Semiarid

Figure 1.--Distribution of Arid Regions in China.

Arid Pastoral Areas in Northwest China

The areas of Northwest China of annual precipitation under 250 mm are often in a drought state all the year round. Their precipitation can only meet the existence of extraordinary drought-resistent plants and their fresh grass yield per mu is only 10-50kg. Most plants are in a state to maintain their lives and barely have growth quantity if they have met a drought year. The farmlands of these areas have a poor productivity. Most parts of the areas are located in the Gobi Desert of strong sandy wind and grave wind erosion.

"Oasis Farming Areas" in Northwest China

The areas of this type have a long farming history. Everywhere has been cultivated as farmland if it has water resources. These lands have become motley oases and have formed a unique ecological system of oasis agriculture in the arid region. The water resources for irrigation are stable because the quantity of snow melt is dependent upon temperature; thus the droughts are lighter in these areas. For example, Houtao area of Inner Mongolia, Yinchuan of Ningxia Autonomous Region, Hexi Corridor of Gansu Province, Shihezi of Xinjiang Autonomous Region, and so on, are important bases to produce grain,crops and economic plants.The key problem there is secondary salinzation of soil, which is common and severe as a result of the dry climate and intense evaporation. Based upon the supply quantity of water resources the oasis agriculture should be rationally developed with intensive management in order to increase the water utilization efficiency and prevent the secondary salinization of soil.

Windy and Semiarid Region in the West Northeast China

This region mainly includes the areas of the middle and lower reaches of the Nong River, Baicheng Prefecture of Jilin Province, Chaoyang and Fuxin Prefectures of Liaoning Province, Shelimu and Zhaowuda Prefectures of Inner Mongolia, the piedmont hills and plains of Xingan and Hulunbeier Prefectures of Inner Mongolia. The region is located in a belt of remarkably weakened southeastern monsoon. The annual precipitation of most of the areas in the region is under 400mm. In this region the spring droughts are serious, mainly because of sparse spring rainfall, bad state of soil moisture before sowing or planting, strong spring wind, and quick loss of soil moisture of soil surface after thawing so that the dry layer of soil is ceaselessly deepened. During spring sowing in grave drought years, the thickness of dry soil is often above 10cm, sometimes above 40cm. The moisture content of the dry layer of light loam would often attain to wilting humidity, and the dry layer would remarkably be deepened, which can gravely affect the turning green of forage grass, sowing, and emergence of seedlings. For white ustalf and sandy soil, because the duration of soil dampness is very short, the spring sowing often can't be completed in the period of melting snow, and mostly must rely on dribbling with a little water or the coming of rainfall. For sandy castanozem, the depth of its dry layer in spring often exceeds 15 cm, and even exceeds 17 cm in extraordinary drought years, so that destruction of seeds by wind often occurs. In late spring, the soil moisture is lost quickly, and strengthens soil drought. The period to get rid of drought due to too deep dry layer is about June 10 to July 10, by rain.
In the west of Northeast China,the frequency of severe spring drought is about 20-30 percent. In the same region the frequency of summer drought is about 20-40 percent; the frequency of successive spring-summer drought is about 20-40 percent.

Semiarid Region in the Middle-South of Inner Mongolia and North of the Loess Plateau

This region includes the south of Xilinguole League and the middle-south of Wulanchabu League of Inner Mongolia, Bashang Prefecture in the north of Hebei Province, the north of Shanxi and Shaanxi province, the south of Ningxia Region and the center of Gansu province. This region of annual precipitation 300-450mm is located in a transitional zone from agriculture to animal husbandry. According to historical data about the droughts and floods of the last 500 years, droughts occurred 102 times in 1468-1973 in Ningxia; on an average, one serious drought in every 5 years, among which successive drought years occurred 26 times, the longest lasting 4-5 yeras.
The localities menaced by serious droughts in Gansu province include 18 counties in its middle part, in a south-to-north zone of relatively sparse rainfall. In most of these counties the precipitation is about 400mm, and the precipitation variability is high.

Semihumid Region Liable to Drought in the Middle-North of the North China Plain

This region mainly includes the center of Hebei province, the northwest of Shandong province and parts of the counties and cities in the northwest of Henan province. In most of these regions the precipitation is about 500-600mm and concentrated in July and August; the precipitation variability is high, the soil fertility is poor, and the soil alkali-salinization is severe. In the center and northwest of Hebei province there are 8-9 spring-drought years in every 10, among which 5-6 have serious spring droughts. The so-called "dog days" drought is centered mainly in the basins of the Sanggan and Yang Rivers, where the drought frequency is 40-55 percent. The center of

the fall drought is mainly Hengshui prefecture, where the drought frequency is 40 percent. The Hai River basin is a drought center of the Huang- Huai-Hai Plain. The successive drought years are 63 percent of all drought years in the basin of Hai River.

In Shandong province, spring droughts are dominant. The northwestern and northern seasides of Shandong province are areas with serious spring droughts and early summer droughts, where the spring rainfall does not attain to 80 mm, the number of successive rainless days may attain to 60-80, and the dry hot wind in early summer often intensifies the drought situation. In the hill areas of northern and western Henan province, the probability of drought in the jointing and earing stages of wheat is 3-6 times in every 10 years.

MEASURES TO MITIGATE DROUGHT

Planting Grass and Trees to Improve Ecological Environment

The areas of northern China having precipitation of about 400 mm are marginally suitable for planting crops and trees. If trees are no irrigation and ground water resources, then most of the poplars planted on large scale would become "dwarfing trees". Thus, in the arid regions the afforestation mainly should be with grass and shrubs. But in some places with good watery condition, some trees may be planted. On arid mountain slopes, drought-resistant shrubs may be planted. In areas of precipitation of about 500 mm, combinations of grass, shrubs and trees or combinations of shrubs and trees may be used.

Building Water Conservancy Projects, and Capital Improvements of Farmland

In areas with favorable conditions, building large-, medium- and small-sized water conservancy projects and gradually enhancing the irrigation level can partially or entirely solve the problem of seasonal drought due to seasonal unbalanced distribution of rainfall. On the dry farmlands, leveling fields, building terraces, ameliorating soil, and enhancing water-holding capacity of soil also can preserve of the rainy-season precipitation for use in the next spring. According to the measurements of the Water conservancy Institute of the Chinese Academy of Sciences, the water-holding capacity of a meter of loess soil, correctly ameliorated and fertilized, can attain to 200-300 mm. In addition, the fertilized soil can improve the development of the root system, enhance "the ability of roots to seek water" and fulfil "the function of fertilizer to regulate water".

Using Effective Measures of Drought-Relief and Soil Moisture Preservation

The measures of drought-relief and soil moisture preservation are the core of dry-land farming. The methods for sowing seeds and effectively using spring soil moisture against drought are as follows: to begin sowing at just the rigt time in order to use the existent soil moisture; to roll on soil surface after sowing in order to conduct the subsoil moisture upward toward the seeds; to sow seeds moderately deeper into soil in order to preserve soil moisture for sprouting; to pour a little water into the soil around seeds in order to give enough soil moisture for sprouting. In China the traditional farming techniques for preserving soil moisture are deep ploughing, harrowing, milling, rolling, and tilling.

Economizing Irrigation Water and Increasing Water Utilization Efficiency

The essential measures of economizing water resources are as follows: to promote sprinkler, drop, and percolation irrigation techniques; to take good measures of canal seepage control; to master the water requirement law of crops in order to irrigate more rationally. As some experiences have pointed out, if it grasps the key periods to irrigate winter wheat in North China. then water can be saved and the economical benefits can be raised. Taking some drought-resistant measures, for instance, using covers of plastic film to reduce the evaporation from soil surface, can greatly raise the water utilization efficiency. According to relevant data, the dry matters produced with 1 ton of water can be only 0.2 kg in the extensive farming, but 0.7-1.2 kg in the intensive farming and 2.4-2.8 kg in the test fields of good conditions. Thus there is a big potential to raise the utilization efficiency of water resources.

Expanding the Area of Drought-Resistant Crops and Regulating the Proportion of Summer Crops to Fall Crops

In the technique system of dry farming, with drought prevention as its core, one selects the drought-resistant crops of stable and high yield, such as kaoliang, foxtail millet, broom corn millet, etc., which need little water for their germination, can be sowed against spring drought, and can quickly restore their growth when they have met rain after undergoing a long drought in the seeding period. The features of precipitation in North China are dry in spring and rainy in summer, which are beneficial to fall crops and unfavorable to summer crops. Hence it would be beneficial to increase the proportion of late fall crops.

THE 1988-89 NATIONAL WATER SUMMARY— A SUMMARY OF FLOODS AND DROUGHTS IN THE UNITED STATES

Richard W. Paulson[1]
Edith B. Chase[1]
John S. Williams[2]
Robert S. Roberts[3]

ABSTRACT

The U.S. Geological Survey's National Water Summary series of reports describes the conditions and characteristics of the Nation's water resources. The latest report—the sixth in the series—is entitled "National Water Summary 1988-89—Hydrologic Events and Floods and Droughts" and focuses on the natural occurrence of floods and droughts as defined from an analysis of stream-discharge data. In addition to summaries of the hydrologic events for water years 1988 and 1989 and articles on the scientific and institutional aspects of floods and droughts, the report contains State-by-State summaries of the most memorable floods and droughts of record. The State summaries show the areal extent and give estimates of the recurrence intervals of these extreme hydrologic events.

INTRODUCTION

The National Water Summary (NWS) series of reports presents information about the Nation's water resources in a nontechnical format. The series is intended for Federal, State, and local officials, and members of the public who have a need to know about the status of water resources, but are not necessarily scientists or engineers. Each report presents information primarily on one aspect or theme of water resources and, by means of standardized text and illustrations, allow a comparison of water-resources conditions across the Nation. Additionally, each report presents information on the hydrologic and meteorologic conditions in the United States for one or more water years, which begin on October 1 and conclude on the following September 30. Themes for the first six NWS reports are water issues (U.S. Geological Survey, 1984), ground-water quantity (U.S. Geological Survey, 1985), surface-water quantity (U.S. Geological Survey, 1986), ground-water quality (U.S. Geological Survey, 1988), water supply and use (U.S. Geological Survey, 1990), and floods and droughts (U.S. Geological Survey, 1991); themes for planned reports are stream water quality and wetlands.

CONTENTS OF NATIONAL WATER SUMMARY

Each NWS report has three principal parts: "Hydrologic Conditions and Water Related Events, " Hydrologic Perspectives on Water Issues," and State-by-State summaries. Each report also contains supplementary reference material that varies with the theme of the report, but can include glossaries, conversion tables, lists of selected chemical names for water-quality contaminants, and maps of water-resources regions and subregions.

Hydrologic Conditions and Water Related Events — The Hydrologic Conditions part of each NWS report describes the hydrologic and meteorologic conditions of the United States during a water year. The first five NWS reports documented these conditions during a single water year, whereas the NWS report on floods and droughts is the first of subsequent reports that will document the conditions for two water years.

1. U.S. Geological Survey, Reston, Virginia
2. U.S. Geological Survey, Denver, Colorado
3. U.S. Geological Survey, Helena, Montana

The annual and seasonal conditions for each year are described. The presentation relies extensively on national maps of streamflow, precipitation, temperature, and the 700-millibar pressure surface; graphs of monthly streamflow for selected rivers and storage for selected reservoirs in the United States; and a map that shows the location of 75-100 discrete hydrologic events, such as floods, spills of petroleum products or other contaminants, landslides, and fishkills. Textual information about each event that is cited on the map is provided in an accompanying table; each table entry of about 100-300 words quantitatively describes lives lost and damage sustained, the size and expected recurrence interval of a flood or rainstorm, the extent of a fishkill, and the quantity and composition of contaminant spills. Additionally, one or more articles about memorable hydrologic events also is included; these articles, which normally are 2 to 4 pages long, provide much more information about the events that are documented in the table of events.

Hydrologic Perspectives on Water Issues — The Hydrologic Perspectives part contains several articles that describe technical and institutional issues on the theme that is presented in the State summaries. These articles provide in-depth information and background about the theme that is discussed in the State summaries. For example, the hydrologic perspectives discussion on water supply and use (U.S. Geological Survey, 1990) contains in-depth articles on agricultural, industrial, and domestic water use; instream flows; and water-use forecasting.

State-by-State Summaries — The State-by-State summaries consist of a 6-10 page summary for each of the 50 States, Puerto Rico, the U.S. Virgin Islands, and the Western Pacific Islands (formerly known as the Trust Territories of the Pacific Islands, Saipan, Guam, and American Samoa). The summary for the District of Columbia is included in the Maryland summary.

Each State summary presents hydrologic information in a standardized format for text, tables, graphs, and maps. Each summary generally consists of an overview of the status of the hydrologic theme in the State, systematic descriptions of the theme in representative areas of the State, and a discussion of Federal, State, and local responsibilities in water-resources management. If possible, the State summaries are organized to complement other U.S. Geological Survey reports that have been published or are in preparation. For example, the State summary discussion on water supply and use (U.S. Geological Survey, 1990) presents county-level ground-, surface-, and total-withdrawal maps that complement State-level withdrawal maps presented in Solley and others (1988).

NATIONAL WATER SUMMARY 1988-89— HYDROLOGIC EVENTS AND FLOODS AND DROUGHTS

The theme of the 1988-89 NWS report is the occurrence of floods and droughts in the United States. These hydrologic events are defined from an analysis of stream-discharge data.

Hydrologic Conditions and Water Related Events, Water Years 1988-89 — For water years 1988 and 1989 (October 1, 1987, through September 30, 1989), 173 hydrologic events are described. In addition, one article, "Storm-Surge Flooding by Hurricane Hugo on the U.S. Virgin Islands, Puerto Rico, and South Carolina, September 1989," discusses the effects and damage of Hurricane Hugo. The article on Hurricane Hugo reports that 26 lives were lost and $9 billion in damage was sustained to United States property as a result of the storm.

Hydrologic Perspectives on Water Issues — Nine articles collectively provide an introduction to some of the hydrologic aspects of floods and droughts and the societal activities that are undertaken to mitigate their effects. These articles are summarized below.

"Climate and Floods" examines the many diverse climate regimes in the United States and the climatic perturbations that cause floods. Although the most-humid drainage basins receive far more moisture than the most-arid basins, both areas are subjected to periodic flooding because, from time to time, the atmosphere delivers more moisture than is expected or can be readily absorbed or stored within the

basins. The moisture is delivered by several short-lived mechanisms, such as convective thunderstorms, tropical storms and hurricanes, extratropical cyclone and frontal passages, and rapid snowmelt. These mechanisms are part of a larger climatic framework that determines the availability and pathways of ocean-derived moisture; this mechanism is presented diagramatically in each State report (fig. 1).

"Climate and Droughts" discusses the long-term deficit in the delivery of moisture by the atmosphere to drainage basins. Droughts are associated closely with persistent atmospheric patterns that deliver less than normal moisture to an area. Atmospheric circulation patterns are affected strongly by the exchange of moisture and heat between the oceans and the atmosphere, and to a lesser extent, by the soil-moisture content or the snow cover of land-surface areas. Understanding the cause of a drought in an area requires knowledge of persistent atmospheric circulation patterns that are driven by sea- and land-surface anomalies beyond the area affected.

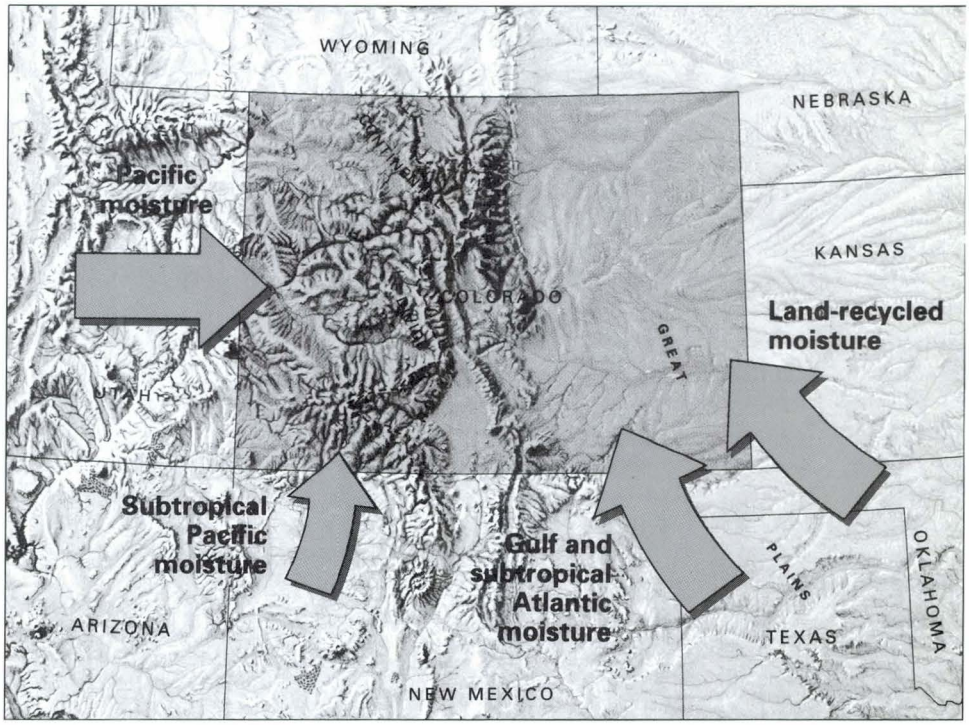

Figure 1. Principal moisture origin and delivery patterns, Colorado. (Sources: Data from Clark, 1989; physiographic diagram from Fenneman, 1946)

"Evapotranspiration and Droughts" discusses the loss of water to the atmosphere through evaporation and transpiration, which is the loss of water from living plant surfaces. Evapotranspiration contributes to the effects of drought because it provides moisture to the atmosphere during time of reduced rainfall. The result is increased moisture deficiency in soil and decreased size of water bodies.

"Paleohydrology and Its Value in Analyzing Floods and Droughts" examines techniques to estimate the frequency and magnitude of extreme hydrologic events that occurred before systematic records of hydrologic and meteorologic data were collected. This period of systematic data collection is about 100 years in some areas of the United States.

Since earliest times, human activities have been affected by hydrologic extremes and societies have attempted to predict, cope with, and mitigate their effects. In modern times in the United States, the Federal Government is involved in the prediction of hydrologic extremes, minimizing their effects, and compensating for loss of property and income. The article "Flood Forecasting and Drought Prediction by the National Weather Service" discusses the role of that agency in forecasting stream discharge. In support of that goal, the National Weather Service operates a network of 13 River Forecast Centers that forecast river discharges and issue flood warnings. It also has developed a Water Resources Forecasting System to help provide drought forecasting capabilities. "Flood Reduction and Drought Functions of the U.S. Army Corps of Engineers" discusses the expanding role of the Federal Government in flood control during the 20th century. Because flooding is the most common and costly natural disaster in the United States, the Congress has appropriated about $25 billion since 1936 to the Corps of Engineers to control floods nationwide. The Corps of Engineers also operates many projects to help mitigate the effects of drought. The article "National Flood Insurance Program—-Twenty Years of Progress Toward Decreas-

ing Nationwide Flood Losses" discusses the Federal Government's national flood insurance program, which is administered by the Federal Emergency Management Agency.

The management and mitigation of extreme hydrologic events at the State and local level differs from State to State; two examples are provided. "Flood Simulation for a Large Reservoir System in the Lower Colorado River Basin, Texas" describes a network of seven dams and reservoirs in the Lower Colorado River Basin in Texas whose operations are simulated by a mathematical model. In contrast to floods, the article "Management of Water Resources for Drought Conditions" indicates that, in most States, society tends to be unwilling to plan for droughts and that many local governments are reactive to them.

State Summaries of Floods and Droughts — Each State summary begins with an overview of the history of the most memorable floods and droughts in the State's history, which is documented more fully in table 1. The overview is followed by a discussion of the general climatology of the State. This discussion includes a map (fig. 1) that shows, by means of a set of one or more vectors, the principal sources of the moisture that is conveyed to the State by the atmosphere. This type of map was prepared for each State by Clark (1989), who identified the Pacific Ocean, the Subtropical Pacific Ocean, the Gulf of Mexico and Subtropical Atlantic Ocean, the Atlantic Ocean, the Northeasterly Atlantic Ocean, the Great Lakes, and Land-Recycled Moisture as sources of moisture. Because moisture-delivery systems are complex and quantitative moisture delivery by these sources is difficult to estimate and portray graphically, only the relative contribution of each source is shown and is designated by the size of the arrows in the figure. A large arrow indicates a primary source of moisture, half-size arrows represent secondary sources, and small arrows represent locally significant sources, such as the Great Lakes. The arrows, which may be straight or curved, are oriented to represent the predominant long-term trajectories of the atmospheric flow of moisture from source to destination.

Table 1. Chronology of major and other memorable floods and droughts in Colorado, 1911–88

[Recurrence interval: The average interval of time within which streamflow will be greater than a particular value for floods or less than a particular value for droughts. Symbols: >, greater than; <less than. Sources: Recurrence intervals calculated from U.S. Geological Survey data; other information from U.S. Geological Survey, State and local reports, and newspapers]

Flood or drought	Date	Area affected (fig. 2)	Recurrence interval (years)	Remarks
Flood	Oct. 4–6, 1911	Rio Grande and San Juan River basins.	>100	Widespread, intense rainfall for 3–5 days. Widespread damage in southwest.
Floods . . .	June 2–17 and Aug. 2, 1921	North Platte, Yampa, White, Roaring Fork, East, Uncompahgre, and Arkansas River basins.	25 to >100	General statewide rainfall and isolated severe thunderstorms and areas of excessive snowmelt.
Drought . .	1930–42	Statewide	20 to >25	Regional.
Floods . . .	July 7 and Sept. 9–10, 1933	South Platte River basin, Plum, Clear, and Bear Creek basins.	50 to 100	Intense localized rainfall.
Flood	May 30–June 1, 1935	Kiowa, Bijou, Fountain, and Monument Creek basins, and South Fork Republican River basin.	20 to 70	Locally intense thunderstorms. Deaths, 13; damage in Colorado Springs and Pueblo.
Flood	Sept. 2–4, 1938	Bear and Clear Creek basins . .	20 to 60	Locally intense thunderstorms.
Flood	Apr. 23–24, 1942	Purgatoire River basin	20 to 40	Intense rainfall combined with snowmelt runoff. Highway and railroad bridges destroyed.
Drought . .	1949–57	Statewide	10 to >25	Regional.
Flood	June 4–16, 1952	Colorado, Yampa, White, and Dolores River basins.	20 to 50	Snowmelt, probably combined with rainfall runoff.
Floods . . .	June 4–July 1, 1957	Arkansas, Roaring Fork, Gunnison, and North Platte River basins.	25 to >100	Snowmelt combined with rainfall runoff.
Drought . .	1958–70	Statewide	<10 to >25	Regional.
Flood	June 14–22, 1965	South Platte and Arkansas River basins.	5 to >100	Widespread intense rainfall for several days. Declared major disaster area. Deaths, 24; damage, $570 million.
Flood	Sept. 5–17, 1970	San Juan and Dolores River basins.	5 to >100	Intense, sustained rainfall. Declared major disaster area. Damage, $2.9 million.
Flood	July 31–Aug. 1, 1976	Big Thompson and Cache la Poudre River basins.	5 to >100	Intense localized rainfall for about 3 hours. Declared major disaster area. Deaths, 144; damage, $39 million.
Drought . .	1976–82	Statewide	<10 to >25	Regional.
Flood	July 15, 1982	Roaring and Fall Rivers	>100	Dam failure. Declared major disaster area. Deaths, 3; damage, $31 million.
Floods . . .	June and July 1983	Colorado, Dolores, and White River basins (June), and Bear Creek basin (July).	10 to >100	Snowmelt combined with rainfall runoff.
Floods . . .	May and June 1984	Colorado, Gunnison, White, Roaring Fork, Uncompahgre, and Yampa River basins.	10 to >100	Snowmelt combined with rainfall runoff. Declared major disaster area.

Areal Extent of Droughts

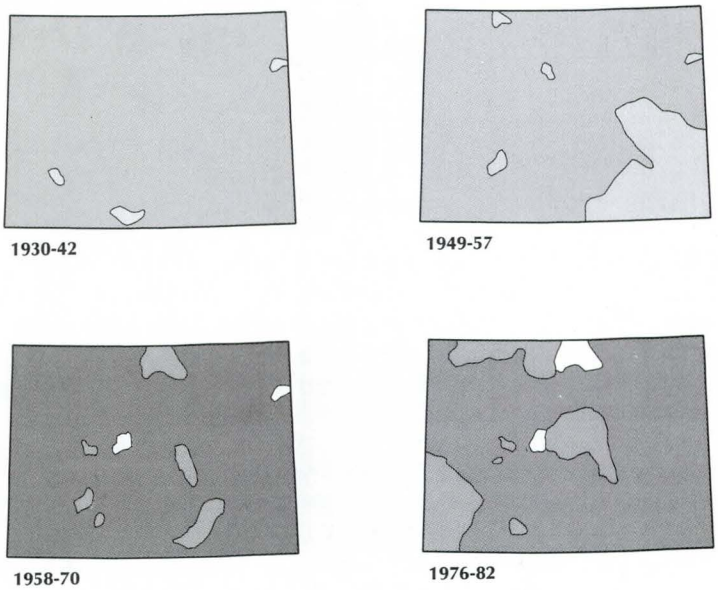

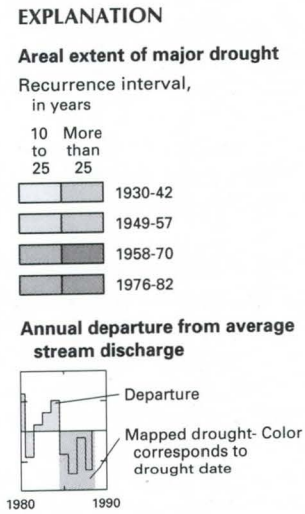

Annual Departure

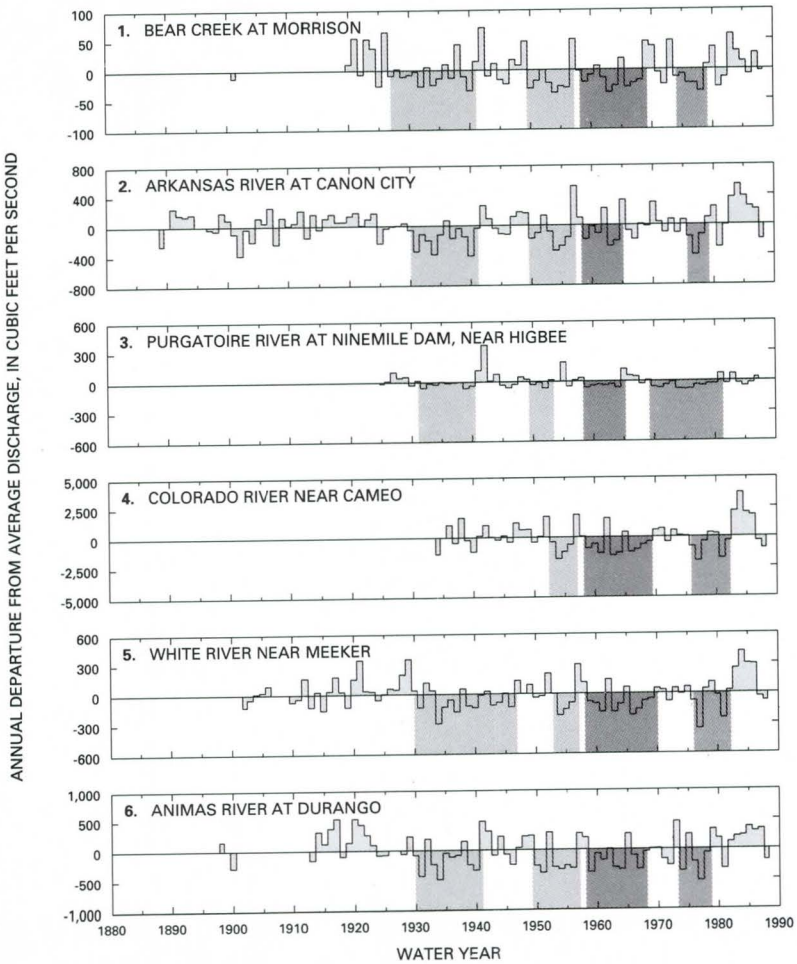

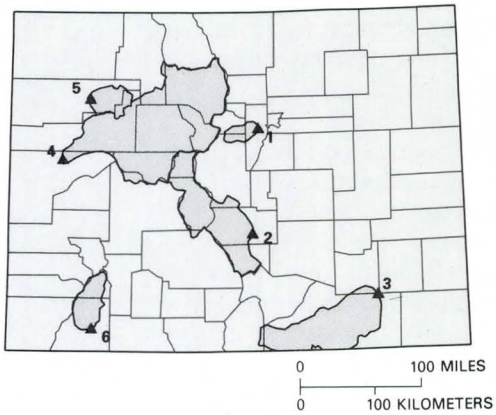

U.S. Geological Survey streamflow-gaging stations and corresponding drainage basins— Numbers refer to graphs

Figure 2. Areal extent of major droughts with a recurrence interval of 10 years or more in Colorado, and annual departure from average stream discharge for selected sites for water years 1889-1988. (Source: Data from U.S. Geological Survey files.)

Although quantitative descriptions of floods typically are based on an analysis of stream-discharge data, droughts may be characterized by analyses of many natural variables, such as stream discharge, precipitation, and soil moisture. The 1988-89 NWS report characterizes droughts from an analysis of stream-discharge data; these stream-discharge analyses are the basis of discussion for the major floods and droughts in each State.

The State summaries are preceded by "Introduction to State Summaries of Floods and Droughts," which includes a description of the method that was used to quantify the severity of floods and droughts in the States. The following discussion about the quantification of droughts is extracted from that article.

> The severity of droughts was estimated from the departure of stream discharge from long-term average discharge. As measured by accumulated departures from long-term average stream discharge, hydrologic drought has three dimensions---intensity, duration, and areal extent. The State summaries characterize intensity and duration of drought at a stream-gaging station by accumulated departures from average stream discharge, in cubic feet per second months, and the areal extent of a drought from the analyses of data from numerous stream-gaging stations.
>
> First, the average discharge for each calendar month was assumed to be the long-term mean stream discharge for that month or, in arid areas, the median monthly discharge. Then, periods of major hydrologic deficits and surpluses were identified from an analysis of the accumulated departures of monthly discharges from mean monthly discharges, beginning from the first month of the period of record (Jennings and Paulson, 1988). For example, on a graph of accumulated departures of monthly discharge from average discharge (fig. 3), the difference between any two accumulated values indicates the deficit or surplus in discharge, relative to the average discharge, between those two times. Note that a sustained downward trend indicates a period of discharge deficit (hydrologic drought) and occurs, in almost all instances, over a multiyear period. For this analysis of droughts, the interest is in quantifying the intensity of deficits, which can be calculated from peak-to-trough differences on the accumulated-departure curve. Segments that represent these peak-to-trough differences in the accumulative-departure curve in figure 3 are the segments of the curve that form the upper boundaries of the shaded areas.

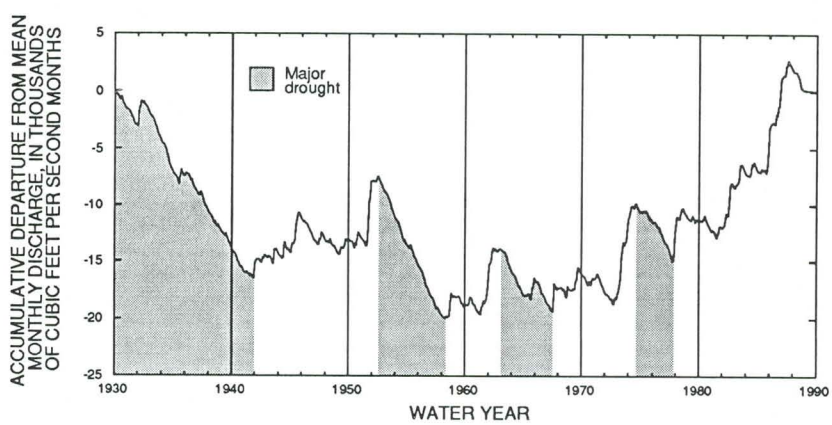

Figure 3. Accumulative departure of monthly stream discharge from long-term mean monthly discharge at a hypothetical stream-gaging station.

> At a given site, hydrologic droughts have three characteristics of interest---duration, intensity, and frequency. Duration and intensity are obtained directly from the accumulated-departure graphs. Accumulated negative departures of a common duration are ranked from largest (most intense) to smallest (least intense). The estimate of drought frequency for a hydrologic drought of given duration is obtained using equation 1, which is adapted to analyze multiyear events (Furness, 1962; Carswell and Bond, 1980):

$$RI = (N-k+2)/m, \qquad (1)$$

> where RI is the recurrence interval, in years; N is the length of the data record, in years; k is the duration of the drought, in years; and m is the rank of the drought. If longer records of discharge or precipitation at nearby sites clearly establish that the rank (m) of the drought is applicable to a longer period than the period of discharge record at the station, then the longer period is used for N, the

length of record. It should be noted that records of stream discharge are relatively short when compared to the long-term multiyear character of great droughts. Thus, calculations for recurrence intervals of drought frequency, based on discharge records alone, are at best only approximate.

For each State, only annual (unaccumulated) departures from average stream discharge at a few stations are shown on bar diagrams (fig. 2). However, the identification and analysis of droughts were based on accumulated monthly departures of stream discharge for many stations in order to define the temporal extent of the drought at the stations and the areal extent of the drought in the State.

Each State summary contains two illustrations that show the time and space characteristics of as many as five floods and as many as five droughts (fig. 2). In the NWS, these are four-color illustrations that show time-series data (peak flow for the illustration about floods and annual departure of stream discharge for the illustration about droughts) for six hydrologic stations in the State. These stations were selected because they monitored streams that are among the least regulated, have the longest periods of record, and represent the varied geographic areas of the State. Each of the major floods and droughts is highlighted (as an annual event if a flood and as a multi-year event if a drought) with a distinctive color, which is found elsewhere in the illustration to define the areal extent of that event on a small-scale State map. The areal delineation of the event is based on analyses of stream-discharge data from many more stations, typically about 40, than the 6 stations whose data are highlighted in the illustration. These illustrations graphically portray how frequently floods and droughts occur at typical hydrologic stations in the State and the areal extent of the most memorable of these events. Figure 2, which is from the Colorado summary, is an example of the drought illustration.

Each State summary also includes a table of characteristics for as many as 20 of the State's most memorable floods and droughts. These characteristics, as is shown in table 1, are date of occurrence, area affected, recurrence interval, and remarks about the effects of the event or the extent of damage. The recurrence interval listed in table 1 is a measure of how frequently in time, on average, the event can be expected to recur. A detailed explanation of recurrence interval also is given in "Introduction to State Summaries of Floods and Droughts."

Finally, a water-management section, which identifies the agencies responsible for flood-plain management, flood-warning systems, and water-use management during drought, and selected references on floods and droughts complete each State summary.

The 1988-89 NWS State summaries conveys the concept that floods and droughts are naturally occurring extreme hydrologic events that recur in time and in spatial extent. Although prediction of their occurrence during a particular period of time is not possible, the probability of their occurrence can be inferred.

REFERENCES CITED

Carswell, W.J., and Bond, S.V., 1980, Multiyear low flow of streams in northeastern Kansas: U.S. Geological Survey Open-File Report 80--734, 26 p.

Clark, D.R., 1989, State diagrams of atmospheric moisture sources and delivery patterns (Contract report prepared by the University of Wisconsin for the U.S. Geological Survey): National Technical Information Service report PB-91-186940, 82p.

Fenneman, N.M., 1946, Physical divisions of the United States: Washington, D.C., U.S. Geological Survey special map, scale 1:7,000,000.

Furness, L.W., 1962, Kansas streamflow characteristics---Part 4, Storage requirements to sustain gross reservoir outflow: Kansas Water Resources Board Technical Report 4, 177 p.

Jennings, M.E., and Paulson, R. W., 1988, Summary of floods and droughts in the United States: American Society of Civil Engineers, National Conference on Hydraulic Engineering, Colorado Springs, Colo., August 8--12, 1988, Proceedings, p. 813--818

Solley, W.B., and others, 1988, Estimated use of water in the United States in 1985: U.S. Geological Survey Circular 1004, 82 p.

U.S. Geological Survey, 1984, National water summary 1983—Hydrologic events and water issues: U.S. Geological Survey Water-Supply Paper 2250, 253 p.

——1985, National water summary 1984—Hydrologic events, selected water-quality trends, and ground-water resources: U.S. Geological Survey Water-Supply Paper 2275, 467 p.

——1986, National water summary 1985—Hydrologic events and surface-water resources: U.S. Geological Survey Water-Supply Paper 2300, 506 p.

——1988, National water summary 1986—Hydrologic events and ground-water quality: U.S. Geological Survey Water-Supply Paper 2325, 560 p.

——1990, National water summary 1987—Hydrologic events and water supply and use: U.S. Geological Survey Water-Supply Paper 2350, 553 p.

——1991, National water summary 1988-89—Hydrologic events and floods and droughts: U.S. Geological Survey Water-Supply Paper 2375, 591 p. [in press]

EXAMINATION OF DRYNESS IN AGRICULTURE WITH MOISTURE BALANCE INDICES

Guan Zhaoyong and Feng Zhiwen

Nanjing Institute of Hydrology and Water Resources, Nanjing, China

ABSTRACT

The "D" index approach of moisture balance used to examine dryness in agriculture is proposed in this paper. This index synthesizes several principal factors, which affect dryness in agriculture, such as precipitation, crop water requirement and pre–growth–stage moisture content. The "D" index is a comparison between the actual water quantity supplied in the crop growth period,and water requirements for keeping crop growth normal. If it generally keeps balance (i.e. $D \approx 1$) , it means that the moisture condition is able to keep crop growth normal. If it can not meet this condition or with larger difference, it means that the crop is in dry ($D < 1$) or waterlogging ($D > 1$) condition. Procedures for calculating the parameters involved in the formula of "D" are introduced in this paper. Taking dry agricultural areas on various natural landscape conditions in Shanxi and Shaanxi provinces as test areas, the full growth period of principal crops (winter wheat, spring corn, summer corn) and the series of "D" values in the key water–demanding periods, from 1961 to 1982 were obtained. With them, the classified indices of agricultural dryness were determined and the occurrence of agricultural dryness and its distribution in time and space were analysed.It is found that it is possible and advantage to characterize agricultural dryness with value "D"and certain precise observed data of moisture content.

INTRODUCTION

Dryness(draught) is the main disaster to agricultural production in North China. For many years, the study of agricultural dryness has been much studied by meteorologists, agricultural experts, and hydrologists. The dryness indices are qantitative indices for measuring the extent and range of dry disaster taking place in some area and period. It is convenient to analyse the freqency,type, and distribution of dryness with the "D" index. From the definition of agricultural dryness, it is considered that in crop growth period, abnormal shortage of precipitation hinders and damages the normal crop growth and decreases the production .

Therefere, agricultural dryness is determined by 3 factors . The first is precipitation, especially precipitation in the crop growth period. The second is the water requirement of the crop ,particularly the water requirement in the key crop growth period . The third is the initial moisture content. Only after considering above principal factors, the real situation of agricultural dryness can be fully expressed.

Shanbei and Guanzhong, in Shaanxi province ,and Shanxi province were studied with "D" index. The total area is 280,000 Km^2. The study area is located in the middle part of the Yellow River basin, and the east part of northwest loess plateau.

This is the main area for producing grain in middle and west China.The shortage of precipitation and variablity of its spatial distribution make dryness occur often and with long duration. In the north part of the area, dryness often occurs in spring and early summer. In the east of Guanzhong and Yuncheng dryness often occurs in summer, seldom in autumn.

BASIC FORMULA

The index formula proposed in the symposium on North China dryness and waterloging [2] is:

$$D = \frac{P - R_c + \bar{\rho}_o / \rho_p + r_g}{W_o + \rho_m / \rho_p}$$

where

P—precipitation in crop growth period,mm;

R_c—surface runoff and percolation to groundwater in crop growth period (precipitation unavailable to crop),mm;

$\bar{\rho}_o$—average soil moisture content at begining of crop growth period;

ρ_p—unit soil moisture in plant root layers per unit of precipitation,% / mm;

r_g—groundwater recharge of soil moisture by upward flow from groundwater during crop growth period;

W_o—water consumed to keep crop growth normal in the growth peoriod, i.e. evaportranspiration of plant and soil,mm

ρ_m—suitable soil moisture content of crop in crop growth period.

In the formula, the denominator is the total water requirement for ensuring crop normal growth .The $P—R_c$in the numerator is precipitation available to crop, which equals precipitation minus runoff and infiltratiion. $\bar{\rho} / \rho_p$ is equivalent to a precipitation depth, transformed from soil moisture content at the beginning of the crop growth period. Total numerator, $P—R_c+\bar{\rho} / \rho_P+r_g$ is the total actual water supply available to crop. If the ratio is at balance value (i.e. $D \approx 1$) it means the moisture is able to keep crop growth normal. If the ratio deviates from the balance, it is regarded that the crop is in dry or waterlogging condition.

The physical definition of the formula is clear, but it is simplified and revised , when it is used in loess plateau(because there $r_g \approx 0$).

Division of experimental area

Because the area is large , the geographic condition is complicated, and the climate difference between north and south part is sharp, we used statistics in sub–divided areas to calculate, analyze and show the distribution principle of agricultural dryness.

The study area was divided into 5 parts (sections).They are: Ⅰ) Shanbei, Ⅱ) Yanbei and Xin Xian, Ⅲ)Jinzhong, Shanxi province, Ⅳ)Guanzhong and Yuncheng, Ⅴ)southeast Shanxi(fig.2)

Determination of calculating period

First we should learn the main crops in each section.The main crops are the crops which are suited to the climate condition and cultivation custom in that area. In Guanzhong, Shaanxi province , Yuncheng, and southeast Shanxi the climate is warm and with a large amount of precipitation. The cultivation custom is crop rotation between winter wheat and summer corn in every year. In south and middle parts of Jinzhong, the main crop is winter wheat, but spring corn in north part of Jinzhong and mountain area.The main crop in most parts of Shanbei and Yanbei is spring corn.

Besides the moisture condition in whole growth period, the key factor to affect crop output is water supply in the key water demanding period,when it is critical for the crop to get water. The type , growth period, and key water demanding period of crops in the 5 sections are summarized in table 1.

Table 1 The cultivation regulation(cropping practice), growth period and key water demanding period of main crops in studied area.

Section	Cultivate regulation	main crops	growth period	key water demanding period
Southeast Shanxi	Two crops a year	Winter wheat Summer corn	last Oct.—May June—Sept.	Mar.—May,Apr., May,July,Aug.
Guanzhong, Yuncheng	Two crops a year	Winter wheat Summer corn	last Oct.—May June—Sept.	Mar.—May,Apr,. May,July,Aug.
Jinzhong	Three crops in two years	Winter wheat Spring corn	last Oct.—May Apr.—Sept.	Mar—May, Apr., May,July,Aug.
Yanbei,Xin Xian	One crop a year	Spring corn	Apr.—Sept.	July,Aug.
Shanbei	One crop a year	Spring corn	Apr.—Sept.	July, Aug.

STATISTICS AND CALCULATION OF PARAMETERS

Precipitation P and initial soil moisture content

Precipitation data were obtained for 43 satations in the study area . Based on the growth periods and key water demanding periods of main crops in each section and its precipitation points, the precipitations in various reference poriods , such as Oct—May, Mar—May , Apr, May , June—Sept, April—September , July, Aug and the full year were calculated respectively and the average precipitation of each section was estimated.

To obtian $\bar{\rho}_o$, the initial soil moisture content in the crop growth period, 41 moisture observation sites were chosen as samples. With the data of initial soil moisture content in every period, the average soil moisture content to the depth of 40 cm was calculated.

Runoff depth

Runoff is ineffective precipitation to crop. Using 1975—1980 daily precipitation data in each section, we chose 1 or 2 typical river basins to calculate regional runoff depth in every period and get the relationship and draw the relative figure between precipitation and runoff coefficient(ratio of runoff / precipitation) for each section. The relations between precipitation and runoff coefficient are shown as figure 1.

Determination of ρ_P

The factors affecting ρ_P are very complex. Here, we collect the observed data, tested in Xizhuang gou, Taiyuan runoff experimental site, from June to september , 1958. The soil moisture content to a depth of 50 cm from surface caused by 1 mm precipitation is 0.11% in Taiyuan, 0.075% (with tested data of 1956) in Yeyugou and the average value is 0.092%. $\rho_p \approx$ 0.09% in Shaanxi province. We use $\rho_p = 0.092\%$ in this paper.

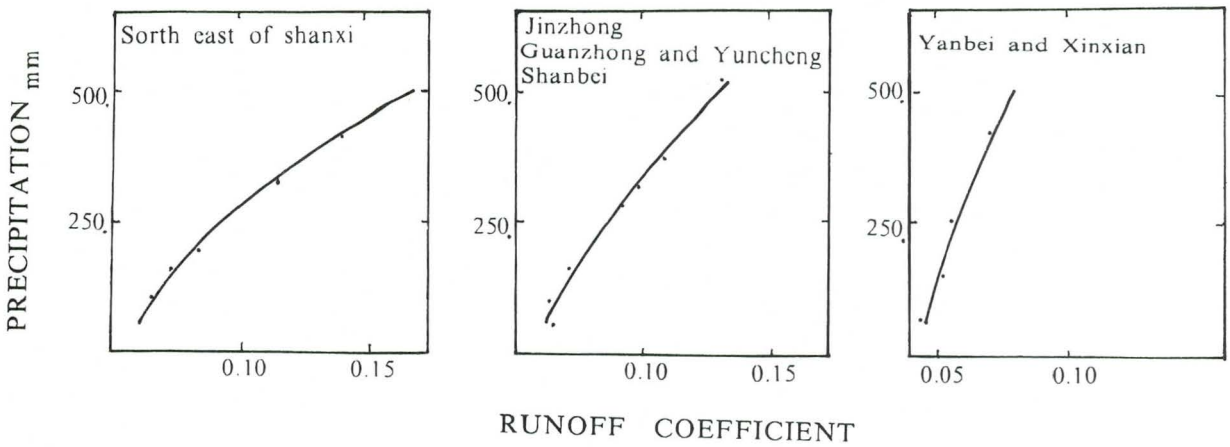

Fig 1 Relation Curve between Precipitation and runoff coefficient

Consumed water quantity and suitable soil moisture content of crop

The consumed water quantity of crop is the total quantity, which maintains normal crop growth and production in the whole crop growth period. It is decided by crop type , property, growing envirenment and agricultural cultivation practices (regulation).

In whole crop growth period, because of difference of climate condition, the crop water requirement varies with time. Generally the crop water requirement is less in the begining and end and large in the middle.The crop water requirementws of main crops are shown in table 2

Table 2 Crop water requirements of main crops

Section	Total consumed water quantity (monthly water demand) (mm)												
	Oct.	Nov.	Dec.	Jan.	Feb.	Mar.	Apr.	May.	Jun.	July	Aug.	Sept.	Total
Southeast Shanxi	25.3	26.3	15.4	15.4	22.7	49.2	111.8	143.0	65.7	116.8	137.1	61.7	790.4
Guanzhong and Yuncheng	32.5	29.1	30.1	30.1	27.2	62.7	100.4	139.8	42.8	112.3	194.7	99.9	901.6
Jinzhong	27.3	26.3	15.4	15.4	22.7	49.2	111.8	143.0	89.4	89.8	102.8	76.0	769.1
Shanbei							2.7	35.1	56.7	180.9	121.5	65.4	462.3
Yanbei and Xinxian	8.9						21.8	67.6	80.1	89.8	102.8	76.0	447.0

ANALYSIS AND EXAMINATION OF RESULT

Analysis of result

With the formula and several parameters, analyzed above,the values of "D" for every crop in every section, every crop growth period, every key water demanding period, from 1961—1982 may be obtained . Some key results are:

1. In 5 sections, taking a year and from Aprl. to Sept. respecticely as statistical duration, the 3 minimum values of"D"and their corresponding years are expressed in table 3. It is clear that the dry years are comparatively concentrated.

Table 3 Table of minimum values of "D" for reference periods of a full year and April to September

name of section		Yanbei and Xinxian		Jinzhong		Shanbei		Guanzhong and Yuncheng		Southeast of Shanxi	
	Statistical duration	Year	D	Year	D	Year	D	Year	D	Year	D
The 3 Years with least value "D"	Year	1963	0.75	1980	0.54	1974	0.71	1972	0.56	1972	0.59
		1965	0.62	1972	0.44	1972	0.71	1980	0.48	1978	0.57
		1972	0.60	1965	0.39	1965	0.66	1977	0.47	1965	0.50
The 3 years with least value "D"	Apr.~Sept.	1975	0.69	1974	0.71	1972	0.61				
		1965	0.66	1965	0.68	1974	0.60				
		1972	0.51	1972	0.67	1965	0.57				

For the March—May reference period in the 3 sections cultivating winter wheat, the largest "D" is not larger than 0.08,which means that the dryness will occur in every spring in Jinzhong . The least "D" for reference period of March–May is 0.30 in 1972.The wheat growth period ,Oct—May, is in dry season. The average value "D" in Oct—May in 22 years is between 0.50 and 0.60. It means that the precipitation can only meet half part of the water demand.

2. Comparing main crops growth period with value "D" of key period year by year for 22 years in every section chosing the reference period with least "D" in a year, and summarizing the frequency of the least value of "D" being in this reference period, is easy to learn the statistical principle of dryness. The table 4 shows the comparison of spring corn growth period and the least "D" in key water demanding period.

Table 4 Comparative table of spring corn growth period and the least "D" in key water demanding period,1961–1982

Section	Reference period	Occurrences of Minimum "D" in reference period in 22 years		The minimim value of "D"
		Number	Percentage	
Shanbei	July	14	70%	0.60
	Aug.	4	20%	0.57
	Apr.~Sept.	2	10%	0.72
Yanbei	Aug.	10	45%	0.65
	Apr.~Sept.	9	41%	0.78
	July	3	14%	0.86
Jinzhong	Aug.	12	55%	0.82
	Apr.~Sept.	7	32%	0.92
	July	3	13%	0.78

* Note: Lack of 2 years data in Shanbei

With the same process as above, the summer corn and winter wheat are analysed. August is the dry season for summer corn , especially in Guanzhong ,Shaanxi province. The possibility of summer dryness is not only great, but serious ; the value of "D" is about 0.50. In other words, the water supply can only meet half of water demand, so it is clear that summer dryness in Guanzhong occurs frequently and seriously.

The general principles, for dryness to take place in wheat growth period are:

① The dryness for wheat in the March–May reference period occurs frequently. Morever, the frequency of dryness taking place in the March —May period is especially high in Jinzhong . Only in southeast Shanxi does early spring dryness seldom occurs .② May is the critical period for wheat to need water. The least values of "D" in Guanzhong and Southeast Shanxi in May are 25% and 40% respectively. This means that, in Guanzhong and Southeast

Shanxi, the dryness in May, occurs once every 2.5—4 years. May dry periods seldom occur in Jinzhong.③The dryness for winter wheat is most serious in Jinzhong, where the average value of "D"is 0.40 , the next most dry condition is in Guanzhong and southeast Shanxi.

3. The analysis of year–average value of"D"in every period (see table 5) can show the average distribution of the dryness in area.Taking a year as a statistical duration, the dryness easily occurs in Jinzhong and Guanzhong, the natural supply water only meet about 60% of crop water requirement.

In Shanbei and Yanbei, because of caltivating a crop a year, the demanding water of crop is less. The multi–year average value"D"is a about 0.90, it is not belong to dryness or is a little bit dry. In spring corn growth period, which is Apr. to Sept., the possibility of dryness occuring in Jinzhong is low, but Shanbei is in dry period, and Yanbei is in the middle condition. The summer corn growth period is not dry in Southeast of Shanxi. It keeps water balance. Summer dryness often takes place in Guanzhong.

Table 5 Growth periods of main crops and their value of"D"

Section		Spring corn	Summer cron	Winter wheat	
	Year	Apr.~Sept.	Jur.~Sept.	Mar.~May	Oct.~May
Shanbei	0.90	0.76			
Yanbei and Xinxian	0.89	0.81			
Jinzhong	0.62	0.92		0.42	0.50
Guanzhong and Yuncheng	0.64		0.74	0.55	0.62
Southeast of Shanxi	0.75		1.02	0.53	0.61

The spatial distribution principle of dryness may be shown with contours of value of "D" for every reference period . We used 1965, 1972 as two typical dry years to draw the contours of value"D"for both whole year and June—September reference periods. Figure 2 expresses the spatial distribution of the value of "D"in a whole year, 1972. There are 3 depressions of value"D"in whole study area (note lack of data in Yuling, Shaanxi province) , and the depressions distribute as a belt . The 3 depressions are in east Guanzhong, Lingfeng, (in south Jinzhong) ,and at Taiyuan—Yangquan. Their values of"D" are less than 0.40. Southwest Shanbei, west Guanzhong and southeast Shanxi are either not dry or only a little bit dry, the "D"values are above 0.60.

Classification of agricultural dryness

Based on the above analysis, and in coordination with observed dry conditions, the indices of "D"of dryness grades in various sections and various growth period of crops are classified as in table 6. Thus, with certain precipitation and initial soil moisture content data in cortain section and period, one can calculate runoff depth, then, calculate value of"D" with the formula, and finally compare with table 6, to classify the relative degree of dryness.

Table 6 Growth period of main crops in every section and the indices of dry grade"D" for whole–year reference period

Section	Reference period	Dryness grade			
		not dry	sliyhtly day	dry	very dry
Yanbei Xingxian and Shanbei	Spring corn growth Period(Apr.~Sept.)	D>1.0	0.80<D<1.0	0.60<D<0.80	D<0.60
	Whole year	D>1.0	0.60<D<1.0		D<0.60
Jinzhong Jingdong and Guanzhong Yuncheng	Winter wheat growth Period(Oct.~May)	D>0.80	0.60<D<0.80	0.40<D<0.60	D<0.40
	Summer corn growth Period(Jun.~Sept.)	D>1.0	0.80<D<1.0	0.60<D<0.80	D<0.60
	Whole year	D>0.80	0.50<D<0.80		D<0.50

Examination of result

Because water is only one factor affecting crop production, the crop production can only be used to examine dry condition in both dry years and waterlogging years.

The "annual comparative growth rate approach" assumes that grain output increases with a stable growth rate. We chose general years for a typical series; the initial and terminal years are neither dry nor waterlogging. We use the data of total grain output, wheat output and corn output, proposed by Shanxi (1961— 1975) , and Shaanxi (1961—1980) , calculate the annual average growth rate of total grain output, and various crops output in every section. The difference between real and calculated output can represent impact of dryness. Comparing the 5 largest difference of annual output and the 5 minimum values of" D" , they are, at least, similar in more than 2 years in Yanbei, Shanbei, Jinzhong, especially in the dry years of 1972 and 1965 . It means that the dry year is the year, in which spring corn output decreases. Additionally, the water condition of key growth demanding period is important to grain output. In most of the years with large negtive difference between actual and calculated output the value of"D"in the key water demanding period is less.

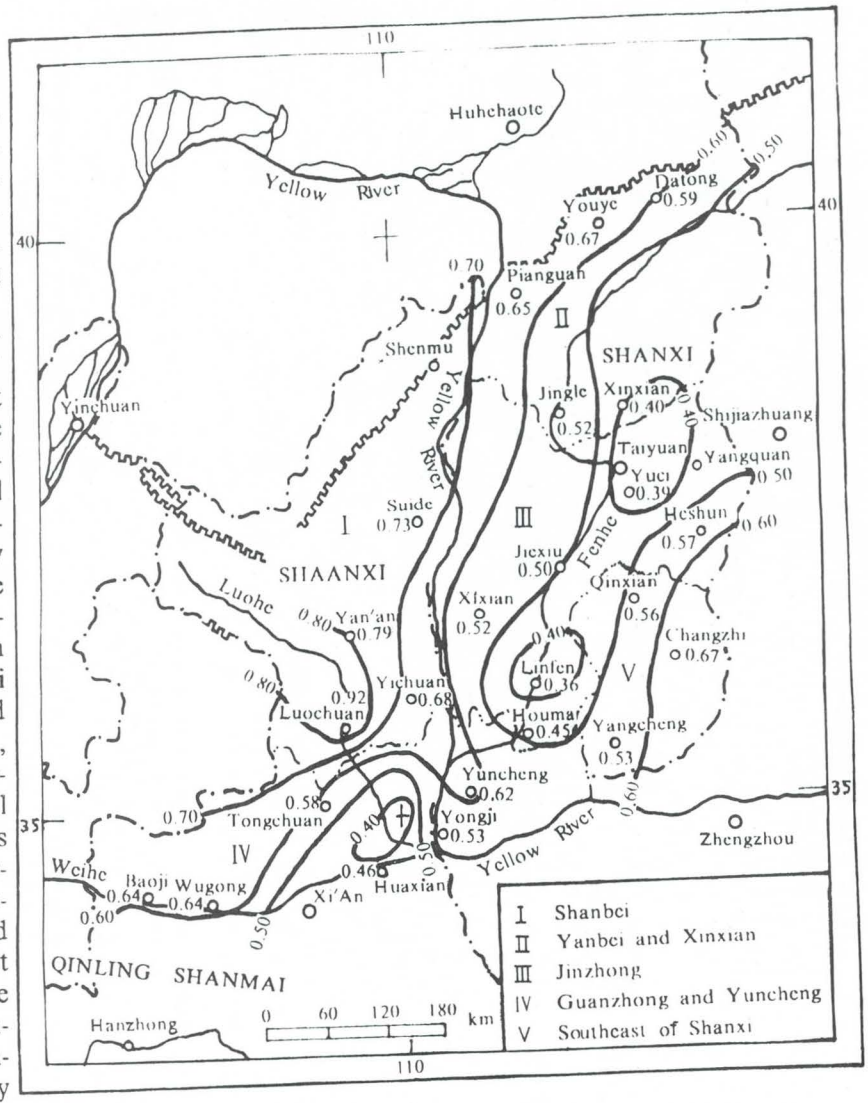

Fig 2 Contour of "D" for Whole Year reference Period 1972

REFERENCE

〔1〕 Agricultural Meterological department, Chinese Agricultural Academy, Dronght–erlief Measures in Northern, Agricultural Press, May 1980.

〔2〕 Office of Yangze River Programme, Hydrological forecasting Approach, Press of water conservancy and electrical power, Sept. 1979.

TRANSFORMATION BETWEEN HYDROLOGICAL DROUGHT AND INDUSTRIAL AND AGRICULTURAL DROUGHT IN SEMI–ARID AREAS

Chen Ze–Zhi

Shanxi General Hydrological Service, Taiyuan, PRC

ABSTRACT

Drought is essentially the shortage of water resources. The transformation between hydrological drought and industrial and agricultural drought is in fact the amount of water transferred between surface runoff and industrial, domestic, and agricultural water consumption. The definition and index of drought are thus put forward in this paper on the basis of the above views. To increase the supply of industrial and agricultural water, Shanxi Province, which is in a semi–arid area and is poor in water resources, has built many irrigation works and water soil conservation projects during the past thirty years, resulting in an increase in infiltrated recharge of precipitation and surface runoff to soil moisture and groundwater, which in turn has increased hydrological drought. The hydrological drought is divided into two types: natural and man–made. According to the water balance principle and the transformation of different kinds of water, the negative relationship between hydrological drought and industrial and agricultural drought is elucidated on the bases of man–made conditions.

INTRODUCTION

Water is the essence of all lives. In arid and semi–arid areas, it is the lifeblood of national economic development. In human activities, the study of hydrology and the development of water resources have important significance to industrial and agricultural development in arid areas. It is also quite essential to improving the ecological environment, and promoting human civilization. In the thesis, the definition and the transformation between hydrological drought and industrial and agricultural drought in semi–arid areas are studied, and a transformation model is put forward on the basis of the natural situations and human productive activities in Shanxi, the characteristics of regulating storage capacity and recharge of streamflow, groundwater and soil water, the enhancement of effective water resources use, and the improvement of agricultural, domestic, and industrial water supply.

GENERAL SITUATION

Shanxi Province is situated in 34–40 ° N lat. and 110–114 ° E long. It has the shape of a parallelogram, with a length from north to south about 600 km, and a width from east to west about 300 km. The total area of the province is $15.63 * 10^4 km^2$. The mountainous area covers 72 percent. The loess plateau and hills make up 11.5 percent of the province; they are mostly distributed over the east bank of the Yellow River and their elevation is about 600–1200 m. Basins and plainland are about 16.5 percent, and are distributed over the middle region between eastern and western mountains.

Due to continental monsoon climate in Shanxi, the average annual precipitation is 523 mm (1956–1984), of which precipitation in the flood season (from July to September) makes up more than 60 percent. The annual evaporation is about 1000 mm and the annual aridity (ratio of annual evaporation to annual precipitation E / P) is bout 2; the climate is semi–arid.

The total average annual water resources amount to $138 * 10^8 m^3$, in which streamflow is $108.6 * 10^8 m^3$. The modulus of annual runoff (runoff per unit area) is $6.9 * 10^4 m^3 / km^2$. The stream runoff per capita is 419 m^3, which is only 3.8 percent of the runoff per capita in the world and 19 percent of the average in China. Shanxi Province is not only lacking in water resources, and domestic and industrial water use, but also suffers serious drought in agriculture.

Shanxi is rich in mineral resources. The coal reserves make up one–third of the country's total. Therefore, Shanxi is a nationally important base of energy resources and coal–based chemical industries.

DEFINITION AND TYPES OF DROUGHT

Drought can be defined as arid climate, little rainfall, abnormal reduction of streamflow, and serious shortage of water supply in a comparatively long period, which makes impacts on domestic, industrial and agricultural production,and even destroys the ecologic environment and disrupts the normal activities of human beings. There are several types of drought, such as industrialdrought, agricultural drought, hydrological drought, and climatic drought. In China, the aridity (K) is taken as the index for climatic drought region division. K shows the degree of air aridity. The annual aridity in semi–arid areas is 1.5–3.49. Agricultural drought is defined as the fact that soil water supply is less than the crop requirement in the crop growing season, which is expressed by dampness (D) in various seasons in Shanxi ($D = P / E$). The industrial drought is that the actual water supply to industrial production is less than the standard water requirement of the process equipments.

The main reason for hydrological drought, agricultural drought, and domestic–industrial water shortage is climatic drought. According to the statistical and historical data, there were 413 drought years in the 525 years from 1464 to 1988. In this period there were 7 exceptional drought years, 80 heavy drought years, and 326 common drought years. The exceptional drought years caused destructive catastrophes. For example, in 1877, the precipitation in the province was only 116 mm, the stream runoff was $29.3 * 10^8 m^3$. Many rivers and lakes were dried–up. The disaster–struck areas covered 84 counties; in 60 of these counties, the harvest failed to reach 30 percent of normal. In the meantime, the nine successive drought years from 1872 to 1880 caused great disaster for the residents.

The stream runoff, groundwater and soil water vary with topography and with soluble permeability of the land surface. In carbonate areas, hydrological drought is very serious. But in some parts of discharging areas, the spring runoff is very large, forming nineteen big natural groundwater reservoirs for concentrated water supply. In lithological sandstone and shale mountainous areas, it is easy to form streamflow. The modulus of annual stream runoff is $(5–16) * 10^4 m^3 / km^2$ in these areas. The groundwater forms the stream base–flow by means of outflow from small springs. The loess plateau and hilly areas are full of gullies; water loss and soil erosion are serious, and the conditions of recharge and storage of groundwater is very poor.

The basins are the best areas to use water resources. The conditions for recharge and storage of groundwater are good in the basins, and 91 percent of the wells in the whole province are located there. The annual exploitable modulus (the exploitable amount of water per unit area) in agricultural wellareas is $(10–50) * 10^4 m^3 / km^2$. In river valleys, where the domestic and industrial water resources are supplied by river infiltration, the annual exploitable modulus is greater than $100 * 10^4 m^3 / km^2$.

HISTORY OF DROUGHT SINCE 1959

The provincial thirty–year plan (1959–1988) for development of industrial and agricultural production and water conservation projects can be divided into three periods, as shown in

Table 1. The first decade was the period during which reservoirs were built and the fields were irrigated by gravity irrigation. At that time, the annual average stream runoff modulus M for the whole province was $8.3 * 10^4 m^3 / km^2$, which can be taken as the basic datum of the natural runoff modulus. The second decade was the period during which groundwater drafts were increased greatly; the industrial and agricultural drought situation was improved significantly. The modulus of stream runoff during this period was $M_{II} = 6.1 * 10^4 m^3 / km^2$. In this period, the supply of permeated precipitation and streamflow recharged groundwater significantly. The third decade was the period of water and soil conservation.The level terraced fields were built in arid or sloping areas, and check dams were built in valleys so as to silt up farmland and to harness small catchments. The stream runoff modulus M_{III} is $4.9 * 10^4 m^3 / km^2$. In this period, the permeated precipitation increased, streamflow decreased, and the agricultural drought situation was improved. The water conservancy projects promoted the development of agricultural production. In 1949, the gross industrial and agricultural output value was $13.4 * 10^8$ RMB yuan, in which the industrial output value occupied only 14.7 percent. In 1984, the gross industrial and agricultural output value was $257.8 * 10^8$ yuan, in which the industrial output value occupied 66.3 percent.

Table 1 The three periods of development of water conservancy projects in Shanxi, 1959–1988.

Period	Years	Annual rainfall P (mm)	Runoff modulus M (m^3 / km^2)	Grain output (kg / ha)	Reservoir storage ($10^4 m^3$)	Annual well yield ($10^4 m^3$)	Water–soil conservation (10^4ha)
I	59–68	533.2	83,000	1,212	338,000	59,000	234.7
II	69–78	500.8	61,000	1,950	421,000	184,000	267.4
III	79–88	487.5	49,000	2,396	420,000	233,000	344.6

HYDROLOGICAL DROUGHT DURING THE THREE PERIODS

Hydrological drought can be defined as the occurrence of annual streamflow that is significantly lower than perennial average streamflow. Hydrological drought is divided into two types, natural and man–made ones, according to its cause and its impact on national economy. Consider the precipitation (P_I) and the runoff modulus (M_I) in the first period in Table 1 as perennial average values. Then compile Table 2 by selecting years with various degrees of rainfall and computing the ratios (G_P, G_M) of P_I and M_I to P_i and M_i for the year i. Because the ratios are defined as $G_P = P_I / P_i$ and $G_M = M_I / M_i$, they reflect the hydrological aridity in year i, relative to the perennial base period I.The larger G_P and G_M, the more serious damage the drought makes.

Table 2 The hydrological drought index for selected years and precipitation amounts, Shanxi. P in mm and M in $10^4 m^3$.

	Precipitatioon ranges (mm)														
	300–400					520–550					590–610				
period	i	P_i	G_P	M_i	G_M	i	P_i	G_P	M_i	G_M	i	P_i	G_P	M_i	G_M
I	65	304	1.75	4.97	1.67	66	522	1.02	7.87	1.05	67	605	0.88	9.92	0.83
II	72	392	1.37	4.11	2.00	76	522	1.02	6.97	1.20	73	595	0.89	7.42	1.12
III	86	346	1.54	3.09	2.69	85	547	0.98	5.19	1.60	88	609	0.87	7.03	1.18

The hydrological drought caused by little rainfall and other natural reasons is called natural hydrological drought, and is expressed by G_P. The hydrological drought caused by overdrafting groundwater and overusing soil water, is called man–made hydrological drought, and is expressed by G_M. If G_P is not very large, but G_M is large, then the industrial, agricultural drought will be modified by man's activities. The severity of drought can be expressed in terms of the numerical values of G_P and G_M as follows: 1.2–1.5, semi–drought;1.5–1.8, drought; > 1.8, heavy drought.

TRANSFORMATION PRINCIPLE AND BASIC MODEL

In a watershed or definite area, no matter how various types of water (precipitation P, surface water Q, groundwater R, soil water W, and evaporation E) transform, the principle of water balance between recharge and discharge will be followed. The basic model of water transformation is formulated as

$$P = Q_{II} + Q_{III} - Q_{I} + R_{II} + R_{III} - R_{I} + W_{II} + E_g + E_s \tag{1}$$

where E_g is evaporation of subterranean water, E_s is evapotranspiration of other types. The subscripts I,II,III denote inflow, regulated outflow and water use, and unregulated outflow, respectively. W_I and W_{III} are zero.

TRANSFORMATION BETWEEN HYDROLOGICAL DROUGHT AND AGRICULTURAL DROUGHT IN ARIDFIELDS

According to the basic model (Eq.1), the model of transformation between agricultural drought in arid fields and hydrological drought is

$$Q_{III} = [P-(Q_{II} + R_{II} + R_{III} + E_s)] - W_{II} = P_A - W_{II} \tag{2}$$

where P_A is the effective precipitation in the transformation between soil storage regulation and surface streamflow (assuming that the remaining elements Q_I, Q_{II}, E_s are practically zero.)

The transformation reflects practically the relationship between the soil water regulated and used (W_{II}) and the surface outflow (Q_{III}) of the water and soil conservation projects in hilly dry land and terraced fields. For a given level of precipitation, if water and soil conservation projects are good, the soil water storage will be large and the agricultural drought will be reduced; however, the yield of surface flow also will be reduced comparatively, and the hydrological drought will increase. For example, in Dazhai Village located in the eastern mountains, there are 53 ha of farmland scattered over sloping fields. Before 1960, the water loss and soil erosion were very serious, and the yield per unit area was only 800 kg / ha. Later, to promote water storage, preservation of soil moisture, and drought resistance, terraced fields which were low inside and high on the verge, with an active earth layer of 0.3 m, were constructed on the sloping fields, and check dams were set up in the gullies. As the result of that, there was no streamflow in normal rainfall condition, and yield per unit area was more than 7500 kg / ha.

As another example, Wangjiagou is located in the Western loess hilly region, with a catchment area of 9.1 km^2, in which sloping fields make up 87 percent. There are 31 gullies. In this region, the annual average precipitation is 506 mm, of which 72 percent is in the flood season. According to the statistics of 216 precipitation events which produced streamflow in

thirty years, 49 percent rainstorms lasted less than 3 hours and caused serious water loss and soil erosion. There were nine years of agricultural drought in ten years and yield per unit area was about 1000 kg / ha. During the past thirty years, twenty–one check dams were set up in Wangjiagou with $80 * 10^4 m^3$ storage capacity; farmland was built and various plants and grass were planted. The streamflow was reduced, and 100 percent of silt loss was overcome. From Table 1, comparing period II with period III, it can be seen that the main reason for the 19.4 percent reduction in streamflow is that the area of preservation of soil moisture was increased by 22.4 percent.

TRANSFORMATION BETWEEN HYDROLOGICAL DROUGHT, AGRICULTURAL DROUGHT IN IRRIGATED FIELDS, AND INDUSTRIAL DROUGHT

According to the basic model, Eq.1, the transformation between hydrological drought, agricultural drought in irrigated fields, and industrial drought is as follows:

$$Q_{III} = [P - (E_s + E_g + W_{II} + Q_{II} - Q_I + R_{III} - R_I)] - R_{II} = P_B - R_{II} \quad (3)$$

where P_B is the effective precipitation in the transformation between water amount for irrigation or industrial supply and surface streamflow. The transformation practically represents the relation between regional regulated runoff and use of groundwater (R_{II}) and surface streamflow ($Q_{II} + Q_{III}$), which are used for agricultural or industrial areas in river valleys. In semi–arid areas,the improvement of industrial water supply depends on groundwater reservoirs, which is related to the direct recharge by streamflow. The larger R_{II} is, the smaller Q_{III}. That is to say, the more the industrial drought is improved, the more serious the hydrological drought. Then, we provided the following two examples.

As an example of agricultural drought, take Fen River, which runs through Taiyuan Basin, and outflows from the Yitang Gorge. The catchment area above theYitang Gorge is about 23,943 km^2, which makes up 20 percent of the basin area.Before 1968, this area was irrigated by means of surface gravity irrigation. The annual streamflow at the outlet of the basin was $8.8 * 10^8 m^3$, but the agricultural drought was still very serious, and the per unit area yield was about 2000 kg / ha. Since the 1970s, the groundwater has been developed greatly, the number of wells has increased to 2000, and the yield per unit area surpassed4000 kg / ha; the highest yield reached 10,000 kg / ha. All of these interacted with each other and strengthened the drought–resistent capacity. In 1986, the annual precipitation in the basin was only 288 mm, so it was a serious drought year. However, because all wells were fully utilized, and groundwater was extracted, it was still a harvest year. However, because of groundwater over–draft, the groundwater table in an area of 3580 km was drawn down 1.74 m. In this year, the annual streamflow at the basin outlet was only $0.85 * 10^8 m^3$. In 1988, it was a high–water year, and infiltration could recharge the groundwater greatly. Only in the flood season, the groundwater table in a 2700 km^2area was restored up to 1.63 m, and the annual streamflow at the basin outlet was about $8.7 * 10^8 m^3$. From Table 1, comparing period II with period I, it can be seen that the main reason for the 26.2 percent reduction of streamflow is the 2000 percent increment in the extracted amount of groundwater.

In another example of industrial drought, the river bed of the Yao River located in the upper part of Yangquan City, contains a loose sedimentary layer with a thickness of less than 36 m, in a river valley of 20 km length and 0.4 km width. The aquifer mainly consists of sandy gravel with an average thickness of about 12 m. Since the 1950s, more than 40 wells recharged by seepage from streams have been drilled in a river bed of 12 km length. The catchment area of the river near the wells is 500 km^2, with annual average streamflow of $5190 * 10^4 m^3$, of which 80 percent appears in the flood season. In the low–water season, the stream is dried up and the groundwater is drawn down to 3–10 m below the surface of the dry river bed. In the

high–water season, the streamflow permeates into the ground and the groundwater table rises again. In 1972, with severe drought, the annual extracted amount of groundwater was $1230 * 10^4 m^3$. The groundwater level dropped more than 10 m and the annual streamflow was $366 * 10^4 m^3$. In 1973, with high water, the groundwater level was raised again and the annual streamflow was $6000 * 10^4 m^3$. Depending on the regulation ability of the aquifer and the recharge of the periodic streamflow, the annual amount of groundwater extracted was $(1000–1700) * 10^4 m^3$, and the extraction modulus was up to $(200–350) * 10^4 m^3 / km^2$. Groundwater from the river–bed aquifer became the main industrial water resources before 1982 for Yangquan City, which had the most serious shortage of water in Shanxi.

A NATIONAL DROUGHT ATLAS FOR THE UNITED STATES OF AMERICA

Gene E. Willeke, Miami University, Oxford, OH; Nathaniel B. Guttman, National Climatic Data Center, Asheville, NC; and Wilbert O. Thomas, U.S. Geological Survey, Reston, VA

ABSTRACT

The National Drought Atlas will provide frequency analysis of precipitation and streamflow for durations of 1 month through five years, for probabilities of occurrence of 0.2, 0.1, and 0.02., and historical summaries of the Palmer Drought Index (Palmer, 1965) and reservoir contents data for principal reservoirs. Frequencies are calculated by the procedure of L-moments; the primary measure of central tendency is the median. Precipitation and temperature data are taken from the Historical Climatology Network for about 1100 stations, and streamflow from 1,700 stations in the U.S. Geological Survey's Hydroclimatic Data Network. Results of the analyses will be displayed in maps, graphs, and tables. For precipitation, a compact presentation of maps of median precipitation together with tables of relationships between the median and each of the frequencies is possible that will enable the user to estimate precipitation at the desired frequency.

INTRODUCTION

The U.S. Army Corps of Engineers was charged in 1989 with the responsibility of conducting a national study of water management during drought. This study was to consider ways to reduce the nation's vulnerability to drought, considering the capabilities and responsibilities of all levels and agencies of government. Responsibility within the Corps of Engineers for conducting this study was given to the Institute for Water Resources.

In the first year of the study, the nature of the drought problem was investigated through questionnaires, workshops, literature reviews, participation in professional society meetings, interviews and correspondence, and special studies conducted by the Advisory Commission on Intergovernmental Relations, Resources for the Future, and the Hydrologic Engineering Center of the Corps of Engineers. Among the conclusions were a) that much of the distress caused by drought was the result of institutional and legal factors, and b) that were technical studies which would be helpful in drought preparedness planning and management of water during drought. (Institute for Water Resources, 1991)

A technical product suggested by study participants and reviewers of draft reports was a national drought atlas. This was deemed desirable in order to provide planners a reliable base of information, using consistent terminology and methodology, that presented information in such a fashion as to indicate the degree of risk involved in various courses of action. The drought atlas will provide an analysis of precipitation, streamflow, the Palmer Drought Index (Palmer, 1965), and reservoir contents data.

The atlas is being prepared by the National Climatic Data Center, the U.S. Geological Survey, and the Institute for Water Resources. The authors of this paper have primary responsibility for the various parts of the atlas. The first author represents the Institute for Water Resources as overall coordinator of the atlas. James R. Wallis and Jon R.M. Hosking of the T. J. Watson Research Center of IBM are providing statistical methodology assistance. Representatives of the U.S. Department of Agriculture (Soil Conservation Service, Forest Service, and the Office of the Secretary), the National Weather Service, the U.S. Bureau of Reclamation, and the Midwestern Regional Climate Center assisted in the planning phase.

A good base of information on several characteristics of drought will enable planners to more quickly and fully understand the nature of the physical aspects of drought. By presenting this information in terms of frequency of occurrence, comparisons between regions of the country can more readily be made. This may facilitate the development of state and national policy pertaining to drought.

CHARACTERISTICS OF DROUGHT

While all hydrologic and climatic phenomena of human interest have a substantial human component, it is especially true of drought. Whereas a flood is usually an unambiguous event, and most observers would agree on when a flood had occurred, the same is not true of drought. A drought occurs when there is not enough water to meet normal demand. The relevant characteristics and dimensions of drought depend on water-use characteristics. For some water uses and users, streamflow is the most important characteristic. For others, it is

precipitation. In yet others, soil moisture is the critical parameter. Whether streamflow, precipitation, or soil moisture is the more relevant characteristic, issues of duration, time of occurrence, and areal extent also may assume major significance. For agriculture, a period of low precipitation in the winter months might be of concern to farmers raising a particular crop, whereas for others, the precipitation of most importance would be in the summer. A municipality dependent on run-of-river flow and with little storage would be severely affected by low flows that may last only a few days or weeks, whereas municipalities that have appreciable water storage capacity would not be concerned unless the period of low streamflow lasted for months or years.

METHODOLOGICAL CONSIDERATIONS

Because the questions most likely to be asked about drought pertain to some aspect of risk, it is desirable to present information in frequency terms. Because planning for drought occurs at many different scales and for many uses, it is also desirable to present information that can be used for a range of durations and areal coverage. A typical question might be something like: "What is the likelihood that a three month period beginning in June will have 60 percent or less of normal precipitation for southwestern Ohio?" It will be possible to answer this and similar questions using information from the atlas. A discussion of methodological issues raised in attempting to provide this information follows.

Data

In general, the longest periods of record available for high quality stations within each region are used. The Historical Climatology Network (HCN), a network of approximately 1,200 stations with data through 1989 (Karl, et al, 1990) for precipitation and the Palmer index. Record lengths are at least 60 years for most stations. Because of data quality issues, not all stations in the HCN are used, because missing data were estimated from nearest neighbors in the HCN, which in some cases are too far apart to be considered reliable for precipitation, and because a month may be included in an HCN record with as many as 9 missing days of precipitation. About 100 stations will be omitted for this atlas because of an excessive number of missing days or because missing data could not be reliably estimated.

For streamflow, a subset of approximately 1,700 stations with data through 1988, prepared for the U.S. Geological Survey's Hydroclimatic Data Network (Landwehr and Slack, 1990), is being used. Record lengths are, on average, shorter than for precipitation, being at least 20 years and averaging about 40 years, but are long enough to support the frequency estimates. Other criteria for selecting stations are that the sites are unregulated with minimal diversion and no significant land use change, i.e., unaffected by human intervention, and that the data are of high quality.

The Palmer Drought Index is being recalculated for each HCN station that has consistent precipitation and temperature data. Because the Palmer Index does not lend itself to averaging over multi-month periods, reporting on the Palmer Index will be the historical percentiles. No frequency distribution will be fitted to this data. For example, one such reported figure might be the following: "During the months of June-August, in southwestern Ohio, the Palmer Index was -3 or lower 10 percent of the time during the 70-yr. period of record."

Duration

Data will be analyzed separately for each calendar month; the calendar or climatic year; consecutive 2-month, 3-month, and 6-month periods; and consecutive 2-year, 3-year, and 5-year periods. Drought durations may, of course, exceed 5 years, and water planners in some places are interested in longer durations. However, it is considered that for an atlas of general applicability, 5 years is a suitable cutoff point. The length of record for many stations is also a factor in choosing the maximum duration. Short records cannot yield estimates of high reliability for long durations, because there are not many 5-year droughts in the record. Those interested in considering longer durations of drought will need to engage in independent analyses.

For durations less than or equal to 1 year, a data series will be prepared for each station with one value for each year of record. For the month of January for a station with 80 years of record, there would be 80

values of total monthly precipitation in the data series. For the multi-month analysis, values will be calculated for all consecutive m-month periods, i.e., m months beginning in January, m months beginning in February, etc.

For periods longer than 12 months, different problems arise as to how to select the items in the data series, and how to make the appropriate probability statement corresponding to the data series. While a final decision has not been made at the time of this writing, two options being considered and tested for developing the precipitation and streamflow data series are the following:

a. Select the lowest m-year (or m times 12 months) moving average in the record as the first item in the data series and remove all years from the remaining record which are dependent on that moving average; then repeatedly select the lowest remaining m-year moving average and remove dependent years until there are no further possibilities; and

b. Divide the record into m separate series of n/m non-overlapping events, where n is the number of years of record, and either select one of these m series or calculate quantiles from each series and average the quantiles. This procedure is equivalent to taking a systematic sample with a random start.

Areal Extent

In general, drought is thought of as a widespread phenomenon, in contrast to a flood, which may have a small areal extent as a result of small, intense storms. However, as area increases within a climatic region, average precipitation or streamflow over the area usually increases, because there is somewhat more likelihood of a precipitation occurring somewhere within this larger area. An attempt will be made to explicitly consider variation of drought intensity with area. Our intent is to select three areas for each region, with smaller sizes in the humid regions and larger sizes in the semi-arid and arid regions. The lower limit will be in the order of 750 to 1,000 sq. mi. and the upper limit in the order of 100,000 sq. mi.

The procedures for obtaining the different areal estimates are still in a testing phase as of this writing. Two basic approaches are available for precipitation. The first is to aggregate the records of adjacent stations into areas approximately equal to the area of concern and then perform the frequency analyses on the aggregated records. The second approach is to perform point data aggregation on a Geographic Information System. In this approach, a raster of varying resolution is defined and used to calculate a weighted average.

Statistical Analysis

The measure of central tendency for all data will be the median. This parameter is chosen rather than the mean because of its stability and robustness, its representativeness of the phenomena under consideration, and its amenability to other aspects of frequency analysis being employed in the study.

The frequency distributions chosen will be guided by the data, using L-moments to estimate the parameters of the distributions. L-moments are an extension of probability weighted moments (Greenwood et al, 1979). The term is a shorthand expression for a linear combination of order statistics. The first L-moment is the mean, the second a measure of dispersion. L-skewness is the ratio of the third L-moment to the second L-moment, and is a measure of skewness. Similarly, L-kurtosis is the ratio of the fourth L-moment to the second L-moment, and is a measure of peakedness or kurtosis. Unlike conventional measures of skewness and kurtosis, the estimates are not affected to the same extent by extreme values. Data points are not cubed or raised to the fourth power. The theory of L-moment analysis is described by Hosking (1990).

Having obtained the L-moments, especially the second, third, and fourth, a plot of values of L-skewness versus L-kurtosis ratios (to the second L-moment) is superimposed on plots of theoretical relations for different frequency distributions. Then, a selection of a frequency distribution is made.

Finally, the data points in the original series are fitted to the selected frequency distribution by use of the L-moments. Values corresponding to average return periods of 2, 5, 10, 20, and 50 years will be presented in the atlas.

Other Parameters

Water managers have noted that reservoir contents would be a desirable addition to the National Drought Atlas. Although reservoir contents are dependent on operating rules for individual reservoirs and systems of reservoirs, precluding frequency analysis of the kind being done for precipitation and streamflow, historical summaries of reservoir contents for major reservoirs will be included. The reported figures will be percentiles of the proportion of normal maximum usable contents of major reservoirs and reservoir systems. The selected reservoirs are likely to be those reported on regularly by the U.S. Geological Survey in the monthly (National Water Conditions, monthly), plus other selected reservoirs and systems proposed by the water management community.

Joint and Conditional Probability

While it is well known that some questions posed by planners and citizens about drought involve consideration of joint and conditional probability, it is not likely that such analyses will be done, because of cost and methodological difficulty. A form of "climatic forecasting" will be possible, however, in which the probabilities of precipitation or streamflow occurring in successive periods are aggregated.

Data Presentation

Wherever possible, a common mode of presentation is planned for all parameters. However, streamflow, which integrates precipitation, evapotranspiration, and water movement through and storage in the soil, cannot be regionalized using the same procedures employed for precipitation. Streamflow analyses will be based on watershed and river basin boundaries.

Finding suitable ways to present the vast amount of information contained in the atlas is challenging. However, it has also led to analysis that shows unanticipated regularities in drought statistics. Combining the questions considered to be most often asked of an atlas that purports to characterize drought with the findings of the study has led to some standard modes of presentation. Some have been used in earlier studies of drought; others are considered original to this atlas.

To illustrate one major mode of presentation, consider calendar year annual precipitation. A map of median annual precipitation can be readily prepared. It is logical to consider preparing a set of maps or tables that would relate particular aspects of low precipitation to these median values. For example, a map or table that gives the ratio of the annual precipitation with an average recurrence interval of once in 20 years over a 10,000 sq. mi. area to the median annual precipitation would enable a planner to pick a location, read values from the maps and/or tables, and estimate the 20-yr. return period annual low precipitation. A first approximation to this map is shown in Figure 1. This map shows the ratio of the 5th percentile of annual precipitation to the median. The values shown on the map are the averages of this ratio for all stations in each state, i.e., the value for Ohio is the average of the ratios for the 25 HCN stations in the state. The 5th percentile is a first approximation to the once-in-20 year event. Considering the length of the precipitation records, at least 60 years for most stations, it is quite a good first approximation. Tabular values will supplement the maps for presenting the ratios, and will be an important mode of presentation for the parameters of interest.

FINDINGS TO DATE

A complete summary of findings would be premature at the time of this writing. However, preliminary work indicates the data may exhibit a degree of regularity unanticipated at the outset of work on the atlas. One early study resulted in the preparation of Figure 1. This analysis, as is stated above, is closely analogous to the ratio of the m-year return period event to the median. The results of this study showed a remarkable degree of regional similarity throughout the United States, with predictable progressions of the ratio from one climatic region to another. The variation of the ratio within states is small, with the exception of some western states.

USE OF ATLAS

The atlas is considered most likely to be used by planners at all levels of government or their consultants, as well as business and industry planners. A planning group can ask a large number of "what-if" questions which can be answered directly from the atlas. They can determine the most likely durations of critical drought, when such droughts are likely to occur, how much reduction from "normal" can be expected in a drought of a given frequency, what droughts have occurred in the region, and what their meteorological characteristics were, both within the period of instrumental records and, for some portions of the country, in the tree ring record.

Information will also be presented on the range of human responses available to cope with drought and reduce the attendant damages.

FORMAT OF ATLAS

The atlas will be a multi-volume document. In the first volume, the purpose and use of the atlas, methodology, and general characteristics of drought will be described. This volume will also contain summary information on some of the most economically and socially important droughts in U.S. history. National summaries of drought characteristics, described more fully in the other volumes, will also be included. A chapter on tree-ring analysis is planned, along with chapters dealing with the meteorological characteristics of drought.

The remaining volumes will be regional summaries. In addition to narrative discussion of droughts and meteorological characteristics in each region, maps, graphs, and tables will summarize drought for each parameter, for ranges of durations, areal extent, and frequencies of occurrence. These volumes, in a four color 11" x 17" wire-bound and edge-reinforced format, will have, in addition to maps, graphs, text, and tables, computer disks in IBM and Macintosh format, that summarize the data, and include the tables and graphs. A compact disk (CD) for the entire atlas is planned, which will include all the regional data.

The initial distribution, expected in 1992, is to be in the range of 10,000 - 15,000 copies. The primary expected audience for the atlas includes federal water agencies, state and local water agencies, consultants, and the academic and research community. Inquiries have, however, been received from the insurance industry, and there are application possibilities for all water users, from marina operators to electric utilities.

THE FUTURE

It has been rightly observed that an atlas represents information as of a moment in time. To continue to be a useful document, it should be updated. While it is true that longer records are generally better than shorter records, the procedures used in the atlas should be an accurate representation of drought occurrence. It is our hope that updates will be made, and that when better methodologies become available, they will be used in subsequent revisions of the atlas.

Among the important improvements that can be made in an atlas such as the one described in this paper is improving the quality of the underlying data sets. This is especially acute for precipitation. Even though there is no better data set than the HCN as of 1991, the HCN's inadequacies are such as to merit additional cleaning and adjustments based on stations close to those in the network. Undertaking joint and conditional probability studies would also be useful, including the joint probability of low precipitation and high temperatures.

Users will undoubtedly find other ways in which the data might have been analyzed or presented. This is one of the reasons data disks are being included in the atlas. It is the hope of the authors that those who find other useful ways of analyzing or presenting data will make their work known to others and us, so that practitioners worldwide may consider these methods when preparing atlases for other regions.

REFERENCES CITED

Greenwood, J.A., Landwehr, J.M., Matalas, N.C., and Wallis, J.R., 1979, Probability weighted moments: definition and relation to parameters of several distributions expressible in inverse form: Water Resources Research, v. 15, p. 1049-1054.

Hosking, J.R.M., 1990, L-moments: analysis and estimation of distributions using linear combinations of order statistics: Journal of the Royal Statistical Society B, v. 52, no. 1, p. 105-124.

Karl, T.R., C.N. Williams, Jr., F.T. Quinlan, and T.A. Boden, 1990, United States historical climatology network (HCN) serial temperature and precipitation data: ORNL/CDIAC-30, NDP-019/R1, Carbon Dioxide Information Analysis Center, Oak Ridge National Lab., Oak Ridge, TN, 377 p.

Institute for Water Resources, April 1991, The National Study of Water Management During Drought: Report on the First Year of Study: U.S. Army Corps of Engineers, Ft. Belvoir, VA, IWR Report 91-P-91.

Landwehr, Jurate M., and James R. Slack, 1990, HCDN (Hydro-climatic data network): A U.S. Geological Survey discharge data set for climatological impact analysis: Symposium on global change systems, American Meterological Society, Feb. 5-9, 1990, Anaheim, California.

National Water Conditions, U.S. Geological Survey, and Department of the Environment, Water Resources Branch, Canada, issued monthly.

Palmer, W.C., 1965, Meteorological drought: Research Paper No. 45, U.S. Weather Bureau, Washington. DC.

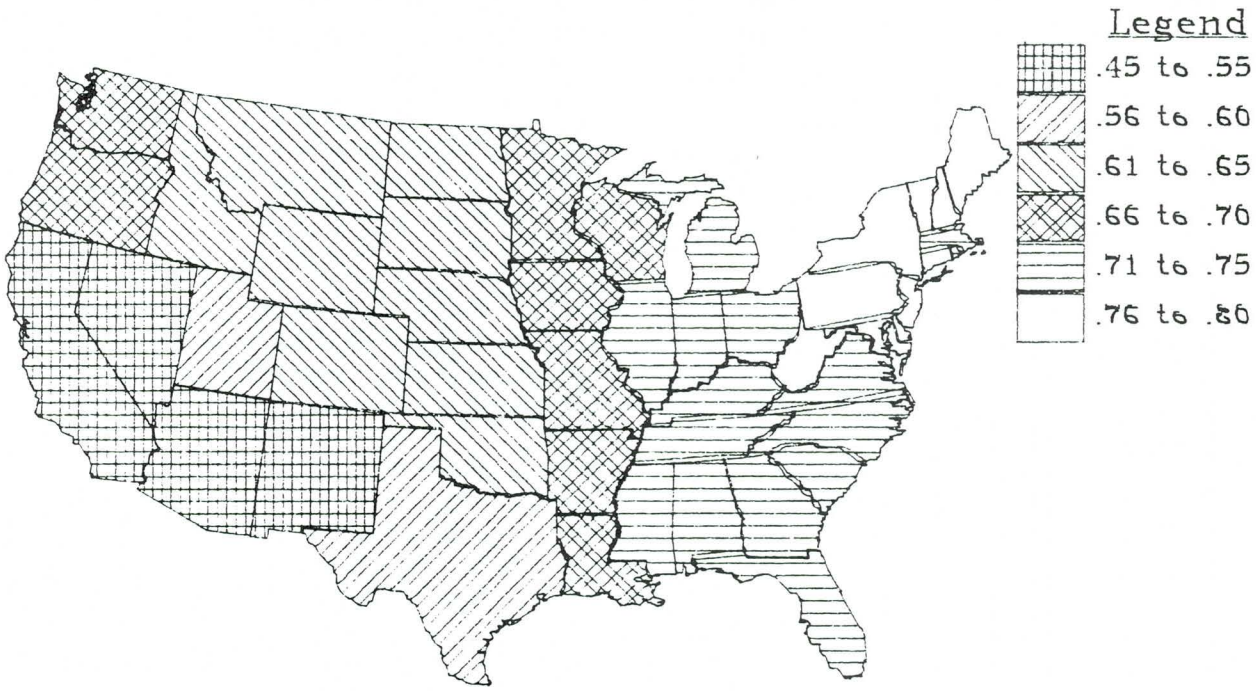

Figure 1. The ratio of the 5-th percentile annual precipitation to the median, regionalized from Historical Climatology Network data.

PREDICTION OF REGIONAL SOIL WATER AND DROUGHT

Li Baoguo

Department of Land Resources Science,
Beijing Agricultural University,
Beijing, 100094, PRC

ABSTRACT

A distributed soil water balance (DSWB) model, has been developed by incorporating a 2-D Cartesian coordinate system (x,y) into the general soil water balance equation. Thus the dynamic spatial distribution of regional soil water can be described and predicted. The DSWB model was implemented by using GIS (geographic information system) techniques. Furthermore, a map of regional soil drought was obtained on the basis of the DSWB model and the needs of the crop for soil water. The above method has been applied in Quzhou, Huang-Huai-Hai fluvial plain, China.

INTRODUCTION

It is difficult to expand the model of soil water dynamics and soil water balance to the regional scale, and obtain everywhere soil water dynamics or distribution dynamics of regional soil water, because the spatial variability of soil water parameters is extreme (Nielsen et al.,1973; Hillel, 1979; Feddes et al., 1988). However, regional irrigation, water resources management, and prediction of drought or waterlogging require the modeling and prediction of regional soil water distribution dynamics. This paper describes the development of a distributed soil water balance (DSWB) model to produce a regional soil drought map.

MODEL ESTABLISHMENT

Principle of DSWB MODEL

Taking into account the integrality of the regional soil water distribution, according to water balance equation and conceptual model of regional water and salt system (Li 1990; Li and Shi 1990), the 2-D Cartesian coordinate system (x,y) was imported into the general soil water balance equation to develop the model for predicting regional soil water content of 1 m deep soil body. The model established was named the DSWB model (DSWB: distributed soil water balance), and can be written as:

---

* *The author gratefully acknowledges the support of K.C. Wong Education Foundation, Hong Kong.*

$$SSW1(x,y)_t = SSW1(x,y)_{t-1} + Ps(x,y)_\tau - ETs(x,y)_\tau + Is(x,y)_\tau + Q_1(x,y)_\tau \quad (1)$$

where (x,y): 2-D Cartesian coordinate; τ: the time period from t-1 to t; $SSW1_t$: the water content of a 1 m deep soil body at time t; $SSW1_{t-1}$: the water content of a 1 m deep soil body at time t-1; Ps: the recharge of precipitation to soil; ETs: evapotranspiration; Is: irrigation amount; Q_1: the upward water flux at depth 1 m. All water volumes are expressed in unit of depth of water over a unit area.
The data set of the water content of 1 m deep soil body at all (x,y) points in the region D is defined as the regional soil water regime ($SSW1_D$). This can be expressed as:

$$SSW1_{Dt} = \{SSW1(x,y)_t \mid (x,y) \in D\} \quad (2)$$

Estimation of the DSWB Model Variables

Ps(x,y) in eqn. (1) is obtained from the local meteorologic station or weather reports, and Is(x,y) is estimated on the basis of the condition of regional water conservancy facilities, crop distribution and irrigation schedule.

Ets(x,y) is given by

$$Ets(x,y)_\tau = K_c(x,y)_\tau \, K_s(x,y)_\tau \, ETM(x,y) \quad (3)$$

where ETM = the potential evapotraspiration, which can be calculated by the Pemman methods, K_c = the crop coefficient, and K_s = soil coefficient. K_s can be determined as follows. Define

$$SSW1(x,y)_\tau = 0.5\,(SSW1(x,y)_{t-1} + SSW1(x,y)_t) \quad (4)$$

$$k = SSW1(x,y)_\tau \,/\, (0.8\, SSW_c(x,y)) \quad (5.1)$$

$$k_0 = SSW_w(x,y) \,/\, (0.8\, SSW_c(x,y)) \quad (5.2)$$

where $SSW_c(x,y)$ and $SSW_w(x,y)$ are the field water capacity and wilting water content, respectively, of a 1 m deep soil body, and depend only on the space coordinate (x,y). Then

$$K_s(x,y) = \begin{cases} 1 & \text{if } k \geq 1 \\ 0 & \text{if } k \leq k_0 \\ k & \text{otherwise} \end{cases} \quad (6)$$

$Q_1(x,y)_\tau$, which is associated with many environmental factors (Li et al., 1988), was estimated by a simple method. This can be expressed as:

$$Q_1(x,y) = Q_{E1}(x,y)_\tau - Q_{I1}(x,y) - Q_{P1}(x,y)_\tau \quad (7)$$

where Q_{E1} = the recharge amount from the soil body below depth 1 m; Q_{I1} = the percolation water amount out of the 1 m deep soil body, which results from irrigation; Q_{P1} = the percolation water amount out of the 1 m deep soil body, which results from precipitation.
Because the surface is very flat in the fluvial plain, if the groundwater

depth is lower than 4 m, The following equations can be assumed (Li, 1990):

$$Q_{E1}(x,y)_\tau = Q_E(x,y)_\tau \qquad (d < 4 \text{ m}) \tag{8}$$

$$Q_{P1}(x,y)_\tau = Q_P(x,y)_\tau \qquad (d < 4 \text{ m}) \tag{9}$$

$$Q_{I1}(x,y)_\tau = Q_I(x,y)_\tau \qquad (d < 4 \text{ m}) \tag{10}$$

where Q_E = the amount of groundwater evaporation; Q_P = the recharge to groundwater resulting from precipitation; Q_I = the recharge to groundwater resulting from irrigation; and d = the groundwater depth.
Q_E, Q_P, and Q_I estimation methods were reported by Li (1989).

Thus $SSW1(x,y)_t$ is calculated by combining equations (1) to (10). Finally, $SSW1_{Dt}$ are obtained by calculating all $SSW1(x,y)_t$ for $(x,y) \in D$.

Drought Prediction

After all $SSW1(x,y)_t$ ($(x,y) \in D$) are predicted, the relative soil water content, which is equal to the ratio of the water amount in a 1 m deep soil body to its field water capacity at (x,y), is defined as the drought index K_d. This can be expressed as:

$$K_d(x,y)_t = SSW1(x,y)_t \ / \ SSW_c(x,y) \tag{11}$$

Generally, different crop systems and different stages of crop growth have different requirements for the value of K_d (Shi, 1984). Comparing $K_d(x,y)$ with crop K_d, which reflects crop growth requirements, we can predict regional soil water drought status.

MODEL IMPLEMENTATION

The DSWB model is implemented by geographic information system (GIS) techniques. This process is shown as figure 1.

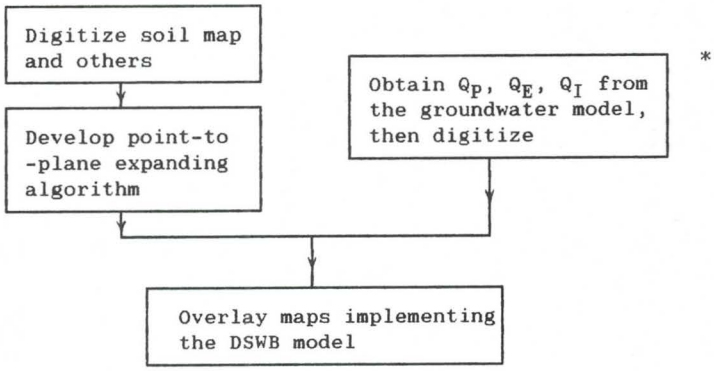

Figure 1.--Model implementation process with GIS

** reported by Li (1989,1990)*

Digitizing maps

The maps (scale=1:50,000), which include the regional soil map, water conservancy facilities map, and others, were digitized. Corresponding to real surface area 50m*50m, each digitized grid square on the maps is 1mm*1mm. using a 16-digit soil-type code, the type of soil series (i.e. soil species), the texture of surface soil, the layer structure of 1 m deep soil body, and other information can be obtained from the digitized regional soil map.

Expanding Data from Point to Plane

The principles of expanding are: (1) Each soil series is considered to have the same soil water properties on the basis of soil series, location in the same geo-environment, and similarity of pedon structure and land use. (2) the nearest-neighbor law of spatial distribution is adopted if there are more than 2 points or no point in the same soil series region. In the light of the two principles, an expanding algorithm from point to plane was developed (Li, 1990). The digitized maps of initial regional soil water ($SSW1_0$) and regional soil water properties (SSW_c, SSW_w) were produced by the expanding algorithm.

Model Execution

The execution process of the DSWB model is shown in Figure 2.

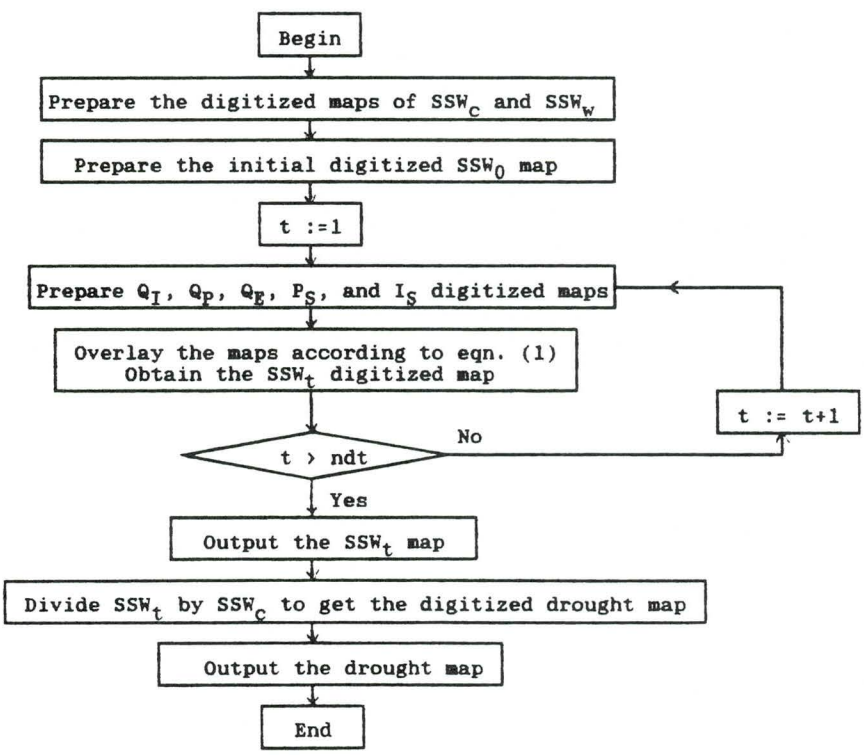

Figure 2.--Flow chart of the DSWB model

MODEL APPLICATION

The DSWB model has been applied in a 253 km^2 experimental area in Quzhou,

Huang-Huai-Hai fluvial plain, China. The crop systems were annually considered as the wheat and corn rotation; K_c were adopted by referring to values given by Tao and Pen (1979), and for each soil texture, SSW_c and SSW_w were measured by sampling in the field. The prediction period is a season and the time step is 5 days. Initial condition could be input to the model again in next time period historical prediction.

Results and Analysis of Historical Prediction

The DSWB model was historically prediction during 8 seasons from 1987 to 1988 in order to calibrate the DSWB model. The surveyed map of the actual content of the 1 m deep soil body and its prediction map can be automatically plotted by computer-driven plotter (Figure 3). The map of soil drought index K_d obtained at same time is presented in Figure 4.

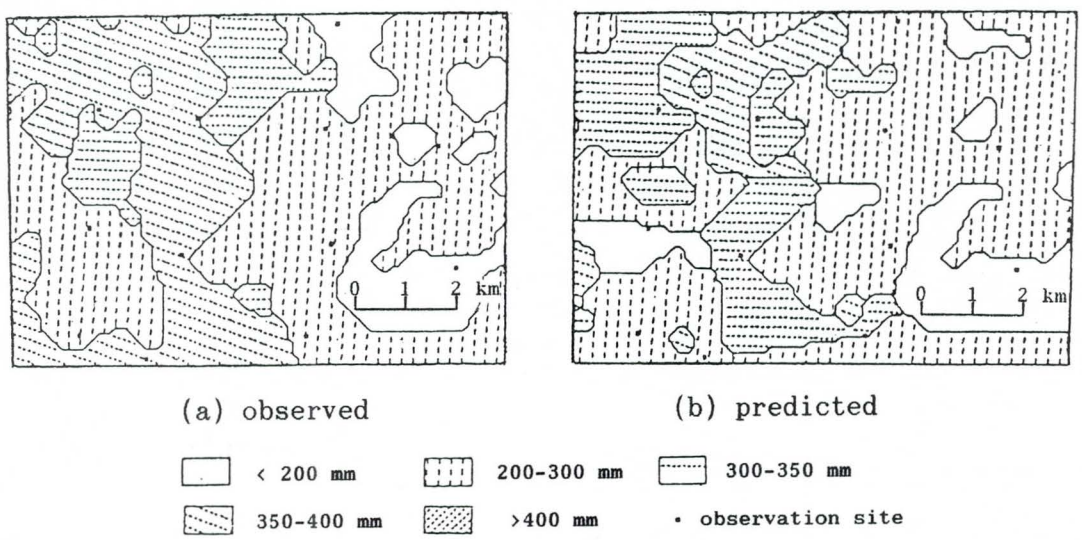

Figure 3.--Maps of water content of 1 m deep soil body, Quzhou experimental area, June 11, 1988. (a part of experimental area is about 60 km^2)

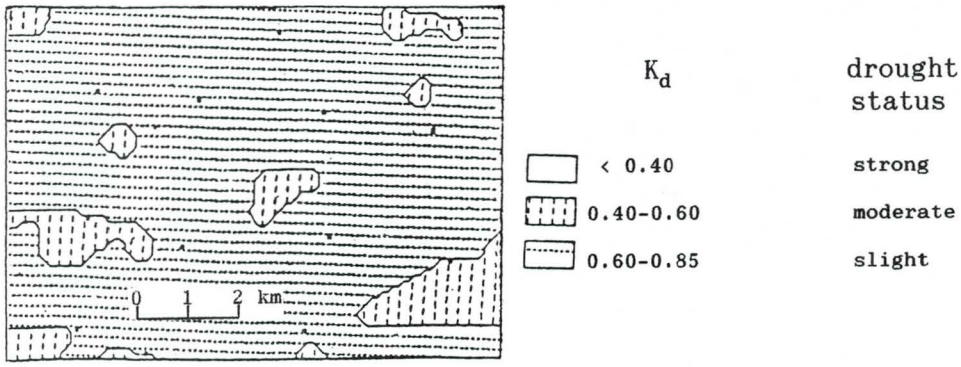

Figure 4.--Prediction map of soil water drought index, K_d, Quzhou experimental area, June 11, 1988.

Based on calibrated of 354 points and times, the absolute error of water content of the 1 m deep soil body is 33.6 mm, and the relative error is 11.7

percent. Considering that the general irrigation requirement is about 75±15 mm for one irrigation, the absolute error is less than half of the irrigation requirement, so the drought prediction accuracy of the DSWB model is acceptable for agricultural practice.

Results and Analysis of Real-Time Prediction

The time period was two seasons in real-time prediction in 1989 assuming that the weather conditions in 1989 were similar to those in 1987. Based on calibration of in the experimental area, the absolute error was 34.9 mm, and the reactive error was 14.1 percent. The accuracy of real-time prediction was slightly lower than that of the historical. Further study is necessary on the real-time prediction.

CONCLUSIONS

1. The 2-D Cartesian coordinate system (x,y) was incorporated into a general water balance equation. The DSWB model, which can be used to predict regional soil water distribution dynamics, has been developed.
2. The DSWB model was implemented using GIS techniques including map digitizing and overlaying, and development of an algorithm for expanding point data to plane data.
3. The DSWB model has been applied to a 253 km^2 experimental area. The relative error is 11.7 percent in the historical prediction and 14.1 in the real-time prediction. The map of regional soil water distribution and regional soil water drought index, can be automatically plotted by computer.

REFERENCES

Feddes R.A., Kabat P., Van Bakel, et al., 1988, Modelling Soil Water Dynamics in the Unsaturated Zone -- State of the Art: J. Hydrol. 100, 69-111.

Hillel D., 1977, Computer Simulation of Soil Physics: Academic Press, New York.

Li Baoguo, 1989, The Dynamics Prediction of Regional Groundwater Table: Trans. of International Symposium on Dynamics of Salt-Affected Soil, Nanjing, China.

Li Baoguo, 1990, Systematic Model for Predicting Dynamics of Regional Water and Salt: Ph.D Thesis, Beijing Agricultural University.

Li Baoguo and Shi Yuanchun, 1990, Modelling for Predicting Seasonal Systematic Dynamics of Regional Water and Salt: Trans. of 14th International Congress of Soil Science. Vol. 6,108-113, Kyoto, Japan.

Li Yunzhu, Chen Yan and Wang Shaoying, 1988, Characteristics and Types of Soil Water Balance on Different Geo-Condition: Trans. of 4th China Soil Physics Congress, Chungking.

Nielsen D.R., Biggar J.W. and Erh. K.T., 1973, Spatial Variability of Field Measured Soil Water Properties: Hilgardia 42, 215-259.

Shi Chengxi, Li Zongsong and Cao Wanjin, 1984, Agricultural Hydrology: Agriculture Press, Beijing.

Tao tsouwien and Pen Puhsiang, 1979, Methods of Computing field evapotranspiration and Variation of soil moisture: Acta Meteorologica Sinica, 37(4), 79-87.

TOPIC B

CHARACTERISTICS OF ARID-REGION HYDROLOGY

FLOOD HYDROLOGY OF ARID BASINS IN SOUTHWESTERN UNITED STATES

By

H.W. Hjalmarson[1]

ABSTRACT

In the arid southwestern United States, summer thunderstorms commonly produce flash floods at low-elevation basins. In northern basins at higher elevations, floods commonly result from snowmelt and rainfall of cyclonic storms. The temporal and spatial variability of floods is particularly acute for streams draining areas of less than 200 square miles. At elevations above 7,500 feet, the magnitude of infrequent flood-peak discharge is significantly less than at lower elevations. Because of the many years of no flow at many gaged streams, there are too few years with flow to reliably define flood-frequency relations.

INTRODUCTION

The topography of the southwestern United States is dominated by the Sierra Nevada to the west and the Rocky Mountains to the east. The crestline of both mountain ranges commonly is more than 10,000 ft; some peaks are in excess of 12,000 ft. Throughout the area, isolated mountains are separated by arid desert plains. Most of the mountain ranges trend north and northwest and commonly rise a few thousand feet above the adjacent alluvial plains.

Major drainage basins include the Colorado River, Rio Grande, and the Great Basin (fig. 1). The large rivers head in high-elevation mountains where precipitation is abundant and then flow through arid deserts. Some flood characteristics of streams that drain areas less than 2,000 mi² are presented in this report. The general relations presented are based on data for 1,336 streamflow gages in and adjacent to the major basins (fig. 1).

Figure 1.—Western United States and selected gaging sites.

Distributary-Flow Areas

Throughout the study area, but especially in southeastern California, southern and western Arizona, and Nevada, alluvial fans (distributary-flow areas) can reduce significantly the amount of floodflow that leaves the basin. Some distributary-flow areas may be noncontributing for most floods. Some of the flood-peak attenuation indicated by comparison of flood-frequency relations for sites on the same stream is related

[1]Hydrologist, U.S. Geological Survey, 375 S. Euclid Avenue, Tucson, Arizona, 85719

to distributary-flow areas in the intervening drainage area. An example is Brawley Wash in southern Arizona in which the 100-year peak discharge decreases from 24,000 to 19,000 ft^3/s between streamflow-gaging stations 09486800 and 09487000 (fig. 1), while the total drainage area increases 68 percent from 463 to 776 mi^2. A large percentage of the potential intervening runoff from the mountains and pediments must traverse many distributary-flow areas. The floodflow divides and combines many times and spreads laterally over the permeable soil. Even during large floods, most of the floodflow peak discharge in the distributary-flow areas is lost to infiltration or attenuation. Floodflow that leaves these distributary-flow areas adds to the peak discharge in Brawley Wash but is of little consequence.

STREAMFLOW

Streamflow at the streamflow-gaging station, 09512200 Salt River Tributary at South Mountain Park, at Phoenix, Arizona (fig. 1), is typical of streams that drain small arid basins in the southern latitudes. For example, all runoff from the 1.75-square-mile basin for water year 1964 occurred in a few hours on October 19, 1963, and August 2, 1964, as a result of thunderstorms (fig. 2). During the 29 years of record at this site, no flow occurred for eight of the water years and 99.5 percent of the days had no flow.

The coefficient of variation (standard deviation/mean) for annual discharges at streamflow-gaging station, Salt River Tributary at South Mountain Park, at Phoenix, Arizona, is 1.9; coefficients of variation for some months were more than 5. During the 29 years of record, no flow occurred during the months of February, April, and May. The coefficient of variation of mean annual discharge at this site is typical for small arid streams in the southern latitudes (fig. 3). The coefficient of variation of mean annual discharge, which is a measure of the ability to detect

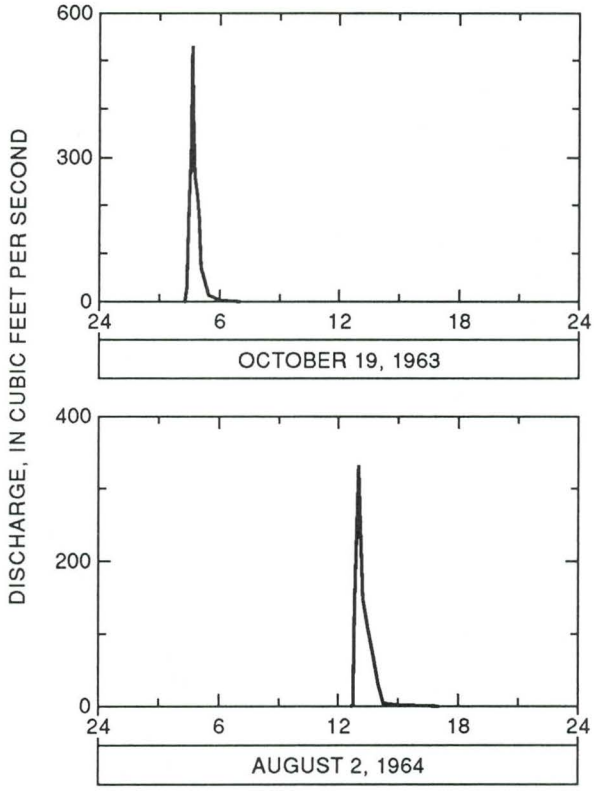

Figure 2.—Storm runoff for water year 1964 at streamflow-gaging station 09512200, Salt River tributary at South Mountain Park, at Phoenix, Arizona.

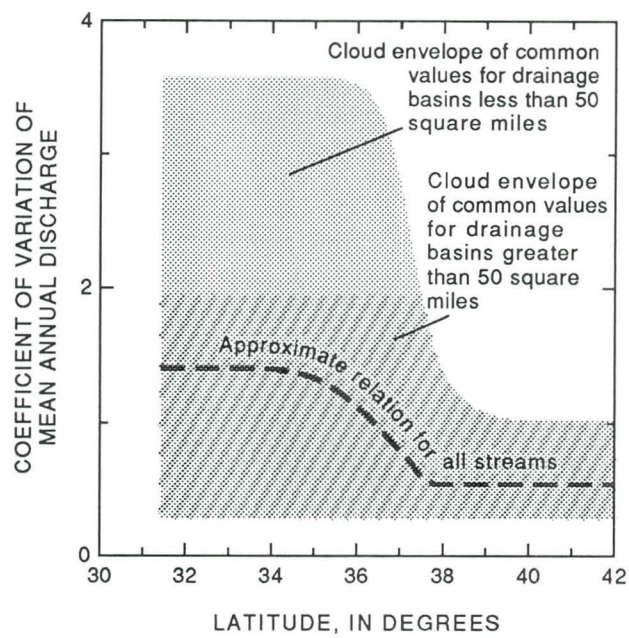

Figure 3.—General relation of coefficient of variation of mean annual discharge to latitude for streams that drain basins of less than 200 square miles.

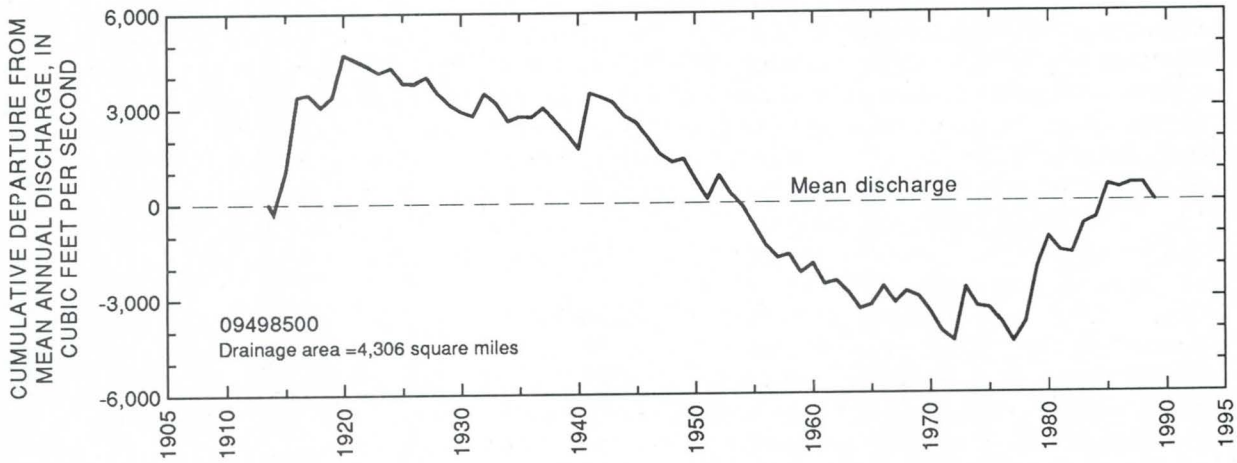

trends of streamflow, is much smaller for streams in the northern latitudes (fig. 3). The coefficient of variation of mean annual discharge commonly is more than 1.0 for small streams in the southern latitudes and less than 1.0 for small streams in the northern latitudes.

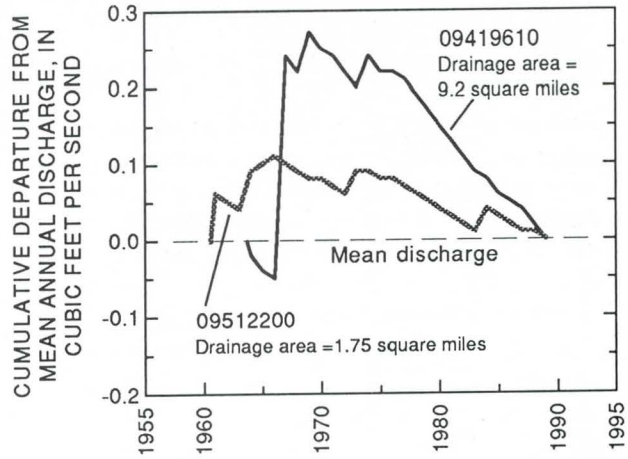

Figure 4.—Cumulative departure from mean annual discharge for indicated sites in the southwestern United States.

The trend of mean annual discharge can be quite different for small ephemeral streams than for large streams that drain large mountainous areas. For example, the cumulative departure from mean annual discharge in figure 4 illustrates differences of runoff patterns. The discharge trends for streamflow-gaging station, 09512200 Salt River Tributary at South Mountain Park, at Phoenix, Arizona, and 09419610 Lee Canyon near Charleston Park, Nevada, which are on small ephemeral streams, are much different from the discharge trends for streamflow-gaging station, 09498500 Salt River near Roosevelt, Arizona. Most of the runoff for station 09419610 was during two storms during water year 1967.

FLOODFLOW

Floodflow in the mountainous areas commonly is in channels confined by steep mountain slopes or V-shaped canyons. Stream channels in the mountains are tributary, and peak discharge increases as the drainage area increases. Floodwater that leaves the mountain fronts can spread over piedmont plains in a complex system of tributary and distributary alluvial channels. In the alluvial plains, the peak discharge can decrease by attenuation and infiltration as the drainage area enlarges.

Desert floods in the southwestern United States commonly result from large amounts of intense rainfall or snowmelt in the steep headwater mountains. Typical floods that result from thunderstorms are characterized by a rapid rise and a rapid cessation of discharge (fig. 2). Typical floods in the northern latitudes that result from snowmelt have a less rapid rise and recession. The floods in the northern latitudes generally are much smaller than those in the

southern latitudes. Typical peak discharges for major floods that are the result of thunderstorms in the southern latitudes are nearly 10 times greater than those in the northern latitudes (fig. 5).

High Elevations

A limiting elevation exists above which large thunderstorm-caused floods are rare. The physical cause of this threshold probably is based on the available energy and moisture in the atmosphere for the convective process. The elevation threshold remains constant at 7,500 ft for all sites south of about 41 degrees latitude, and decreases north of that latitude. North of 41 degrees latitude, the threshold is approximately a flat plane sloping about 300 ft for each degree of latitude. For example, at 42 degrees latitude, the threshold is 7,200 ft; and at 43 degrees, it is 6,900 ft. The unit peak discharge for sites south of 41 degrees latitude commonly is greater than the unit peak discharge for sites north of 41 degrees latitude (fig. 6). North of 41 degrees latitude, the unit peaks were less than 300 $(ft^3/s)/mi^2$, and most were less than 100 $(ft^3/s)/mi^2$. All the peaks greater than 100 $(ft^3/s)/mi^2$ were the result of rainfall. Below 100 $(ft^3/s)/mi^2$, peaks are the result of a mix of rainfall and snowmelt. North of 41 degrees, most of the peaks are the result of snowmelt.

Flood-Frequency Relations

The shape of flood-frequency relations for sites is assumed to have limitations. The expected slope of the relation is positive because peak discharge logically increases with decreasing probability of occurrence. The expected shape of the relation is a straight line or a smooth curve in log-probability space. The fitted relation is expected to visually agree

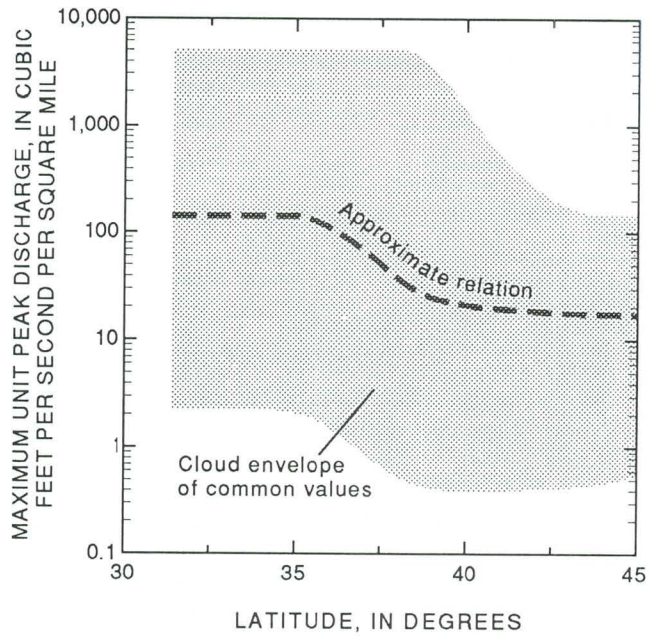

Figure 5.—Relation of maximum unit peak discharge at gaging stations to latitude for unregulated streams that drain basins of less than 200 square miles.

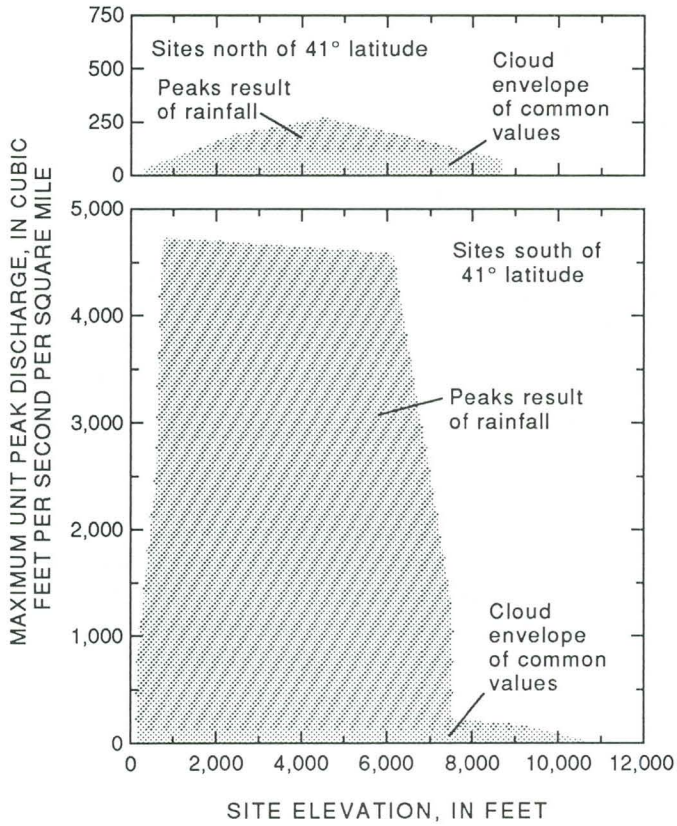

Figure 6.—Relation of maximum unit peak discharge of record to site elevation.

with the plotted data; for example, persistent departures between the smaller annual peaks and the relation are not considered a satisfactory fit. Where the plot of data does not have the expected appearance or does not appear to satisfactorily fit using the flood-frequency relation, adjustments can be made to the fitting method.

Doglegs

The fitting of three-parameter flood-frequency relations to series of annual peaks for streams that drain arid basins has many pitfalls. Flood-frequency relations and the *dogleg*-appearing plots of annual peaks for two gaging stations are typical of an arid region in the southwestern United States (fig. 7). The off-center positioning of the data points on the plotting grid indicates that a significant number of the annual maxima equal zero; station 09415560 had 5 years of no flow, and station 10172902 had 9 years of no flow. In addition, the dogleg configuration of the remaining data points indicates that the data should not be fitted with a three-parameter relation and perhaps two distinct flow-generating mechanisms are involved.

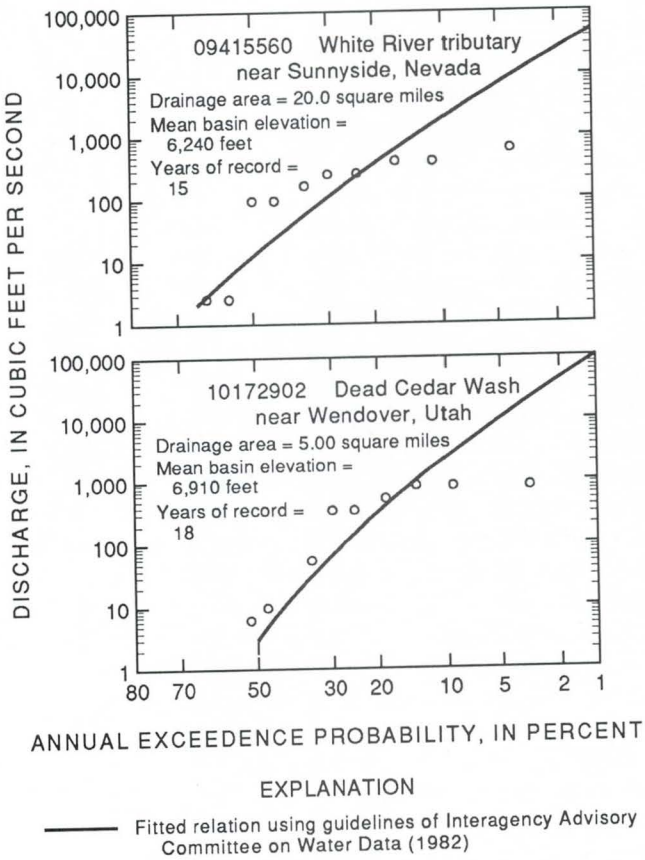

Figure 7.—Flood-frequency relations for selected gaging stations in the southwestern United States.

The fitted curves have excessive standard deviation (slope) and excessive negative skewness (curvature); the fitted curves do not appear to properly reflect the statistical characteristics of the flood events, and hydrologic judgments are required. The solid curves in figure 7 were obtained by mathematical application of a statistical fitting procedure without consideration of the hydrologic character of the data (Interagency Advisory Committee on Water Data, 1982).

Low-Discharge Threshold

Low outliers can have an adverse effect on computed flood-frequency relations by causing a large negative skew coefficient that can distort the frequency relation by flattening the upper end of the curve. Low outliers are small peak discharges that depart from the low end of the fitted relation. For many sites, the departure of the small peaks from the curve may be related to physical characteristics of the stream channel upstream from the streamflow-gaging station. These departures should be called hydrologic low outliers to emphasize that they are defined by hydrologic considerations, such as infiltration into alluvial stream channels rather than by statistical tests. The recommended procedure for computing flood-frequency relations includes a statistical test and adjustment for low outliers. Small peaks often are identified as low outliers and appropriate adjustments are made. The low outliers are truncated and a conditional probability adjustment is made to obtain the final relation. Although this statistical procedure frequently is successful in making appropriate adjustments for low outliers, it is not always

successful, and computed results must be examined for hydrologic low outliers.

The effect of using small annual peaks for the definition of a flood-frequency relation can be large as shown by the relations for the streamflow-gaging station, 09480000 Santa Cruz River near Lochiel, Arizona (fig. 8). The 100-year discharge for the unadjusted curve is 5,200 ft^3/s or about one-third of the discharge for the curve with the low-discharge threshold adjustment. The unadjusted curve is far below the two largest annual peaks; no known physical characteristic of the drainage basin can be used to explain flattening of the flood-frequency relation for large floods. Also, the unadjusted curve gives a 100-year discharge that is about one-quarter of the discharge using a regional modification. The use of the low-discharge threshold of 450 ft^3/s, which is greater than 5 of the 41 annual peaks, results in a flood-frequency relation that better fits the data. Also, for this station, the default statistical adjustment produced a satisfactory relation.

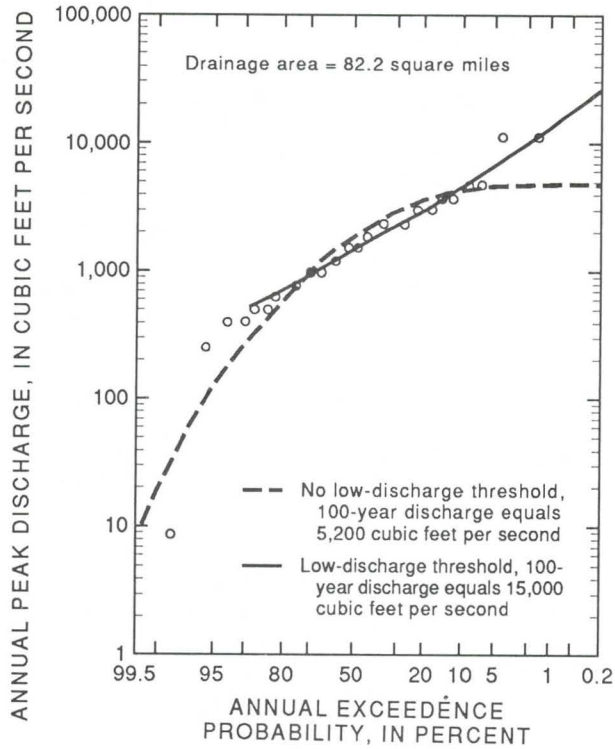

Figure 8.—Flood-frequency relations for streamflow-gaging station, 09480000 Santa Cruz River near Lochiel, Arizona.

SUMMARY

Small streams in the northern latitudes commonly flow in direct response to snowmelt and rainfall. Small streams in the southern latitudes commonly flow in direct response to thunderstorms and flow only a few hours during a typical year. The coefficient of variation of mean annual discharge commonly is more than 1.0 for small streams in the southern latitudes and less than 1.0 for small streams in the northern latitudes. The variation of runoff is much greater for small streams than for large streams. In the southern latitudes at elevations above 7,500 ft, the magnitude of infrequent flood-peak discharge is significantly less than that at lower elevations.

For many gaging stations, the fitted flood-frequency relations do not visually agree with the plotted annual peaks. The plot of the annual peaks commonly has a dogleg appearance that cannot be fit by a single three-parameter flood-frequency relation. Small peak discharges that depart from the low end of the fitted relation are common on ephemeral streams where loss of floodflow to channel infiltration is large. Truncation of these low outliers and the use of a conditional probability adjustment to obtain the final frequency relation results in reasonably appearing fitted relations.

REFERENCE

Interagency Advisory Committee on Water Data, 1982, Guidelines for determining flood flow frequency: Washington, D.C., Interagency Advisory Committee on Water data, Hydrology Subcommittee, Bulletin 17B, 28 p., 14 appendices.

HYDROLOGICAL CHARACTERISTICS OF THE SEMI-ARID HAIHE RIVER BASIN, CHINA

Feng Yan

Haihe River Water Conservancy Commission, Ministry of Water Resources, Tianjin, P.R.China

ABSTRACT

The Haihe River Basin belongs to the semi-arid region. The yearly and seasonal variations of runoff in the basin are extreme compared to those of other large river basins in China, and have aggravated the drought problem of the basin. The peak flow of the Haihe River Basin has reached record-high levels in China, and the modulus of peak flow is even much larger than that of other arid regions in the world. Drought problems in the Haihe River Basin have caused many adverse influences on many aspects. Annual runoff of the Haihe River Basin is being reduced due to the severe over-exploitation of groundwater. It is estimated that the reduction of runoff will become more serious in the future.

BRIEF INTRODUCTION TO THE HAIHE RIVER BASIN

The Haihe River Basin is located in the north of China between East longitude 112° and 120°, North latitude 35° and 43°. There are mountains and plateau in the north and west, but the broad North China Plain exists in the south and east in the basin.

The Haihe River Basin is composed of two large river systems, the Haihe River and Luanhe River. The former system consists Jiyunhe, Chaobaihe, Northern Grand Canal, Yongdinghe, Daqinhe, Ziyahe, Zhangweihe and Southern Grand Canal, Tuhaihe and Majahe Rivers. The latter system consists of the Luanhe River and others along the coast in the east of Hebei Province. The catchment area is 31800 km^2, 166 million mu arable land (1 ha=15 mu), and a population of 110 millions.

SEVERITY OF DROUGHT

Severe Shortage of Water Resources

The average annual runoff per capita in the Haihe River Basin is 262 m , which is the smallest value in China's seven largest river basin. It only accounts for 11% of nationwide average, 3% of world average and 37% of the Yellow River Basin average. The runoff per mu of arable land is 173 m , being only 10%, 7% and 48% of nationwide, world, and Yellow River Basin values respectively (Table 1) . Therefore, in order to meet past, current, and increasing future water demands, the Haihe River Basin needs transfers of water from the Yellow River.

Table 1. Regional water resources characteristics of rivers in China and the world
[Data compiled from IPDWCHP (1987)]

Nation, river or region (1)	Annual runoff (10^9 m) (2)	(mm) (3)	Population (10^6) (4)	Water resourses per person (5)	Arable land (10^6 mu) (6)	Water resources per mu (7)	(5)/9000 (8)	(7)/2350 (9)
Brazil	5,190	609	144	36,000	486	11,700	4.00	4.98
U.S.S.R.	4,710	211	285	16,500	3,400	1,290	1.83	0.55
Canada	3,120	313	26	12,000	654	4,770	1.33	2.03
America	2,970	317	248	12,000	2,840	1,050	1.33	0.45
Indonesia	2,810	1,480	174	16,100	213	13,200	1.78	5.62
China	2,710	284	1100	2,470	1,500	1,810	0.27	0.77
India	1,780	514	720	2,470	2,470	720	0.27	0.31
Japan	547	1,470	123	4,450	65	8,420	0.49	3.58
World	468,000	314	5200	9,000	19,900	2,350	1.00	1.00
Yangtze R.	951	526	379	2,510	352	2,700	0.28	1.15
Zhujiang R.	334	751	82	4,070	70	4,770	0.45	2.03
Songhua R.	76.2	137	51	1,490	157	485	0.17	0.21
Yellow R.	65.8	87.5	92	715	182	362	0.08	0.15
Huaihe R.	62.2	231	142	438	185	336	0.05	0.14
Haihe R.	28.8	90.5	110	262	166	173	0.03	0.07
Liaohe R.	14.8	64.6	34	435	66	224	0.05	0.10
Inland R.	116	34.5	23	4,980	89	1,300	0.55	0.05

The average annual water transfer from the Yellow River to the Haihe River Basin was 630 million m^3 shortly after the People's Victory Canal in north Henan Province was built in 1952. When water use in Tianjin met difficulties in 1972-1982, the People's Victory Canal was used to transfer 1000 million m^3 to Tianjin. Another water transfer project from the Yellow River to north Shandong Province was completed in 1955. From 1980 to 1989, average annual water transfer has been 4500 million m^3, accounting for 17% of the annual runoff in the Haihe River Basin.

Serious Consequences of the River

Earth Subsidence

In order to meet the necessary water use for both living and production, groundwater has to be heavily exploited. In the past, the groundwater depth below land surface in the Haihe River Basin Plain was 2-3 m, but now is below 10 m. In some cities, the groundwater table has declined to 30 m below the land surface. A large groundwater cone of depression has formed in Tianjin and the maximum to depth water in the center of the cone has reached 95 m. The accumulated volume of over-exploited water in the Haihe River Basin has exceeded 25 billion m^3. The groundwater aquifer of the Western Suburbs in Beijing has been in a dry state. The ground surface in Tanggu and Hangu has subsided below sea level. The maximum surface subsidence in Tianjin since 1959 has added up to over 2 m.

Lake Baiyangdian Drying Up

Because of severe shortage of surface runoff, Lake Baiyangdian, ever called the "bright pearl of North China", has run dry 5 times between 1966 and 1983; it ran dry for five consecutive years during 1983-1987. At the same time, the water ecological environment deteriorates day by day and water pollution in rivers beomes more serious. The contents of fluorine, alkali and iodine in drinking water for Cangzhou and Hengshui cities have largely exceeded the acceptable limits for drinking water preseribed by the state. Such a serious situation has endangered the sustenance of the local residents.

Infiltration Losses of the Haihe River

In 1988, the Haihe River Basin experienced a middle-sized flood after suffering from drought for many consecutive years. The river bed had become a sand belt due to no passage of water in the river course for 10 years. The river bed in the plain area is composed of sand and fine sand. Depth to groundwater on both sides of the river was from 10 m to 20 m. When water passes through the river course in the plain region, it must meet the requirment of infiltration in river bed. After river bed was saturated with water, water started side infiltration to both sides. As a result, water loss was great. Water loss along the river course can reach 4.2 to 8.3 million m^3 per km , based on the analysis of the flood regime of Hutuo & Zhulong River.

Sediment in the Tidal Estuary and Reaches

The water quantities emptying into the Bohai Sea have been reduced due to the surface runoff shortage. Because of this, about 12 tidal reaches and the tidal estuary of the Haihe River Basin have been silted up with the total sediment volume of 56.3 million m^3. Now the discharge capacity of the Haihe River Basin estuary is only 60-70% of the original design capacity. Flood prevention and navigation have been influenced greatly.

"Red Tide" Phenomena in the Bohai Bay

From August to October in 1989, drought & water pollution of the Haihe River Basin caused successive "red tide" phenomena in the Bohai Bay. The red tides lasted so long a time, influenced so larger areas and caused such heavy losses that such an event has seldom occurred in the history of our country.

GREAT VARIATION OF RUNOFF

The annual and seasonal variations of runoff have certain effects upon the drought. Their variational extent determines the severity of drought.

Annual Variation of Runoff

The relation between coefficient of variation C_v of annual runoff and catchment area F (km^2) for major rivers in China is as follows

$$C_v = \alpha F^{-0.15} \qquad (1)$$

The coefficients α of some basins are listed below (Table 2).

Table 2. Hydrological characteristics of river basins in China

Basin	α	β	γ	R_0/R (%)
Songhua R.	2.6	81	0.096	28.8
Liaohe R.	2.6	108	0.024	22.3
Haihe R.	2.6	108	0.024	13.0
Yellow R.	2.0	54	0.043	19.4
Huaihe R.	2.6	128	0.096	22.8
Yangtze R.	1.4	43	0.039	37.0
Zhujiang R.	1.4	43	0.039	32.6
Inland R.	1.0	29	0.003	22.1

Although the Haihe, Liaohe and Yellow Rivers all belong to the semi-arid region, the values of α for the Haihe and Liaohe Rivers are 2.6 whereas that of the Yellow River is 2.0. The drought for the former is more severe than that for the latter.
The ratio of the largest annual runoff and the smallest annual runoff is K . The relation between K_r and catchment area F is as follows

$$K_r = \beta F^{-0.25} \qquad (2)$$

The coefficient β for the Haihe River is larger than the Yellow River (Table 2).

Seasonal Variation of Runoff

The smallest average monthly runoff in a year, R , reflects the flow discharge in low-water years in the basin to some extent, because the runoff in the low-water period is relatively steady from year to year. The relation between R_{min} ($10^9 m^3$) and catchment area F is:

$$R_{min} = \gamma F \qquad (3)$$

The coefficients γ of the basins are listed in Table 2. The smallest monthly runoff of the Haihe River and Liaohe River is smaller than that of the Yellow River, although they all belong to the semi-arid region.
The agricultural sector is a major water user. The ratio of runoff in the crop growth period (from April to June) to annual runoff influences the severity of drought. The ratio of April-June runoff to annual runoff in each basin is shown as R_0/R in Table 2. The value of R_0/R of the Haihe River Basin is the smallest in China, thus showing that the problem of drought is most serious in that basin.
The decreasing runoff due to ground-water exploitation will make the problem of drought in the Haihe River Basin much more serious. For this reason, water is diverted from the Yellow River to the Haihe River, although they belong to the same semi-arid region.

SEVERITY OF FLOOD MENACE

The yearly and seasonal variations of runoff are large; the floods as well

as the droughts causing these variations also are extreme. For example, a flood with peak discharge of 42000 m^3/s occurred in an area of 50000 km^2 in the Haihe River Basin in August 1963. This is one of the greatest floods from catchments of this size in China and the world (Table 3).

Table 3. Observed maximum discharge records in China and the world.
[Data compiled from Rodier and Roche (1984) and Feng Yan (1990)]

No.	River & observing location	Catchment area (km^2)	Maximum discharge (m^3/s)	Date
1	Haihe R. Nandihe Xitaiyu	127	3,990	1963
2	Taiwan Zhushuixi Tongtou	259	7,780	1979
3	Huaihe R. Zhentonhe Baoshan	578	9,550	1975
4	Huaihe R. Ruhe Bangqiao	762	13,000	1975
5	Huaihe R. Ganjiaghe Guanzhai	1,120	14,700	1975
6	Hainan Nandujiang Shongtao	1,440	15,700	1977
7	Taiwan Wuxi Dadu	1,980	18,300	1959
8	Hainan Changhuajiang Baoqiao	4,630	20,000	1963
9	Yalujiang R. Yunfeng	11,300	23,900	1960
10	Yangtze R. Qujiang Fengtan	16,600	26,700	1965
11	Yangtze R. Peijiang Xiaoheba	29,600	28,700	1981
12	Qiantang R. Fuchunjiang Lucifu	31,500	29,000	1955
13	Yangtze R. Hanjiang Ankang	38,700	31,000	1983
14	Haihe R. Luanhe Luanxian	44,100	34,000	1962
15	Haihe R. Jingguang railway line between Ziya R. & Daqing R.	50,000	42,000	1963
1	Quinne New Caledonia (France)	143	4,000	1975
2	Quaieme New Caledonia (France)	330	10,400	1981
3	Cithuatlan, Mexico	1,370	13,500	1959
4	Niyodo, Japan	1,560	13,510	1963
5	West Nueces, Texas, USA	1,800	15,600	1935
6	Shingu, Japan	2,350	19,000	1959
7	Eel, California, USA	8,060	21,300	1964
8	Pecos, Texas, USA	9,100	26,800	1954
9	Toedonggang, North Korea	12,200	29,000	1967
10	Han, South Korea	23,900	37,000	1925
11	Mangoky, Madagascar	50,000	38,000	1933
12	Marmada, India	88,000	69,400	1970

The relation between average annual peak modular discharge q_m ($m^3/s/km^2$) and annual runoff depth R (mm) in the Haihe River Basin is:

$$q_m = 0.004R^{1.4} \qquad (4)$$

However, this expression for other arid regions in the world has a coefficient of 0.0023 and an exponent of 0.38. Hence the value of q_m for the Haihe River Basin is much greater.
The relation between q_m and catchmend area F in the Haihe River Basin is:

$$q_m = 63F^{-0.67} \qquad (5)$$

For the other arid regions, the coefficient of this expression is 1.22 and the exponent is -0.42. The value of q_m for the Haihe River Basin is again much larger.
The coefficient of variation in the Haihe River Basin is C_v= 1.0-2.0. This value is the largest in China and much larger than that of other arid regions in the world (C_v = 0.58-0.74).

FREQUENCY AND PERSISTENCE OF WATER-LOGGING AND DROUGHT

The Haihe River Basin historically had the name of "Nine Droughts in Ten Years". According to historical data, there were 439 drought years from 1470 to 1989 (520 years). The frequency of drought is 84.4%. Moreover, there were always consecutive drought years. The consecutive drought with duration of 2 years or more makes up 88.2% of the total. Droughts of 3 or more consecutive years make up 47.2% of the total.There were also consecutive droughts in 9 years from 1521 to 1529 (Table 4).

Table 4. Drought disaster statistics of Haihe River Basin from 1470 to 1989

Area affected	Drought duration (years)									Total years
	1	2	3	4	5	6	7	8	9	
Whole basin	48	15	8	2	0	0	1	0	0	117
Part of basin	4	75	25	8	5	2	1	1	1	322
Total	52	90	33	10	5	2	2	1	1	439

Although many water conservancy projects had been buit since the founding of the People's Republic of China, drought disaster still influences industry, agriculture and urban developments. According to incomplete statistics from 1950 to 1979, the average annual disaster affected area in the Haihe River Basin was 21 million mu. The largest disaster affected area was 79.5 million mu in 1963, which covered 50% of the total cultivated land in the Haihe River Basin.
In the nonflood season (from October to May next year), a drought period with less than 5 mm precipitation per day occurs for 120-150 consecutive days in the basin. In the most serious cases, there was no rainfall in 240-250 days, or even no penetrating rainfall in the whole year when the basin was in severe drought situation. Drought occurred in almost every spring, and frequently occurred in summer. There were many years when spring drought and summer drought occurred consecutively.
In the 581 years from 1368 to 1948, the Haihe River Basin had 383 water disasters, 2 disasters per 3 years on average, according to the historical data.Based on the data of 403 years from 1546 to 1948,Beijing suffered from 12 water loggings, including 5 events in which the city was inundated. Tianjing suffered from 13 water loggings including 9 inundations. These resulted in great losses of people's lives and property.
Based on the data series of 30 years from 1950 to 1979, average annual water logged area is 21 million mu. The most serious water-logging occurred in 1963, with a water-logged area of 75 million mu, which was almost equal to the maximum area of drought.

TREND OF DROUGHT IN THE HAIHE RIVER BASIN

According to the long series of hydrological data from selected representative stations, annual runoff in the 1980s was obviously less than that in the past. The precipitation of the Haihe River Basin in the 1980s was 85% of that in the 1970s. Annual runoff in the 1980s is only 55% of that in the 1970s. This trend is shown in Table 5.

Table 5. Yearly variative tendency of runoff and precipitation ($10^9 m^3$)

Time period	Haihe R. Runoff	Basin Precip	Guanting	Miyun	Huangbizhuang	Panjiakou	Yuecheng
1920-29			1.59	1.83	1.25		
1930-39			1.47	1.64	(1.50)	2.57	
1940-49			1.54	1.07	(2.34)	2.32	1.48
1950-59	37.5	195.4	2.44	2.12	3.39	3.06	1.96
1960-69	28.7	178.5	1.96	1.23	2.78	2.05	2.05
1970-79	25.8	174.6	1.71	1.38	1.59	2.47	1.84
1980-84	14.2	148.0	1.53	0.77	1.38	1.65	1.05
1985-89						1.48	
Average	26.4	174.3	1.76	1.48	2.20	2.45	1.83
F (km^2)	318000		43400	15800	23400	33700	18100

CONCLUSIONS

The surface water resources per capita in the Haihe River Bisin is the least in the seven largest river basins in China. Therefore, it is reasonable to divert water from the Yellow River. Because the annual and seasonal variations of runoff of the Haihe River Basin are most obvious, the flood in the basin is also the largest in the basins of the country. It is unique that both drought and flood are most serious in the whole country. This paper is helpful to deepen the understanding of the drought and flood in the basin and provide a scientific base to prevent floods and droughts of the Haihe River Basin in the future.

REFERENCES

Feng Yan, 1990, Dual Nature of Water Resources & the Potential for Forecasting: The Hydrological Basis for Water resources Management. IAHS Publication No. 197, P.461-468.

Institute of Planning & Design for Water Conservancy & Hydroelectric Power, Ministry of Water Resources and Electric Power, 1987, The Utilization of Water Resources in China (in Chinese), P.36.

Rodier, J.A., and Roche, M., 1984, World Catalogue of Maximum Observed Floods. IAHS Publication No.143, P.354.

PRELIMINARY INVESTIGATION FOR CHARACTERIZATION OF DROUGHT AND STREAMFLOW IN THE WESTERN GREAT BASIN--DISTINGUISHING CLIMATE CHANGE FROM NATURAL VARIABILITY

Alex Pupacko

U.S. Geological Survey, Carson City, Nevada

ABSTRACT

Analysis of streamflow records for the West Fork of the Carson River at Woodfords, California, indicates that the prolonged current 4-year drought (1987-90) is not unusual and that similar drought periods have occurred in 1959-62 and 1976-79. Records also indicate significant differences in the quantity and timing of streamflow between the periods 1939-64 and 1965-90. For the latter period, mean annual streamflow has increased about 12 percent and streamflow variability has increased. The increases are evident in both summer and winter seasons for the latter period. Mean monthly streamflow for the summer months (June-September) has increased about 26 percent and mean monthly streamflow for the winter months (January-March) has increased by about 37 percent. Mean streamflow in April and May has not changed significantly between the two periods.

INTRODUCTION

Results from theoretical studies indicate that global temperatures will rise during the next century as a result of increased concentrations of carbon dioxide and other atmospheric "greenhouse" gases (Mitchell, 1989). General Circulation Models indicate that global warming will promote global changes in circulation that could alter patterns of hydrologic cycles (Schaake, 1990). The U.S. Geological Survey (USGS), as part of its Global Change Research Program, is studying the potential effects of plausible climate change on the water resources of several river systems in the western United States. The Carson River basin, in California and Nevada, is one of those being studied to determine the sensitivity of water resources to potential climate change. This basin has had less-than-average streamflow for 4 consecutive years, 1987-90. Future climate changes might increase the potential for drought and other variations in the hydrologic system. Before hydrologic responses to climate change can be simulated, the current hydrologic system must be defined. This paper provides preliminary results for determining if changes have occurred in the quantity and timing of streamflow during the period of record (1939-90) for a representative stream in the western Great Basin. This paper provides an example of the difficulty in distinguishing real change from natural variability.

DESCRIPTION OF STUDY AREA

The headwaters of the Carson River are located in the eastern Sierra Nevada of California. From there, the river flows northward and eastward to its terminus in the Carson Sink in western Nevada (fig. 1). The basin interfaces two climate zones: the sub-humid Sierra Nevada range and the arid Great Basin. The watershed of the Upper Carson River is predominantly natural and undisturbed and is representative of natural runoff processes for the area.

The USGS has continuously monitored streamflow on the West Fork of the Carson River at Woodfords, Calif. (Station 10310000), for 52 years, beginning in October 1938. Analysis of historical streamflow records indicates that the current 4-year drought (1987-90) is not unusual and that similar droughts have occurred several times in the recent (recorded) past. Although the climate of the region has changed during the millennia, current water-management systems are a function of supply and demand over recent decades. Thus, trends in the recent historical record are more important than paleoclimatic trends to water-resource managers.

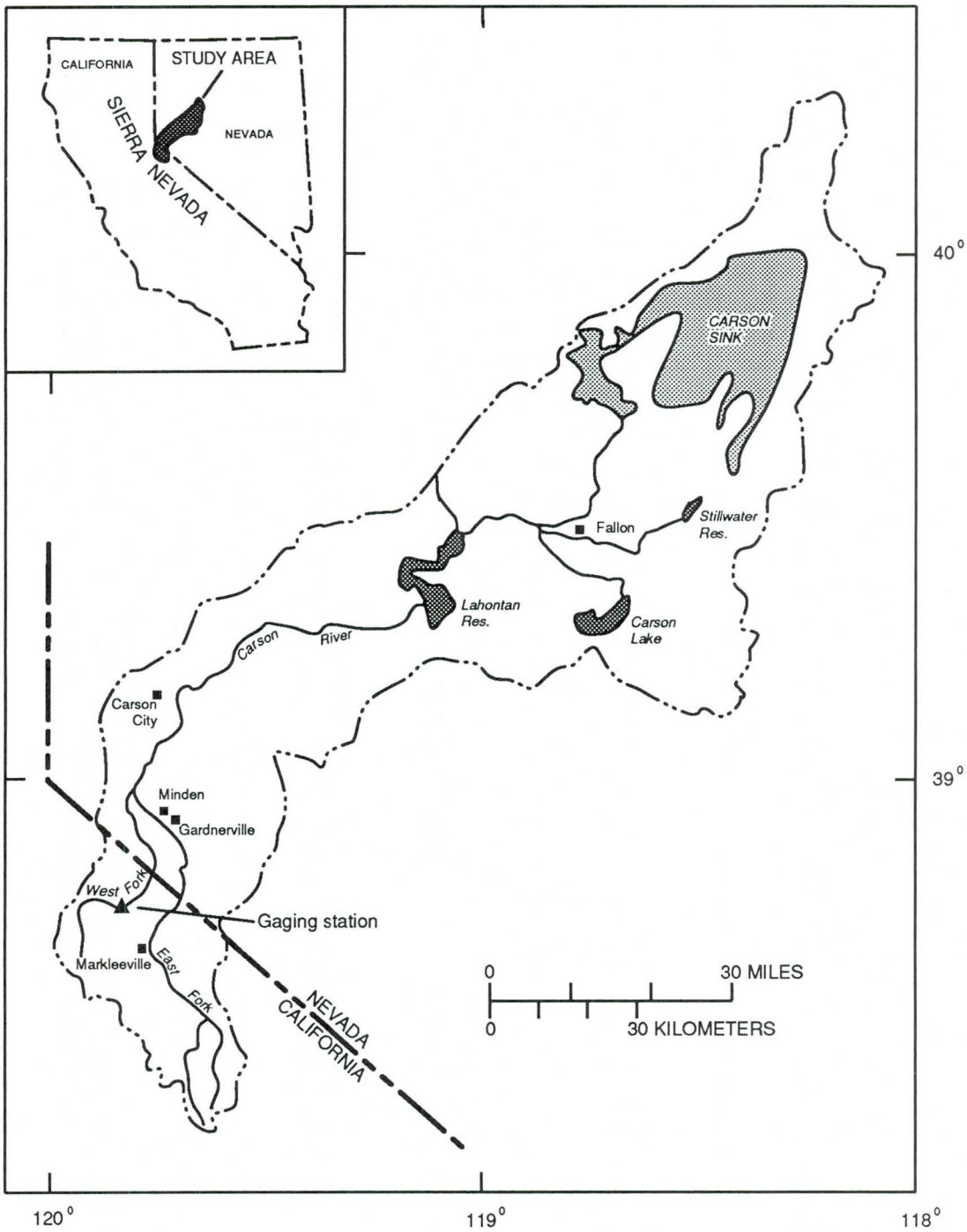

FIGURE 1.--Location of Carson River Basin and gaging station on West Fork Carson River at Woodfords, California.

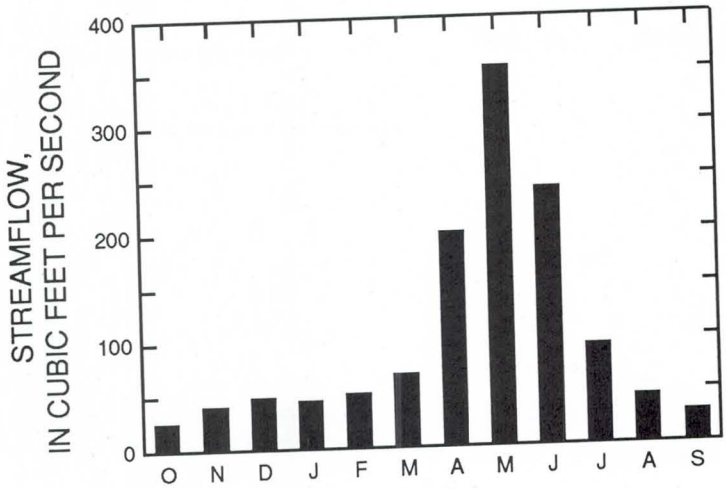

FIGURE 2.--Mean monthly streamflow for West Fork Carson River at Woodfords, water years 1939-90.

Most precipitation in the headwaters of the Carson River falls in the winter as snow. Runoff from melting of the winter snowpack usually occurs in the spring and early summer, causing increased streamflow (fig. 2).

About 65 percent of the annual streamflow in the Carson River at Woodfords occurs during April, May, and June. About 29 percent of the annual streamflow occurs during May. Streamflow is characterized by extreme variability from season to season and from year to year (fig. 3). Figure 3A shows daily mean streamflow for the period of record. Streamflow varies greatly, with minimum daily flows of less than 10 ft^3/s usually occurring in the late summer, and maximum daily flows at times over 1,000 ft^3/s during the spring snowmelt. Mean streamflow for the period of record (1939-90) is about 103 ft^3/s. Streamflow varies greatly from year to year and annual streamflow has a large range, from a minimum of 26.1 ft^3/s in 1977 to a high of 243 ft^3/s in 1983. Figure 3B shows annual mean streamflow for the period of record.

DISCUSSION

Periods of extended drought in the basin, defined here as below normal annual streamflow for 4 or more consecutive years, are not unusual. Records indicate that periods similar to the current (1987-90) extended drought have occurred in 1959-62 and 1976-79. Streamflow for the period 1987-90 averaged about 56 percent of the mean for the period of record. Streamflow for the periods 1959-62 and 1976-79 were 58 percent and 62 percent of normal, respectively. The records indicate, however, that changes in the hydrology of the basin may have occurred during the period of record, 1939-90. Since 1965, mean annual streamflow and streamflow variability have increased, and timing of seasonal runoff has changed, compared with the period 1939-64.

Cumulative annual streamflow for the West Fork Carson River is plotted in figure 4A. A general increase in the slope of the curve from the mean of 1939-64 is evident beginning about the 1965 water year. Streamflow was about 12 percent greater for the period 1965-90 than for the period 1939-64.

Table 1 shows statistics for mean annual streamflow for the two periods and the combined period. In addition to increased streamflow during the period 1965-90, variability has increased also.

Increased streamflow for the period 1965-90 is evident also in the monthly distributions. Figure 4B shows cumulative mean monthly streamflow for March. The slope of the curve increases significantly about 1965. The March mean for the period 1939-64 is 53.5 ft^3/s. The March mean for the period 1965-90 is 82.9 ft^3/s, an increase of about 55 percent. Variability of streamflow for most months also has increased in the 1965-90 period, as shown in table 1. Figure 4C shows cumulative streamflow for the month of May. Mean May streamflow remained the same between the two periods; however, variability of May streamflow has increased about 10 percent for 1965-90 compared with 1939-64. Cumulative mean streamflow for October is shown in figure 4D. October is usually the lowest flow period and table 1 indicates an increase in mean October streamflow of about 12 percent for the period 1965-90, compared with 1939-64.

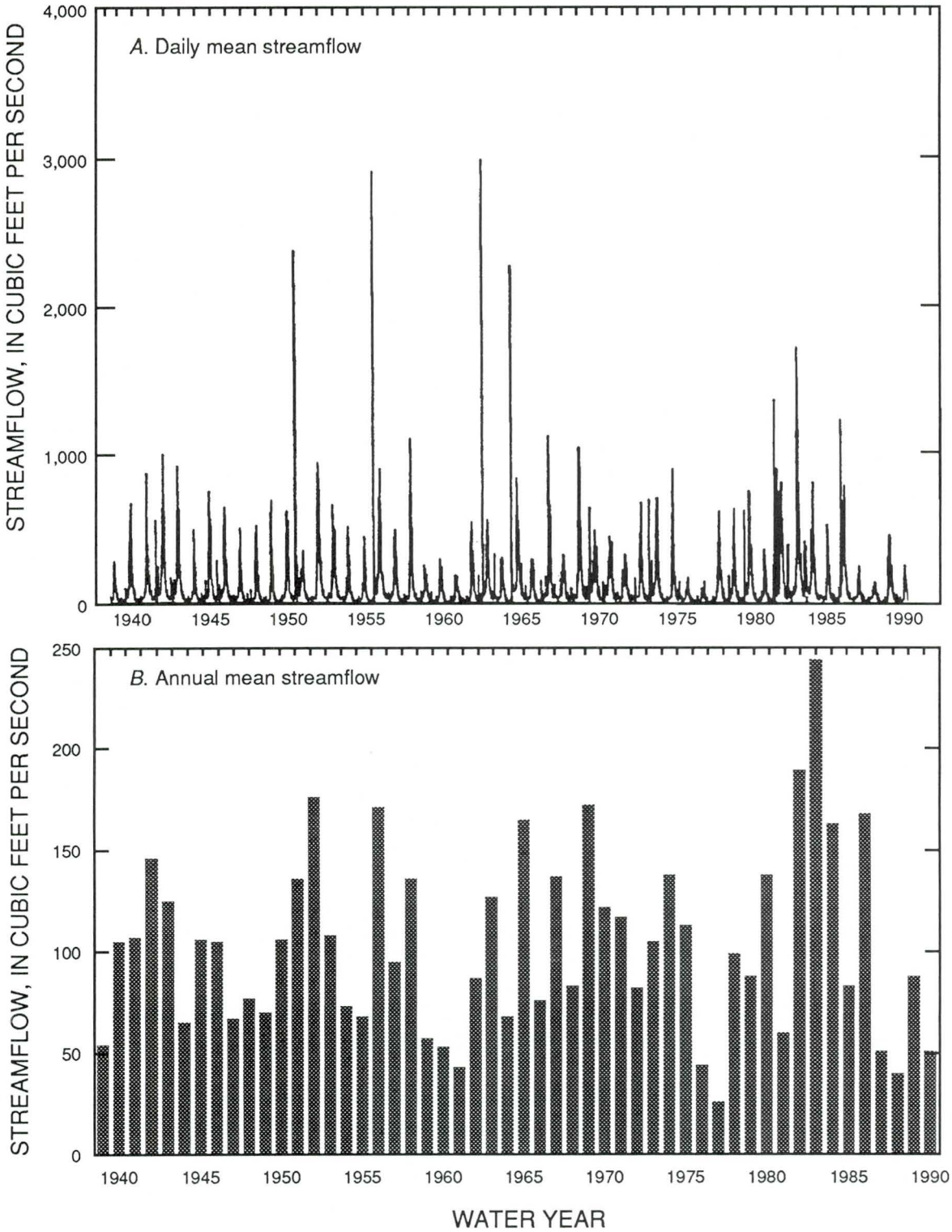

FIGURE 3.--Variability of (*A*) daily mean and (*B*) annual mean streamflow for West Fork Carson River at Woodfords, 1939-90.

TABLE 1.--Streamflow statistics for the West Fork Carson River at Woodfords, California

[ft^3/s, cubic feet per second]

Water years	Mean streamflow (ft^3/s)	Standard deviation (ft^3/s)	Mean Coefficient of variation	Mean streamflow (ft^3/s)	Standard deviation (ft^3/s)	Mean Coefficient of variation
		Annual			May	
1939-64	97.3	36	0.37	354	166	0.47
1965-90	109	53	.48	354	184	.52
1939-90	103	45	.44	354	173	.49
		March			October	
1939-64	53.5	22.8	0.43	24.5	8.1	0.33
1965-90	82.9	53.4	.64	27.5	15.2	.55
1939-90	68.2	43.2	.63	26.0	12.2	.47

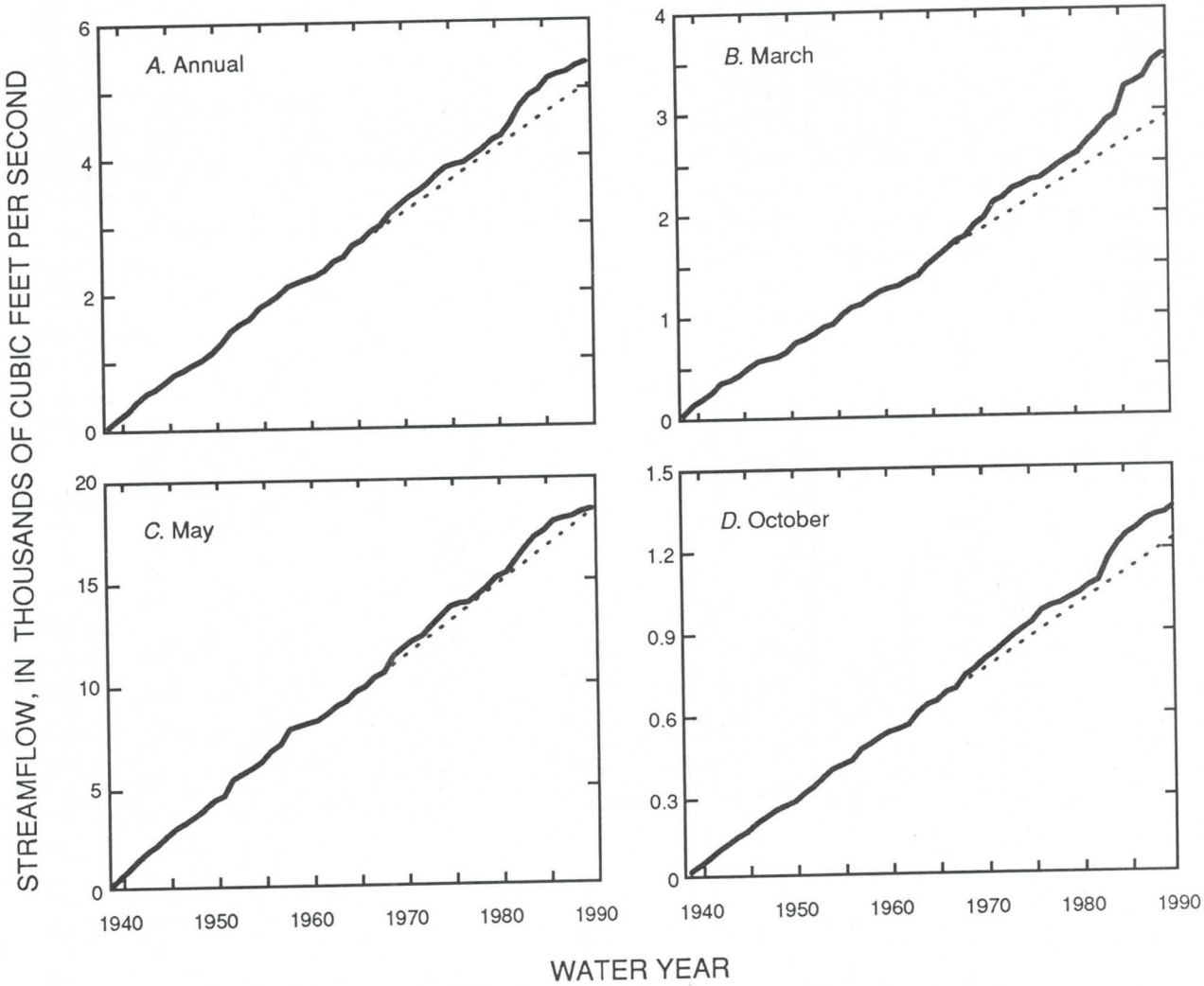

FIGURE 4.--Cumulative mean streamflow for West Fork Carson River at Woodfords, 1939-90: (*A*) Annual, (*B*) March, (*C*) May, (*D*) October. Dotted line is extension of 1939-64 mean.

TABLE 2.--Mean monthly streamflow between water-years 1939-64 and 1965-90 for the West Fork Carson River at Woodfords, California

Months	Streamflow (cubic feet per second) Water years 1939-64	Water year 1965-90	Percent increase
June	219	260	19
July	79	107	35
August	38	50	32
September	24	34	42
Average	90	113	26
January	39	51	31
February	47	55	17
March	53	83	57
Average	46	63	37

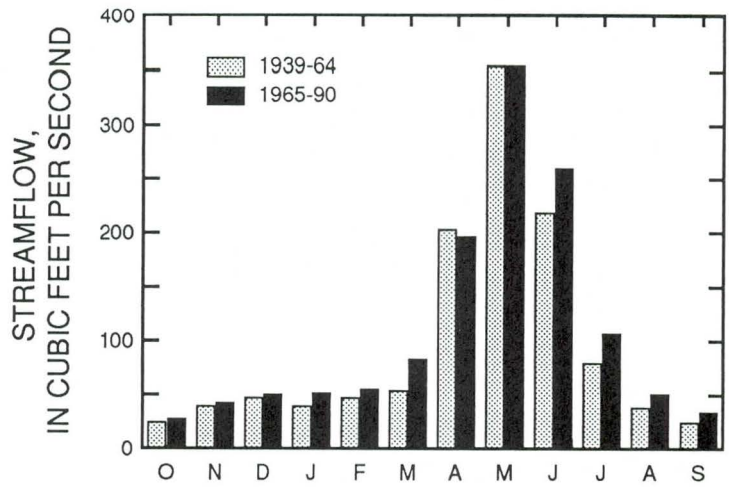

FIGURE 5.--Mean monthly streamflow for West Fork Carson River at Woodfords, for periods 1939-64 and 1965-90.

Analysis of streamflow records for the period of record (1939-90) indicates an increase in mean monthly streamflow for all months except April and May (fig. 5) and some significant changes in timing of runoff. Mean annual streamflow for the periods 1939-64 and 1965-90 are different at a significance level of 0.35. Mean October streamflows for the two periods are different at a significance level of 0.38. Mean March streamflows for the two periods are different at a significance level of 0.01. The March statistics are strong indicators for a change taking place. Annual statistics are not strong indicators for change. Increase in March streamflow might indicate that a change in timing of runoff has occurred in recent decades as a result of earlier snowmelt. This possibility needs investigation. Figure 5 shows a comparison of mean monthly streamflow for the periods 1939-64 and 1965-90. The graph shows an increase in streamflow during winter months for the 1965-90 period. The high runoff months of April and May do not show an increase. April streamflow has decreased for the 1965-90 period and there is no difference between the two periods for May. Streamflow during the summer months, June through September, increased about 26 percent during the period 1965-90 compared with the period 1939-64. January, February, and March had increases in mean monthly streamflow for the period 1965-90. Streamflow for these winter months increased about 37 percent during the 1965-90 period compared with 1939-64. Table 2 summarizes the differences.

The reasons for these apparent changes in runoff are not known at this time. They could be related to changes in global temperature and circulation patterns, indeed a real change in climate. Changes in land cover, particularly forest growth, also could have a significant influence on changes in streamflow. Changes also could be a function of normal variability, reflected in the series of consecutive extremely wet years in the 1960's, 1970's, and 1980's. These influences, and others, are being investigated by the U.S. Geological Survey Global Change Research Program.

REFERENCES CITED

Mitchell, J.F.B., 1989, The "greenhouse" effect and climate change: Reviews of Geophysics, v. 27, no. 1, p. 115-140.

Schaake, J.S., 1990, From "Climate to Flow," *in* Waggoner, P.E., ed., Climate change and water resources: John Wiley & Sons, New York, p. 177-206.

RAINSTORM CHARACTERISTICS IN THE ARID AREA OF CHINA

Wang Jiaqi

Nanjing Institute of Hydrology and Water Resources, Nanjing, China

ABSTRACT

The character of rainstorms in arid areas, including semi–arid areas, is obviously different from that in humid areas. On the basis of abundant observed and field–investigated rainfall data in the arid area of China, an important fact is revealed by the analysis: that there were also heavy rainstorms in the arid area . The difference of rainstorm charateristics between the arid area and the humid area of China is discussed. Results show that in the arid area extraordinary rainstorms,which have long duration, large area,and large flood volume, are very rare, but that when rainfall does occur, the short duration point and small–area rainfall depths and flood peak discharges of small basins are sometimes unusually intense. Because the rainstorm character and the precipitation measurement conditions are obviously different between the arid area and the humid area, the methods of design storm and Probable Maximum Precipitation (PMP) estimation in the arid area should also differ from the usual methods used in humid area.

INTRODUCTION

Purpose of Study

The average annual precipitation in the arid or semi–arid area of China is very small. The main hydrologic regime of the area is drought. Raingage stations are few and far between. Rainstorms and floods are rare, and extreme floods disasters are frequently not observed. The precipitation in the area has large interannual and seasonal variation , and extraordinary rainstorms with short duration, small area, and high intensity can happen at a few places in a few years. Some of the rainfall depths exceed those recorded in the humid area of South China. A few rainfall records with short duration even approach world's highest records and can cause serious flood disasters. It is thus necessary to conduct rainstorm studies in the arid area.

Arid area of China

According to geographic division researches (Central Weather Bureau,1979; Academia Sinica, 1984; Bureau of Hydrology , 1987) , several indices for distinguishing the arid, semi–arid areas and the humid, semi–humid areas of China have been adopted. They are: dryness (ratio of annual maximum evaporation capacity from plant–covered surface to annual precipitation) = 1.5, drought index (ratio of annual water surface evaporation to annual precipitation) = 3, annual precipitation = 400—500 mm , annual evaporation capacity from water surface = 1200 mm, annual runoff depth = 50 mm, annual runoff coefficient = 0.1, etc. The arid and semi–arid area of China are distributed in the northern and western parts, which are mainly situated in the interior of Eurasia and are far from oceans.

This area basically includes the largest region and its adjacent districts delimited individually by the above mentioned various indices for the arid and semi–arid area.

In this paper, the studied area is limited to the northern arid and semi–arid region; Xizang (Tibet) and Yunnan are not included. This area is called "arid area" for short. In this area, the surface elevations are generally higher than 1000m in the east plateaus and west basins. The average precipitable water above ground surface anywhere is less than 15 mm (Bureau of Hydrology, 1987) while it is as much as about 40 mm in South China. The arid area is rarely influenced by monsoons. The most frequent rain–producing weather system is a cold front from the northwest. For about half of the area , the mean annual precipitation is less than 100 mm. It is only 5.9 mm at Toksun station, Xinjiang (Northwest Teachers College and Map Press, 1984) ; this is the minimum . The coefficient of variation of annual precipitation for most stations in the arid area is over 0.3 (Burean of Hydrology 1987) . The mean number of annual precipitation days is generally less than 80 and is less than 10 in the center portion . The mean annual water surface evaporation is larger than 1200 mm in most parts and even higher than 2000 mm in the center section .

POINT RAINFALL DEPTH

Point rainfall depth means the rainfall depth observed or field–investigated at a station or a place. The characteristic of point rainstorm in the arid area can be described in terms of the relationships of rainfall depth–frequency and rainfall depth – duration .

A rainstorm is a rare event in the arid area. The mean annual number of rainstorm days (days with daily rainfall $>$ 50 mm) is less than 0.1 in the western part (west of 105 ° E) and is about 0.5 – 1 in the eastern part of the arid area, but is over 10 in the most humid area of China. The mean of annual maximum 24–hour rainfall depth is about 50 – 70 mm in the eastern part of the arid area and is less than 10 mm in the center section, but is over 200 mm in the coastal belt of South China. Although the mean of annual maximun 24–hour rainfall depth is slight in the arid area, the coefficient of variation is generally greater than 0.6 and is over 0.8 in the center area. Many extraordinary rainstorm have been observed and investigated. The record 24–hour rainfall depth exceeds 200 mm in each province and autonomous region. Several records of 400 – 600 mm have been investigated at places in the eastern area, and the value of 1400 mm at Muduocaidang, Inner Mongolia, set the highest rainfall depth record in the mainland of China. Some ratios of the maximum 24–hour observed or investigated rainfall depth to the mean of annual precipitation at nearby locations exceed 1.0 in the arid area, and the maximum ratio even reaches 4.1.

Rainfall amounts are concentrated generally in a limited duration in the arid area and the ratio of rainfall depth in short duration to total rainfall depth is higher than the ratio in humid area. The coefficient of variation C_v of short–duration rainfall is larger than that of long–duration rainfall in arid areas and this trend is just opposite to that in humid areas. Therefore, the extraordinary rainfall and rare frequency rainfall with short duration are extremely heavy in the arid area. The total duration of such storms is usually shorter than 10 hr and is mainly concentrated in 3 – 6 hr (see table 1) . The rainfall records with short–duration between 0.5 — 10 hr in the arid area can be higher than that in the humid area by 30 — 70% and near the world's records (WMO, 1986) . A host of facts have proved that heavy rainstorms with short duration actually occur in the arid area in spite of their main character of water shortage.

Table 1. Maximum point rainfall depth – duration in the arid area

Location	Date	Duration	Rainfall Depth (mm)
Heiyukou, Shaanxi	May 27, 1973	5 min	59.1
Meidonggou, Shanxi	July 1, 1971	5 min	53.1
Danianzi, Inner Mongolia	May 26, 1982	20 min	120.*
Xiaoyeba, Qinghai	June 19, 1976	30 min	240.*
Sikeshugou, Hebei	July 3, 1974	30 min	280.*
Shangdi, Inner Mongolia	July 3, 1975	1 hr	401.*
Anjihai, Xingiang	June 24,1981	1 hr	240.*
Dashicao, Shaanxi	June 20,1981	1.1 hr	273.
Gaojiahe, Gansu	Aug.12,1985	1.2 hr	440.*
Boligou,Hebei	June 25, 1973	1.5 hr	430.*
Yujiawanzi, Inner Mongolia	July 19, 1975	2 hr	489.*
Bainaobao, Hebei	June 25, 1972	2.5 hr	550.*
Duan Jiazhuang, Hebei	June 28, 1973	3 hr	600.*
Zhangjiafangzi, Inner Mongolia	July 19, 1959	3.5 hr	600.*
Taocunbao, Shanxi	Aug.10, 1970	5 hr	600.*
Muduocaidang, Inner Mogolia	Aug.1, 1977	10 hr	1400.*

* investigated data

AREAL RAINSTORM

The areal distribution characteristics of rainstorms in the arid area are small area, high rate of decrease of rainfall depth with distance, limited rainfall volume, and low areal average rainfall depth.

Most of the rainstorms in arid areas are of small scale and limited rain area (see figure 1). The rain area enclosed by a 24–hour isohyet of 50 mm is usually less than 1000 km^2. For example, it was only 103 km^2 for the storm at Anjihai, Xinjiang, 1981. The largest area was 24,600 km^2 for the storm at Muduocaidang, Inner Mongolia, 1977. But the maximum areas have exceeded 200,000 km^2 in the middle–latitude humid area of China.

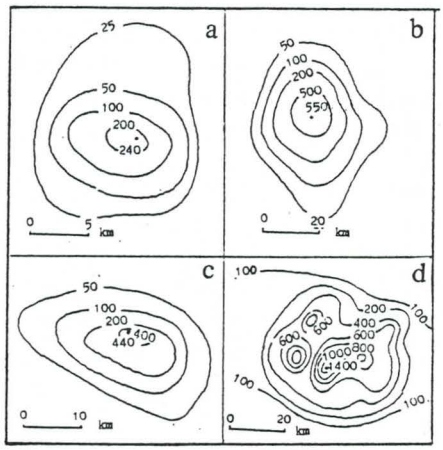

Figure 1. —Typical isohyets of rainstorms in arid area

a Anjihai,Xinjiang June 29,1981 1 hr
b Bainaobao,Hebei June 25,1972 2.5 hr
c Gaojiahe, Gansu Aug. 12,1985 1.2 hr
d Muduocaidang, Inner Mongolia Aug.1,1977 10 hr

The shape of the closed isohyet is nearly circular for small scale storms and in the center sections of larger scale storms. The generalized storm pattern is an ellipse and the shape ratio (ratio of major to minor axis) is usually between 1.0 and 2.0 in arid area. This ratio is not only less than the generalized value of 2 to 3 for the storms for the whole of China but also lower than the recommended

value 2.5 in the United States (Hansen and others, 1982).

In arid areas, the rate of decrease of rainfall depth with increasing distance from the center of a storm is distinctly higher than that in humid areas. According to the hypothesis that the isohyet is a circle, the relationship between the rainfall depth H of an isohyet and its generalized radius R can be established (see figure 2). R can be computed from the area A of closed isohyet by the formula $R = (A/\pi)^{0.5} = 0.564\ A^{0.5}$. The generalized radius R for an isohyet in arid areas is shorter than that in humid areas for 24–hour rainfall and is much smaller for long–duration rainfall. For example, for the isohyet of 750 mm, R is about 8 km for the storm Muduocaidang (arid area) and is 90 km for the storm (with long–duration) Nishi, Hunan (humid area), 1935.

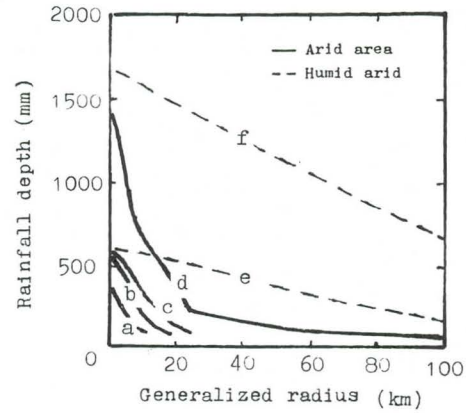

Figure 2. —Relation between rainfall depth of isohyet and generalized radius

a Xilinhot b Baorcijiu
c Bainaobao d Muduocaidang
e Nishi,1–day f Nishi,7–days

In comparison with the humid area, the precipitation volume of a storm in arid area is far smaller. The 24–hour precipitation volume of a storm with rainfall over 50 mm is less than 1 km^3 in most cases and the largest volume is only 3.2 km^3 in the arid area. But the maximum value can reach 21.7 km^3 in the humid area.

The comparison of maximum depth–area–duration records between the arid area (see table 2) and the whole of China (Wang, 1985) indicates that most items of China's records are contributed by arid area storms when duration < 12 hr and area < 3000 km^2. But the record depths in the arid area are far smaller than those in the humid area for storms with long durations and large areas.

Table 2. Maximum depth–area–duration record in the arid area of China

Duration (hr)	areal average rainfall depth (mm) Area (km^2)					
	Point	100	300	1000	3000	10000
1	401	267	167			
3	600	422	316			
6	840	630	512	405	240	127
12	1400	1050	854	675	400	212
24	1400	1050	854	675	400	222

FLOODS

The characteristics of rainstorms can be well demonstrated by characteristics of floods in the arid area. A comparison of the envelope values of maximum observed flood peak discharge and 7 day flood volume data for the river basins with areas smaller than 100,000 km^2 have been made between the eastern arid area where the storms and floods are serious, including Hebei, Shanxi, Inner Mongolia, Shaanxi, Gansu and Ningxia, and the humid area in South China including Zhejiang, Anhui, Fujian,. Taiwan, Jiangxi, Hunan, Guangdong, Guangxi and Hainan (see fignre 3 and 4).

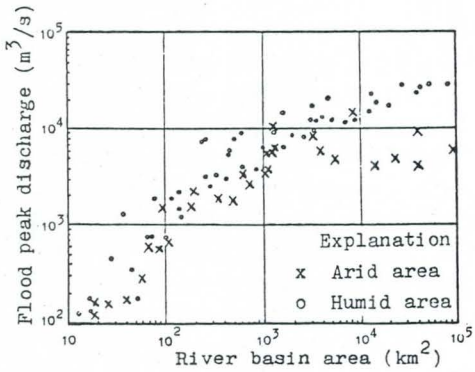

Figure 3. —Relation between maximum flood peak discharge and river basin area

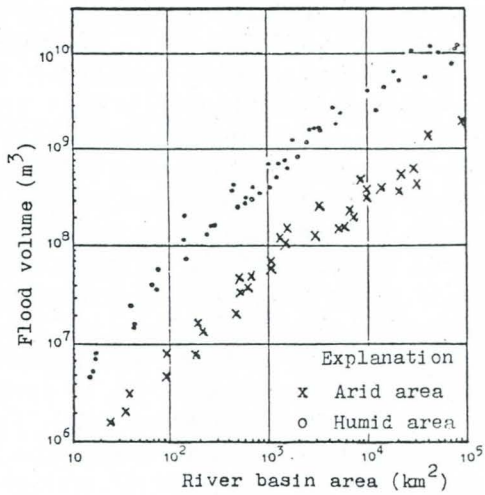

Figure 4. —Relation between maximum 7–day flood volume and river basin area

Figure 3 shows that the records of maximum observed flood peak discharges in the arid area are close to the records in the humid area when the area is smaller than 1500 km^2, and they are obviously smaller than those in the humid area when the area is larger than 1500 km^2. This phenomenon proves again that extraordinary rainstorms actually occur in the arid area and that the rainfall extreme values with small area and short duration are very similar to the values in the humid area, but that the rainfall extreme values with large area and long duration are distinctly smaller than those in the humid area.

The maximum 7–day flood volume includes basically the great majority of surface runoff caused by 1 to 2–day storms. Figure 4 illustrates that the relationships between the records of maximum observed 7–day flood volumes and the areas are expressed in two separate envelope belts for the arid and humid areas when the area of basin is within 100,000 km^2. The records for different scales of area from the arid area are far smaller that those from the humid area and the former is only about 10% of the latter. The figure shows that the areal rainfall in the arid area is distinctly smaller than that in the humid area and thus that both the temporal and spatial distributions of most rainstorms in the arid area are concentrated.

ESTIMATION OF DESIGN STORM AND PMP

The precipitation–measurement conditions and rainstorm characteristics in the arid area are obviously different from those in the humid area, therefore, the estimation methods of design storm and PMP (probable maximum precipitation) in the arid area should be also differentiated from the usual methods used in the humid area.

In the arid area, rainfall gages are unusually sparse. Most rainfall stations are not equipped with recording gages and the number of observed years is generally below 40. The rainstorms in the arid area are often characterized by large spatial variability, severe temporal variation and especially large variation from year to year. In general, the exact locations of storm centers have not been found, the heaviest rainfall intensities persisting in extremely short durations have not been observed, and the extraordinary storms are difficult to observe.

Therefore, the estimation of design storms and PMP using traditional methods cannot give precise values.

Studies of the estimation methods of design storm and PMP for arid area were developed in several countries (WMO, 1986). The study results in China show that some ideas are important to improve the estimation. (1) Field investigation work for extraordinary storms must be emphasized. Up to now, the investigated data of the tens of valuable extreme storms have been applied in design and research works in China and some of them are extracted in this paper. The results indicate that the province investigated maximum rainfall records are about 1.5 to 5 times as high as maximum observed rainfall records in arid China. (2) Regional synthetic analysis for the statistical parameters and design values of storms is an efficient way to utilize the limited data. The representativeness of rainfall data series for single station is poor and the first item (maximum rainfall depth) in the data series of a station is greatly different from that of nearby stations. Therefore, all of the heavy rainstorm data must be studied as a unit in a region where the hydrologic characteristics are homogeneous. The outliers of storms should be studied carefully and their transposition and adjustment to the adjacent area should be made rationally. (3) Particular requirements for specific estimation methods in arid areas must be considered. For instance, if only the areal average rainfall depth for total duration of a design storm is given, the estimation of the design flood will not be accurate. Therefore, the temporal pattern (hyetograph) and areal pattern (isohyet) should be supplied simultaneously. In addition, to suit the special conditions in arid areas, the selection of frequency distribution types, the methods of moisture maximization for the estimation of PMP, etc, need further study and improvement.

REFERENCES

Academia Sinica, 1984, Physical Geography for China—Climate, Science Press, Beijing, 161 p. (in Chinese)

Bureau of Hydrology, 1987, Water Resources Assessment for China, Water Resources and Eletric Power Press, Beijing, 194 p. (in Chinese)

Central Weather Bureau, 1979, Climatic Maps for the People's Republic of China, Map Press, Beijing, 226 p. (in Chinese)

Hansen, E. M., Schreiner, L. C., and Miller, J. F., 1982, Application of Probable Maximum Precipitation Estimates—United States East of the 105th Meridian: Hydrometeorological Report No. 52, National Weather Service, NOAA, US Department of Commerce, Washington, D. C., 168 p.

Northwest Teachers College and Map Press, 1984, Maps of Physical Geography for China, Map Press, Beijing, p. 60 (in Chinese)

Wang, Jiaqi, 1985, Maximum Depth–Area–Duration Records for China: Journal of Hydrology, No. 1, p.44—45. (in Chinese)

WMO, 1986, Manual for Estimation of Probable Maximum Precipitation, 2nd Edition, WMO—No. 332, Geneva, 269 p.

EFFECTS OF GLOBAL CLIMATE CHANGE ON EROSION STABILITY IN ARID ENVIRONMENTS USING WEPP

Richard H. Hawkins and Vicente L. Lopes, School of Renewable Natural Resources, University of Arizona, Tucson, Arizona

Ronald A. Parker and Mark A. Weltz, U.S. Department of Agriculture, Agricultural Research Service, Beltsville, Maryland, and Tucson, Arizona.

ABSTRACT

The notion of climate change requires accompanying weather changes. In most arid situations the regimen of rainstorm depth, intensity and duration govern erosion and runoff patterns. Using the 10 percent overall level of increased rainfalls suggested by General Circulation Model outputs, three alternative forms of achieving this increase are synthesized, and their effects on erosion patterns and intermittent runoff are modeled. Forms of rainfall increases are 1) more events (same intensity patterns and event durations); 2) longer events (same intensity patterns and number of events); 3) higher intensities (same durations and number of events). These are stochastically generated as a part of climate simulation for 20 100-year periods, and used as input to model erosion and event runoff with WEPP (Water Erosion Prediction Project), a recently developed U.S. Department of Agriculture erosion simulation model. An erosion scenario using Tombstone, Arizona climate and a nearby watershed is evaluated. Increases in both runoff and erosion occur in all cases, but especially so when event intensities are modified upwards. The ability (or inability) of such models to mimic the interrelationships between soil properties, hydrology, erosion, and plant cover and growth are discussed, as are implications for future modelling efforts.

INTRODUCTION

Background: Most literature on global change stresses the long term and wide area effects on water supply and vegetation communities. For example, General Circulation Model (GCM) output is on the order of 200 miles square, and water resource modeling derived from it is often on a monthly time step. However, in most arid lands, the processes over smaller areas and shorter durations are important. Weather, in the form of rainstorm events, is the entire water input to the landscape, and is the sole source of water for runoff, erosion, soil moisture, and ground water recharge. This occurs in short durations over small areas, and is sensitive to such rainstorm event details as amount, intensity, and duration. These internal storm characteristics will govern how erosion and runoff patterns will be altered. This matter is almost entirely absent in global climate change concerns, and will be examined here.

Strategy: The recently developed Water Erosion Prediction Project (WEPP) model will be applied to a semiarid hillslope watershed, and the inputs so adjusted to reflect the possible different forms of rainfall delivery to meet an increased overall rainfall depth of 10%, a figure often suggested from GCM studies. The differences in model output will be taken to be the effects of the altered rainfall.

METHODS

WEPP: The basic tool used in this work was the hillslope version (90.92) of the Water Erosion Prediction Project (WEPP) model. This model is the product of a five year interagency development effort by the U.S. Department of Agriculture and other agencies, and has been described in considerable detail elsewhere (Lane and Nearing, 1989). In the interests of space economy, only a minimum of the necessary background will be supplied here.

The WEPP model simulates daily climate (weather) to drive the model's hydrology, erosion, and plant growth components. The hillslope version contains an overland flow hydrology component and erosion model. The hydrology component is driven by rainfall excess using the Green and Ampt equation, with adjustments in parameters for soil and cover properties. The erosion model computes erosion in interrill areas, and detachment, transport, and deposition in rill areas. Interrill erosion is modeled as particle detachment by raindrop impact and delivery to rills. The interrill detachment is proportional to the square of the rainfall intensity, incorporating parameters to account for the effects of ground cover, canopy cover, and soil erodibility (Lane and others, 1987). Rill erosion is modeled as detachment, transport and deposition by concentrated flow, and is based upon the flow's capacity to detach and transport soil particles, including the sediment delivery from the interrill areas. Net detachment occurs when hydraulic shear exceeds critical shear and when sediment load is less than transport capacity. Net deposition occurs when sediment load is greater than transport capacity (Lopes and others, 1989).

Location: The location chosen is the semiarid landscape in the vicinity of Tombstone, Arizona, the site of the Walnut Gulch Experimental Watershed, a long-term research facility for the study of arid land hydrology and erosion (Renard, 1970), operated by U.S. Department of Agriculture, Agricultural Research Service. This area is at the northwestern extreme of the Chihuahuan desert, which is typified by low rainfalls (ca 5-15 in/yr, or 130-140 mm/yr) with a bimodal seasonal distribution and shrub dominated plant communities.

Land: The land characteristics were excerpted from those of a specific small watershed, "Lucky Hills #103", which is 9.1 acres (3.68 ha) in size, and is located about 2 miles (3 km) northeast of Tombstone, Arizona, at an elevation of about 4500 ft (1372 m). A 100 meter long hillslope 50 m wide and with an S-shaped slope configuration with successive slope gradients of five, ten, and five percent was used, with no channel component. The soils are in the Stronghold series, a gravelly-cobbly sandy loam surface texture with an erosion pavement. The vegetation is dominated by creosotebush, whitethorn acacia, and tarbush. The canopy cover is 39%, and the ground cover is 78%, of which 70% is rocks above 2mm in diameter. The area has not been grazed for the past 20 years, but

had prior long-term continuous grazing since the late 1800s. All these attributes of land and climate are representative of the general area (with the exception of the recent grazing exclusion), and their parameter representations were used in the WEPP erosion simulations.

Climate: Long term (20 year) data from Tombstone were used to estimate the parameters of the stochastic climate generator, "CLIGEN" (Nicks and Lane, 1989). Storm event characteristics are simulated through preservation of seasonal and monthly wet day - dry day characteristics, and - within a wet day - the duration, and intensity characteristics of the event. The long term average target rainfall was 294 mm/yr, or about 11.6 in/yr.

Climate Change: The study examined the effects of overall rainfall increases of 10 percent, a rough figure often suggested by GCM studies. This rainfall increase, assumed to be a manifestation of climate change, could occur in three separate forms in rainfall events: 1) 10 percent more storm events of the same duration and intensity patterns; 2) 10 percent longer storms, but of the same number and intensity, and 3) 10 percent more intense storms, but the same number and durations. It could also occur in combinations of the above, but these were not studied here.

Simulation of these three altered conditions was done by adjusting the descriptive statistical parameters in the WEPP climate generating routine. However, modeling the case of 10 percent more rainy days required changing the transition probabilities to produce 10 percent more wet days. This was done on both the dry-wet and wet-wet cases, and required multiplying them by the factor (1+b)/[1-(Pr(W/D)-Pr(W/W)*b], where b is the fractional increase, here taken at 0.10. The transitions to dry days was merely subtracted in the transition matrix. Thus, the following overall procedure was used:

1. Generate the daily sequences with 10 percent more storms (wet days), using the above described adjustments to the transition probabilities. This is the "10 percent more storms case".

2. For the standard or base condition of NO climate change, delete the rainfall for every 11th wet day, thus leaving 100 percent of normal, or the "base" condition.

3. For the case of 10 percent higher intensities, use the data from condition 2 above, but merely multiply the simulated event depth by 1.10. The event duration is preserved, but the intensity is increased by 10 percent.

4. For the case of 10 percent longer storms, again use the data from condition 2 above, but multiply the simulated event depth *and* duration by 1.10. This preserves the intensity, and the storms are 10 percent longer in duration.

These specific procedures, which were chosen to preserve comparability between the data sets for each century, did create some compromises to reality. In the initial step (#1 above), the wet-dry day probabilities were adjusted uniformly throughout the year, thus ignoring any seasonal changes which might occur under a climate change, or differences for wet days or dry days. In step #2, making every 11th wet day a dry day fails to recapture the

original population target transition probabilities. However, the total error is small, and was ignored here. Also, CLIGEN simulates only a single event per wet day, while in reality, multiple events do occur. In the Tombstone area the average is 1.75 events per wet day (Econopouly et al, 1990).

A total of 20 100-year sets were simulated for Case 1 (10 percent more storms). Conversion to Cases 2, 3, and 4 was done as described above within the WEPP model once individual data sets were read. The four cases were run in the WEPP model for the 20 sequences of 100 years each, a total of 80 scenarios.

RESULTS AND DISCUSSION

The results, greatly reduced, are given in summary form in the following table:

Table 1. Average annual values for the 20-100 year simulations.

Case	--------Rainfall---------		-------Runoff---------		Erosion
	Number of Events	Depth (mm)	Number of Events	Depth (mm)	(kg/ha)
Base	38.07	307.47	20.25	140.87	410.0
More	41.87	338.38	22.33	155.56	460.0
Longer	38.07	338.22	21.03	159.55	481.2
Intensity	38.07	338.22	21.69	165.42	529.4

According to the simulations, the increased rainfall did indeed increase the erosion rate. As shown in Table 1, the intensity case resulted in the greatest increases in erosion, amounting to an average of 29.1% over the base condition. Because the detachment portion of the erosion process (which makes the material available for transport by overland flow) is a function of the intensity squared, a potential increase on the order of 1.1^2-1.0 = 21% might be expected from this source process alone. The additional increase seen indicates the presence of other processes, specifically rill erosion, in this situation.

Figure 1 displays the general nature of the results, and shows the relationship with the base climatic conditions. The most benign form of rainfall increase is simply more storms (wet days), and this produces a basement effect of 10% increase in erosion as a minimum. Most impacts are non-linear with total rainfall depth.

This experience highlights some limitations of the WEPP model for this application. The model does not carry out a conservation-of-mass accounting on the soil profile, and thus does not mimic any hillslope evolution or soil armoring. The plant growth component does not carry over any long term changes: dynamics of cover and canopy apply only within a single year. Thus, it would not be possible to simulate the interacting effects of changing plant community on erosion with a climate of optimum erosion to verify the well-known

Langbein-Schumm (1958) relationship. As mentioned previously, the climate generating scheme produces only a single event per wet day.

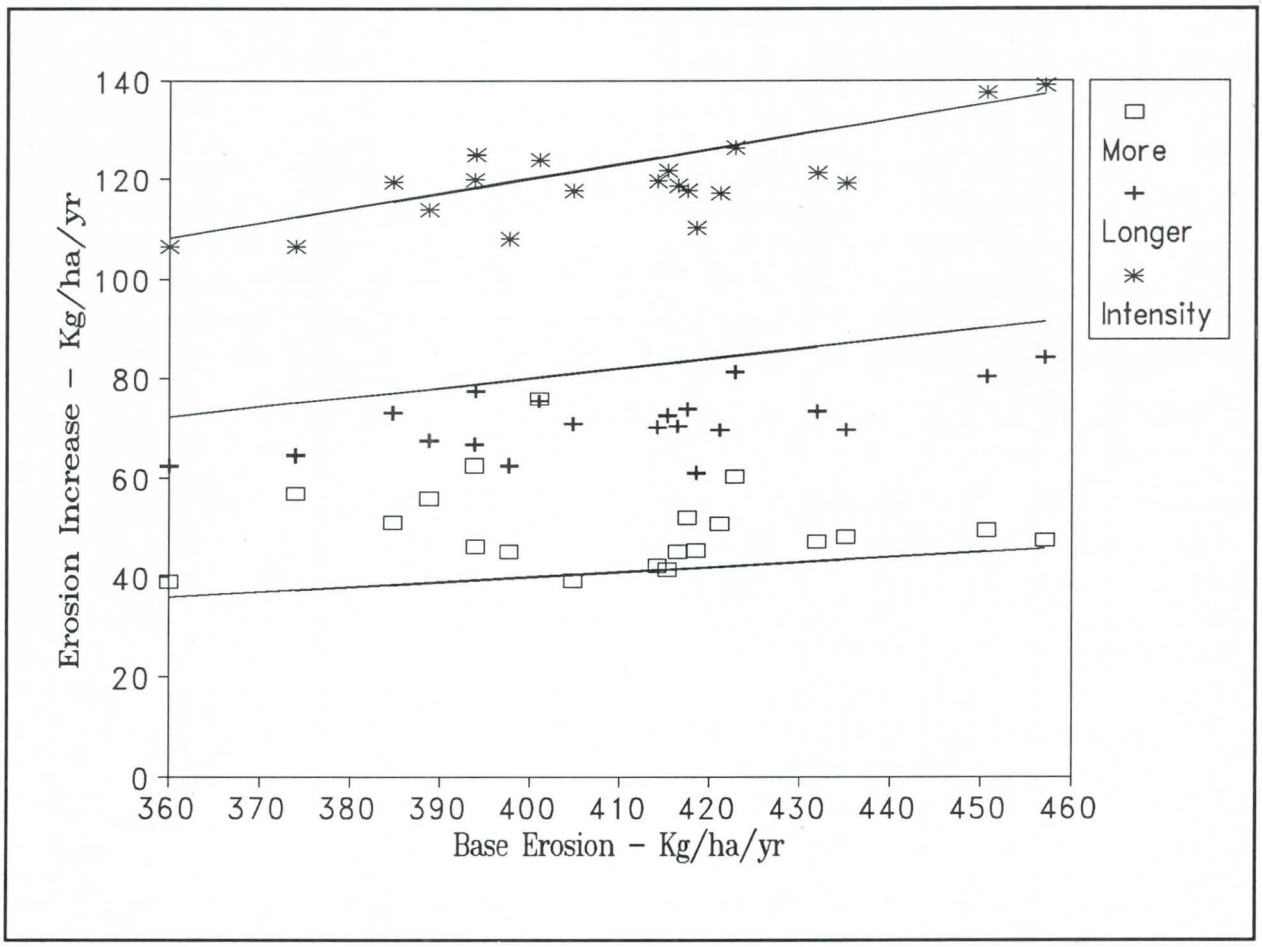

Figure 1. Simulated average erosion rates increases in Kg/ha/yr for centuries for three different scenarios of a 10 percent increase in rainfall at Tombstone, Arizona as a function of the base erosion rate. The three lines shown are, from bottom to top, 10, 20 and 30 percent erosion increases from the base condition.

The simulations for the Walnut Gulch case presented some specific difficulties. The simulated runoff is much higher than that actually experienced at similar sites in the Walnut Gulch area. Analyses of on-site gage records indicates about 25 mm/yr might be expected for these conditions, with an accompanying erosion of about 0.61 Tons/acre/yr, or 1365 Kilograms/hectare/year (Simanton et al, 1980). As shown in Table 1, the model gave about 141 mm/yr and 410 Kg/ha/yr respectively. Post-simulation analysis suggests that a source of these aberrations might be in the accounting for the effects of soil surface and profile rock content on infiltration properties, and in specific limitations in the weather generating routines. These experiences give a basis for enhancing future versions of WEPP.

The work here suggests several possible variations. The effects of seasonal distribution of additional rainfalls might be an avenue of fruitful inquiry, insofar as the

summer storms are the more intense and productive of erosion episodes. Assessing the climate change effects on larger drainages which include more substantial channel processes would be an obvious extension of the work here. Also, an important consideration in this area is the regional groundwater recharge, which occurs almost entirely from these intermittent events, but which occurs almost entirely the larger downstream channels not considered here.

A general conclusion from this study is that these simulation techniques are useful within the acknowledged limits of the model. Erosion variation can be expected to be non-linear with increased rainfall in any form. Simply having more storms of the same characteristics will create the minimum effect. More intense storms will create the maximum effect, and longer storms will produce an intermediate effect. From this experience, it might also be expected that rainfall decreases would produce similar negative responses.

REFERENCES

Econopouly, T.W., D.R. Davis, and D.A. Woolhiser. 1990. Parameter Transferability for a Daily Rainfall Disaggregation Model. Journal of Hydrology v118, p208-228.

Lane, L.J., Foster, G.R., and A.D. Nicks 1987. Use of Fundamental Erosion Mechanics in Erosion Prediction. Paper Presented to the American Society of Agricultural Engineering, Chicago, Ill. 10pp.

Lane, L.J., and M.A. Nearing (eds). 1989. USDA - Water Erosion Prediction Project: Hillslope Profile Model Documentation. NSERL Report No.2, USDA-ARS National Soil Erosion Laboratory, West Lafayette, Indiana, 47907. ca 200pp.

Langbein, W.B. and S.A. Schumm. 1958. Yield of Sediment in Relation to Mean Annual Precipitation. Trans. Amer. Geophys. Union v39, p1076-1084.

Lopes, V.L., Nearing, M.A., Foster, G.R., Finkner, S.C., and J.E. Gilley. 1989. The Water Erosion Prediction Project: Erosion Processes. in Proceedings National Water Conference, Newark, Delaware. Amer. Soc. Civ. Eng., New York. p503-510.

Nicks, A.D., and L.J. Lane. 1989. Weather Generator. in Lane, L.J., and M.A. Nearing (eds). 1989. USDA - Water Erosion Prediction Project: Hillslope Profile Model Documentation. NSERL Report No.2, USDA-ARS National Soil Erosion Laboratory, West Lafayette, Indiana, 47907. pp 2.1-2.19.

Renard, K.G. 1970. The Hydrology of Semiarid Rangeland Watersheds. ARS 41-162. 26pp.

Simanton, J.R., H.B. Osborne, and K.G. Renard. 1980. Application of the USLE to Southwestern Rangelands. in Hydrology and Water Resources in Arizona and the Southwest; Proceedings of the 1980 Meetings of the Arizona Section, American Water Resources Association and the Hydrology Section, Arizona- Nevada Academy of Science.

HYDROLOGY OF AQUIFER RECHARGE IN ARID REGIONS

by

H. J. Morel-Seytoux[1], Chuan-Mian Zhang[2],
Cinzia Miracapillo[3] and Hassan Khadr[4]

ABSTRACT

The understanding of the physics that govern water movement, either natural or artificially induced, toward an aquifer is crucial to proper management of water resources in arid regions. That movement may be in an unsaturated or saturated state. The proper minimal description of these phenomena is presented. The selected descriptions retain the essence of the phenomena, that is, they fully account for the significant interactions between the components of the hydrologic cycle.

INTRODUCTION

Conjunctive management of surface and ground waters becomes important when the exchange between them is rapid. For example, it is estimated that 0.3 billion m^3 are discharged annually from the Nile delta aquifer to the Mediterranean Sea (Samir Farid, 1985). However, two-thirds of this amount is first returned to the Nile (primarily the Rosetta branch) within the middle third of the delta and then discharged to the sea as streamflow (Samir Farid, 1985). It is clear that for proper management of a stream-aquifer system the discharge and exchange mechanisms must be well understood and correctly described.

DEFINITION OF RECHARGE

Recharge is viewed in this article as the general phenomenon of replenishment of groundwater from a surface source (supply). The transfer of water from the surface supply to the aquifer may take place from a supply source such as a stream, a lake, a canal, a ditch, a basin, a pit, or a trench *directly* into a saturated aquifer, which can be either phreatic or confined. The term *seepage* is often used in this context. If no delay occurs, the seepage rate (the rate of loss of water from the river, the lake, etc.) becomes the recharge rate (rate of gain of storage in the aquifer). Under these conditions the water supply source is said to be in *hydraulic connection* with the aquifer.

---

[1]Professor, Department of Civil Engineering, Colorado State University, Fort Collins, CO 80523
[2]Hydrogeologist, Woodward Clyde Consultants, Denver, Colorado
[3]College of Engineering, University of Rome, La Sapienza, Italy
[4]Department of Civil and Irrigation Engineering, University of Cairo, Egypt

In other instances the water loss from the surface supply (irrigation furrow, sprinkler system, rain, snowmelt, flooding wadi) will penetrate the soil (infiltrate) and first replenish an unsaturated zone extending between the source and the aquifer.

RECHARGE VIA VADOSE ZONE

A relatively simple analytical procedure has been developed to predict aquifer recharge. The procedure accounts for the difference in specific yield in the zones below the recharge pond and away from it. It also accounts for its variation in time. It accounts for aquifer anisotropy. However, because the solution is approximate, the emphasis in this article is on testing its validity.

Simplified Mathematical Formulation of the Problem

The mound profile below the circular basin is approximated by a plateau at a distance z_{rf} above the initial water table level (the position of the reflected front) and by the profile h(r,t) in region not below the basin. The origin of the r-axis is at the center of the circular basin of radius R. The rapid change in water table elevation in the region of sharp curvature of the flow is represented by a finite drop at r = R from the value of $z_{rf}(t)$ to h(R,T). The problem is decomposed into two parts: (1) the determination of the evolution of the mound elevation h(r,t), due to a prescribed lateral specific discharge (discharge per unit circular length along the entire depth of the aquifer) q(t) at r = R, and (2) the evolution of the reflected front $z_{rf}(t)$ given a prescribed velocity r(t) (recharge rate) and specific discharge q(t). Then the two solutions which both depend on the unknown q(t), the transmitted flux from the aquifer below the recharge area to the aquifer away from it, are coupled through a third equation, the matching equation, that relates the variables $z_{rf}(t)$, q(t) and h(R,t). Details of the procedures have appeared in the literature (e.g., Morel-Seytoux and Miracapillo, 1988).

Determination of the Transmitted Flux

Using the flow net approach (e.g., Morel-Seytoux, 1985), the recharge rate q(t) can be expressed by an integrated form of Darcy's law. To evaluate the head drop at the interface between the two unidimensional flow regions, the water table below the irrigated area can be approximated by a horizontal line at a height z_{rf} above the initial water table level. On the other hand, to represent the steep gradient about r = R, it is necessary to have a stationary front at r = R. In other words, the limit of h(r,t) as r tends to R from the positive side is $h(R,t) \neq z_{rf}(t)$. Consequently, the head drop between the horizontal recharge circle and the cylindrical lateral boundary (at r = R) is:

$$\Delta H(t) = z_{rf}(t) - h(R,t) \tag{1}$$

Eventually after some approximations (Morel-Seytoux and Miracapillo, 1988) one obtains a formula for the recharge rate:

$$q = \frac{Q}{2\pi R} = \frac{\frac{1}{2}T_V q_H + T q_V + h K_V q_H}{T_V + T + q_H + K_H z_{rf}} \tag{2}$$

where e is mean saturated thickness and for brevity the following quantities are defined:

$$T_V = K_V R \; ; \; T = K_H e \; ; \; q_H = K_H[z_{rf} - h(R, t)] \; ; \; q_V = K_V[z_{rf} - h(R, t)] \tag{3}$$

Coupling of the Various Components

Under the assumption that R and e are large compared with $z_{rf}(t)$ and h(R,t), Eq. (2) can be further simplified to the final form:

$$q = K[z_{rf}(t) - h(R, t)] \tag{4}$$

where K is an effective conductivity related to the hydraulic conductivities in the horizontal and vertical directions K_H and K_V and to the geometrical characteristics R and e, namely:

$$K = \frac{1}{2}\frac{R + 2e}{\frac{R}{K_H} + \frac{e}{K_V}} = \frac{(0.5R + e) K_H K_V}{R K_V + e K_H} \tag{5}$$

Eventually, after elimination of the other variables of state an integro-differential equation for the unknown q(t) obtains:

$$q(t) + \frac{2K}{R}\int_o^t \frac{q(\tau)\, d\tau}{[\tilde{\theta} - \theta(\tau)]} + K\int_o^t K_h(R, t-\tau)\frac{\partial q(\tau)}{\partial \tau} d\tau = K\int_o^t \frac{r(\tau)\, d\tau)}{\tilde{\theta} - \theta(\tau)} \tag{6}$$

where $\tilde{\theta}$ is water content at natural saturation, $\theta(t)$ is a mean water content in the saturated zone above the reflected front, $K_h(R,t)$ is a unit step response of head in the aquifer away from the recharge area due to the lateral flux and r(t) is the recharge rate. This equation is discretized and easily solved numerically (Morel-Seytoux and Miracapillo, 1988). Part of the real problem is to determine r(t) and $\theta(t)$ given the infiltration i(t) at the ground surface. In this paper, they are assumed known. A methodology to calculate these quantities is described in a separate document (Morel-Seytoux and Miracapillo, 1988).

Comparison with a Three Dimensional Saturated-Unsaturated Groundwater Model

Figure 1 displays a comparison between field observations (Bianchi and Haskell, 1968), results from a 3-dimensional numerical model and from the approximate analytical procedure. In both cases the fit is quite reasonable, given some uncertainty in the accuracy and reliability of the observations. One can conclude that either method is adequate and thus one may as well use the simpler procedure.

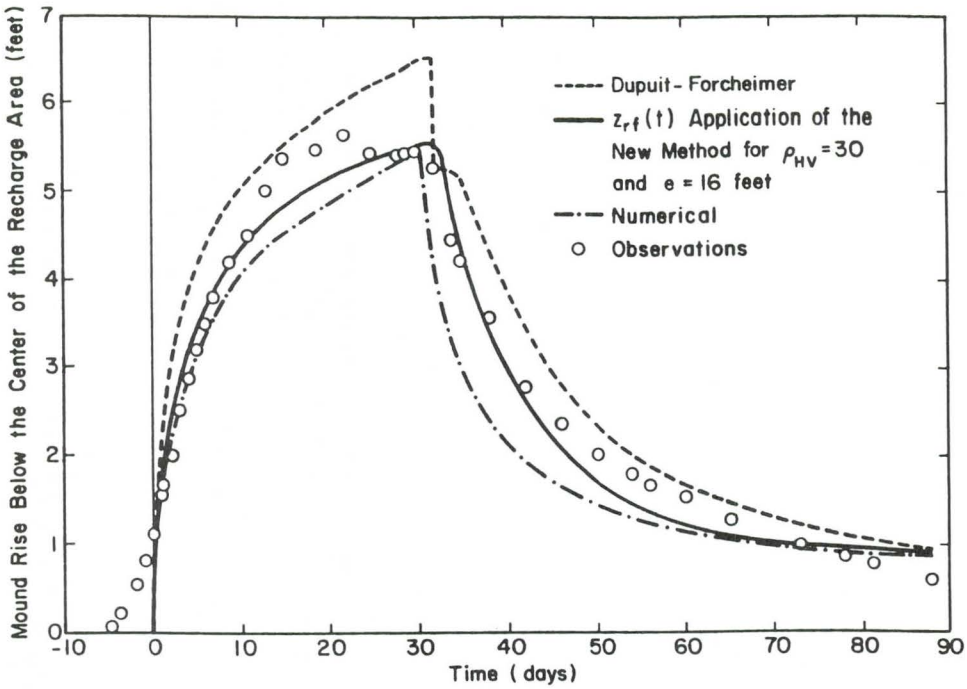

Figure 1. Comparison of Observed Mound Heights with Calculated Ones Using the Three-Dimensional Numerical Model and the Analytical Procedure.

RECHARGE UNDER CONDITION OF HYDRAULIC CONNECTION

Partial Penetration and Vertical Flow

Given that interest lies in the overall discharge (seepage or actual return flow) and not in the detailed velocity field, the quantity of concern to characterize the exchange flux is the conductance of the system between two potential surfaces. At a sufficient distance away from the stream cross-section the flow will tend to become again essentially horizontal. At such distance, say C, the equipotential surface is vertical. An approximate method to determine the conductance of the flow system between two potential surfaces is the method of flow nets (e.g., Morel-Seytoux, 1985). In its crudest form the method yields for the discharge the expression:

$$Q_R = KL\left(\frac{W_P + 2e}{e + 2C}\right)(h-\zeta) \tag{7}$$

where K is a representative hydraulic conductivity for the region between the two equipotential surfaces, L is the length of the river reach of concern, W_P is the wetted perimeter of the cross-section, e is a representative (mean) saturated thickness of the aquifer for the region, C is a distance at which the equipotential surface is essentially vertical, h is water table head (potential) at distance C and ζ is river head (potential) both measured from the same horizontal datum. The coefficient of $(h-\zeta)$ in Eq. (7) has been called "reach transmissivity," denoted Γ because it has dimensions of a transmissivity (area per time) and it depends on the geometric characteristics of the reach and on the aquifer properties in the vicinity of the reach.

To apply Eq. (7) one must estimate C. Theoretical and experimental studies have shown that C should be of the order of 5W where W is the top width of the cross-section (usually an adequate approximation for the wetted perimeter, W_P). Thus, the practical formula for applications to estimate the reach transmissivity from field data is:

$$\Gamma = KL\left(\frac{W_P + 2e}{e + 10W_P}\right) \approx \frac{T}{e} L\left(\frac{W + 2e}{e + 10W}\right) \tag{8}$$

Equations (7) and (8) were used to estimate return flows along the South Platte river and the practical validity of Eq. (8) was verified by streamflow data on inflow and outflow from the channel reach (e.g., Morel-Seytoux, 1985).

Anisotropy and Clogging

Equation (8) was derived under the assumption that the aquifer is isotropic. Usually the horizontal conductivity K_H is much larger than the vertical one K_V. Under such conditions the method of flow nets yields the more general formula (Morel-Seytoux and Miracapillo, 1988):

$$\Gamma = \frac{T_H}{e} L\left[\frac{W_P + 2e}{10W_P + \rho_{HV} e}\right] \tag{9}$$

where T_H is horizontal aquifer transmissivity (i.e. eK_H) and $\rho_{HV} = \frac{K_H}{K_V}$ is a measure of anisotropy. In addition, the streambed is often clogged. Over a thickness z_c, the hydraulic conductivity is K_c. In such a situation a more general formula yields:

$$\Gamma_c = \Gamma\left[1 + z_c \frac{\Gamma}{W_P} L K_c\right]^{-1} \tag{10}$$

where in this equation Γ is given by Eq. (9). In the remainder of this article it is understood that T stands for T_H and the symbol T will be used exclusively for horizontal aquifer transmissivity.

Grid Size Selection

From the discussion of the previous sections and the magnitude of the parameter $C (\approx 5W_P)$, it is apparent that the grid size cannot be independent of the width of the river because the mean water table elevation in the cell must be a representative value of the water table elevation at some $5W_P$ away from river center. For this reason, one must select for the grid size a value of the order of at least 10 W_P. This is a practical size in most situations. It provides a means of predicting return flow with good accuracy without having to use a grid size of the order of W_P. There will be cases, however, where a grid size of order 10 W_P is not acceptable. For example, in the case of the Nile River in Upper Egypt (Attia, 1974) the alluvial aquifer is so narrow that a single grid of size 2 or 3 W_P would cover the entire width of the alluvial aquifer. The model would then be essentially a one-dimensional groundwater model. It would still describe properly the stream-aquifer interaction. If one wished to predict water table elevations in the near vicinity of the river it

might be necessary to use a grid size of the order of W_P. In this case the reach transmissivity formula must be modified to the form:

$$\Gamma = LW_P \frac{T}{e} \left(\frac{K_c}{z_c K_H + \rho_{HV} K_c \frac{e}{2}} \right) \tag{11}$$

This formula accounts for clogging and anisotropy, but does not account for additional head loss due to the abrupt change from vertical to horizontal flow direction. In most situations such a detailed water table elevation profile is not needed. For a situation such as the Nile River to account for the three dimensional character of the flow it may be necessary to use a cell size smaller than W_P (say one fifth of W_P). In this case W_P in Eq. (11) would be replaced by the grid width, a fraction of W_P.

CONCLUSIONS

The approximate analytical solution is quite simple to exploit. However, simplicity of application is not the only virtue of a predictive tool. It should be sufficiently accurate and complete to represent reality. The three-way comparison with observations and results from a complex three-dimensional model shows that the simple model performs adequately.

In the case of hydraulic connection, the use of simplistic boundary conditions for the exchange between stream and aquifer may lead to unrealistic values of seepage and, in fact, artificial creation of water. Modeling of the river flows and a water balance for surface waters must be included in the analysis of the system.

REFERENCES

Attia, Fatma, 1974. "Parameters and Characteristics of the Groundwater Reservoir in Upper Egypt," M.S. thesis, Faculty of Engineering, Cairo University 159 pages.

Bianchi, W. C. and E. E. Haskell, 1968. Field Observations Compared with the Dupuit-Forchheimer Theory for Mound Heights under a Recharge Basin, Water Resour. Res., 4 (5), 1049-1057.

Farid, Samir, 1985. "Management of the Groundwater System in the Nile Delta," Ph.D. dissertation, Faculty of Engineering, Cairo University, 300 pages.

Morel-Seytoux, H. J., 1985. Conjunctive Use of Surface and Ground Waters, Chapter in Artificial Recharge of Groundwater, T. Asano, editor, Butterworth Publishers, Boston, 35-68.

Morel-Seytoux, H. J. and C. Miracapillo, 1988. "Prediction of Infiltration, Mound Development and Aquifer Recharge from a Spreading Basin or an Intermittent Stream" Hydrology Days Publications, 1005 Country Club Road, Fort Collins, Colorado 80524, 96 pages.

ANALYSIS AND FORECAST OF THE WATER QUALITY STATE OF MAIN RIVERS IN XINJIANG

Hao Yu–Ling
Xinjiang University

ABSTRACT

This paper discusses the water quality state of the main rivers in Xinjiang. It is important to Understand the water quality state of the main rivers in Xinjiang. Adopting current methods, an evaluation of water qualities on ten and more main rivers within Xinjiang which have data from water quality monitors has been made in this paper.Proceeding to the next step,the state of the water quality in the low water season has been explained also. On the basis of the above research we obtained the arrangement or ranking of pollutants of the main rivers. In the final part of the paper, using the Chinese scientist Professor Ju–lung Deng's Grey System Theory, we conducted a forecast of water quality. The thinking and the concrete working methods which this paper presents will possess a reference value for other arid and semi–arid areas.

INTRODUCTION

Xinjiang lies deep in the interior of Eurasia. It is a standard arid and semi–arid area. For a long time people were concerned only with the amount of water resources, and did not pay attention to water qualities until about the last ten years. In general, as to the water quality of the surface water in Xinjiang, it is good before flowing out of the mountain basins, while after flowing out of the moutains it gradually becomes poor. Especially, the river waters near the citics have been contaminated by varying degrees. Connecting with the peculiarity of the oasis economy of Xinjiang, the effect of human activities is shown clearly. In the low water season,the pollution which was brought by man–made effects frequently becomes heavier. Water is a sensitive factor in the arid area.The water quality in low water season is an even more sensitive factor. Connecting with its naturally formative mechanism, it is especially easy to bring about exhaustion of water resources from loss of water quality.

CHARACTERISTICS OF WATER QUALITY OF RIVERS IN XINJIANG

(1) The topographic structure of basins being surrouded by mountains in Xinjiang and the wild ecological environment determined that the weaker earth surface runoff was grown.Though there are 500 and more rivers,they are mostly creeks of low water volume, short flowing distance and strong seasonality. These rivers collect more and more water volume within the area which the run–off was formed. where the water flows out of the mountain catchment, the water volume reaches its largest, but diminishes continuously after flowing out of the mountains. (This is different from the general rule of China's inland rivers.) When rivers flow out of the mountains, they are contaminated by human activities on the one hand and the water volume gradually becomes less on the other hand, and their ability of cleaning themselves reduces. Rivers in Xinjiang have therefore the peculiarity that the water quality becomes poor with increasing flow distance.

(2) The rivers in Xinjiang rise mostly in the mountinous districts which lie in the basin periphery, and they have no other alternative but to converge toward depressions, so as to form a centripetal water system without outlet (except the Ili He River and the Ertix He River) . The pollutants and varied toxic and harmful matter entering the centripetal water system are hard to drain

away. The pollutants which are discharged into the water bodies of the exterior rivers in China's inland, may cause harm with the area of lower reaches of river or ocean, but in Xinjiang the pollutants which are discharged into the water bodies basically deposit or bring about pollution in local area.

(3) The earth surface water and ground water in Xinjiang originate from the same source and they are prone to transform into each other. Although this mutual transformation undoubtedly is an advantage for using water volume, as to water quality, a mutual transformation brings a mutual transmission and transference of pollutants, especially some organic toxic matter of lasting poisonousness and some heavy metal elements hard to dissolve, between the earth surface water and ground water.

(4) So far as the water quality change along the water course being concerned, after flowing out of the moutains, due to leaking, scattering and disappearing and evaparation, rivers have a concentrating effect, causing the degree of mineralization to increase continuously, and human activities make pollution worse. Especially in the lower reaches of irrigation areas, a large amount of agricultural chemical fertilizer on the farmland is brought into the river water through draining off water from farmland. Also, the high–concentration water of alkali washing,which was drained away from the salinized soil and returned to the river course, causes the degree of mineralization of river water to increase markedly. The mineralizing degree was extremely high in the lower reaches of rivers, where the current nearly dried up. The change of water quality along the river course is greater than that for the mountainous creeks, which have less water volume and shorter flow distances.

(5) The fundamental state of the surface water quality in Xinjiang at present is as follows. The rivers such as the Ili He River, Ke Zi He River and Manas He River,in which the runoff volume is large, are basically uncontaminated. Other rivers, such as the Shui Mo He River, which is close to the city of Urumqi, and the Ke Lan He River, which is close to the city of Altay, which lie nearby the city, or which have small runoff volume, or many factories on both banks or at the upper reaches, or which receive directly the discharge of polluted water, were polluted seriously. Other rivers,lakes and reservoirs that the above–mentioned rivers empty into or connect with, are polluted too. The cause that brought about the man–made serious pollution was that in some large and middle cities in Xinjiang, several 10 thousand to several 100 thousand tons of untreated waste water discharged every day into the rivers, lakes and reservoirs nearby or permeated into the ground. Thus the surface water and ground water were polluted in varying degrees.

METHODS AND ELEMENTS OF EVALUATION

This paper adopts Nemerow's (1978) synthetic index method to conduct the water quality evaluation of rivers. This index summarizes the ratios of pollutant concentrations to water quality standards. The water quality standard of evaluation (except the controlling section of the Shui Mo He River) adopted entirely the second grade of the Quality Standard of Earth Surface Water (GB3838–83) of China, and the remaining items were evaluated under The Standard of Producing Drinking Water (GB5749–85), but the third grade of (GB3838–83) was adopted to evaluate the controlling section of the Shui Mo He River. To adopt the methods and elements like this ensures both the unified comparableness and the differentiation of the rivers of different function. The classification of environmental quality of surface water is shown in Table 1.

Table 1 **Classification of Surface Water Quality**

Value Pi	<0.70	0.71–0.90	0.91–1.50	1.51–3.00	>3.00
Grade	I	II	III	IV	V
The State of Water Quality	Clean Water Quality	Cleanner Water Qualily	Light Polluted Water Quality	Moderate Polluted Water Quality	Heavy Polluted Water Quality

RESULTS OF EVALUATION AND ANALYSIS

(1) The Synthetic index of the river water quality.

Every river has one contrasting section(D) and one or two controlling sections(K) . There is a consuming and diminishing section(X) also in some rivers, which belongs to additive one of determining. The contrasting section was set up mostly in upper reaches or river source to reflect the original value of river water quality and to use it as contrasting to the contaminated state at the controlling section. The controlling section was mostly selected in the middle or lower reaches of a river. It can control and determine the great part of pollutants of that river. Table 2 is the yearly synthetic index of water quality in the controlling section of the main rivers in Xinjiang. One can see from the Table that the river which was polluted most seriously over the years is the Shui Mo He River. The mean values of the synthetic index of water quality over the years were taken to show their water quality state, and are listed in the table 2.

Table 2 Table of Water Quality Synthetic Index at the Controlling Section of the Main Rivers in Xinjiang

Year / River	1982	1983	1984	1985	1986	1987	1988	mean	remarks
Urumqi He	0.73	1.00	0.76	0.87	0.80	0.92	0.64	0.81	Grade II
Shuimo He	6.77	2.21	1.43	2.70	2.95	4.66	7.40	4.02	Grade V
Manas He	1.01	1.43	0.36	0.73	1.42	0.66	0.59	0.89	Grade II
Ili He	1.68	1.57	0.63	0.68	1.58	0.75	0.74	1.10	Grade III
Kaidu He	0.36	0.56	0.61	0.58	0.58	0.63	0.59	0.56	Grade I
Kongque He	0.38	0.62	1.05	0.87	0.86	1.08	0.84	0.81	Grade II
Kezi He	0.62	0.82	0.86	0.77	0.81	0.84	0.87	0.80	Grade II
Tuman He	0.84	1.13	1.01	1.05	0.99	1.09	1.02	1.02	Grade III
Baiyang He	0.75	1.56	0.52	0.56	0.68	1.18	0.82	0.87	Grade II
Kelan He			5.96	3.44	0.77	1.23	0.72	2.42	Grade IV
Ertix He				1.17	1.55	0.66	0.60	1.00	Grade III
Tarim He				1.75	1.09	1.14		1.33	Grade III
Yarkant He				0.71	0.75	1.33		0.93	Grade III

(2) To show water quality difference of each period of a same river and water quality difference of the same period of different rivers,according to the result of calculation, the mean value over the years of water quality synthetic index of the low, high and moderate water season is listed for comparison (See Table 3). The water quality synthetic index and its mean value in low, high and maderate water seasons in the place of controlling section is listed in Table 3: The arrangement of water quality comtamination in low, high and moderate three water seasons of the same river was carried out. In addition, the level of water quality contamination among the rivers in the low water season also was arranged.

One can see from Table 3 that the best water quality is in the Urumqi He River and the Kai Du He River. The worst water qualities in low water season are Shui Mo He River and the Manas He River.

The rivers above–mentioned together with the Shui Mo He River,the Ili He River, the Kong Que He River, the Ke Zi He River, etc.. are all the main rivers of receiving pollutants within Xinjiang. When these rivers flowed by the vicinity of cities, several million cubic metres of waste and polluted water were discharged into them every year. But because of the Ili He River and the Kong

Table 3 Table of Water Quality Synthetic Index of Each Season at the Place of Controlling Section of Each River

River	Periods \ Year	1984	1985	1986	1987	1988	mean	Arrangement in Order of Three Stages of This River	Arrangement of Contamination of Each River in low Water Season	remarks
Urumgi He	Low water season	0.60					0.60	3	Ⅸ	Grade Ⅰ
	High water season	0.66	0.68	0.81	0.92	0.76	0.77	2		
	Moderate water season	0.81	1.05	0.85	0.92	0.53	0.83	1		
Shuimo He	Low water season		2.84	4.50	3.65	6.40	4.35	3	Ⅰ	Grade Ⅴ
	High water season			4.42	7.38		5.90	1		
	Moderate water season		3.11	2.15	3.43	9.25	4.49	2		
Manas He	Low water season	0.72	0.73	4.25	0.85	0.82	1.47	1	Ⅱ	Grade Ⅲ
	High water season	0.51	1.01	0.54	0.64	1.41	0.82	2		
	Moderate water season	0.44	0.44	0.87		0.70	0.61	3		
Ili He	Low water season	1.01	0.62	2.79	0.77	0.74	1.19	2	Ⅲ	Grade Ⅲ
	High water season	0.66	1.14	0.92	0.97	1.40	1.02	3		
	Moderate water season	0.76		1.91			1.34	1		
Kaidu He	Low water season	0.59	0.81	0.59	0.69	1.46	0.83	1	Ⅷ	Grade Ⅱ
	High water season	0.62	0.55	0.56	0.63	0.92	0.66	2		
	Moderate water season	0.60	0.62	0.59	0.61	0.54	0.59	3		
Kongque He	Low water season	0.97	0.65	1.77	0.90	0.79	1.02	3	Ⅴ	Grade Ⅲ
	High water season	1.48	1.36	0.73	1.47	0.81	1.71	2		
	Moderate water season	1.14	1.86	1.09	0.98	0.92	1.20	1		
Kezi He	Low water season		0.85	0.92	0.88	0.84	0.87	2	Ⅶ	Grade Ⅱ
	High water season		1.26	0.70	0.79	0.93	0.92	1		
	Moderate water season		0.84	0.80	0.91	0.84	0.85	3		
Tuman He	Low water season			1.06	1.00	1.33	1.13	1	Ⅳ	Grade Ⅲ
	High water season			0.89	1.22	0.94	1.02	3		
	Moderate water season			1.03	1.09	1.05	1.06	2		
Baiyang He	Low water season			0.51	1.69	0.72	0.97	2	Ⅵ	Grade Ⅲ
	High water season			1.14	1.52	1.39	1.35	1		
	Moderate water season			0.59	0.45	0.66	0.57	3		

Que He River are big in water volume and currents are swift, only in the vincinity of cities, was contamination brought about generally. The water qualities did not differ greatly in high and low water seasons, even in the period of generating water sometimes, the water quality is more poor than that in low water season yet. On the one hand, the rate of flow is large, the ability of diffusing and diluting is strong in high water season and, moreover, the water temperature and sunshine are high and strong respectively. Therefore the complement of dissolved oxygen(DO) and the chemical and organic decompositions of pollutants are all able to quicken, thus raising the ability of self–purification of water body. On the other hand, one should see that the productive activities are vigorous in high water season in some cities and towns. Many seasonal industrial enterprises such as sugar making, food making, industry of building materials and processing hides and so on went all into operation, thus bringing about great volume of industrial waste water, which were discharged into rivers, making the contamination of water quality more serious. Advantageous and disadvantageous factors were almost synchronous and, moreover, the seasonal discharging of waste water changed relatively large and had not regularity again among years. This agrees with the change of water quality index in each stage in Table 3.

(3) The Characteristic of Contamination in Low Water Season

Making an average of many years for the branch Ii value of each pollutant, and the ranking order of the pollutants in low water season and year–round were listed as Table 4 below.

From Table 4, one can see that the kind of pollutants of many years average in low water season in each river and the kind of pollutants of many years average year–round of that river. Only the sequence of arrangement is

different.The sequences of the pollutants of many years average at the place of controlling section, which has been arranged in the Table,are exactly the principal pollutants of that river and its sequence of contamination.

Table 4 The Arrangement of Pollutants in Low Water Season and Many Years of Each River

Rivers	Order / Ii / Season	1	2	3	4	5	6	mean value
Urumqi He	mean value in low water	PH	Volatile phenol	BOD_5	total hardness	COD	fluorine	
	season	0.83	0.80	0.48	0.43	0.30	0.27	0.518
	mean value	PH	BOD_5	COD	Cr^{+6}	Volatile phenol	Ammoniacal nitrogen	
	of years	1.02	0.74	0.56	0.457	0.455	0.45	0.614
Shuimo He	mean value in low water	NO_2–N	NH_3–N	Volatile phenol	COD	BOD_5	total hardness	
	season	4.92	4.70	3.75	3.30	2.88	1.39	3.49
	mean value	COD	NH_3–N	BOD_5	NO_2–N	Volatile phenol	total hardness	
	of years	4.00	3.83	3.49	3.05	2.00	1.52	2.982
Manas He	mean value in low water	Volatile phenol	Cr^{+6}	PH	mercury	fluorine	COD	
	season	1.41	0.89	0.74	0.44	0.34	0.338	0.693
	mean value	mercury	PH	Cr^{+6}	COD	Volatile phenol	BOD_5	
	of years	0.826	0.63	0.566	0.47	0.44	0.289	0.537
Ili He	mean value in low water	COD	PH	Volatile phenol	Cr^{+6}	BOD_5	total hardness	
	season	1.32	0.74	0.65	0.565	0.556	0.51	0.724
	mean value	COD	PH	Cr^{+6}	Volatile phenol	BOD_5	total hardness	
	of years	1.316	0.765	0.764	0.63	0.61	0.476	0.760
Kaidu He	mean value in low water	PH	fluorine	BOD_5	total hardness	COD	NH_3–N	
	season	0.82	0.538	0.517	0.32	0.31	0.27	0.463
	mean value	PH	BOD_5	COD	total hardness	fluorine	NH_3–N	
	of years	0.715	0.447	0.36	0.33	0.30	0.22	0.395
Kongque He	mean value in low water	BOD_5	COD	PH	total hardness	NH_3–N	fluorine	
	season	1.065	1.054	0.744	0.63	0.564	0.337	0.732
	mean value	COD	PH	total hardness	BOD_5	NH_3–N	fluorine	
	of years	1.11	0.79	0.76	0.60	0.48	0.41	0.692
Kizi He	mean value in low water	total hardness	PH	BOD_5	COD	Volatile phenol	fluorine	
	season	1.21	0.74	0.59	0.43	0.33	0.23	0.588
	mean value	total hardness	PH	COD	Cr^{+6}	BOD_5	fluorine	
	of years	1.11	0.60	0.369	0.34	0.29	0.21	0.487
Tuman He	mean value in low water	total hardness	PH	BOD_5	COD	NH_3–N	Cr^{+6}	
	season	1.46	0.62	0.57	0.31	0.29	0.24	0.582
	mean value	total hardness	PH	COD	fluorine	BOD_5	Cr^{+6}	
	of years	1.425	0.53	0.42	0.37	0.36	0.32	0.571
Baiyang He	mean value in low water	COD	BOD_5	Cr^{+6}	PH	total hardness	fluorine	
	season	1.35	0.76	0.38	0.33	0.322	0.32	0.577
	mean volue	COD	BOD_5	mercury	PH	NH_3–N	total hardness	
	of years	1.17	0.72	0.65	0.61	0.36	0.34	0.642
Klan He	mean volue	COD	BOD_5	Cr^{+6}	Volatile phenol	NH_3–N	PH	
	of years	3.20	1.43	0.97	0.64	0.54	0.40	1.197
Ertix He	mean volue	Cr^{+6}	NH_3–N	COD	Cyanide	BOD_5	PH	
	of years	0.96	0.95	0.937	0.42	0.37	0.267	0.651
Tarim He	mean volue	total hardnes	Cr^{+6}	PH	NH_3–N	COD	mercury	
	of years	1.51	1.40	0.97	0.47	0.38	0.20	0.822
Yarkant He	mean volue	Volatile phenol	Cr^{+6}	PH	total hardness	NH_3–N	mercury	
	of years	1.00	0.95	0.87	0.42	0.35	0.30	0.648

FORECAST OF STREAM WATER QUALITY

The Chinese Scientist Ju–lung Deng's theory of Grey System (1982) was adopted when the author conducted the forecast of the stream water qualities. As space is limited, only a part of the forecasting value and error of stream water qualities are listed in Table 5. Except for one or two values in Table 5, the great part of forecasting value and error are less 10%. As the tendency of water qualities changes, it may be used as reference.

CONCLUSIONS

(1) The water qualities of most main rivers in Xinjiang are better, having clean and cleaner water qualities. To protect the good water qualities of these rivers have to be done from now on.

(2) According to the investigation, the organic pollutants are mostly principal in the industrial waste water of the whole of Xinjiang. Secondly, the volatile phenol and three nitrogen pollutants are more either. Among the discharging substances of the heavy metal, $Cr^{+6}$was discharged more and then mercury and arsenic etc.. This rather tallies with Table 4.

Table 5 The Forecasting Value of Water Quality Index Pi at the place of Controlling Section of Each River

River	Pi \ Year	82	83	84	85	86	87	88	89	90	91	92	93	94	95
Urumqi He	Actual Value	0.73	1.00	0.76	0.87	0.80	0.92	0.64							
	Forecasting Value				0.890	0.832	0.780	0.677	0.641	0.605	0.569	0.534	0.500	0.469	0.439
	Errors (%)				−2.299	−4.078	15.22	−5.78							
Ili He	Actual Value	1.68	1.57	0.63	0.68	1.58	0.75	0.74							
	Forecasting Value						0.68	0.73	0.776	0.824	0.869	0.913	0.956	0.998	1.040
	Errors (%)						9.33	1.35							
Kaidu He	Actual Value	0.36	0.56	0.61	0.58	0.58	0.63	0.59							
	Forecasting Value			0.582	0.588	0.594	0.600	0.606	0.612	0.619	0.625	0.632	0.638	0.644	0.651
	Errors (%)			4.590	−1.379	−2.413	4.761	−2.711							
Kongque He	Actual Value	0.38	0.62	1.05	0.87	0.86	1.08	0.84							
	Forecasting Value			0.982	0.960	0.939	0.918	0.897	0.878	0.858	0.839	0.820	0.802	0.784	0.767
	Errors (%)			6.48	−10.34	−9.19	14.95	−6.79							

(3) Water is the sensitive factor in arid area.The problem of water quality is even more the most sensitive factor. The mean main pollutants of many years in low water season of each river and the yearly main pollutants of many years were similar. There are differences only in the order of arrangement. This shows that the water quality state in low water season has an important influence on the yearly water quality. But the index of water quality of the mean main pollutants of many years in low water season in most rivers will be large to the water quality index of the mean main pollutants of many years of that river all the year round (the mean value column of Table 4) . This shows that the contamination of water quality in low water season is heavier than the yearly mean contamination. Therefore, to control the water quality in the low–water season has thus become the key to controlling and improving the yearly water quality.

REFERENCES

Tang Qicheng: 1985. The basic characteristics of hydrology of arid area of China. The natural geography of arid area of China. Science Press Beijing

Gao Zhizhang. Wang Yijian: 1988. The Scientific Countermeasure of Ecological Environment in 2000 in Xinjiang. Journal of Environmental Protection in Xinjiang.1988.No.3

Hao Yuling: 1990. An Analysis on Water Quality of Water Resources in Ili Prefecture in Xinjiang. Hohhot, China: "International Symposium on the Arid land Resources and Environment" selected works of paper V01. I. Journal of Arid Land Resources and Environment.1990.Vo1.4.No.3

Lu Lachang:1988.The Ecosystem Characteristics of the Inland Basin of the Northwest China––Taking Tarim River Basin As An Example.Journal of Arid Land Resources and Environment.1988.Vo1.2 No.3

Deng Julung: 1987. The Basic Working Method of the Gray System. Central China Science and Engineering University Press Wuhan.China

IRRIGATION INDUCED WATER QUALITY PROBLEMS IN THE WESTERN UNITED STATES

Herman R. Feltz
U.S. Geological Survey
Reston, Virginia 22092
U.S.A.

ABSTRACT

In response to concerns expressed by the U.S. Congress over contamination at the Kesterson National Wildlife Refuge in California, the Department of the Interior (DOI) initiated a program in 1985 to identify the nature and extent of irrigation-induced water-quality problems that might exist in other areas of the western United States. A Task Group prepared a comprehensive plan for reviewing irrigation-drainage concerns for areas where the DOI has responsibility. These concerns relate to three specific responsibilities: (1) irrigation or drainage facilities constructed or managed by the Department, (2) national wildlife refuges managed by the Department, and (3) other migratory-bird or endangered-species management areas that receive water from Department-funded projects.

As the program evolved, it has become a five-phase process: (1) Site Identification, (2) Reconnaissance Investigations, (3) Detailed Studies, (4) Planning, and (5) Remediation. Projects conducted under phases 1-3 are carried out by study teams composed of scientists from the U.S. Geological Survey (USGS), the U.S. Fish and Wildlife Service (FWS), the U.S. Bureau of Reclamation (BOR), and the U.S. Bureau of Indian Affairs. A USGS scientist heads each study team. Activities for phases 4 and 5 are conducted by the BOR.

Media investigated at each location (fig. 1) include surface and ground water, bottom sediment, and biota. Results of completed and active reconnaissance-level investigations and detailed studies have led to several generalizations about areas where problems have been detected: (1) Irrigation drainage problems are prevalent in the western United States; (2) Elevated concentrations of trace elements and pesticides have been detected in some of the study areas; (3) Areas underlain by alkaline, oxidized soils that contain elevated concentrations of trace elements, may become problem areas when irrigation water is applied; (4) Selenium, boron, arsenic, and mercury are the constituents found most often at elevated concentrations in water, bottom sediment, and biota; (5) Concentrations of arsenic and selenium tend to vary inversely; (6) Contamination problems are mostly area specific; and (7) The highest concentrations of the constituents of concern occur in closed drainage basins.

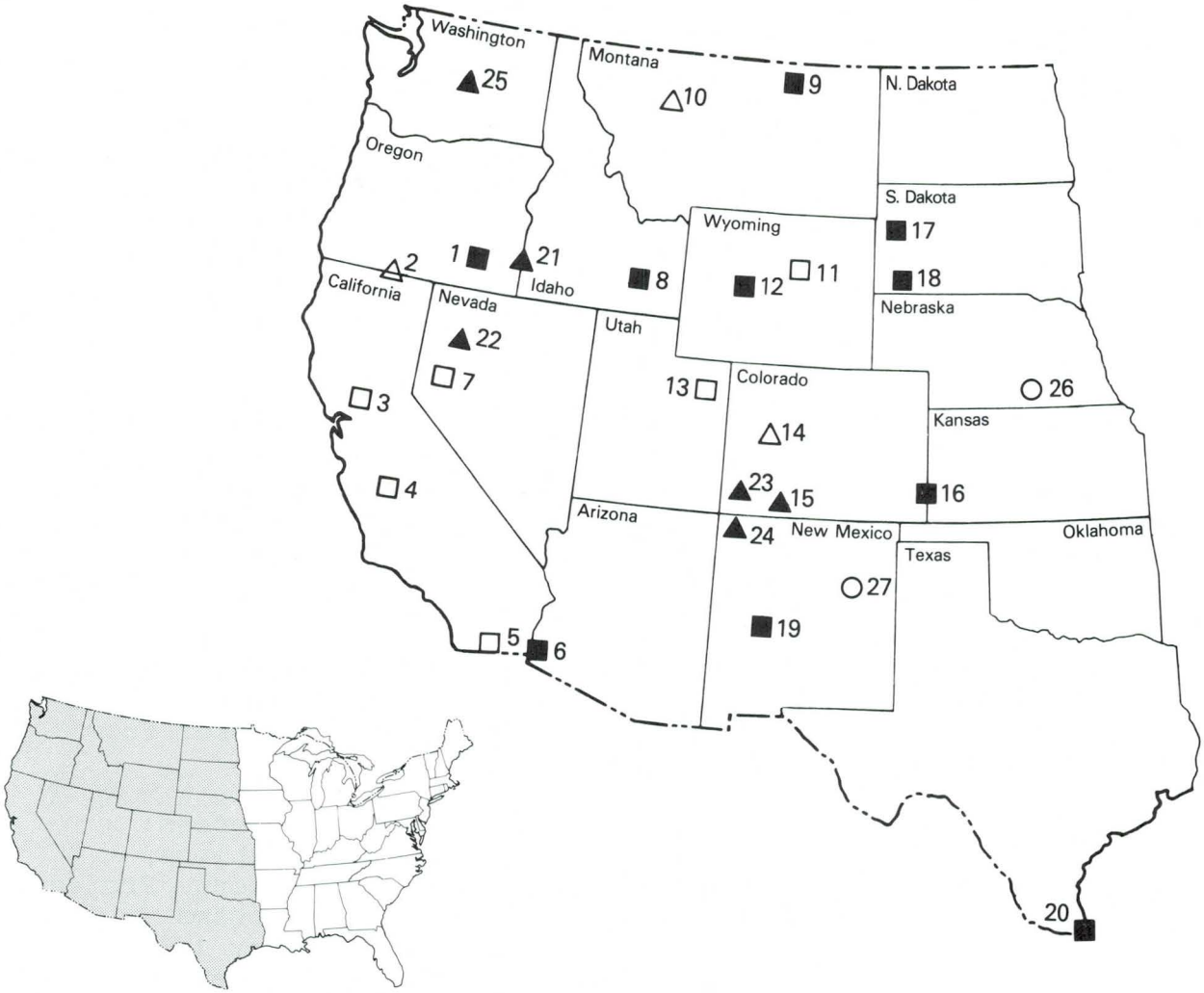

EXPLANATION

■ RECONNAISSANCE INVESTIGATIONS COMPLETED

1. Malheur National Wildlife Refuge, Oreg.
3. Sacramento Refuge Complex, Calif.
4. Tulare Lake Bed Area, Calif.
6. Lower Colorado River Valley, Calif./Ariz.
8. American Falls Reservoir, Idaho
9. Milk River Basin, Mont.
12. Riverton Reclamation Project, Wyo.
15. Pine River Area, Colo.
16. Middle Arkansas River Basin, Colo./Kans.
17. Belle Fourche Reclamation Project, S. Dak.
18. Angostura Reclamation Unit, S. Dak.
19. Middle Rio Grande and Bosque del Apache National Wildlife Refuge, N. Mex.
20. Lower Rio Grande Valley and Laguna Atascosa National Wildlife Refuge, Tex.

□ RECONNAISSANCE AND DETAILED STUDIES COMPLETED

5. Salton Sea Area, Calif.
7. Stillwater Wildlife Mgmt. Area, Nev.
11. Kendrick Reclamation Project Area, Wyo.
13. Middle Green River Basin, Utah

▲ RECONNAISSANCE INVESTIGATIONS UNDERWAY

21. Owyhee-Vale Projects, Oreg./Idaho
22. Humboldt Wildlife Mgmt. Area, Nev.
23. Dolores Project, Colo.
24. San Juan River Area, N. Mex.
25. Middle Columbia Basin, Wash.

△ RECONNAISSANCE COMPLETED AND DETAILED STUDIES UNDERWAY

2. Klamath Basin Refuge Complex, Calif./Oreg.
10. Sun River Area, Mont.
14. Gunnison River Basin/Grand Valley Project, Colo.

○ POTENTIAL RECONNAISSANCE INVESTIGATIONS

26. Bostwick Division, Nebr./Kans.
27. Upper Pecos Basin, N. Mex.

Fig. 1 Locations and names of study areas.

SURFACE-WATER CHEMICAL CHANGES DUE TO HUMAN ACTIVITIES IN THE TARIM BASIN

Wei Zhongyi

Institute of Geography, Chinese Academy of Sciences, Beijing

ABSTRACT

Based on the distribution pattern of the surface water chemical characteristics of the Tarim Basin with time and space, the impact of human activities is analysed. The effect of building large water projects and large-scale reclaiming on the Tarim River and Lake Bosten is especially displayed.

INTRODUCTION

The Tarim Basin, located in Xinjiang Uygur Autonomous Region, is the largest inland basin in chana, and belongs to typical arid area. Its water system includes all the rivers from the South Tianshan Mountains and the north Kunlun Mountains to the Tarim Basin. The tributaries to the Tarim River are only the Aksu River, the Yarkant River and the Hotan River.

Water is one of the most sensitive factors in arid zone, and the surface water chemical characteristics are especially important. The study of surface-water chemical characteristics is hence very important for the utilization of its water resources and the protection of its ecology and environment in arid zone.

THE BASIC CHARACTERISTICS OF THE SURFACE WATER CHEMISTRY

The Vertical Distribution Pattern

The composition of the surface water chemistry is controlled by the zonal geographic conditions. In the Tarim Basin, the climatic and hydrological characteristics vary vertically with the terrain which is from mountains to plains, so the surface water chemical characteristics are accordingly vertically changed. The mountainous river water mostly consists of low mineralization hydrocarbonate. With the increasing of the downstream distance, the hydrochemical types are more and more complex and the mineralization is higher and higher. In the midstream reach of the river, the water easily becomes sulfate water and in the downstream reach therefore, high mineralization sulfate and / or chloride water. The formation of this situation is also due to the river having received natural regression water and to the basin's intensive evaporation and concentration. So the vertical distribution pattern of the surface water chemical characteristics of the Tarim Basin is that the mineralization increases from upstream reach to downstream reach and from mountainous basin to plainous basin, as shown in Fig.1. From Fig.1, the mineralization (dissolved solids) is read as 0.1–0.2 gram per liter (g / L) in the foot of north Kunlun Mountains, increases to 0.2–0.5g / L, 0.5–1.0g / L and 1.0–3.0g / L downstream and lastly becomes 3 g / L in Lake Taitema at the end of the river. The hydrochemical type varies from hydrocarbonate water near the north foot of the Kunlun Mountains to sulfate water and chloride water downstream.

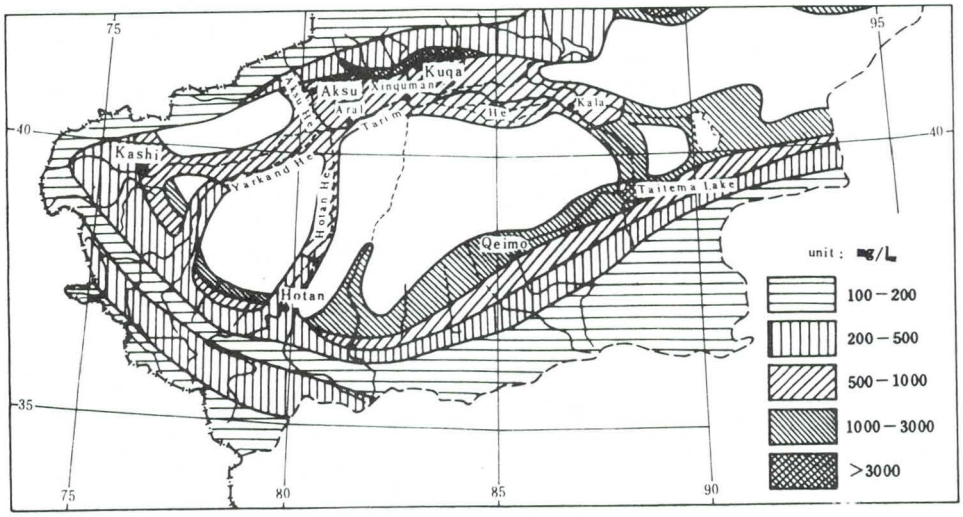

Fig.1. Map showing mineralization (dissolved solids) of the rivers in the Tarim Basin.

The Seasonal Variation of River Chemistry

The seasonal variation of the Tarim River chemistry depends on the seasonal variation of river discharge, which again depends on the precipitation and temperature of the mountainous area. The seasonal snow of middle mountainous area begins to melt from April each year, the process of which will be quickened with the going up of the temperature.It is the melted snow that makes some rivers appear spring floods in May. Till summer (from June to August) the water discharge from the melted snow in alpine and the concentrated water of rainfall result in the summer floods(Han Qing,1985).

Generally, the mineralization of river water is low during floods, but high during the dry season. This is mainly because of groundwater supply. In the Muzhate River, for example, the mineralization during dry seasin is 0.29–0.48g / L, the water chemical type is HCO_3–SO_4–Ca–Na or SO_4–HCO_3–Na–Ca, but during floods the mineralization becomes 0.27–0.36g / L and the hydrochemical type is HCO_3–SO_4–Ca–Na.

The River Water Mineralization and its Ion Conmponent

The ion component of river water varies with the flow route, river runoff and mineralization. There is a certain relationship between river runoff and ion flow and between river runoff and ion total amount. The mineralization generally decreases with increasing runoff discharge. At the Aral station of the Tarim River, for instance, the mineralization of the river water becomes about 0.5g / L when the river discharge is up to $90m^3$ / sec. But the highest value is 5.4g/L during low water.

The mineralization of the river water has a direct bearing on its ion composition. When the mineralization is less than 0.3g / L. the anions of river water take $HCO_3^-$and cations take Ca^{2+}as the dominant factor. But when the mineralization increases to 0.5–1.0g / L, SO_4^{2+}increases, and $Ca^{2+}$and $Mg^{2+}$are accordingly increased: Once the mineralization reaches 1.0g / L, the amount of Cl^-takes the lead in anions. Na^+ increases rapidly but HCO_3^-, $Ca^{2+}$and Mg^{2+}increase slowly.

THE EVOLUTION OF THE TARIM RIVER QUALITY

Large scale reclamation and irrigation began in the Tarim Basin in 1958. The irrigation water drains into the Tarim River. The area of the cultivated land is 20 million

hectares. The reclaimed zone along the Tarim River was mostly produced from the first step terrace, old delta and the edge of alluvial fan where the discharge water passage is impeded and the mineralization of the ground water is high. The soil types before cultivation are relict soil, salinized meadow soil, salinized Huyang soil and solonchak, in which the salinity is high. Salt uashing is done to ameliorate soil for cultivating.

The salinity of cultivated land will continuously decrease with salt washing. After soil desalinization, with less salinity accumulating in the oasis land, more will discharge into river channel with salt washing process. The evolution of the Tarim River water quality is as follows.

According to the water sample analysis of the Sayar station in September of 1958 and the Algan station in April of 1959 by the Comprehensive Survey Team of Xinjiang, Chinese Academy of Sciences, the mineralization of the Tarim River water then was as low as 0.48–0.7g / L. From the data of the Aral station by the Wasteland Survey Team of Xinjiang from May to October in 1958, the mineralization of the Tarim River water was also shown as low as 0.45–0.99g / L. Therefore the Tarim River water in 1950's can be regarded as low mineralization fresh water. Owing to human activities for the next three decades, the water quality of the Tarim River has vastly changed. The details are as follows.

The Water Quality Evolution of the Upstream Reach of the Tarim River

From the data of the Aksu hydrology station, the mineralization of the Aral station in the upstream reach of the Tarim River from May of 1960 to January of 1961 was mostly less than 1g / L and 1.28g / L only in May. The hydrochemical type was HCO_3–Ca–Na. The mineralization during this period was slightly higher than that in 1958. On the basis of the data from the early 1960's to the middle 1970's, however, the mineralization of the Tarim River increased by five to eight times during low water. The gap of the mineralization between low water and floods also increased continously. Fig2 shows the comparison of the mineralization of the Aral station in the Tarim between 1960 and 1977.

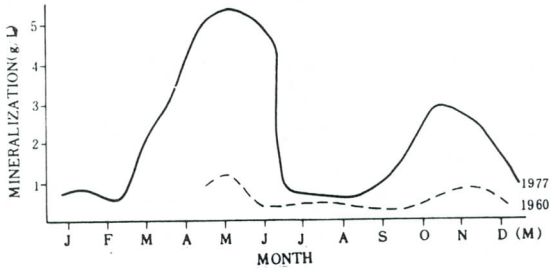

Fig.2. Mineralization in the Tarim river between 1966 and 1977(Aral station)

The former stands for the variation before reclamation of land and the latter stands for that after reclamation of land. The two curves in Fig2 demonstrate that the mineralization of 1977 was totally higher than that of 1966. The difference between floods and dry season in 1966 was a bit but in 1977 was large(Han Qing, 1980).

Based on the data of the Aral station in the Tarim River in 1960, 1965 to 1966, 1985 to 1986, the relationship between river discharge and mineralization is shown as Fig3. It is displayed that the curve of 1965 is close to that of 1960, which demonstrates only a trifling change of the mineralization taken during this period. Only in dry season, there was an obvious difference, in which the mineralization is slightly increased. In the period from 1985 to 1986, however, the range of the variation was large, and the highest valus of the mineralization was more than 6 g / L. A clear conclusion is hence that for these two decades, human activities, especially large–scale land reclamation, made the mineralization of the Tarim River water obviously increase and the water quality deteriorate.

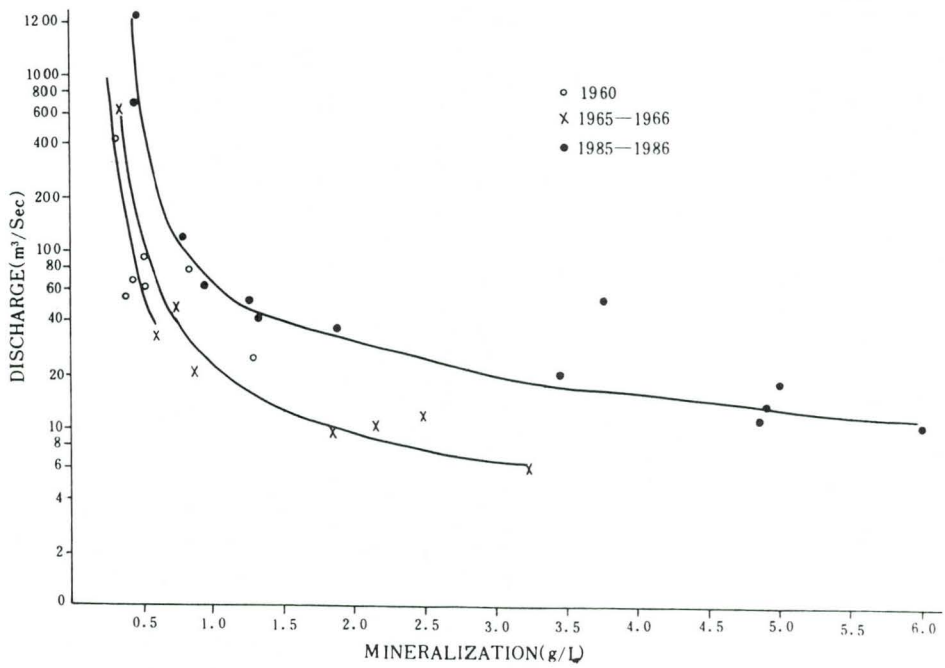

Fig.3. Correlation of mineralization and discharge of the Tarim river (Aral station)

The Water Quality Evolution of the midstream reach (the Xinquman station) of the Tarim River

The Xinquman station of the Tarim River lies 180 kilometers eastward of the Aral station. Based on the station data of 1965, 1985 to 1986, the relationship between the mineralization and discharge is shown as Fig4. Under the condition of the same discharge,the mineralization of the Tarim River water from 1985 to 1986 is higher than that of 1965 according to Fig.4. The difference reflects the range of the increase during the two decades. When the discharge is more than 50 m^3/s, the two curves are close to each other,which shows the mineralization in this case had · little change.When the discharge is less than $50m^3/s$, the scope of the variation of the mineralization is wide and the yearly variation during low water is obvious. It is also shown from Fig 4 that the higher the river water mineralization, the bigger the gap between the two curves. This is enough to illustrate that the river water mineralization during the dry season in the 1980's is higher than that in the 1960's.

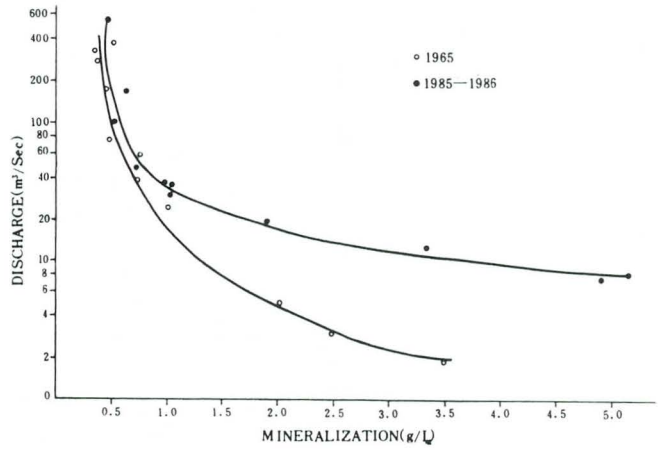

Fig.4. Correlation of mineralization and discharge of the Tarim river (Xinquman station)

The Water Quality Evolution of the Downstream Reach (the Kala Station)of the Tarim River

The Kala station lies in the downstream reach of the Tarim River and 487 kilometers eastward of the Xinquman station. There was no river water chemical field data during the 1950's and 1960's.From the data from November 1976 to October 1977 by the Wasteland Survey Team of Xinjiang in the Kala station, there were 7 months in which the river water mineralization is more than 1 g / L. The highest value is 3.19 g/ L, which appeared in the middle of June. The low mineralization, i.e. less than 1 g/ L, arose in the floods after August and the medium and low water between March and April, in which there was no discharge from upstream reach and the water supply depended on the recession of the ground water along the bank. The mineralization during floods from November to Febuary and dry season from May to July is 1–3 g / L.

Based on the river water chemical field data of the Kala station from July of 1986 to June of 1987,there were 11 months when river water mineralization was more than 1 g/ L. Only in August of floods the mineralization was less than 1 g/ L. The yearly mean river water mineralization is 1.56 g / L, which is higher than that of 1977, i.e. 1.4 g/ L. It is shown that the total variant tendency of river water mineralization is slightly increasing. The highest value 2.86 g / L (June) is less than that in the period from 1976 to 1977 and the lowest value 0.82 g / L (August) is higher than that in the period from 1976 to 1977, i.e. 0.7 g / L (from April to October).

The most important reason of the salinization of the Tarim River water is large–scale reclamation in this area since 1958. The irrigation discharge water gives the Tarim River large amounts of salinity. It is estimated that the salinity discharged into the reach upstream of the Alar station is several million tons per year. The mineralization in the discharge ditches of the old Aksu irrgational area (developed before 1949) was 1–3 g / L and 3–15 g / L after 1949.

THE SALINIZITION OF LAKE BOSTEN AND THE CAUSE OF FORMATION

Lake Bosten is located in the lowest area of Yanqi Basin of southTianshan Mountains. Being once the biggest inland fresh lake in China, it is the largest non–closed lake. Water flows into the lake from the Kaidu River and flows out from the southwest of the lake into the Kongque River. With vast water surface, its length from east to west is about 55 kilometers and width from south to north is about 20–25 kilometers. When the lake water level is 1084 meters, the lake area is 1,000 sq kilometers and the volume is 8.15 billion cubic meters.

The lake Water Salinization Process

According to the investigated data of 1958 by the Comprehensive Survey Team of Xinjiang, China Academy of Sciences, Lake Bosten then belonged to low mineralization fresh lake. Its mineralization was less than 0.4 g / L and the hydrochemical type was HCO_3–Mg–Ca. The mineralization in the west part of the lake was only 0.25 g / L due to the discharge of the Kaidu River and in the east part, where there is no inlet, the value is slightly higher but is still only 0.38 g / L (H.T.Kudznezof and Tang Qicheng,1959).

The investigated data from over 80 water samplings of 1975 by the Wasteland Survey Team of Xinjiang shows that the mineralization and water chemical type were tremendously changed. The mean mineralization of the lake water was 1.44 g / L, which shows that the water then was brackish. The hydrochemical type was SO_4–CL–Na–Mg or SO_4–CL–HCO_3–Mg. The mineralization during these 17 years has increased 1 g / L more than that before, and the yearly rate of increase is 0.06 g / L. The distribution of the lake water mineralization is shown as Fig.5 (Qu Yaoguang and Others, 1986).

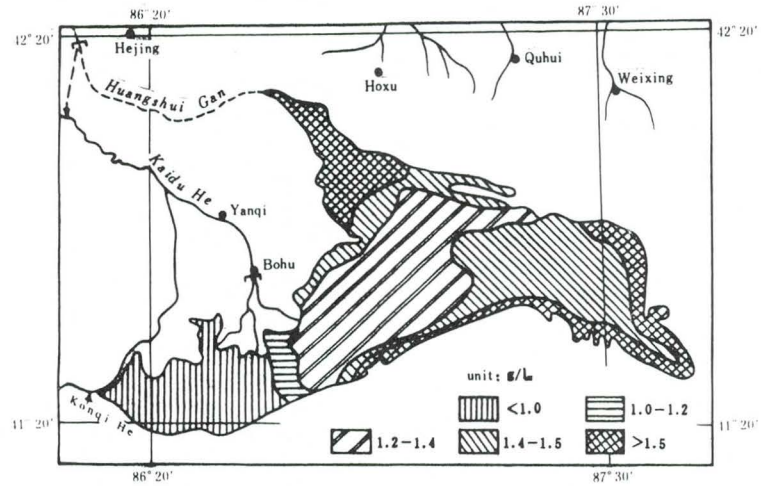

Fig.5. Map of the mineralization distribution of Bosten Lake

The mineralization in the west part of the lake is slightly low as 1.0–1.4 g / L due to the discharge of the Kaidu River. In southeast and south inshore is 1.5–1.7 g / L. The mineralization in the northwest part of the lake which is the confluence of Huangshuigan Ditch is slightly high, ie 1.8–2.6 g / L. Seven water samplings were collected again by the Wasteland Survey Team in May of 1980 and the mean mineralization was shown as 1.72 g / L. In 1981, the Kaidu River Comprehansive Survey Team of Xinjiang collected 71 lake water samplings. The mean mineralization weighted by area was 1.8 g / L. From the data above, the mean yearly rate of increase of mineralization from 1975 to 1981 was 0.08 g / L. Afterwards, lake water samplings were collected by the Territory Renovating Special Team of Bazhou in Xinjiang from 1983 to 1984, the number of which varied from 39 to 84. The values of the mean mineranlization of the lake water were all in the range of 1.81–1.86 g / L. It is shown that although the mineralization of the lake has slightly increased since 1980, the yearly rate of increase has obviously decreased, the value being only 0.02 g / L. So the salinizating speed of the lake in this period is low.

In a word, the lake water has indeed been salinized since the 1950's. To protect the lake emergency measures must be taken.

The Reason of the Salinization of the Lake Water and the Preventive Measures to be Taken

Lake Bosten is the confluence of the surface water, ground water and farmland discharge water of Yanqi Basin. There were only 8670 hectares cultivated land in 1949. The area of the cultivated land has been increasing since large–scale reclamation began in the basin in 1959, and was 82700 hectares in 1980 which is about 10 times of that in 1949. The new reclaimed area is mostly produced from the edge of diluvial fan or the delta downstream of the Kaidu River and alluvial plain. In these areas, the salinity is very high. Therefore, to improve the soil, salt washing measures must be taken. The amount of the salt washing water discharged into Lake Bosten each year is about 0.46 billion m^3, (estimated by the Institute of Soil and Fertilizer, Xinjiang Agriculture Academy in 1982), and the total salinity discharged into the lake is 1.0855 million tons, over 40% of which is from farmland discharge water. This is the important reason that results in the rapid salinization of Lake Bosten water. Moreover, the amount of diverted water for farmland irrigation from the lake has been increasing since 1949, until in 1980 it was up to 1.46 billion m^3, which radically reduced the amount of water in the lake.

Reduction of discharge water from salt washing and an increase in the fresh water inflow to the lake will reduce further salinization of Lake Bosten. One of the best meas-

ures is to open up the ground water of Yanqi Basin which is rich in ground water resources and has excellent conditions for exploitation. On the one hand the amount of recharge ground water is 1590 million m^3 per year, the beneficial condition to develop well irrigation and ground water engineering. On the other hand the amount of the ground water exploited is only 47 million m^3 per year which is 5% of the extracting resources (Wei Zhongyi and Tang Qicheng 1987).

REFERENCE

1.The Comprehensive Survey Team of Xinjiang, Chinese Academy of Sciences, Xinjiang Hydrogeography, Sciences Press. 1966

2.Han Qing, Hydrochemistry and Hydrogeographic Chemistry in the South Foot of Tianshan Mountains, The Physiography of Chinese Arid Area. Sciences Press, 1985.

3.Han Qing, The Variation and Control Measures of Water Quality of the Tarim Basin after Reclaiming, Geography Journal, Beijing, Vol 35. No 3. 1980.

4.H.T.Kudznezof, Tang Qicheng, The Introduction of Hydrochemistry of the Rivers in East Tianshan Mountains, The Natural Conditions of the Xinjiang Uygur Autonomous Region (Symposium), Science Press, 1959.

5.Qu Yaoguang et.al, The Salinization of Lake Bosten and the control, The Symposium of the Third National Academic Conference of Chinese Geography Union, Science Press, 1986

6.Wei Zhongyi, Tang Qicheng, The Hydrologic Effect after Developing the Water Resources of Northwest Arid Area and the Variation of Utility Model, Natural Resources Journal, Beijing, Vol.2 No 3, 1987.

CONCENTRATION AND DISTRIBUTION OF SELENIUM ASSOCIATED WITH IRRIGATION DRAINAGE IN THE WESTERN UNITED STATES

R. A. Engberg

Department of the Interior, Washington, D.C.

ABSTRACT

Concentrations, distribution and sources of selenium from irrigated lands were studied between 1986 and 1990 at 20 reconnaissance project areas in western States under the Department of the Interior's National Irrigation Water Quality Program. Samples of water, bottom sediment, whole-body fish, and bird livers for analysis of selenium concentrations were collected before, during, and after irrigation season from streams, canals, lakes, and groundwater in each project area. Selenium concentrations in water ranged from less than the reporting limit of 1 microgram per liter in 42 percent of the 586 samples collected to 4,800 micrograms per liter from a well in the Pine River Area in southern Colorado. Selenium concentrations in 223 samples of bottom sediment ranged from less than the reporting limit of 0.1 microgram per gram to 85 micrograms per gram in a sample from the Middle Green River Basin in Utah. Selenium concentrations in whole-body fish (all species) ranged from 0.1 to 50 micrograms per gram dry weight with the maximum concentration observed in a carp from the Gunnison River Basin in western Colorado. Selenium concentrations in bird livers (all species) ranged from less than 0.32 to 170 micrograms per gram dry weight with the maximum concentration observed in the liver of an avocet from the Kendrick Reclamation Project Area in Wyoming.

INTRODUCTION

Water quality problems related to elevated concentrations of dissolved solids in irrigation drainwater occur in many areas of the United States. In 1983, the link between irrigation drainwater and elevated concentrations of selenium was made after waterfowl deaths, deformities, and reproductive failures at Kesterson Reservoir in California were observed. The Department of the Interior in 1985 began the National Irrigation Water Quality Program (NIWQP) to determine whether problems of selenium and other inorganic or organic trace constituents in irrigation drainwater similar to those at Kesterson Reservoir existed in other western States.

Reconnaissance investigations were completed for 20 areas (Figure 1) between the years 1986 and 1990. Reconnaissance investigations are field-sampling studies to determine levels of potentially toxic constituents in the water, bottom sediment, and biota of the study areas. Samples generally were collected before, during, and after the irrigation season. Samples were analyzed for major and trace constituents and in some cases, for pesticides.

CONCENTRATIONS AND DISTRIBUTION OF SELENIUM

Selenium has been detected in samples of water, bottom sediment, or biota from all 20 reconnaissance study areas. Although selenium is the constituent that has the greatest potential for toxic effects on biota in most of the study areas, other trace constituents are of concern in some areas.

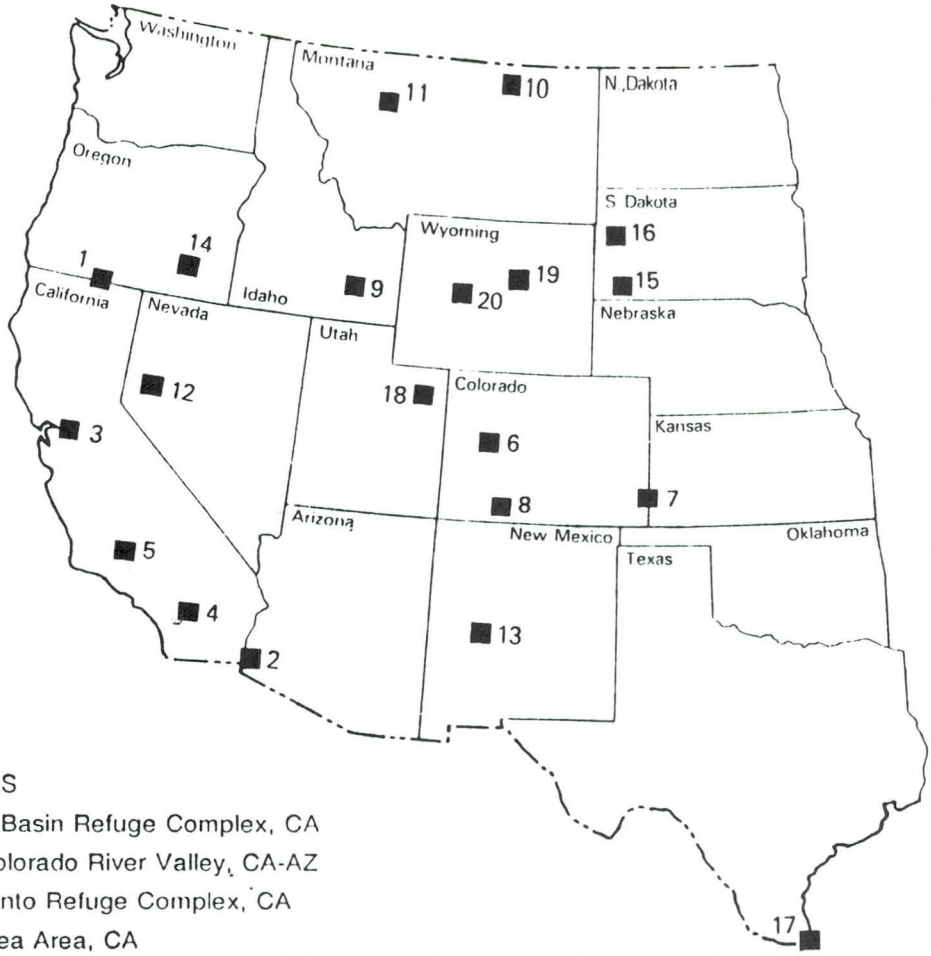

STUDY SITES

1. Klamath Basin Refuge Complex, CA
2. Lower Colorado River Valley, CA-AZ
3. Sacramento Refuge Complex, CA
4. Salton Sea Area, CA
5. Tulare Lake Bed Area, CA
6. Gunnison River Basin, CO
7. Middle Arkansas River Basin, CO-KS
8. Pine River Area, CO
9. American Falls Reservoir, ID
10. Milk River Basin, MT
11. Sun River Area, MT
12. Stillwater Wildlife Management Area, NV
13. Middle Rio Grande and Bosque del Apache National Wildlife Refuge, NM
14. Malheur National Wildlife Refuge, OR
15. Angostura Reclamation Unit, SD
16. Belle Fourche Reclamation Project, SD
17. Lower Rio Grande and Laguna Atascosa National Wildlife Refuge, TX
18. Middle Green River Basin, UT
19. Kendrick Reclamation Project Area, WY
20. Riverton Reclamation Project, WY

Figure 1: Locations of reconnaissance areas, National Irrigation Water Quality Program, 1986-1990

Table 1. Selenium concentrations in water from reconnaissance study areas. [Units are micrograms per liter (ug/l). Analytical reporting limit is 1 ug/l. Study areas are keyed to Figure 1.]

Study Area	Abbreviated Name	Number of Samples	Range of observed concentrations (ug/l)	Median	Number of observations less than reporting limit
1	Klamath	18	< 1	< 1	18
2	Lower Colorado	14	< 1 - 2	2	3
3	Sacramento	28	< 1	< 1	27
4	Salton Sea	12	1 - 300	19	0
5	Tulare	12	< 1 - 390	35	5
6	Gunnison	37	< 1 - 320	12	5
7	Arkansas River	26	1 - 52	6	0
8	Pine River	69	< 1 - 4800	2	26
9	American Falls	18	< 1 - 6	<1	13
10	Milk River	16	< 1 - 1	<1	15
11	Sun River	27	< 1 - 580	2	8
12	Stillwater	78	< 1 - 1	< 1	71
13	Middle Rio Grande	29	< 1 - 1	< 1	28
14	Malheur	22	< 1	< 1	22
15	Angostura	34	< 1 - 16	3	2
16	Belle Fourche	41	< 1 - 34	3	2
17	Lower Rio Grande	16	< 1 - 2	< 1	10
18	Green River	43	< 1 - 140	17	8
19	Kendrick	24	< 1 - 300	8	4
20	Riverton	26	< 1 - 12	2	4

Selenium in Water

Analytical results of selenium in water for all sampling sites from 20 reconnaissance study areas are presented in Table 1. Sampling sites in each area include irrigation drainwater, irrigation supply, ground water, receiving water sites (streams, wetlands, etc.) and reference sites. For comparison between study areas, results of water samples from all sources in each area are grouped for discussion with the understanding that they provide the widest spectrum of selenium concentrations that may occur in water in that area. Analytical results were provided by the U.S. Geological Survey Water Resources Division Central Laboratory in Denver, Colorado. Study areas in Table 1 are keyed by number and abbreviated name to Figure 1. Results presented in Table 1 and in all following tables are from data available in U.S. Geological Survey files and/or in the following publications: Study area 1, Sorenson and Schwarzbach (1991); 2, Radtke and others (1988); 4, Setmire and others (1988);

5, Schroeder and others (1988); 9, Low and Mullins (1990); 10, Lambing and others (1988); 11, Knapton and others (1988); 12, Hoffman and others (1990); 15, Green and Sowards (1991); 16, Roddy and others (1991); 17, Wells and others (1988); 18 Stephens and others (1988); 19, Peterson and others (1988); and 20, Peterson and others (1991). Reconnaissance investigation reports are in preparation or in review for study areas 3,6,7,8,13, and 14. These reports like those referenced above are planned for release as U.S. Geological Survey Water-Resources Investigations Reports.

Selenium concentrations in a total of 590 water samples from all reconnaissance study areas range from less than the reporting limit of 1 ug/l to 4800 ug/l in a sample collected from a shallow well in the Pine River Area. A total of 271 samples (46 percent) from 18 of the 20 areas had concentrations of less than the detection limit and the minimum selenium concentration for all areas was at or below the reporting limit. At the Klamath, Sacramento, and Malheur study areas, no selenium was detected in any water samples. At the Milk River, Stillwater, Lower Colorado, Middle Rio Grande and Lower Rio Grande areas, maximum selenium concentrations were 2 ug/l or less. Selenium concentrations were less than 5 ug/l in approximately 70 percent of all samples from all areas. The median selenium concentration was less than 1 ug/l at the Klamath, Sacramento, American Falls, Milk River, Stillwater, Malheur and Lower Rio Grande areas. The median value of 35 ug/l selenium for the Tulare area exceeds the U.S. Environmental Protection Agency (EPA) (1987) acute criterion for protection of freshwater aquatic life of 20 ug/l. The median values of 19, 12, and 17 ug/l selenium for the Salton Sea, Gunnison, and Middle Green areas, respectively, exceed the EPA (1986b) drinking water standard of 10 ug/l. Fewer than 10 percent of all samples from all areas had concentrations of selenium greater than 20 ug/l and these concentrations were found in samples from only nine areas. Large concentrations of selenium (>100 ug/l) were found in 18 samples (3 percent) from seven areas (Salton Sea, Tulare, Gunnison, Pine River, Sun River, Middle Green, and Kendrick).

In general, selenium concentrations in water in those areas where large concentrations (>100 ug/l) were found were not distributed evenly throughout the area and tended to be found principally in drainwater, ground water, or wetlands and associated ponds in or near areas of known selenium "hot spots." For example, in the Pine River area, out of a total of 69 samples, ten samples of ground water were collected with selenium concentrations ranging from 30 to 4800 ug/l. Ground water sampling on the other hand was biased to a known seleniferous area. Conversely, 26 out of the 59 samples collected at surface water sites in the Pine River area had selenium concentrations less than the detection limit of 1 ug/l. The median concentration for all samples from the Pine River area was 2 ug/l.

Selenium in Bottom Sediment

Analytical results of selenium in bottom sediment (Table 2) represent only the fine material (<0.062 millimeters in diameter) in surficial sediment (upper 50 millimeters). Samples were collected from streams and wetlands during conditions of low streamflow in each area, most frequently following irrigation season (October-November). Samples were sieved either in the field or in the laboratory and results were determined on both the fine material and the larger-size material between 0.062 millimeters and 2 millimeters in diameter. Because of the greater surface exposure of fine material, most transport of trace

constituents by sediment probably occurs in this phase. Only these data are discussed herein. Study areas in Table 2 are keyed by number to Figure 1. Analyses of bottom sediment samples were provided by the U.S. Geological Survey Geologic Division Laboratory in Denver, Colorado.

A total of 221 bottom sediment samples were collected from all areas and analyzed for total selenium concentrations. Compared to an upper limit of the expected 95 percent baseline range of 1.4 micrograms per gram (ug/g) dry weight (Feltz and others, 1991) for selenium in soils of the western United states, selenium concentrations in about 22 percent of the samples exceeded the baseline. Selenium concentrations in bottom sediment from all sites in the Klamath, Sacramento, Pine River, Milk River, Sun River, Stillwater, Malheur, and

Table 2. Total selenium concentrations in bottom sediment less than 0.062 millimeters from reconnaissance study area. [Units are micrograms per gram (ug/g) dry weight. Analytical reporting limit is 0.1 ug/g.]

Study Area	Abbreviated Name	Number of Samples	Range of observed concentrations (ug/g)	Median	Number of observations less than reporting limit
1	Klamath	13	0.1 - 0.7	0.6	0
2	Lower Colorado	12	<0.1 - 7.1	0.9	1
3	Sacramento	13	0.1 -.4	0.2	0
4	Salton Sea	17	0.1 - 3.3	0.7	0
5	Tulare	9	<0.1 - 19	0.2	1
6	Gunnison	6	1.5 - 41	2.2	0
7	Arkansas River	13	0.5 - 5.4	1.3	0
8	Pine River	10	0.2 - 0.8	0.5	0
9	American Falls	9	0.1 - 1.9	0.4	0
10	Milk River	6	0.3 - 6.7	0.4	0
11	Sun River	14	0.3 - 0.6	0.8	0
12	Stillwater	17	<0.1 - 1.2	0.5	1
13	Middle Rio Grande	11	0.2 - 0.4	0.3	0
14	Malheur	5	0.1 - 0.6	0.2	0
15	Angostura	9	0.6 - 14	1.0	0
16	Belle Fourche	10	0.6 - 2.8	0.9	0
17	Lower Rio Grande	15	0.3 - 0.7	0.4	0
18	Green River	9	<0.1 - 85	7.1	1
19	Kendrick	9	0.9 - 25	2.5	0
20	Riverton	14	0.1 - 3.0	0.4	0

Lower Rio Grande areas did not exceed the baseline. Conversely, selenium concentrations in all samples collected from the Gunnison area and nearly all samples from the Middle Green and Kendrick areas did exceed the baseline.

Median selenium concentrations for these three areas are 2.2, 7.1, and 2.5 ug/g respectively. Median concentrations do not exceed the baseline for any of the other areas. The maximum concentration of 85 ug/g was found in a sample from the Middle Green River Basin in Utah (area 18).

In some areas, elevated selenium concentrations in bottom sediment tend to correspond to elevated selenium concentrations in water (Gunnison, Middle Arkansas, Middle Green, and Kendrick areas). In the Klamath, Sacramento, and Malheur areas, where selenium concentrations in all water samples were less than the reporting limit, median concentrations of selenium in bottom sediment ranged from 0.2 - 0.6 ug/g and maximum concentrations ranged from 0.4 - 0.7 ug/g, all of which are considerably less than the baseline. These concentrations of selenium probably can be considered naturally occurring and at background levels.

Selenium in Fish

Analytical results of selenium in whole-body fish samples for all sampling sites from all reconnaissance study areas are presented in Table 3. Study areas are keyed by number to Figure 1 and all values represent selenium concentrations in micrograms per gram dry weight for whole-body fish samples. Results from all species from cold-water sport fish to warm-water bottom feeders collected from each area are combined in the data table. Analytical results were provided by Fish and Wildlife Service laboratories or their contract laboratories.

A total of 911 individual or composite fish samples from all areas were analyzed for total selenium concentrations. Concentrations ranged from 0.1 ug/g dry weight in a Utah sucker from the American Falls Reservoir to 50 ug/g dry weight in a carp from the Gunnison River Basin. Baumann and May (1984) indicate a threshold concentration of about 8.0 ug/g dry weight selenium for adverse reproductive effects in fish. Approximately 16 percent of all samples from all areas had concentrations exceeding 8 ug/g selenium, dry weight. Selenium concentrations for all samples from all sites in the Sacramento, Klamath, Tulare, American Falls, Milk River, Middle Rio Grande, Malheur, Belle Fourche, and Lower Rio Grande were less than 8 ug/g. In contrast, selenium concentrations in 58 percent of all samples collected from the Middle Arkansas area (median 11 ug/g) and in 80 percent of all samples collected from the Middle Green area (median 20 ug/g) were greater than 8 ug/g.

Although it was assumed that species-to-species differences in selenium uptake might occur, concentrations of selenium generally varied narrowly among all species collected at the same sampling site in areas where high concentrations of selenium in fish samples occurred. In many cases, however, average concentrations in all fish at one site varied widely with average concentrations in all fish at a different site in the same area. This indicates that all species of fish tend to accumulate selenium similarly in their body tissues and that the availability or nonavailability of selenium to the food chain is responsible for the differences in accumulation of selenium in fish among sites.

Table 3. Selenium concentrations in fish (all species) from reconnaissance study areas. Units are micrograms per dry weight (ug/g). [Analytical reporting limit is 0.1 ug/g.]

Study Area	Abbreviated Name	Number of Samples	Range of observed concentrations (ug/g)	Median	Percent of samples with concentrations >8.0 ug/g
1	Klamath	19	0.43 - 1.2	0.70	0
2	Lower Colorado	31	2.4 - 16	6.1	32
3	Sacramento	27	0.50 - 2.0	1.4	0
4	Salton Sea	25	3.5 - 20	7.7	48
5	Tulare	33	0.60 - 4.3	1.5	0
6	Gunnison	55	1.3 - 50	5.0	27
7	Arkansas River	59	2.1 - 20	11	58
8	Pine River	153	0.92 - 16	4.2	16
9	American Falls	10	0.1 - 2.6	1.0	0
10	Milk River	2	2.3 - 2.5	2.4	0
11	Sun River	8	2.2 - 48	2.5	25
12	Stillwater	98	0.69 - 11	1.7	3.1
13	Middle Rio Grande	14	0.57 - 1.7	0.96	0
14	Malheur	11	0.66 - 3.1	2.0	0
15	Angostura	126	2.1 - 13	4.4	8.6
16	Belle Fourche	128	1.4 - 5.3	2.8	0
17	Lower Rio Grande	22	0.59 - 3.4	1.7	0
18	Green River	10	3.1 - 31	20	80
19	Kendrick	11	1.9 - 49	6.1	27
20	Riverton	69	0.48 - 15	5.9	28

Generally, for areas and sites within areas where elevated concentrations of selenium occurred in fish samples, elevated concentrations also occurred in water and bottom sediment. A comparison of median values indicated that concentrations of selenium in fish were higher than in water and in bottom sediment in all areas. This indicates that bioaccumulation of selenium occurs in all areas. Bioaccumulation is greatest in the Gunnison, Middle Green, and Kendrick areas, where the largest amounts of selenium occur in water and in bottom sediment.

Table 4. Selenium concentrations in bird livers (all species) from reconnaissance study areas. [Units are micrograms per gram (ug/g) dry weight. Analytical reporting limit is 0.1 ug/g. NA = not available.]

Study Area	Abbreviated Name	Number of Samples	Range of Observed concentrations (ug/g)	Median (ug/g)	Percent of sampled with concentrations greater than 9 ug/g	30 ug/g
1	Klamath	15	2.8 - 16	4.2	13	0
2	Lower Colorado	0	-	-	-	-
3	Sacramento	52	1.5 - 11	3.7	1.9	0
4	Salton Sea	23	6.7 - 42	19	78	4.3
5	Tulare	10	26 - 120	> 30	100	NA
6	Gunnison	17	6.5 - 84	31	88	53
7	Arkansas River	78	< .32 - 56	16	69	14
8	Pine River	9	4.2 - 50	6.8	44	22
9	American Falls	10	0.80 - 42	8.0	40	20
10	Milk River	14	2.1 - 7.4	3.4	0	0
11	Sun River	15	2.3 - 46	25	80	33
12	Stillwater	239	1.0 - 48	6.9	38	7.1
13	Middle Rio Grande	24	0.85 - 9.1	3.7	4.2	0
14	Malheur	15	3.9 - 36	14	80	6.7
15	Angostura	0	-	-	-	-
16	Bell Fourche	8	6.5 - 28	12	50	0
17	Lower Rio Grande	0	-	-	-	-
18	Green River	17	2.0 - 43	7.1	35	12
19	Kendrick	12	13 - 170	30	100	58
20	Riverton	32	1.3 - 35	9.0	51	2.9

Selenium in Bird Livers

Analytical results of selenium in livers from all waterfowl collected at sampling sites in 17 reconnaissance study areas are presented in Table 4. Study areas in Table 4 are keyed by number to Figure 1 and all values represent selenium in micrograms per gram dry weight. Samples were not collected from the Lower Colorado, Angostura, and Lower Rio Grande areas. Results from all species from which livers were collected and analyzed, including ducks, shorebirds, raptors, and others, are combined in the data from each area. Analyses of livers from both adult and juvenile birds are included in Table 4. It is understood that there may be species-to-species differences in selenium uptake and that this artificial grouping may interfere with interpretation of the data. Analytical results were provided by Fish and Wildlife Service laboratories or their contract laboratories.

Livers from a total of 590 adult and juvenile birds collected from the 17 areas were analyzed for total selenium concentrations. Ranges of observed selenium concentrations and median values are compared to a level of 9 ug/g dry weight, which is the lower concentration of a range of 9 - 41 ug/g associated with adverse reproductive effects in mallards, including reduced egg laying and survival of chicks, according to Heinz and others (1987). Ranges and medians also are compared to a level of 30 ug/g dry weight above which embryonic deformities in birds are likely to occur (Skorupa and others, 1990).

Selenium concentrations in bird livers ranged from <0.32 ug/g dry weight in the liver of a coot from the Middle Arkansas River Basin to 170 ug/g dry weight in the liver of an avocet from the Kendrick Reclamation Project Area. Selenium concentrations were less than 9 ug/g in livers of all birds collected from the Milk River area. The selenium concentration (9.1 ug/g) in the liver of one bird from the Middle Rio Grande area exceeded 9 ug/g. Median selenium concentrations were less than 9 ug/g for these areas as well as for the Klamath, Sacramento, Pine River, American Falls, Stillwater, Middle Green, and Riverton areas. Median selenium concentrations exceeded 9 ug/g for 7 areas and were 30 ug/g or greater for the Tulare, Gunnison and Kendrick areas. Selenium concentrations in bird livers exceeded 30 ug/g in approximately 10 percent of all birds from all areas and exceeded 9 ug/g in approximately 46 percent of all birds. Deformed birds were found in the Tulare, Sun River, Stillwater, Middle Green, and Kendrick areas but the cause of the deformities in the birds at the Stillwater area may be a trace constituent other than selenium.

Some birds collected at 16 of the 17 sites accumulated selenium in their livers in potentially harmful quantities (> 9 ug/g). This occurred even in areas where selenium concentrations in other sampled media generally were low. This shows that selenium is readily bioaccumulated. Because mostly adult birds were collected, there is no way to know for certain whether the selenium in the liver was obtained at nearby sites, or from sites in other areas long distances away. However, the sampling programs were set up such that only adult birds thought to have arrived in the areas several weeks earlier were collected.

SOURCES OF SELENIUM

Cretaceous-age marine shales probably are the original sources for selenium in 16 of the 20 areas studied. This may be a direct or indirect relationship. For example, the Cretaceous-age Cody Shale underlies part of the Kendrick area and some soils formed directly on the shale. Selenium accumulating plants are found in the area. Large concentrations of selenium, presumably leached from the soil, were found both in water and bottom sediment samples from the area and in whole fish and livers of some of the birds collected from the area. Conversely, the Salton Sea area is an example of Cretaceous-age shales as an indirect source of selenium. No selenium sources occur in the vicinity of the Salton Sea area, but small amounts of selenium are contained in irrigation water diverted to the All-American Canal from the Colorado River. Selenium in the Colorado River is from Cretaceous-age deposits located in the Colorado River Basin upstream of the All American Canal diversion. Evaporative concentration of the irrigation water is the mechanism responsible for elevated selenium concentrations in water, bottom sediment and biota in the Salton Sea area.

Permian-age deposits, lacustrine deposits, and Cenozoic-age volcanic deposits may be sources for extremely limited amounts of selenium in the other four areas.

GENERAL OBSERVATIONS

Several observations based on data from all 20 areas are summarized below:

1) In areas where large concentrations of selenium in water were found, concentrations were not widely distributed over the area, but were found principally in drainwater, ground water, ponds, or wetlands.
2) Elevated selenium concentrations in bottom sediment generally tend to correspond with elevated selenium concentrations in water.
3) All species of fish sampled tend to accumulate selenium in their body tissues.
4) Comparisons of median selenium concentrations in water and in fish tissue, and in bottom sediment and fish tissue indicate that bioaccumulation of selenium occurs in all areas.
5) The normal ratio of median bird liver selenium concentration to bottom sediment selenium concentration appears to be in the 7:1 to 31:1 range.
6) Cretaceous-age marine shales are the principal sources of selenium in 16 of the 20 areas studied.
7) The potential for irrigation-induced water quality problems is enhanced in areas where closed drainage basins or sinks occur. Evaporative concentration of selenium may occur in these and other areas.
8) Climatic conditions, including variations in rainfall and streamflow, may affect the potential for irrigation-induced water quality problems from selenium and other trace constituent concentrations.

REFERENCES CITED

Baumann, P. C., and May, T. W., 1984, Selenium residues in fish from inland waters of the United States: in Workshop proceedings, The effects of trace elements on aquatic ecosystems, March 23-24, 1982, Raleigh, North Carolina: Electric Power Research Institute, Palo Alto, California, p. 7-1 to 7-16.

Feltz, H. R., Sylvester, M. A., and Engberg, R. A., 1991, Reconnaissance investigations of the effects of irrigation drainage on water quality, bottom sediment, and biota in the western United States: Proceedings, Toxic Substances Hydrology Technical meeting, March 11-15, 1991, Monterey, California, in press.

Heinz, G. H., Hoffman, D. J., Krynitsky, A. J., and Weller, D.M.G., 1987, Reproduction in mallards fed selenium: Environmental Toxicology and Chemistry, v.6, p. 001-011.

Greene, E. A., and Sowards, C. L., 1991, Reconnaissance investigation of water quality, bottom sediment, and biota associated with irrigation drainage in the Angostura Reclamation Project area, South Dakota 1988-89: U.S. Geological Survey Water-Resources Investigations Report 90-4152, 75p.

Hoffman, R. J., Hallock, R. J., Rowe, T. G., Lico, M. S., Burge, H. L., and Thompson, S. P., 1990, Reconnaissance investigations of water-quality, bottom sediment and biota associated with irrigation drainage in and near Stillwater Wildlife Management Area, Churchill County, Nevada, 1986-87: U.S. Geological Survey Water-Resources Investigations Report 89-4105, 150 p.

Knapton, J. R., Jones, W. E. and Sutphin, J. W., 1988, Reconnaissance investigation of water quality, bottom sediment, and biota associated with irrigation drainage in the Sun River Area, West-Central Montana, 1986-87: U.S. Geological Survey Water-Resources Investigations Report 87-4244, 78 p.

Lambing, J. H., Jones, W. E. and Sutphin, J. W., 1988, Reconnaissance investigation of water quality, bottom sediment, and biota associated with irrigation drainage in the Bowdoin National Wildlife Refuge and adjacent areas of the Milk River Basin, Northeastern Montana, 1986-87: U.S. Geological Survey Water-Resources Investigations Report 87-4243, 71 p.

Low, W. H., and Mullins, W. H., 1990, Reconnaissance investigation of water quality, bottom sediment, and biota associated with irrigation drainage in the American Falls Reservoir area, Idaho 1988-89: U.S. Geological Survey Water-Resources Investigations Report 90-4120, 78 p.

Peterson, D. A., Jones, W. E. and Morton, A. G., 1988, Reconnaissance investigation of water quality, bottom sediment, and biota associated with irrigation drainage in the Kendrick Reclamation Project area, Wyoming, 1986-87: U.S. Geological Survey Water-Resources Investigations Report 87-4255, 57 p.

Peterson, D. A., Harms, T. F., Ramirez, Jr., P., Allen, G.T., and Christenson, A. H., 1991, Reconnaissance investigation of water quality, bottom sediment, and biota associated with irrigation drainage in the Riverton area, Wyoming 1988-89: U.S. Geological Survey Water-Resources Investigations Report 90-4187, 84 p.

Presser, T. S., and Swain, W. C., 1991, Geochemical evidence for Se mobilization by the weathering of pyritic shale, San Joaquin Valley, California, U.S.A.: Applied Geochemistry, vol. 5, p. 703-717.

Radtke, D. B., Kepner, W G. and Effertz, R. J., 1988, Reconnaissance investigation of water quality, bottom sediment, and biota associated with irrigation drainage in the Lower Colorado River Valley, Arizona, California, and Nevada, 1986-87: U.S. Geological Survey Water-Resources Investigations Report 88-4002, 77 p.

IMPACT OF WATER RESOURCES UTILIZATION ON THE ECOLOGICAL ENVIRONMENT IN THE XINJIANG ARID REGION, CHINA

Zhou Tianxiang and Tang Minda

Xinjiang University , Urumqi , Xinjiang , China

ABSTRACT

Under the influence of natural and human factors, the utilization of water resource in Xinjiang has evidently shown a tendency that may be called " hydrotropism". Several new artificial ecological systems have formed as a result of various ways of water resource use. For this reason, a series of questions regarding environmental changes are raised. On the basis of summing up former experience, this article makes a synthetic environmental evaluation of the main problems in the utilization of water resources in Xinjiang, and then seeks laws to provide a scientific basis for rational development and utilization of water resources in Xinjiang.

INTRODUCTION

Surrounded with mountains, Xinjiang is located in the center of Eurasia. With little rainfall and a fragile environment, it is the largest inland arid area of China and one of the famous arid areas in the world. Total water resources (including surface and ground water) in Xinjiang is nearly 88. 0 billion m^3 per year, of which available groundwater is 25. 2 billion m^3. At present, most of water resource used are provided by surface water (as much as 46 billion m^3 per year), which is 47. 4 percent of total water resource in Xinjiang. With the development of the economy, the influence of the use of water on the environment of the Xinjiang arid area has become greater and greater. Overexploitation and misuse of water resources commonly make environmental deterioration irreversable. In order to achieve the best economic, social and environmental benefit, it has become imperative to study the patterns of water usage in Xinjiang. the results of such a study would hopefully provide information to assit in avoiding waste and making wise use of this limited and precious resource.

THE TREND OF SUCCESSION OF DEVELOPMENT AND UTILIZATION OF WATER RESOURCE IN XINJIANG DETERMINED THE MACROPATTERN OF THE ECOLOGICAL ENVIRONMENT

Water is the prerequisite for the development and utilization of every kind of resources in Xinjiang . The state and degree of the development and utilization of water resources control and affect the development of the

regional economy and prosperity of the society. For thousands of years, such maxims of existence as, "Where there is water, there is everything," and, "Water is the lifeblood," have governed people's development and use of the limited water resource in arid areas, and have made people's action a distinct tendency, which can be called "hydrotropism". The "hydrotropism" tendency shows as follows in Xinjiang.

From the View of the Whole Region, the Tendency is toward the Northwest

If we draw a line from Cele (the east of Hotan) to Yanqi to Qitai, dividing Xinjiang into two part of similar area, we find that the annual basin yield in the northwest part is 73. 75 billion m^3, which accounts for 93 percent of the whole basin yield in Xinjiang, whereas the yield of the southeast part is 5. 55 billion m^3, which accounts for only 7 percent. Such a distribution pattern of water resource makes people move to the northwest. For example, in the northwest, in places such as Altai, Yili, Aksu and kashi, the cultivated area is larger.

In the Range of Drainage Area, the Tendency is towards the Area within the Upper or Middle Reaches of the River

There are 570 rivers of all sizes and 270 springs in Xinjiang. Generally, the sources of the river discharge are stable; they make up the main part of the water resources in Xinjiang and are regarded as the "lifeline" of arid areas. Along these lifelines, there grow a series of oases like beads on a string. With the development of social production, people rely more and more on the lifeline and their wants become higher and higher. Being near the mountain area where runoff is formed, those who are in the upper and middle reaches of the river can get water at a high water—supply provision ratio; high—water — consuming actions such as diverting water to reclaim wasteland, flood irrigating, and developing mining or manufacturing industry can be seen frequently. However, getting water at lower and lower water—supply provision ratios, areas within the lower reaches of the rivers are facing serious problems. The Tarim River in the southern Xinjiang is a typical example.

The Tarim River has the natural function of diverting water. It divert part of the water in Tarim Basin from the western part of the basin (which accounts for 55 percent of whole area and 82 percent of the yield) to the east, and plays an important role in maintaining the ecological environment in the eastern part of the Tarim Basin. But with large quantities of water diverted and retained within the upper reaches of the river and large water —consuming actions within the upper and middle reaches of the river [table 1], the river discharge in the lower reaches not only becomes smaller and smaller, but even cut up as well. For instance, the river bed between Yinsu and Taitema lake has become dry completely since 1972; the river course within the lower reaches has shortened by 180km. The former terminal lakes Luobopo and Taitema don't exist any more. The primeval Populus diversifolia forest along the middle and lower reaches of Tarim River has been damaged severely; its area is 250,000 ha smaller than before, which is larger than the whole afforestation area of all irrigated regions in the Tarim Basin in the past 30 years. Even the famous "Green Corridor" in the lower reaches of Tarim River faces the danger being engualfed by the desert. Conditions of other rivers such as the Kongque, Manasi and Kuitun Rivers are similar to that of Tarim River.

Table 1. —Annual water consumption in the upper and middle reaches of the Tarim River

Location	Distance (km)	Consumption ($10^6 m^3$)	Consumption ($10^6 m^3$/km)	Consumption (Percentage of Alaer flow)
Alaer—Xinqiman (middle of the upper reaches)	180	820	4.56	16.5
Xinqiman—Great Dam (end of the upper reaches)	284	1140	4.01	22.9
Great Dam—Kala (the middle reaches)	315	2150	6.83	43.2
Alaer—kala (Total)	779	4110	5.28	82.5

Data Source: [Chen (1988)]

From the View of Region Types, the Tendency is toward the Oases

The oases are the core regions where people of Xinjiang live and work, they are the main base of the agriculture and industry in Xinjiang. With the development of economy, more and more water resources are put into the oases, in order to get better benefits with less investment. The area of man—made oases was 13,000km² in 1949 and is 58,700km² now (1991) (4.5 times larger). These artificial ecosystems, with excellent functions and reasonable structures, are being in further perfection. But, unfortunately, the conditions of the edges of these oases are unsatisfactory. For instance, the desert forest of Haloxylon in th southern Junggar Basin has retreated about 20 — 30km, while the desert forest of Tamarix and Populus diversifolia at the edge of the Tarim Basin has retreated even more. The vegetation zone between Hotan Oasis and the desert is almost completely destroyed.

INTENSIFIED HUMAN INFLUENCE OF THE VARIOUS WAYS OF THE WATER RESOURCE USED IN XINJIANG

In addition to the influence of the "hydrotropism" tendency, the various methods of water resource used on the ecological environment. In Xinjiang, as in other arid zones, the secondary salinization of soil involved in excess water application (waterlogging) and the desertification of soil involved in water resource exhaustion are two main environmental problems commonly encountered in development and utilization of water resources.

Influence of Surface Water Resource Utilization on Ecological Environment

Effect of Reservoir Construction on Environment

Besides storing up floodwater in summer and surplus water during

springrunoff to adjust the contradictory seasonal patterns of water supply and demand, reservoirs are built also to store up groundwater drawn from upstream well fields. When abstracting groundwater in Xinjiang, people often build well fields on the piedmont alluvial and diluvial fan areas, where shallow groundwater is plentiful and wells were concentrately digged. For exemple, in the Qingeda well field on the diluvial fan areas besid the Urumqi River, groundwater has been abstracted and stored up in the Mongjin Reservoir to meet the needs of Wujiaqu irrigation district. 480 reservoirs have been built in Xinjiang, the maximum storage capacity of which is 5. 5 billion m^3; the water surface area has increased by about 2000 km^2. Reservoirs in Xinjiang actually provide 6. 3 billion m^3 of water per year, which irrigate a cultivated land area of 653,000 ha.

Since reservoirs in mountain areas are situated on runoff — forming districts, location of reservoirs in the mountains is advantageous to adjustment of the water resources in the whole basin. But in the mountain areas in Xinjiang there exist disadvantageous factors such as complex geologic conditions, etc. Therefore, the absolute majority of reservoirs built are built in the piains. Plains reservoirs are generally situated form diluvial fan to alluvial plain. The reservoirs main influences on the environment are:

(1). The large reservoir surface gives rise to great moisture evaporation. As a result, much moisture is lost. This may change the microclimate of the irrigation districtions in arid zones. In terms of its influence on climate, water surface of reservoirs in Xinjiang corresponds to over 2000 km^2 of forest.

(2). Although leakage around reservoir dam has brought about disadvantageous influence on the rise of groundwater table and the salinization of soil, its improvement of the environment is often neglected. First, leakage plays an adjustment and supply role on abstracting groundwater in lower reaches. According to the observation data of well No. 24—A near Wulabe reservoir, the depth to groundwater was 0. 34m in 1964 and 0. 19m in 1979, which corresponds to a water—table rise of an average of 0. 01m per year. Although this well belongs to an overdevelopment district of groundwater, owing to benefitting from reservoir leakage supply, dynamic state of groundwater tends to equilibrium, and a great decline in groundwater is averted. Second, The leakage has played a desalination role on the quality of groundwater in the lower reaches. For example, in the past twenty years, in spite of overdraft, the quality of groundwater at Guojia village below Hongyanchi Reservoir in Xinjiang has not fundamentally worsened and sometimes even has improved: the degree of mineralization is 0. 2 — 0. 3g/l; hardness is 122. 71—210. 35 mg/l as $CaCO_3$.

(3). If plains reservoirs are not emptied, it is possible for them to be utilizated synthetically, such as, for breeding fish in the reservoirs and for afforestation around them. At the same time, the reservoir district is also an ideal place for tourism and recreation in arid zones. For instance, the Forest Park at Mongjin Reservoir in Urumqi is used in this way.

(4). The problem that can't be overlooked is that plains reservoirs have caused a series of bad influences on natural ecological environment such as, groundwater table rise in the lower districts, great moisture evaporation losses, and secondary salinization. In addition , under the circumstance of water being contaminated in the upper reaches and entering reservoirs, the polluted area is enlarged, thereby doing harm to people's product and life in the irrigation districts. According to the investigation

statistics for 1,427 enterprises by the Environmental Protection Authority (1985), the total discharge of industrial waste water in Xinjiang is 145 million tons, the majority of which is not treated and discharged directly into river courses and reservoirs. thereby causing surface water and groundwater to be polluted to some degree.

As discussed above, in the light of hydrological characteristics of river in arid zones in Xinjiang, and in order to make the best use of the water resources, building different kind of reservoirs according to local conditions is still one of the main remedies for shortage of water resources. At the same time, there is also the precondition of protecting the weak ecolgical envionment in Xinjiang and preventing desertification. Since building reservoirs is often an engineering activity which changes the natural condition, detailed knowledge of natural conditions and environmental evaluation are indispensable to making the right decision.

Effect of Rivre's Drying up on Environment

When water demand in the upper and middle reaches is continuously increased or utilization is out of control, it is inevitable for the river to become intermittent or dry up in the lower reaches. After rivers have dried up, the groundwater table in the lower reaches descends by a great extent at first. For example, the ground water level in the Tarim river has descended from the original 3—5m depth to 8—13 now(1991), and the quality of the groundwater also has been getting worse. Second, owing to shortage of water, vegetation has withered and died, and desertification has been intensified. Of 86 counties and cities in Xinjiang, 53 have been threatened by sand. in the middle and lower reaches of the Tarim River and the lower reaches of the Kongque River, desertified lands take up about 61. 6 percent of the areas. Third, riverbed in the lower reaches have shrunk, and terminal lakes of rivers have become salt or dry; for example, Luobupo, Taitema, Edean, and Manasi lakes, and others, are dissipating one after another. Surfaces of some lakes are gradually getting small. At present, the area of all lakes in Xinjiang is only 52 percent of the lake area in the 1950's. Moreover, banks of rivers and lake basin areas have become barren land.

Influence on Ecological Environment and Agricultural Production by Abstraction and Utilization of Groundwater

Environmental Problems Engendered by Irrational Utilization of Groundwater Resources

Excess draft of groundwater causes the groundwater table to fall dramatically and also makes the quality of groundwater become worse. In the past thirty years, groundwater levels throughout the middle and upper part of the piedmont plain on the north side of the Tianshan Mountains have descended between 3m and 10m. The increasing rate of use of river water results in the reduction of groundwater recharge and spring discharge, and even in the exhaustion in the overflow zones. The discharge from springs in the Urumqi River basin was 206 million m^3 in 1959 and 61 million m^3 in 1981, a decrease of 70 percent. Groundwater overdraft not only will cause groundwater levels to drop generally, but also will make the quality of groundwater salty and worse. For example, in the past twenty years, the hardness in the Urumqi River has risen by 262. 94—368. 12mg/l as $CaCO_3$ and degree of mineralization by 0. 5—0. 8g/l. The concentration of NO_3^-

has increased by 7. 6—79. 2 mg/l in the past four years. Particularly, in cities and towns, where groundwater has been abstracted to a high extent for industry, a great amount of waste water which is discharged by industries and living has, by means of percolation, directly polluted surface river and phreatic waters.

In addition, as discussed above, oversupply of water in the form of irrigation will cause groundwater tables to rise, which can give rise to saltmarshes. At present, the area of salinization land in Xinjiang is over one million hectares, and has increased by 1/3 from the end of 1950's.

The Measures of Protecting Ecological Environment in the Use of Groundwater

In those districts where groundwater level is higher and salinization of soil is serious, the groundwater irrigation and well drainage can be carried out. This not only makes the best use of limited water resource and increases irrigation areas, but also lowers ground water levels in the irrigation districts so as to improve the salinized soil. This measure turns disadvantage into advantage and has led to improved ecological environment in arid zones. For example, Wujiaqu irrigation district, situated on the alluvial plain in the lower reaches of the Urumqi River, originally was severely afflicated by salinization. Since 1978, owing to carrying out the groundwater irrigation and well drainage, the salt content of the soil has decreased year after year, cultivated land area has increased several times, and grain yield has rapidly increased.

REFERENCES

Chen Qichou, 1988, Rational Distribution of Water Resource Utilization Tarim River's Main Current: ARID LAND GEOGRAPHY, vol. 11, NO. 4, p11—16.

China Academy of Science, Comprehensive Survey Team for Resource Exploitation in Xinjiang, 1989, The Rational Utilization and Balance Between Supply and Need of Water Resource in Xinjiang: Science Press, p50—55.

Zhou Tianxiang, 1987, The Ralationship Between the Utilization of Water Resource and Ecological Environment in the Urumqi River Basin of Xinjiang: Journal of Arid Land Resource and Environment, vol. 1, NO. 1, p64—77.

MEASUREMENTS OF VAPOR PRESSURE OVER NATURAL VEGETATION AT A HIGH DESERT SITE IN SOUTHEASTERN ARIZONA

by A.M. Sturrock, Jr.

U.S. Geological Survey
Stennis Space Center, Mississippi

and W.D. Nichols

U.S. Geological Survey
Carson City, Nevada

ABSTRACT

Vapor pressure over natural vegetation was computed from measurements of air temperature, relative humidity, and dew point at a site near Tombstone, Arizona, during a 16-day period from July 27 through August 11, 1990. These measurements were made as part of a larger field experiment to measure evapotranspiration above natural vegetation.

Three sets of sensors mounted at 2 and 3 meters above the ground were used to determine the vapor pressure gradient from measurements of air temperature and relative humidity or dew-point temperature. The first sensor set is nonventilated and uses platinum resistance thermometers to measure air temperature and a capacitance bridge to measure changes in relative humidity. The second set, also nonventilated, uses platinum resistance thermometers for measuring air temperature and measures relative humidity as a function of the capacitance change in a thin polymer film as it absorbs moisture. The third set, a ventilated unit, uses chromel-constantan thermocouples to measure air temperature and a single ventilated, cooled-mirror dew-point hygrometer to determine the dew-point temperature of the air.

The hourly vapor pressure computed using the ventilated unit measurements was considered the most accurate of the three sets. Therefore, the hourly measured values of vapor pressure from the nonventilated units, computed from air temperatures and relative humidity, were compared to the hourly values from the ventilated unit, computed from air and dew-point temperatures. For approximately 40 hours, from 1600 hours on August 9, 1990, to 0900 hours on August 11, 1990, the 3-meter nonventilated units were positioned at the 2-meter height, so that all four units could be compared with the 2-meter, ventilated unit. Results of this comparison, for a vapor pressure range from 0.954 to 1.936 kilopascals, show a mean vapor pressure difference between the ventilated and nonventilated units of -0.044 kilopascals with a maximum difference of +0.048 and a minimum difference of -0.152 kilopascals. Considering this excellent agreement, these nonventilated or naturally ventilated units warrant additional test and evaluation. A low-cost, low-maintenance, naturally ventilated unit for measuring vapor pressure offers several advantages for remote study sites.

INTRODUCTION

Purpose and Scope

One of the most difficult environmental variables to measure is the moisture content of the atmosphere. In past evaporation studies, a wide variety of sensors, from simple sling psychrometers to complex dew-point hygrometers, have been used to determine vapor pressure. At remote study locations, it is desirable to have sensors that do not require alternating-current (ac) voltage, do not require forced ventilation, and maintain their calibrations over long periods of time. Two sensors that fit the above criteria were selected for an evaluation test with an accepted standard sensor. This report discusses the results of that study.

Description of the Study Site

The study site, called Lucky Hills, is located 3.2 kilometers (2 miles) north of highway 90 at the west end of Tombstone, Arizona. The topography at this site can be described as gently rolling hills incised by steep drainage channels. The vegetation is mixed grass-brush rangeland, typical of southeastern Arizona.

SENSOR MEASUREMENTS

Reference-unit vapor concentration is measured by a single ventilated, cooled-mirror dew-point hygrometer. Air samples from two heights are routed to the cooled mirror through teflon filters that exclude liquid water and dust. Every two minutes, the air drawn to the mirror is switched from one height to the other. A 40-second interval is allowed for the mirror to stabilize at the new dew point; 1 minute and 20 seconds of measurement is collected for each 2-minute cycle. A single low-power dc pump aspirates the system. Air temperature is measured at the same two heights with 76 μm-diameter chromel-constantan thermocouples. The thermocouples are not aspirated. The sampling interval for air temperature, dew-point temperature, and vapor pressure is one second. These measurements are averaged for the 20-minute data output interval.

The vapor concentration also was measured with two different nonventilated units that use a combined humidity-temperature probe. The relative humidity sensor of the first unit is connected to a capacitive bridge. The output from this bridge is then fed into an amplification and linearization circuit that converts the output to relative humidity. Air temperature is measured with a platinum resistance thermometer. The sensors are protected against dust and other contaminants by a replaceable membrane filter. The unit is further protected from direct solar radiation and precipitation by a multi-plate radiation shield.

The second nonventilated unit also uses a combined humidty and temperature probe to measure vapor concentration. In this unit, relative humidity is measured as a function of the capacitance change in a thin polymer film as it absorbs moisture. A platinum resistance thermometer measures air temperature. As with the above sensors, this unit uses a membrane filter to protect the sensors from dust and other contaminants and a multi-plate radiation shield to protect from solar radiation and precipitation.

Both nonventilated units require 10 to 15 seconds to respond to changes in relative humidity; therefore, the sampling interval was set to 20 seconds. These measurements are averaged for the 20-minute data output interval.

DISCUSSION

As part of a larger field experiment to determine evapotranspiration using remotely sensed information, ground-truth measurements of air temperature, relative humidity, and dew-point temperature profiles were collected and used in the computation of the vapor pressure of the air at 2- and 3-meter heights above the land surface. All sensors were connected to microloggers capable of measuring at the 1- and 20-second sampling intervals of the hygrometers. The measurements averaged over the 20-minute data output interval were used in the calculation of hourly and daily vapor pressure values. These 20-minute averages are this study's most in-depth evaluation of the data and were used in constructing the comparative analysis of the hourly and daily averages.

Table 1 lists the daily values of air temperature and relative humidity for July 28 - August 8, 1990, for the sensors at the 2- and 3-meter heights. Columns 1-4 give daily values from the nonventilated capacitance bridge units and columns 5-8 give daily values from the nonventilated polymer film units. Because of the poor agreement of air temperature between the nonventilated units (differences of as much as four percent), the last two columns of table 1 list the daily air temperature values from the dew-point hygrometer unit. In previous studies, the ventilated unit had been used as a state-of-the-art sensor and was used in this study as a standard of comparison for the untested nonventilated units. The close agreement between the daily values of air temperature of the capacitance bridge units and the dew-point unit (differences of less than one percent), indicates that the air temperature reading from the polymer film unit is incorrect. The agreement between average daily relative humidity values at the 2- and 3-meter heights for both nonventilated units is good. For the 12-day period, daily values at each height are within one percent of each other. There were no dew-point temperature data from the ventilated unit during this time period.

As a means of comparing changes in both the temperature and vapor pressure of the air, all sensors except the 3-meter sensor on the dew-point ventilated unit were positioned at the 2-meter level for a period of approximately 40 hours from 1600 hours on August 9 to 0900 hours on August 11. Tables 2 and 3 present hourly and daily values of air temperature and vapor pressure for the 24-hour period for August 10. Table 2 lists the hourly values of air temperature from the capacitance bridge units and the 2-meter dew-point unit. Also listed, for comparative purposes, are the hourly relative humidity values from the four nonventilated units. Again, the air temperature values from the polymer film units were suspect and are not listed.

The agreement of hourly values of air temperature for the two capacitance bridge units is considered good. The daily temperature values for August 10 are within 0.06 °C of each other; and hourly temperature value differences range from -0.517 °C at 0700 hours to +.050 °C at 1800 hours, the approximate times of sunrise and sunset when temperature values are changing very rapidly. A comparison of these hourly values from the capacitance bridge units with air temperatures from the dew-point unit reveals that the greatest differences again occur in the morning hours between 0800 and 1000 hours; the differences between the daily values of the three units are less than 0.2 °C. Differences between averaged hourly values from the four relative humidity units listed in table 2 range from less than one percent to almost three percent. The agreement between like units was almost exact. Differences between values from the capacitance bridge units ranged from +0.83 percent at 0700 hours to -1.94 percent at 2200 hours, and differences between values

Table 1.--Average daily values of air temperature and relative humidity at 2 and 3 meters for July 28 - August 8, 1990

[Ta, temperature; RH, relative humidity; °C, degrees Celsius; %, percent; m, meters; numbers in parentheses indicate column numbers]

	Nonventilated sensor with capacitance bridge				Nonventilated sensor with polymer film				Ventilated sensors with dew-point hygrometer	
	At 2 m		At 3 m		At 2 m		At 3 m		At 2 m	At 3 m
1990 Date	Ta (°C)	RH (%)	Ta (°C)	RH (%)	Ta (°C)	RH (%)	Ta (°C)	RH (%)	Ta (°C)	Ta (°C)
	(1)	(2)	(3)	(4)	(5)	(6)	(7)	(8)	(9)	(10)
July 28	25.30	39.19	25.36	40.26	26.09	38.86	24.74	40.09	25.07	25.09
29	25.06	43.28	25.04	44.89	25.85	43.27	24.44	44.94	24.79	24.73
30	23.52	47.12	23.55	48.48	24.27	47.33	22.89	48.82	23.33	23.33
31	24.18	47.17	24.16	48.82	24.97	47.44	23.52	49.17	23.95	23.89
Aug. 1	20.27	71.77	20.24	73.79	21.01	72.66	19.61	74.15	20.18	20.13
2	20.04	78.38	20.03	79.68	20.87	78.87	19.51	79.90	20.03	20.00
3	20.56	75.26	20.60	76.47	21.41	75.80	20.07	76.31	20.65	20.66
4	22.81	60.51	22.81	61.61	23.71	60.70	22.32	61.22	22.70	22.65
5	22.47	59.30	22.51	60.65	23.24	59.86	21.84	60.94	22.36	22.31
6	19.19	74.85	19.27	76.11	19.98	75.86	18.64	76.93	19.19	19.19
7	20.23	72.28	20.22	73.93	21.05	72.91	19.61	74.09	20.16	20.06
8	21.97	62.91	21.97	64.54	22.78	63.58	21.33	64.71	21.84	21.73
Avg.	22.13	61.00	22.15	62.43	22.94	61.43	21.54	62.61	22.02	21.98

Table 2.--*Average hourly values of air temperature and relative humidity at 2 meters for August 10, 1990*

[CB, nonventilated sensor using capacitance bridge; DP, ventilated sensor using dew point; PF, nonventilated sensor using polymer film; °C, degrees Celsius; %, percent; numbers in parentheses indicate column numbers]

Hour	Air temperature (°C)			Relative humidity (%)				
	CB (1)	CB (2)	DP (3)	CB (4)	CB (5)	PF (6)	PF (7)	DP (8)
1	17.78	17.83	17.85	76.40	77.90	78.10	79.60	80.50
2	17.80	17.85	17.87	75.30	76.80	76.67	78.40	79.10
3	17.87	17.95	17.95	74.97	76.20	76.30	77.83	78.90
4	17.25	17.32	17.33	76.63	78.50	78.80	80.23	81.10
5	17.19	17.26	17.34	76.69	78.43	78.83	80.23	80.90
6	16.76	16.86	16.99	78.30	80.00	80.57	81.73	83.10
7	17.54	18.06	17.86	78.33	77.50	78.67	77.80	81.40
8	21.62	22.02	21.45	66.49	66.03	63.56	64.52	70.20
9	25.15	25.50	24.52	51.55	52.70	49.56	50.53	57.30
10	28.33	28.35	27.91	32.42	33.50	33.09	34.01	36.30
11	29.47	29.51	29.18	29.19	30.19	29.72	30.67	31.70
12	30.15	30.24	29.88	27.45	28.31	27.57	28.59	29.20
13	30.57	30.65	30.50	27.64	28.41	27.77	28.85	29.10
14	31.82	31.84	31.68	23.37	23.80	22.44	23.35	24.80
15	32.28	32.30	32.12	18.94	19.26	18.17	18.92	19.90
16	32.31	32.32	32.05	19.47	19.95	18.77	19.54	20.50
17	31.90	31.88	31.57	21.05	21.73	20.42	21.25	22.30
18	30.58	30.53	30.21	23.29	24.14	22.76	23.81	24.90
19	28.34	28.38	27.96	28.22	29.32	29.05	30.14	30.30
20	25.19	25.26	24.89	35.61	37.37	37.41	38.42	38.70
21	23.60	23.69	23.43	37.97	39.28	39.05	40.03	40.60
22	21.67	21.73	21.47	44.06	46.00	45.25	46.30	47.10
23	21.49	21.56	21.47	45.08	46.24	45.32	46.37	47.40
24	21.63	21.71	21.60	44.40	45.56	44.73	45.79	46.90
Avg.	24.51	24.567	24.38	46.37	47.38	46.77	47.79	49.30

Table 3.--*Average hourly values of vapor pressure at 2 meters for August 10, 1990 (in kilopascals)*

[numbers in parentheses indicate column numbers]

Hour	Vapor pressure in Kilopascals					
	Nonventilated sensor with capacitance bridge		Column 1 minus Column 2	Ventilated sensor with dewpoint hygrometer	Column 4 minus Column 1	Column 4 minus Column 2
	(1)	(2)	(3)	(4)	(5)	(6)
1	1.554	1.590	-0.036	1.648	+0.094	+0.058
2	1.533	1.569	-0.036	1.623	+0.090	+0.054
3	1.534	1.566	-0.032	1.627	+0.093	+0.061
4	1.508	1.551	-0.043	1.607	+0.099	+0.056
5	1.507	1.544	-0.037	1.605	+0.098	+0.061
6	1.493	1.536	-0.043	1.603	+0.110	+0.067
7	1.570	1.604	-0.034	1.669	+0.099	+0.065
8	1.712	1.744	-0.032	1.800	+0.088	+0.056
9	1.642	1.715	-0.073	1.768	+0.126	+0.053
10	1.249	1.292	-0.043	1.367	+0.118	+0.075
11	1.201	1.245	-0.044	1.288	+0.087	+0.043
12	1.176	1.219	-0.043	1.233	+0.057	+0.014
13	1.213	1.253	-0.040	1.272	+0.059	+0.019
14	1.100	1.121	-0.021	1.161	+0.061	+0.040
15	.916	.932	-0.016	.957	+0.041	+0.025
16	.943	.967	-0.024	.980	+0.037	+0.013
17	.996	1.027	-0.031	1.036	+0.040	+0.009
18	1.021	1.056	-0.035	1.070	+0.049	+0.014
19	1.086	1.130	-0.044	1.147	+0.061	+0.017
20	1.140	1.202	-0.062	1.221	+0.081	+0.019
21	1.106	1.151	-0.045	1.178	+0.072	+0.027
22	1.139	1.193	-0.054	1.208	+0.069	+0.015
23	1.154	1.189	-0.035	1.216	+0.062	+0.027
24	1.147	1.183	-0.036	1.212	+0.065	+0.029
Avg.	1.277	1.316		1.354		

from the polymer film units ranged from +0.87 percent at 0700 hours to -1.73 percent at 0200 hours, giving net total ranges of 2.80 and 2.60 percent, respectively. The daily maximum difference between the readings from the four units was less than 1.5 percent. The last column of table 2 lists average hourly relative humidity values from the dew-point unit. These values were back calculated from hourly values of air temperature and vapor pressure and are presented only for a relative comparison to the other values.

The average hourly values of vapor pressure of the air for August 10 from the capacitance bridge and ventilated dew-point units are listed in table 3 in columns 1, 2, and 4, respectively. Vapor pressure values in columns 1 and 2 are from the measurements of the 2- and 3-meter capacitance bridges, respectively, which are now both positioned at the 2-meter level for this comparison with the 2-meter dew point unit. The average hourly vapor pressure from the capacitance bridge units is derived from air temperature and relative humidity readings taken at 20-second intervals that are summed and averaged over 20-minute periods. The vapor pressure for the ventilated dew-point unit is determined from air temperature and dew-point temperature readings taken at 1-second intervals that are summed and averaged over 20-minute periods. Thus, for all units, the 20-minute data are summed and averaged, which yields the hourly and daily values of vapor pressure.

Columns 3, 5, and 6 of table 3 give the differences between the hourly vapor pressure values of the individual capacitance bridge units and comparisons of these values to the hourly values from the dew-point unit. The difference between the hourly values of the capacitance bridge units presented in column 3 is considered small. The maximum difference of -0.73 kilopascals occurs at 0900 hours during the early morning hours when temperatures are changing rapidly. The average daily values are within 0.04 kilopascals. Columns 5 and 6 list the differences between the hourly vapor pressure from the capacitance bridge units and the hourly values from the dew-point unit. The maximum difference of 0.126 kilopascals between the two units occurs at 0900 hours for the 2-meter height. The primary and secondary maximum differences for both units occur in the early morning between 0600 and 1000 hours. The average daily differences between the capacitance units and the dew-point unit are 0.04 and 0.08 kilopascals for the 3-meter and 2-meter heights, respectively.

From the discussion above, it is apparent that, although malfunctions occurred for the air temperature sensor of the polymer film units, the performance of the capacitance bridge units was satisfactory over the total study period. Because the correlation between the four relative humidity sensors of the nonventilated units was considered good, it was concluded after the data analysis that a modified nonventilated polymer film unit using a thermistor for measuring air temperature would be procured and tested concurrently with the capacitance bridge units.

Future plans include testing of state-of-the-art ventilated and nonventilated units in both hot humid and cold dry environments. It is anticipated that these tests may lead to the identification of a low cost unit that does not require ac or additional battery power, needs no ventilation, and yields an accurate measurement of vapor pressure.

EVAPORATION PROPERTIES AND ESTIMATES IN THE LANDLOCKED ARID REGION IN XINJIANG, CHINA

Zhang Guowei and Zhou Yuchao

Xinjiang Hydrology Bureau, Urumqi, China

ABSTRACT

Xinjiang, the western part of China, is landlocked and far from oceans and has an arid climate. Evaporation properties in Xinjiang are in close relation with its unique natural and geographic conditions. As a result, the mountain areas are runoff-forming areas where precipitation is greater than evaporation; the plains below the river mouths are runoff-dissipating areas where actual evaporation is far greater than precipitation; and the broad desert areas are no-runoff areas where precipitation is completely consumed by evaporation. The experimental studies on evaporation and the available estimation methods for the evaporation from water surface, land and groundwater are presented.

INTRODUCTION

Xinjiang, situated in the center of Eurasia, represents a typical arid climate characterized by extremely dry air, low precipitation, wide ranges of air temperature, and high evaporation rates. However, the three mountain ranges, namely Altai, Tianshan and Kalakunlun, scattered in Xinjiang from north to south, intercept a large amount of water vapor passing above Xinjiang. This leads to plentiful precipitation in mountain areas, where low temperature and high elevation provide favorable conditions for water retention and glacier development. Hence, runoff is generally produced in mountain areas and dissipated in sloping plains below the river mouths, and no runoff exists in desert areas. Under such particular climatic and geographic conditions, accurate measurement and estimation of evaporation are very important for water balance analysis and assessment of available water resources. This paper describes experimental studies on evaporation observation, evaporation properties and evaporation estimates in Xinjiang.

EVAPORATION MEASUREMENT AND EXPERIMENTAL STUDY

Observation Network

The observation of evaporation was started in the 1950's in Xinjiang. The major instrument for surface water evaporation measurement is the 20cm-diameter(ø20) evaporimeter. So far, a total of 225 such evaporimeters have been installed over Xinjiang. Most are located at river mouths and in towns in the plains. In addition, there are 33 evaporimeters of model E601 installed in Xinjiang. The E601 evaporimeter, which has a water surface of 3000cm^2 with a water protection ring on it, is recommended for evaporation measurement in hydrological stations by the Ministry of Water Resources PRC.

Experimental Study

An experimental station for evaporation measurement was built in 1958 at the Hadipo hydrological station (43°47'N, 87°15'E, el.966m) on the Toutun River, which originates on the north slope of the Tianshan Mountains. This experimental station incorporates a large evaporation basin of $20m^2$ area and thirteen small evaporimeters of various kinds. The purpose of this experimental station is to provide comparative measurements between various kinds of evaporimeters for determining conversion factors between them and to find the correlations between evaporation and climatological elements.

In 1982, the Xinjiang Geography Institute of China Science Academy built a water-balance experimental station in the southern part of Xinjiang, where the Hetian, Yerkant and Aksu Rivers join together to form the Tarim River (40°27'N, 80°45'E, el.1028m). In this station there are a $20m^2$ evaporation basin and other evaporimeters, and the observation and study for soil evaporation, crop consumption use and evapotranspiration of wild plants are carried out.

On the plain of the lower part of the Sangong River on the north slope of the Tianshan Mountains, there is a groundwater study plot (44°17'N, 87°55'E, el.475m) established in 1982. In this plot 43 cylinders were set in soil for the study of groundwater evaporation from different kinds of soils with different groundwater levels.

EVAPORATION ESTIMATES

Estimates of Water Surface Evaporation

There are three methods for evaporation estimates currently used in Xinjiang. They are: (1) conversion factor analysis based on observed data from evaporimeters; (2) an empirical formula derived by correlation analysis with climatological elements; (3) the Penman equation.

Conversion Factor Analysis

Measurements from small-size evaporimeters will be subject to larger values of evaporation than measurements from large water bodies. To correct the measured evaporation, it is necessary to determine conversion factors (K) between the small-size evaporimeters and the large $20m^2$ evaporation basin (E_{20}), expressed as $K_1 = E_{20}/E_{\phi 20}$ for ø20cm evaporimeters and $K_2 = E_{20}/E_{601}$ for E601 evaporimeters.

It is found that the conversion factors are significantly affected by the climatic elements in arid regions where the evaporation process has some properties different from those in wet regions. According to the study of Wu(1984) on K, the evaporation rate in small waters (say in small-size evaporimeters) increases rapidly in daytime as water temperature goes up and decreases at night as water temperature falls; on the other hand, large waters (say in $20m^2$ evaporation basin) show little change of evaporation rate between day and night because of heat storage regulation with which the water absorbs heat in daytime and releases heat at night. Consequently, the conversion factor K_1 shows large variation from day to night because the evaporation in ø20cm evaporimeters changes dramatically within the day; the K_2 shows insignificant variation from day to night due to more water contained in E601 evaporimeters. See Table 1 for the diurnal variations of K's. Moreover, the effects of great variation of air temperature through the

whole year on K must be taken into account when K is determined on a monthly basis. Table 2 gives the monthly variations of K's with time and location.

Table 1. -- Diurnal variation of K in Tarim water balance station (1983)

month	$K_1 = E_{20} / E_{ø20}$ night	daytime	all day	$K_2 = E_{20} / E_{601}$ night	daytime	all day
Jun.	1.062	0.376	0.564	0.740	0.650	0.694
Jul.	1.407	0.378	0.614	0.791	0.693	0.740
Aug.	1.424	0.430	0.640	0.772	0.730	0.749
Sep.	1.872	0.402	0.668	0.880	0.697	0.779
Oct.	3.217	0.440	0.766	0.941	0.798	0.862
mean	1.795	0.407	0.650	0.825	0.714	0.764

Table 2. -- Monthly variation of K in Hadipo and Tarim stations

station	K	Apr.	May.	Jun.	Jul.	Aug.	Sep.	Oct.	mean
Hadipo exp. st.	K_1	0.49	0.54	0.55	0.55	0.55	0.62	0.70	0.56
(north Xinjiang)	K_2	--	0.78	0.82	0.79	0.81	0.79	0.90	0.82
Tarim wat. bala.	K_1	0.51	0.51	0.56	0.60	0.61	0.65	0.71	0.59
(south Xinjiang)	K_2	--	--	--	--	--	--	--	--

Empirical Formula

Wang and Wang(1988) developed an empirical formula for evaporation estimates in Xinjiang using monthly mean temperature, as following:

$$E = A\ B^T \qquad [1]$$

where E is the monthly evaporation in ø20cm evaporimeters (mm); T is the monthly mean temperature(°C); A and B are parameters. According to the climatic characteristics of the year in Xinjiang, three seasons were defined for the correlation analysis; they are: November - February, March - June and July - October. The correlation analysis for the three periods was carried out respectively by using the data of 24,575 months in 104 meteorological stations all over Xinjiang. It is found that the parameters A and B vary with season and location, so that seasonal isoline maps of A and B have been made for practical use. However, the estimation from this formula must be corrected by conversion factors of K_1.

Penman Equation

The Penman equation can be expressed in the following form:

$$E_o = (\delta R_n + \Gamma E_a) / (\delta + \Gamma) \qquad [2]$$

in which, E_o is the evaporation from open water surface (mm/day); R_n is the net solar radiation; δ is the slope of the saturated vapor pressure curve at air temperature t_a; Γ is the psychometric constant; and E_a is the aerodynamic evaporation expressed as: $E_a = C(e_a - e_d)(1 + U/100)$, where C is

equal to 0.35; (e_a - e_d) is the difference between saturated and ambient vapor pressures; and U is the wind speed at 2 meters.

Zhang(1986) studied the Penman equation with the evaporation data from the $20m^2$ evaporation basin in the Hadipo station, and made a modification to Penman equation based on the following suggestions: (1) since the factor Γ/δ is a function of air temperature and atmospheric pressure, it should be corrected according to elevations; (2) an accurate estimate of R_n can be achieved by an empirical formula derived with the climatological data in Xinjiang; (3) the C in the formula for E_a can be an empirical coefficient term related to the turbulent functions and the stability of the atmospheric boundary layer, which vary with different seasons; (4) The Penman equation does not involve the function of heat storage of water, which cannot be neglected in arid regions. As a result, it will over-estimate evaporation in the period of air temperature increase due to the function of heat storage in water, and on the contrary, will under-estimate in the period of air temperature decrease due to the heat release from water. Therefore it is necessary to take the heat storage in water into account in a modified Penman equation. Yet, to calculate the heat flux of water is extremely difficult. A simple way to deal with the problem is to incorporate the function of the heat storage in water into the coefficient term C. It is found that C is related to the difference of monthly mean temperatures: increasing temperatures result in a smaller C in spring; decreasing temperatures yield a greater C in fall, and in July to August the temperature difference is insignificant and C remains 0.35 as taken by Penman equation.

The results of the modified Penman equation were compared with estimates from observed data and with results from the original Penman equation, see Table 3, with the estimates of the mean evaporation of the Hadipo evaporation experimental station in 1960 - 1984, which yields satisfactory error. The modified Penman equation also gives sound results when applied in other 41 meteorological stations. This indicates that the modified Penman equation is suitable for arid regions.

Table 3. -- comparison between estimated and observed mean evaporation, in mm, in Hadipo station, 1960 -1984.

	Apr.	May.	Jun.	Jul.	Aug.	Sep.	Oct.	Total
observed evap.	82.3	130.7	156.3	182.8	169.2	118.7	65.5	905.5
origi. Penman eq.	92.7	139.4	164.1	175.0	149.2	97.1	47.3	864.8
modif. Penman eq.	82.8	128.9	158.1	184.7	165.2	121.1	67.1	907.9

Estimates of Groundwater Evaporation

Groundwater evaporation is essentially subject to climatological factors, soil type in the unsaturated zone, and depth to groundwater table. Since the water surface evaporation reflects the climatological factors, the groundwater evaporation coefficient (defined as the ratio of groundwater evaporation to surface water evaporation) is introduced for estimating the groundwater evaporation. This coefficient is determined on the basis of experimental studies carried out in Xinjiang such as the study at the Songong groundwater evaporation experimental station. Table 4 shows that the sand soil gives larger coefficients than the clay soil when the groundwater table is higher, the groundwater evaporation is small at the depth of 3.0-4.0 of groundwater tables.

Table 4. -- Groundwater evaporation coefficient in Xinjiang

depth to ground water tables (m)	sand soil		clay soil	
	north of Xinjiang	south of Xinjiang	north of Xinjiang	south of Xinjiang
0 - 1.0	0.12 - 0.24	0.10 - 0.18	0.073-0.122	0.06 -0.098
1.0 - 2.0	0.06 - 0.11	0.05 - 0.10	0.03 -0.015	0.018-0.036
2.0 - 3.0	0.03 - 0.05	0.018-0.036	0.012-0.049	0.006-0.012
3.0 - 5.0	< 0.012	< 0.012	< 0.006	< 0.006

Estimates of Land Surface Evaporation

The river basins in Xinjiang can be generally classified into three types according to climatological conditions: runoff-forming area in mountains, runoff-dissipating area in plains below river mouths, and no-runoff area in deserts. For a given river basin, the land-surface evaporation in each type of area can be obtained by the following water balance equations:

mountain area: $$E_m = P_m - R \quad [3]$$

plains area: $$E_p = P_p + R \quad [4]$$

desert area: $$E_d = P_d \quad [5]$$

where E_m, E_p and E_d are the land-surface evaporations; P_m, P_p and P_d are the precipitations; and R is the runoff from the mountain area.

To find a possible method for estimating land evaporation in mountain areas, the Urumqi river basin is selected, where sufficient precipitation data in mountain area are available, the formula developed by Dr. Fu (Wu and Zhang, 1986) the water balance method are used in this river basin.

Water Balance Method

The water balance equation in the mountain area of the Urumqi river basin can be expressed as follows:

$$E = P - R - \Delta V - \Delta B_I \quad [6]$$

where E is the land-surface evaporation; P is the precipitation; R is the runoff; ΔV is the change of water storage; and ΔB_I is the equilibrium of glacial material, with all terms above in (mm).

Fu's Formula

Dr. Fu's formula for land-surface evaporation estimates is given in the following form:

$$E = E_o\{ 1 + P/E_o - [1 + (P/E_o)^m]^{1/m} \} \quad [7]$$

where E_o is the potential evaporation (mm); m is a land-surface parameter including permeability, vegetation and slope. When m = 1, it represents the condition of steep slope, impermeable soil and no vegetation. For this basin m is taken as 2.0, which represents a condition of steep slope, permeable soil, and good vegetation.

The estimations made by Fu's formula for the annual land evaporation from 1984 through 1987 in the mountain area of the Urumqi river basin in comparison with the water balance method have a maximum error of 12% and an error of 0.5% for the average of this four years. In 1986 the observation of land-surface evaporation in the headwater area was carried out by the Tianshan glacier experimental station; the observed land evaporation in this area was 270.3mm and close to the value of 278.8mm estimated by using Fu's formula. This indicates that Fu's formula is feasible for land evaporation estimates in the mountain area of Xinjiang.

EVAPORATION PROPERTIES IN XINJIANG

The evaporation from water surfaces in Xinjiang can essentially reflect the potential evaporation, which increases from mountain areas to plains, from west to east and from north to south. Since Xinjiang is landlocked with highly arid climate, the actual amount of evaporation depends on the water supply. Consequently, the distribution of evaporation in space is essentially in accordance with the distribution of the precipitation in space and the water supply conditions in certain area. Table 5 lists the land evaporations distributed over Xinjiang.

Table 5. -- Distribution of land evaporation in Xinjiang

region	area (km^2)	precip. (10^9 m^3)	evap. from	evap. (10^9 m^3)	percent (%)
runoff-forming area	710,000	204.8	glaciers	2.4	1.05
			mountain areas	116.0	50.8
			subtotal	118.4	51.9
runoff-dissipating area	100,000	8.5	precipitation	7.1	3.1
			used surface water	28.2	12.4
			used groundwater	8.2	3.6
			lakes	5.5	2.4
			groundwater	31.3	13.7
			subtotal	80.3	35.7
no-runoff area	837,000	29.6	precipitation	29.6	12.9
whole Xinjiang	1,647,000	242.9	total	228.3	100

REFERENCES

Wang, Jiqiang and Wang, Butian (1988) Correlation Analysis between Water Surface Evaporation and Monthly Mean Temperature in Xinjiang: China Journal of Geography in Arid Region, Vol.7, No.4.

Wu, Hekang and Zhang, Zhiming (1986) Meteorology: Water Resources Press, Beijing, p.168-171.

Wu, Shenyan (1984) Estimates of Conversion Factor K of Evaporations in Arid Regions: China Journal of Xinjiang Geography, Vol.7, No.8.

Zhang, Guowei (1986) Test and Modification to Penman Equation Applied in Landlocked Arid Regions: China Journal of Xinjiang University, 1986 No.4.

ESTIMATING EVAPOTRANSPIRATION BY PHREATOPHYTES IN AREAS OF SHALLOW GROUND WATER IN A HIGH DESERT VALLEY

William D. Nichols

U.S. Geological Survey, Carson City, Nevada

Abstract

Given a continuous supply of ground water, phreatophytes and other vegetation growing in areas of shallow ground water may be expected to behave as a well-watered crop. Energy budget data collected over greasewood growing where ground water is about 2 meters below land surface and over sagebrush and rabbitbrush growing in areas where ground water is about 3.5 meters below land surface are used to develop and calibrate models for estimating latent heat flux and evapotranspiration from measured net radiation and soil heat flux.

Introduction

Phreatophytes are the major consumer of ground water by vegetation in the arid and semiarid western United States. Greasewood is a particularly ubiquitous phreatophyte over the northern Great Basin. Determination of reasonable water budgets for this area is dependent largely on the reasonableness of estimates of evapotranspiration by greasewood as well as other, less prevelant, phreatophytes. Although a number of field studies have been conducted to determine evapotranspiration rates from these plants, methods for estimating daily and seasonal evapotranspiration have not been developed and few data are available upon which to base such estimates.

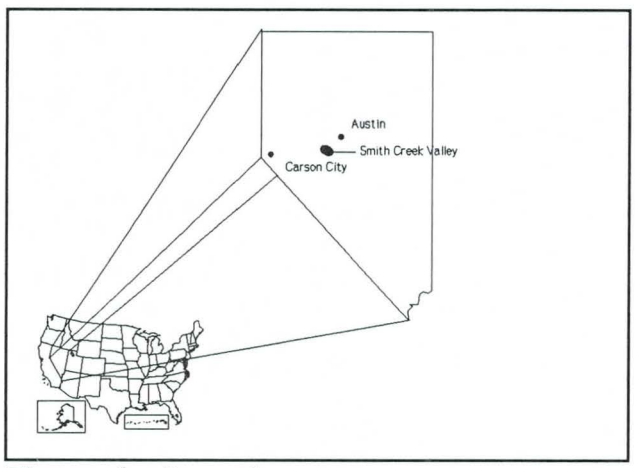

Figure 1. Location map

Energy balance field studies were conducted in Smith Creek Valley, Nevada (fig. 1) in the west-central Great Basin over stands of greasewood growing in areas where the water table is less than two meters below land surface and in stands off mixed sagebrush and rabbitbrush growing in areas where the water table is less than four meters below land surface. These studies were conducted for 5- to 10-day periods in May, July, and August, 1988; from May 25 to September 7, 1989; and from May 24 to July 1, 1990. They were conducted to better define the use of ground water by phreatophytes, and to determine if methods could be developed for estimating evapotranspiration at basin and regional scales. Evaluation of the results of these studies has indicated that phreatophytes growing under these conditions behave as a well-watered crop, and that the transpiration of ground water by these plants can be predicted within reasonable limits of accurracy.

Smith Creek Valley is located in central Nevada, about 196 km east of Carson City, Nevada, and 41 km southwest of Austin, Nevada. It is a semiarid hydrologically-closed basin covering about 1500 km^2 with a playa that covers about 44 km^2. The playa is at an altitude of about 1850 m; the surrounding mountain ranges rise to 3000 m.

Two sites were repeatedly instrumented during the course of the study. The first site occupied in August, 1988, from May to September, 1989, and from May to July, 1990 is located 170 m west of the playa. The vegetation at this site is greasewood (Sarcobatus spp.), with a plant density of about 25-30 per cent and a crown height of about 0.7 m. The water level at this site is 1.8 m below land surface. A second site, located about 2 km northwest of the playa, was occupied in late May and late July 1988, and from May to July, 1990. The vegetation at this site is predominantly sagebrush (Artemisia spp.) with some rabbitbrush (Chrysothamus spp.) with a plant density of 35-40 per cent and a crown height of about 0.8 m. The ground-water level at this site is between 3 and 4 m below land surface.

Methods and Data

Data needed to solve the energy budget - Bowen ratio equation were collected at each site. This method uses measurements of temperature and vapor pressure of the air at two heights above the canopy to determine the ratio of sensible to latent heat fluxes, which is defined as the Bowen ratio (Brutsaert, 1982, p.209)

$$\beta = H / \lambda E \tag{1}$$

and

$$\beta = pc_p(T_1 - T_2) / \lambda\epsilon(e_1 - e_2) \tag{2}$$

where

β = Bowen ratio
H = sensible heat flux, W/m^2
λ = latent heat of vaporization, J/kg
E = evapotranspiration, kg/m^2s
p = atmospheric pressure, kPa
c_p= specific heat of air at constant pressure, J/kg K
T_1, T_2= air temperature at heights 1 and 2 above the canopy, °C
e_1, e_2= vapor pressure of air at heights 1 and 2, kPa
ϵ = ratio of molecular weight of water to weight of dry air

The Bowen ratio, together with measurements of net radiation and soil heat flux, is then used to solve the energy budget equation, given by

$$\lambda E = Rn - G - H \tag{3}$$

Substituting equation 1 into equation 3 leads to

$$\lambda E = (Rn - G) / (1 + \beta) \tag{4}$$

where

Rn = net radiation, W/m^2

G = soil heat flux, W/m^2

Data collected for this study included air temperature and vapor pressure at two heights above the canopy, incident and reflected short-wave radiation, incident and emitted long-wave radiation, soil heat flux, and soil temperature needed to correct the flux term for heat storage in the soil layer above the flux plate. Net radiation was calculated from the four measured components of the radiation budget.

Analysis

The data and equations discussed above were used to calculate energy budgets for each site for all of the measurement periods. Typical examples are shown in figure 2. Evaluation of these energy budgets for different time intervals over the 3-year period suggested a seasonally decreasing latent heat flux rate at the greasewood site. The maximum flux rate at this site of about 350 W/m^2 was observed in late May and early June; this rate decreased steadily through the

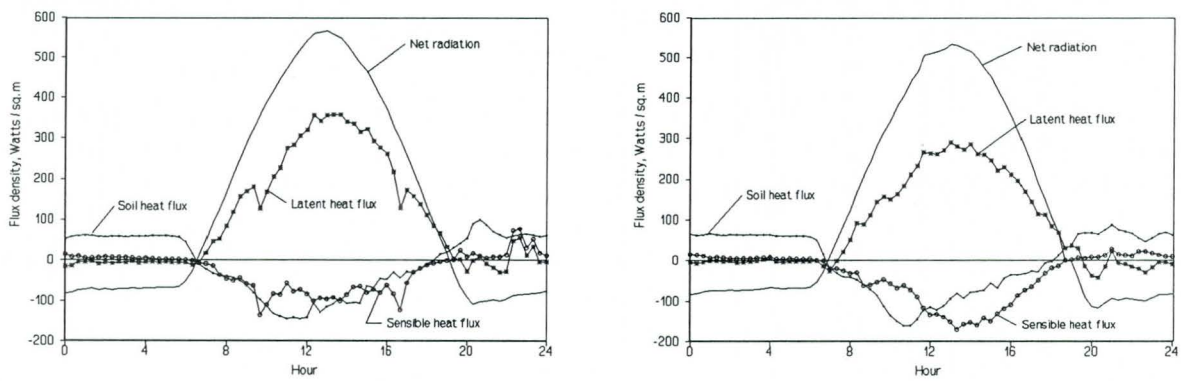

Figure 2. Energy budget at greasewood site, Smith Creek Valley for A) June 18, 1989 and B) July 29, 1989

summer to an observed minimum of about 180 W/m^2 by early September. Fewer data are available for the sagebrush site, but a similar uniformity in latent heat flux rates appears to occur there also. The rates are significantly lower than at the greasewood site, with a maximum rate of about 200 W/m^2 occuring in late May declining to about 100 W/m^2 by late July. Data for this site are not available for August or September. The only time this uniformly decreasing rate is not seen at either site is on a day of, and several days following, convective storm precpitation. On these days, latent heat flux rates are very high as water evaporates from the bare soil; the rate rapidly decreases over the next 5 to 7 days until it has returned to about the same as before the precipitation.

This area of Nevada has experienced severe to extreme drought conditions since 1987, the year before the field studies began. Soil moisture content at the sites was approximately the same in May and July, 1988, in May and September, 1989, and in May 1990. In other words, there was no significant year-to-year change in near-surface soil moisture content over the 3 years of data collection. This suggests that soil moisture in the soil between land surface and the water table at the two sites is supplied primarily by ground water throughout the

summer months, and that the observed latent heat flux represents primarily the transpiration of ground water by greasewood and sagebrush. The uniformly decreasing rate further suggests that these shrubs are responding as a well-watered crop, and are transpiring in a predictable manner controlled primarily by the available energy.

Preliminary analysis using three different simple linear regression models demonstrated a strong correlation between latent heat flux and 1) incident solar radiation, 2) incident solar radiation less soil heat flux, and 3) net radiation less soil heat flux, with the third model yielding the best results. This model is given by

$$\lambda E = b(Rn - G) + 10.0 \tag{5}$$

where Rn and G are known values of net radiation and soil heat flux. The coefficient b is a function of time and decreases from early June into early September. The value is easily determined with a linear regression equation that uses the day number as the time factor. For the greasewood site

$$b = 1.08 - .00215(day\ number) \tag{6}$$

and for the sagebrush site, although fewer data are available,

$$b = .4936 - .00164(day\ number) \tag{7}$$

where day number is the number of the day of the year, with January 1 being day number 1

Comparison of estimated latent heat flux values based on equation 5 with measured values indicated that, while daily average values were reasonably close, equation 5 somewhat overestimates flux values in the morning and late afternoon hours and underestimates during midday hours. This suggests that the latent heat flux may be better estimated using an equation more appropriate to a periodic function. Further consideration indicated that if the observed latent heat flux is a function only of the available energy, then it is analogous to soil heat flux and can be estimated by a Fourier series of the form (Kirkham and Powers, 1972, p.474)

$$\lambda E = B_0 + \sum_{n=1}^{\infty} A_0 \left[A_n \sin(n\omega t) - B_n \cos(n\omega t)\right] \tag{8}$$

where ω is $2\pi/p$, p is the period (in this case 24 hr), and the coefficients A_n and B_n are given by

$$A_n = \frac{4}{p} \sum_{i=1}^{N} (Rn_i - G_i) \left[\sin \frac{n\pi t_i}{(p/2)}\right] \Delta t \tag{9}$$

$$B_n = \frac{4}{p} \sum_{i=1}^{N} (Rn_i - G_i) \left[\cos \frac{n\pi t_i}{(p/2)}\right] \Delta t \tag{10}$$

and

$$B_0 = [(\overline{Rn - G}) / 2] - C \tag{11}$$

where Rn and G are known values of net radiation and soil heat flux at time t and C is a correction term to reduce the mean value of (Rn − G). Coefficients determined by trail-and-error matching of graphs of estimated and measured latent heat flux using the above equations and data from late June, early August and early September, 1989, demonstrated that both A_0 and C are functions of time, with A_0 showing a linear decrease from late May to early September and C increasing linearly over the same period. Both of these variable are easily determined with a linear regression equation that uses the day number as the time factor. For the greasewood site in Smith Creek Valley these variables are

$$A_0 = .60925 - .00135\ (day\ number) \tag{12}$$

and

$$C = 21.29 + .0562\ (day\ number) \tag{13}$$

For the sagebrush site in Smith Creek Valley the variables are

$$A_0 = .20745 - .00045\ (day\ number) \tag{14}$$

and

$$C = 100.0 + .056\ (day\ number) \tag{15}$$

Discussion

The latent heat fluxes estimated by equations 5 and 8 are compared with measured latent heat fluxes for the greasewood site in Smith Creek Valley for days in June and July, 1989 in figure 3, and for the sagebrush site for a day in June, 1990 in figure 4. It is important to understand that the coefficients for these model solutions are calibrated for these sites which have minimal soil-water evaporation and generally shallow ground-water conditions. The applicability of

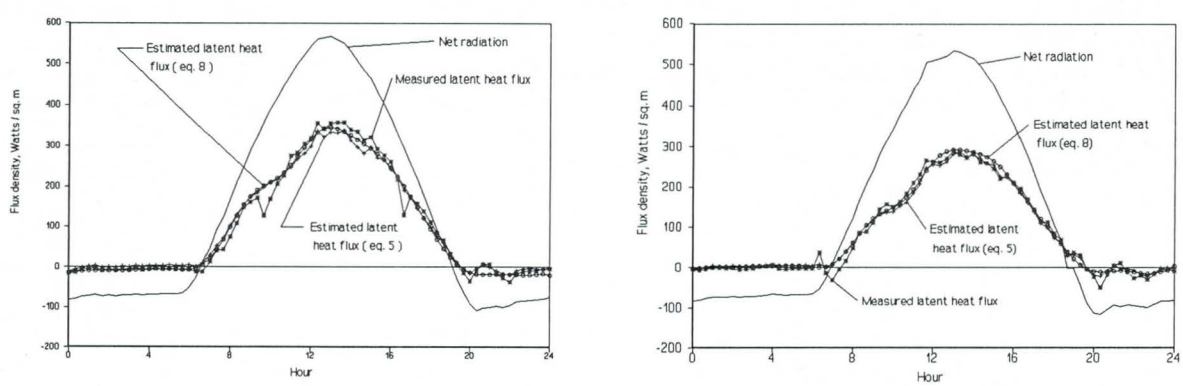

Figure 3. Comparison of measured and estimated latent heat flux at greaswood site for A) June 18, 1989, B) July 29,1989,

the models and coefficients to other climatic regions has not yet been determined. However, for the conditions at the study sites, the estimated flux values compare very well with measured values. Table 1 compares mean daily values of measured and estimated flux rates and evapotranspiration rates for selected dates. Mean daily flux and evapotranspiration rates estimated by equation 5 are within 8 percent of measured values and those estimated by equation 8 are within 5 percent. Instantaneous 20-minute values calculated by equation 5 are within 10 percent of measured 20-minute values, while those calculated by equation 8 are within about 6 percent. Both equations yield suitably accurrate mean daily values; equation 8 gives somewhat better

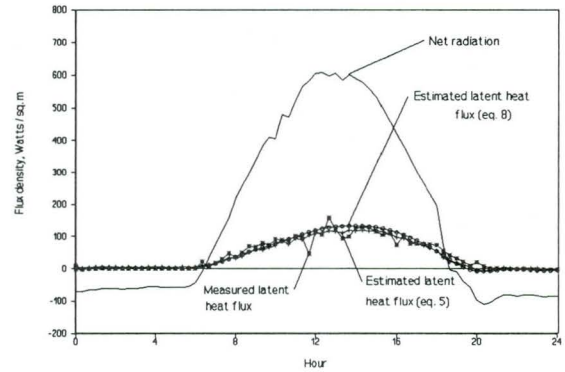

Figure 4. Measured and estimated latent heat flux for sagebrush site, June 4, 1990

Table 1.--*Measured and estimated mean daily values of latent heat flux, evapotranspiration, and Bowen ratios for selected dates.*

	Date			
	June 1989		July 1989	
	18	19	6	29
Flux, W/m^2				
Measured	202.1	207.4	168.3	171.7
Equation 5	202.8	207.3	173.2	164.9
Equation 8	200.2	204.4	169.8	158.7
Evapotranspiration, mm				
Measured	7.15	7.34	5.95	6.08
Equation 5	7.18	7.34	6.13	5.83
Equation 8	7.09	7.15	6.01	5.62
Bowen ratio				
Measured	0.3593	0.3881	0.4144	0.4575
Equation 5	0.3543	0.3583	0.3836	0.4698
Equation 8	0.3329	0.3266	0.4085	0.5280
Correlation coefficient				
Equation 5	0.991	0.991	0.994	0.992
Equation 8	0.992	0.995	0.996	0.995

results for 20-minute time periods. Equation 5 can be solved with a single value of net radiation and soil heat flux; equation 8 requires 24 hours of hourly or 20-minute data to calculate the Fourier coefficients.

Using the equations presented above, it is now possible to estimate daily latent heat flux rates from greasewood and sagebrush growing in areas were ground water is within 4 m of land surface using only values of net radiation and soil heat flux. It remains to be determined if the value of the variables b, A_0 and C are general and apply to all occurrences of greasewood as well as sagebrush utilizing ground water or if these values change with different climatic regions, canopy density, depths to ground water, ground-water quality, and soil types.

References Cited

Brutsaert, W., 1982, Evaporation into the atmosphere: Boston, Mass., R. Reidel Publishing Co., 229 p.

Kirkham, D., and Powers, W.L., 1972, Advanced soil physics: New York, N.Y., John Wiley and Sons, Inc., 534 p.

TOPIC C

MONITORING AND FORECASTING

A SIMPLIFIED APPROACH FOR EVALUATING EVAPORATION USING SATELLITE-BASED REMOTELY SENSED DATA

M. Susan Moran and Ray D. Jackson

USDA-ARS U.S. Water Conservation Laboratory, Phoenix, Az. 85044 USA

ABSTRACT

Latent heat flux density (LE: the product of the heat of vaporization L and the rate of evaporation E) was estimated for an agricultural area near Maricopa, Arizona, using Landsat Thematic Mapper (TM) spectral data with on-site measurements of solar irradiance, air temperature, wind speed and vapor pressure. Simplified methods for the atmospheric correction of TM visible and thermal data and for the determination of aerodynamic resistance were tested that may prove useful in an operational mode. The satellite-based estimates of LE differed from ground-based Bowen ratio measurements by less than 10 percent in fields of cotton and alfalfa.

INTRODUCTION

Evaporation of water from the earth's surface is of vital importance for agricultural applications and is also of interest in the areas of atmospheric circulation, global climate change, and regional hydrology. However, obtaining information about surface evaporation is limited by the lack of convenient, accurate methods for estimation over large areas. Conventional methods such as weighing lysimeters (van Bavel and Myers, 1962) and eddy-correlation or Bowen-ratio methods (Gay and Greenberg, 1985; Swinbank, 1951) provide a reasonably accurate means of measuring actual evaporation on a hourly or daily basis, but resulting data may not be valid beyond the immediate vicinity of the apparatus. One method of mapping the spatial distribution of evaporation on regional or local scales is to use remotely-sensed spectral data for evaluation of latent heat flux density (LE: the product of the heat of vaporization L and the rate of evaporation E) based on surface energy balance.

Jackson (1985) proposed that, on a local scale, the surface-dependent components of the energy balance (reflected radiation and surface temperature) could be measured remotely and combined with on-site meteorological measurements (solar and sky radiation, air temperature, wind speed, and vapor pressure) to evaluate three terms of the energy balance equation and obtain LE as a residual. This technique was successfully applied to mature agricultural fields using ground-, aircraft- and satellite-based sensors (Reginato and others, 1985; Jackson and others, 1987; Moran and others, 1990) and, with some refinements, to an arid rangeland site (Moran and others, 1991b). However, in each case, the application was dependent upon on-site measurements of some field characteristics, such as surface aerodynamic roughness and plant height, and, in the case of the satellite-based application, measurements of atmospheric optical depth and water content.

In this analysis, new methods are tested for estimation of aerodynamic properties of the surface and atmospheric correction of satellite sensor

output, in order to circumvent the need for detailed atmospheric and field-scale agronomic measurements. These simplified methods may be useful in the development of an operational system for assessment of regional evaporation[1].

REMOTE ENERGY BALANCE METHOD

The method for estimating energy balance components from remote sensors and ground-based meteorological instruments is based on the evaluation of a one-dimensional form of the energy balance equation,

$$LE = R_N - G - H, \tag{1}$$

where R_N is the net radiant flux density, G is soil heat flux density, H is sensible heat flux density, and values of LE, G and H are positive when directed away from the surface.

Net radiant flux density is the sum of incoming and outgoing radiant flux densities,

$$Rn = R_{S\downarrow} - R_{S\uparrow} + R_{L\downarrow} - R_{L\uparrow}, \tag{2}$$

where the subscripts S and L signify shortwave radiation (0.15 to 4 μm) and longwave radiation (> 4 μm), respectively, and the arrows indicate the flux direction (↓=incoming, ↑=outgoing). $R_{S\downarrow}$ can be measured directly with a calibrated pyranometer and $R_{L\downarrow}$ can be estimated from ground-based measurements of air temperature and vapor pressure (Jackson and others, 1985). The outgoing terms ($R_{S\uparrow}$ and $R_{L\uparrow}$) can be inferred from data collected with down-looking multispectral sensors (Jackson, 1984; Jackson and others, 1987).

The G term can be determined by a relation between G/R_N and surface reflectance factors in the red and near-infrared (NIR) spectral bands (Jackson and others, 1987). The relation has the form

$$G/R_N = 0.583e^{-2.13ND}, \tag{3}$$

where ND is the normalized difference [(NIR-red)/(NIR+red)], a spectral index that estimates the amount of vegetation present. This expression is limited to clear sky conditions and midday hours.

The sensible heat flux density can be expressed as

$$H = \rho c_P(T_S - T_A)/r_A, \tag{4}$$

where ρc_P is the volumetric heat capacity ($\approx$1200 J m^{-3} C^{-1}), T_S and T_A are surface and air temperatures (C), respectively, and r_A is a stability-corrected aerodynamic resistance (s m^{-1}) (adapted from Mahrt and Ek, 1984) which is a function of T_S, T_A, wind speed (U), the height above the surface at which the wind speed and air temperature are measured, and the aerodynamic parameters: surface roughness (z_O) and displacement (d).

ATMOSPHERIC CORRECTION AND DETERMINATION OF AERODYNAMIC RESISTANCE

An effort was made to apply the remote energy balance method with a minimum of on-site measurement requirements. In this section, conventional

---

[1] In this text, the term evaporation is used instead of evapotranspiration to refer to the evaporation of water from soils and plants. Penman (1963) pointed out that the term evapotranspiration is a misnomer because water is *transpired* to the plant leaves but it *evaporates* from the stomatal cavities.

methods for correcting atmospheric effects and determining resistance to heat transfer are briefly outlined and possible operational methods are proposed.

Atmospheric Correction, Visible and NIR Data

In previous applications of the remote energy balance method, atmospheric corrections to satellite digital data were made by measuring atmospheric optical depth on the day of satellite overpass and using a radiative transfer code (RTC) to compute the relationship between surface reflectance and radiance at the sensor (Holm and others, 1989). This procedure is too expensive and time consuming to be used on a regular basis. Moran and others (1991a) found that, though the most accurate results were obtained using RTCs with on-site measurements of optical depths, acceptable results (±0.02 reflectance) were achieved using RTCs with reasonable estimates of atmospheric conditions. They proposed that a simple RTC, such as Lowtran7 (Kneizys and others, 1988), could be used with available modeled atmospheres to retrieve acceptable estimates of surface reflectance from satellite sensor digital data.

Atmospheric Correction, Thermal Data

Atmospheric correction of Landsat thermal data has principally involved complex atmospheric correction models with measurements of atmospheric soundings (Byrnes and Schott, 1986). Atmospheric soundings must be made on site, concurrent with the satellite overpass; non-local and non-coincident radiosonde data can result in errors in estimation of surface temperature as large as 12 °C (Wukelic and others, 1989). A simple statistical regression of image data with simultaneously acquired surface temperatures has been proposed to circumvent the need for radiosonde measurements (Malaret and others, 1985). Moran (1990) conducted a comparison of correction methods based on Landsat thermal data (TM6) and measurements of T_s acquired using aircraft-based sensors. They found that linear regressions of measured T_s and TM6 digital numbers provided satellite-based estimates of T_s to within ±1.2 °C of measured values.

Remote Estimation of z_0 and d

The common practice of estimating z_0 and d from plant height (Brutsaert, 1975) is difficult for large, diverse areas where plant height (h) is rarely known and not easily estimated from satellite-based spectral data. However, ratios of z_0/h and d/h are related to plant density (Shaw and Pereira, 1982), a parameter that can be estimated from remote spectral data (Tucker, 1979). Moran (1990) determined empirical relations between z_0 and d and the ratio of NIR and red reflectance factors based on measurements over a one-year period in an alfalfa field,

$$z_0 = e^{\{-0.769 + 0.181\ (NIR/red)\}}, \text{ and} \tag{5}$$

$$d = e^{\{0.951 + 0.176\ (NIR/red)\}}. \tag{6}$$

When applied to cotton and wheat fields in Arizona, the uncertainty in H associated with the error in remote estimates of z_0 and d was ±25 percent.

EXPERIMENTAL SITE AND PROCEDURE

The experimental site was the University of Arizona Maricopa Agricultural Center (MAC), located about 48 km south of Phoenix. From April

1985 to June 1986, meteorological measurements were made on each day of the Landsat-5 overpass, weather and equipment permitting. Data used in the following analysis were limited to two dates when Landsat Thematic Mapper (TM) data were acquired and Bowen-ratio data were collected, and to fields in which the Bowen-ratio equipment (Gay and Greenberg, 1985) was located, i.e., in a cotton field (0.27 X 1.6 km) on 23 July 1985 and an alfalfa field (0.14 X 0.8 km) on 24 June 1986. A portable micrometeorological station, located in the same field as the Bowen-ratio equipment, recorded incoming solar radiation, wet- and dry-bulb air temperatures, and wind speed (at 1.5 m) at 6-second intervals. Fluctuations of the 6-second wind speed values were reduced by smoothing the data with a 30-point (3-minute) running average.

Energy fluxes, R_N, G and H, were computed using the remote energy balance method according to procedures described by Moran and others (1990), with several modifications designed to enhance operational utility. The Landsat visible and NIR digital data were converted to radiance values using the Lowtran7 code with the standard atmospheric models, as proposed by Moran and others (1991a). The surface temperatures were retrieved from TM thermal data using empirical regression equations based on a small sample of TM digital data and corresponding surface temperature measurements (Moran, 1990). Resistance to sensible heat transfer (r_A) was computed using Mahrt and Ek's (1984) equations with values of z_0 and d based on the NIR/red ratio (Eqs. 5 and 6). These enhancements to the model eliminated the need for on-site measurements of optical depth, atmospheric water vapor, and plant height.

RESULTS AND DISCUSSION

A comparison of remote estimates of R_N, G, H, and LE with values measured using the Bowen-ratio apparatus is shown in Figure 1. The bars indicate values at the location of the Bowen-ratio apparatus.

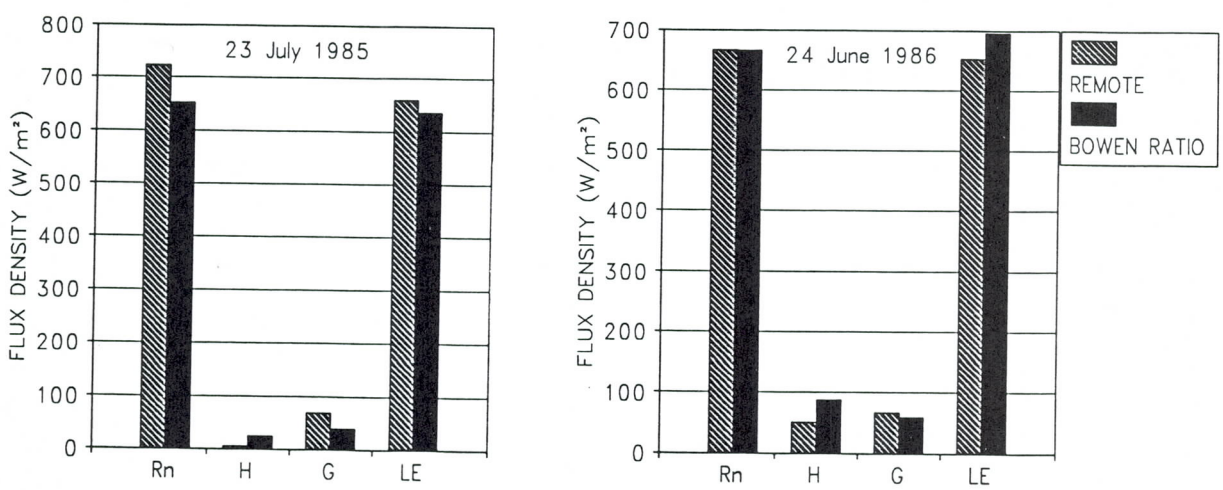

Figure 1.--Estimates of net radiant flux density (R_N), sensible heat flux density (H), soil heat flux density (G), and latent heat flux density (LE) (W m^{-2}) at the location of the Bowen-ratio apparatus in the cotton field on 23 July 1985 and in the alfalfa field on 24 June 1986.

Of the four energy balance components, LE and R_N are the largest values for cropped fields; values of H and G are often an order of magnitude smaller than LE and R_N. Thus, the accuracy of the estimate of R_N will have the greatest effect on the accuracy of LE. Although relative differences between remote and Bowen-ratio estimates of G and H were large, the differences between LE values (3.6 percent for cotton and -6.2 percent for alfalfa) were still within ±10 percent. This uncertainty is comparable to the uncertainty of conventional ground-based instruments (Kanemasu and others, 1987).

The results reported here indicate that a satellite-based technique will yield values of LE from full-cover cropped fields that compare well with values measured with the Bowen-ratio method. However, there are still several aspects of the remote energy balance method that need further attention before it can be applied on an operational basis.

Atmospheric correction of TM thermal data is presently based on a concurrent set of measurements of T_S over a variety of surfaces. This procedure would obviously be inconvenient if the method were to be used on an operational basis. Ideally, a correction technique should be based on information that is readily available from conventional weather stations or from the satellite digital data.

Estimations of surface roughness and aerodynamic resistance are currently based on an empirical relation with the NIR/red reflectance ratio. This relation was developed from data collected in an experimental alfalfa field. Although the accuracy was acceptable, the results were considered to be crop-specific and not necessarily applicable to other crops.

Finally, there are difficulties in extrapolating ground-based measurements of T_A and U over complex terrain. Both T_A and U are sensitive to local topography and changes in surface cover. For example, Brown and Owen-Joyce (1991) reported differences in T_A of 3 °C between instruments located in an irrigated cotton field and an adjacent fallow field.

REFERENCES CITED

Brown, P.W. and Owen-Joyce, S.J., 1991, Remote sensing and evapotranspiration estimates: influence of ground-based meteorological data: U.S./P.R.C. Bilateral Symp. on Droughts and Arid-Region Hydrology, Tucson, Az., (in press).

Brutsaert, W.H., 1975, Comments on surface roughness parameters and the height of dense vegetation: J. Meteorol. Soc. Jpn., vol. 53, p. 96-97.

Byrnes, A.E. and Schott, J.R., 1986, Correction of thermal imagery for atmospheric effects using aircraft measurement and atmospheric modeling techniques: Applied Optics, vol. 25, p. 2563-2570.

Gay, L.W., and Greenberg, R.J., 1985, The AZET battery-powered Bowen ratio system: Proc. of the 17th Conf. on Agric. and Forest. Meteorol., Scottsdale, Az., Amer. Meteorol. Soc., Boston, Ma., p. 181-182.

Holm, R.G., Moran, M.S., Jackson, R.D., Slater, P.N., Yuan, B., and Biggar, S.F., 1989, Surface reflectance factor retrieval from Thematic Mapper data: Rem. Sens. of Environ. vol. 27, p. 47-57.

Jackson, R.D., 1984, Total reflected solar radiation calculated from multiband sensor data: Agric. and For. Meteorol., vol. 33, p.163-175.

Jackson, R.D., 1985, Evaluating evapotranspiration at local and regional scales: Proc. of the I.E.E.E., vol. 73, p. 1086-1096.

Jackson, R.D., Moran, M.S., Gay, L.W. and Raymond, L.H., 1987, Evaluating evaporation from field crops using airborne radiometry and ground-based meteorological data: Irrig. Sci., vol. 8, p. 81-90.

Jackson, R.D., Pinter, P.J. Jr. and Reginato, R.J., 1985, Net radiation calculated from remote multispectral and ground station meteorological data: Agric. For. Meteorol., vol. 35, p. 153-164.

Kanemasu, E.T., Asrar, G., Nie, D., Watts, D., Fritschen, L., Gay, L., Weaver, H., Tanner, B., Tanner, M., Green, J. and Stannard, P., 1987, Inter- and intra-sensor comparisons among Bowen-ratio and eddy correlation instruments: Intl. Symp. on Flow and Transport in The Natural Environ.: Advances and Applications, Canberra, Australia.

Kneizys, F.X., Shettle, E.P., Abreu, L.W., Chetwynd, J.H., Anderson, G.P., Gallery, W.O., Selby, J.E.A., and Clough, S.A., 1988, Users Guide to LOWTRAN 7: Report AFGL-TR-88-0177, AFRCL, Bedford, Mass., 137 p.

Mahrt, L., and Ek, M., 1984, The influence of atmospheric stability on potential evaporation: J. Climate and Appl. Meteorol., vol. 23, p. 222-234.

Malaret E., Bartolucci, L.A., Lozano, D.F., Anuta, P.E. and McGillen, C.D., 1985, Landsat-4 and Landsat-5 Thematic Mapper data quality analysis: Photogramm. Eng. Rem. Sens., vol. 51, p. 1407-1416.

Moran, M.S., 1990, A satellite-based approach for evaluation of the spatial distribution of evapotranspiration from agricultural lands: Ph.D. Dissertation, Univ. of Ariz., Tucson, Az. 223 p.

Moran, M.S., Jackson, R.D., Raymond, L.H., Gay, L.W. and Slater, P.N., 1990, Mapping surface energy balance components by combining Landsat Thematic Mapper and ground-based meteorological data: Rem. Sens. of Environ., vol. 30, p. 77-87.

Moran, M.S., Jackson, R.D., Slater, P.N. and Teillet, P.M., 1991a, Comparison of atmospheric correction procedures for visible and near-infrared satellite sensor output: 5th Intl. Coll. on Phys. Meas. and Signatures in Rem. Sens., Courchevel, France (in press).

Moran, M.S., Kustas, W.P., Vidal, A., Stannard, D.I. and J. Blanford, 1991b, Use of ground-based remotely sensed data from surface energy balance calculations during Monsoon'90: IEEE Geosci. and Rem. Sens. Symp., Helsinki, Finland, (in press).

Penman, H.L., 1963, Vegetation and hydrology: Tech. Commun. No. 53, Commonwealth Bur. of Soils, Harpenden, 123 p.

Reginato, R.J., Jackson, R.D., and Pinter, P.J., Jr., 1985, Evaporation calculated from remote multispectral and ground station meteorological data: Rem. Sens. of Environ., vol. 18, p. 75-89.

Shaw, R.H. and Pereira, A.R., 1982, Aerodynamic roughness of a plant canopy: a numerical experiment: Agric. Meteorol., vol. 26, p. 51-65.

Swinbank, W.C., 1951, The measurement of vertical transfer of heat and water vapor by eddies in the lower atmosphere: J. Meteorol., vol. 8, p. 135-145.

Tucker, C.J., 1979, Red and photographic infrared linear combinations for monitoring vegetation: Rem. Sens. Environ., vol. 8, p. 127-150.

van Bavel, C.H.M. and Myers, L.E., 1962, An automatic weighing lysimeter: Agric. Eng., vol. 43, p.580-583 and p. 586-588.

Wukelic, G.E., Gibbons, D.E., Martucci, L.M. and Foote, H.P., 1989, Radiometric calibration of Landsat Thematic Mapper thermal band: Rem. Sens. of Environ., vol. 28, p. 339-347.

REMOTE SENSING AND EVAPOTRANSPIRATION ESTIMATES: INFLUENCE OF GROUND-BASED METEOROLOGICAL DATA

Paul W. Brown

University of Arizona, Tucson, AZ

Sandra J. Owen-Joyce

U.S. Geological Survey, Tucson, AZ

ABSTRACT

Models that use instantaneous remotely sensed multispectral data for regional evapotranspiration (ET) assessment estimate ET in terms of latent heat flux (LE) and require ground-based meteorological data. The quality and acquisition interval of ground-based meteorological data can limit the accuracy of the LE estimates. In this study, portable meteorological stations were established over cotton plants and fallow ground to provide the ground-based meteorological data needed to investigate (1) how the acquisition interval of ground-based data affects LE estimates and (2) whether point-source ground-based data can be used to estimate regional LE. Instantaneous (1-minute), 15-minute mean, and 59-minute mean values of air temperature and wind speed were combined with instantaneous values of net radiation and canopy temperature and were input into an ET model; the resulting LE estimates were compared. The period over which air temperature and wind speed were averaged did not have a major effect on LE estimation. Brief periods of high or low wind speed did, at times, create instantaneous LE estimates that differed considerably from those estimated with the 15- and 59-minute averages. Surface characteristics did affect air temperature and wind speed and, thus, limited the ability to transfer data to other sites with different surface conditions. Futhermore, when measurements of air temperature and wind speed are transferred to a different surface, the measurement height can have a major effect on sensible heat flux and thus on LE estimation. Adjustments in wind speed or height might be necessary to transfer wind-speed data to a different surface. However, reasonably accurate results were obtained when air temperature and wind speed obtained over one surface were used to estimate LE of a second similar surface; differences in wind speed, air temperature, and height were minimal and produced only small differences in LE.

INTRODUCTION

Economic growth in many parts of the United States and the world hinges on the availability of adequate supplies of water. In the Southwest, rapid population growth and widespread irrigation have raised concerns over the long-term reliability of water supplies. These concerns have fueled legislative and political pressures to manage large-scale irrigation projects efficiently.

Accurate, near-real-time information on crop evapotranspiration (ET) could be one means of improving the overall efficiency of an irrigation project. The information has potential uses at the grower and project level. Growers can use ET information in conjunction with irrigation-scheduling programs to optimize the use of irrigation water in crop production; managers of irrigation projects can use ET information to anticipate and schedule water deliveries.

Current methods of estimating ET typically use a simple model that requires some form of ground-based weather data as input. Most commonly used ET models are not highly accurate, particularly when used to estimate ET on a regional basis. The use of remote-sensing techniques has been suggested as a method of improving regional ET estimation. Recent research indicates that remotely sensed emitted and reflected electromagnetic radiation

(multispectral data), combined with ground-based meteorological data, can provide accurate estimates of ET (Hatfield and others, 1983; Jackson and others, 1983; 1987; Reginato and others, 1985). Jackson and others (1987) and Reginato and others (1985) suggest that a major limitation to the accuracy of ET estimates rests in the ground-based meteorological data.

Ground-based meteorological data are available in the Southwest because of the presence of automated weather-station networks (Brown, 1987; 1989), many of which provide weather-based information to agricultural clientele. Nearly all agricultural weather networks collect and disseminate data on solar radiation, temperature, wind, and humidity—parameters currently used to estimate ET using remote-sensing methods. Questions remain, however, on how to combine ground-based data and remotely sensed data correctly to ensure accurate regional ET estimates. One area of concern relates to the required acquisition interval of ground-based data. Most weather networks provide data for hourly intervals while the data captured by remote-sensing platforms (satellite or aircraft) are virtually instantaneous. The acquisition interval of ground-based meteorological data might need to be adjusted to effectively use remote-sensing techniques to estimate regional ET. A second area of concern relates to how well point-source ground-based data can describe weather conditions over an entire region. Automated weather stations typically are 20 to 50 km apart and located over and adjacent to a variety of surfaces ranging from sparse range and fallow ground to well-watered turf or alfalfa. The spatial reliability of the data obtained from these point-source stations is of critical concern and could become the major limitation to the use of remote-sensing techniques to estimate regional ET.

Groups of portable meteorological stations were established over agricultural fields during the summer of 1989 to investigate two specific questions. First, how does placement and exposure of the weather station affect the usefulness of the resulting data for input in remote-sensing ET models? Second, how does the acquisition interval affect the usefulness of ground-based weather data for remote-sensing ET estimation? This paper presents the results of these studies.

METHODS

Ground-Based Meteorological Data

Ground-based meteorological stations were installed in five agricultural fields on and to the south of the University of Arizona Maricopa Agricultural Center (MAC) between day of year (DOY) 239 (Aug. 27) and 256 (Sept. 13) in 1989 (fig. 1). MAC is about 45 km south of Phoenix. Stations were installed in cotton fields managed by MAC (MAC), Mr. Pat Murphree (MUR), Ak Chin Farms (AK), and Mr. John Smith (SMI). A fifth station was installed in a fallow field at MAC (FAL). All stations were positioned to provide a fetch-to-instrument height ratio of at least 100:1 in the direction of the prevailing winds.

Each station consisted of a tripod tower, an auxiliary sensor support mast, a datalogger, attendant sensors, and equipment necessary to store incoming data on cassette tape. Meteorological data acquired by each station consisted of air temperature (T_a), relative humidity (RH), wind speed (U), solar radiation (SR), and net radiation (R_n). Sensors used to measure T_a, RH, and U were installed 1.5 m above the top of the canopy in the cotton fields and 1.5 m above the soil surface in the fallow field. Net radiometers were installed 1.0 m above the canopy/soil surface, and pyranometers were installed between 0.75 and 1.5 m above the canopy/soil surface. An infrared thermometer (IRT, 15° field of view) was installed at MUR to provide surface temperature (T_s). The IRT, which was calibrated at a U.S. Water Conservation Laboratory, was mounted 1.3 m above the canopy and oriented to provide a nadir view of the canopy. Output from all sensors was sampled once each minute by automatic dataloggers.

The cotton at all locations had reached cutout (in-season cessation of flowering) at the start of the study. Consequently, the cotton, although green and healthy, was not growing vertically to any extent. Canopy height remained 1.35, 1.15, 0.95, and 1.0 m at MAC, MUR, AK, and SMI, respectively, for the duration of the study.

ET Estimation

The ET model of Jackson and others (1987) and Reginato and others (1985) was chosen for evaluation in this study. The model is based on the energy balance equation

$$LE = R_n - G - H, \qquad (1)$$

where LE is the latent heat flux, R_n is the net radiation, G is the soil heat flux, and H the sensible heat flux. Net radiation generally is estimated using a combination of remotely sensed multispectral data and ground-based meteorological data (Jackson and others, 1985; Moran and others, 1989). However, because multispectral data were not available for this study, the R_n measured at the meteorological stations was used for LE estimation. G was estimated by letting G equal $0.1R_n$ on the basis of the results of W.P. Kustas and C.S.T. Daughtry (written commun., U.S. Agricultural Research Service, 1988). Sensible heat flux is calculated using the equation

$$H = \rho C_p(T_s - T_a)/r_a, \qquad (2)$$

where ρC_p is the volumetric heat capacity (~1150 J/kg/°K at 25°C at MAC elevation), T_s is the surface temperature, T_a is the air temperature, and r_a is the aerodynamic resistance. The value for r_a is determined using the formula of Mahrt and Ek (1984):

For $(T_s - T_a) < 0$ (stable)

$$r_a = \{\ln[(z-d+z_o)/z_o]/k\}^2(1+15Ri)(1+5Ri)^{1/2}/U \qquad (3)$$

For $(T_s - T_a) > 0$ (unstable)

$$r_a = \{\ln[(z-d+z_o)/z_o]/k\}^2\{1-15Ri/[1+C(-Ri)^{1/2}]\}^{-1}/U, \qquad (4)$$

where z is the height above the ground surface at which U and T_a are measured; d is the displacement height; z_o is the surface roughness; k is von Karman's constant (0.4); Ri is the Richardson number calculated as

$$Ri = g(T_a - T_s)(z-d)/T_aU^2, \qquad (5)$$

where g is the acceleration due to gravity; U is the windspeed; and

$$C = 75k^2[(z-d+z_o)/z_o]^{1/2}/\{\ln[(z-d+z_o)/z_o]\}^2. \qquad (6)$$

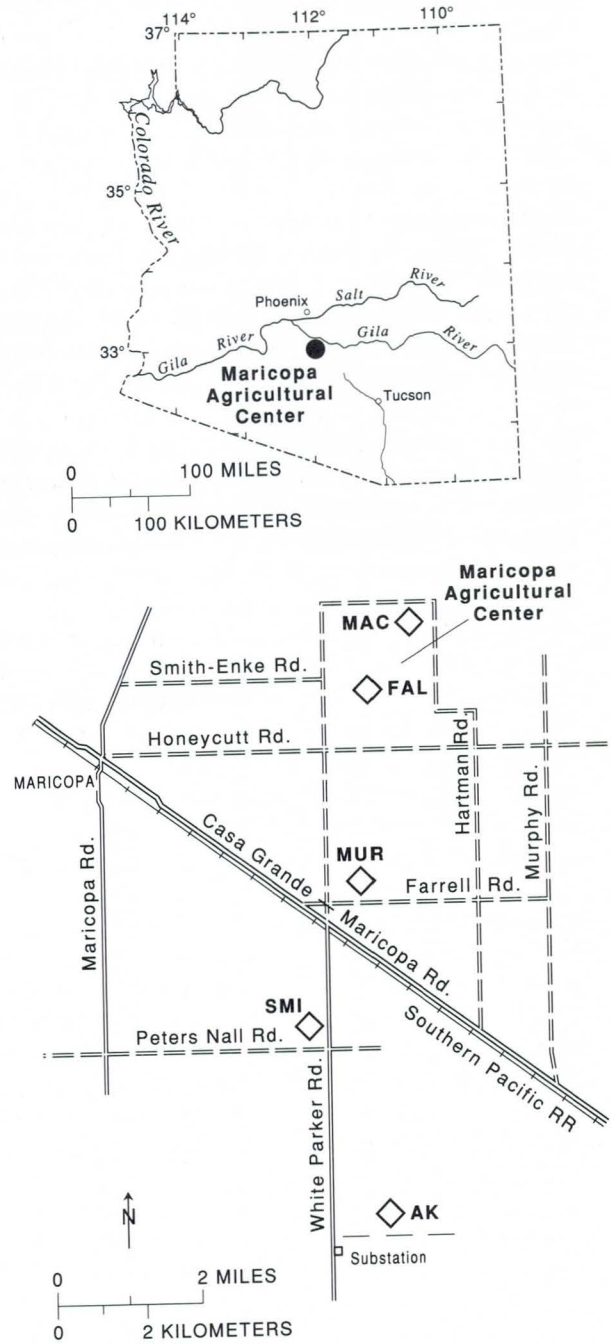

Figure 1.—Location of ground-based meteorological stations.

The d and z_o terms required in eqs. 3-6 were estimated from canopy height (h) using the relations d = 0.63h and z_o = 0.13h as reported by Montieth (1973).

LE Evaluations and Analysis

The acquisition interval of T_a and U data was evaluated for its effect on LE as computed by the Jackson model. The evaluations were performed at 10:30, 11:30, 12:30, 13:30 and 14:30 m.s.t. on DOY 239, 247, 255 and 256. Instantaneous (1-minute) values of R_n, T_s, T_a, and U obtained in the MUR field at each of the times were input into eqs. 1-6 to obtain instantaneous LE values (LE_i).

Next, the instantaneous T_a and U values were replaced in eqs. 1-6 with T_a and U obtained by averaging over 15- and 59-minute periods. Each averaging period contained the central measurement minute (10:30, 11:30, ...) plus an equal number of T_a and U values obtained prior to and after the central minute. For example, a 15-minute average value for 10:30 used data collected from 10:23 through 10:37; a 59-minute average value for the same time was computed from data collected between 10:01 and 11:00. The LE values obtained using the 15- and 59-minute means of T_a and U (LE15 and LE59) were then compared with LE_i.

The entire process of calculating LE_i and evaluating the effects of time averaging T_a and U were repeated using T_a and U data obtained from the FAL, MAC, AK, and SMI locations. This analysis provided an opportunity to evaluate whether ground-based meteorological data acquired over similar and (or) dissimilar surfaces can be transferred across a distance of 14 km (fig. 1). The measurement height (z) of the T_a and U sensors at FAL, MAC, AK and SMI differed from that at the MUR field. For this analysis, the z used in eqs. 3-6 to estimate H was that of the sensors used to obtain T_a and U, not the z at MUR.

COMPARISON RESULTS AND DISCUSSION

The results presented here illustrate some of the potential problems associated with using ground-based meteorological data in ET models designed to use remotely sensed multispectral data. Data from DOY 239 were found to be representative of the overall results of this study and are presented to show the effects of data-acquisition interval and surface conditions on LE estimation.

The characteristics of the underlying surface affected both T_a and U. T_a and U were consistently higher over fallow ground than over the cotton fields (figs. 2 and 3). When averaged over 15-minute midday periods, T_a over FAL generally was 1-3°C warmer than T_a obtained over cotton (fig. 2). Similarly, midday mean U typically was 0.5-1.0 m/s higher than U obtained over cotton (fig. 3). T_a and U compared reasonably well across the four cotton fields. Midday means of T_a were within 2°C in most situations and frequently within 1°C. Mean U over the four cotton fields typically was within 0.5 m/s, although in some cases mean U differed by more than 1.0 m/s.

The averaging period for T_a and U did affect the resulting LE estimations, but the effects were not systematic in one direction or the other (high or low). In general, the effect of time averaging was small, averaging less than 50 W/m^2 in most cases; however, in one case, LE_i was nearly 150 W/m^2 greater than LE15 and LE59 (fig. 4, 13:30). In this case, the instantaneous U value was much greater than the 15- and 59-minute mean U value. Throughout this study, when LE15 and LE59 were significantly different from LE_i, these differences were caused by fluctuations in U. T_a proved to be much less variable and tended to change in a nearly linear fashion over the averaging periods. As a result, the effect of time averaging of T_a on LE estimates was not great.

The characteristics of the underlying surfaces determined whether T_a and U obtained over one field could be transferred to another field for use in estimation of LE. The worst-case scenario resulted when T_a and U from a fallow field were used to estimate LE over cotton. The higher T_a and U and the lower z value over the fallow field, when merged with R_n and T_s from MUR and inserted into eqs. 3-6, resulted in higher calculated H, which results in much higher LE estimates than would be computed using local wind and temperature data (fig. 5). This enhanced level of H could be minimized to some extent by either (1) making a correction in z when transferring the T_a and U from a fallow field to cotton, or (2) adjusting U for changes in surface roughness and atmospheric stability.

Use of T_a and U obtained over one cotton field to estimate LE over a second cotton field appears more promising. In most cases, LE estimates made with T_a and U from other cotton fields were within 15 percent of LE computed

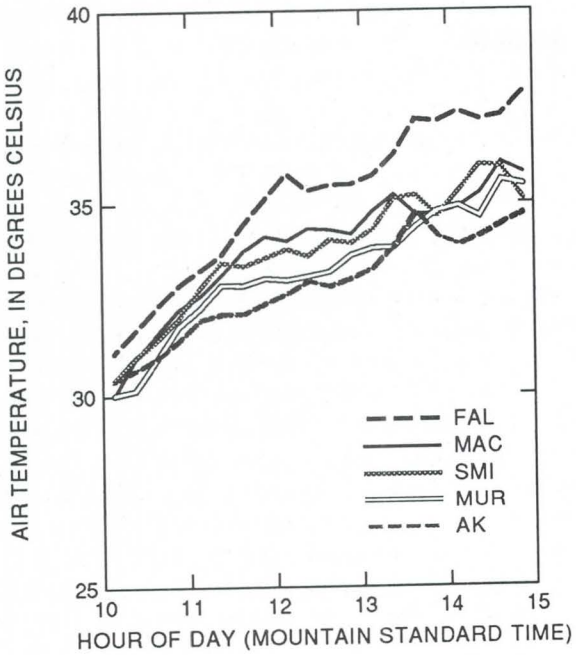

Figure 2.—Fifteen-minute mean values of midday air temperature obtained from ground-based meteorological stations located over fallow ground (FAL) and four different cotton fields (MAC, MUR, AK, and SMI) on August 27, 1989 (DOY 239).

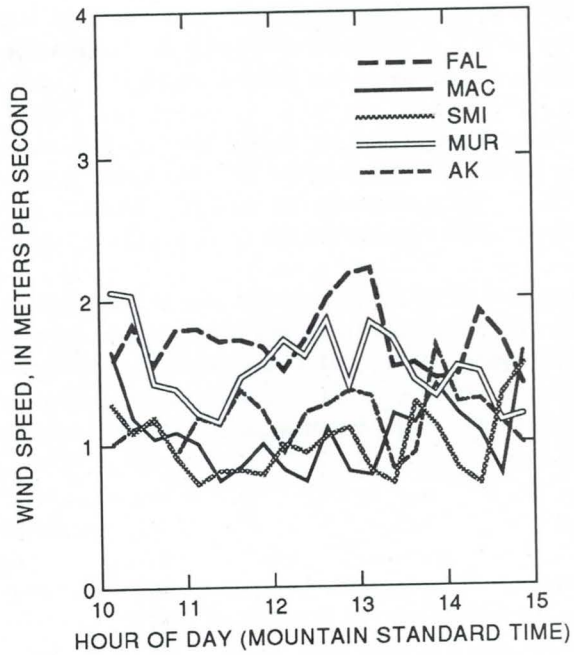

Figure 3.—Fifteen-minute mean values of midday wind speed obtained from ground-based meteorological stations located over fallow ground (FAL) and four different cotton fields (MAC, MUR, AK, and SMI) on August 27, 1989 (DOY 239).

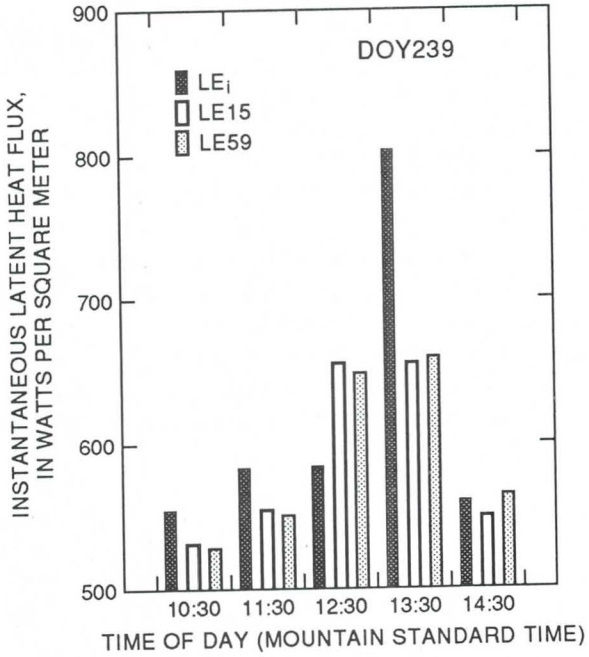

Figure 4.—Latent heat flux (LE) estimates made for MUR using instantaneous latent heat flux (LE_i) as well as 15- and 59-minute mean values (LE15 and LE59) of air temperature (T_a) and wind speed (U) obtained at MUR.

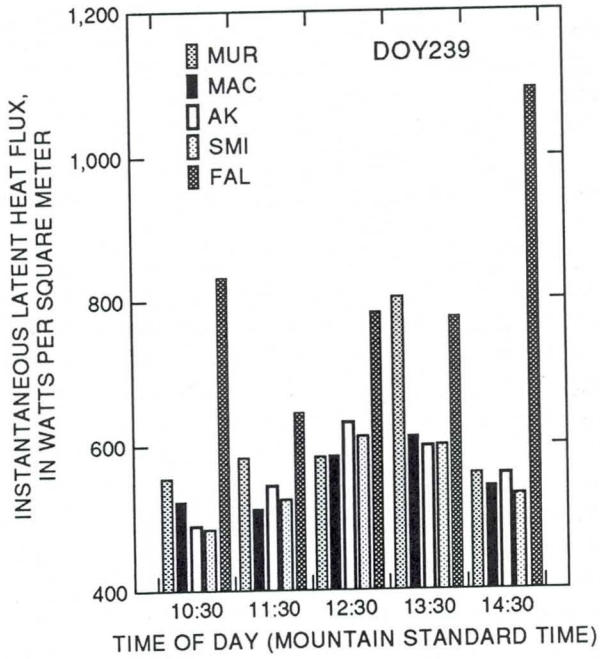

Figure 5.—Midday instantaneous latent heat flux (LE_i) estimates for MUR made using instantaneous values of air temperature (T_a) and wind speed (U) from the MUR, MAC, AK, SMI, and FAL stations.

with local T_a and U data (fig. 5). In some cases, large differences in U caused large differences in LE estimates, even when T_a and U were obtained over similar surfaces (fig. 5 at 13:30). These across-location U differences, on occasion, exceeded 2 m/s, particularly when U was averaged over short periods.

To summarize, this study shows that both data acquisition interval and placement of meteorological stations can affect LE as computed by the Jackson model. The concern raised here pertaining to the effect of short acquisition intervals on LE estimates may well be unfounded, given that the procedures used to estimate H are based on profile theory, which requires the use of U and (T_s-T_a) values that are averaged over a period of at least 15 minutes.

Placement of meteorological stations, or more correctly, the condition of underlying and surrounding surfaces, did affect the data collected. T_a and U acquired on the same farm (MAC and FAL), but over dissimilar surfaces, differed much more than T_a and U acquired from cotton fields separated by a distance of about 14 km. Successful extrapolation of ground-based meteorological data across a region probably will depend more on whether surface characteristics at the station are representative of regional surface conditions rather than on distance from the station.

REFERENCES

Brown, P.W., 1987, Using a computer bulletin board as an agricultural weather information system: Preprint Vol. 18th Conf. Agric. & For. Meteor. and 8th Conf. Biometeor. and Aerobiology. 14-18 Sept. 1987. W. Lafayette, IN. Amer. Meteor. Soc. Boston, MA. p. 67-69.

Brown, P.W., 1989, Accessing the Arizona Meteorological Network by computer: Ext. Rpt. 8733, Univ. of Arizona, College of Agriculture, Tucson, AZ, 26 p.

Hatfield, J.L., Perrier, A., and Jackson, R.D., 1983, Estimation of evapotranspiration at one time-of-day using remotely sensed surface temperatures: Agric. Water Mgmt., v. 7, pp. 341-350.

Jackson, R.D., Hatfield, J.L., Reginato, R.J., Idso, S.B., and Pinter, Jr., P.J., 1983, Estimation of daily evapotranspiration from one time-of-day measurements: Agric. Water Mgmt., v. 7, pp. 351-362.

Jackson, R.D., Pinter, P.J., and Reginato, R.J., 1985, Net radiation calculated from remote multispectral and ground station meteorological data: Agric. and For. Meteor., v. 35, pp. 153-164.

Jackson, R.D., Moran, M.S., Gay, L.W., and Raymond, L.H., 1987, Evaluating evaporation from field crops using airborne radiometry and ground-based meteorological data: Irr. Sci., v. 8, pp. 81-90.

Mahrt, L., and Ek, M., 1984, The influence of atmospheric stability on potential evaporation: J. Climate and Appl. Meteorology, v. 23, pp. 222-234.

Montieth, J.L., 1973, Principles of environmental physics: London, Edward Arnold, 241 p.

Moran, M.S., Jackson, R.D., Raymond, L.H., Gay, L.W., and Slater, P.N., 1989, Mapping surface energy balance components by combining Landsat Thematic Mapper and ground-based meteorological data: Remote Sens. Environ., v. 30, pp. 77-87.

Reginato, R.J., Jackson, R.D., and Pinter, Jr., P.J., 1985, Evapotranspiration calculated from remote multispectral and ground station meteorological data: Remote Sensing of Environment, v. 18, pp. 75-89.

CLIMATOLOGICAL ANALYSIS OF SEASONAL SNOW RESOURCES IN THE QILIAN MOUNTAINS OF NORTH CHINA

Chen Qian and Chen Tianyu

Lanzhou Institute of Arid Meteorology,Lanzhou,Gansu

ABSTRACT

In this paper, snow parameters retrieved from the NOAA AVHRR data during October 1986 — September 1988 with the data of daily depths and density of snow cover and snow days at 26 weather stations from 1951 to 1988 in the Qilian Mountains region have been contrasted for correcting the retrieved snow parameters. The distributions of mean depth and frequency of snow cover have been obtained. Mean snow storage, snowfall and snowmelt runoff for every river basin in this region is estimated.

INTRODUCTION

Snow resources are a very important fresh water supply in North China . Snowmelt–runoff from the Qilian Mountains feeds many of the Hexi and Qaidam continental rivers and provides water for irrigation in these arid regions. About one half of the water that sustains agricuture, industry and domestic water supply in springs at oases in the Hexi corridor is derived from snowmelt water of the Qilian Mountains. The difference between water supply and consumption is especially severe in the Heihe and Shiyang River basins. The water shortage rate is 9% in median years (p = 50%) and 14% in middle dry years(p = 75%). Therefore, it should be noted that measures for saving on water are formulated based on analysis of seasonal snow resources in the Qilian Mountains region, in order to prevent the downstream Shiyang River basins from desertification. On the other hand,any climatic change is certain to be related to change of snow cover in Northern Hemisphere, especially in the Qinghai–Xizang Plateau. Any change of snow resources will have an important influence on the environment and hydrological regimes of all of China. Therefore, the snow cover has been the focus of climatologists' interests during recent decades.

METHODOLOGY AND RETRIEVED MODEL

In order to estimate accurately the area of stable snow cover, altitudes of snow lines, and space distribution of snow depth and snow storage,we have used the NOAA–9 and 10 AVHRR data during October 1986 — september 1988. and landsurface altitudes on a corresponding 1.2 minutes of latitude × longitude grid to retrieve snow cover parameters.

Normalization.

The radiometric information of Channels 1 and 2 of AVHRR flown on the NOAA polar orbiters has no onboard calibration capability. Therefore, a methodology was developed which used the earth's surface as a target, The Badanjilin desert area,which has minimum seasonal change of surface character was adopted as the target to monitor the radiometric calibration. Channel 1 of NOAA–9 has displayed signs of sensor degradtion (Brest et al.,1988). The correction factor is 0.4 percent month. Overflight times of

both satellites NOAA−9 and 10 are different. The error of the cosine of solar zenith angle correction must be revised. In view of above all of these factors, linear regression equations for channels 1 and 2 of NOAA−9 to normalize them to NOAA−10 are as follows:

$$Ch.1(N-10) = 1.3627 + 0.9303 \times (1.075 + 0.004 \times Mon) \times Ch.1(N-9) \quad (1)$$
$$Ch.2(N-10) = 3.6519 + 0.7673 \times Ch.2(N-9) \quad (2)$$

where Ch.1(N−10), Ch.1(N−9), Ch.2(N−10) and Ch.2(N−9) are albedos of Channels 1 and 2 of both satellites NOAA−10 and NOAA−9, respectively,and Mon is number of months from October 1986 (For example,for April 1987, Mon equals 6).

Calculating Snow Cover Areas.

The thresholds of snow cover estimation are albedo of Ch.1 > = 30% and (Ch1.1−Ch.2) > = 0. The albedo of snow cover is the same as that of clouds in visible(Ch.1), but the brightness temperature on cloud tops is lower than that on the surface of snow cover. According to different temperature of both, we could identify cloud.

Estimation of Snow Depth and Snow Equivalent.

The following equation is used for estimation of snow depths

$$Sz = 1.575 \times [0.152 \times Ch.1 + 0.157 \times (Ch.1 - Ch.2) - 3.343] \quad (3)$$

where Sz is snow depth(cm),Ch.1 and Ch.2 are normalized albedos of Channels 1 and 2, respectively.
In order to estimate snow water equivalent,snow density must be recognized.525 samples of fresh snow density were selected from 16 weather stations in 1951−− 1988.The average fresh snow density equalled 0.12 g / cm³. An approximate equation of snow density increasing with time in the Qilian Mountains region has been established as follows:

$$\rho n = 0.12 \times (n+1)^{0.16} \quad (4)$$

where ρn is snow density n days after snowfall. Regional snow water equivalent estimation can be written as follows:

$$SWE = \sum_{i=1}^{N} Sz \times \rho n \times 10^4 \times 4.9457 \times cos\varphi \quad (5)$$

where SWE is snow water equivalent(m^3),N is grid number of snow cover in a river basin, φ is latitude. Using the boundary of the river basin as input to the computer,snow and snowmelt water equivalents are estimated. The derived model is presented by Chen Qian et al(1990).
In order to obtain representative mean values on climate from snow parameters retrieved from NOAA AVHRR data, statistical relationships were determined between mean values of the retrieved parameters and observed values of snow depth and snow cover frequency data at 17 weather stations with more than 28 years of record. Based on data on daily depth and density of snow and snow days at 26 weather stations from 1951 to 1988, using monthly and annual cumulative daily depth, seasonal and annual variations of snow cover have been analyzed. Time−space distribution of snow density has been analyzed for estimation of snow water equivalent.

CLASSIFICATION, DEMARCATION, AND SPATIAL DISTRIBUTION OF SNOW COVER

According to classification of snow cover in China by Li Peiji et al (1983),snow is divided into three types: firn, seasonal stable and unstable snow cover. The snow cover frequency is defined as the number of snow days as a percentage of the total days. The seasonal stable and unstable snow covers are demarcated

by apparent frequency 40% at 1.2 minutes of latitude × longitude grid points. It is defined that the frequency of snow cover more than 40% is called stable seasonal snow cover. Fig.1 is frequency distribution of snow cover.

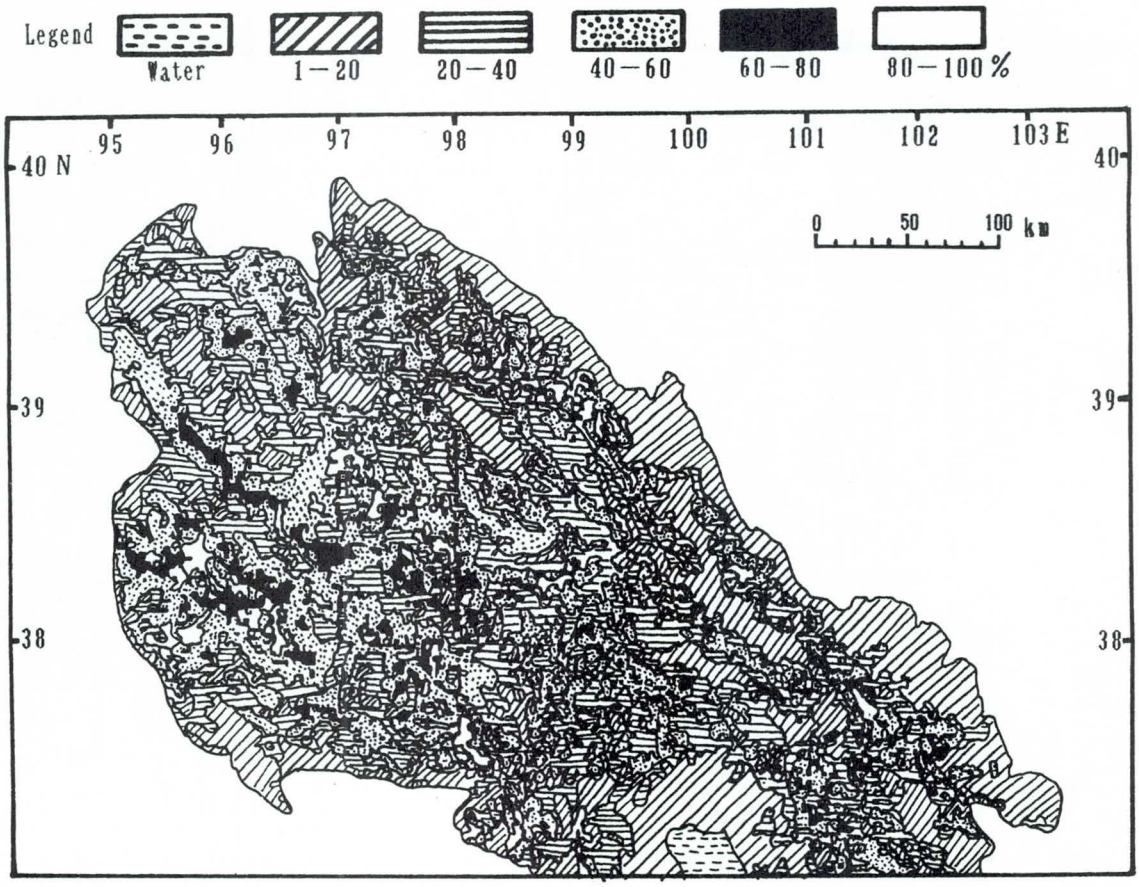

Fig.1—Frequency distribution of snow cover in the Qilian Mountains retrieved from satellite AVHRR data in spring (April—May).

Mean area of stable snow cover during September — May made up 38.7 percent of total area of the Qilian Mountains region. The minimum area occurs in winter and maximum in autumn. Snow cover increases in Spe.–Nov. diminishes in Dec.–Feb and increases again in March –May.The monsoon climate is responsible. The snowfall recharge is much less than the snow dissipation in winter. Therefore,the snow storage is reduced from fall to winter. In spring,the snowfall recharge is much more then the snowmelt that so the snow storage increases again. The highest mean altitude of the snow line is 4085m in winter and the lowest is 3991(from 3425 to 4367)m in spring.In the whole Qilian Mountains region the minimum mean altitude of snowline during September — May occurs in the Shiyang River basins and the maximum in Har Lake basin. Distribution of Firn is in separate patches in the alpine region; their total area is 1972.5 km^2. As much as 1334.7 km^2(67.7 percent) of the total firn area lies in Hexi continental river basins. (Wang Zontai et al, 1981)The detail data of various types of snow cover in every river basin of the QiLian Mountains region are shown in table 1.

The statistical relationships between the mean snow depth at 17 weather stations during 1951—1988 and retrievals data in 1986—1988 have been establish- ed. Then distribution of mean depth of many years with 2x2 km resolution has been made (fig.2). It is shown that the space distribution of snow depth is influenced by altitude and terrain (orograpic effect). Snow depth is increased with altitude. Thicker

Table 1.--Areas of firn and seasonal stable snow cover and altitudes of firn lines and snow lines in every river basin in Qilian Mountains region.

River system	River basins	Area Km^2	Firn region			April-May			Dec.-Feb.			Sep.-May		
			Area Km^2	%	firn lines m.	Area Km^2	%	snow lines m.	Area Km^2	%	snow lines m.	Area Km^2	%	snow lines m.
Sule He	Dang He	15115	259.74	1.7	4887	6752	44.7	4022	4494	29.7	4124	6440	42.6	4057
	Changma He	11417	554.81	4.9	4765	5256	46.1	4035	3435	30.1	4088	4904	42.9	4082
	Shiyou and baiyang He	5327	34.83	0.9	4670	1068	20.0	3800	613	11.5		1010	19.0	
	Subtotal	31859	849.38	2.7	4798	13076	41.0	4009	8542	26.8		12354	38.8	
Hei He	Beida He	6969	136.67	2.0	4630	2293	32.9	3943	1240	17.8	4064	2018	29.0	3998
	Hongshuiba He	1605	130.84	8.2	4705	643	40.4	3728	218	13.6	4247	438	27.3	3994
	Fengle He	568	23.25	4.1	4665									
	Maying He	619	19.52	3.1	4515	468	15.7	3626	64	2.1		420	14.1	
	Bailang He et.	1800	15.13		4450									
	Liyuan He	2211	16.18	0.7	4550	482	21.8	3621	81	3.7	3806	263	11.9	3893
	Hei He	10330	59.00	0.6	4440	3201	31.0	3905	1528	14.8	3991	2902	28.1	3946
	Suyou He et.al	2825	19.96	0.7	4500	443	15.7	3630	63	2.2		405	14.3	
	Subtotal	26927	420.55	1.6	4580	7535	28.0	3851	3194	11.9		6446	23.9	
Shiyang He	Xida He and Dongda He	2729	34.43	2.1	4375	712	26.1	3680	77	2.8		583	21.4	
	Xiying He	1455	19.80	1.4	4260	451	31.0	3765	192	13.2	3836	372	25.6	3823
	Jinta He	1005	6.73	0.7	4300	231	23.0	3612	35	3.5	3801	198	19.7	3469
	Zamu He	902	3.86	0.4	4260	341	37.8	3666	47	5.2	3867	232	25.7	3745
	Huangyang He	884	0			193	21.8	3674	24	2.7	3738	143	16.2	3640
	Gulang He	991	0			160	16.1	3680	20	2.0		191	19.3	
	Subtotal	7966	64.82	0.8	4312	2088	26.2	3688	395	5.0		1717	21.6	
total/mean		66752	1334.75	2.0	4706	22701	34.0	3913	12131	18.2	3986	20517	30.7	3916
%		47.0	67.7			41.9			29.8			37.3		
Cotinental Lake	Har Hu	4952	89.27	1.8	4905	3391	68.5	4381	3569	72.1	4347	3729	75.3	4383
	Northern Qinghai	23012	13.29	0.06	4775	6574	28.6	4111	4117	17.9	4163	7134	31.0	4145
	Subtotal	27964	102.56	0.4	4888	9965	35.6	4203	7686	27.5	4196	10863	38.8	4190
Chaidam		30721	494.22	1.6	4965	15982	52.0	4102	17217	56.0	4256	17417	56.7	4153
total/mean		58685	596.78	1.0	4969	25947	44.2	4141	24903	42.4	4227	28280	48.2	4169
%		41.3	30.2			47.8			61.1			51.5		
Datong and Huangshui		16631	40.97	0.25	4610	5613	33.8	3976	3705	22.3	3961	6168	37.1	3960
%		11.7	2.1			10.3			9.1			11.2		
total of Qilian Mt.or mean		142068	1972.5	1.4	4790	54261	38.2	4028	40739	28.7	4085	54965	38.7	4029

snow cover occurs on north–east slopes and thinner on south–west slopes.In spring the maximun space variability of snow depth (Cv = 0.73) occurs in the Liyan River basin where terrain is precipitous and the minimum Cv of 0.19 occurs in the Har Lake plains. (The space variability,Cv,is defined as the coefficient of variation, $Cv = \sigma / Sz$) where σ is the standard deviation of snow depths based on just the snow–covered grid points and for the Qilian Mountains region as a whole, the mean snow depth is 4.3cm during September—May.The minimum occurs in the Liyan River basin and maximum in the Har Lake. During March — May, mean snow depth is 5.6cm in all of the Qilian Mountains region extending from 3.9 to 8.9cm in different river basins. The maximum mean depth of 29 cm occurs at south slope of the Tuanjie summit(5808 m) of Shulenanshan. Total area of snow cover more than 15 cm deep is only 538 km^2in winter,which accounted for 0.38% of the whole Qilian Mountains region.Thickness of the mean snow depth

of river basins increases from east to west in the Qilian Mountains. Thick snow covers are concentrated in alpine regions where altitude is more than 4000 m. The high–altitude terrain receives much more snowfall than the lowlands.

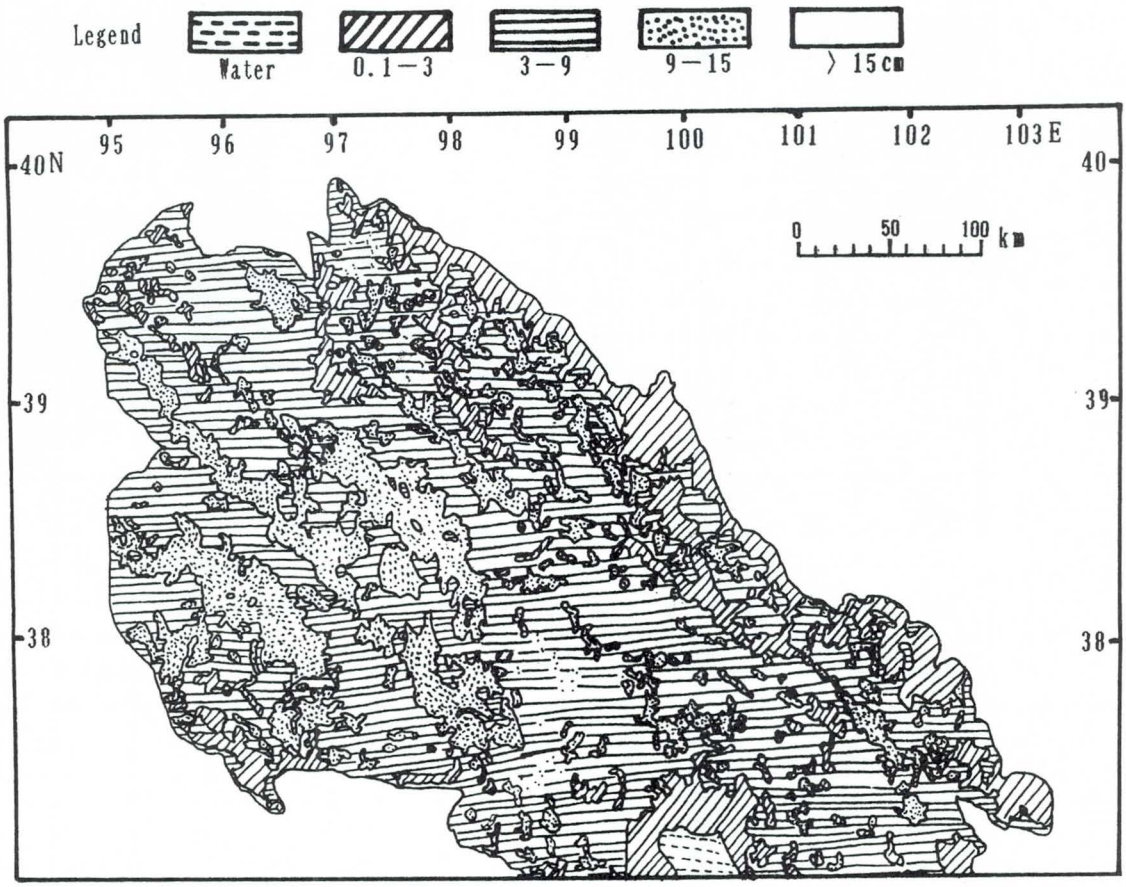

Fig.2.—Mean distribution of snow depth in the Qilian Mountains retrieved from satellite AVHRR data in spring (April–May)

FEATURES OF SNOW RESOURCES

Annual mean snow water equivalents, snowfall amounts (Li,1987), and mean snowmelt runoff in every river basin in the Qilian Mountains region are shown in table 2. In spring the maximum snow water storage amounts ($7.76 \times 10^8 m^3$, 44% of the total for the Qilian Mountains region) occur in the Hexi continental river basins; the minimum ($1.984 \times 10^8 m^3$) occurs in the Datong and Huanshui river basins. It is shown that most of the snow resources for fresh water supply and consumption of the Qilian Mountains region are supplied by the Hexi river basins.

In all of Qilian Mountains region the mean annual amount of snowfall is $160.5 \times 10^8 m^3$, and the mean snow water storage(from September to May) is $12.9 \times 10^8 m^3$,which accounted for 8.0% of the mean annual snowfall. The minimum snow storage, $10.6 \times 10^8 m^3$, occurs in winter and the maximum, $17.5 \times 10^8 m^3$, which accounts for 10.9% of the mean annual snowfall, occurs in spring. This percentage is different from place to place. The maximum occurs in the Qaidam River basins and the minimum in the Shiyan River basins. In spring, snowmelt runoff only accounts for 7.8% of annual snow–fall. It is notable that snowmelt runoff accounts for 71.2% of snow storage in spring. In the Shiyang and Datong basins, the snowmelt runoff is greater than the spring snow storage. This seems unreasonable, however, snow melting

Table 2.--Annual snowfall, snow storage and spring runoff of snowmelt production in every river basin in Qilian Mt. region. (unit: $\times 10^8 m^3$)

River system	River basins	Hydrologic station	Annual snowfall		mean snow storage Weter equivalent				spring runoff of snowmelt	
			amount	% a)	Sep.-May	% b)	April-May	% b)	Surface-water discharge	% b)
Sule He	Dang He	Dangchengwan	19.98	12.4	1.4521	7.3	2.0213	10.1	0.358	1.8
	Changma He	Changmabao	19.09	11.9	1.0876	5.7	1.6147	8.5	0.634	3.3
	Shiyou and Baiyang He	Yumen Baiyanghe	4.82	3.0	0.4966	10.3	0.6478	13.4	0.169	3.5
	Subtotal		43.89	27.3	3.0363	6.9	4.2838	9.8	1.161	2.6
Hei He	Taolai He	Binggou	9.09	5.6	0.5751	6.3	0.8588	9.4	0.259	2.8
	Hongshuiba	Xindi	1.79	1.1	0.1279	7.1	0.1978	11.1	0.171	9.5
	Fenglehe to Bailang He	Fengle He Hongwanxia	3.14	2.0	0.1535	4.9	0.1972	6.3	0.348	11.1
	Liyuan He	Gangoumen	2.91	1.8	0.1253	4.3	0.1948	6.7	0.154	5.3
	Hei He	Yingluoxia	12.65	7.9	0.8021	6.3	1.1415	9.0	1.407	11.1
	Suyouhe to Mayinghe	Suyoukou	4.55	2.8	0.1460	3.2	0.1864	4.1	0.675	14.8
	Subtotal	Wafangcheng Shuangshusi	34.06	21.2	1.9299	5.7	2.7765	8.2	3.014	8.8
Shiyang He	Xida and Dongda He	Chajianmen Shagousi	3.59	2.2	0.1275	3.6	0.1871	5.2	0.534	14.9
	Xiying He	Jiutiaoling			0.1018		0.1379		0.551	
	Jinta He	Qingzywan Xiawan			0.0650		0.1011		0.171	
	Zamu He	Zamusi	3.36	2.1	0.0730	8.9	0.1030	12.6	0.421	40.2
	Huangyang He	Shajingtai			0.0594		0.0820		0.210	
	Gulang He	Gulang	1.44	0.9	0.0548	3.8	0.0871	6.0	0.133	9.2
	Subtotal		8.39	5.2	0.4815	5.7	0.6982	8.3	2.020	24.1
total			86.34	53.8	5.4477	6.3	7.7565	9.0	6.195	7.2
Lake	Har Hu		7.83	4.9	0.5456	7.0	0.8504	10.9	0.116	
	Northern Qinghaihu	Buhahekou Gangcha Haeygai	20.74	12.9	1.8182	8.7	2.5828	12.5	1.504	7.2
	Subtotal		28.57	17.8	2.3638	8.3	3.4332	12.0	1.620	5.7
Chaidam river			26.81	16.7	3.6816	13.7	4.3295	16.1	1.0598	4.0
total			55.38	34.5	6.0454	10.9	7.7627	14.0	2.680	4.8
Huang shui	Datong He	Tiantangsi							2.7655	
	Beichuan He	Qiaotou							0.7617	
	Huangshui	Haiyan							0.0591	
	total		18.80	11.7	1.4285	7.6	1.9835	10.6	3.5863	19.1
total of Qilian Mt.			160.52	100	12.9216	8.0	17.5047	10.9	12.461	7.8
total of China			3451.80	4.7					235.70	5.3

a) Percentage of Qilian mountains total.

b) Percentage of aunual snowfall for basin.

and recharge occur several times during snowmelt season. Therefore, daily snow storages are a wavylike curve, not a monotone decreasing depletion curve shown by Hall (1985). For this reason, snow storage before snowmelt of early–spring, SWo, should be increased by cumulative recharge production of daily snowmelt, $\sum$ SWi. The total is defined as accumulated snow storage $\sum$ SW as follows:

$$\sum SW = SWo + \sum_{i=1}^{n} SWi \tag{6}$$

where N is snow recharge days. The accumulated snow storage in spring is $22.2 \times 10^8 m^3$in Hexi River basins, which is 26% of mean annual snowfall. Snowmelt runoff accounts for about 28% of the accumulated snow storage in spring. It is considered that more than 70% melt water is consumed by evaporation and infitration in spring. It is necessary to improve snow storage conditions by afforestation and planted grass to considerable dry soil.

REFERENCES

Brest,C.L and Rossow, W.B., 1988,Radiometric Monitoring and Calibration of NOAA AVHRR Channel 1 Data: Proceedings of the International Radiation Symposium,Lille, Franc, P.245—247.

Chen Qian et al, 1990, Retrieval of Snow–cover Parameters Using AVHRR Data Over Qilian Mountains: J.Glaciology and Geocrylogy Vol.12 (4) P.281–292.

Hall, D.K and Martinec, J., 1985, Remote Sensing of Ice and Snow: Chapman and Hall Ltd, 1985, P.47—49.

Li Peiji and Mi Desheng, 1983,Distribution of Snow Cover in China: J.Glaciology and Geocryology, Vo1.5 (4) P.9—18.

Li Peiji, 1987, Seasonal Snow Resources and their Fluctuations in China: Large– scale Effects of Seasonal Snowcover, IAHS Publication No.166 P.93—104.

Wang Zontai et al,1981,Glacier Inventory of China I Qilian Mountains.

Developing an Index of Hydrologic Drought for the Gunnison River Basin, Colorado

R.S. Parker

U.S. Geological Survey

ABSTRACT

Because the principal areas that supply water and areas where water is used are separated by considerable distances in the Colorado River basin, hydrologic drought assessment is difficult. Typically, water is supplied by mountain basins, such as the Gunnison River basin, Colorado; and much of the water demand is from the lower Colorado River basin in Arizona and California. Characterizing drought within the Gunnison River basin presents problems because of variability in water supply and demand. Recognizing that runoff largely is derived from snowmelt, a method of evaluating the probability that annual streamflow will be less than some threshold amount (an assumed hydrologic drought indicator) is defined by linear regression relating annual streamflow to February, March, and April snowpack. The method is detailed for the East River, a tributary of the Gunnison River, and identifies considerations for a study recently initiated to evaluate the sensitivity of the water resource to potential changes in climate in the Gunnison River basin.

INTRODUCTION

Hydrologic drought assessment is difficult for the Colorado River basin because most of the water supply is derived from mountains in the upper part of the basin, but much of the water demand is located in the lower part of the basin. Hydrologic drought assessment needs to evaluate natural and man-induced factors which affect water supply and water demand. In the Colorado River basin, many of the demands are far removed from the major snowpacks that provide most of the water supply. The Gunnison River basin has a drainage area of 20,534 km^2. It is a mountain basin that supplies much of the water to the Colorado River system. Because the basin is an important supplier of water to such a large river system, the sensitivity of the water resource of the Gunnison River basin to changes in climate is being evaluated in a joint U.S. Geological Survey/Bureau of Reclamation study. An assessment of drought within the basin and its effects on downstream water users, relative to changes in climatic factors such as precipitation or air temperature, is an important part of this joint study.

Characterizing drought within the Gunnison River basin is complex because of the variability of climatic and hydrologic factors used to determine drought. This variability results, in part, from the dramatic changes in elevation (elevation ranges from 1,410 m to 4,400 m). The Palmer Index (Palmer, 1965), is a drought index routinely published for 344 climatic regions in the United States by the Federal government (see for example U.S.

Department of Commerce and U.S. Department of Agriculture, 1981). This index is calculated for only five regions in the State of Colorado, and all of the Colorado River drainage in the State is lumped into one climatic region. A number of criticisms have been made about the methodology used in the Palmer Index (Alley, 1984). In addition, the lumping of this diverse region into a single value can be a significant problem. To provide more homogeneous areas for calculating the Palmer Index, a Colorado Palmer Index was developed (Doesken and others, 1983). This index does not modify the original algorithm but subdivides the State into 25 regions to provide areas that are more climatically uniform. The Gunnison River basin is part of three separate regions (lower valleys, upper valleys, and mountains) in the Colorado Palmer Index. One of the main attributes used to separate regions in the Colorado Palmer Index is elevation because the algorithm does not make allowances for the snowpack, nor the time lag in available water from snowmelt, in water-balance calculations.

To define the surface-water conditions in mountain basins that have a large component of snowmelt, a surface water supply index (SWSI) was developed (Shafer and Dezman, 1982) that incorporates components of snowpack, streamflow, precipitation, and reservoir storage. Each of these components is weighted by the relative importance of the component in a particular basin. Past record of snowpack, streamflow, precipitation, and reservoir storage are evaluated by deriving a frequency analysis of each component. Scaling is done to provide an index that ranges between ±4.2. The SWSI and the Colorado Palmer Index are calculated monthly for the major drainage basins in the State of Colorado to aid State and Federal agencies in assessing drought conditions.

The recognition that water from the Gunnison River basin is primarily derived from snowmelt provides opportunities to assess downstream drought conditions early in the water year. This paper details a method for evaluating the probability of annual streamflow being less than a threshold amount using the measurements of snow courses in the winter months of the water year. The method described helps to detail the physical-hydrology and water-use components that will need attention in the joint U.S. Geological Survey/Bureau of Reclamation study.

The East River basin is a 749-km^2 tributary drainage of the Gunnison River (fig. 1). This basin was chosen for study because it is relatively free from anthropogenic influences. The East River basin is one of the headwater tributaries of the Gunnison River and reflects many of the streamflow characteristics of the total basin. With additional work on gaged streamflows at the outlet of the Gunnison River basin to evaluate reservoir storage, interbasin transfers, diversions, and irrigation, the analysis described here could be extended to the entire Gunnison River basin.

The annual mean discharge from 1911-22 and 1935-90 is shown in figure 2 for the gage at the outlet of the East River. The distribution of annual flows for the period of record follows a normal distribution (probability of the Shapiro-Wilk test is 0.743). The mean annual discharge is 9.55 m^3/s with a standard deviation of 2.85 m^3/s. There appears to be little serial correlation between the annual flow of a given year and the annual flow lagged 1 year ($r=0.14$) or 2 years ($r=0.00$). The dominance of snowmelt on the annual hydrograph is seen by examining the hydrograph of the mean of the daily mean discharges (fig. 3) for the 68-year period of record (1911-1922 and 1935-1990).

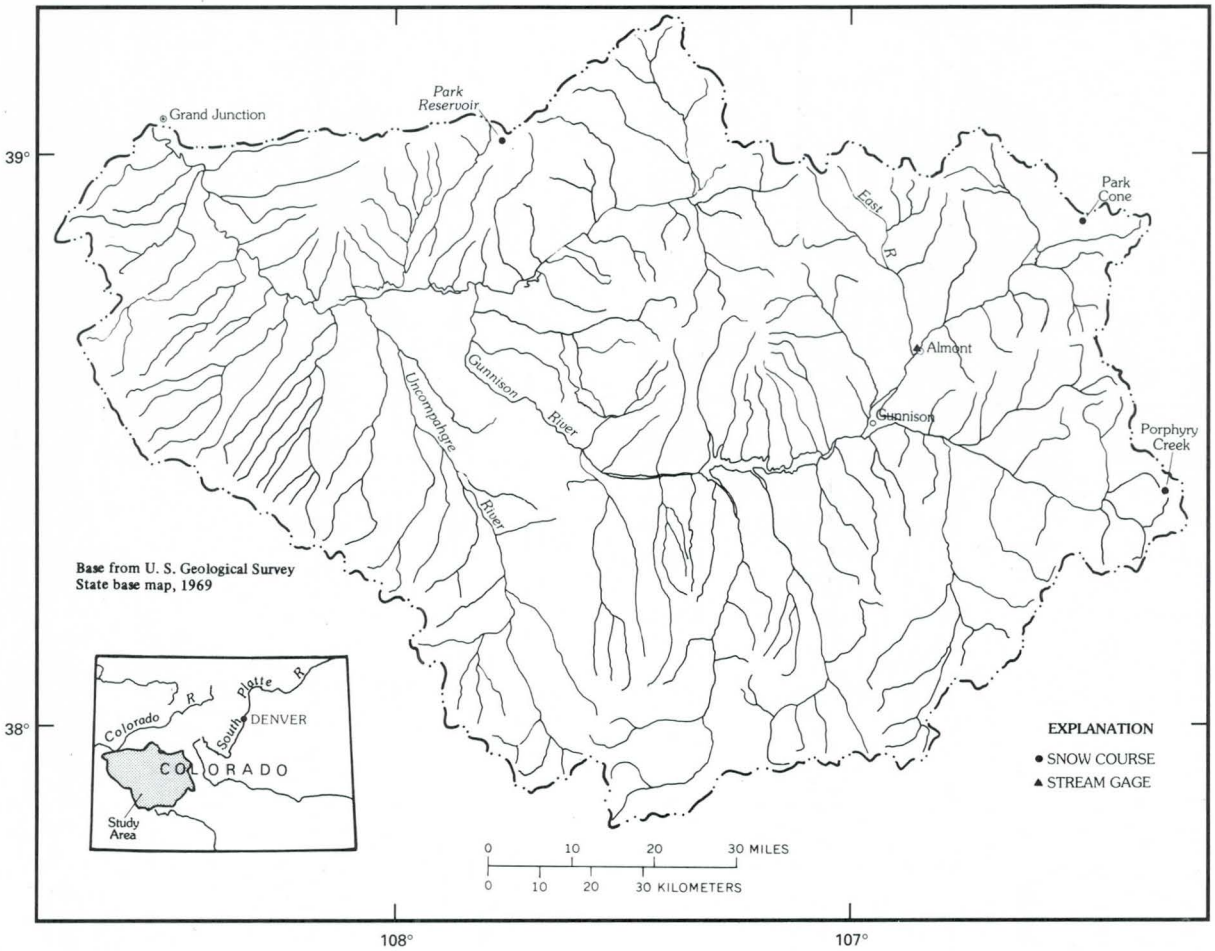

Figure 1.--The Gunnison River basin, including the East River drainage basin and snow courses used in the analysis.

To identify a drought index, an annual streamflow that is exceeded more than 70 percent of the time is assumed to signify drought conditions. It is emphasized that this is an assumed threshold, and that much more analysis is needed to define appropriate threshold conditions. Assuming a normal distribution, the threshold for annual streamflows is 8.04 m^3/s.

Three snow courses, Park Cone (elevation 2,925 m), Park Reservoir (elevation 3,035 m), and Porphyry Creek (elevation 3,280 m), are located near the East River drainage basin and provide data on the water equivalent of the snowpack (fig. 1). These three snow courses are used in the SWSI to index snowpack conditions in the Gunnison River basin, and record is available from 1936 to the present for Park Cone and from 1940 to the present for the other two sites. These snow courses are measured at the beginning of February, March, and April. In the analysis that follows, the mean snowpack-water equivalent of the three sites for each month is used.

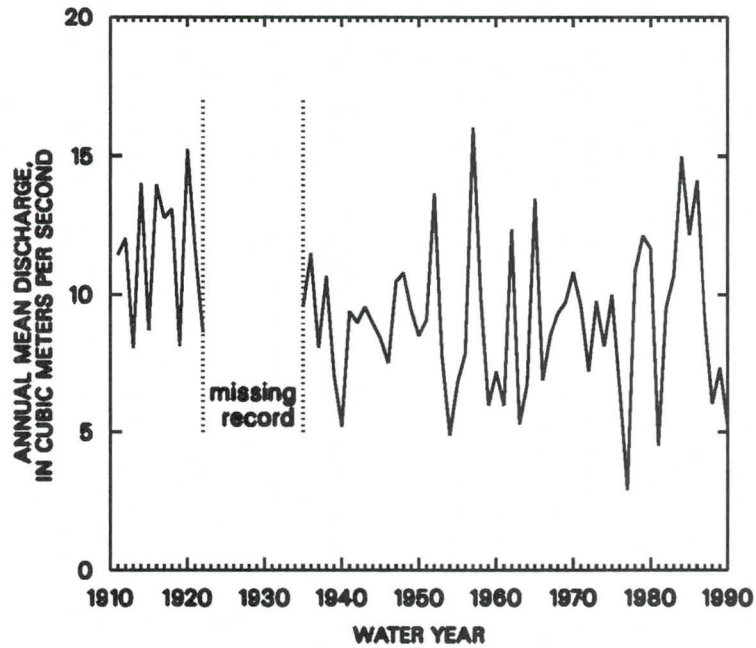

Figure 2.--Annual mean discharge for the period of record for the gaging station East River at Almont, Colorado.

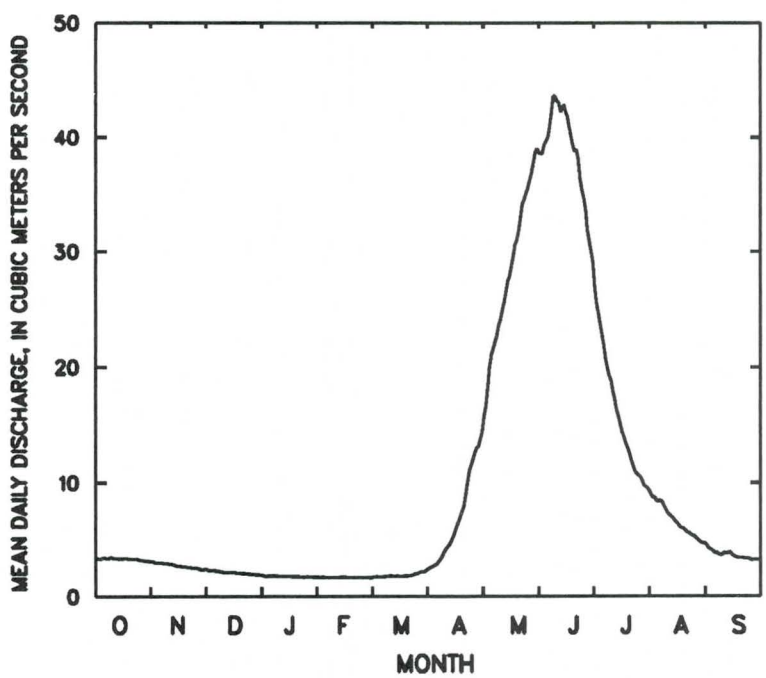

Figure 3.--Annual hydrograph of the mean of the daily mean discharges for the period of record for East River at Almont, Colorado.

METHOD

To define a drought index with respect to snowpack, a relation between annual streamflow and water equivalent of the snowpack was established for the East River. A linear relation between the annual mean streamflow of the East River (Q) and the mean water equivalent of the snowpack (P) is:

$$Q = a+bP, \tag{1}$$

where a and b are regression coefficients.

If P is defined as the mean of the three snow courses for April, the relation is between the annual runoff and a measure of the peak of the snowpack (fig. 4). This relation (table 1) has a standard error of 1.54 m^3/sec and an r^2 of 0.71. Using this relation to predict annual runoff assumes that (1) the mean of the three snow courses adequately depicts the spatial distribution of snow in the basin, (2) the measurement for April defines the peak of the snowpack, and (3) all runoff produced in the basin is from snow. These three assumptions are violated to some extent, and scatter in the relation results.

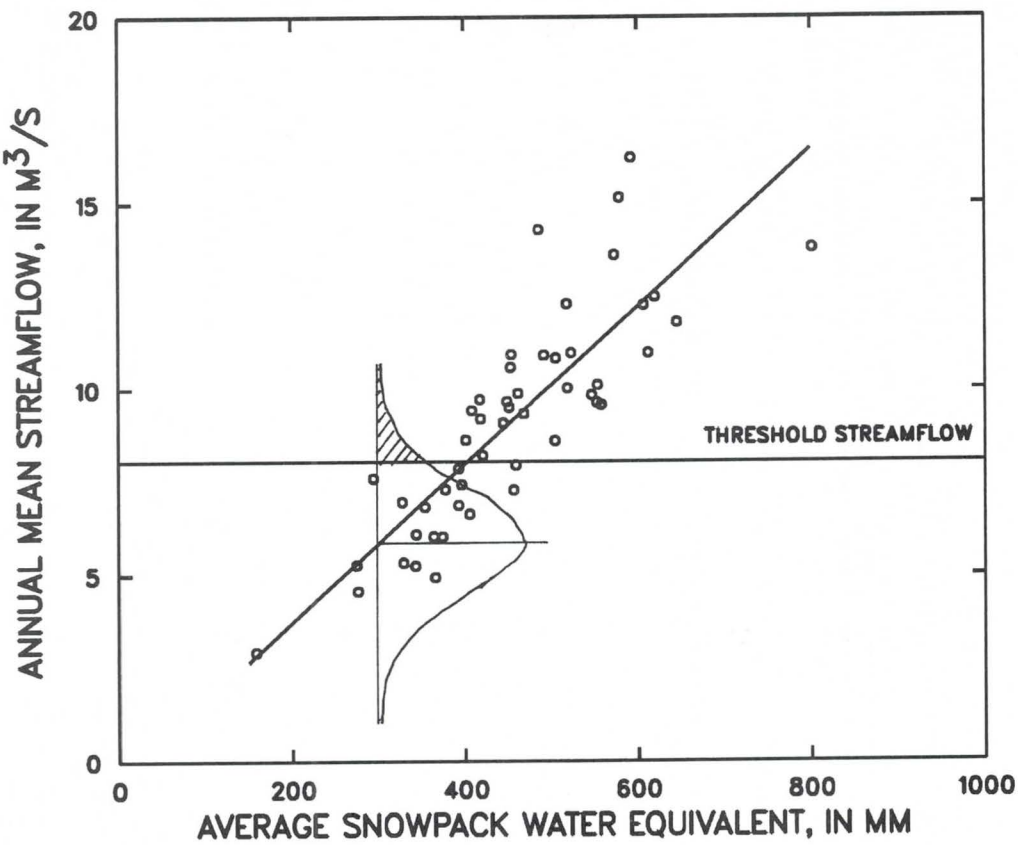

Figure 4.--The relation between annual mean streamflow for the gaging station East River at Almont, Colorado, and the mean snowpack water equivalent of three snow courses for April for the period 1940-90. The geometry between the standard normal distribution for a predicted value of snowpack and the threshold streamflow is shown.

If annual streamflow of less than 8.04 m^3/sec is assumed to yield hydrologic drought conditions, it would be useful to determine whether this drought condition will occur in a given year by examination of the mean of three snow-course values in April. Prediction of values of Q follows the assumption of linear regression that for a given value of the independent variable (P) the dependent values (Q) are normally distributed about a mean (a+bP) with a standard deviation equal to the standard error of the regression model (s). The probability of occurrence of the drought condition (D) can be computed for a given value P by evaluating the standard normal probability at the standardized-deviate value of:

$$z = \frac{D - (a+bP)}{s}. \qquad (2)$$

Figure 4 shows the relation between the regression equation and the drought threshold for a mean April snowpack-water equivalent value of 300 mm. The probability of occurrence of a drought condition is 0.926 (non-shaded area for the normal curve in fig. 4) for this situation.

To provide probability estimates for the assumed drought threshold earlier in the water year, relations between annual mean streamflow (Q) and the mean water equivalent of the snowpack (P) for the first of February and first of March can be used, and probabilities can be defined for a drought threshold for relations developed using snowpack measurements of February and March. The coefficients and statistics for the regression equations for February, March, and April are listed in table 1. The probabilities of occurrence of the drought threshold for each of the three months are plotted in figure 5. The three curves representing the three months are similar in shape. The standard error does decrease through time (table 1), and is lowest for April, as information is gained on the water content of the snowpack in the drainage basin (Tangborn and Rasmussen, 1976).

Table 1.--Regression equations for annual streamflow of the East River (Q) and mean water equivalent of the snowpack (P) for the linear equation Q = a+bP showing the standard error of the estimate (s) and the coefficient of determination (r^2).

Month of snow measurements	Number of measurements	a	b	s	r^2
February	45	1.33	0.030	1.669	0.66
March	48	-.25	.026	1.653	.67
April	51	-.50	.021	1.545	.71

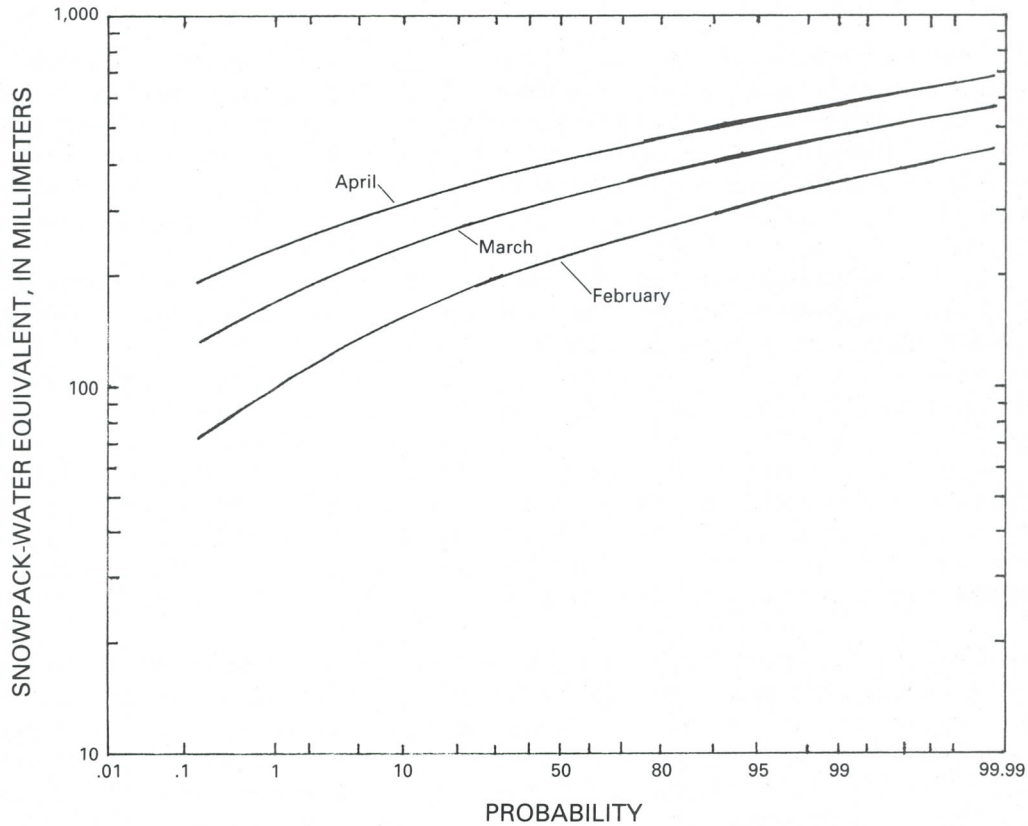

Figure 5.--The probability that annual streamflow will exceed the assumed drought threshold (8.04 m3/s) for given values of mean snowpack water equivalents for February, March, and April, East River at Almont, Colorado.

DISCUSSION

Runoff from the East River basin is dominated by snowmelt, suggesting a well-defined relation between the snowpack and annual runoff. However, using the mean of data from three snow courses does not adequately depict the spatial variability of the basin's snowpack. The correlation coefficients among the three snow courses for April for the period of record range from 0.59 to 0.65. In examining time-invariant factors of winter precipitation in the Upper Colorado River Basin, Peck and Schaake (1987) found that elevation accounted for 25 percent of the variance; when local conditions at the measurement site (rise, exposure, orientation, and zone of environment) were included, the variance estimate was improved to 40 percent. They concluded that additional improvements were possible by including an orographic precipitation model to better represent the meteorology. The use of a regression equation does not provide for the distribution of runoff in time and space. Further refinements in estimating runoff can occur by use of watershed models. The use of conceptual models in runoff processes provide the potential for using The National Weather Service's Extended Streamflow Prediction (ESP) procedure (Twedt and others, 1977). This procedure has the advantage of providing the probability distribution of a given threshold in terms of the physical processes interpolated by a watershed model. In ESP, current conditions are evaluated within the context of the historic data.

A more complex issue may be to identify the threshold values that represent hydrologic drought. For a basin such as the Gunnison, this means categorizing the water use and water rights both within the basin and downstream. Within the joint U.S. Geological Survey/Bureau of Reclamation study, this implies routing water through the basin to determine water availability.

For high-altitude basins that supply substantial water to downstream users, standard methods of determining drought that are based on within-basin precipitation and within-basin demand are not sufficient. Water demands commonly are external to the basin, and therefore some minimum flow criterion becomes a hydrologic drought indicator. The minimum flow, or threshold, was assumed in the example given here, but the study now being conducted will focus on water-use and water-rights requirements that lead to a rational definition of one or a series of streamflow thresholds.

REFERENCES

Alley, W.M., 1984, The Palmer drought severity index -- limitations and assumptions: Journal of Climate and Applied Meteorology, v. 23, p. 1100-1109.

Doesken, N.J., Kleist, J.D., and McKee, T.B., 1983, Use of the Palmer Index and other water supply indexes for drought monitoring in Colorado: Colorado State University Department of Atmospheric Science, Climatology Report No. 83-3, Colorado State University, Ft. Collins, Colo., 71 p.

Palmer, W.C., 1965, Meteorological drought: U.S. Weather Bureau Research Paper No. 45, Washington. D.C., 58 p.

Peck, E.L., and Schaake, J.C., Jr., 1987, Network design for water supply forecasting in the west: Proceedings American Water Resources Association 23rd Annual Conference and Symposium, November, Salt Lake City, Utah.

Shafer, B.A., and Dezman, L.E., 1982, Development of a surface water supply index (SWSI) to assess the severity of drought conditions in snowpack runoff areas: Proceedings, Western Snow Conference, Reno, Nevada, p. 164-175.

Tangborn, W.V., and Rasmussen, L.A., 1976, Hydrology of the North Cascades region, Washington. 2. A proposed hydrometeorological streamflow prediction method: Water Resources Research, v. 12, no. 2, p. 203-216.

Twedt, T.M., Schaake, J.C., Jr., and Peck, E.L., 1977, National Weather Service Extended Streamflow Prediction: Proceedings, Western Snow Conference, Albuquerque, New Mexico, 9 p.

U.S. Department of Commerce and U. S. Department of Agriculture, 1981, Weekly weather and crop bulletin: v. 69, no. 31, NOAA/USDA Joint Weekly Agricultural Weather Facility, Washington, D.C., 1 volume.

FORECASTING DRY-SEASON DROUGHT AND RUNOFF IN CHINA

Zhang Fuyi
Hydrological Forecasting and
Water Control Center
Ministry of Water Resources, PRC, Beijing

ABSTRACT

This paper discusses the importance of the forecasting of drought and runoff in the dry season, analyzes the factors governing the development of drought, expounds the time of occurrence and characteristics of river runoff in the dry season, and introduces some methods for drought and runoff forecasting in the dry season.

INTRODUCTION

China is situated in the southeastern side of the Eurasian continent and covers 3 regions with high, medium and low latitudes. Due to the influence of monsoons and physiographic conditions, temporal and spatial distributions of precipitation vary greatly and change from year to year. Thus, drought and waterlogging frequantly occur. According to historical data, 1056 great droughts occurred between 206 BC and AD 1949. That is to say, drought occurred every 2 years in average. Agriculture is often influenced by drought. Therefore, the analysis and forecasting is very important for lessening the effects of drought.

Rainstorms and floods occur frequently in China during summer and fall, which is called the flood period. After this period there is a low-water period, which often lasts from October to March in the southern part of China and from October to May in the north. During the low water period, river runoff is low, while the various industries and agriculture need water very much. That means, there is a contradiction between supply and demand during this period. Consequently, it is important to make forecasts of dry-season runoff for working out a plan for irrigation, generating electricity, navigations and water supply in urban areas, in order to ensure the steady development of the national economy. Here, some methods for drought and runoff forecasting in the dry season are introduced as follows.

DROUGHT FORECASTING

Drought conditions are a reflection of shortage of water in the growth period of crops. When soil moisture cannot meet the need of crop growth, the crops will decrease in yield or wither and have no yield. Obviously, suitable soil moisture is one of the essential conditions for crops growth. Therefore, soil moisture or other water indices can be used as the basis for forecasting the occurrence and development of drought.

1. Index Method of Soil Moisture

In the growth period, crops need soil moisture in a certain range. If

the soil moisture goes below or above this range, it is necessary to provide irrigation or drainage for the steady and high yield of crops. According to the data of the irrigation experiment for crops in Hebei Province of China, the suitable soil moisture in the various growth phases of wheat should be within 60-90% of field moisture capacity (Table 1).

The field moisture capacity varies with the soil type. In the area of North China, for example, the field moisture capacity is different in various kinds of soil (Table 2).

Table 1 Suitable Soil Moisture Ranges for the Various Growth Phases of Wheat
(Agriculture Univ. of Hebei Prov., 1978)

Growth Phase	Suitable Soil Moisture Range (percentage of maximum field moisture capacity)
Stage of Turning Green	60-85
Jointing Stage	45-100
Boot and Heading Stage	65-90
Florescence	60-90

Table 2 Maximum Field Moisture Capacity in Various Kinds of Soil (percent)
(Agriculture Univ. of Hebei Prov., 1978)

Sand Loam	Light Loam	Loam	Heavy Loam	Light Clay	Clay
22-30	22-28	22-28	22-28	28-32	25-35

When soil moisture is less than 60% of field moisture capacity, drought will appear. Soil moisture is influenced by many factors, such as precipitation, evapotranspiration, soil characteristics, kind of crops, depth of groundwater, irrigation and drainage. Within a specified time interval, the increase or decrease in soil moisture can calculated with the equation of water balance as following:

$$\Delta \rho = \sum F - F_d - E + G$$
$$\sum F = P - Is - R$$

So

$$\Delta \rho = P - Is - R - F_d - E + G \qquad (1)$$

in which, $\Delta \rho$ indicates the change of soil moisture from the beginning to the end of the interval, $\sum F$ shows the total infiltration flow within the interval, F_d indicates the infiltration flow at the deep layer under crops, E shows the evapotranspiration, P indicates precipitation, Is shows the interception by crops, R indicates the depth of surface runoff and G shows groundwater capillary rise in the root zone during the interval. When precipitation does not produce surface runoff and groundwateris not influential, Equation (1) can be simplified as following:

$$\Delta \rho = P - E \qquad (2)$$

Based on observed data, a relation between soil moisture at earlier and later stages can be construced with the precipitation and month as parameters (Fig. 1). When making forecasts, the figure can be used for calculating soil moisture changes.

2. Water Balance Index Method

Whether the crops suffer from drought will be determined by the need for water, the precipitation and the soil moisture at the beginning of the growth period. If there is a basic balance between the supply and consumption of water in the growth period, the crops will grow in normal condition; if not, the crops will suffer drought or waterlogging. Therefore, based on the observed data of drought and analysis of the water balance in the cultivated soil, a comprehensive index of drought condition can be determined as the standard to analyse and forecast drought conditions. In the early 1960's, an equation of drought and waterlogging has been given out as following:

$$D = (P - Rc + \rho o / \rho p + Rg) / (Wo + \rho m / \rho p) \qquad (3)$$

in which, D indicates the drought and waterlogging index of the crops at the end of a growth period, P shows precipitation in the growth period, Rc indicates ineffective precipitation (surface runoff from precipitation and infiltration flow in deep layer), ρo shows the soil moisture in the layer of root distribution at the beginning of growth period, ρp indicates the increased soil moisture resulting from precipitation of 1 millimeter in the layer of root distribution, Rg shows supply of groundwater in growth period, Wo indicates the evapotranspiration from crops and soil, ρm shows the suitable soil moisture for normal crop growth in growth period.

The comprehensive index of drought condition can be obtained from the values of D calculated with Equation (3) and the observed data of drought condition together (Table 3).

Table 3 The Comprehensive Index of Drought Condition

Drought	Subdrought	Normal	Sub-waterlogging
$D < 0.5$	$0.5<D<0.8$	$0.8<D<1.3$	$D > 1.3$

RUNOFF FORECASTING IN THE DRY SEASON

In China at present, the common method for runoff forecasting in the dry season is to forecast the total runoff and the runoff process according to either the depletion-curve regulation of runoff or the water storage in the river network and the initial runoff. For the rivers with more precipitation or ice, some factors influencing runoff in dry season should be considered, such as river freezing and thawing and precipitation in the prediction period. There are several methods as follows:

1. The Method of Depletion Curve

During the dry season, a large part of the runoff in rivers is produced by the decrease of water storage. So, the runoff and guaranteed discharge in

rivers in the dry season can be forecast according to depletion regulation. The most simple depletion regulation can be indicated by the depletion equation for the groundwater layer:

$$Q_t = Q_0 e^{-\beta t} \tag{4}$$

in which, Q_t(m^3/s) is the outflow of groundwater during the time t after the beginning of depletion, Qo(m^3/s) is the outflow of groundwater at the beginning of depletion, β is the coefficient of depletion.

Depletion curves of groundwater in a river basin can be obtained according to the observed data of depletion during the dry season. According to the equation of depletion, $\beta = (\ln Qo - \ln Q_t)/t$, which can be calculated as shown in Table 4. The β is the average value from 0 to t. If the discharge in an adjacent time period is used, β' for this duration will be obtained, as shown in Table 4.

The distribution of β in Table 4 indicates that the values of β obtained from the observed data of depletion frequently are not constant. The value of β is bigger in the earlier stages of depletion while the value decreases and approaches a steady state in later stages of depletion. The reason is that the outflow produced by a given decrease of water storage in the river in the earlier stage of depletion is larger in proportion to the discharge at the outlet section than at later stages of depletion. According to the analysis of the data of the depletion in dry season from the Luanhao Hydrological Station on the Honghe River in Yunnan Province of China, the average value of β from 0 to t not only changes along with the change of t, but also relates to the discharge at the beginning of depletion. The larger the discharge, the bigger the corresponding value of β (Fig. 2). In forecasting depletion, a relation of β versus t can be inserted in the figure according to the condition of discharge at the beginning of depletion in order to calculate the depletion at various times during the prediction period.

Table 4 Calculation of Depletion Coefficient of the Groundwater at the Xixian Hydrology Station in the Huai River Basin

t date	Q (m^3/s)	lnQ	$\ln Qo - \ln Q_t$	β (day^{-1})	$\ln Qt - \ln Q_{t+1}$	β' (day^{-1})
0	68.5	4.23				
10	27.5	3.31	0.92	0.092	0.92	0.092
20	14.3	2.66	1.57	0.078	0.65	0.065
30	8.2	2.10	2.13	0.071	0.56	0.056
40	4.8	1.57	2.66	0.067	0.53	0.053
50	2.85	1.05	3.18	0.064	0.52	0.052

Because β is not a constant, a graph for depletion forecasting usually will be drawn to simplify the calculation. There are several common figures for depletion forecasting, as follows:

(1) Figure of relation $Q_{t+1} = f(Q_t)$

The figure of relation $Q_{t+1} = f(Q_t)$ (Fig. 3) is identical in concept with

the curve of depletion. In the figure, the slope of the curve linking the original point and other points is the ratio of the discharges in the adjacent interval of the depletion curve, i.e. $Q_t/Q_{t+1}=Q_0 e^{-\beta t}/Q_0 e^{-\beta(t+1)}=e^{\beta}$. The change of the slope also indicates the change of β in the depletion period. When the discharge is great, the slope is large and the value of β is big; when the discharge is small, the slope and the value of β are small. This is identical with the change of β calculated from the depletion equation.

(2) Figure of relation $Q_t = f(Q_o, t)$

Because the value not only changes along with the change of time (t) but relates to the discharge at the beginning of depletion, the figure of relation between the discharge of depletion at the same time, Q_t and the discharge at the beginning of depletion Q_o (Fig. 4).

2. The Method of Water Storage in River Network

The storage water discharged from the river network of a river basin generally is more than the supply of groundwater in the prediction period. During the period with less precipitation, the long-term runoff forecasting in the dry period can be based on the storage volume in the river network. During the period with abundant precipitation, the inflow will have much influence on the runoff in the prediction period. At this time, we should consider the runoff at the outlet section as transformed from precipitation. Based on the concept of water balance, the total runoff through the outlet section in the prediction period can be calculated with the following equation:

$$\sum Q = W_t + \sum Qsw + \sum Qgw \qquad (5)$$

in which, $\sum Q$ is the total runoff through the outlet section in the prediction period (Δt), W_t is the storage volume in the river network when the concentration time is equal to Δt, and $\sum Qsw$, $\sum Qgw$ are the surface-water and net ground-water inflows into the river network during Δt. If we let Δt equal to the concentration time, the W_t in Equation (5) will indicate the storage volume in the river network.

The storage volume in the river network is the sum of water storage in the various river reaches. The channel storage in various river reaches can be obtained from observed hydrological data or by checking the channel storage curve.

During the earlier stage of the depletion of a flow event in the river basin, the outflow of groundwater makes us a small proportion of the flow and there is a close relation between groundwater and storage water in the river network. When no precipitation occurs in the prediction period, the runoff at the outlet section can be forecast by using the relation of $\sum Q = f(W_t)$, as shown in Fig. 5.

CONCLUSION

It is effective to use the calculation of water balance for drought forecasting. In China, better precision is obtained by a depletion curve in the forecasting of runoff in the dry season. This technique will have a bright future for high precision if water storage in the river network is used for forecasting runoff in the dry season in large river basins. The forecasting precision will be improved if the characteristics of distribution of storage water in river network are used.

REFERENCES

1. Hydrology Department, Hydraulic Engineering College of East China, 1962, Hydrological Forecasting: Industry Publishing House of China, Beijing

2. Agriculture University of Hebei Province, 1978, Farmland Irrigation: Science Publishing House, Beijing

3. Water Conservancy Commission for the Yangtze River, 1979, The Method of Hydrological Forecasting: Publishing House of Water Resources and Electric Power, Beijing

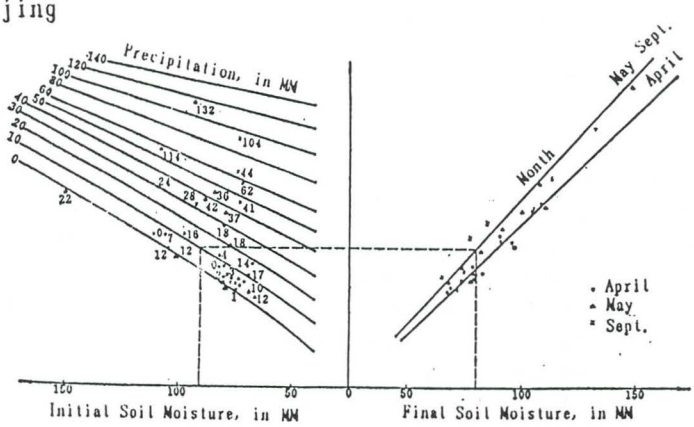

Fig. 1 Relation Curve of Initial and Final Soil Moistures at the Taiyuan Hydrological Station

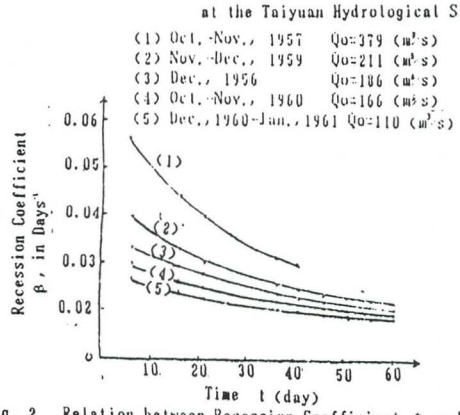

Fig. 2 Relation between Recession Coefficient β and Time for Luanhao Hydrological Station on the Honghe River, Yunnan Province

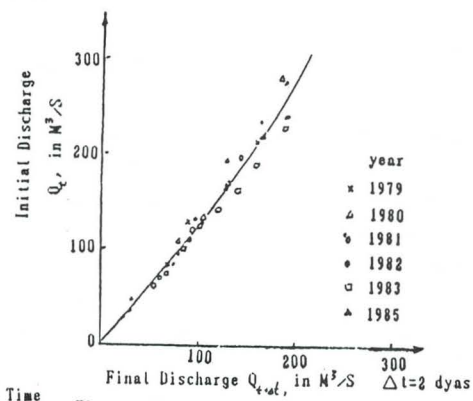

Fig. 3 Relation of the Depletion Curve $Q_t \sim Q_{t+\Delta t}$ for Huaibin Hydrological Station on Huai River, Henan Province

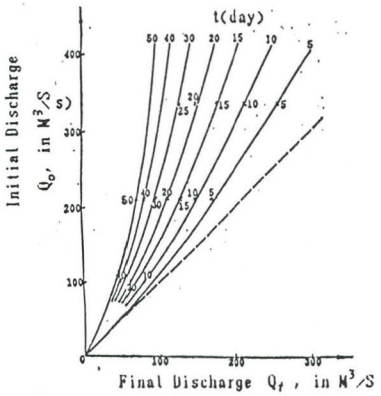

Fig. 4 Relation of Depletion Curve $Q_o=f(Q_t, t)$ for Luanhao Hydrological Station on the Honghe River, Yunnan Province

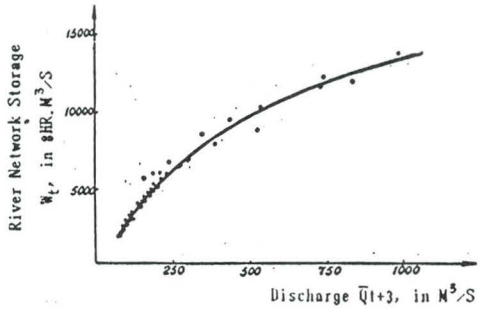

Fig. 5 Relation of $\overline{Q}_{t+3}=f(W_t)$ for Lijiadu Hydrological Station on the Wuhe River, Jiangxi Province

LOW STREAMFLOW FORECAST MODEL FOR LONGYANGXIA HYDROPOWER STATION ON THE YELLOW RIVER

Yang Baiyin and Sun Hanxian

Northwest Hydropower Investigation and Design Institute. Xian, China

ABSTRACT

Low streamflow forecast plays very important roles in reservoir operation and regulation, water quality control, and water supply for domestic, agricultural and industrial uses. Taking the Longyangxia Reservoir on the Yellow River as an example, this article presents a low streamflow forecast model. This model consists of different time intervals and considers different antecedent forecast variables. Using the forecast results of various computation methods, a synthetic fuzzy evaluation model for October and a recession analysis model for the interval from November to March of the next year are established. Through examination most relative errors are lower than 10 percent and the qualification ratio with relative errors less than 20 percent is over 90 percent.

INTRODUCTION

The Longyangxia Reservoir, with a storage capacity of 27.6 billion m^3 and having the function of pluriennial regulation, is the most-upstream large reservoir on the upper Yellow River. The accurate forecast of the Longyangxia reservoir inflow in dry seasons not only can make the most of the reservoir itself but also plays a very important role in proper regulation of the downstream cascade reservoirs so as to obtain maximum benefit in the power system. Therefore, dry season flow forecast models are developed for the Longyangxia Hydropower Station.

SYNTHETIC FUZZY EVALUATION MODEL OF OCTOBER RUNOFF FORECAST RESULTS BY MULTIPLE METHODS

Description of the Problem

As for the runoff of a river, though the preceding affecting factors are various and complicated, they are still integral, correlative and sequential in nature. Thus in the past two or three decades, with the rapid development and popularization of stochastic processes, information theory, multivariate analysis techniques, time series analysis, and computing techniques, the forecast method of probabilistic statistics has rapidly matured. Two major classes of statistical forecast methods have taken shape, namely the time series analysis method, in which the runoff series themselves are taken as linear or nonlinear, and the multivariate analysis method, in which the preceding affecting factors are taken as its starting point. In recent years the other runoff forecast models, have been developed, which apply fuzzy mathematics theory (Wang, 1983) and grey system theory (Deng, 1985), for instance the fuzzy cluster model and the grey dynamic

model GM(n, h), to hydrological phenomena (Yang, 1988, 1989).

Since the factors considered by the various methods and their structural principles are different, their forecast results also differ from one another remarkably. Under these circumstances, it is very difficult to determine the final forecast result. For this reason, the synthetic fuzzy evaluation model of forecast results by multiple methods is suggested in this paper.

Structure of Forecast Model

If the result of each forecast method is taken as a factor, there is not a pure reflection process between the forecast result and the runoff but rather a multiplex fuzzy relation between them. Therefore, by first establishing the matrix of fuzzy relation between each single-method forecast result and the runoff, then finding the weighting set of the various methods, and finally establishing the synthetic forecast matrix by weighting the single-method forecast result matrices, synthetic evaluation can be realized by synthetic fuzzy operation.

$\underset{\sim}{B}$ is assumed to be the fuzzy subset on the runoff domain Z, $\underset{\sim}{B} \in F(Z)$; $\underset{\sim}{A}$ the fuzzy subset on the factor domain Y; and $\underset{\sim}{R}$ the fuzzy relation between the runoff and the forecast results by various forecast methods, $\underset{\sim}{R} \in F(Y \times Z)$.

By classifying the runoff and forecast results into a number of discrete grades the fuzzy relation matrix of the single-method forecast result can be established

$$\underset{\sim}{R}(Y_t, Z) = \begin{pmatrix} r_{11} & r_{12} & \cdots & r_{1l} \\ r_{21} & r_{22} & \cdots & r_{2l} \\ \cdots & \cdots & & \\ r_{k1} & r_{k2} & \cdots & r_{kl} \end{pmatrix} ; \qquad r_{ij} = M_{ij} \Big/ \sum_{j=1}^{l} M_{ij} \qquad (2\text{-}1)$$

where l represents the number of grades of runoff; t the forecast method index; k the number of grades of forecast result; M_{ij} the number of times that Grade j runoff appeared affer a Grade i forecast.

The main purpose of determining the weight distribution of the various forecast methods is to make the weight distribution represent the forecast accuracy of the various models. At present, there are many methods for determining the weight distribution. In this paper, the weight distribution $\underset{\sim}{A}$ of the various methods is determined on the basis of the fuzzy relation matrix for single-method forecast result; the formula is

$$a_t = \sum_{i=1}^{k} \left[\max_{j=1,2,\cdots,l} (M_{ij}) \right] \Big/ \sum_{t=1}^{m} \sum_{i=1}^{k} \left[\max_{j=1,2,\cdots,l} (M_{ij}) \right] ; \qquad \underset{\sim}{A} = (a_1\ a_2 \cdots a_m) \qquad (2\text{-}2)$$

where m is the number of forecast methods.

If the forecast results of the various models for a given forecast year are denoted by Y_t $(t=1,\cdots,m)$ and the corresponding forecast grades are denoted by i_t $(t=1,\cdots,m)$, then a synthetic evaluation matrix can be formed by combining appropriate rows of the single-method fuzzy-relation matrix $\underset{\sim}{R}(Y_t, Z)$, as follow:

$$\underset{\sim}{R} = \begin{pmatrix} r_{i_1 1} & r_{i_1 2} & \cdots & r_{i_1 l} \\ r_{i_2 1} & r_{i_2 2} & \cdots & r_{i_2 l} \\ \cdots & \cdots & & \\ r_{i_m 1} & r_{i_m 2} & \cdots & r_{i_m l} \end{pmatrix}$$

where $r_{i_t j}$ is the element of matrix $\underset{\sim}{R}(Y_t, Z)$ located at column j and row i corresponding to the forecast value Y . According to the resultant operation rule of fuzzy mathematics, the output information of runoff $\underset{\sim}{B}$ is obtained.

$$\underset{\sim}{B} = \underset{\sim}{A} \circ \underset{\sim}{R} = (b_1 \ b_2 \cdots b_l), \quad b_j = \bigvee_{i=1}^{m} (a_i \wedge r_{ij}) \qquad (2\text{-}3)$$

where the meaning of operation "o" is fuzzy-relation computation of composition, "$\vee$" and "$\wedge$" are defined as: $a \vee b = \max(a, b)$, $a \wedge b = \min(a, b)$.
Corresponding to $\underset{\sim}{B}$, the following forecast model is established

$$b = \bigvee_{j=1}^{l} b_j = \max (b_1 \ b_2 \cdots b_l) \qquad (2\text{-}4)$$

where b is the maximum subordination degree of the runoff appearing in the j corresponding interval for the forecast year, and the corresponding interval is taken as the forecast interval. Since the forecast results of several methods may appear in the forecast interval, in order to represent the forecast result more concentrately, the average value of the forecast results of the various methods appearing in the forecast interval is taken as the forecast value of the year.

October Forecast Model for Longyangxia

The streamflow in October at Longyangxia is mainly affected by the preceding rainfall, runoff and weather system. Five statistical analysis models, including stepwise regression (hereinafter represented by Y_1), tendency surface analysis(Y_2, orthogoal transformation method (Lou and Xing, 1987)), fuzzy cluster analysis (Y_3), mixed analysis of periodic mean superposition and time series (Y_4) and grey dynamic analysis GM (1,1) (Y_5), are established on the basis of the measured hydrological and meteorological data from 1959 to 1988. Through analysis of relevant factors, the forecast models are obtained as follows.

Stepwise Regression Model

$$Y_1 = 3105.15 + 7.59X_1 - 49.15X_2 + 0.22X_3 \qquad (2\text{-}5)$$

where X_1 is the areal rainfall in September above Longyangxia; X_2 height of the 500 mb average monthly geopotential meter (40° N, 130° E) in March; X_3 the average monthly discharge (m^3/s) in August at Longyangxia. Through checking the equation is statistically significant and the multiple correlation coefficient is 0.916.

Tendency Surface Analysis Model

$$Y_2 = 1842.86 - 1.8503X_1 - 7.9217X_2 + 0.0007X_1X_2 + 0.0037X_1^2 + 0.0670X_2^2 \qquad (2\text{-}6)$$

Where X_1 is the average discharge (m^3/s) in August at Longyangxia; X_2 the areal rainfall (mm) in September above Longyangxia. The multiple coefficient is 0.809, the computed F value is 9.05, which is higher than the theoretical value $F_{0.05}$; thus the equation is valid.

Fuzzy Cluster Analysis Model

The runoff at Longyongxia is divided into five grades, namely "high", "less high", "normal", "less low" and "low" waters, and the corresponding deviation from the mean is greater than 130 percent, 111-130 percent, 91-110 percent, 71-90 percent and less than or equal to 70 percent respectively. The forecast factors are chosen as follows: X_1 — the average discharge (m^3/s) in September at Longyangxia; X_2 — the areal rainfall (mm) in September above Longyangxia; X_3 — the zonal circulation index in August in Asia (45-65° N, 60-150° E); X_4 — height (m) of 500 mb average monthly geopotential (40° N, 130° E) in March.

The cluster analysis is conducted according to the various factors composition of each runoff grade and the cluster centers; the parameters of the subordinative function of the forecast scheme of each grade are obtained. The forecast model is

$$a_{\underset{\sim}{M_i}}(X) = \max\{0,\ 1-\alpha_i \| X - B_i \|^2\};\ \underset{\sim}{M} = \sum_{i=1}^{m} \underset{\sim}{M_i}\ ;\ a_{\underset{\sim}{M}}(X) = \bigvee_{i=1}^{m} a_{\underset{\sim}{M_i}}(X) \qquad (2\text{-}7)$$

Where $\underset{\sim}{B}$ is cluster center, $\underset{\sim}{M_i}$ is fuzzy subset, X is a factors composition, and α_i is parameter of the subordinative function. Y_3 is the value of the forecast interval, corresponding to $a_{\underset{\sim}{M}}$. The qualification ratio of the model's forecast may be up to 93 percent.

Mixed Model of Periodic Mean Superposition and Time Series
The periodic superposition model is

$$(Y_4) = \overline{Z} + \sum_{j=1}^{n} P_{j,t} + \varepsilon_t \qquad (2\text{-}8)$$

where $\overline{Z}$ is the average value of actual runoff, $P_{j,t}$ is the j-th periodic component of runoff in year t ($j=1,\cdots,n$), and ε_t is the random component. Through periodic analysis, the significant periods are determined to be 10, 4 and 14 years respectively (the results of computation are omitted). The residual series model is the autoregressive AR (5) model:

$$\varepsilon_t = -0.1272\,\varepsilon_{t-1} - 0.198\,\varepsilon_{t-2} + 0.0297\,\varepsilon_{t-3} - 0.2409\,\varepsilon_{t-4} - 0.3026\,\varepsilon_{t-5} \qquad (2\text{-}9)$$

Grey Dynamic GM (1,1) Model.
The grey dynamic GM (1,1) model (Deng, 1985) is

$$dY_t^{(1)}/dt + a(\otimes)Y_t^{(1)} = b(\otimes) \qquad (2\text{-}10)$$

Where $Y_t^{(1)} = \sum_{j=1}^{t} Z_j$ is the accumulation value of actual runoff from Z_1 to Z_t, t is the time, Z_j is the actual runoff in year j ($j=1,\cdots,n$), and $a(\otimes)$, $b(\otimes)$ are grey parameters that can be estimated by the least square method. From equation 2-10, we can obtaine the forecast model

$$Y_{t+1}^{(1)} = 139799.06\ \exp\{0.007636\ t\} + 427524.23\ \exp\{0.001572\ (t-1)\} - 566244.13;$$

$$(Y_5)'_{t+1} = Y_{t+1}^{(1)} - Y_t^{(1)} \qquad (2\text{-}11)$$

The model is modified directly by the periodic analysis method (use the trigonometric fuction) in respect to the residual items. The correlation degree of the modified model (Y_5), r=0.8, is up to the accuracy requirement.

Based on the back-cast results of above forecast models, the fuzzy relation matrix between the forecast result and the measured runoff is established by applying equation 2-1. From thoes fuzzy relation matrices and by applying equation 2-2, the weight distribution of the various methods is calculated as $\underset{\sim}{A}$=(0.194, 0.183, 0.290, 0.150, 0.183). The runoff forecast model in October at Longyangxia is thus obtained.

Check of Model

The models established do not include 1988 and now the trial forecasts are conducted with respect to the average discharge in October of 1988. The forecast-results grades of the foregoing five models are 3; 4; 2; 3 and 2 in order. In accordance with the single-method fuzzy-relation matrices and the above

forecast results, the October fuzzy synthetic evaluation matrix is established and the resultant operation is conducted

$$\underset{\sim}{B} = \underset{\sim}{A} \circ \underset{\sim}{R} = (0.183 \quad 0.290 \quad 0.194 \quad 0.194 \quad 0.183)$$

$b = \bigvee_{j=1}^{5} B_j = 0.290$ appears at grade 2 or the less-high flow and its subordination degree is close to the normal flow. The average of the forecast results of the two methods that appeared at the less-high flow interval (grade 2), the forecast value, is calculated to be 1277 m^3/s; the actual discharge is 1280 m^3/s and the relative error of the forecast value is −0.2 percent. The October runoff back-cast of 30 years from 1959 to 1988 is conducted with the present model. The qualification ratio for relative errors less than 30 percent is 100 percent and that of the relative error less than 20 percent is 90 percent. In accordance with the hydrological forecast specification in China, both qualification ratios of 100 percent and 90 percent have high accuracy and belong to superior forecast schemes, and can be used as operation forecast schemes.

NOVEMBER-MARCH RUNOFF FORECAST MODEL

This section describes the mid — and long-term forecasting of the runoff at Longyangxia from November to March of the next year, including monthly forecasting, and continuous forecasting of the average discharge of each month, when the average discharge in October is known.

Recession Forecast Model

The recession analysis method has a wide scope of application. The following recession equation is commonly used:

$$Q_t = Q_0 \, e^{-\alpha t} \qquad (3\text{-}1)$$

where Q_0 is the initial recession discharge, Q_t is the discharge at t, α is the recession coefficient, and t is the time.

Determination of Recession Coefficient

The measured monthly discharge of 30 years at Longyangxia on the upper Yellow River is analyzed with the October mean discharge as the initial discharge. From October to December the river basin still has much surface and subsurface water and the surface water recession is closely related with the initial discharge, that is to say, the higher is the initial discharge, the steeper is the depletion curve. Therefore the October mean discharge is divided into five grades(same as fuzzy cluster analysis).

Since the recession rules of surface water, subsurface water and underground water are obviously different, their recession coefficient values are also different. Through analysis, four recession stages can be defined from November to March of the next year and four different values are adopted. A typical depletion curve is shown in figure 1. From the figure it can be seen when the March mean discharge is forecasted from the February mean discharge, the value of the exponential α is negative. This is because high air temperature results in some snowmelt runoff and makes the discharge rise in an exponential law from February to March.

Qualification Ratio of Continuous Forecast

The continuous forecast is made by starting with the known October mean discharge and using the recession coefficient to forecast the November mean discharge first and then to forecast the December mean discharge from the November forecast discharge. (When the October mean discharge is lower than 500 m^3/s, α =0.33 for November and December). The forecast is thus propagated month to month until the March mean discharge has been computed. In accordance with the hydrological forecast specification in China, the present forecast scheme is 100 percent up to the standard. Evaluated according to the standard for inland and arid areas (in which the permissible error of monthly water volume forecast is 20 percent of the measured value), its total qualification ratio is 92 percent and it belongs to superior forecast scheme.

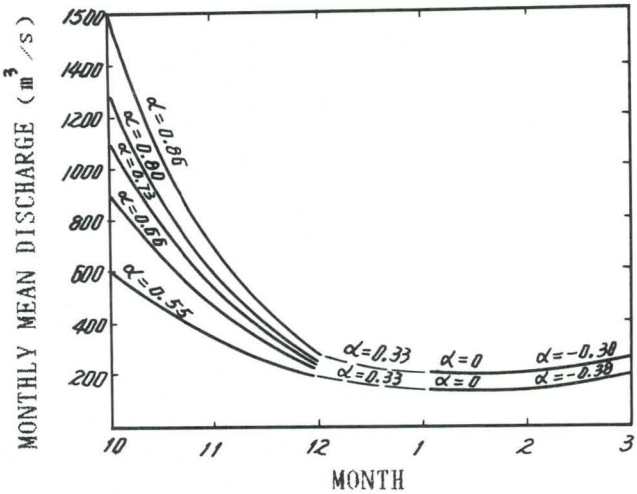

Figure 1. -- Recession curves for low water at Longyangxia

The qualification ratio of continuous forecast for March is obviously lower than that for the other months. This resulted mainly from the error accumulation of continuous forecast and the random error of the February forecast value. In order to partially eliminate the above errors, a regression equation for March and November-February mean discharge is established as follows:

$$Y_3 = 0.398\ Y_{11-12} + 135.1 \qquad (3-3)$$

where Y_3 is the March mean discharge, Y_{11-12} is the November—February mean flow. The March mean discharge is forecasted by introducing the forecasted Y_{11-12} into the above equation. In this way the qualification ratio of March forecast is improved to 93.3 percent and the relative error of most years is reduced to some extent.

To sum up, for continuous forecast of November--March mean discharges from the October mean discharge, the monthly qualification ratio and the total qualification ratio are 93.3 percent and can be used for operational forecasting.

REFERENCES

Wang Peizhuang, 1983, Fuzzy Sets Theory and Its Applaction: Scientific and Technologcal publishing House, Shanghai.

East China Water Conservancy College, 1984, Mid and Long Term Hydrological Forecast: East China Water Conservancy College press, Nanjing.

Deng Julong, 1985, Grey System: National Defence Industry Publishing House, Beijing.

Luo Jiyu and Xing Ying, 1987, Economic Statistical Analysis Method and Prediction: Qinghua University Press, Beijing.

Yang Baiyin, 1988, Longyangxia Dry Season Runoff Forecast by Synthetic Fuzzy Evaluation: Preceedings of Symposium on Northwest China Arid and Semiarid Hydrology, Xi'an.

Yang Baiyin, 1989, Fuzzy Cluster Method of Long-term Runoff Forecast for the Longyangxia Hydropower Station: Hydrology, No2, (in Chinese).

TOPIC D

FREQUENCY ANALYSIS, REGIONALIZATION, AND STOCHASTIC ANALYSIS

ESTIMATING LOW-FLOW CHARACTERISTICS AT GAGING STATIONS AND THROUGH THE USE OF BASE-FLOW MEASUREMENTS

W. O. Thomas, Jr. and J. R. Stedinger

U. S. Geological Survey, Reston, Virginia
Cornell University, Ithaca, New York

ABSTRACT

Various low-flow characteristics are needed for water-management decisions. Techniques are described for estimating low-flow characteristics at gaging stations and at partial-record stations through the use of base-flow measurements. A partial-record station is defined as a station at which only discharge measurements during periods of base flow (that is, ground-water contribution to streamflow) are available. The techniques for estimating low-flow characteristics are illustrated using observed data. The relative accuracy of these estimated characteristics is discussed.

INTRODUCTION

Low-flow characteristics are a required component in many water-resource analyses relating to waste dilution, municipal and industrial water supplies, aquatic habitat protection, and agricultural irrigation demands. Traditionally, the U.S. Geological Survey (USGS) has provided users estimates of the D-day, T-year low flows, such as the 7-day, 10-year low flow. The 7-day, 10-year low flow is defined as the **annual** minimum flow for 7 consecutive days that is exceeded in 9 of 10 years. This value is used by about half of the State regulatory agencies in the United States for the management of water quality in receiving streams (Environmental Protection Agency (EPA), 1986). Low flows of other durations and frequencies are used in some States. Recently some different low-flow characteristics have been suggested and used in hydrologic analyses and these characteristics are briefly discussed herein.

LOW-FLOW CHARACTERISTICS

The estimation of low-flow characteristics within the USGS has historically been oriented toward defining the magnitude and frequency of annual D-day events, such as the 7-day, 10-year low flow. In these analyses, the D-day events are the minimum arithmetic average over D consecutive days of flow within each year. The use of annual values lends itself to frequency analysis which requires the events to be random, independent, and free of trends.

Recently, EPA (1986) has suggested the use of biologically-based design flows for evaluating water-quality effects on aquatic life and ecosystems and risk to human health. For this purpose, EPA has suggested computing, from daily flows, harmonic means rather than arithmetic means as used in the annual D-day low flows. The harmonic mean, which is the reciprocal of the average of the reciprocals of daily flows, was recommended because the concentration of pollutants in the stream is inversely related to the magnitude of flow. The biologically-based design flow for aquatic life is computed by searching the

entire daily-flow record and determining how frequently harmonic means of D-day durations are less than the prespecified design flow. With this approach, there may be no events or one or more events per year less than the design flow. The biologically-based design flow for human health is computed as the harmonic mean of the daily flows for the period of record (Rossman, 1990).

Low-flow characteristics based on average streamflow for d consecutive years, where d is greater than 1, are also useful for defining the magnitude and frequency of droughts that exceed one year in duration. The USGS National Water Summary for 1988-89 describes the magnitude and frequency of several multi-year droughts that have occurred in each State. Jennings and Paulson (1988) describe the methodology used in this analysis. A drought atlas being prepared by the U. S. Army Corps of Engineers also provides statistics on the magnitude and frequency of multi-year droughts (Willeke and others, 1991).

FREQUENCY ANALYSIS AT GAGING STATIONS

Analysis of Annual D-day Events

The discussion of frequency analysis of low-flow characteristics at gaging stations will be oriented to the analysis of annual D-day events. These are the types of analyses most frequently made by USGS and for which procedures are better established. The frequency analysis of biologically-based design flows and d-year low flows is not described.

The USGS determines the magnitude and frequency of annual minimum D-day low flows by first fitting a Pearson Type III distribution to the logarithms of the annual D-day events. This computed frequency curve is adjusted graphically if the data, based on Weibull plotting positions, do not appear to fit the Pearson Type III distribution (Riggs, 1972). The USGS utilizes a computer program (A193) for performing the frequency analysis (Hutchison, 1975; Lumb and others, 1990). Tasker (1987) has demonstrated that fitting a Pearson Type III distribution to the logarithms of the annual D-day events is as good or superior to three other alternative approaches for defining low-flow frequency for streams in Virginia.

Ten or more years of data should be used in the frequency analysis. The annual events should be evaluated for trends or serial correlation to determine if the data are suitable for frequency analysis. Hirsch and others (1982) describe a nonparametric Kendall test useful for detecting monotonic trends. The serial correlation, as computed in the USGS low-flow program, can be used to assess the independence of the annual D-day low flows. Tasker and Gilroy (1982) provide guidance on how to adjust for the effect of serial correlation.

An Example of At-Site Frequency Analysis

An example of fitting a Pearson Type III frequency curve to the logarithms of the annual 7-day low flows for Little Mahoning Creek near McCormick, PA (03034500) is given in figure 1. For this particular example, the Pearson Type III distribution appears to adequately fit the data. Selected D-day, T-year low-flow characteristics ($Q_{D,T}$) are computed using the equation:

$$\log Q_{D,T} = M + KS \qquad (1)$$

where

M = mean of the logarithms of the annual D-day events
S = standard deviation of the logarithms of the annual D-day events
K = Pearson Type III frequency factor for a skewness of G and a recurrence interval of T (nonexceedance probability of p = 1/T).

For the example in figure 1, M = 0.648 log units, S = 0.359 log units, and G = -0.181 giving K = -1.30 for T = 10 years. When substituted in equation 1, one obtains a $Q_{7,10}$ of 1.5 ft^3/s.

Zero values are not consistent with the logarithmic transformation used in the Pearson Type III frequency analysis. When zero values do occur in a sample, a conditional probability adjustment is made to estimate the D-day, T-year low flow. In the USGS low-flow program (A193), the computation is performed as follows. The mean (M), standard deviation (S) and skewness (G) are computed based on the logarithms of the nonzero values in the sample. These statistics are used in conjunction with a new Pearson Type III frequency factor (K^*) to compute $Q_{D,T}^*$ based on the entire sample including zero values (W.H. Kirby, USGS, personal commun., 1987). The new equation is:

$$\log Q_{D,T}^* = M + K^* S \qquad (2)$$

where

$Q_{D,T}^*$ = D-day, T-year low flow estimate, in ft^3/s, based on inclusion of zero flows

K^* = Pearson Type III frequency factor for a skewness of G and nonexceedance probability of

$$p^* = \left(\frac{1}{T}\left(\frac{N}{n}\right) - \frac{N-n}{n}\right) = 1 - \frac{N}{n}\left(\frac{T-1}{T}\right) \qquad (3)$$

where N = total number of events in sample
n = number of non-zero events
N-n = number of zero events

ESTIMATING LOW-FLOW CHARACTERISTICS FROM BASE-FLOW MEASUREMENTS

Estimation of Characteristics

Low-flow characteristics are often needed at locations other than at gaging stations. Riggs (1972) suggested that base-flow measurements be obtained at the site of interest and correlated with concurrent daily flows at a nearby gaged site with a long flow record. The base-flow measurements and the concurrent daily flows can be used to establish a relation between flows at the two sites. That relation and the statistical properties of flows at the gaged site can be used to estimate low-flow characteristics at the partial-record site. This technique will be illustrated in estimating D-day, T-year low-flow characteristics.

A typical relation between concurrent flows is given in figure 2. For the purpose of the example, Little Mahoning Creek at McCormick, PA (drainage area = 87.4 square miles) is assumed to be a partial-record station at which only 10 base-flow measurements are available to estimate the D-day, T-year low flows. (In fact, daily-flow record for the period 1941-83 is available and was used to define the frequency curve for annual 7-day low flows shown in figure 1.) Buffalo Creek near Freeport, PA (03049000, drainage area = 137 square miles) is chosen as the long-term index site with daily-flow record for the period 1942-83. The relation shown in figure 2 was computed by ordinary least squares regression using the logarithms of the concurrent flows (for base-flow periods in 1962-63) and is as follows:

$$\log Q_{0345} = 0.298 + 0.557 \ (\log Q_{0490}) \qquad (4)$$

where

Q_{0345} = base-flow measurement at Little Mahoning Creek, in ft^3/s

Q_{0490} = concurrent daily flow at Buffalo Creek, in ft^3/s

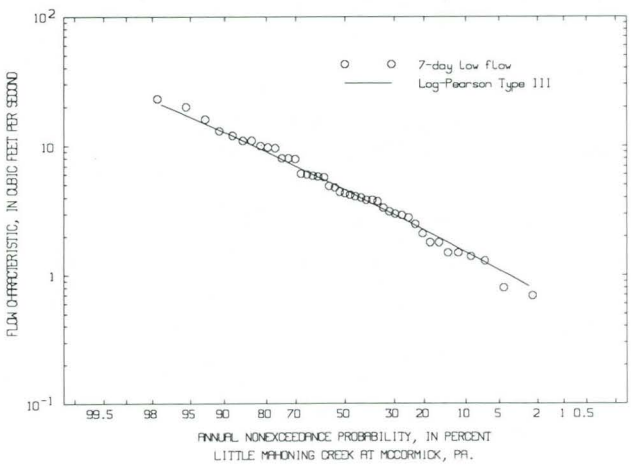

Figure 1.--Log-Pearson Type III frequency curve for 7-day low flow for Little Mahoning Creek at McCormick, PA.

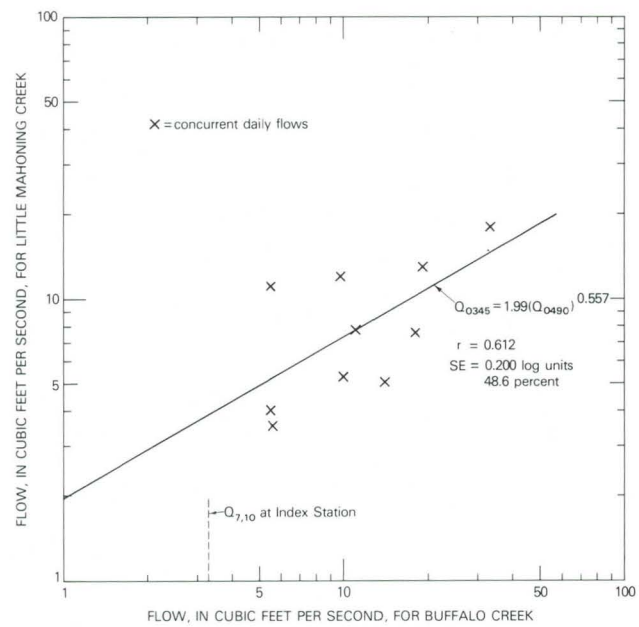

Figure 2.--Relation between concurrent daily flows for Little Mahoning Creek and Buffalo Creek.

In equation 4, 0.298 corresponds to the regression constant a and 0.557 corresponds to the regression coefficient b. The standard error of estimate (SE) of equation 4 is 0.200 log units (48.6 percent) and the correlation coeffficient (r) is 0.612.

Riggs (1972) suggested that graphical techniques should be used to establish the relation in figure 2 and to estimate D-day, T-year low flows at partial-record stations. Stedinger and Thomas (1985) described a method that utilized the ordinary least square regression relation in figure 2 and suggested that the mean and variance of the annual D-day events be estimated at the partial-record site by the following equation:

$$\hat{\mu}_y = a + b\,M \tag{5a}$$

$$\hat{\sigma}_y^{\,2} = b^2\,S^2 + (SE)^2\left[1 - \frac{S^2}{(L-1)\,(SX)^2}\right] \tag{5b}$$

where

$\hat{\mu}_y$ and $\hat{\sigma}_y^{\,2}$ are the estimated mean and variance of logarithms of annual D-day low flows at the partial-record site
a and b are the regression constant and coefficient for the log-linear relation in figure 2 and equation 4
L is the number of base-flow measurements
SX is the standard deviation of the logarithms of the concurrent daily flows at the index station
M and S are previously defined.

The D-day, T-year low flows are then estimated by the following equation, assuming the logarithms of the annual 7-day minimums follow a Pearson Type III distribution:

$$\hat{Y}_{D,T} = \hat{\mu}_y + K_y\,\hat{\sigma}_y \tag{6}$$

where

$\hat{Y}_{D,T}$ is the D-day, T-year low flow, in log units
K_y is the Pearson Type III frequency factor for recurrence interval T estimated using G from the index site
$\hat{\mu}_y$ and $\hat{\sigma}_y$ are defined above.

An important assumption in the use of a relation like equation 4 is that the relation between concurrent annual D-day low flows at the two sites is essentially the same as the relation between concurrent daily flows. If a relation similar to equation 4 is used to estimate D-day, T-year low flows in excess of say 30 days duration, the analyst should evaluate the applicability of this assumption.

An Example Using One Index Station

An example of estimating the 7-day, 10-year low flow at Little Mahoning Creek is given to illustrate the technique described by Stedinger and Thomas (1985). The required input for equation 5 is as follows: a = 0.298 log units, b = 0.557, and SE = 0.200 log units from equation 4; statistics for Buffalo Creek (index station), M = 0.875 log units, S = 0.287 log units, G = 0.296, K = -1.242 (for T = 10 years), and SX = 0.262 log units.

Using this input and equation 5, $\hat{\mu}_y$ and $\hat{\sigma}_y$ are estimated to be 0.785 and 0.245 log units, respectively. The 7-day, 10-year low flow in logarithmic units

($\hat{Y}_{7,10}$) for little Mahoning Creek is 0.481 log units which corresponds to a $Q_{7,10}$ of 3.0 ft^3/s. This estimate of 3.0 ft^3/s can be compared to the value of 1.5 ft^3/s computed earlier using the actual gage record (equation 1).

Equation 5 can be extended to include more than one index station. The multi-index equation, analogous to equation 5, for up to k index stations is:

$$\hat{\mu}_y = b_0 + b_1 M_1 + b_2 M_2 + \ldots + b_k M_k, \tag{7a}$$

$$\hat{\sigma}_y^2 = b^T V_{xx} b + (SE)^2\{1 - \text{trace}[V_{xx}(S_{xx})^{-1}]\} \tag{7b}$$

where

b_i = regression coefficients
M_i = mean of logarithms of annual D-day events at index station i
V_{xx} = covariance matrix of annual D-day events at the index stations
S_{xx} = sum of squares of concurrent daily flows at the index stations
trace = sum of diagonal elements of the matrix $[V_{xx}(S_{xx})^{-1}]$.

The b and b^T (transpose of b) in equation 7b are now vectors of regression coefficients with dimension k+1, respectively. The V_{xx} covariance matrix is defined using the longest period of **concurrent** annual D-day events at all the index stations being used in the analysis. The S_{xx} sum of squares matrix is defined from the **concurrent** daily flows from all the index stations that are used in defining the relation analogous to figure 2 and equation 4 for one index station.

An Example Using Two Index Stations

For the purpose of illustration, the 7-day, 10-year low flow will be estimated for Little Mahoning Creek using two index stations. A second station, Crooked Creek at Idaho, PA (03038000, drainage area = 191 square miles), will be used in addition to Buffalo Creek from the previous example. A new equation is recomputed using 10 base-flow measurements and concurrent daily flows (for baseflow periods in 1962-63) for both index stations. The two-index station equation, analogous to equation 4, is:

$$\log Q_{0345} = -1.013 + 0.719 (\log Q_{0490}) + 0.953 (\log Q_{0380}) \tag{8}$$

where

Q_{0380} = concurrent daily flow at Crooked Creek, in ft^3/s.

The regression coefficients of -1.013, 0.719 and 0.953 correspond to b_0, b_1, and b_2, respectively, in equation 7. The standard error of estimate for equation 8 is 0.119 log units (28 percent) and the correlation coefficient is 0.897. Using equation 7, the regression coefficients from equation 8, and the statistics from the two index stations, the new estimates of $\hat{\mu}_y$ and $\hat{\sigma}_y$ are 0.723 and 0.480 log units, respectively. By use of equation 6 with a K_y value of -1.25 (average of two index stations), $Q_{7,10}$ becomes 1.3 ft^3/s. These results and those from the one-index-station example are summarized below.

Table 1.-- Summary of low-flow statistics for Little Mahoning Creek (03034500)

	One index station	Two index stations	Station value (03034500)
r	0.612	0.897	-----
SE (log units)	0.200	0.119	-----
$\hat{\mu}_y$ (log units	0.785	0.723	0.648
$\hat{\sigma}_y$ (log units	0.245	0.480	0.359
K_y (T = 10 years)	-1.242	-1.250	-1.300
$Q_{7,10}$ (ft^3/s)	3.0	1.3	1.5

Stedinger and Thomas (1985) caution against the use of the linear model in equation 4 to directly transfer the $Q_{7,10}$ at the index station to the partial-record station. They discuss why this approach tends to, on average, overestimate $Q_{7,10}$ because of the "regression effect." As an example, if the $Q_{7,10}$ value of 3.3 ft^3/s for Buffalo Creek (index station) is used in figure 2, the estimated $Q_{7,10}$ for Little Mahoning Creek is nearly 3.9 ft^3/s. This value is higher than any of the estimates of $Q_{7,10}$ given in the above table.

Accuracy of Characteristics

In any statistical analysis, it is usually worthwhile and informative to compute the uncertainty of the estimated statistic. The standard error of the three estimates of $Q_{7,10}$ in the above table can be computed and compared in the following manner. The time-sampling error in the station value of 1.5 ft^3/s can be computed by methods described by Kite (1988) under the assumption that the logarithms of the annual 7-day events are Pearson Type III distributed and there is no significant measurement error in the data. By use of the at-site standard deviation (0.359) and skew (-0.181), and the length of record (43 years), a standard error of 16 percent is computed for the station value of $Q_{7,10}$ by using equation 9-56 from Kite (1988) as follows:

$$\text{standard error} = \frac{0.359}{\sqrt{43}}(1.26) = 0.0690 \text{ log units} = 16 \text{ percent} \qquad (9)$$

where

the factor 1.26 is based on a skew of -0.181 and T = 10 years.

The standard error of the estimated $Q_{7,10}$ using one index station can be estimated from the following equation derived by Stedinger and Thomas (1985):

$$\left[SE \left[\hat{Y}_{D,T} \right] \right]^2 \cong$$

$$\frac{(SE)^2}{L-1} \left[1 + \frac{(M-\bar{X})^2}{(SX)^2} + \frac{K_y^{\,2}}{2\hat{\sigma}_y^{\,2}} \left[(SE)^2 + \frac{2b^2S^4}{(SX)^2} \right] + \frac{2bK_y(M-\bar{X})S^2}{\hat{\sigma}_y(SX)^2} \right]$$

$$+ \frac{b^2S^2}{N-1} \left[1 + \frac{b^2K_y^{\,2}S^2}{2\hat{\sigma}_y^{\,2}} \right] \qquad (10)$$

where SE $\left[\hat{Y}_{D,T} \right]$ is the standard error of the D-day T-year low-flow estimate (in log units) at the partial-record site, $\bar{X}$ is the mean of the logarithms of the concurrent daily flows at the index station and all other variables are previously defined. From equation 10, SE $\left[\hat{Y}_{D,T} \right]$ is computed to be 0.175 log units, corresponding to a standard error of 42 percent for the 3.0 ft^3/s estimate of $Q_{7,10}$ for Little Mahoning Creek.

Equation 10 can also be extended to allow use of more than one index station (J. R. Stedinger and W. O. Thomas, Jr., unpublished manuscript). The derivation of the equation is not discussed here. A standard error of 26 percent was computed for the estimated $Q_{7,10}$ (1.3 ft^3/s) based on two index stations. The estimated reduction in standard error from 42 percent (for one index station) to 26 percent is a measure of the improvement in the accuracy of the estimate of $Q_{7,10}$ obtained by using an additional index station. Both of these standard errors can be compared to the 16 percent standard error based on 43 years of annual 7-day events at the site.

REFERENCES CITED

Environmental Protection Agency, 1986, Technical Guidance Manual for Performing Waste Load Allocation, Book VI, Design Conditions: Chapter 1, Stream Design Flow for Steady-State Modeling: Environmental Protection Agency, Washington, D.C.

Hirsch, R. H., Slack, J. R., and Smith, R. A., 1982, Techniques of trend analysis for monthly water quality data: Water-Resources Research, v. 18, no. 1, p. 107-121.

Hutchison, N. E., 1975, WATSTORE User's Guide, v. 1, Chapter IV, Section G, Daily Values Statistics (Programs A969 and A193): U.S. Geological Survey Open-File Report 75-426.

Jennings, M. E., and Paulson, R. W., 1988, Summary of floods and droughts in the United States: Proceedings of the American Society of Civil Engineers, 1988 National Conference on Hydraulic Engineering, Colorado Springs, Colorado, August 8-12, 1988, p. 813-818.

Kite, G. W., 1988, Frequency and risk analyses in hydrology: Water-Resources Publications, Littleton, Colorado, 257 p.

Lumb, A. M., Kittle, J. L., Jr., and Flynn, K. M., 1990, Users manual for ANNIE, a computer program for interactive hydrologic analyses and data management: U.S. Geological Survey Water-Resources Investigations 89-4080, 236 p.

Riggs, H. C., 1972, Low flow investigations: U.S. Geological Survey Techniques of Water-Resources Investigations, Book 4, Chapter B1, 18 p.

Rossman, L. A., 1990, Design stream flows based on harmonic means: American Society of Civil Engineers Journal of Hydraulic Engineering, v. 116, no. 7, p. 946-950.

Stedinger, J. R., and Thomas, W. O., Jr., 1985, Low-flow frequency estimation using base-flow measurements: U.S. Geological Survey Open-File Report 85-95.

Tasker, G. D., 1987, A comparison of methods for estimating low flow characteristics of streams: Water-Resources Bulletin, v. 23, no. 6, p. 1077-1083.

Tasker, G. D. and Gilroy, E. J., 1982, Comparison of estimators of standard deviation for hydrologic time series: Water-Resources Research, v. 18, no. 5, p. 1503-1508.

Willeke, G. E., Guttman, Nathaniel, and Thomas, W. O., Jr., 1991, A national drought atlas for the United States of America: Proceedings of the USA-PRC Bilateral Symposium on Droughts and Arid-Region Hydrology, Tucson, Arizona, September 16-20, 1991.

FREQUENCY DISDRIBUTION FOR HYDROLOGIC SAMPLES WITH ZERO EVENTS

Shan-Xu Wang

Bureau of Hydrology, Yangtse Valley Planning Office
Wuhan 430010, CHINA

ABSTRACT

Conventional hydrologic frequency analysis is based on an assumption that the hydrologic variable under study follows a continuous distribution, which is not the case in arid and semi-arid regions where the hydrologic series, such as annual low flow, monthly precipitation in dry seasons, etc; often contain several zero events resulting from regional climate-hydrologic regime. As a result, the conventional frequency estimation method and distribution families in hydrologic literature are no longer applicable. In this study a discontinuous distribution with discontinuity at zero value is recommended to fit these series, which consists of a continuous positive component and a non-zero probability mass placed on zero value. Further, a method for estimating snch a discontinuous frequency distribution (exceedance probability) is proposed based on statistical theory. Case study demonstrates the suitability of the distribution and estimation method.

INTRODUCTION

It is often encountered in analysing hydrologic observations in arid and semi-arid regions that some series contain zero events resulting from regional Climate-hydrologic regime. From viewpoint of probability theory, this phenomenon can be characterized by placing a non-zero probability mass on zero value, i.e. $pr\{Y=0\}\neq 0$. Therefore, distributions of these random variables would be discontinuous with discontinuity at zero value and violate the basic assumption of continuity in conventional frequency analysis. As a result, the regular method and distribution families are no longer valid for analysing such series in the arid and semi-arid regions.

Jin(1964), Jennings and Benson(1969), among others, proposed methods for determining frequencies for non-zero values of the series. However, contribution of the probability of zero events to the distribution and its parameter estimation were not explicitly discussed. Recently, Woo and Wu (1989) reported that many annual flood records of the rivers of the Canadian prairies have zero flows. They considered the occurrence of zero and non-zero events to be mutually exclusive and expressed the distribution as a sum of the two parts, probability of zero events $p(0)$ and $[1-P(0)]\cdot[P(Q\leqslant X|Q>0)]$. They fitted the non-zero portion by procedures used for conventional flood series.

In this study, a discontinuous distribution with discontinuity at zero value is recommended to fit such hydrologic series. The study consists of: (1) basic properties of the distribution and its moments and parameter expressions; (2) conditional distribution of order statistics with positive values, their plotting positions and fitting procedure; (3) estimation of zero

event probability; and (4)distribution transformation and design event determination, Finally, an actual sample is analysed to illustrate the application of the proposed estimation method.

DISTRIBUTION AND ITS MATHEMATICAL CHARACTERS

It is well known that the distribution function of any random variable, regardless of whether it is continuous or not, is monotonic. Based on properties of the monotonic function in real variable function theory, the distribution function of the hydrologic random variable under study takes the form of

$$F(y)=F_c(y)+P_r\{Y=0\} \qquad 0\leqslant y<+\infty \tag{1}$$

where $F(\cdot)$ and $Fc(\cdot)$ stand for the distribution function of the random variable Y and its positive component, respectively.

When $y>0$, $F(y)$ is continuous with derivative

$$f_c(y)=dF(y)/dy=dF_c(y)/dy \qquad 0<y<+\infty \tag{2}$$

but

$$\int_{-\infty}^{+\infty} f_c(t)dt < 1$$

$f_c(y)$ does not meet the condition to be a probability density function (abbreviate to "pdf" from now on).

When $y=0$,

$$dF(y)/dy \rightarrow \infty \tag{4}$$

indicating that the zero value is a discontinuity of $F(y)$.

From eq.(1),

$$\int_{-\infty}^{+\infty} dF(y)=P_r\{Y=0\}+\int_{+0}^{+\infty} f_c(t)dt=1 \tag{5}$$

$F(y)$ meets the necessary condition to be a distribution function.

The moments of the distribution $F(y)$ can be derived as follows:

$$m_r=\int_{-\infty}^{+\infty} y^r dF(y)=y^r\Big|_{y=0}[F(+0)-F(0)]+\int_{+0}^{+\infty} y^r f_c(y)dy$$

$$=\int_{+0}^{+\infty} y^r f_c(y)dy=m_{cr} \qquad r=1,2,\cdots \tag{6}$$

and

$$u_r=\int_{-x}^{+\infty} (y-m_1)^r dF(y)=(y-m_1)^r\Big|_{y=0}[F(+0)-F(0)]+\int_{+0}^{+\infty}(y-m_1)^r f_c(y)dy$$

$$=(-1)^r m_1^r P_r\{Y=0\}+u_{cr} \qquad r=2,3,\cdots \tag{7}$$

where m_r、u_r and m_{cr}、u_{cr} are, respectively, the rth original、central moments of $F(y)$and those of its positive component $F_c(y)$.

From eqs. (6)and(7), it can be seen that the original moments of the

distribution F(y)are equal to those of its positive component $F_c(y)$, while it is not the case for the central moments. The probability of occurrence of the zero events contributes only to the central moments.

The first three moments can then be expressed as

$$m_1 = m_{c1}$$
$$u_2 = m_1^2 \, P_r\{Y=0\} + u_{c2} \qquad (8)$$
$$u_3 = -m_1^3 \, P_r\{Y=0\} + u_{c3}$$

Further, one can obtain the coefficient of variation and the skewness

$$C_v = \sqrt{u_2} / m_1 = \sqrt{m_1^2 \, P_r\{Y=0\} + u_{c2}} / m_1 \qquad (9)$$

and

$$C_s = u_3 / u_2^{1.5} = (-m_1^3 \, P_r\{Y=0\} + u_{c3}) / (m_1^2 \, P_r\{Y=0\} + u_{c2})^{1.5} \qquad (10)$$

respectively.

Inspection of eqs. (8)−(10) yields that the probability $Pr\{Y=0\}$ always positively contributes to Cv, while negatively to Cs.

FREQUENCY ANALYSIS PROCEDURES

In practice, the problem to solve is how to infer the above distrbution, F(y), or frequency distribution, P(y) (in terms of exceedance probability), with discontinuity at Y=0, on the basis of an observed record with several zero values so as to obtain quantile estimates for design purposes. According to the previous description of the distribution, the inference may be carried out by estimating the positive component, which is continuous, and the probability $Pr\{Y=0\}$. However, it should be noted here that the positive component is not a full−definite distribution so that the conventional procedures including plotting position formulae and distribution families cannot be used. The proper procedures will be described in the following.

Conditional Frequency Distribution

From eq(5), the probability of event Y>0 would be

$$P_r\{Y>0\} = \int_{+0}^{+\infty} f_c(t)dt = 1 - P_r\{Y=0\} \qquad (11)$$

The conditional distribution and frequency distribution on Y>0 can then be written as (Cramer 1946)

$$F'(y|y>0) = F_c(y) / (1 - P_r\{Y=0\}) \qquad (12)$$

and

$$P'(y|y>0) = P_c(y) / (1 - P_r\{Y=0\}) \qquad (13)$$

respectively, in which $P_c(y) = 1 - F_c(y)$. $F'(\cdot)$ and $P'(\cdot)$ are in general termed as truncated distibution and truncated frequency distribution, with pdf

$$f'(y|y>0) = f_c(y) / (1 - P_r\{Y=0\}) \qquad (14)$$

which meets

$$\int_0^{+\infty} f'(t|t>0)dt = 1 \qquad (15)$$

Using eq.(12), eq.(1) can be rewritten as

$$F(y)=P_r\{Y=0\}+(1-P_r\{Y=0\})F'(y|y>0) \qquad (16)$$

which coincides with that in Woo and Wu (1989).

Eq.(16) indicates that estimation of F(y) (or P(y)) can be carried out by estimating probability $P_r\{Y=0\}$ and the conditional distribution function $F'(y|y>0)$ (or $P'(y|y>0)$), which meets the necessary condition to be a distribution function. Hence, our major attention will center on developing a fitting procedure for F' or P'.

Plotting Positions for Conditional Frequency Distribution

Surpose we have obtained a consecutively observed hydrologic sample of size n $(y_1, \cdots, y_K, 0, \cdots, 0)$ in descending order, where $y_1, \cdots, y_K$ are all positive while the remainder are n−k zero values.

Obviously, empirical frequency distribution conditional on $Y>0$ can be plotted by using the first k positive order statistics. Based on theorem of conditional distribution of the order statistics (Chen and Fong et al, 1989), the conditional distribution, on $Y>0$, of the first k order statistics of the sample of size n drawn from distribution F(y) is equivalent to the distribution of the ranked sample of size k drawn from the conditional distribution $F'(y|y>0)$. The theorem lays the theoretical foundation for estimating the conditional frequency distribution on the basis of the first k order statistics $(y_1, \cdots, y_K)$.

According to order statistics theory, the joint pdf of the ranked sample $(y_1, \cdots, y_K)$ is then

$$h'(y_1, \cdots, y_K)=K!\prod_{i=0}^{k} f'(y_i|y_i>0) \qquad (17)$$

Further, for any individual m, $m=1, \cdots, k$, the pdf of the mth order statistic y_m is

$$h'_m(y_m)=m\binom{k}{m}P'^{\,m-1}_m(1-P'_m)^{k-m}f'(y_m|y_m>0) \qquad (18)$$

where $P_m'=P'(y_m|y_m>0)$, the conditional probability of exceeding y_m.

Analogously, the joint pdf of the conditional exceedance probabilities $(P'_1, \cdots, P'_K)$ and the pdf of any P'_m are

$$g'(P_1', \cdots, P_K')=K! \qquad (19)$$

and

$$g_m'(P_m')=m\binom{k}{m}P_m'^{\,m-1}(1-P_m')^{k-m} \qquad (20)$$

respectively.

From eq. (20), as in the derivation of the Weibull formula, the expectations of the P_m'

$$E(P_m')=\int_0^1 P_m' g_m'(P_m')dP_m'=\frac{m}{k+1} \qquad m=1, \cdots, k \qquad (21)$$

can then be adopted as plotting positions for $(y_1, \cdots, y_K)$.

Type of Conditional Frequency Distribution

To fit the empirical distribution plotted by eq.(21), it is necessary to choose a proper distribution type. According to the properties of the conditional distribution (see eq.(12)–(14)), with origin at zero value, the Pearson Type 3 distribution constrained by $C_s' = 2C_v'$ may be an appropriate candidate. Its pdf is shown as

$$f(y) = \frac{b^a}{\Gamma(a)} y^{a-1} e^{-by} \qquad 0 \leq y < +\infty \tag{22}$$

where a and b are positive parameters, and $\Gamma(\cdot)$ stands for Gamma function. With eq.(22) the random variable y can be expressed as usual

$$y(P') = m_1' [1 + C_v' \phi(P', C_s')] \tag{23}$$

where: ϕ is frequency factor of the Pearson Type 3 distribution;

m_1', C_v' and C_s' are the mean value, coefficient of variation and skewness, respectively. And

$$a = 4 / C_s'^2 \tag{24}$$

$$b = 2 / (m_1' C_v' C_s')$$

The parameters m_1', C_v' and C_s' (hence a and b) can be estimated by applying a conventional fitting procedure to $y_1, \cdots, y_K$.

Estimation of Positive Component

Estimating $P'(y|y>0)$, the estimator of the positive component $P_c(y)$ can then be obtained using eq.(13) when probability $P_r\{Y=0\}$ has been known. While $P_r\{Y=0\}$ can be estimated with a classical estimator

$$P_0^* = (n-k)/n \tag{25}$$

which leads to estimator

$$P_c^*(y) = (k/n)\, P'^*(y|y>0) \tag{26}$$

Eq.(26) indicates that the estimator of the positive component $P_c(y)$ can be obtained by multiplying the estimator of conditional frequency distribution $P'(y|y>0)$ by a factor of k/n, which has been got previously. Since $k<n$, then $P_c^*(y)$ is always less than $P'^*(y|y>0)$.

Accordingly, its first three noments m_{c1}, u_{c2} and u_{c3} can also be derived as follows

$$m_{c1} = \int_{+0}^{+\infty} y f_c(y) dy = (1 - P_r\{r=0\}) \int_{+0}^{+\infty} y f'(y|y>0) dy = (1 - P_r\{Y=0\}) a/b \tag{27}$$

$$u_{c2} = \int_{+0}^{+\infty} (y - m_{c1})^2 f_c(y) dy$$

$$= 1/b^2 \, [(1 - P_r\{Y=0\}) a + (P_r\{Y=0\})^2 (1 - P_r\{Y=0\}) a^2] \tag{28}$$

$$u_{c3} = \int_{+0}^{+\infty} (y - m_{c1})^3 f_c(y) dy = 1/b^3 \, [2(1 - P_r\{Y=0\}) a + 3P_r\{Y=0\}(1 - P_r\{Y=0\}) a^2$$

$$+ (P_r\{Y=0\})^3 (1 - P_r\{Y=0\}) a^3] \tag{29}$$

Inserting eq.(25) into eqs.(27)—(29) yields estimators

$$m_{c1}^* = ka^* / nb^* \quad (30)$$

$$u_{c2}^* = (k / nb^{*2})[a^* + (n-k)^2 a^{*2} / n^2] \quad (31)$$

$$u_{c3}^* = (k / nb^{*2})[2a^* + 3(n-k)a^{*2} + (n-k)^3 a^{*3} / n^3] \quad (32)$$

where a^* and b^* are the estimators of the parameters a and b of the conditional frequency distribution given previously.

Combination of $P_c^*(y)$ and P_0^* yields the fitted frequency distribution $P^*(y)$, as shown in Fig.1.

Based on the fitted frequency distribution estimated above, the magnitude of the design event of given return period can then be estimated:

(1) If the design frequency P is less than k/n, the design event $y(P)>0$ and can be interpolated on $P_c^*(y)$ directly or on $P'^*(y|y>0)$ with frequency kP/n;

(2) If design frequency P is larger than or equal to k/n, $y(P)=0$.

CASE STUDY

The proposed discontinuous distribution (or frequency distribution) and its estimation procedure have been used to analyse the December monthly precipitation series at Lugouqiao gauge, in North China, with $n=51$ (from 1918 to 1970 with data missing in 1937 and 1948) and $k=37$ (i. e. 14 zero values). The procedure and results are summarized as follows:

(1) Estimating the probability $P_r\{Y=0\}$ by eq.(25): $P_0^*=0.27451$;

(2) Estimating the conditional frequency distribution $P'(y|y>0)$:

Plot 37 positive values on probability paper by eq.(21),

The Pearson Type 3 distribution with $C_s'=2C_v'$ is adopted to fit these plots by using a constrained Least Squares fitting procedure (Bard 1974). The estimated parameters are:

$m_1'^*=5.656$ $C_v'^*=1.525$ $C_s'^*=3.050$ $a^*=0.429992$ $b^*=0.076024$

(3) Estimating the positive component $P_c(y)$:

$P_c^*(y)$ is obtained by diminishing the abscissa (exceedance probability) of $P'^*(y|y>0)$ by the factor k/n, as shown in Fig.1. Its moment estimators are:

$m_{c1}^*=4.10337$ $u_{c2}^*=55.72363$ $u_{c3}^*=1674.06251$

(4) Estimating frequency distribution $P(y)$:

$P^*(y)$ is obtained by combining $P_c^*(y)$ and the line segment paralell to the abscissa, from (0.72549, 0) to (1,0), representing P_0^* with connection at (0.72549, 0), see Fig.1, with its moments and parameters as

$m_1^*=4.10337$ $u_2^*=55.72363$ $u_3^*=1655.09631$ $C_v^*=1.8931$ $C_s^*=3.5306$

using eqs.(8)—(10).

SUMMARY

Occurrence of the zero events in hydrologic series in the arid and semi-arid regions reflects the regional climate-hydrology regime. A non-zero

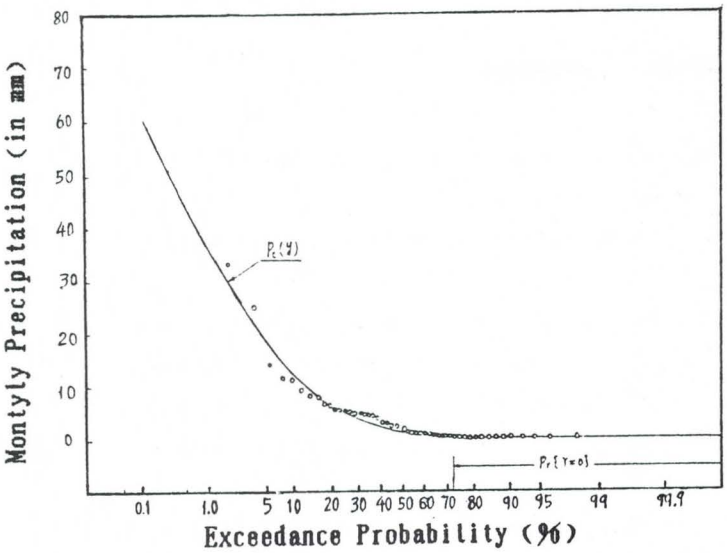

Fig. 1.

Discontinuous Frequency Distribution $P^m(y)$ (transformed from $P'^m(y|y>0)$)

∘ data plots by $\frac{m}{n+1}$, $n=51$

probability mass should be placed on the zero value. As a result, the conventional distribution families and the estimation methods in hydrology literature are no longer appropriate for determining their frequencies. A discontinuous distribution with discontinuity at zero value would be a proper probabilistic tool to fit them. The impact of the probability $P_r\{Y=0\}$ on mathematical characters is not negligible.

The fitting procedures of the frequency distribution can be conducted by fitting a continuous distribution with zero origin to the positive order statistics and estimating the probability of zero events.

The proposed estimation method in this study may be applicable to dry regions throughout the world.

REFERENCES

Bard, Yonathan, 1974, Nonlinear Parameter Estimation, Academic Press, New York.

Chen, Xi-Ru, Fong, Zhao-Ben, Li, Guo-Ying and Tao, Bo, 1989, Non-Parametric Statistics (in Chinese), Shanghai Science-Techonlogy Press, Shanghai, China.

Cramer, H., 1946, Mathematical Methods of Statistics, Princeton Univ. Press.

Jennings, M. E and Benson, M.A, 1969, Frequency Curves for Annual Flood Series with Some Zero Events or Incomplete Data, Water Resources Research, Vol.5, No.1, P.276-280.

Jin, Guang-Yan, 1964, The Principle and Methods for Hydrologic Computations (in Chinese), Industry Press, Beijing, China.

Woo, Ming-Ko and Wu, Kai, 1989, Fitting Annual Floods with Zero-Flows, Canadian Water Resources Journal, Vol.14, No.2, P.10-16.

ESTIMATING LOW FLOW CHARACTERISTICS OF STREAMS AT UNGAGED SITES

Gary D. Tasker

U. S. Geological Survey, Reston, Virginia

ABSTRACT

Regional regression models that relate flow characteristics at gaged sites to physiographic and meteorological characteristics of the drainage basins are sometimes used to estimate flow characteristics at ungaged sites. One problem often encountered in developing regional low flow regressions, especially in semi-arid regions, is that many observed flows are zero. In order to deal with this problem a regional logistic regression relating probability of zero flow at gaged sites to basin characteristics at the sites is developed. A second problem encountered in developing regional low flow regressions is how to properly weight observations in the analysis. To deal with this problem an estimated generalized-least squares procedure is used to determine weights based on length of record, proximity to other gages in the analysis, and whether a site has continuous record or low flows estimated by correlation of base flow measurements. Combining these two methods with conditional probability adjustments yields a solution to the problem of estimating low flow characteristics at ungaged sites.

INTRODUCTION

Low flow characteristics of streams are used in planning and design of water supplies, analyzing environmental and economic impacts, modeling stream water quality, and improving the general level of understanding of stream systems. Hydrologists often use regional regression methods to estimate low flow characteristics at sites where no flow information is available. Regional regression methods relate observed flow characteristics at gaged sites to basin characteristics of the site, such as drainage area, soil type, average precipitation amounts, or aquifer characteristics. Practical problems encountered in trying to develop regional regression models of low flow characteristics include how to deal with observations of minimum flows of zero and how to properly include data observed at sites with short records or partial-record sites where only low flow data, such as base flow measurements, are available. The first problem is approached as a logistic regression problem and the second is approached as a generalized-least-squares regression problem.

LOGISTIC REGRESSION TO ESTIMATE PROBABILITY OF ZERO FLOW

At many streams in the United States the minimum flow for a year is zero. To estimate the probability of having a minimum of zero at an ungaged site a regional logistic regression model (Cox, 1970) that relates probability of a zero minimum at a site to physical, meteorological, and geological characteristics of the watershed may be developed. Consider a collection of p basin characteristics denoted by the vector $\boldsymbol{x}' = (x_1, x_2, \ldots, x_p)$. Let $\pi(\mathbf{x})$ denote the probability that the annual minimum flow associated with a duration, such as 7-day, 30-day, or 90-day, is nonzero. Then the multiple logistic regression model is given by the equation

$$g(\boldsymbol{x}) = \beta_0 + \beta_1 x_1 + \beta_2 x_2 + \ldots + \beta_p x_p$$

in which

$$\pi(\boldsymbol{x}) = \frac{e^{g(\boldsymbol{x})}}{1 + e^{g(\boldsymbol{x})}}$$

Using sample data collected at stream gages in the area, the unknown b's are estimated by maximizing the log likelihood function

$$L(\beta) = \sum_{i=1}^{n} \{ y_i ln[\pi(\boldsymbol{x})] + (1 - y_i) ln[1 - \pi(\boldsymbol{x})] \}$$

in which $y_i = 1$ if an observed annual minimum is nonzero in year i and $y_i = 0$ if an observed annual minimum is zero and n is the total number of observations at all sites.

GENERALIZED LEAST SQUARES REGRESSION TO ESTIMATE LOW FLOW STATISTICS

Low flow at a site may be characterized by an index of low flow such as the 30-day, 10-year low flow, which is the discharge having a 10-year recurrence interval derived from a frequency curve of lowest average flow for thirty consecutive days in a year. A popular and useful distribution for estimating low flow characteristics such as the 30-day, 10-year low flow is the Log- Pearson III (LPIII) distribution. At ungaged sites the parameters needed to estimate a percentage point from a LPIII can be determined from regional regression models relating the mean, standard deviation, and skewness coefficient at a site to watershed characteristics. The data used to estimate the regression coefficients, β, are flow data collected at stream gages in the region and at partial-record sites where a number of base flow have been made and correlated with a long record (Stedinger and Thomas, 1985).

The accuracy of an estimate of a flow characteristic based on recorded or measured flows may vary greatly from site to site depending upon, among other things, the length of record at a gaged site or number of base flow measurements at a partial- record site. Other factors that affect accuracy include natural variability of flow and degree of autocorrelation in annual minimum flows. Ordinary least squares regression is not appropriate when the response variable, in this case the low flow characteristic, is not observed with equal accuracy at all sites used in the regression.

Recently, Stedinger and Tasker (1985, 1986) documented the value of an estimated generalized least squares (EGLS) regression procedure for regional regression of streamflow characteristics. The EGLS method can be applied in separate regional regressions to develop models for the skewness coefficient, standard deviation of annual minimums, and mean of annual minimums. After suitable transformation of variables, the EGLS regression model may be written as

$$\mathbf{Y} = \mathbf{X}\beta + \mathbf{e}$$

where **Y** is a $mx1$ vector of flow characteristics at m sites, **X** is an mxp matrix of (p-1) basin characteristics augmented by a column of 1's, β is a $px1$ vector of regression parameters to be estimated, and **e** is a $mx1$ vector of errors. The EGLS estimator of β is

$$\beta = (\mathbf{X}^T\Lambda^{-1}\mathbf{X})^{-1}\mathbf{X}^T\Lambda^{-1}\mathbf{Y}$$

where it is assumed that the errors have zero mean E[**e**]=**0**, and covariance E[$\mathbf{ee}^T$]=Λ.

The operational difficulty with this equation is that Λ is unknown and must be estimated from the data at hand. Stedinger and Tasker (1985) proposed that Λ be estimated as

$$\Lambda = u^2\mathbf{I} + \mathbf{V}$$

where u^2 is an estimate of the model error variance due to an imperfect model, **I** is the identity matrix, and **V** is an mxm matrix of sampling covariances that depend on record length, natural variability of the flow characteristic, cross correlation of sample response variables, and which flow characteristic is being estimated.

For regional skew coefficient the elements of **V** can be approximated by

$$(skew)\, v_{ij} = \begin{cases} 6n_i(n_i-1)\,(1+\frac{6}{n_i})^2\,\{(n_i-2)\,(n_i+1)\,(n_i+3)\}^{-1} \text{ (for i=j)} \\ \qquad or \\ 0 \text{ (for i} \neq \text{j)} \end{cases}$$

where n is the length of record at site i (Tasker and Stedinger, 1986). For the regional standard deviation regression, the elements of V can be approximated by

$$(\text{std dev})\, v_{ij} = \begin{cases} 0.5s_i^2\,(1+0.75G_i^2)\,n_i^{-1} \text{ (for i=j)} \\ \qquad or \\ 0.5m_{ij}r_{ij}s_is_j\,(n_in_j)^{-1}\,[r_{ij}+0.75G_iG_j] \text{ ((for i} \neq j) \end{cases}$$

where G_i and s_i are regional estimates of skewness coefficient and standard deviation, respectively, at site i, m_{ij} is the concurrent record length and r_{ij} is the cross correlation coefficient of annual minimums between sites i and j. The cross correlations, r_{ij}, are estimated as a function of distance between sites (Tasker and Stedinger, 1989).

For regional mean regression, the elements of **V** can be approximated by

$$(mean)\, v_{ij} = \begin{cases} s_i^2 n_i^{-1} & \text{(for i=j)} \\ & or \\ \dfrac{m_{ij} r_{ij} s_i s_j}{n_i n_j} & (\text{ for i} \neq j) \end{cases}$$

The regression coefficient, β, are found by an iterative search to find β that minimizes model error variance, u^2 (Stedinger and Tasker, 1985). For partial-record sites and autocorrelated data an effective record length, *n'*, is substituted for *n* in the above equations.

ESTIMATE OF T-YEAR LOW FLOW

To make an estimate of a T-year low flow characteristic, such as the 30-day, 10-year minimum, requires a conditional probability adjustment if the probability of nonzero minimum is less than 1.0. Suppose F(z) is the unconditional probability that flow Z does not exceed z. For the 10-year recurrence interval, F(z)=0.1. Let F*(z) denote the probability that Z does not exceed z, conditioned on nonzero values of Z. The relationship between F*(z) and F(z) is

$$F^*(z) = \frac{F(z) - 1 + \pi(x)}{\pi(x)}$$

The value of π(x) is estimated from the regional logistic regression described above. If the value of F*(z) is negative, then the estimated T-year flow is zero. Otherwise, the T-year low flow, Z can be estimated by

$$\log(Z_T) = M_z + K^* S_z,$$

in which M_z and S_z are regional estimates of the mean and standard deviation, respectively, of the logs of the nonzero flows as determined by the GLS regression methods described above, and K is the Pearson III percentage point (Harter, 1969) associated with a regional skew and exceedence probability F*(z).

SUMMARY

Two critical problems developing operational regional regression models for low flow characteristics are addressed. The first problem of how to treat regions in which many annual minimum flows are zero is addressed as a regional logistic regression that relates the probability of observing zero minimum flow at a site to physiographic characteristics of the watershed. The second problem, how to account for unequal variances in the observed response variable, is addressed as an estimated generalized-least-squares regression problem. The generalized- least squares approach accounts for sites with different lengths of record, autocorrelated annual minimums, cross correlation of low flow characteristics, and different types of gages (continuous-record or

partial-record). Combining these two approaches with conditional probability adjustments allows one to make regional estimates of T-year low flow characteristics in regions where minimum flows are often zero.

REFERENCES CITED

Cox, D. R., 1970, *The Analysis of Binary Data*: London, Chapman and Hall, 225 p.

Harter, H. L., 1969, A new table of percentage points of the Pearson type III distribution: *Technometrics*, v. 11, no. 1, p. 177-186.

Stedinger, J. R., and Tasker, G. D., 1985, Regional hydrologic analysis 1: *Water Resources Research*, v. 21, no. 9, p. 1421- 1432.

Stedinger, J. R., and Tasker, G. D., 1986, Regional hydrologic analysis 2: *Water Resources Research*, v. 22, no. 10, p. 1487- 1499.

Stedinger, J. R., and Thomas, W. O., 1985, Low-flow frequency estimation using base flow measurements: U. S. Geological Survey Open-File Report 85-95, 22 p.

Tasker, G. D., and Stedinger, J. R., 1986, Regional skew with weighted LS regression: *Journal Water Resources Planning and Management*, v. 112, no. 2, p. 225-237.

Tasker, G. D., and Stedinger, J. R., 1989, An operational GLS model for hydrologic regression: *Journal of Hydrology,* vol. 111, p. 361-375.

STOCHASTIC ANALYSIS OF DROUGHT PROPERTIES OF THE MAIN RIVERS IN CHINA

Yang Rongfu, Ding Jing, and Deng Yuren

Chengdu University of Science and Technology, Chengdu

ABSTRACT

Based on the observed data of annual runoff of the main rivers in China, the stochastic properties of negative run lengths (NRL) considered as indices indicating the quantitative degree of hydrologic drought have been examined. The final results obtained in this paper can be summarized as follows: 1. Pearson Type III distribution may be used to describe the statistical properties of NRL on the main rivers in China; 2. Mean NRL has a close relation to first-order autoregressive coefficient r(1) of annual runoff. 3. Maximum NRL within a period can be taken as a measure of drought severity. Its occurrence probability may be reasonably estimated by using a stochastic simulation approach.

INTRODUCTION

A drought is recognized as a natural phenomenon which is characterized by the fact that demanded water quantity surpasses natural supply. However, on its definitions and quantitative indices (Dracup et al, 1980) there is no general agreement. In order to examine drought properties of the main rivers in China, NRL is chosen as an index indicating the quantitative degree of a drought. In this paper NRL is defined by persistent duration of annual runoff related to negative deviation from mean annual runoff. The choice of NRL is due to its clear concept, convenient computation and ability in comparison.

Based on a large number of observed data on main rivers in China, the statistical properties of NRL such as distribution, mean value, and maximum value have been examined in this paper. The distribution type of NRL is explored and identified by using a station-year method. The expression of mean NRL related to r(1) is developed according to the observed data. Moreover, the statistical properties of maximum NRL is deduced by using stochastic simulation approach.

THE PROPERTIES OF DROUGHT VARIATIONS ON MAIN RIVERS IN CHINA

Probabilistic Distribution of NRL

177 samples of NRL were obtained according to the data observed at 177 stations. NRL is characterized by the persistence of annual flow and it will have a close relation to r(1). Our research (Deng et al, 1990a) has shown that r(1) represents a special property that is characteristic of a region. Three regions may be classified according to the magnitudes of r(1) in China: large value, small value, and negative value. Based on the three regions, 177 stations were separated into three groups. For each group (region) the statistical properties of NRL may be considered similar. Thus the samples of

NRL obtained from the stations situated at the same region can be pooled to construct a combined sample by virtue of which the probability of NRL is computed as

$$P (L \geq j) = w / n \qquad (1)$$

where L is NRL (a random variable), j is length (in years), w is the total number of NRL lengths which are greater than or equal to j, and n is the total number of NRL in the combined sample. By using the station-year method, three empirical probabilistic distributions of NRL corresponding to the three regions can be developed. Pearson Type III (P3) and log-normal (L-N) distributions were separately fitted to the empirical data. The parameters of the two distributions were estimated by probability weighted moment (PWM) method (Ding et al, 1989). Moreover, a large sample of NRL pooled from all stations concerned in this study was applied to develop a comprehensive probabilistic distribution for the whole country. All results associated with station-year method are listed in Table 1. Table 1 shows that:

Table 1. --Properties of probabilistic distribution of NRL in China

Regions	Total number of NRL	Distri-bution	Parameters			j related to P(L≥j) (in year)						
			EL	Cv	Cs	0.2%	0.5%	1%	2%	5%	10%	20%
		Empirical				20.0	13.0	11.0	10.0	7.0	6.0	5.0
Large	431	P3	2.89	0.89	2.4	17.5	14.8	12.7	10.8	8.1	6.1	4.2
r(1)		L-N	2.89	0.97	4.3	22.2	17.2	13.9	11.0	7.8	5.8	4.0
		Empirical				14.0	11.0	9.0	7.0	6.0	5.0	4.0
Small	501	P3	2.30	0.82	2.6	13.3	11.2	9.6	8.1	6.1	4.6	3.2
r(1)		L-N	2.30	0.90	4.9	17.2	13.1	10.5	8.3	5.9	4.3	3.1
		Empirical				11.0	9.0	7.0	6.0	4.0	4.0	3.0
Negative	520	P3	1.86	0.76	3.1	10.7	8.9	7.6	6.3	4.7	3.5	2.4
r(1)		L-N	1.86	0.89	8.1	14.8	10.8	8.4	6.4	4.4	3.2	2.3
		Empirical				14.0	11.0	10.8	8.0	6.0	5.0	4.0
Compre-	1452	P3	2.32	0.87	2.8	14.5	12.1	10.4	8.6	6.4	4.7	3.2
hensive		L-N	2.32	0.99	6.3	19.5	14.6	11.4	8.8	6.1	4.4	3.0

(1) P3 distribution demonstrates a better fitting to empirical distribution of NRL than L-N distribution does for all regions listed in Table 1.
(2) The distribution of NRL for the comprehensive region characterizes the general statistical properties of NRL of the main rivers in China.
(3) The statistical parameters of NRL vary regularly with r(1); that is, as r(1) decreases, the average (EL) and variation coefficient (Cv) of NRL decrease, while the skewness coefficient (Cs) increases.
(4) NRL in large-value region of r(1) is greater than that in the small-value and negative-value regions for a given probability P.

The variation properties of expectation of NRL (EL) and maximum NRL (L_N)

The analyses in 177 observed samples has indicated that EL has

significant relation to r(1) and Cs of annual runoff. By using stepwise regressive method the following equation may be obtained

$$EL = 1.85 + 2.25 * r(1) + 0.65 * Cs \quad (2)$$

The multiple regression coefficient is 0.69.

The relation between L_N and statistical parameters of 177 observed sequences shows that L_N not only has close relation to Cs and r(1) but also has relation to sample size N, which can be expressed as the following equation

$$L_N = 3.23 + 0.03 * N + 4.09 * r(1) + 1.48 * Cs \quad (3)$$

The multiple regression coefficient is 0.60. Eqs. (2) and (3) are reasonable and have the configurations in common with the results obtained by Yevjevich (Yevjevich, 1972).

PROBABILITY ESTIMATION OF SEVERE DROUGHT

The probability of severe drought could be defined as either $P(L_N \geq j)$ or $P(L \geq C)$, where C indicates a critical length. We try to indicate how to estimate $P(L_N \geq j)$ and $P(L \geq C)$ based on the observed data on two large rivers in China by using stochastic simulation method.

The stochastic modeling of annual runoff sequences

The analysis by Deng et al (1990a) has shown that annual runoff sequence at Harbin Station located on Shonghua River can be described by the following ARMA(2,2) model

$$X_t = 171.9 + 1.190 * X_{t-1} - 0.333 * X_{t-2} + \delta_t - 0.997 * \delta_{t-1} + 0.357 * \delta_{t-2} \quad (4)$$

where X_t stands for annual stream flow at time t, δ_t is independent P3 random variable with mean zero, variance 189,000 and skewness coefficient 0.610.

Table 2. --Diagnostic checks of stochastic models of annual runoff at Harbin and Shanxian Stations

Station	Sequence	Mean (m^3/s)	Cv	Cs	r_1	r_2	r_3	r_4	r_5	EL (yr)
Harbin	Observed	1205	0.40	0.53	0.36	0.31	0.31	0.30	0.16	3.2
	Simulated	1203	0.40	0.48	0.34	0.33	0.31	0.26	0.19	2.8
Sanxian	Observed	1323	0.28	0.56	0.16	0.13	0.37	-0.02	-0.01	2.6
	Simulated	1323	0.27	0.57	0.16	0.12	0.34	0.05	0.03	2.4

Note: Simulated size is 10,000 years; r_1, r_2, ..., r_5 are the 1st, 2nd, ..., 5th order autocorrelation coefficients respectively.

The analysis by Deng et al (1990a) has shown that the annual runoff sequence at Shanxian Station located on Yellow River is characterized by a

significant 3-year periodicity. And a combined model was adopted and expressed as

$$X_t = U_x + \sum_{j=1}^{H} A_j \sin(w_j + \theta_j) + Y_t \quad (5)$$

where X_t stands for annual stream flow at time t, U_x is mean, Y_t stands for a stationary autocorrelated sequence with mean zero, H is the number of harmonics, and A_j, w_j, and θ_j are the amplitude, angular frequency, and phase of the j-th harmonic respectively. In order to preserve the statistical properties of the observed sequence, a new method for estimating parameters of the combined model has been proposed, which is based on the following equations (Deng et al, 1990b)

$$\sigma_x^2 = 0.5 * \sum_{j=1}^{H} A_j^2 + \sigma_y^2 \quad (6)$$

$$Cs_x = Cs_y * (\sigma_y / \sigma_x)^3 \quad (7)$$

$$\rho_x(\tau) = (\rho_y(\tau) * \sigma_y^2 + 0.5 * \sum_{j=1}^{H} A_j^2 \cos w_j\tau)/\sigma_x^2 \quad (8)$$

where σ_x, Cs_x, and $\rho_x(\tau)$ are mean, skewness coefficient, and lag-τ autocorrelation coefficient of variable X, and σ_y, Cs_y, and $\rho_y(\tau)$ are mean, skewness coefficient, and lag-τ autocorrelation coefficient of variable Y respectively. The rest have been defined before.

Based on the observed data at Shanxian Station spectral analysis was used and the significant harmonic with 3-year period was identified; A, w, and θ were estimated by traditional procedure. Finally parameters of sequence Y were calculated from the estimates of sequence X by using Eqs. (6), (7), and (8). And the traditional procedure was applied to develop a stationary model for Y. The final combined model at Shanxian Station is expressed as

$$X_t = -71.6 * \cos(2/3*\pi*t) + 139.1 * \sin(2/3*\pi*t) + 1323 + Y_t \quad (9)$$

$$Y_t = 0.154 * Y_{t-1} + 0.107 * Y_{t-2} + 0.246 * Y_{t-3} + \delta_t \quad (10)$$

where δ_t is independent P3 random variable with mean zero, variance 104,500, and skewness 0.793.

These two models have been tested in various aspects. The results of diagnostic check are listed in Table 2. Table 2 shows that the stochastic models at Harbin and Shanxian Stations perform well in preserving their statistical properties. So these models can be used to simulate annual stream flow sequences and estimate the probabilities of the famous droughts that occurred at these two stations.

The estimation of the probability of maximum NRL in a certain period $P(L_N \geq j)$

1000 samples of annual stream flow at Harbin Station, each with size 100, were simulated by Eq. (4) and the maximum NRL of each sample was evaluated. Thus the number of occurrences of the event that $L_{100} \geq 13$ also was calculated. The following equation could approximately be used to estimate its probability

$$P(L_{100} \geq 13) = S / 1000 \quad (11)$$

where S is the number of occurrences of the event $L_{100} \geq 13$. Similarly, the

probability that the maximum NRL is greater than or equal to 13 years in size 200 $P(L_{200} \geq 13)$ can also be estimated. So can $P(L_{100} \geq 11)$ and $P(L_{200} \geq 11)$ for Shanxian Station. All the results are listed in Table 3.

Table 3. --Probabilities of severe droughts in 100- and 200-year records estimated by various methods at Shanxian and Harbin stations

Station		100-year record			200-year record		
		Sen's	Empirical	Simulated	Sen's	Empirical	Simulated
Shanxian	$P(L_N \geq 11)$	0.250	0.169	0.227	0.438	0.309	0.468
Harbin	$P(L_N \geq 13)$	0.263	0.196	0.245	0.457	0.353	0.498

Note: The results from simulation method were calculated based on 1000 samples of size 100 and 500 samples of size 200.

Under certain assumptions, Sen (1980) and Güven (1983) obtained the following equations.

$$P(L_N \geq j) = 1 - \exp[-N * q * (1 - h) * h^{j-2}] \quad (12)$$

$$P(L_N \geq j) = 1 - \exp(h_N - h^{j-1}) \quad (13)$$

where $q = P(X \leq X_0)$, X_0 is a given constant crossing level, $h = P(X_i \leq X_0 | X_{i-1} \leq X_0)$ is the conditional probability, and h_N is the average number of occurrences of drought years ($X_i \leq X_0$) during N years.

For convenience sake, Eqs. (12) and (13) are referred to as Sen's method and empirical method respectively. Based on the observed data at Harbin and Shanxian stations, the parameters of Eqs. (12) and (13) were estimated and the probability $P(j \geq 13)$ (Harbin) and $P(j \geq 11)$ (Shanxian) were calculated. The results are also listed in Table 3.

Sen's method and empirical method may fail to take into account special characteristic properties of the annual sequence concerned because they were deduced based only on general considerations. In contrast, the stochastic simulation method does well in reproducing the important characteristic properties of the annual runoff sequence. Therefore, the estimator of $P(L_N \geq j)$ by using the simulation method may be more reliable than that by using Sen's method and empirical method.

The estimation of probability of critical NRL $P(L \geq C)$

A large number of simulated sequences were produced by using the developed stochastic models at Harbin and Shanxian stations respectively. The probability $P(L \geq C)$ was estimated by analyzing the lengths of all simulated negative runs and using Eq. (1) and listed in Table 4.

Table 4. --Simulated probability distribution of negative run length $P(L \geq C)$ at Harbin and Shanxian stations

C (in years)	3	4	5	6	7	8	9	10	11	12	13	14	15	16	17	18	19
Shanxian (%)	33	23	16	12	9	7	5	4	3	2.5	2.0	1.4	1.1	0.8	0.6	0.5	0.4
Harbin (%)	26	18	13	8	6	4	3	2	1.5	1.0	0.7	0.5	0.4	0.3	0.2	0.1	0.07

The estimation of return period of certain NRL $T(L \geq j)$ and the relation between $P(L_N \geq j)$ and $P(L \geq j)$

It is clear that in Eq. (1) the probability $P(L \geq j)$ is conditional on the event that NRL occurs; but NRL does not occur in every year. So the return period $T(L \geq j)$ is not equal to $1/P(L \geq j)$. In fact, if the time span m (in year) is known in which one NRL occurs on average, the return period $T(L \geq j)$ could be calculated from $P(L \geq j)$ by the following equation

$$T(L \geq j) = m/(P(L \geq j) \tag{14}$$

Generally, m can be estimated from historic data or a long simulated sequence as follows

$$m = M/n \tag{15}$$

where M is the length of a sequence (in years) and n is the number of NRL in the sequence.

From the simulated sequence at Harbin Station m=5.2 was obtained and Table 4 shows $p(L \geq 13) = 2\%$, therefore the return period $T(L \geq 13) = 260$ years. Similarly, from the simulated sequence at Shanxian Station m=4.35 was computed and Table 4 shows $P(L \geq 11) = 1.5\%$, so $T(L \geq 11) = 290$ years. Based on historical documents, the return period of the event of $L \geq 11$ occurring at Shanxian Station may be 200 years, that is, $T(L \geq 11) = 200$ years (Shi, 1989).

If variable NRL is independent, the following equation could be approximately deduced

$$P(L_N \geq j) = 1 - [1 - P(L \geq j)]^{\frac{N}{m}} \tag{16}$$

REFERENCES

Deng, Y., Ding J., & Yang R., 1990a, Preliminary Research on the Regular Parttens of Annual Runoff Sequences on Main Rivers in China, Water Science Advances, Vol. 1, No. 1, in Chinese.

Deng, Y., Ding J., & Yang R., 1990b, Preliminary Research on the Stochastic Models Suitable for Annual Runoff Sequences on Main Rivers in China, Geographic Science, accepted, in Chinese.

Ding, J., Song D., & Yang R., 1989, Further Research on Application on Probability Weighted Moments in Estimating Parameters of Pearson Type Three Distribution, Journal of Hydrology, Vol. 110.

Dracup, J. A., et al, 1980, On the Definition of Droughts, Water Resources Research, Vol. 16, No. 2.

Güven, O., 1983, Simplified Semiempirical Approach to Probabilities of Extreme Hydrologic Droughts, Water Resources Research, Vol. 19, No. 2.

Sen, Z., 1976, Wet and Dry Periods of Annual Flow Series, Journal of Hydraulics Div. ASCE, 102(HY10).

Sen, Z., 1980, Statistical Analysis of Hydrologic Critical Droughts, Journal of Hydraulics Div., ASCE, 106(HY10).

Shi, F., et al, 1989, Research Report about the Extreme Drought of Yellow River During 1922 and 1932, Yellow River Water Conservancy Institute, in Chinese.

Yevjevich, V., 1972, Stochastic Processes in Hydrology, Water Resources Publications, U.S.A.

STREAMFLOW DROUGHT STATISTICS BY STOCHASTIC SIMULATION

Jose D. Salas and Magdy W. Abdelmohsen

Hydrology and Water Resources Program
Colorado State University
Fort Collins, Colorado 80523

ABSTRACT

Determining drought statistics by stochastic methods usually requires modeling and simulation of the hydrologic processes under consideration. This paper reports research currently being carried out for modeling and simulation of seasonal streamflow processes which can preserve seasonal as well as longer term (annual) statistical properties without the usual disaggregation approach. The model is called the multiplicative periodic ARMA (XPARMA) process. Applications of the new model for simulating monthly flows of the Nile River and comparisons with well known alternative models have been made to reproduce not only basic statistics such as means and covariances, but storage and drought statistics as well. Preliminary results indicate that the new model reproduces long term statistics better than the more commonly used models.

INTRODUCTION

One of the desirable properties of stochastic models of seasonal flows is the ability for preservation of both seasonal and annual statistics. However, such dual preservation of statistics is difficult to achieve. Two basic approaches have been followed in the literature for modeling and generation of seasonal flows. The first has been to model and generate the seasonal flows directly; while the second has been to model and generate annual flows first, then to obtain the seasonal flows by disaggregation.

A typical example of the first approach is the so-called PAR(1) model or periodic lag-1 autoregressive process (Thomas and Fiering, 1962). Higher order processes such as PAR(2) or PAR(3) processes have also been suggested (Yevjevich, 1972). Likewise, low order periodic autoregressive moving average models such as the PARMA(1,1) models have been proposed for the same purpose (Tao and Delleur, 1976; Hirsch, 1979; Salas et al., 1980; Salas et al., 1982). However, despite the fact that the PARMA(1,1) model has more structure than the low-order PAR model, results obtained by Obeysekera and Salas (1986) showed that these models generally are not able to capture the desired historical annual flow properties when annual flows are obtained from seasonal flows.

The second approach for generating seasonal flows is the so-called disaggregation approach (Valencia and Schaake, 1973) in which annual flows are modeled and generated first to make sure that the annual statistics are reproduced, and then the generated annual flows are disaggregated into seasonal flows in such a way that the seasonal statistics are also reproduced. This approach was suggested in order to get around the problem alluded to in the first approach as noted in the previous paragraph. The disaggregation approach has become quite popular in operational hydrology and a number of variations and improvements have been suggested in literature (see, for instance, Lane, 1979; Salas et al., 1980; Loucks et al., 1981; Stedinger and Vogel, 1984; Stedinger et al., 1985; Grygier and Stedinger, 1988; Santos and Salas, 1991). While the advantages of the disaggregation approach are quite clear from the practical standpoint, one may not be satisfied from the theoretical standpoint since it is only logical that if a model applied directly to the seasonal flows fails to reproduce the statistics at the aggregated level (annual), it must be because the model was not right in the first place. This paper presents a model which, when applied directly to the seasonal flows, is in a better position to reproduce the annual statistics than the usual PAR or PARMA models.

MODEL DESCRIPTION

In order to define the new model we will first describe the usual ARMA and PARMA models and some needed notation. The stationary ARMA(p,q) process (Box and Jenkins, 1976; Brockwell and Davis, 1987) may be expressed as

$$\phi(B)\ y_t = \theta(B)\ \varepsilon_t \tag{1}$$

in which y_t = original stationary process with mean zero, ε_t = normal uncorrelated noise with mean zero and variance $\sigma^2(\varepsilon)$, and $\phi(B)$ and $\theta(B)$ are operators defined as

$$\phi(B) = 1 - (\phi_1 B + \phi_2 B^2 + \ldots + \phi_p B^p) \tag{2a}$$

$$\theta(B) = 1 - (\theta_1 B + \theta_2 B^2 + \ldots + \theta_q B^q) \tag{2b}$$

with $B^j z_t = z_{t-j}$.

Likewise, the PARMA(p,q) process may be expressed as (Salas et al., 1980)

$$\phi_\tau(B)\ \xi_{\nu,\tau} = \theta_\tau(B)\ \varepsilon_{\nu,\tau} \tag{3}$$

where $\xi_{\nu,\tau}$ = periodic correlated process with mean zero, $\varepsilon_{\nu,\tau}$ = uncorrelated normal process with mean zero and variance $\sigma^2_\tau(\varepsilon)$, ν is the year and τ is the season, $\phi_\tau(B)$ and $\theta_\tau(B)$ are operators defined as

$$\phi_\tau(B) = 1 - \left(\phi_{1,\tau} B + \phi_{2,\tau} B^2 + \ldots + \phi_{p,\tau} B^p\right) \tag{4a}$$

$$\theta_\tau(B) = 1 - \left(\theta_{1,\tau} B + \theta_{2,\tau} B^2 + \ldots + \theta_{q,\tau} B^q\right) \tag{4b}$$

with $B^j z_{\nu,\tau} = z_{\nu,\tau-j}$ for $j \leq \tau$, otherwise $B^j z_{\nu,\tau} = z_{\nu-1,\omega+\tau-j}$.

Now, Box and Jenkins (1976) suggested a multiplicative model which could be useful for seasonal series. Let us assume that the underlying seasonal series (after removing the seasonal mean) is denoted by y_t. We will fit an ARMA(P,Q)$_\omega$ model to this series as

$$\Phi(B^\omega)\ y_t = \Theta(B^\omega)\ \xi_t \tag{5}$$

in which ξ_t = correlated normal process with mean zero and variance $\sigma^2(\xi)$, and $\Phi(B^\omega)$ and $\Theta(B^\omega)$ are operators defined as

$$\Phi(B^\omega) = 1 - \left(\Phi_1\ B^\omega + \Phi_2\ B^{2\omega} + \ldots + \Phi_P\ B^{P\omega}\right) \tag{6a}$$

$$\Theta(B^\omega) = 1 - \left(\Theta_1\ B^\omega + \Theta_2\ B^{2\omega} + \ldots + \Theta_Q\ B^{Q\omega}\right) \tag{6b}$$

For instance, suppose P = 2 and Q = 0, then model (5) can be rewritten as

$$y_t = \Phi_1\ y_{t-\omega} + \Phi_2\ y_{t-2\omega} + \xi_t$$

In other words, the model is like an ARMA(2,0) process, but defined over blocks of ω seasons (years). Recall that t is time in seasons. Let us further assume that the residual ξ_t of Eq. (5) can be modeled by an ARMA(p,q) process as

$$\phi(B)\ \xi_t = \theta(B)\ \varepsilon_t \tag{7}$$

Finally, combining Eqs. (5) and (7) we have

$$\Phi(B^\omega)\ \phi(B)\ y_t = \Theta(B^\omega)\ \theta(B)\ \varepsilon_t \tag{8}$$

which is the stationary multiplicative ARMA(p,q)x(P,Q)$_\omega$ process.

The drawback with the foregoing multiplicative model for modeling seasonal processes is that there is no provision for reproducing seasonal or periodic variance-covariance structure. Therefore, the new model to be defined here must incorporate such periodic features. Thus, the multiplicative PARMA (XPARMA) process may be expressed

$$\Phi_\tau(B^\omega)\ \phi_\tau(B)\ y_{\nu,\tau} = \Theta_\tau(B^\omega)\ \theta_\tau(B)\ \varepsilon_{\nu,\tau} \tag{9}$$

for which $y_{\nu,\tau}$ = periodic series after removing the seasonal mean, $\varepsilon_{\nu,\tau}$ = normal uncorrelated series with mean zero and variance $\sigma^2_\tau(\varepsilon)$, and $\Phi_\tau(B^\omega)$ and $\Theta_\tau(B^\omega)$ are defined as

$$\Phi_\tau(B^\omega) = 1 - \left(\Phi_{1,\tau}\ B^\omega + \Phi_{2,\tau}\ B^{2\omega} + \ldots + \Phi_{P,\tau}\ B^{P\omega}\right) \tag{10a}$$

$$\Theta_\tau(B^\omega) = 1 - \left(\Theta_{1,\tau}\ B^\omega + \Theta_{2,\tau}\ B^{2\omega} + \ldots + \Theta_{Q,\tau}\ B^{Q\omega}\right) \tag{10b}$$

For instance, the multiplicative PARMA(1,1)x(1,1)$_\omega$ process is written as

$$y_{\nu,\tau} = \Phi_{1,\tau}\, y_{\nu-1,\tau} + \phi_{1,\tau}\, y_{\nu,\tau-1} - \Phi_{1,\tau}\, \phi_{1,\tau}\, y_{\nu-1,\tau-1} + \varepsilon_{\nu,\tau} - \Theta_{1,\tau}\, \varepsilon_{\nu-1,\tau} - \theta_{1,\tau}\, \varepsilon_{\nu,\tau-1} + \Theta_{1,\tau}\, \theta_{1,\tau}\, \varepsilon_{\nu-1,\tau-1} \tag{11}$$

MODELING THE NILE RIVER FLOWS

Monthly flows of the Nile River at Aswan for the period 1871-1989 were used for testing the proposed model. The original data showed significant skewness so the logarithmic transformation was used and the subsequent modeling was done in the log-transformed domain. The PAR(1), PARMA(1,1) and XPARMA(1,1)x(1,1)$_{12}$ models were fitted to the log-transformed data and the model parameters were obtained by least squares.

For each model, one hundred samples of the same length as the historical record were generated. The seasonal and annual statistics were then computed from each sample, from which generated mean and standard deviations of each statistic were obtained. They were compared with similar statistics obtained from the historical record. The statistics for comparison included monthly statistics such as mean, standard deviation, skewness coefficient, and lag-1 and lag-2 month-to-month correlations, and annual statistics such as mean, standard deviation, skewness coefficient, correlogram, adjusted range, Hurst K coefficient and length of longest drought. In addition, year-to-year annual correlograms computed for each month were determined and compared. It would be too lengthy to show all results obtained, thus only a few of the statistics will be shown. In general, all models performed quite well in reproducing monthly statistics. As usual, monthly skewness values are not well reproduced by all models because the simple log-transformation does not completely remove skewness. But because the concern was with variance-covariance structure and other long term statistics, the skewness was not considered a major problem.

Nile River flows show significant year-to-year dependence structure for monthly flows as well as significant dependence structure of annual flows. The first can be seen, for instance, in the correlogram of figure 1 for the month of May and the annual correlogram can be seen in figure 2. Figure 1 also shows the correlogram derived from the generated flows based on the PAR(1) and XPARMA(1,1)x(1,1)$_{12}$ models. It is clearly seen that the former model cannot reproduce the type of dependence structure of May flows while the latter model does a good job of this. Generally, this is the case for the correlograms for all months of the year. Also, figure 2 shows that the correlogram of annual flows, derived from the generated PAR(1) flows, is quite different from the historical ones, while the annual correlogram derived from the generated XPARMA(1,1)x(1,1)$_{12}$ flows resembles quite well the correlogram of the historical record. In addition, correlograms obtained from the PARMA(1,1) model, while better than those of the PAR(1) model, still were significantly different than the historical correlograms.

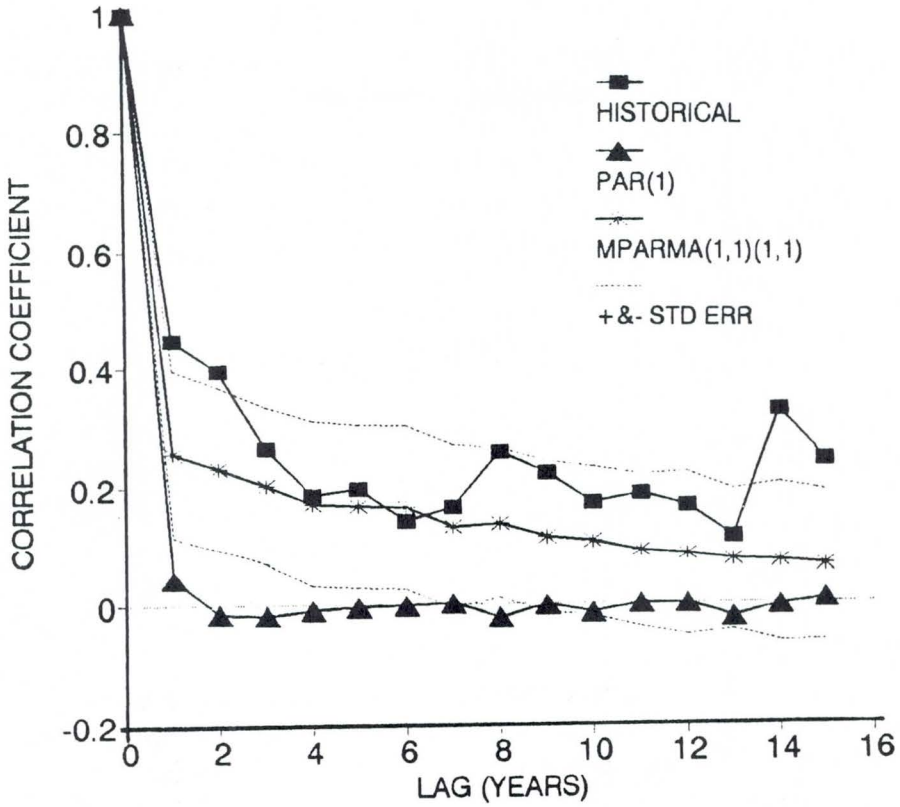

Figure 1. Year-to-year correlogram for Nile River May flows (1871-1989).

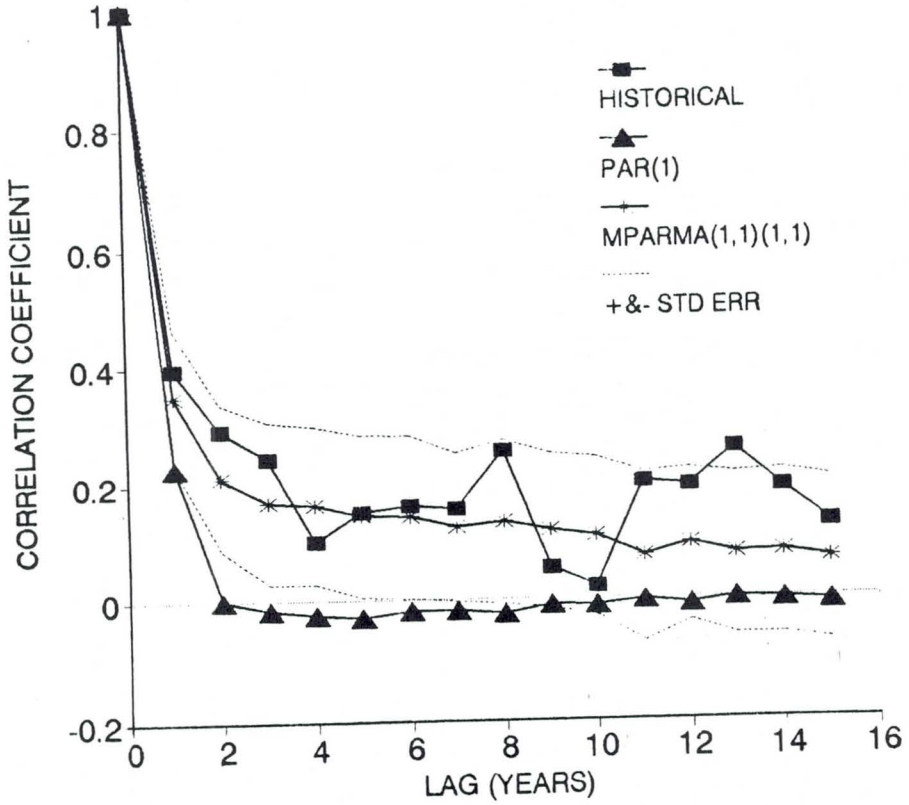

Figure 2. Correlogram for Nile River annual flows (1871-1989).

Normally, one would like to see comparisons made based on other statistics as well. Table 1 summarizes the annual statistics obtained from the historical record and those derived from the generated PAR(1), PARMA(1,1) and XPARMA(1,1)x$(1,1)_{12}$ monthly flows. Once again, the table shows that the adjusted range, Hurst K coefficient and longest drought statistics derived based on the latter model are quire comparable to the historical ones while this is not the case for the other two models.

CONCLUSIONS

Results obtained up to now are quite encouraging. They indicate that it is possible to find stochastic models of monthly flows which can preserve both monthly and annual statistics without resorting to disaggregation. The multiplicative PARMA model presented herein appears to have such attributes.

Table 1 Comparison of generated and historical annual statistics for Nile River flows at Aswan.

Models		Mean $10^9 m^3$	Standard Deviation $10^9 m^3$	Skewness Coefficient	Longest Drought (Years)	Adjusted Range	Hurst K
PAR(1)							
	MEAN	88.470	15.787	0.539	7.660	14.629	0.651
	STD	1.946	1.267	0.264	1.955	3.085	0.052
PARMA(1,1)							
	MEAN	88.473	15.162	0.536	7.680	13.824	0.637
	STD	1.713	1.209	0.253	1.836	3.040	0.055
XPARMA(1,1)$(1,1)_{12}$							
	MEAN	88.891	15.749	0.509	10.640	24.995	0.779
	STD	10.790	2.608	0.228	3.899	6.460	0.067
Historical		88.278	14.600	0.246	11.000	28.562	0.820

Acknowledgement. The research leading to this paper was partly funded by an agreement with the U.S. Bureau of Reclamation on Simulation and Optimization of Operation of the High Aswan Dam and by the project Prediction of Droughts in Agricultural Regions of Colorado, Agricultural Experiment Station, Grant No. 645.

REFERENCES CITED

Box, G.E.P. and Jenkins, G., 1976, Time Series Analysis, Forecasting and Control: Holden-Day, San Francisco, 553 p.

Brockwell, P. and Davis, R., 1987. Time Series: Theory and Methods: Springer-Verlag, New York, 519 p.

Grygier, J.C., and Stedinger, J.R., 1988. Condensed disaggregation procedures and conservation corrections for stochastic hydrology: Water Resources Research, 24(10), p. 1574-1584.

Hirsch, R.M., 1979. Synthetic hydrology and water supply reliability: Water Resources Research 15(6), p. 1603-1615.

Lane, W.L., 1979. Applied stochastic techniques (Last Computer Package) user manual, U.S. Bureau of Reclamation, Denver, Colorado.

Loucks, D.P., Stedinger, J.R. and Haith, D.A., 1981. Water Resource Systems Planning and Analysis: Prentice Hall, Inc., New Jersey, 559 p.

Obeysekera, J.T.B. and Salas, J.D., 1986. Modeling of aggregated hydrologic time series: J. Hydrol., 86, p. 197-219.

Salas, J.D., Boes, D.C. and Smith, R.A., 1982. Estimation of ARMA models with seasonal parameters: Water Resources Research, 18(4), p. 1006-1010.

Salas, J.D., Delleur, J.W., Yevjevich, V. and Lane, W., 1980. Applied Modeling of Hydrologic Time Series: Water Resources Publications, Littleton, Colorado, 484 p.

Santos, E. and Salas, J.D., 1991. Stepwise disaggregation scheme for synthetic hydrology: ASCE J. of Hydraulic Engineering. (Accepted for publication).

Stedinger, J.R., and Vogel, M.R., 1984. Disaggregation procedures for generating serially correlated flow vectors: Water Resources Research, 20(1), p. 47-56

Stedinger, J.R., Pei, D. and Cohn, T., 1985. A condensed disaggregation model for incorporating parameter uncertainty into monthly reservoir simulations: Water Resources Research, 21(5), p. 665-675

Tao, P.C. and Delleur, J.W., 1976. Seasonal and nonseasonal ARMA models in hydrology, ASCE J. Hydraulics Div., 102(HY10), p. 1541-1559.

Thomas, H.A. and Fiering, M.B., 1962. Mathematical synthesis of streamflow sequences for the analysis of river basins by simulation, in Design of Water Resources Systems, edited by A. Mass et al.: Harvard University Press, Cambridge, Mass.

Valencia, D. and Schaake, J.C., 1973. Disaggregation processes in stochastic hydrology: Water Resources Research, 9(3), p. 580-585.

Yevjevich, V., 1972. Stochastic Processes in Hydrology: Water Resources Publications, Littleton, Colorado, 276 p.

SYNTHETIC STREAMFLOWS FOR GLOBAL CLIMATE CHANGE

William L. Lane

U.S. Bureau of Reclamation, Denver, Colorado

ABSTRACT

Monthly streamflows for five locations in Colorado are statistically analyzed and parameters estimated for the stochastic generation of synthetic data. The stochastically generated data are being used in a study of the influence of global climate change on the operations of the Colorado-Big Thompson Project. The statistical time series analysis of the observed data is covered in detail. The analysis was carried out using the Bureau of Reclamation's computer package for stochastic hydrology. This study represents the first use and testing of a newly written personal computer version of that particular software. The use of the data for operations studies is described along with the techniques for the adjustment of the data to account for climatic change. The purpose of the overall study is to examine the effects of climate change on project water supply, water shortages, and droughts.

INTRODUCTION

This paper documents the stochastic hydrology aspects of a global climate change study that is being performed under the Bureau of Reclamation's Global Climate Change Response Program (GCCRP). Under the GCCRP, several other studies are also underway (Bureau of Reclamation, 1990). This particular study deals with the Bureau of Reclamation Colorado-Big Thompson Project and is oriented towards the changes in timing and quantity of the water supply due to climate change and how those changes will affect the project operation. The Colorado-Big Thompson project is one of the largest and most complex natural resource developments operated and managed by the Bureau of Reclamation. The development consists of over 100 structures integrated into a transmountain water diversion system which provides water supplies to parts of northeastern Colorado. The project involves over 2500 square miles in Colorado. The structures store, regulate and divert water from the Colorado River on the western slope of the Continental Divide to the eastern slope of the Rocky Mountains. The project provides supplemental water for irrigation of about 720,000 acres of land in addition to water for municipal and industrial use, hydroelectric power, and water-oriented recreation (Bureau of Reclamation, 1981). Project operations include many advanced features such as pump back storage for maximizing power benefits, remote sensing and transbasin diversions. The project water supply results primarily from snowmelt runoff from high altitude mountainous regions. The supply is sensitive to snowfall, snowpack, snowmelt, and related climatic factors. Climate change would have an immediate effect on these factors with a resulting impact on the operation

and efficiency of the Colorado-Big Thompson Project and perhaps a dramatic effect on the project water supply.

Although there appears to still be a great debate as to the magnitude of impending climate change, there now seems to be some consensus that global climate change is taking place. The cause of this change is assumed to be due to changes in the gasses in the atmosphere, primarily a buildup of carbon dioxide. Much of the change appears to be directly linked to the activities of man (Houghton and Woodwell, 1989). Schneider (1989) provides a good introduction to global climate change. Berner (1990) gives insight into the carbon cycle on earth. Several scientists, Kite (1989) for example, have looked for evidence of trends in various time series due to climatic changes, but generally they have been without conclusive results. Jones and Wigley (1990) review some of the problems and concerns involved in the measurements of the primary data that is being used today as supportive evidence for the climatic change theory. Many scientists and engineers has taken the position that it is best to be prepared well in advance for the entire range of future changes to the climate (Trefil, 1990). White (1990), while pointing out that the existence and magnitude of climatic change is debatable, states that society should act to "blunt the impact in the face of this uncertainty." It is in this vein that this study is performed.

One aspect of the Colorado -Big Thompson study is to perform operation studies for the project using scenarios of potential future water supplies. The future water supply scenarios are generated using stochastic techniques and time series models. The time series modeling is the specific feature addressed by this paper. Stochastically generated sequences of water supply will be used to study the operation of the project under both current climatic conditions and conditions reflecting global climate change. Each sequence of generated data is designed to behave in the same statistical manner. Although each sequence is different, the statistical behavior of the sequences is such that they all appear to come from the same parent process and differ only by the sampling variation that would be expected. All of the sequences can be treated as equally likely future scenarios. The various stochastic sequences will insure that operational policies are tested under a variety of possible future conditions, not simply the one historical sequence, an average condition, or one or two "worst case" scenarios. This paper addresses the problem of the time series analysis of the observed data under the current climatic conditions.

The time series analysis of the data is performed using standard approaches that have successfully been used for the last decade (Salas et al., 1980). The computer software used for this study was developed over ten years ago and the basic approach and techniques have remained the same (Lane, 1979). This study provided an opportunity to apply a personal computer version of that software (Lane and Frevert, 1989). The approach uses both spatial and temporal disaggregation modeling with linear autoregressive models used for the annual key series. All of the models are linear models and the data is transformed to normal during the analysis process. An inverse transform is performed during the data generation phase to insure preservation of the original distribution. The generated data is designed to preserve, in an expected value sense, the relevant statistical properties of the recorded data. These properties include annual and seasonal means, variances, serial correlations, and lagged and concurrent cross correlations. This preservation

is accomplished through the use of mathematical models that randomly generate sequences with the desired properties. The differences between traces or sequences are due only to what is often termed "sampling variations." These sampling variations are really the natural variation that is to be expected in the actual future flows. It is this preservation of the "natural variation" that makes stochastic hydrology techniques valuable. This process makes available a virtually unlimited number of different possible future traces. Further, each trace may be treated as "equally likely" which means that the frequency or probability of any aspect of an operations study may be easily estimated.

The water supply for the Colorado-Big Thompson Project is represented in this study at five locations or stations: inflow to Willow Creek Reservoir, inflow to Granby Reservoir, inflow to Green Mountain Reservoir, Big Thompson River at Estes Park, and Big Thompson River at the Canyon Mouth. The flows at the Big Thompson River at the Canyon Mouth are the increment of Big Thompson flow accumulated between Estes Park and the canyon mouth. The total of the five stations is modeled as a sixth station. All of the basic recorded data have been adjusted to natural values, that is undepleted, unregulated values, by adding, to the recorded data, the diversions and adjusting for storage effects. All of the data came from the Colorado-Big Thompson Project Office data base. The stations have in common 42 years of concurrent flows, 1948 to 1989.

STATISTICAL CHARACTERISTICS OF THE OBSERVED DATA

The data sets were analyzed in several different ways to determine the appropriate form of modeling. Analysis was performed for all of the five stations plus the sixth station created to represent the sum of the original five. The various analyses were used to assure that no errors or abnormalities existed in the data. Data for the Granby station was also analyzed for the entire period of record which was from 1928-1989. This was done to check to insure that the concurrent period, 1948-1989, was indeed a representative sample. The coefficients of variation and coefficients of skew were found to have negligible differences between the two periods, while the means differed by less than two percent.

Of the five stations involved in this study, the highest flow is the inflow to Green Mountain. Although this station is important to the operation of the Colorado-Big Thompson Project, its flows do not contribute as directly to the available water supply as do the other four stations. The next highest flows are the inflow to Granby. This station could be considered the primary station of importance to this study. The Big Thompson River at Estes Park, located in the upper portion of the basin, is at a very high elevation and has a very well defined snowmelt behavior. This station has very nearly normally distributed annual flow with only an insignificant amount of skew, as would be expected. Its coefficient of skew is only one tenth. The lower part of the Big Thompson on the other hand shows annual flows that are much nearer to being log normally distributed. The other four stations have annual skews which are midway between that of the normal and log normal distributions. The coefficients of variation for all of the stations were consistently near 0.3 as is expected for streams in this region. The only exception is the flow for the Big Thompson at the Canyon Mouth. Since flows for this station are

calculated as incremental flows, the higher coefficient of variation was not unexpected.

Most of the flow, about 70%, is observed in three months of the year: typically, either April, May and June, or May, June and July. The pattern of flow is a snowmelt dominated pattern with very little flow outside of the snowmelt season. The highest five consecutive months in each year start with either March or April and end with either July or August and typically contain about 90-95% of the annual flow. Both the seasonal means and the seasonal standard deviations reflect the same pattern throughout the year with a near constant coefficient of variation of about 0.3. The runoff pattern is the same as might be expected in basins with very little natural storage and annual carryover. This is also supported by the relatively small annual lag one correlations and relatively sharp recessions of the snowmelt hydrographs. The low flow months are often very near zero flow.

All of the annual lag zero cross correlations are extremely high with values usually 0.85 or larger. These high values are not particularly unusual for snowmelt dominated streams within a close geographic region. The cross correlations, as expected, are lower for the incremental flow station, the Big Thompson River at the Canyon Mouth. There also is a minor but obvious change in the statistical behavior between data from different sides of the continental divide. Slightly stronger correlations exist between stations which are on the same side of the divide. The annual lag one serial and cross correlations varied from near zero to 0.2. Annual lag two correlations are near zero.

Seasonal lag zero cross correlations are very strong as a result of the dominant snowmelt. The seasonal lag one serial and cross correlations also show a strong relationship for the high flow months due to snowmelt and an even slightly stronger relationship for the low flow months (especially October through February) which seem to be largely dictated by the recession of the snowmelt hydrograph. Autocorrelations for the monthly data show significant values for several lags, generally back as far as the previous peak month. Again the strong snowmelt behavior with little or no significant runoff due to rainfall seems to adequately describe this behavior.

In order to render the annual data into normally distributed data, transformations were utilized. For the annual data, a square root transformation was adequate except for the data for the Big Thompson at Estes which was already normally distributed and did not require any transformation.

Seasonal distributions tend to be less like the normal distribution than the annual distribution. The monthly distributions are almost always highly positively skewed. Generally the log normal distribution is indicated in all but the highest flow months. A logarithmic transformation was required in most months to reduce the data to a nearly normal distribution. A three parameter log normal distribution was used for many of the months in order to reasonably fit both the upper and lower tails of the distributions. All correlations, annual and seasonal, were checked both before and after transformations and found to be linear. Since the time series models will not preserve nonlinear correlations, it is important that the transformed data being modeled have linear relationships. In addition, double mass plots were used to check for changes in the relationships with time.

MODELLING AND GENERATION OF FLOWS

The transformed values for the total flow at the five stations, that is, the transformed data for the sixth station, was analyzed and found to be reasonably well represented by an annual autoregressive lag one model as also were each of the individual stations. In no case was a lag two or lag three annual model justified. Likewise, moving average models were not found to be appropriate for the annual correlation structure observed for these stations.

A linear autoregressive lag one, AR(1), model was chosen to generate flows for the sixth station, the total annual flows. A spatial disaggregation model was used to reduce the total into annual flows at the five actual stations. The model preserves the lag zero and lag one correlations among the stations. The data treated by the model is assumed to be normally distributed. Therefore, the observed data was transformed by an appropriate transformation before analysis. The AR(1) and disaggregation models produce data that is normally distributed. The inverse transform is applied to this normally distributed data to obtain generated flows. The parameters of the model are obtained using method of moments estimation. The modeling techniques used are covered in Salas et al. (1980) and the computer software used is documented in Lane and Frevert (1989).

A trace of 1,000 years was used to examine generated means and standard deviations; the observed discrepancies were well within the expected sampling variations. For the annual means, the discrepancies were all less than one half percent. In addition, the appropriate correlations and distribution attributes were also examined and found to be adequately preserved. A 10,000 year trace was also generated and found to preserve the intended statistics.

The monthly flows for all five stations were generated using a condensed seasonal disaggregation model (Salas et al., 1980). This model reduces the annual flows at the stations to monthly values, while preserving lag one and lag zero cross correlations among the monthly flows and also correlations with the current annual flows. Again, transformations are used to preserve the distribution properties and all the parameters are estimated by method of moments techniques.

A comparison of seasonal means and standard deviations was made between generated data and corresponding observed values. The same trace was used as for the annual statistics comparison. Again, the deviations are well within expected sampling variations. As was done with the annual flows, the appropriate monthly correlations and distribution attributes were also examined and found to be adequately preserved. The long term generated annual means differed by less than one half percent while the monthly means were generally within one percent of the observed values.

In this study of climate change, the basic climate and runoff changes will be treated outside the operations model. Climate change will be accommodated through the use of altered flows input to the model. There are two basic approaches for providing modified data that reflects climatic change. One approach is to adjust the basic hydrology data to reflect the climate change. The second approach is to adjust the statistics for the stochastic generation.

Both of these will be considered as the study progresses.

CONCLUSIONS

The use of stochastic data for studying the impacts of global climate change on the operation of the Colorado-Big Thompson Project is a viable approach. This approach adequately preserves all of the important time series features that were noted in the observed records while allowing for the desired sampling variability in generated traces. This allows the project operations to be examined without the bias that would be inherent in using the observed data alone.

The stochastic approach also allows for more options and versatility in the study of the effects of global climate change. Assumed or potential changes in the climate may be relatively easily accounted for through the manipulation of the time series parameters. Changes may also be treated by adjusting the observed data and reanalyzing the time series properties.

REFERENCES CITED

Berner, R. A., and Lasaga, A. C., 1990, Modeling the Geochemical Carbon Cycle: Scientific American, vol. 260, no. 3, p. 74-81.

Bureau of Reclamation, 1990, Global Climate Change Response Program, List of projects for fiscal year 1990: Bureau of Reclamation, Denver, Colorado.

Bureau of Reclamation, 1981, Project Data, A Water Resources Technical Publication, United States Department of Interior: United States Government Printing Office, Denver, Colorado.

Houghton, R. A., and Woodwell, G. M., 1989, Global Climatic Change: Scientific American, vol. 260, no. 4, p. 36-44.

Jones, P. D., and Wigley, T. M. L., 1990, Global Warming Trends: Scientific American, vol. 263, no. 2, p. 84-91.

Kite, G., 1989, Use of Time Series Analysis to Detect Climatic Change: Journal of Hydrology, 111, p. 259-279.

Lane, W. L., 1979, Applied Stochastic Techniques, User Manual: Bureau of Reclamation, Denver, Colorado.

Lane, W. L. and Frevert, D. K., 1989, Applied Stochastic Techniques (Personal Computer Version), User Manual: Bureau of Reclamation, Denver, Colorado.

Salas, J. D., Delleur, J. W., Yevjevich, V., and Lane, W. L., 1980, Applied Modeling of Hydrologic Time Series: Water Resources Publications, Littleton, Colorado, 484 p.

Schneider, S. H., 1989, The Changing Climate: Scientific American, vol. 261, no. 3, p. 70-79.

Trefil, J., 1990, Modeling Earth's Future Climate Requires both Science and Guesswork: Smithsonian, vol. 21, no. 9, p. 28-37.

White, R. M., 1990. The Great Climate Debate: Scientific American, vol. 263, no. 1, p. 36-43.

PRELIMINARY ANALYSIS OF STREAMFLOW DROUGHT CHARACTERISTICS IN THE MIDDLEREACH OF THE YELLOW RIVER

Li Changxing, Shen Jin, and Fan Rongsheng

School of Water Resource and Hydroelectric Engineering
Shaanxi Institute of Mechanical Engineering, Xian

ABSTRACT

In this paper, based on the data of annual streamflow and low folws, collected from the eleven stations on the main stem and tributaries in the middlereach of the Yellow River, the characteristics of time and space variation concerning the dificiency and low flows of streamflow were analyzed and expounded in detail from the concept of streamflow drought. The results can be used as a reference for further study and application.

INTRODUCTION

Drought means water shortage. Water is of vital importance to the existence of mankind. There have been studies of historical drought and waterlogging since the 1950's in China. But because of the slow velocity, long duration, low frequency, and the long-term and complex mechanism in drought occurrence, it is difficult to predict droughts quantitatively. Therefore, there are not many works available for studying drought.

In recent years, the conflict of water supply and demand have became more and more critical. In order to analyze and understand the occurrence of drought quantitatively, to serve the production and life of mankind direcly, study on hydrologic drought was initiated by hydrologists. Hydrologic drought is a hydrologic phenomenon in which natural precipitation, streamflow and groundwater flow below the normal available values are persistent and widespread The objectives of this paper are to analyze the characteristics of streamflow deficit and low flows, which is an important aspect of hydrololgic drought study.

There is arid and semi-arid climate in the middlereach of the Yellow River, Streamflow is the main source of irrigation, navigation, water power, sewage drainage, and underground water recharge of this region. It is very significant to study the basic characteristics and regularities of streamflow drought for development, utilization and protection of water resources, and for guaranteeing and promoting the development of industry and agriculture.

CONCEPT AND BRIEF ACCOUNT OF STREAMFLOW DROUGHT STUDY

Streamflow drought is a phenomenon in which natural streamflow is below the long-term mean annual runoff. It is classified into two types: multiyear and annual. The follwing parameters are used to represent streamflow drought: deficit volume S, deficit duration T, deficit flow M, and, correspondingly, maximum deficit volume MS, maximum deficit duration MT and maximum deficit flow MM. The S means the total volume by which the natural streamflow is below the long-term mean runoff during the continuous period of deficit duration T, and the deficit volume within a unit duration is the def-

icit flow M. The meanings and relationships of S, T and M are given in figure I.
Generally, the frequency analysis method is used in study of stream flow drought. The frequency characteristics of two indices, deficit volume and duration, which are both stochastical varibles, with independent and identically distributed values in each year, are mainly researched. Because of shorter hydrological sequences at present, there are two types of methods for frequency analysis: direct and indirect methods. The direct method uses a probability distribution model to determine frequency characteristics directly from observed values of deficit volume and deficit duration. There are some commonly used probability distributions, such as the normal, log−normal, exponential and Pearson Type Ⅲ distributions. The indirect method uses a stochastic model based on the statistical nature of historical data to generate the streamflow sequence, and then some apropriate methods are used to analyze and test the drought events which come from the generated sequences.

TIME AND SPACE VARIATION CHARACTERISTICS OF STREAMFLOW DROUGHT

Analysis of Multiyear Drought

Some basic aspects of eleven main−stem and tributary stations from which the data was selected are given in bable 1. The statistical results of multiyear deficit volume in eight of the stations in which the continuous data record is over 20 years and continuous deficit period is over 5 times are also given in table 1.

Table 1. − −Basic aspects of stations and statistical results of multiyear deficit volume. [S and N represent the mean multiyear deficit volume (yr. m^3/S) and the years of data record respectively. C_v and C_s are variation coefficient and skew coefficient of sequence S respectively. T_a represents the mean value of drought duration T]

River	Station	Area (Km^2)	N (yr)	S (yr. m^3/S)	C_v	C_s	T_a (yr)	MS (yr. m^3/S)	MT (yr)
main stem	Wubu	433514	22	200.31	0.85	1.42	1.71	525.40	4
	Longmen	497561	47	382.65	0.88	1.07	1.85	1168.24	4
	Tongguan	682141	19	− −	− −	− −	− −	− − −	−
tributary	Zhaoshiku	15325	20	− −	− −	− −	− −	− − −	−
	Ganguyi	5891	21	2.16	0.50	1.00	1.5	4.54	3
	Wenjiachuan	8045	20	15.42	0.52	1.98	2.2	29.92	4
	Gaojiachuan	3253	18	− −	− −	− −	− −	− − −	−
	Gaoshiyan	1263	20	2.28	0.45	0.01	1.57	4.01	3
	XianYang	46827	47	89.50	1.12	2.09	1.77	324.7	4
	Zhuangtou	25154	38	15.61	0.55	0.91	2.63	32.00	5

As can be seen from the table, the variation coefficient of deficit volume, C_v, ranges from 0.45 to 1.18; its mean is 0.77 among the stations. The C_v of two stations, Xiangyang and Zhangjiashan, are relatively large; and that of another three stations, Ganguyi, Wenjiachuan and Gaoshiyan are small; at two main−stem stations of the Yellow River, Longmen and Wubu, the C_v is in the middle. The skew coefficient C_s ranges between 0.01 and 2.03, the average is 1.23; the C_s of Gaoshiyan is the smallest and that of Xianyang is the largest relatively. The range of C_s/C_v is from 0.02 to 3.81. The Pearson Type Ⅲ gives a good fit to all of the data with the exception of Gaoshiyan's data which conforms with the normal distribution by means of frequency analysis and χ^2 test. An example of results of frequency analysis of multiyear deficit volume is given in

figure 2.

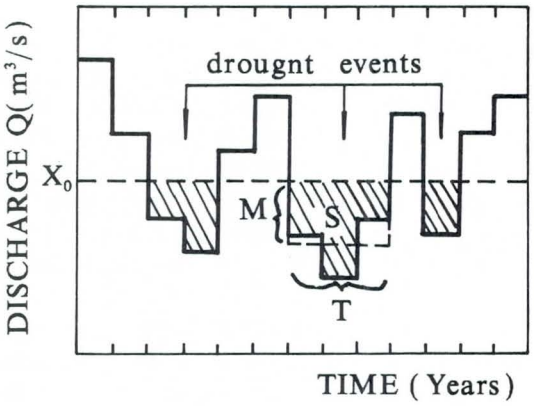

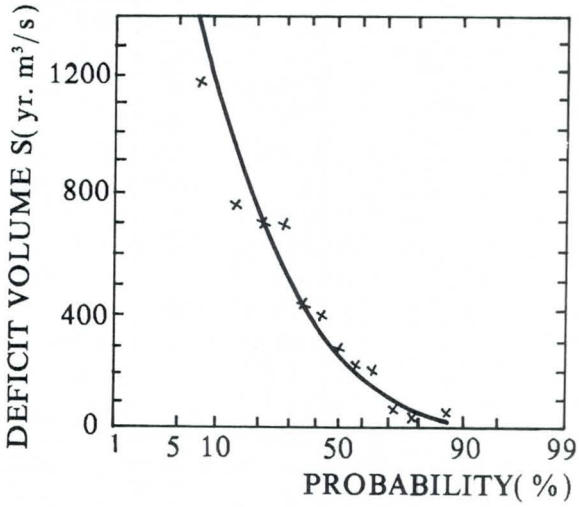

Fig. 1 – – Sketch of streamflow drought event definition
M deficit flow
S deficit volume
T deficit duration

Fig. 2 – – Frequency Curve of multiyear deficit volume at Longmen station

"x" observed
– fitted

Analysis of Annual Drought

Table 2 gives the statistical results for annual deficit flow of seven stations in the main – stem and tributaries of the middlereach of the Yellow River. $\overline{M}$ represents the annual mean deficit flow (m_3/s). As can be seen in the table, the variation range of C_v is from 0.44 to 0.65, its mean is 0.53; the C_s ranges from 0.29 to 1.54, the average value is 0.82; C_s/C_v ranges between 0.52 and 2.91. There is no evident regional characteristics for variation of C_v and C_s for annual deficits as compared with the variation of multiyear deficit volume, but the value and range of variation are on the decrease evidently. According to the results of frequency analysis and test, the variation of annual deficit flow at each station is good for fitting the Pearson Type Ⅲ distribution. Figure 3 gives the frequency curve of annual deficit flow with the data of Tongguan station.

Table2 – – Statistical results of annual deficit flow
[C_v and C_s are variation coefficient and skew coefficient of annual deficit sequence respectively. N_p represents the mean annual deficit period.]

Station	$\overline{M}$ (m^3/S)	C_v	C_s	N_p	MM (mon. m^3/s)	MT (mon.)
Wubu	291.89	0.44	0.81	2.8	621	7
Longmen	333.16	0.54	1.31	3.0	933	7
Tongguan	399.73	0.47	1.05	2.6	853	7
GanguYi	3.02	0.53	1.54	2.5	7.98	6
Zhaoshiku	2.78	0.56	0.29	3.2	6.21	5
Gaojiachuan	1.86	0.65	0.37	3.3	4.7	4
Wenjiachuan	11.43	0.49	0.38	2.9	22.6	6

The analysis results show that there are generally 2 to 4 deficit periods in each station

every year. Maximum deficit duration is generally 7 months. Annual mean deficit flow generally increases with the increase of catchment area. The maximum annual deficit flow varies in the range from 4.7 to 933 mon. m^3/s.

Space Variation of Deficit Flow

In order to take further study on space variation of deficit flow, correlation analysis was made between the Tongguan station (main station) and the rest of the stations (relative stations). The results show that the variation of coefficient has no evident relation to distance and watershed area. But the climate conditions and station locations have large effect on variation of correlation coefficient. For example, the Wubu, Longmen, and Tongguan stations are all situated on the main-stem of the Yellow River; there is a systematic relation of inflow and outflow for runoff formation so that the correlations are relatively high. The Xianyang, Zhangjiashan, and Zhuangtou stations are located on the main tributary of the Yellow River, their flow forms a large proportion of the runoff of Tongguan station so that the correlation also is relatively high. But there are small amounts of mean annual precipitation, and large amounts of soil-water erosion and groundwater recharge in the rest of the stations, such as Zhaoshiku, Ganguyi, Wenjiachuan, and Gaojiashan, which are close to the border of desert, so the correlation of their data is not good. Moreover, the correlation coefficient in some individual stations is even a negative value.

TIME AND SPACE VARIATION CHARACTERISTICS OF LOW FLOW

Statistical Analysis of Daily and Monthly low Flows

The statistical analysis results of daily and monthly low flows are shown in table 3, the daily and monthly low flows are the lowest mean flow for any day and any month of the year respectively. Because the daily and monthly low flows were zero in more than 10 of 20 years record at Gaoshiyan, the statistical parameters are hardly representative of variation characteristics of daily and monthly low flows in this station, and are not given in ghe table.

Table 3--Statistical results of daily and monthly low flows

Station	Mean Q(m^3/s)		C_v		C_s		α		β(m^3/s)	
	Day	Mon.	Day	Mon.	Day	Mon.	Day	Mon.	Day	Mon.
Wubu	130.26	271.09	0.40	0.36	0.66	0.11	2.23	2.61	149.92	307.60
Longmen	163.28	332.40	0.31	0.30	0.35	0.60	3.26	3.46	183.01	369.88
Tongguan	238.16	436.24	0.37	0.26	0.04	−0.38	2.45	3.34	271.94	489.38
Zhaoshiku	3.66	10.94	0.50	0.21	−0.31	0.02	1.00	4.69	4.72	11.95
Ganguyi	0.20	1.02	0.84	0.41	0.50	0.92	0.46	2.48	0.42	1.17
Wenjiachuan	0.66	4.48	1.27	0.36	3.22	0.42	0.75	2.76	0.88	5.06
Gaojiachuan	3.57	8.11	0.41	0.14	0.12	0.14	2.20	7.06	4.10	8.64
Xianyang	21.22	40.21	0.73	0.49	0.90	0.21	1.37	1.83	23.45	46.04
Zhangjishan	3.02	7.03	0.92	0.71	1.47	0.72	1.24	1.11	3.32	7.99
Zhuangtou	4.40	7.54	0.47	0.41	0.20	−0.37	2.05	2.03	5.03	8.73

As can be seen from the table, the C_v of mean daily low flow ranges between 0.31 and 1.27; the average is 0.62. The variation range of C_s is from −0.32 to 3.22; the mean is 0.72. C_s/C_v varies in the range of −0.62 to 2.53. The average level of C_v and C_s in three

main tributary stations, Xianyang, Zhangjiashan and Zhuangtou, is higher than that of another three main-stem stations, Wubu, Longmen and Tongguan. The variation range of C_v and C_s is the largest in rest of the stations.

It is noticeable that the average of daily mean low flow in Gaojiachuan is higher than that of Wenjiachuan and Ganguyi and approaches that of Zhaoshiku. The catchment area of Gaojiachuan is the smallest in these four stations and over 3 times smaller than that of Zhaoshiku. From the view of geographic location, Gaojiachuan is in the north of the studied region and the formation of its low flow is affected by the variation of climate and precipitation to a large extent. Maybe, the only reason to explain this phenomenou is the contribution of groundwater discharge to low flow, which means that the recharge and regulation function of groundwater on the watershed of Gaojiachuan is more efficient than that on the other watersheds.

The C_v of monthly low flow ranges from 0.14 to 0.71; and the average is 0.36. The variation range of C_s is between -0.38 and 0.72; and the mean is 0.24. The value of C_s/C_v varies from -1.46 to 2.24. The value and range of C_v and C_s is evidently decreased as compared with that of daily low flow. Especially, the variation of C_v and C_s in four stations, Zhaoshiku, Ganguyi, Wenjiachuan and Gaojiachuan, is smaller than that in the sequence of daily low flow at the same stations.

Frequency Analysis of Low Flow

The occurrence of low flow is a kind of extreme hydrological situation, and generally has a good fit with the Extreme-value Type Ⅲ distribution. It was found that all of the data, daily and monthly low flow sequences, from the ten statios except for the Gaoshiyan, conforms quite well with the two parameters Extreme-value Ⅲ distribution by frequency analysis and χ^2 test. The distribution function is

$$F(X) = 1 - \exp[1 - (x/\beta)^{\alpha}] \quad 0 < x < \infty \qquad \alpha, \beta > 0 \tag{1}$$

where, α and β are distribution parameters. There are some methods, such as moments and maximum likelihood that are commonly used to estimate the value of α and β, but it is not convenient in practice to use these methods bicause cut-and-try solutions are

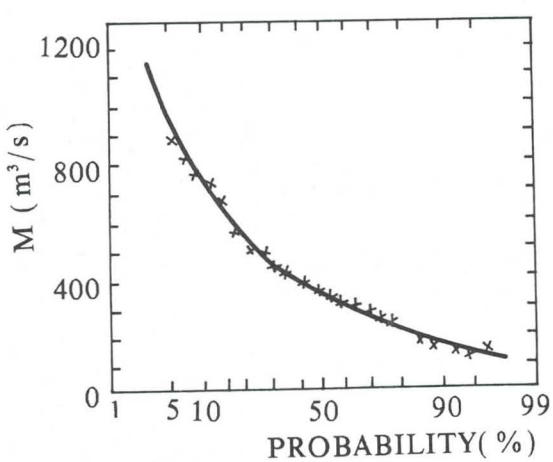

Fig. 3.--Frequency curve of annual deficit flow at Tongguan station
"x" boserved
-fitted

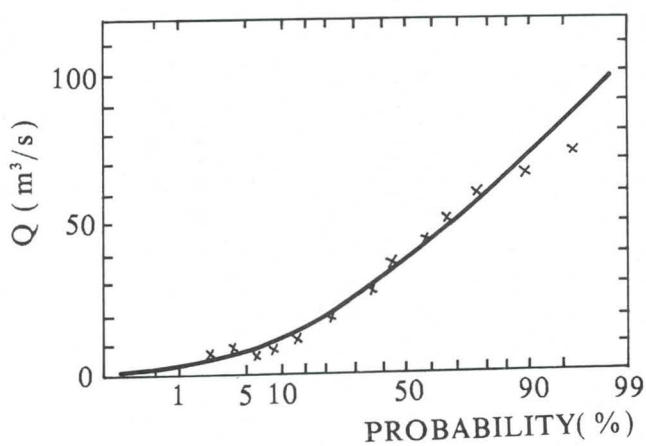

Fig. 4.--Frequency curve of monthly mean low flow at Xiangyang station
"x" observed
-fitted

needed. If we make logarithm transformation two times for equation (1), we can get a linear form of it as follow:

$$Y = aZ + b \tag{2}$$

where $Y = \ln\{\ln[1/[1-F(x)]]\}$

$Z = \ln(x)$; $a = \alpha$; $b = -\alpha \cdot \ln\beta$

Therefore, it is convenient to estimate the parameter by least square method. For comparison, the curve-fitting method by visual estimation was used to estimate the parameters, and it was found that the least square method gave a better fit. The value of estimated parameters are given in table 3 for daily and monthly low flows.

As can be seen from bable 3, variation of parameter β is in direct proportion to the sequence Q, which shows that β represents the average level to some extent, and determines the location of the distribution of the random variable. The variation of α is approximately in inverse proportion to the variation of C_v and C_s; especially, it is evident that α increases with the decrease of C_v, which shows that α represents the concentration characteristics of the distribution. Curve-fitting result is given in Figure 4 for monthly low flow sequence of Xiangyang station.

RELATIONS OF STREAMFLOW DROUGHT TO LOW FLOWS

Theoretically, there is a direct causative realtionship between maximum annual deficit flow MM and mean daily or monthly low flows because the MM is practically the parts below the long-term mean annual runoff and above the mean daily or monthly low flows. Therefore, correlation analysis was made on the synchronized sequences between the maximum annual deficit flow and daily or monthly low flows among the eleven stations in this paper. The results show that all of the correlation coefficients are relatively small. For daily low flows, the maximum correlation coefficient is only 0.51 (at Longmen station); minimum correlation coefficient is −0.25 (at Wenjiachuan). For monthly low flow sequences, maximum correlation coefficient is only 0.42 (at Tongguan); minimum correlation coefficient is −0.35 (at Ganguyi). In addition, the data at most of the stations shows negative corrrelation as compared with the sequences of daily low flows, which means that the larger the deficit flow, the smaller the low flow, and this result relatively conforms to the concept of physical causality. But there is not a good correlation between the sequences of maximum annual deficit flow and daily or monthly low flow as a whole. For revealing the relationship of physical causality, it is not enough only to do correlation analysis.

REFERENCES

Li Changxing, 1990, Characteristics of Drought of River Runoff in Middle Reaches of the Yellow River: Northwest Water Resources and Water Engineeting (in Chinese), No. 2, 35−41

Li Changxing, 1990, Review on Study of Hydrologic Drought: Scientific and Technological Information on Hydrology (in Chinese) No. 1, 1−4.

AN EVENT-BASED MODEL OF PRECIPITATION FOR ANALYZING OCCURRENCE AND SEVERITY OF SUMMER DROUGHTS IN SOUTHERN ARIZONA AND NEW MEXICO

By

Vicente L. Lopes, School of Renewable Natural Resources, University of Arizona, Tucson, Arizona

Martin M. Fogel, School of Renewable Natural Resources, University of Arizona, Tucson, Arizona

Lucien Duckstein, Systems and Industrial Engineering, University of Arizona, Tucson, Arizona

Bisher M. Imam, School of Renewable Natural Resources, University of Arizona, Tucson, Arizona

ABSTRACT

Any definition of drought considers that precipitation, directly or by implication, is below normal for a prolonged duration at a single site or over a region. This paper uses this concept and an event-based stochastic model to generate sequences of summer thunderstorm events for determining conditional probabilities of occurrence and severity of periods with below-normal precipitation. The effect of elevation, which is of particular importance for the occurrence of summer rainfall events, was also considered. An effort was made to define a statistical index to describe occurrence and severity of droughts in southern Arizona and New Mexico. An analysis of the drought index was performed for twenty 100-year sequences of synthetic precipitation data for various elevations.

INTRODUCTION

Purpose and Scope

The purposes of this paper are:

1. To provide a stochastic system framework for analyzing the frequency and severity of drought phenomena in southern Arizona and New Mexico.

2. To devise an index to describe occurrence and severity of summer droughts in southern Arizona and New Mexico.

Scrutiny of past events and present developments such as climate changes have increased concerns about drought in Arizona and New Mexico. The southwestern states of Arizona and New Mexico have the potential of becoming more vulnerable to the effects of prolonged dry periods because of their expanding population. Dry periods that in the past might have had negligible effects may in the future have more serious consequences on these states' populations, agriculture, industry, wildlife and native vegetation.

Drought is an elusive concept, difficult to define and apply, particularly in arid environments such as in Arizona and New Mexico. The problem of drought definition is caused by conflicting concepts from different viewpoints. For example, from a meteorological viewpoint (Palmer 1965), drought is a period when precipitation is significantly less than a critical value. From a hydrologic view point (Yevjevich 1967), drought occurs when there is a period with below-normal streamflow and a depleted reservoir storage. From an agricultural view point (Newman 1978), drought is defined as a period during which soil moisture is insufficient to support crop production. Other drought definitions emphasize socioeconomic factors such as the availability of desired quantities of water at desired costs (Riefler 1978). Although the preceding definitions differ according to the nature of the water shortage, they all refer, directly or by implication, to a scarcity of precipitation during extended periods at a single site or over a region.

Various indices and formulas have been devised to define and measure drought. The Palmer index (Palmer 1965) is best suited for conditions in the Midwest. Seeking a more appropriate index for the West, Colorado officials devised a Surface Water Supply Index (Arroyo 1991) which has been adapted to situations in other states, including Oregon and Montana. Some officials (Arroyo 1991) believe that Arizona and New Mexico should develop an index suitable to their environmental conditions.

DROUGHT ANALYSIS

A necessary component of a drought analysis is specification of the method by which drought events will be abstracted from a time series of precipitation events. The method employed here uses an event-based stochastic model to generate twenty 100-year sequences of summer thunderstorm events for determining probabilities of summer seasons with below-normal precipitation. The effect of elevation, which is of particular importance for the occurrence of thunderstorm rainfall events, was also considered in the analysis. A statistical analysis of the periods with below- normal precipitation was performed for the 20 sequences of synthetic precipitation data. A drought- severity index suitable to the environmental conditions of southern Arizona and New Mexico was defined.

Event-Based Precipitation Modeling

Stochastic event-based precipitation models are characterized by at least two classes of random variables and their probability distribution functions. First, there is the random number of events or alternatively, the interarrival time between events. Second, there is a description of the event characteristic such as storm depth, duration or maximum intensity

for a specified period of time.

In this paper, the event-based modeling approach described by Fogel and Duckstein (1969) was adopted. The approach is based on statistical analysis of summer thunderstorm events in southern Arizona and New Mexico (Fogel et al. 1971). In this model, the simulation is conducted on two different interactive scales. First, the overall characteristics of the monsoon season, which include the number of storms per season (N), the starting day of the season (D_1), and the length of the season (L). Second, the individual storm characteristics, which include the maximum rainfall depth at the storm center (R_{max}), and the interarrival time between two consecutive storms. The number of storms per season is drawn from a Poisson distribution with a mean that is related to the mean elevation of the watershed (Fogel and Hyun 1990). Monsoon season starting date (D_1), and length (L) are drawn from normal distributions with means and standard deviations that vary regionally (Fogel and Hyun 1990). They are considered to be independent of elevation. Once the seasonal variables are defined, each storm within the season is generated by computing the time separating the storm from the beginning of the season. This is done by drawing (N-2) uniform deviates and placing them in ascending order. The uniform deviates are then multiplied by the length of the season and the time location of each storm is identified. The above procedure generates an exponentially distributed interarrival time between two consecutive storms. Storm duration and intensity variations are not accounted for in this model. The next step is to generate maximum storm depth at the storm center. One possible probability distribution of R_{max} for southern Arizona and New Mexico, is the gamma distribution (Fogel 1979).

In this study, the mean and standard deviation of R_{max} were assumed to be independent of elevation due to insufficient information about the nature of this dependency. The conversion of maximum depth into total precipitation was approached by assuming a bell shaped storm. The shape factors for each storm were given by a function of the maximum storm depth (Fogel and Hyun 1990). The volume under the bell was calculated and distributed uniformly over the watershed area. The seasonal precipitation was calculated by repeating the process for all storms during the season and summing them up. The values of the simulation statistics used for the different random variables described in the model are shown in Table 1. These are characteristic values describing summer precipitation conditions in southern Arizona and New Mexico.

Drought Index

Recognizing that both the total amounts of seasonal rainfall and the number of events that result in this total are significant indicators of a dry season, we propose the following statistical index as a descriptor of drought occurrence and severity in southern Arizona and New Mexico:

$$S_i = \begin{cases} (1 - R_i/R_o)(1 - N_i/N_o) & \text{if } Ni<N_o \text{ and } R_i<R_o \\ 0 & \text{otherwise} \end{cases} \qquad (1)$$

where S_i is the statistical drought-severity index for the i-th season, R_i is the total rainfall for the i-th season, R_o is the long-term average seasonal rainfall, N_i is the number of rainfall events for the i-th season, N_o is the long-term average number of events per season, and I is the number of seasons. Notice that by including the number of events per season in Eq. 1, we account for the effect of interarrival time between events in determining drought severity. A drought-severity index equal to 1 defines the most severe seasonal drought in terms of total absence of precipitation ($R_i = 0$ and $N_i = 0$). The severity of this phenomenon would increase drastically with its prolonged duration over the following seasons.

Table 1. Values of simulation statistics of random variables

Variable	Distribution	Parameters
Mean Elevation (ft)	-----	1500, 1800, 2200, 2600, 3000, 4200, 4800
Number of events per season	Poisson	$\mu_{1500} = 5.6$, $\mu_{1800} = 11.6$, $\mu_{2200} = 19.6$, $\mu_{2600} = 27.6$, $\mu_{3000} = 35.6$, $\mu_{4200} = 59.5$, $\mu_{4800} = 71.5$
Maximum Storm Depth	Gamma	$\mu = 1.06$ in, $\sigma = 0.63$ in
Season Length	Normal	$\mu = 95$ days, $\sigma = 15$ days
Starting Day	Normal	$\mu = 185^1$, $\sigma = 10$ days

[1] Julian date

Table 2. Probabilities of drought occurrence and drought Index statistics for various elevations

Elevation (ft)	Occurrences	Pr	$\mu(S_i)$	$\sigma(S_i)$	Max(S_i)
1500	537	0.2685	0.0511	0.0566	0.4167
1800	515	0.2575	0.0377	0.0422	0.2859
2200	519	0.2595	0.0261	0.0332	0.2555
2600	521	0.2605	0.0218	0.0263	0.1760
3000	525	0.2625	0.0210	0.0245	0.2036
4200	521	0.2506	0.0149	0.0171	0.1099
4800	525	0.2625	0.0146	0.0153	0.0844

Twenty sequences of one hundred summer seasons were generated following the above criteria for seven different elevations, ranging from 1500 ft to 4800 ft. For each elevation, the total seasonal precipitation was calculated by adding the precipitation for each storm within the season. The average number of storms and the average total seasonal precipitation were computed from the 2000 seasons for each elevation. The drought index for each season was calculated using Eq. 1. At each elevation, the probability of drought occurrence was determined as the number of occurrences of $S_i > 0$ divided by the total number of seasons. The conditional probabilities of drought severity exceeding a specified value (if a drought occurs) were developed by ranking values of S_i for each elevation and performing a maximum value analysis on the ranked sequences. The result of this analysis is shown in Fig. 1. Multiplying the latter value by the proper value from Table 2 yields the absolute probability of occurrence of a drought with a given severity index.

DISCUSSION AND CONCLUSIONS

The second and third columns of Table 2 show that summer droughts, independent of their severity, have the same likelihood of occurrence for all elevations. The probability of drought occurrence ranges from 0.2505 to 0.2685 with no significant differences between elevations (column 3). However, Table 2 shows that elevation is an important parameter in determining the maximum severity of summer droughts. The drought index ranges from 0.42 at 1500 ft to 0.084 at 4800 ft. The fact that the mean number of storm events/area/season increases with elevation contributes significantly to the observation of decreasing drought severity as elevation increases. Fig. 2 shows the joint distribution of number of rainfall events (N) per season and the total rainfall (R) for twenty 100-season sequences at two different elevations (1500 and 4200 ft.). Notice that N and R are highly correlated. The size of the cluster at 1500 ft is considerably smaller than that at 4200 ft elevation. This indicates that at higher elevations we can expect higher deviations from the mean values for both parameters. Lower number of events and higher variability in total precipitation are the reasons for the occurrence of more severe droughts at lower elevations.

The following conclusions can be drawn from this study:

1. The occurrence and severity of a dry season can be described in terms of a statistical index related to the number of storms and
the total precipitation during the season.

2. Periods of below-long-term-average precipitation and number of precipitation events per season have the same likelihood of occurrence for all elevations. However, elevation is an important parameter in determining the severity of summer droughts in southern Arizona and New Mexico.

3. Further research is needed to determine the influence of elevation on the maximum rainfall depth at the storm center (R_{max}), the starting day of the season (D_1), and the length of the season (L).

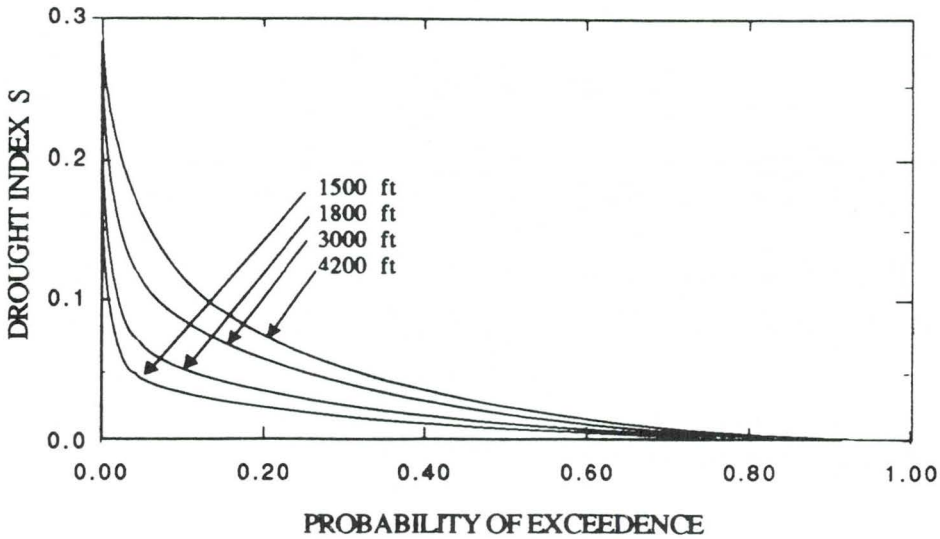

Fig. 1.- Conditional Probability of exceedence for drought severity index given the mean elevation of the watershed.

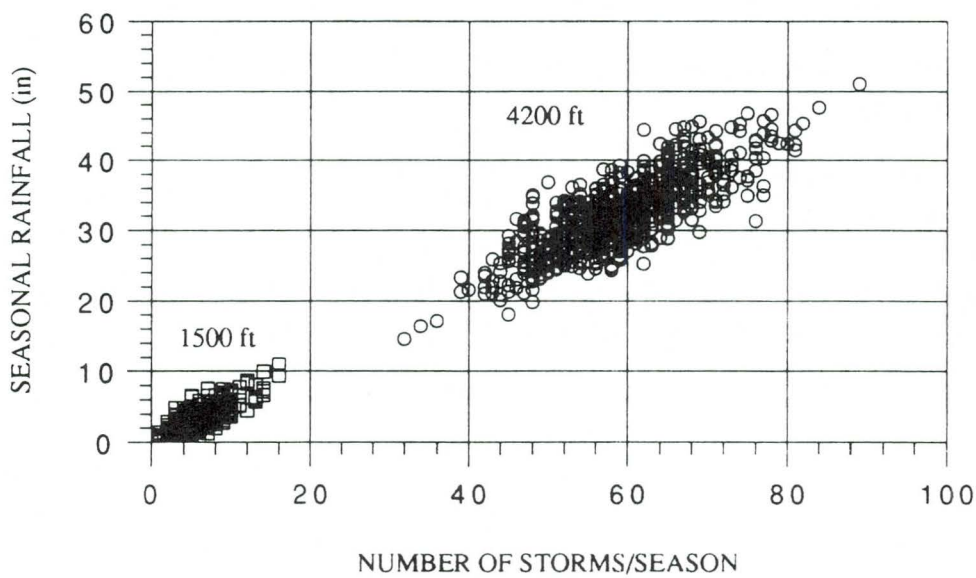

Fig. 2.- Conditional distribution of number of storm events/season and total seasonal precipitation.

REFERENCES CITED

Arroyo. 1991. Drought planning - preparing for dry spells, even in the desert. Water Resources Research Center, The University of Arizona, Vol. 4. No. 4.

Fogel, M. M. 1979. Precipitation in the desert. In: D. D. Evans and J. L. Thames (eds.). Water in desert ecosystems. Dowden, Hutchinson and Ross, Inc., Stroudsburg, PA, pp. 365-391.

Fogel, M. M. and Duckstein, L. 1969. Point rainfall frequencies in convective storms. Water Resources Research, 5(6):1129-1137.

Fogel, M. M., Duckstein, L. and Kisiel, C. C. 1971. Space-time validation of a thunderstorm rainfall model. Water Resources Research, 7(2):309-316.

Fogel, M. M. and Hyun K. K. 1990. Simulating spatially varied thunderstorm rainfall. In: Proceedings, ASCE Intl. Symp., Hydraulics/Hydrology of Arid Lands, San Diego, CA, pp. 513-518.

Newman, J. E. 1978. Drought impacts on American agricultural productivity. In: Rosenberg, N. J. (ed.). 1978. North American Droughts. AAAS Selected Symposium, No. 15, pp. 43-61.

Palmer, W. C. 1965. Meteorological Drought. Research Paper No. 45, U.S. Department of Commerce, Washington, D.C., 58 pp.

Riefler, R. F. 1978. Drought: an economic perspective. In: Rosenberg, N. J. (ed.). 1978. North American Droughts. AAAS Selected Symposium, No. 15, pp. 43-61.

Yevjevich, V. M. 1967. An objective approach to definitions and investigations of continental hydrological droughts. Hydrology Paper No. 23, Colorado State Univ., Fort Collins, Co.

DROUGHTS AND FLOODS IN NORTH AND EAST CHINA, 1380-1989AD

Wang Shaowu, Wang Guoxue and Zhang Zuomei
Department of Geophysics, Peking University, Beijing

ABSTRACT

The considerable impact of droughts on the crop yield in China is emphasized. Two drought/flood grade series were reconstructed for the period 1380 to 1989 from the documentary evidence. The series characterize the variations of summer rainfall in North and East China respectively. Power spectra show that there was not significant trend in either series, but that a 5-year cycle was prominent for the last 600 year period. The predominance of variations between warm-dry and cold-wet climate is noticeable, when the drought/flood series are compared with the temperature series reconstructed in earlier papers. The Little Ice Age was characterized by the cold-wet climate in China. Abrupt changes in drought/flood variations were examined by using the technique of t-test. The abrupt drying in 1616 in East China and in 1916 in North China, and the abrupt wetting in early Qing Dynasty(1644AD) over whole country were identified.

INTRODUCTION

Cultivated area in China during the period 1978-1989 averaged 112.6 million ha(hectares), 30% of which usually suffered from assorted disasters.Among them, the drought predominated over the others.The sown area and the area suffering from disasters for the period 1978-1989 are outlined in Table1. The percentage of sown area with disasters, and the percentage of disaster-affected area with droughts or floods are given in parentheses. Table1 shows that the area with drought in most cases makes up more than half of the area with disasters.

According to the National Bureau of Statistics (1990), the average crop yield was 2.6 t/ha in 1978; it rose to 3.6 t/ha in 1989(Fig.1). Of course, technical progress and improvement of social conditions are reponsible for the generally increasing trend of the crop yield. Therefore, a linear trend was removed from the crop yield series, though one could not guarantee that the impact of technology and society was a linear one. Then, the series without trend was regarded as the meteorological yield, which depends mainly on meteorological conditions.

Figure 2 shows the meteorological yield and the areas with disasters, droughts, and floods. The greatest correlation coefficient was found between the meteorological yield and the area with droughts(-0.77). Aforemetioned data provided good evidence of the predominant role taken by the droughts in determining the crop yield in China. Therefore, the studies on the drought/flood history will supply important information for understanding the possible causes of natural variability of crop yield, which has considerable significance in improving the agriculture production, and for management of hydrological facilities.

Table 1 Sown area and the area with disasters (in million hectares)

year	Area sown	Area suffering disaster (%)		Area suffering drought (%)[1]		Area suffering floods (%)[1]	
1978	150.10	50.79	(33.8)	40.17	(79.1)	2.85	(5.6)
1979	148.48	39.37	(26.5)	24.65	(62.6)	6.76	(17.2)
1980	146.38	44.53	(30.4)	26.11	(58.6)	9.15	(20.5)
1981	145.16	39.79	(27.4)	25.69	(64.6)	8.62	(21.7)
1982	144.75	33.13	(22.9)	20.70	(62.5)	8.36	(25.2)
1983	143.99	34.71	(24.1)	16.09	(46.4)	12.16	(35.0)
1984	144.22	31.89	(22.1)	15.82	(49.6)	10.63	(33.3)
1985	143.63	44.37	(30.9)	22.99	(51.8)	14.20	(32.0)
1986	144.20	47.14	(32.7)	31.04	(65.8)	9.16	(19.4)
1987	144.96	42.09	(29.0)	24.92	(59.2)	8.69	(20.6)
1988	144.87	50.87	(35.1)	32.90	(64.7)	11.95	(23.5)
1989	146.55	46.99	(32.1)	29.36	(62.5)	11.33	(24.1)
mean	145.61	42.14	(28.9)	25.87	(60.6)	9.49	(23.2)

1 Area in drought or flood as percentage of area suffering disaster.

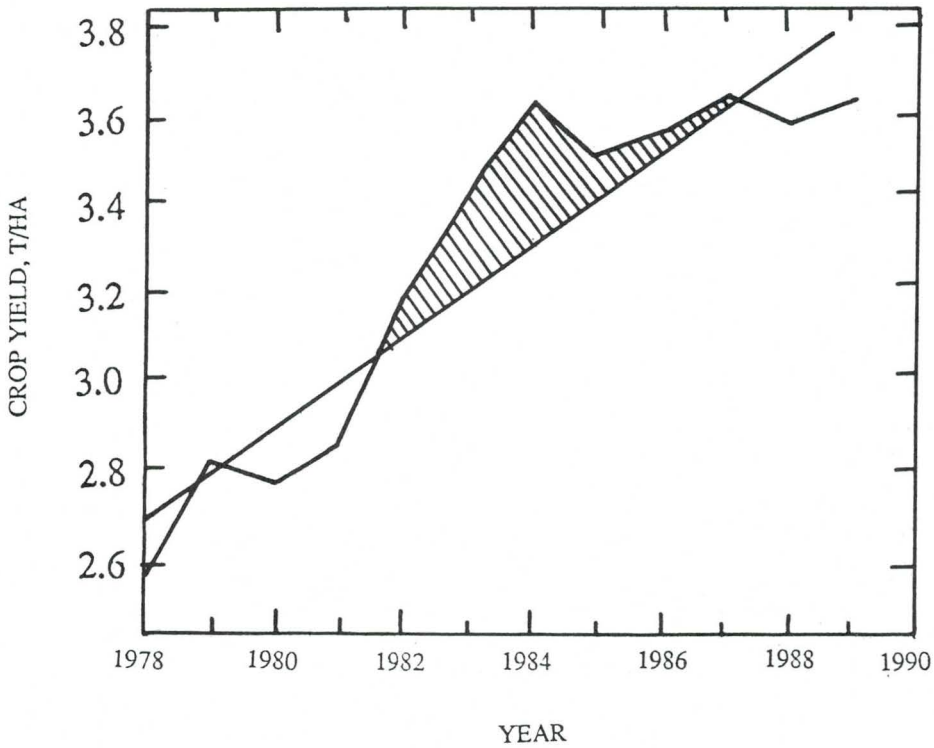

Fig.1 Crop yield in China, 1978-1989 (in t/ha)

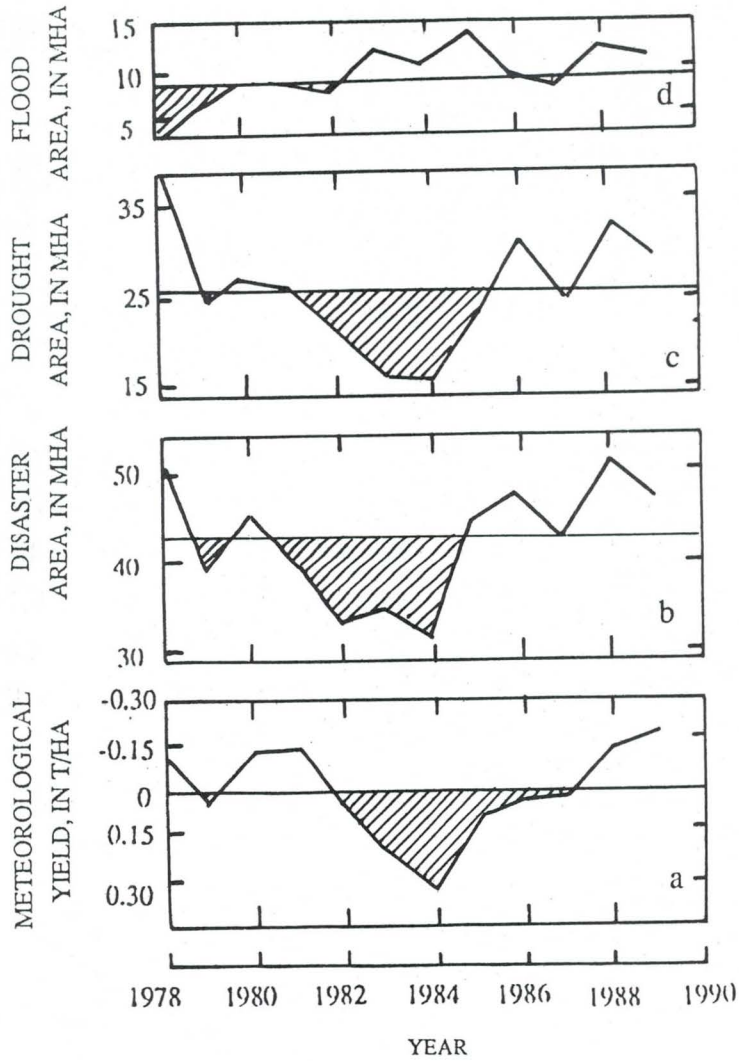

Fig.2 Meteorological yields(a), area with disasters(b), area with droughts(c), and area with floods(d), 1978-1989.

DATA

Observational rainfall data in China are limited generally to the present century and are filled with considerable gaps in war time. So, historical documents had been used in reconstruction of the rainfall series before the instrumental time(Wang and Zhao, 1981).

First, the summer rainfall(June to August) anomalies based on a normal period of 1951-1980 in China were classified into five grades according to their frequency distribution, so that grade 1(very wet) and grade 5 (very dry) have a frequency of 12.5% and each of the other three grades, grade 2 -wet, grade 3 -normal and grade 4 -dry, have a frequency of 25%. Then average anomalies of each grade were found and given in Table2

with only minor modification and rounding the numbers.

Second, the assorted descriptions of droughts and floods contained in the local chronicles were classified also into five grades, considering the duration and severity of the phenomena presented in the documents and comparisons with the rainfall observations when both historical documents and instrumental observations were available. The definitions are briefly outlined in Table 3. Then, the series was extended backward to 1380AD for two regions, each of them containing five key stations:

North China: Beijing, Shijiazhuang, Taiyuan, Jinan and Zhengzhou.
East China: Bengbu, Nanjing, Shanghai, Jiujiang and Wuhan.

Table 2 Definition of drought/flood grades by rainfall observations

grade	rainfall anomaly (percent of normal)
1	R > 50%
2	25% < R < 50%
3	-25% < R < 25%
4	-50% < R <-25%
5	R < -50%

Table 3 Definition of drought/flood grades by historical documents

grade	content
1	severe flood, prolonged rain from summer to autumn, raining for about twenty days, boating over the land, torrential rain with a meter deep of water on the ground
2	flood, flood in summer, torrential rain, flood in summer but drought in autumn, flood in summer but drought in spring
3	good harvest, flood and drought, no data
4	drought with locust, hail, drought, no rain until July
5	severe drought, no rain until August, no rain in the whole year, scene of utter desolation after drought

RESULTS

Because of limited space we cannot provide details in describing the drought/flood variations in the 600-year period. Only three key points are noted: the periodicity, the abruptness of drought/flood variations, and the relationship of drought/flood to the change of temperatures.

Power spectra were calculated for the drought/flood grade series. The maximum lag was 100 and the length of the series was 610. The spectra showed that there is no significant trend in the series: the power in low frequency band is relatively weak. The only peak in the spectrum of East China which is significant at the 95% confidence level is found in the 5.1 year cycle band. A similar(5.0 year) cycle occurs in the spectrum of North China. The 10.5 year cycle is even stronger than the 5.0 year one in North China.

The second interesting character worthy of note is the close correlation between the reconstructed summer rainfall and the temperature. Recently, the ten-year mean temperature anomalies of North and East China have been estimated on the basis of historical documents(Wang,1990; Wang and Wang,1990). The two temperature series were correlated with the ten-year-mean grades found in present paper. A significant correlation coefficient(-0.46) was found for North China(N=61). This means that warm-dry or cold-wet climates have predominated for the last 600-year period. Figure 3 shows the ten-year-mean anomalies of summer rainfall and temperature. The ten-year mean grades were transformed into rainfall anomalies according to Table 2. The correlation coefficient for East China was less significant (-0.24). However, the cold-wet climate was prominent before 20th century even though the maximum of rainfall was not always accompanied by a minimum of temperature. The summer rainfall was generally plentiful in both North and East China before the 20th century, while the temperature was low. It implies that the climate in the Little Ice Age was in general characterized as a cold-wet one in China.

Finally, the abruptness in drought/flood variations was examined. The t-test was performed for successive pairs of thirty -year periods. For example, the grades for thirty years 1380-1409 were compared with those for 1410-1439. The t- value was denoted on 1410. The t-value series is regarded as indicating abrupt change only if the t-value is significant at the 99% confidence level. A positive t-value indicates drying(changing from wet to dry conditions); a negative one indicates wetting(changing from dry to wet). Only three(four) times of drying and two(two) times of wetting were identified for North(East) China; the years when the abrupt change occurred are given in Table 4.

The drying after 1916, and the wetting after 1644(beginning of Qing Dynasty) in North China can also be found in figure 3. It is unnecessary to go into details.

Table 4 Chronology of abrupt changes in summer rainfall

	Drying	Wetting
North China	1483, 1572, 1916	1514, 1644
East China	1433, 1520, 1616, 1852	1550,1647

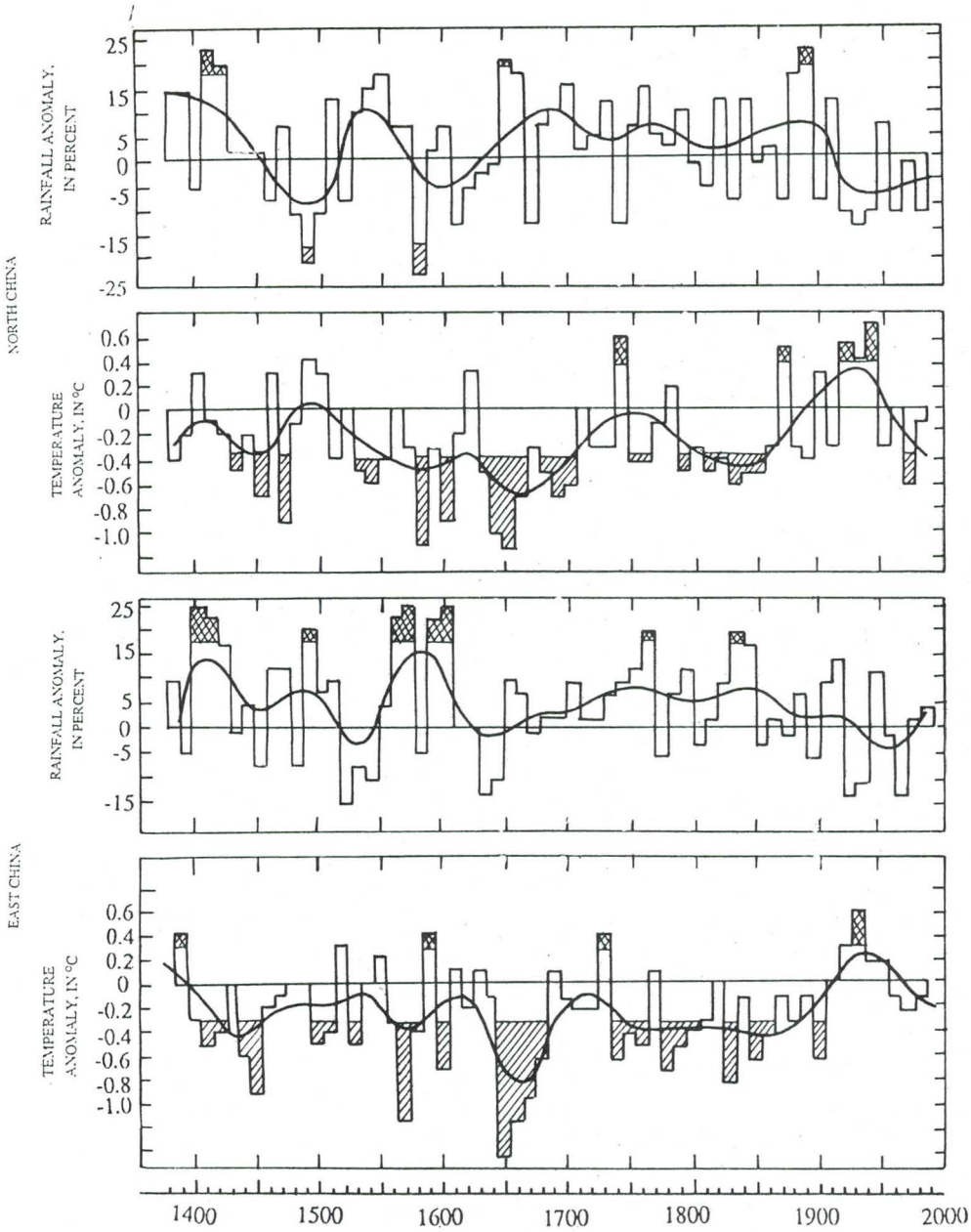

Fig. 3. Ten-year mean summer rainfall and temperature anomalies in North (upper panel) and East (lower panel) China, 1380s-1980s. Normal: 1880s-1970s. Curve is 50-year running mean. Anomalies significant at 95% of confidence level are shaded

REFERENCES

National Bureau of Statistics, 1990: A Statistical Survey of China, Chinese Press of Statistics.

Wang Shaowu and Zhao Zongci, 1981: Drought and floods in China, 1470-1979, in "Climate and History", edited by T.M. L. Wigley et al., Cambridge University Press, 271-288.

Wang Shaowu and Wang Risheng, 1990: Seasonal and annual temperature variations since 1470AD in East China, Acta Meteoro. Sinica, 4, 428-439.

Wang Shaowu, 1990: Reconstruction of temperature series of North China from 1380s to 1980s, Scientia Sinica, (series B), 33, 553-560.

TREE RINGS AND THE SEVERITY OF HYDROLOGIC DROUGHT

David Meko

Laboratory of Tree-Ring Research, University of Arizona
Tucson, Arizona

ABSTRACT

Runs analysis is applied to tree-ring data in the southwestern United states to mark off periods of widespread drought to A.D. 1600. Widespread drought, as measured by spatial coverage of negative growth departures, was notably absent for the 19-year period 1905-1923. The second longest drought-free interval (9 years) also occurred in the twentieth century (1937-1945). Extremes in drought duration and severity occurred in previous centuries. Runs results were compared with tree-ring reconstructions of annual flow for two important water-supply areas for southern California -- the Upper Colorado River Basin and the Sierras of California. Widespread droughts lasting at least seven years corresponded to unusually low reconstructed flows on the Colorado River. The results underscore the need to look beyond the instrumental period to understand the natural variability of drought.

INTRODUCTION

The accurate reconstruction of drought area from tree rings requires a dense network of sites and a strong drought signal in individual tree-ring series. After decades of field collections, the tree-ring network is perhaps most suitable for this purpose in the semiarid southwestern United States (Stockton et al. 1985). Spatial patterns of drought are also especially relevant to water resources management in the Southwest, where users commonly import water from widely separate sources. In this paper, runs analysis (Salas et al., 1980) is applied to tree-ring data to describe time variations in spatial coverage of drought in the southwestern United States to A.D. 1600. Corresponding variations in water availability are inferred by comparing runs results with previously generated annual flow reconstructions for the Upper Colorado River Basin and the Four Rivers Index of northern California.

SPATIAL EXTENT OF DENDROCLIMATOLOGICAL DROUGHT

"Drought" is defined here in a dendrochronological sense as a negative departure from normal of tree growth averaged over a specified area. A network of 121 tree-ring chronologies covering the years 1600-1962 was assembled and grouped into twenty-eight 2° latitude by 3° longitude grid cells (Figure 1). An annual index of the area in dendroclimatological drought was then derived by the following steps: (1) tree-ring indices were averaged over all chronologies in a given cell, (2) any cell with an average tree-ring index more than 0.5 standard deviations below its long-term mean in a given year was designated as a "dry cell", (3) the number of dry cells N_t in each year was tabulated, and (4) any year with greater than the long-term median number of dry cells was defined as a year of "widespread" drought. This particular definition, though arbitrary, provides a relative measure by which spatial coverage of drought in the twentieth century can be compared with coverage in earlier years.

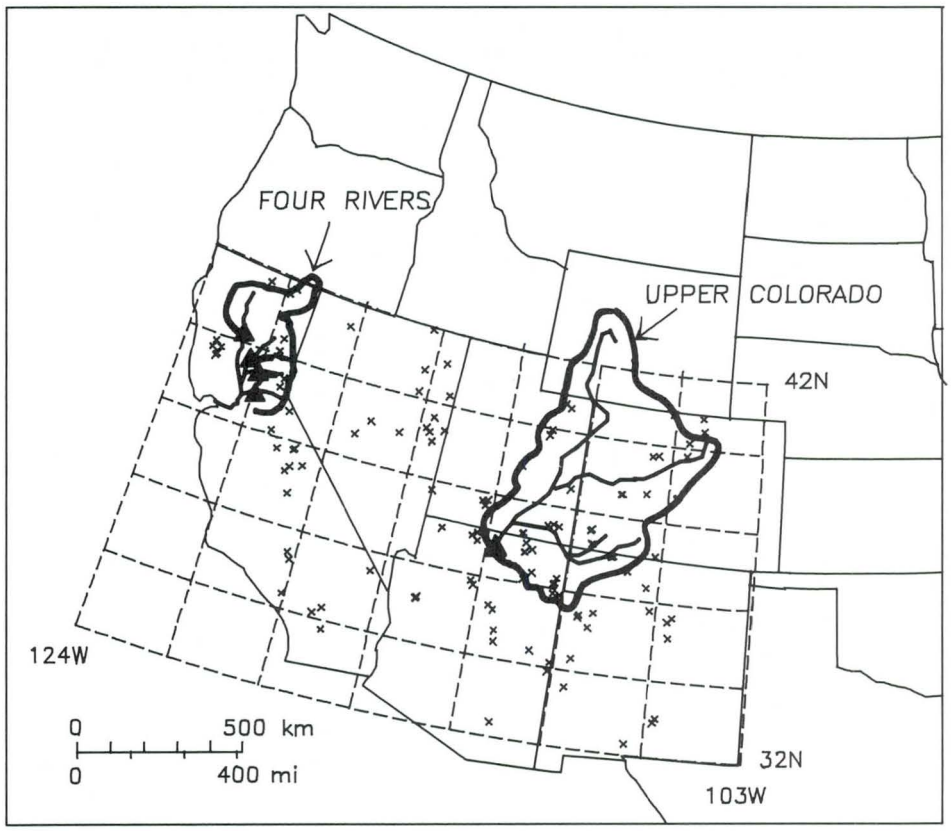

Figure 1. Map showing grid, tree-ring sites (x's), river basins (heavy solid), and stream gages (triangles).

The time series N_t measures the waxing and waning of drought area (Figure 2). A year with more than five dry cells (median of N_t) is an occurrence of widespread drought. In the terminology of runs analysis, a hydrologic drought is characterized by its duration, severity, and magnitude (Salas et al., 1980; Dracup et al., 1980). The duration, or run-length is the number of consecutive years below the threshold line. The severity, or run-sum, is the cumulative area of the curve below the threshold. The magnitude, or run-sum divided by run-length, is the average area below the threshold. Because the time series represents an area in this application,

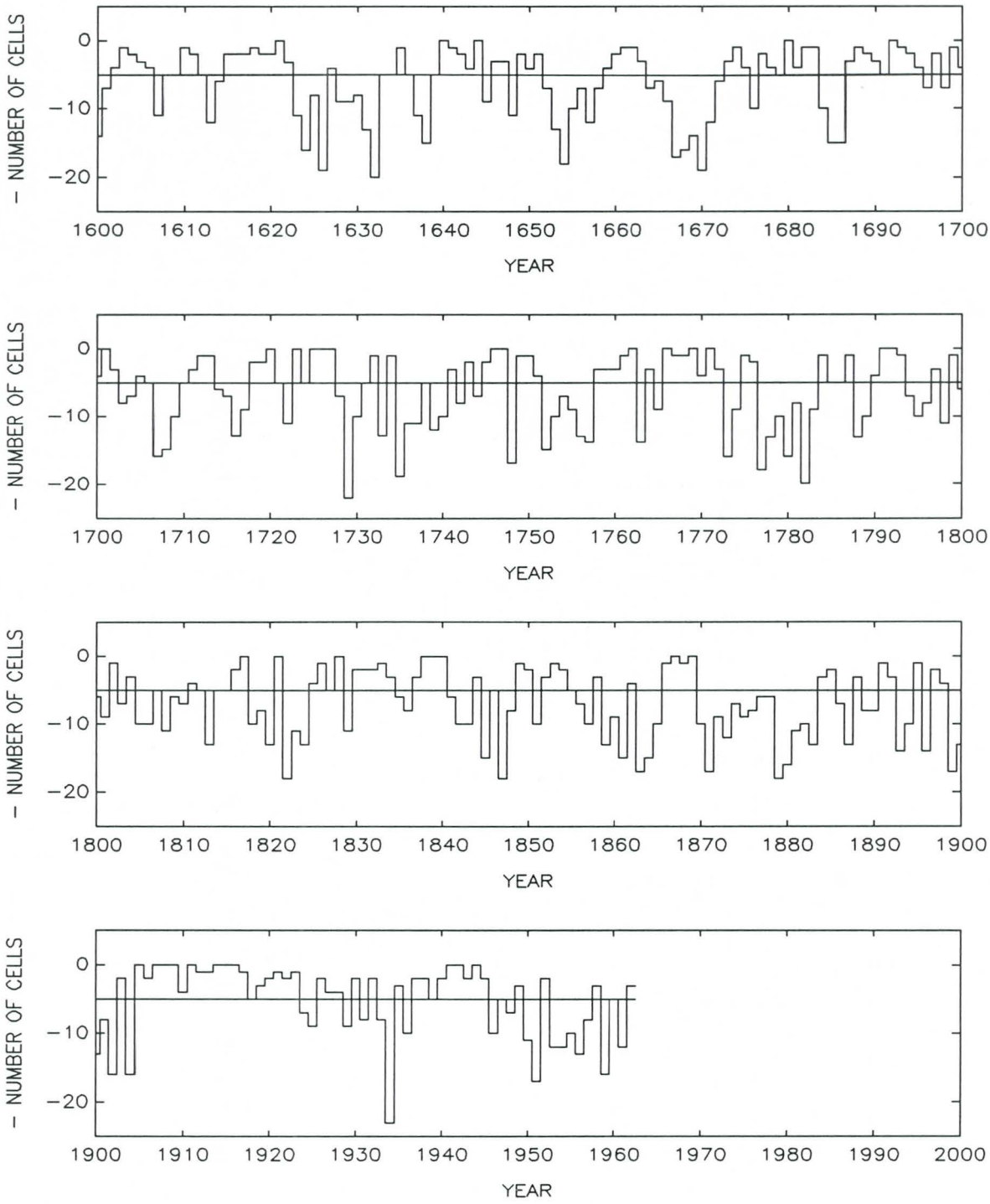

Figure 2. Number of inferred dry latitude-longitude cells, A.D. 1600-1962. Sign of ordinate has been changed to make drought a downward departure. Horizontal line marks threshold for widespread drought as defined in text.

severity is a cumulative measure of spatial drought coverage, and magnitude is the average annual spatial coverage.

The twentieth century has three distinct periods of recurrent or persistent drought separated by two drought-free periods (Figure 2). After a 4-year drought at the turn of the century, 1899-1902, widespread drought was notably absent for 19 years from 1905-23, the longest drought-free period in the tree-ring record. The next-longest drought-free period back to A.D. 1600 was nine years, occurring once in the modern record (1937-1945), and once in the seventeenth century (1687-1695). Although the maximum single-year spatial coverage of drought was reached in the twentieth century (23 cells, in 1934), previous centuries had extremes in drought duration and severity. The four most severe droughts in the long-term record were as follows:

YEARS	LENGTH	RUN-SUM (SEVERITY)
1870-1883	14	82
1664-1672	9	61
1777-1783	7	59
1652-1658	7	39

Drought ranking is sensitive to the choice of threshold defining widespread drought. For example, if the threshold were 6 dry cells instead of 5, the 14-year drought starting in 1870 would be split into two shorter droughts.

COMPARISON WITH HYDROLOGIC RECONSTRUCTIONS

How do the runs properties of drought area relate to water availability in the western United States? This question can be answered indirectly by comparing the runs series of Figure 2 with tree-ring reconstructions of annual flow for specific river basins. Reconstructions selected are those for the Colorado River at Lee's Ferry (Stockton and Jacoby, 1976) and the Four Rivers Index (reconstruction A2) of the Sacramento River Basin, northern California (Earle and Fritts, 1986). Both regions contribute greatly to the water supply of metropolitan southern California (Harris, 1990). Runoff-producing areas of the two basins are separated by about 700-1,500 km (Figure 1). Mean annual virgin flows based on the gaged record, 1906-1985, are nearly equal: 15.1 maf/yr for the Colorado River at Lee's Ferry and 17.2 maf/yr for the Four Rivers Index. Both reconstructions cover more than 400 years. The Colorado River reconstruction is the more accurate as measured by calibration-period statistics: 75% variance explained as opposed to 45% (Stockton and Jacoby, 1976; Earle and Fritts, 1986).

Reconstructions were first smoothed to 20-year moving averages to discount relatively short droughts whose effects would be mitigated by the large reservoir storage capacity in the Colorado river system. Smoothed values are plotted at the beginning year of the corresponding 20-year period in Figure 3. The moving-average series are referred to as CR and FRI in the discussion that follows. Both moving averages are extremely variable, with

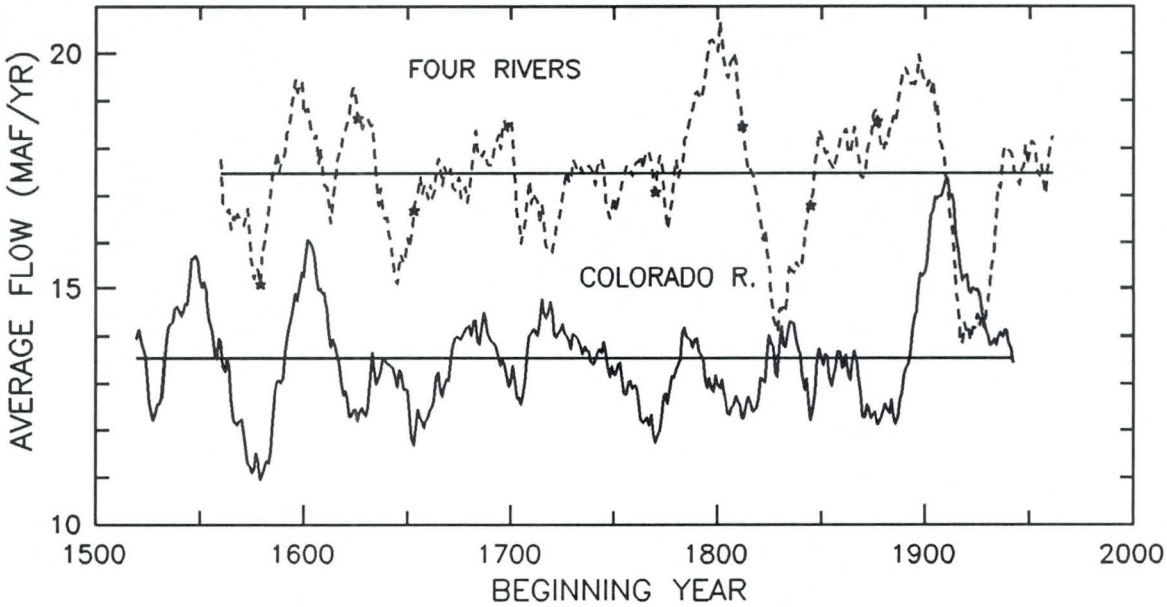

Figure 3. Time series plots of 20-year moving average reconstructed flow of Four Rivers Index of northern California, and Colorado River at Lee's Ferry. Values are plotted at the beginning years of 20-year periods. Horizontal lines mark long-term reconstructed means. Stars on Four Rivers plot mark timing of seven lowest values (non-overlapping periods only) in Colorado River plot. Sources of annual reconstructed series are Stockton and Jacoby (1976) and Earle and Fritts (1986)

ranges exceeding 6 maf/yr. The twentieth century is unusual in having both the highest value for CR and the lowest for FRI. To test for synchrony in drought periods in the two widely separate basins, the 7 lowest **non-overlapping** 20-year means in CR were defined as key hydrologic droughts on the Colorado River. Key CR droughts are marked for reference by the stars on the corresponding time series plot of FRI. The lack of synchrony in low-flow periods in the two basins is immediately obvious from the plots in Figure 3. Some CR key droughts fall opposite low flows in FRI (e.g., 1579-1598), and others opposite high flows (e.g., 1626-1645).

The early-1900s anomaly noted previously in the drought-area series (Figure 2) is also prominent in CR. The beginning year of the highest 20-year-mean reconstructed flow on the Colorado River (1905) is also the beginning year of the longest recorded period without widespread drought as

defined by the runs analysis. The CR and drought-area plots also agree in indicating that the current century is not representative of the most severe drought conditions of the past 400 years. None of the 7 CR droughts fall in the twentieth century.

The drought-area series and basin-specific flow reconstructions suggest that drought variability in the western United States cannot be adequately modeled by hydrologic data from the instrumental period. Tree ring analysis such as performed here can flag bias in such models. Alternatively, long-term time series of drought variables (e.g., runs quantities) can be reconstructed directly by calibrating tree rings with flow series. Where suitably long or sensitive tree-ring chronologies are lacking, it might be possible to indirectly infer the drought history of a particular hydrologic series from the spatial variations in tree growth over a much larger region encompassing the basin. Such an approach would exploit the tendency for precipitation anomalies associated with severe drought to be spatially coherent.

Acknowledgements. I thank W. R. Boggess and C. W. Stockton for their helpful suggestions on the manuscript. The research was supported by National Science Foundation Grant ATM-88-14675.

REFERENCES

Dracup, J.A., Lee, K.S., and Paulson, E.G., 1980, On the definition of droughts: Water Resources Research, vol. 16, no. 2, p. 297-302.

Earle, Christopher J., and Fritts, Harold C., 1986, Reconstructing riverflow in the Sacramento Basin since 1560: Report prepared for California Department of Water Resources under Agreement No. DWR B-55395.

Harris, Richard W., 1990, Southern California's water resources: an assessment of future supply and demand with projected drought effects: Master's Thesis (draft), University of California, Los Angeles.

Salas, Jose D., Delleur, Jacques W., Yevjevich, Vujica M., and Lane, William L., 1980, Applied modeling of hydrologic time series: Water Resources Publications, Littleton, Colorado, 484 p.

Stockton, Charles W., and Jacoby, Gordon C., 1976, Long-term surface-water supply and streamflow trends in the Upper Colorado River Basin: Lake Powell Research Project Bulletin No. 18, National Science Foundation.

ANNUAL RUNOFF SERIES EXTENSION AND RUNOFF VARIATIONS IN LANZHOU-SANMENXIA REACH OF YELLOW RIVER, CHINA

Ma Xiufeng, Wang Yunzhang, Huo Shiqing

Hydrologic Bureau, Yellow River Conservancy Commission
Zhengzhou, Henan Province

ABSTRACT

This paper deals with runoff series extended from 1919 to 1749 on the basis of relations among natural annual runoff, a dryness and wetness index, and three groups of tree ring indices in Lanzhou-Sanmenxia reach of the Yellow River. Analyses of phases and periodic features of historic runoff variation are also discussed.

INTRODUCTION

The Lanzhou-Sanmenxia reach of the Yellow River("reach" for short hereinafter) lies at 33.5°-42°N lat. and 104°-113°E long. (see Fig.1) with a catchment area of nearly 0.466×10^6 km^2, comprising 64% of the total upper and middle Yellow River Basin. Only its southern part, abundant in water resources, belongs to semi-humid climate region, most of the remaining area has arid or semi-arid climate, where there is a shorter rainfall period, less yearly precipitation, and more variable precipitation than in the other. The annual runoff in the reach is less than 18×10^9 m^3, which is 31% of the total of the upper and middle river. Owing to the arid climate, scanty rainfall and insufficient water resources, the development of production in industry, agriculture, forestry and animal husbandry there is seriously influenced, bringing much trouble in harnessing the Yellow River.

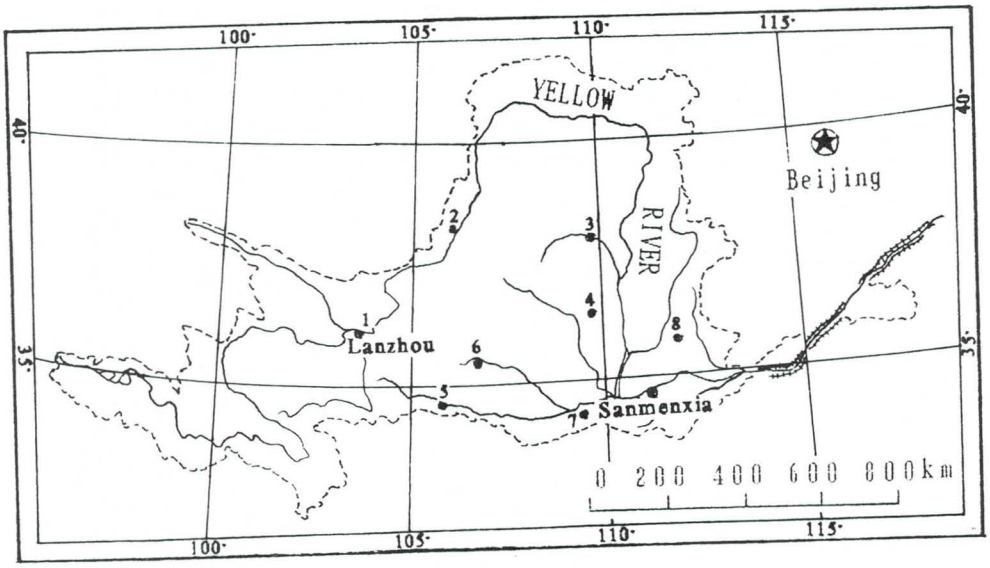

Figure 1.--Yellow River Basin sketch map, showing Hydrometric stations of Lanzhou(1), Yinchuan(2), Yulin(3), Yanan(4), Tianshui(5), Pingliang(6), Xi'an(7), and linfen(8)

Because of historic reasons, only short series of hydrometric and meteorological data are available, but there exist many historical accounts on flooding and drought, and data from tree rings. In light of those data and their statistical relations, a runoff series was reconstructed and extended to 1749 and a preliminary analysis on characteristics of historic runoff variations was conducted.

1.BASIC DATA

1.1 Runoff

The runoff difference between Sanmenxia and Lanzhou hydrometric stations can be regarded as the water inflow in the reach. A runoff series for the reach from 1919 to 1989 can be calculated approximately, based on the data of observed runoff, water consumption for irrigation and reservoir storage, and discharge conditions in major hydrometric stations.

1.2 Dryness and Wetness Grade Data

Making use of dryness and wetness grade data available in Reference[1], in which missing and inexact records for a few stations were reconstructed and revised with reference to "Chronological List of Major Historic Flooding & Drought in Yellow River Basin", and of the data since 1980 provided by prof. Zhang Xiangong, meterological Research Institute of State Meterological Administration, a dryness and wetness index for 8 hydrometric stations of Lanzhou, Yinchuan, Yulin, Yanan, Tianshui, Pingliang, Xi'an, Linfen in the years of 1749 to 1989 was developed. The index values or grades are explained in section 3.1.

1.3 Tree Ring Data

Studies show that tree rings in arid or semi-arid regions can provide fairly good information about climate and hydrology; thus, reconstruction and extension of hydrologic series can be done by using tree-ring indices related to climate and runoff in the basin (Reference 4).

Through correlation analysis on runoff from 1919 to 1974 and on several ten groups of tree rings, it was discovered that the runoff has quite good positive correlations with tree-ring indices of many groups, in particular, closly correlated to the following three groups:

a.Growth rings of cypress at Liyuan village of Huanglin county.
Meteorological Station of Shaanxi Meteorological Office in cooperation with Scientific Research Institute of State Meteorological Office in June 1975 collected some data at Liyuan Village of Huanglin County, Shaanxi Province, where the slope dips 15° southward, 930m above sea level. After reading and revising calculation, the tree-ring series from 1648 to 1974 was obtained.

b.Spruce growth rings at Luanchaigou of Helanshan Mountain.
Climatic Reference Office of Ningxia Meteorological Office in June 1985 collected some data at Luanchaigou, western side of Helanshan Mountain with slope of 32° at elevation 2705m. After reading, original ring-width series

were selected, then three programs-RWLIST, IUDEX, SUMAC-developed by Arizona Tree Ring Research Lab. of U.S.A were used for calculation, and the spruce tree-ring series of 1736 through 1984 was established.

c.Pine growth-ring index on Huashan Mountain.
In cooperation with the Climatic Research Institute of State Meteorological Administration, the Shaanxi Meteorological Research Institute collected data at the top of western Huashan Mountain at an elevation of 2063.8m in May 1984. Tree-ring indices from 1460 though 1984 were obtained after reading and calculation.

2. EXTENSION AND EXAMINATION OF RUNOFF SERIES

Statistical results indicate that the runoff in the reach is not only consistent with tendency of drought and waterlogging, but also fairly related to three groups of tree-ring as mentioned above. For instance, the correlation coefficient of natural runoff from 1919 to 1974 with dryness and wetness index is as high as 0.72 and the correlations with tree-ring indices of the aforesaid groups are 0.42, 0.35, 0.32, respectively, all their degrees of confidence exceeding 0.02. Thus, a regression equation can be established with terms of natural annual runoff(W), dryness and wetness index(X_1), and tree-ring indices of pine(X_2), cypress(X_3), and spruce(X_4). By substituting historical values of $X_{1,2,3,4}$ into the equation, reconstruction and extension of runoff series can be realized. Specific procedures are as follows:

a.In view of non-unity dimensions of runoff, dryness and weteness index, and tree-ring indices, they first should be standardized by using the formulas:

$$X_j'(i)=(X_j(i)-\overline{X_j})/\sigma_j \qquad \begin{cases} j=1,2,3,4 \\ i=1,2,3,...226 \end{cases}$$

$$W'(i)=(W(i)-\overline{W})/\sigma_W \qquad (i=1,2,3,...,56)$$

where, $X_j'(i)$ and $W'(i)$ stand for the annual values of $X_{1,2,3,4}$ and W respectively after standardization; $\overline{X_j'}$ and σ_j stand for mean value and standard deviation of $X_{1,2,3,4}$; and $\overline{W}$ and σ_w stand for mean value and standard deviation of W.

b. An equation with multiple correlation coefficient of 0.78 is obtained by regression calculation:

$$W^*=-0.538X_1+0.281X_2+0.199X_3+0.151X_4$$

c. Calculate W^* for 1749 through 1918 by substitution of historic standardized values of $X'_{1,2,3,4}$ into the above equation.

d. Compute the runoff W:

$$W(i)=W^*(i)\times\sigma_W+\overline{W} \qquad (i=1,2,3,...,170)$$

then, the runoff of 1749 to 1918 can be obtained (see Table 1).

Table 1--Result of runoff extension in the reach from 1749 to 1918 (Unit:10^9m^3)

Year	0	1	2	3	4	5	6	7	8	9
1740										20.9
1750	16.9	24.7	20.0	21.3	14.3	18.5	21.7	17.9	15.9	15.9
1760	25.5	26.7	16.2	20.9	28.6	16.4	23.4	28.0	38.3	22.0
1770	17.8	23.6	23.5	19.4	19.1	22.6	20.7	20.5	19.7	17.4
1780	17.0	19.7	19.2	17.7	15.9	15.9	16.9	22.3	12.2	15.9
1790	17.1	15.5	13.9	14.8	13.3	11.1	10.3	11.8	18.4	16.5
1800	15.3	13.3	16.0	13.2	13.8	10.5	15.9	15.0	15.4	15.9
1810	12.6	19.2	15.5	12.5	15.1	16.8	14.3	12.2	15.5	24.5
1820	17.9	21.9	20.0	18.7	12.3	15.1	14.9	15.9	11.8	14.0
1830	16.2	14.5	13.4	9.1	10.9	12.5	10.4	12.1	14.7	12.5
1840	15.5	15.1	16.7	18.2	22.4	14.0	10.6	14.4	20.6	19.4
1850	20.4	23.4	19.0	19.7	24.4	20.2	16.2	12.6	18.0	13.3
1860	23.0	18.7	14.5	18.1	18.6	14.8	21.3	15.6	18.3	17.8
1870	15.3	17.6	16.0	17.2	13.4	14.9	15.7	11.6	14.5	14.2
1880	17.7	12.2	17.3	21.0	20.4	17.8	16.0	20.9	17.1	22.6
1890	17.4	18.5	12.0	18.8	19.3	20.1	19.0	21.9	19.1	15.6
1900	8.9	11.7	15.5	18.3	17.5	16.3	18.2	19.3	15.5	15.6
1910	18.0	18.8	14.2	22.0	22.4	16.3	14.5	18.6	16.4	

Consistency of the extended and original runoff series was checked with the "U" statistic. For the extended series, U=-1.238 and for a given degree of confidence α=0.05, Uα=1.96. As $|U|$=1.238<1.96, the extended runoff series is well consistent with its original one.

3. CLASSIFICATION AND STAGE ANALYSIS OF RUNOFF

3.1. Classification of runoff

For convenience of statistics and analysis, natural annual runoff in the reach is divided into five grades, i.e. extremely wet, slightly wet, normal, slightly dry and extremely dry. The classification standard in Reference [1] is determined by the following formulas:

Extremely wet yaer (Grade 1): $W > \overline{W} + 1.17\sigma$

Slightly wet year (Grade 2): $\overline{W} + 1.17\sigma \geq W > \overline{W} + 0.33\sigma$

Normal year (Grade 3): $\overline{W} + 0.33\sigma \geq W > \overline{W} - 0.33\sigma$

Slightly dry year (Grade 4): $\overline{W} - 0.33\sigma \geq W > \overline{W} - 1.17\sigma$

Extremely dry year (Grade 5): $\overline{W} - 1.17\sigma \geq W$

in which, W, W and $\sigma\alpha$ refer to natural annual runoff, mean value (17.36×10^9m^3), and standard deviation (4.43×10^9m^3). Their classified range and climatic probability are shown in Table 2.

Table 2-Classified Range & Climatic Probability of Natural Annual Runoff in Lanzhou--Sanmenxia Reach, 1749-1989.

Grade	1	2	3	4	5
Runoff range (10^9m^3)	W>22.6	22.6--18.8	18.7--15.9	15.8--12.2	W<12.2
Frequency	28	51	70	65	27
Climatic probability(%)	11.6	21.2	29.0	27.0	11.2

Table 2 shows that the frequency of the runoff in normal year (grade 3) is the highest and that the frequency in dry years (grades 4 and 5) is a little higher than that of wet years (grades 1 and 2). That is, the frequency of slightly dry years is nearly 6% higher than that of slightly wet years, while the frequencies of extremely dry and extremely wet years are equal.

3.2. Analysis of wet and dry stages

Based on runoff data for successive years, analysis of 10-year moving averages reveals that historical variation of the runoff appears in clear stages and it experiences 4 wet and 3 dry stages among the 237 years up to 1985 (Tables 3 and 4).

Table-3 Characteristic Values of Historic Variation of Runoff in Wet Stages

Item Start-stop year	Years	Frequency of grade 1	2	3	4	5	Mean runoff (10^9m^3)
1749-1787	39	10	14	14	1	0	20.4
1848-1866	19	3	7	5	4	0	18.7
1883-1898	16	1	8	6	0	1	18.9
1933-1985	53	13	14	13	9	4	19.5
Average	32	6.8	10.8	9.5	3.5	1.3	19.4
Frequency (%)		21.4	33.9	29.7	10.9	4.1	
Climatic probability*(%)		11.6	21.2	29.0	27.0	11.2	

* From Table 2

Table 4-Characteristic Values of Historic Variation of Runoff in Dry Stages

Item Start-stop year	Years	Frequency of grade 1	2	3	4	5	Mean runoff (10^9m^3)
1788-1847	60	1	4	14	31	10	14.8
1867-1882	16	0	0	7	8	1	15.6
1899-1932	34	0	3	11	10	10	14.7
Average	37	0.3	2.3	10.6	16.3	7.0	15.0
Frequency (%)		0.1	6.2	28.6	44.2	18.9	
Climatic probability*(%)		11.6	21.2	29.0	27.0	11.2	

* From Table 2.

Tables 3 and 4 show that the longest duration of wet stage is 53 years and the shortest 16, averaging 32 years; while the longest dry stage lasts 60 years and the shortest 16, averaging 37 years. The average runoff of wet stage is 29.3% higher than the dry.

Comparing and analysing frequency difference of the runoff in both stages, their continuous and alternative features can be clearly seen: in wet

stage, frequency of the runoff of grades 1 and 2 is 55.3%, nearly 8 times that of the dry (6.3%), whereas, grades 4 and 5 in dry stage have frequency of 63.1%, more then 3 times of the wet(15%). Runoff is in dry stage now, starting from 1986. The dry stage is expected to cover a minimum of ten years until another wet stage comes.

4. POWER SPECTRUM ANALYSIS OF RUNOFF VARIATION

In accordance with sample lag correlation coefficient in Reference [2], the power spectrum of the runoff was calculated using 45 years as the maximum lag time length(Fig.2). There are 5 wave crests with corresponding periods of 90, 3, 2.4, 3.9 and 2.1 years. The first two are very outstanding; hence it can be concluded that the runoff change has a marked periodic feature.

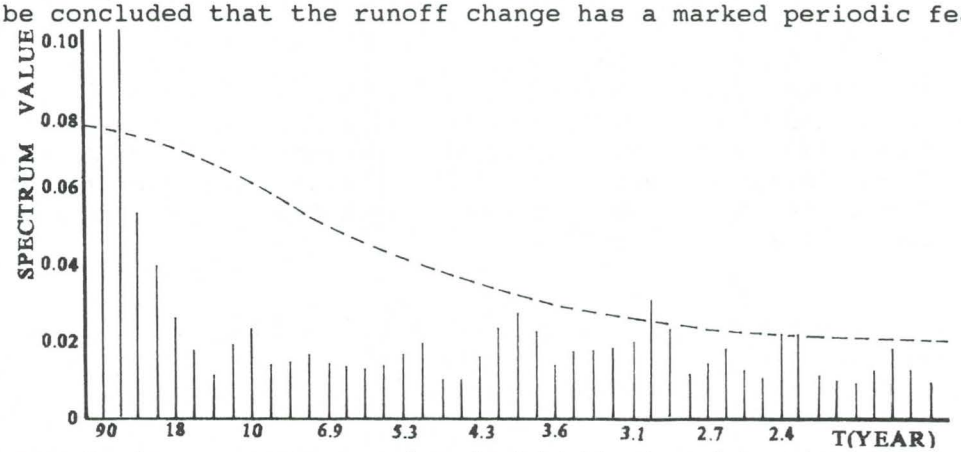

Figure 2--Power spectrum value (solid line) and testing critical value (dotted line) if $\alpha=0.5$

The author is of the opinion that the 90-years period can be called a century period, which may relate to that of solar activity, the 3-to-4-years period, consistent with the oscillation period of subtropical high pressure, reflects air-sea interaction and the 2 years period is undoubtedly associated with the well-know quasi-two-year period of atomspheric circulation and weather. It should be pointed out that only a preliminary trial on runoff extension has been made according to the data on dryness and wetness and tree rings. As the dryness and wetness grade is mainly based on the occurrence of disasters in both stations and adjacent areas, further studies are needed to prove the reasonableness of the regression analysis and the representativeness of tree-ring data used in the paper, even though the latter in arid or semi-arid region can reveal better hydrologic and climatic information.

REFERENCES

[1] Meteorologic Research Institute of State Meteorological Administration, 1981, Drought and Waterlogging Map of China in Recent 500 years: Cartographic Publishing House, Beijing.

[2] Huang Jiayou, Li Huang, 1984, Analysis on Meteorologic Spectrum: Meteorological Press, Beijing.

[3] Zhang Xiangong, Climatic Oscillation of Subtropical High Pressure in West Pacific Ocean: Journal of Meteorologic Research Institute, vol.3, no.1, p.1-8.

[4] Wu Xiangding, 1990, Tree Rings and Climate Variations: Meteorological Press, Beijing.

RECURRENCE PROBABILITY OF 11-YEAR CONTINUOUS LOW WATER PERIOD (1922-1932 A.D.) IN THE YELLOW RIVER

Shi Fucheng , Wang Guoan , Mu Ping , MA Guian , Gao Zhiding

Reconnaissance, Planning and Design Institute,
Yellow River Conservancy Commission, Zhengzhou

ABSTRACT

1922-1932 A.D.was a continuous water period 11 years long in the Yellow River Basin. Based on the measured data of the water-level scale at Qingtongxia and Wanjintan from the beginning of the eighteenth century (the Qing Dynasty) and the water regime reports to the Emperor by administrators, this paper estimates high and low water regime for the past 200 years. Combining these estimates with stochastic hydrology calculation, it is concluded that the recurrence period of the continuous low water period (1922-1932) is 200 years at least. The conclusion is rather important to recognizing year-to-year variation of the Yellow River water resources and to development and use of Yellow River water resources.

The earlest modern hydrologic station in the Yellow River Basin is Shanxian xian Station (see Figure 1). It has had 70 years of measured data from 1919 so far. In this 70 years, 1922-1932 was a continuous low-water period 11-year long (see Figure 2). The average annual water quantity of 1922-1932 was only 75 percent of the annual average water quantity. Each year's water quantity of 1922-1932 is shown in Table 1. In the past planning and hydraulic engineering design of the Yellow River Basin, the recurrence probability of the 11-year low water period has been considered as one time each 70 years.

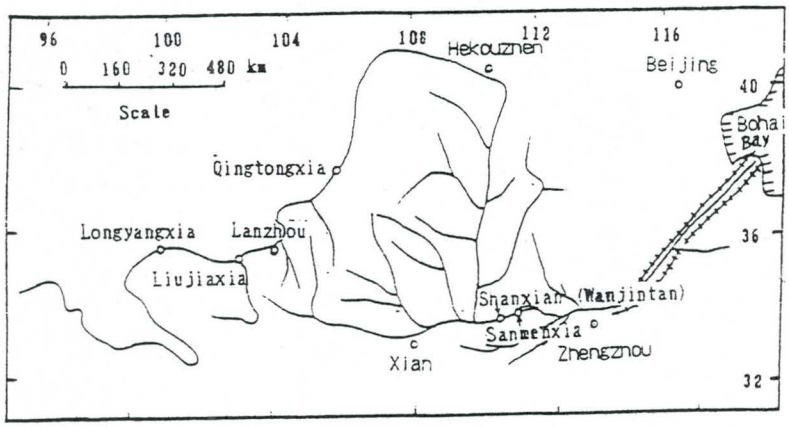

Figure 1.—The Yellow River Basin

Since the founding of new China (1949), eight hydraulic projects have been built in the main Yellow River. Hydro-electric resources and irrigation with the Yellow River water were developed. But because there was abovesaid 11-year low water period, it is not advantageous to the development of water resources and hydroenergy. Soon some new hydraulic projects will be built in

the main river and tributaries in the Yellow River, and industrial and agricultural water consumption will be further increased. It will make utilization and distribution of the Yellow River water resources more and more short

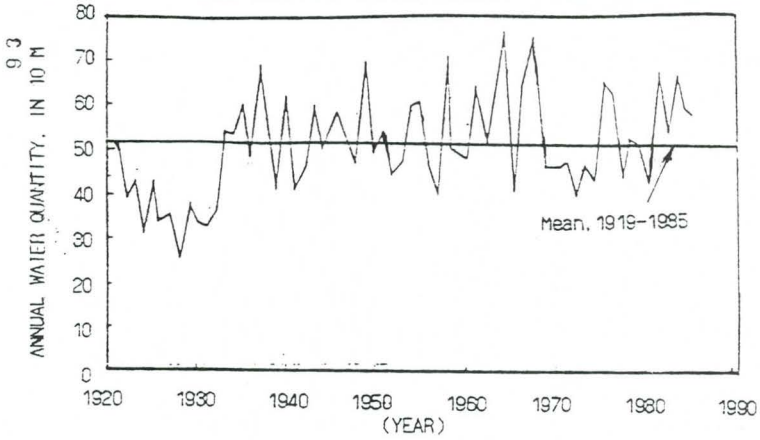

Figure 2.—Series of Shanxian station in the Yellow River

Table 1.- Measured and natural annual water quantity at Shanxian Station, 1922-1932

unit : $10^9 m^3$

year	1922 to 1923	1923 to 1924	1924 to 1925	1925 to 1926	1926 to 1927	1927 to 1928	1928 to 1929	1929 to 1930	1930 to 1931	1931 to 1932	1932 to 1933	average for 11 years	1919 to 1980 average
measured	34.1	39.1	26.7	38.6	30.0	31.9	19.8	33.4	29.3	27.7	31.4	31.1	41.4
natural*	37.8	42.8	30.4	42.5	33.6	35.7	23.9	37.7	33.7	32.1	35.8	35.1	50.2

*the natural year water quantity equals that the irrigation water quantity plus measuring year water quantity

Therefore,the problems of the 11-year low water period, especially its recurrence probability, is more and more important and has received a good deal of attention. Prof.Ding Jing has guided the section of stochastic hydrological calculation in this paper, and the authors express their deep thanks to him.

The western end of the Yellow River basin is the Bayankele Mountain in the Qinghai-Tibet plateau and the eastern part is to Bohai Bay. The area of the Yellow River basin is 752,000 km^2. The larger part of the Yellow River basin is located in the dry or semidry region of north-western China. Its annual average precipitation is 476 mm. The precipitation distribution gradually decreases from south-east to north-west. Annual precipitation in the southern end of the basin (northern slope of Qin Mountain) may be 800-900 mm, but in the northern end of the basin (Inner Mongolia) may be only about 150 mm. From Table 1.average annual runoff is 50.2* $10^9 m^3$. Average annual sediment discharge is 1.6* 10^9 T at Shanxian Station. The concentration of suspended load of the Yellow River is the largest in the world. Above 60% of annual water quantity and 80% of annual sediment load in the Yellow River are produced in the 4-month flood season from July to October. It may greatly increase short degree of the Yellow River water resources.

There are thousands of years of culture history in the Yellow River basin,

but in the world the Yellow River is famous for its serious flood disasters in the past. For thousands of years the people of the Yellow River basin have struggled against flood or drought disasters, so there are many historical relics that provide evidence about flood and drought disasters, and there are many flood and drought situation records in many geographical and historical references and works. For example, Li Daoyuan (466-527 A.D.), in the North Wei dynasty, recorded in his works that high water reached a level of 4 Zhang 5 Chi (about 10.9 m) on the stone cliff of the Yihe River, a tributary of the Yellow River, in 223 A.D. (Huangchu 4 year of Emperor Weiwendi). According to the level the flood peak discharge is calculated as 20,000 m^3/s . This data have been used in Lohun Reservoir at the upper Yihe River.

After founding of new China in 1949, hydrologists have discovered that there were seasonal water level scales at Qingtogxia of the upper Yellow River and at Wanjintan of the middle Yellow River in the beginning of the Qing dynasty (about 1700 A.D.). At present, annual records of the seasonal water level scales are collected as precious relics in the Forbidden City Museum.

Qingtongxia is at upper reaches of the Yellow River (see Figure 1), which may control 60% water quantity of the Yellow River. According to our textual research, the water level scale of Qing dynasty at Qingtongxia was set in 1709 A.D. (Emperor Kangxi 48 year). Wanjintan is at middle reaches of the Yellow River, which may control 90% water quantity of the Yellow River. Its water level scale was set in 1765 A.D. (Emperor Qianlong 30 year). These water levels were measured from July to October every year. When the flood level rose over one Chi (0.32 m), horses were rapidly ridden for passing on the information to the lower Yellow River, station by station, so that the people of the lower Yellow River could prepare struggling against flood. According to texual research, the Qingtongxia water level scale of Qing Dynasty was near the present Qingtongxia Hydrologic Station, which was set in 1939. The Wanjintan water level scale was set near the Shanxian Hydrologic Station.

Water measurements of Qing dynasty recorded and reported only the rising limb of the flood and not the falling limb. According to measurement data statistics, the water quantity of flood season may be over 60% the water quantity of the whole year, so relations between the flood rising Chi number of every year's flood season and the water quantity of whole year may be established at Qingtongxia and Shanxian Hydrologic Stations (See Figure 3 and 4). Then the water quantity and flood-drought situation of each year may be estimated from the measured water level data of Qing dynasty by use of Figure 3 and 4.

The relation on Figure 3 is rather good; its point distribution appears band shaped. This is because the rainfall area is very large, rainfall intensity is small, rainfall duration is rather long, which produces floods with duration of 30-40 days and with similar flood hydrograph shape in the basin area above Qingtongxia Station. The relation on Figure 4 is rather bad. Its point distribution appears in confusion. This is because the flood peaks at Shanxian Station are formed from short duration storms in the Hekouzhen--Shanxian subregion in the middle reaches of the Yellow River, its rising Chi number of flood depends on storm area, rainfall intensity etc. In some years its storm intensity was very large but duration was rather short. Flood peak was rapidly rising and falling. The rising water level of flood was high but water quantity of flood was not large, so the flood point on Figure 4 tend to the left side. In other years, the rising water level of flood was low but the quantity was large. The flood hydrograph had low and fat shape or there were many of flood rising events. So the flood point on Figure 4 tend to the right side.

The governor of Henan Province (as the head of a province at present)

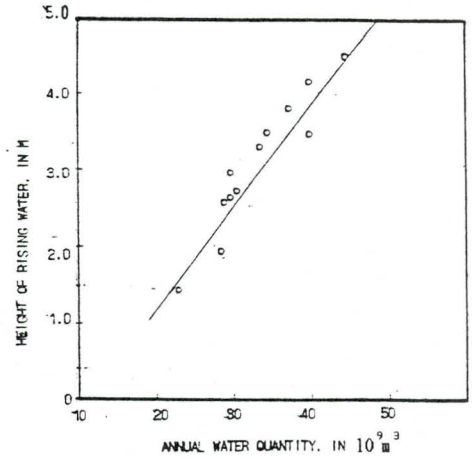

Figure 3.—Relation between the hight of the rising limb of the flood and the annual water quantity at Qingtongxia

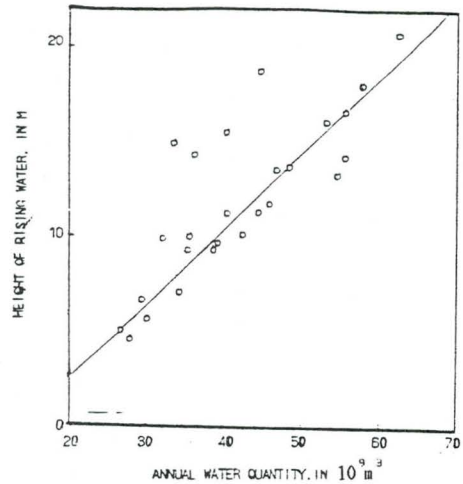

Figure 4.—Relation between the hight of the rising limb of the flood and the annual water quantity at Shanxian

Wu Zhongxi had reported to the Emperor in a letter the setting and measuring situation of Qingtongxia water level scale : ".....There are 10 Chinese words on the water level, the height of each word is 1 Chi (0.32 m), the water surface usually was one Zhang (3.2 m) from the bottom of the water level scale, but in this year the flood level has been one Zhang and eight Chi (5.76 m), its recurrence period is over 3 years. However, it is very rare that the flood submerges all the 10 words. " From the report, the highest word of Qingtongxia water level scale corresponded with 10 Chi (3.2 m), the zero point of the scale corresponded with low water surface and under the low water surface the water depth usually was one Zhang (3.2 m).

At present collected years in which there was measured data and rising water level are shown on Figure 5.

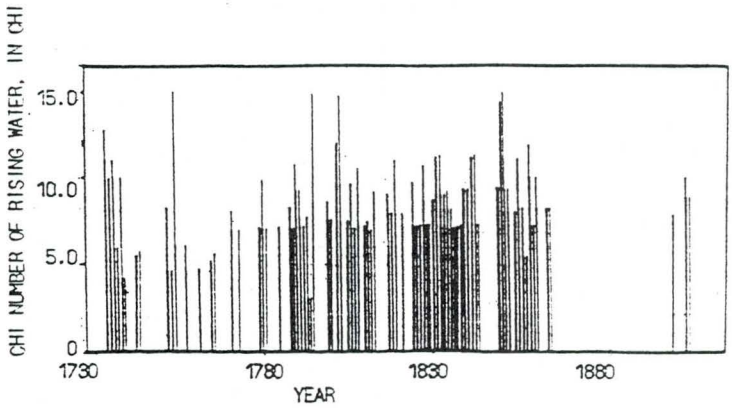

Figure 5.—Annual height of rising water at Qingtongxia, 1736-1860

Because Qingtongxia Station controls over 60% of water quantity in the whole basin, using rising water level data of each year in Figure 5, water quantity and flood-drought situation of each year may be estimated from Figure 3. It can basically represent the flood-drought situation of water quantity in the whole basin.

Through the above relations, the water quantity of each year in 1736-1860 A.D. can be estimated. The most plentiful water years were 1755, 1796 and 1850; their annual water quantity might be about $47*10^9 m^3$. The lowest water years were 1741 and 1749; their annual water quantity might be $20*10^9 m^3$. The average annual water quantity is $32.4*10^9 m^3$. During the period of measured annual water quantity at Qingtongxia Station 1939-1967, before operation of Liujiaxia reservoir, the most plentiful water years were 1946, with a $45.26*10^9 m^3$ water quantity, and 1967, with a $45.1*10^9 m^3$ water quantity; the lowest water year were 1965, with a $21.6*10^9 m^3$ water quantity, and 1941, with a $23*10^9 m^3$ water quantity. The average annual water quantity of the 29 years 1939-1967 was $31.9*10^9 m^3$. From contrast and analysis of above said annual water quantity characteristics, the flood-drought situation of annual water quantity that was estimated from water level data of Qing dynasty scale at Qingtongxia may be qualitatively credible.

According to the ratio of annual natural water quantity to average annual natural water quantity, the flood-drought situation can be divided 5 classes:

Table 2.- Definition of flood-drought classes

Annual quantity , percent of average	>=130	111-130	91-110	71-90	<71
Flood-drought class	very plenty	plenty	middle	low	very low

From Figure 5, it can be shown that there were many unmeasured water level years in 1736-1780 A.D., but measured data basically were continuous in the 80 years, 1780-1860 A.D., which had the longest (7 years) continuous low water period.

In 1860-1919 A.D. (Shanxian Station began measuring in 1919 A.D.) there were only a few years of measured data, so measured data of Wanjintan water level scale and the water regime reports of administrators are used for estimating the flood-drought situation in 1860-1919 A.D.

According to synthetic review of Wanjintan water level data and the reports of administrators, there was not more than 10 years long low water period in the water regime of 1860-1919 A.D. So it may be considered that the 11-year long low water period of 1922-1932 A.D. was the only 11-year-long low water period in 1780-1985 A.D. or 200 years.

In contrast to water regime of the Changjiang River and the Haihe River, the rain regime of coast area of south-eastern China, and the rainfall of Kashimir of west end of Qinghai-Tibet plateau, the 11 year continuous low water period of 1922-1932 A.D. could be attributed to weather situation abnormal in large scale.

Using stochastic hydrologic methods, a 10 thousand year runoff series was simulated based on the 70 year measured runoff series at Shanxian Station. The comparison between the measured series and simulation series with 10 thousand years is shown as Table 3.

From Table 3 the statistical characteristics of measured and simulated series are very close, except for skewness coefficient. Recurrence times and probabilities of continuous low water periods of different lengths in the simulated 10 thousand years runoff series are shown as Table 4.

From Table 4 the recurrence probability of an 11-year or longer continuous low-water period is about one time in 250 years.

At the Hongze Lake in the Huihe River Basin, adjacent to the Yellow River

basin, a water level scale has been set since 1736 A.D. and there are a lot of measured data (reference 2). Though many natural and artificial factors affected the water regime of the Hongze Lake, these data measured in 200 years can reflect the historical flood-drought situation of the Huihe River Basin. In the 200 years, of data the longest continuous low-level period was from 1922 to 1930 A.D., so the recurrence probability of the continuous low-level period also is one time in 200 years in the Huihe River.

Table 3.- Comparison of statistic characteristics between measured series and simulated series

series	average water quantity $10^9 m^3$	deviation coefficient Cv	skewness coefficient Cs	standard deviation	auto-relation coefficient r1	r2	r3
measured	50.22	0.237	0.421	11.90	0.252	0.237	0.439
simulated	50.25	0.238	0.501	11.98	0.265	0.240	0.436
relative error %	0.1	0.42	28.5	0.67	5.1	1.26	6.8

Table 4.- Recurrence intervals and probabilities of continuous low-water periods of different length

Length of low water period in years (L)	Accumulated number of occurrences >=L (n)	Accumulated probability	Recurrence interval in years (10000/n)
5	136	0.0136	73.5
6	104	0.0104	96.1
7	84	0.0084	119
8	73	0.0073	137
9	52	0.0052	192
10	46	0.0046	217
11	40	0.0040	250
12	26	0.0026	385
13	22	0.0022	455
15	11	0.0011	909

In some papers, scholars consider the changing period of sunspots to be 11 years, 22 years, century, and double century (reference3,4). The 200-year recurrence interval of the 11-year continuous low-water period in the Yellow River basin could be related with double-century period of sunspots by primary analysis, because the solar activities are a principal factor affecting atmospheric circulation and and long-term climate change.

Thus the recurrence period of the 1922-1932 year continuous low-water period in the Yellow River is at least 200 years, based on measured data of Qingtongxia and Wanjintan water level scale set in Qing dynasty, 250 years based on simulation by stochastic hydrologic methods, and 200 years based on solar activity period and large scale climatic background. Finally its recurrence period is determined as 200 years by synthetic choice.

After determining that the recurrence period of the 1922-1932 continuous low water period is 200 years, instead of 70 years since 1919, using extraordinary value calculating formula in hydrology we estimate average value and

Cv of annual water quantities at Shanxian, Lanzhou and Guide Stations again.

Supposing that the average value of 120 years water quantity before 1919 A.D. would equal the average value of present measured series without 1922-1932 low water period, we have:

$$\bar{X}=\frac{1}{N}(XN+\frac{N-11}{n}\sum_{i=1}^{n}Xi)$$

$$Cv=\{1/(N-1)*[\sum_{i=1}^{n}(XNi/\bar{X}-1)^2+(N-11)/n*\sum_{i=1}^{n}(Xi/\bar{X}-1)]^2\}^{1/2}$$

where XN is the sum of 1922-1932 A.D. year water quantity;
XNi is the annual measured water quantity from 1922 to 1932;
N is 200 years;
n equals the number of years in the measured series, minus 11.

Average values and Cv of this calculated results (N=200 years) and original results (N= 70 years) at Shanxian, Lanzhou and Guide Station is shown as Table 5.

Table 5.- Average value and Cv of 200 years and 70 years *

station	N = 200 years X ($10^9 m^3$)	Cv	N = 70 years X ($10^9 m^3$)	Cv
Shanxian	52.9	0.20	50.2	0.23
Lanzhou	34.3	0.19	32.7	0.22
Guide	21.8	0.22	20.4	0.22

* 200 years and 70 years are recurrence period of the 1922-1932 A.D. continuous low water period.

From Figure 5, when the recurrence period of the 1922-1932 A.D. sequent low-water period is considered as 200 year instead of 70 years, the average value of each station is increased and the Cv value is decreased. For example, the average value of Shanxian Station is $52.9*10^9 m^3$ instead of $50.2*10^9 m^3$, about 5% increased. Cv value is 0.20 instead of 0.23, so the series tends more stable. It is more important that the result of this paper makes us reassess flood-drought changing of water resources in the Yellow River Basin. So several feasible schemes for increasing using water index and hydroelectric index can be considered.

REFERENCES

1. Ding Jing, Deng Yuren, 1988, Stochastic hydrology: Press of Cheng Du University of Science and Technology, Chengdu.
2. Guo Shu, 1982, The water level at the Hongze Lake in two hundred years: The Proceedings of Water Conservancy and Hydroelectric Power Research.
3. Zhang Jiacheng, Zhu Mingdao and Zhang Xiangong, 1976, Climatic changing and its causes: Science Press, Beijing.
4. Wang Shaowu, Zhao Zongci, 1976, The foundation of long-term weather forecast: Shanghai Science and Technology Press.

ANALYSIS OF PERSISTENCE OF HYDROLOGICAL DROUGHT ON THE UPPER YELLOW RIVER, CHINA

Wang Weidi Sun Hanxian Shi Jiabin

Northwest Investigation and Design Institute, Xi'an, China

ABSTRACT

By using four kinds of hydrological data from observed, investigated, historical and synthetic series, a comprehensive analysis of drought persistence is made in this article. The results confirm that the persistence of hydrological drought on the upper Yellow River exists, that the 11-year drought from 1922 to 1932 did occur on the upper Yellow River. The frequency analysis for yearly runoff of various lengths of persistence has been made with synthetic series. It shows that the recurrence period of the 1922-1932 drought persistence is far larger than that estimated before.

INTRODUCTION

Drought persistence was found from analysis of the hydrological data of Shanxian (Sanmenxia) Gauge Station on the middle Yellow River. The persistence of the 11-year drought from 1922 to 1932 is especially remarkable. But there are not any hydrological data to verify whether there was also a synchronous or similar phenomenon on the upper Yellow River. In the catchment planning, this question becomes more important due to the existence of a multi-year regulated reservoir--Longyangxia Reservoir.

A joint group, consisting of members from six units (Beijing Investigation and Design Institute, Water Conservancy Committee of the Yellow River, Institute of Water Conservancy Research, Institute of Geography, Institute of Glacier and Frozen Earth, and Northwest Investigation and Design Institute, simplified as Six Units later on) carried out a thorough investigation, from June to August, 1968, along the upper and middle reaches of the river and offered a technical report.

While doing the computation of engineering hydrology for the Longyangxia Project, the Six-Units report was used to interpolate and extrapolate the observed series. As for the probability of this drought persistence, only a rough analysis had been made. A schematic drawing of the catchment is shown in Fig.1, and the drought of 1922 to 1932 is shown in Fig.2.

RELIABILITY OF THE EXISTENCE OF DROUGHT PERSISTENCE

Generality of Drought Persistence

The problem of drought persistence is a phenomenon of global nature. Drought persistence over vast areas have often occurred in the world. Some majority opinions have been obtained. Especially, the works of Hydrological Aspects of Drought (Beran and Rodier, 1985) have drawn some important conclusions on the basis of introducing many facts and by summarizing comprehensively the works done previously. Among them, the most important opinions are: a. Drought may last a long persistence period rather than a random event; b. In bydrologic data, the probability of a drought year following another drought year is larger than in a random series; c. Gauge station groups display more persistence than individuals;

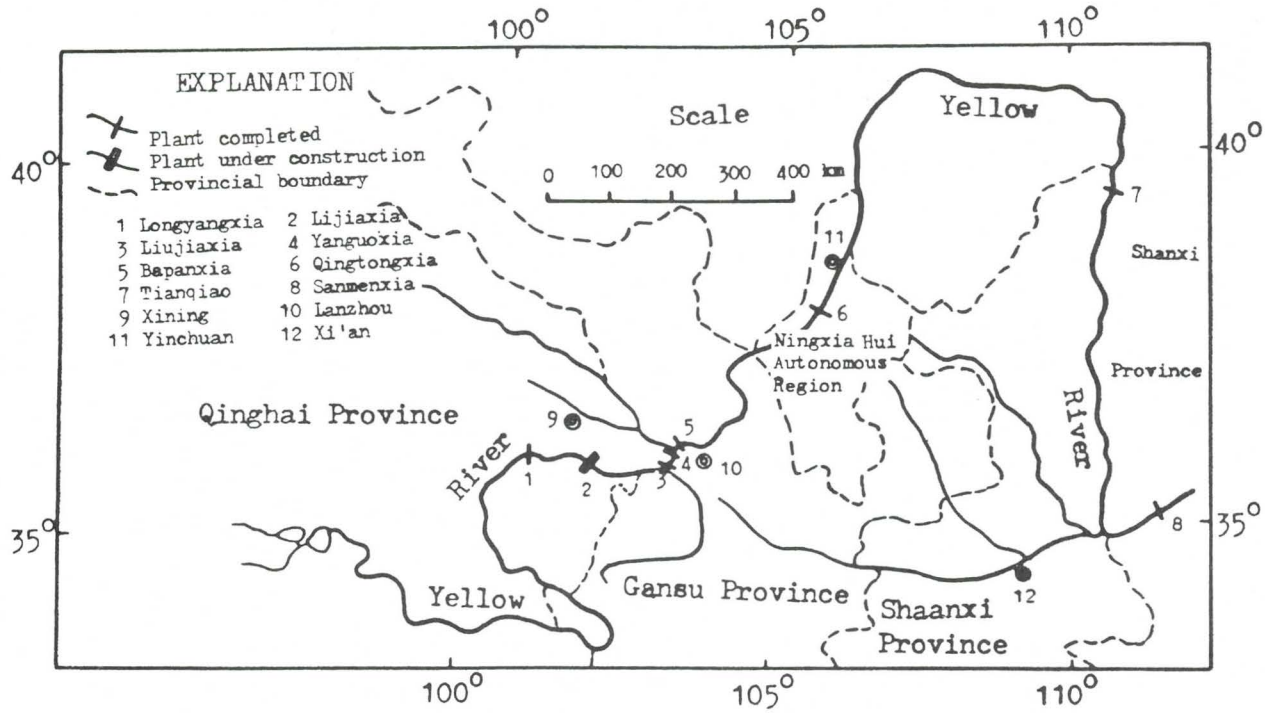

Figure 1. --Schematic drawing of the upper and middle Yellow River

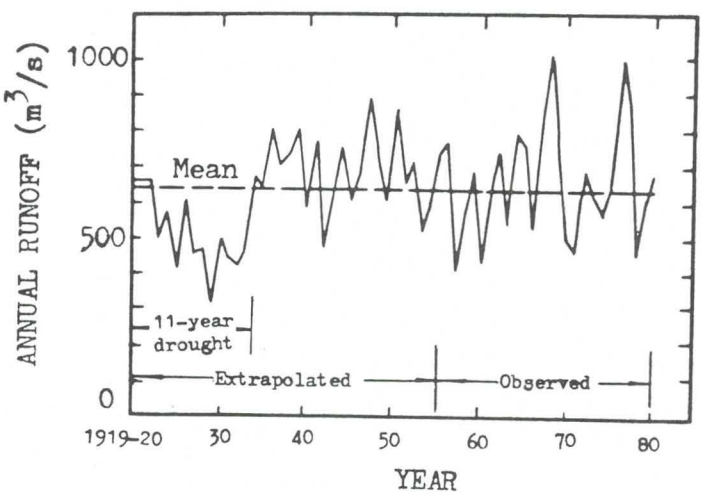

Figure 2. --Annual runoff process at Longyangxia

d. Drought persistence is more obvious in arid areas. These phenomena were also found in China. Hence, the 11-year drought persistence on the upper Yellow River is not a highly particular exception.

Investigation and Verification of the 11-year Drought Persistence

In 1968, a joint group of six units made a 3-month in-depth hydrological investigation (the Six-Units study) along the Yellow River from Shanxian Station at the middle reach to Maqiu Station at the upper reach. They visited 450

inhabitants and herdsmen and looked over many historical documents related with drought events. They divided water regimes into 5 degrees from wet to dry years (Table 1) and after analysis recognized that an 11-year drought persistence existed on the upper Yellow River synchronously with that on the middle reach.

Table 1. Classification of wet-dry degrees

Degree	Six-Units report	Deviation from mean Album	EXPLANATION
1	$1.30\bar{Q} \leqslant Q_i$	$(\bar{R}+1.17\sigma) \leqslant R_i$	Q_i--Yearly runoff, i-th year
2	$11.11\bar{Q} \leqslant Q_i < 1.30\bar{Q}$	$(\bar{R}+0.33\sigma) \leqslant R_i < (\bar{R}+1.17\sigma)$	$\bar{Q}$--Mean of yearly runoff
3	$0.91\bar{Q} \leqslant Q_i < 1.11\bar{Q}$	$(\bar{R}-0.33\sigma) \leqslant R_i < (\bar{R}+0.33\sigma)$	R_i--Precipitation, May to Sept.
4	$0.71\bar{Q} \leqslant Q_i < 0.91\bar{Q}$	$(\bar{R}-1.17\sigma) \leqslant R_i < (\bar{R}-0.33\sigma)$	for i-th year
5	$Q_i < 0.71\bar{Q}$	$R_i < (\bar{R}-1.17\sigma)$	$\bar{R}$--Mean of precipitation σ--Standard deviation

Later, in 1976, when doing the planning and designing for the Longyangxia Hydropower Project on the upper Yellow River, we rechecked the investigation report by the Six Units and recognized it fundamentallyreliable. From these data, the observed yearly runoff series of Guide Gauge Station, representative station for the project, are extrapolated. The feasibility of extrapolating the non-observed yearly runoff data from the middle Yellow River is based on the fact that there exist very close relationships between the series of the two reaches. The correlation coefficient between runoff at Lanzhou and Shanxian is 0.876 and that between Longyangxia and Lanzhou is 0.915. The total amount of yearly runoff at Lanzhou is nearly 62% of that at Shanxian in average, and the amount of Longyangxia is nearly 65% of that at Lanzhou. According to statistical analysis, the corresponding probability that the yearly runoffs of Shanxian and Lanzhou are simutaneously smaller than their mean values is as high as 96%.

A Historical Verification from Meteorological Data

The Album of Wet and Dry Years Distribution in China in the Recent 500 Years (Central Weather Bureau and Institute of Meteorology, 1981, simplified as "Album" later on) is a nationwide scientific cooperative work that provides a comprehensive compilation of historical data. We have discovered that some data from the Album may be taken as a powerful verification and complement for the conclusion of the report of the Six Units.

In the Album, there are some years of missing data due to very long ages of examination, especially in Northwest China. Among them, the data are best at Xi'an, fair at Lanzhou and Yinchuan, and poor at Xining. Nevertheless, they are still significant as an independent verification qualitatively. In the Album, the regimes are divided into five degrees from wet to dry years with wettest year for the 1st degree and driest year for the 5th degree (Table 1). Typical drought events over large areas for approximately 10-year persistence are identified and the average value of the four stations mentioned above is used as a synthetic index. Some conclusions drawn from this analysis are as follows:

1. The 1922-1932 drought is a long-persisting drought with vast areas. It fundamentallycorresponds with the yearly runoff process of Guide Station at the same period as shown in Fig.3. Except in 1931, all the points lie on the side of drought.

2. In Northwest China, there are other persistent drought years, and some of them are even longer in duration. For example, a 18-year persistence occurred in 1481-1498, a 16-year persistence in 1627-1642, a 13-year persistence in 1710 - 1722, and a 12-year persistence in 1857-1868. All of them show that the persistence in 1922-1932 is not an exception.

3. It is worthy to notice the example of the persistence in 1857 - 1868. In these 12 years, Lanzhou, Xining and Yinchuan experienced below-normal yearly rainfalls, but the rainfalls at Xi'an, situated in the middle Yellow River, were wet for 3 years, normal for 5 years and dry for 4 years. On the whole, it is not an obvious drought persistence of weather. Nevertheless, it is an hydrological drought of runoff on the middle Yellow River in the series of 232 years from the report of the Six Units. This shows that the drought persistence of runoff on the upper Yellow River seriously affects that of the middle Yellow River.

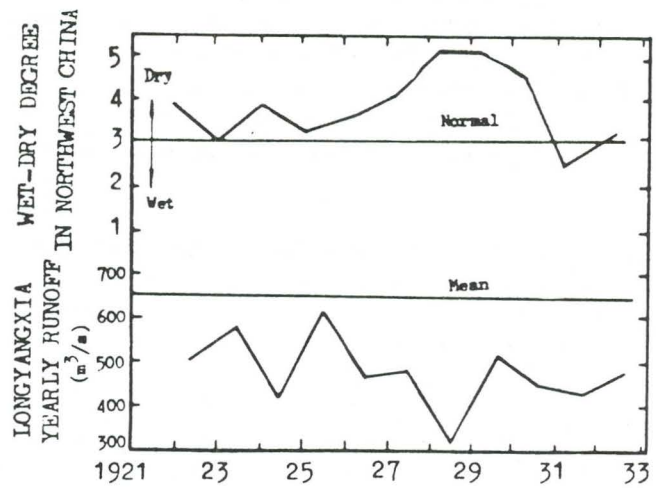

Figure 3. —Comparison of the processes of runoff and precipitation index on the upper Yellow River

FREQUENCY ANALYSIS FOR DROUGHT PERSISTENCE

Analysis Based on Observed and Historical Records

According to the observed series: Length of the series is 70 years, while there is only one occurrence of drought persistence longer than 10 years. The return period is nearly 70 years. According to the Six-Units Report: There are 232 Years of historical data of water regime with a few years missing. Drought persistence longer than 10 years occurred 3-4 times. Hence the return period is nearly 60-80 years. According to the Album: There are 4-5 times of occurrences of more than 10-year drought persistence in 500 years; hence the return period is nearly 100-125 years.

The three results given above offer a fuzzy view point of the return period of the drought persistence. Although they have important meaning for reference, they are of little use in hydropower design because they lack a relationship with the severity of drought.

Analysis Based on Synthetic Series

Generation and Checkup of the Synthetic Series of Yearly Runoff

Because the yearly runoff at the upper Yellow River is comparatively steady with small variance, a simple autoregressive model of lag-one is adopted:

$$Q_t = \bar{Q} + R_1 (Q_{t-1} - \bar{Q}) + T_t S(1-R_1^2)^{1/2} \qquad (1)$$

where Q_t is the synthetic yearly runoff in the t-th year, $\bar{Q}$ is the mean value of the observed yearly runoff, R_1 is the lag-one correlation coefficient of the series, S is the standard deviation of the series and T_t is the stochastic variable of normal distribution after skew modification (Sun and Wang, 1986).

A series of yearly runoff for the Longyangxia Project was thus generated with a length of 10150 years. A statistical checkup are shown in Table 2 and 3.

Table 2. Statistical examination of synthetic yearly runoff series of the Longyangxia Reservoir inflow

Series	mean value (m^3/s)	Cv	Cs	R_1
Observed	649.8	0.233	0.261	0.298
Synthetic	650.1	0.233	0.223	0.313

Table 3. Comparison of transition probabilities for observed and synthetic series of the Longyangxia Reservoir inflow

Wet-dry degree	1	2	3	4	5
1	22.8/33.3	30.3/33.1	29.7/16.7	15.0/16.7	2.3 /0
2	15.4/0	27.7/33.3	32.3/20.0	19.7/40.0	4.9 /6.7
3	9.0/16.7	22.1/27.8	32.9/33.3	26.4/16.7	9.6 /5.6
4	5.6/ 6.2	16.6/18.7	32.7/37.5	30.2/18.7	15.0/18.7
5	3.0/0	12.9/0	25.9/33.3	36.2/50.0	20.1/16.7

Note: Numerator--synthetic series; Denominator--observed series.

Frequency Analysis of Yearly Runoff Drought Persistence

In the synthetic series of 10150 years, n-year-mean value ($\bar{Q}n$)of persisting Periods n=1, 3, 5, 8, 11 and 15 years are calculated and they are arranged in order from small to big values for each sub-series of n persisting years. Data groups (drought events) for each sub-series are selected such that the mean value $\bar{Q}n$ is equal or less than the mean value $\bar{Q}_n$, i.e. $\bar{Q}_n \leq \bar{Q}_n$, forming a partial series. The empirical frequency P and corresponding return period T are calculated by the formula of mathematical expectation:

$$P = M/(N+1) \qquad (2)$$

and

$$T = (N+1)/M \qquad (3)$$

where M is the order of arrangement of a certain persistence series and N is the total years of the synthetic series, i.e. 10150.

Ploting mean flows of n-year drought persistence against P or T, a group of frequency curves may be established (Fig.4), by which design values for reservoir and water energy may be obtained quantitatively.

PRELIMINARY EXAMINATION OF RESERVOIR AND WATER ENERGY DESIGN FOR THE LONGYANGXIA PROJECT

The Longyangxia Hydropower Project is situated on the main branch of the upper Yellow River, Qinghai Province, China. The catchment area is 131420 km^2 with a mean flow of 650 m^3/s. The damheight is 178m with a total reservoir capacity of $27.6\times10^9 m^3$, of which the effective capacity amounts to $19.35\times10^9 m^3$, with a coefficient of reservoir capacity up to 0.94. The project is equipped with an installed hydroelectric capacity 1280 MW. It was completed in 1989 and operates satisfactorily.

The representative gauge station, Guide, was established in 1954. The yearly runoff series was extended to 1919. The return period of 1922-1932 drought was roughly estimated to be 60 years. Among the 11 years, the yearly runoff of the first 6 years was taken as design standard and the following 5 years as a power-reducing period. Correspondingly, the total reservoir capacity was divided into three parts: the yearly regulation capacity, the multi-year regulation capacity, and the reserve capacity, for which the reduced-output period was designed and which occupies a considerable percentage of the total capacity.

The return period of the mean flow 478m^3/s of the 11-year drought persistence is nearly 1000 years according to Fig.4. The severity of that drought is extremely rare. Taking its return period as 60 years, the length of the observed record, is obviously too short. But what is the reliability of taking its return period as long as 1000 years?

In addition to the fair preservation of statistical characteristics of the synthetic series, the authors also compared the drought severity with those of the famous drought persistence on 13 large river catchments in China. If the severity is expressed with the coefficient of deviation Qn/Q_N, the drought persistence from 1922 to 1932 on the upper Yellow River is the second most severe event, except for one more severe persistence which occurred on the Song-Hua River in Northeast China.

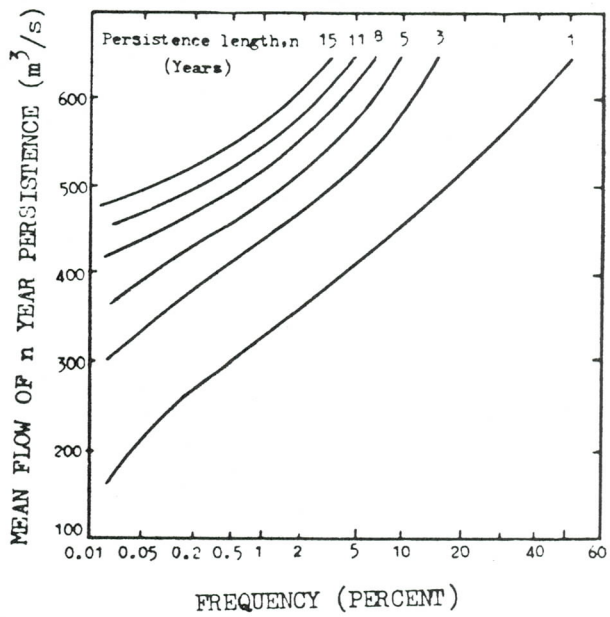

Figure 4. —Frequency curves of simulated annual runoff for n-year drought persistence at Longyangxia

The deviation coefficient of the 11-year persistence on the upper Yellow River is 73.5 % while the average value for the 13 rivers is 81.2%. If the coefficient of deviation be raised from 73.5% to 81.2% with its corresponding average yearly runoff raised from 478m^3/s to 527 m^3/s, the return period would be only 180 years.

REFERENCES

Beran, M.A. and Rodier, J.A., 1985, Hydrological Aspects of Drought, P.5-11: Studies and reports in hydrology, Unesco/WMO, 1985.

Central Weather Bureau and Institute of Meteorology, China, 1981, Album of Dry and Wet Years' Distribution in China in the Recent 500 Years: Cartographic Publishing House, Beijing.

Sun Hanxian and Wang Ruishen, 1986, On Runoff Stochastic Modeling for the upper Yellow River and Its Preliminary Application, (in Chinese): Hydrology, v.5, p.10-18.

TOPIC E

WATER-RESOURCE MODELING AND MANAGEMENT

RESERVOIR SIZING CRITERIA FOR BUREAU OF RECLAMATION PROJECTS

Eldon L. Johns, P.E.

Bureau of Reclamation, Denver, Colorado

ABSTRACT

Fundamental to project formulation and engineering is the hydrologic analysis used to arrive at the optimum reservoir size. The Bureau of Reclamation reservoir sizing criteria were developed following generally accepted engineering methods, based on many years of experience on a large number of projects. However, some of the criteria are based on heuristic guidelines, and the origins of these guidelines were never formally documented. The existing reservoir sizing criteria were recently reviewed (CH2M Hill, 1990) and were found to be adequate for most preliminary studies. Presently the existing irrigation shortage criteria allow for a 50 percent water shortage in a single critical year and/or an accumulative shortage of 100 percent in 10 consecutive years. Municipal and industrial water users would suffer no appreciable shortages. In the case of advanced or detailed studies, the following changes were recommended: In the future, these heuristic rules may be replaced by the use of an economically based model that will measure the economic impact of various shortage levels. Other changes under consideration include (1) using stochastic hydrology in place of deterministic hydrology, and (2) requiring municipal, industrial and other uses to share in any anticipated shortages.

INTRODUCTION

The United States Bureau of Reclamation (Reclamation), an agency within the United States Department of the Interior, has responsibility for water and related land resource development and management in the arid Western United States. Increased emphasis has been placed on efficient project planning and operation. Reclamation has therefore undertaken a research program to determine whether changing reservoir sizing criteria would improve the economic viability of planned projects. A recent review (CH2M Hill, 1990) covered the following aspects of Reclamation reservoir sizing procedures: (1) water supply or inflow hydrology, (2) estimates of project water requirements, (3) estimates of reservoir losses, and (4) reservoir operating criteria. Each of these factors is discussed below.

WATER SUPPLY HYDROLOGY

Deterministic hydrology has been used for almost all water resource studies up to this time. This type of hydrology has the advantage of being easily understood and is readily accepted. However, a crucial problem that

periodically presents itself is the lack of a complete or adequate historical record. For example, streamflow records may not exist for a critically low-flow period such as the 1930's. A key question is how much streamflow data is needed to properly portray the water supply and anticipated reservoir operation with that water supply. Although specific Reclamation criteria do not exist, there are "common sense" rules that apply. There should be enough data to cover both periods of high and low runoff or supply. The data set should also be adjusted for historical depletion so that the entire period of record reflects either no development (virgin condition) or present development. The virgin condition data set can be adjusted to any desired level of development in the operation study. The data set that is adjusted to present level can be used directly with no further adjustment, but has to be adjusted periodically to bring it up to date. Examples of situations where adjustment may be needed would be for irrigation development over a period of time, where a storage impoundment was constructed above the gauging station, or to reflect changes in base flow due to ground water pumping. Stochastic generation of flow data (Lane and Frevert, 1988) may be appropriate in cases when historical (gauged) data are extremely limited. It may allow consideration of extreme conditions that are not in the historical record, although stochastic generation of water supply quantities usually removes some of the "coarseness" found in historic flow patterns. Future Reclamation studies will incorporate more stochastic analyses. Missing or incomplete data can also be estimated from correlations with nearby weather stations or stream gauges.

PROJECT WATER REQUIREMENTS

Accurate estimates of project water requirements are essential for proper reservoir sizing. (It is beyond the scope of this paper to discuss the water requirement estimating procedures in detail.) The water requirements can be furnished by the project sponsor or be derived from theoretical procedures. Many of the estimating procedures are empirical in nature. Examples of such methods used to estimate irrigation water use are the Blaney-Criddle Method, Jensen-Haise Method and Penman Method (Jensen, 1983). Irrigation water requirements exhibit both seasonal and year-to-year variation in most situations. An exception is the extreme arid areas such as southern Arizona or California where effective rainfall is negligible and temperatures vary little from year to year; in this area a single typical yearly demand pattern can adequately represent any or all years in a hydrologic sequence. However, in areas where temperature and rainfall do vary from year to year, it is important to reflect this variation in the reservoir sizing analysis. Municipal or industrial water requirements are generally supplied by the water using entity and are often based on population growth projections and per capita water usage. These too can have significant seasonal and year-to-year variation, particularly where lawn and garden irrigation is significant. Water requirements must also be estimated or determined for other project functions such as instream flows.

RESERVOIR LOSSES

In many cases reservoir losses are minor. Nevertheless, the estimates of these losses should be as accurate as possible. Evaporation is the largest

loss from most reservoirs. It can be estimated based on National Weather Service evaporation pan data, adjusting these to lake or free water surface conditions. Appropriate adjustments may also be made to account for the pre-reservoir evaporation losses from the reservoir area. It should also be kept in mind that the amount of evaporation will vary directly with the surface area of the reservoir, which varies with the amount of water in storage. Seepage loss depends upon geologic conditions, type of dam and height of dam. Like evaporation, seepage varies with the amount of water in storage. Estimates of seepage can be based on experience considering similar dams and geology. Once a reservoir is in place, the evaporation and seepage losses from a reservoir can be determined or verified using an inflow-outflow budget for the reservoir. Generally these losses are not large relative to the total amount of water involved in the budget. In many cases, these losses can be estimated simply as a percentage of the reservoir inflow. The reservoir losses discussed above are water supply losses and are relatively constant throughout the project life. In contrast, the loss due to reservoir sedimentation is a loss of storage space and this loss accumulates throughout the life of the project. Techniques for estimating the reservoir storage loss due to sedimentation are found in a Reclamation technical guideline (Strand and Pemberton, 1982). Reclamation requires that provisions be made for sediment storage space whenever the anticipated sediment accumulation during the economic life of the project exceeds five percent of the total reservoir capacity. A 100-year period of economic analysis and sediment accumulation is typically used. In planning studies simulating the operation of a reservoir, an average (50 year for a 100 year economic analysis) value can be used for the sediment accumulation. If the reservoir location has unusual geologic conditions that may result in significant bank storage this may have to be taken into account. Examples include karst limestone or sandstone formations. The actual amount of storage in such formations may have to be determined from water budgets.

RESERVOIR OPERATING CRITERIA (OPERATION STUDY)

Operation studies are conducted to simulate the contemplated project operation and to size the reservoir(s). These are water budget or water-accounting models which operate on a monthly time increment. Some are generic computer models but in most instances a simulation model must be custom-tailored for specific physical situations. An example of a typical operation study can be found in a recent project planning report (U.S. Department of the Interior, 1979). The simulation model compares project water supply with project demand, accounting for losses and constraints. The constraints can be physical, such as maximum reservoir size or a tunnel or channel capacity. The constraints can also be legal or institutional, such as downstream water rights or minimum flows for instream uses. The operation study is used to determine the project water supply shortage. By simulating reservoir operations for a number of scenarios of varying demand and reservoir size, for example, the "optimum" reservoir size is determined. Of all the parameters that affect reservoir size, water supply shortage criteria seemed to merit the principal focus of the review. The following discusses existing Reclamation planning criteria.

Sizing a project to supply 100 percent of the projected water demand for all uses at all times is generally not economical. Consequently, a small degree

of acceptable water supply shortage during drought periods improves the economic justification. The recent review (CH2M Hill, 1990) revealed that longstanding heuristic "guidelines" had been relied on almost universally by Reclamation engineers and hydrologists. The guidelines allow an irrigation shortage of 50 percent of the annual demand in the most critical year and a maximum cumulative shortage of 100 percent of the annual demand in a consecutive 10-year period. The criteria also allow no municipal and industrial shortages. Although specific shortage criteria were not formally documented, it is in evidence in numerous planning reports and in some guidelines. Shortage criteria for other project purposes such as instream flow were not quantified, although it was generally acknowledged that shortages would have to be experienced under certain conditions. It should be kept in mind that infrequent shortages, even if they are severe, are likely to be tolerated. Frequent, nuisance-like shortages will not be tolerated. Even though the shortage criteria may be met, numerous small shortages will probably be unacceptable to the water users. Therefore, certain discretion must be used by the hydrologist or engineer in determining the exact shortage criteria. The following illustrates another way that shortage criteria can be tailored to specific situations. Perennial crops, especially those having high investment costs, such as orchards or vineyards, may require less severe shortage criteria. There have been instances where shortages were limited to only 25-30 percent in the most critical year for orchards. This demonstrates early attempts to tie the shortage criteria to economics.

Recently, significant advances have been made toward a means of measuring the economic losses due to water supply shortages. A linear programming model (CH2M Hill,1990) was developed to accomplish this. The key to the model is the use of production functions that describe the incremental amount of production resulting from an incremental increase in the amount of irrigation water applied. The model also accounts for certain management strategies that may be employed by irrigators in critical drought years. For example, an irrigator may elect to use a limited water supply only on the crops that would net him the highest return. Little or no water would be used on lower return crops or crops that are more drought tolerant, such as alfalfa, while crops having a high economic investment, such as orchards, would be fully irrigated. Chances are the alfalfa would not die, although a number of cuttings (harvests) may be lost. The incorporation of such management strategies makes the model results more realistic. The use of this economic model together with the operation study allows the water supply shortage criteria to be tailored to the unique conditions of individual projects. Eventually, when a large number of reservoirs are successfully sized using the economic model, enough data will be gathered to revise the heuristic rules.

Reclamation's criterion allowing for essentially no municipal and industrial shortages is similar to that of other agencies and has been widely used in the past. Various water resource agencies now believe that some municipal and industrial shortages, especially in the outside residential water use, should be allowable. This was evidenced by voluntary conservation measures and cutbacks experienced by many municipal and industrial users during the severe droughts of the 1970's. Some believe that the municipal and industrial users should share shortages equally with all other users. The aforementioned economic model could be employed to evaluate these shortages as well. Recent legislation in various Western States allows instream minimum flows to be established. In most cases, it is expected that this use will experience

shortages along with other users. It may be more difficult to evaluate shortages related to instream flow uses using only economic tools, however.

CONCLUSIONS

The shortage criteria and reservoir sizing procedure review will be considered in future Reclamation planning and in evaluating the operation of Reclamation projects. Consideration will be given primarily to: (1) increasing the use of stochastic techniques, (2) requiring users other than irrigators to share to some degree in a water supply shortage (this would include municipal and industrial and instream flow uses), and (3) use of the economic optimization model developed by CH2M Hill to assist in determining the appropriate shortage level for each user sector and for local project conditions. The heuristic rules will continue to be used, primarily in preliminary studies, until experience is gained with the alternative methods explained above.

REFERENCES CITED

CH2M Hill, 1990, Review of Water Supply Shortage Criteria and Reservoir Sizing Criteria; Summary Report and four appendixes: United States Department of the Interior, Bureau of Reclamation, Denver, Colorado.

Jensen, M. E.(Ed.), 1983, Design and Operation of Farm Irrigation Systems: American Society of Agricultural Engineers Monograph No. 3, ASAE, St. Joseph, Michigan, pp 189-232.

Lane, W. L. and Frevert, D. K., 1988, Applied Stochastic Techniques User's Manual: United States Department of the Interior, Bureau of Reclamation, Denver, Colorado.

Strand, R. I. and Pemberton, E. L., 1982, Reservoir Sedimentation - Technical Guideline for Bureau of Reclamation: United States Department of the Interior, Bureau of Reclamation, Denver, Colorado.

United States Department of the Interior, 1979, Definite Plan Report, Animas-La Plata Project, Colorado-New Mexico. Appendix B, Water Supply: Water and Power Resources Service (Bureau of Reclamation).

QUANTIFYING MARKETABLE HYDROPOWER AT RECLAMATION POWERPLANTS GIVING RECOGNITION TO PERIODS OF DROUGHT

Craig R. Phillips

Bureau of Reclamation, Denver, Colorado

ABSTRACT

The quantities of electrical energy committed for delivery from Bureau of Reclamation hydroelectric powerplants are determined by using computer simulations to estimate future generation and by selecting generation to be committed based on acceptable risk levels. The occurrence of particularly severe drought periods may raise questions of whether the hydrologic record used to determine existing resource commitments contained droughts of comparable severity. Examination of circumstances for two Bureau of Reclamation projects for which the recent droughts have been especially severe (Central Valley Project and Colorado River Storage Project) reveals that, although generation has been at adverse levels (near the most severe anticipated), generation during the droughts appears to have been within the range of expectations considered in previous computer simulations. If the current droughts persist, however, clear effects on average energy expectations are likely.

INTRODUCTION

The Bureau of Reclamation (Reclamation) has about 50 hydroelectric powerplants in operation in its five regions of the 17 western states. These plants have a combined capacity of about 14,000 MW (Megawatts) and have generated an annual average of about 20,000 GWh (Gigawatthours) over the past 80 years. Average generation for recent periods has been greater since more plants exist today than existed in the earlier years. In the past 10 years, annual generation has ranged from 36,000 to 59,000 GWh. The Figure 1 map shows the locations of Reclamation's hydro plants and the boundaries of its five regions: the Pacific Northwest (PN), Mid-Pacific (MP), Lower Colorado (LC), Upper Colorado (UC), and Great Plains (GP) Regions.

The electric power generated at Reclamation's hydro plants is marketed to wholesale customers by the Western Area Power Administration (WAPA) and the Bonneville Power Administration (BPA). BPA markets power generated in the Pacific Northwest Region and WAPA markets power generated in Reclamation's other regions.

Each of these Power Marketing Administrations (PMAs) estimate the future availability of capacity and energy from Reclamation's hydro plants to enable the preparation of contracts for "firm" commitments to deliver electrical energy. Risk assessments must be made, based on analyses of possible future hydrological patterns and resulting electrical generation, in order to quantify the generation to be provided as firm. The power marketing contracts contain provisions regarding responsibilities for obtaining alternative power supplies during periods of low generation due to low water supplies. The occurence of especially severe and/or lengthy drought periods may raise

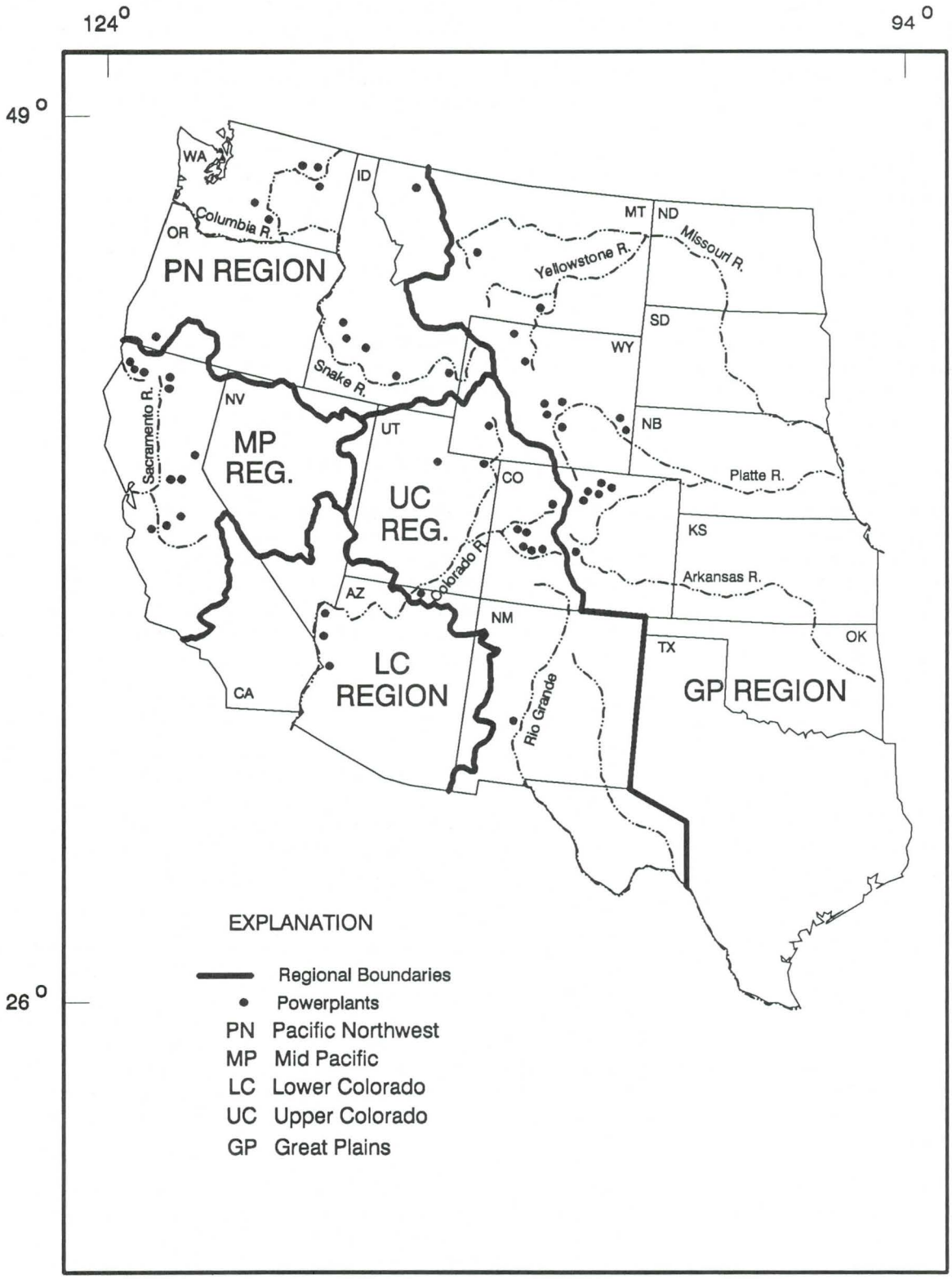

Fig. 1. Bureau of Reclamation Regional boundaries and hydropower plant locations

questions of whether events of such severity were considered in previous projections of available resources or whether incorporation of the new drought information into the hydrologic data base would affect estimates of available electrical resources. Therefore, when such severe events occur, a re-examination of expected power resources, incorporating the new drought information, can be instructive.

This paper discusses procedures used in determining marketable firm energy for two example projects within WAPA's marketing area. Recent droughts have been particularly severe for those two projects -- the Central Valley Project (CVP) in California's Sacramento River Basin and the Colorado River Storage Project (CRSP) in the upper Colorado River Basin. Perspective is provided on the severity of the recent droughts in light of historic water supplies. Next, generation by those projects during the recent droughts is compared to previous projections of energy generation. Finally, conclusions are drawn regarding the impact on energy projections of incorporating the new drought information into the hydrologic data base.

QUANTIFYING FUTURE ENERGY GENERATION

The amount of electrical energy available on a long-term basis from Reclamation's powerplants is typically quantified through joint efforts between Reclamation and the PMAs. Reclamation's river basin computer models are often used in projecting the availability of energy (Bureau of Reclamation, Mid Pacific Region, Simulation Model H164; and Upper Colorado Region, Colorado River Simulation System). WAPA then typically determines the amount of the electrical resource to commit contractually, based on risk assessments (WAPA, 1989). Long-term firm energy commitments are most often based on the "average" energy projected by the computer models.

CVP power is marketed by WAPA's Sacramento Area, the boundaries of which generally correspond with those of Reclamation's Mid-Pacific Region. The power is generated by Reclamation powerplants in the Sacramento and Trinity River basins. CVP firm energy is marketed on an annual basis. There are 10 CVP powerplants ranging in capacity from 578 MW at Shasta Powerplant on the Sacramento River to 17 MW at Nimbus Powerplant on the American River. Total CVP capacity is 2,038 MW.

CRSP power is marketed by WAPA's Salt Lake City Area, the boundaries of which generally correspond with those of Reclamation's Upper Colorado Region. The power is generated by Reclamation powerplants in the Upper Colorado River basin. The firm energy is marketed on a seasonal basis with the winter season running from October through March and the summer season running from April through September. Six powerplants produce power marketed by the CRSP. They range in capacity from 1,300 MW at Glen Canyon Powerplant on the Colorado River to 13 MW at Fontenelle Powerplant on the Green River. Total project capacity is 1,715 MW.

Figure 2 shows the expected energy generation frequencies from the computer simulation studies (WAPA, 1989) for each of the projects. The CVP generation is based on an 82-year simulation study, using 1899 to 1981 hydrologic data. The CRSP generation is based on a 78-year simulation study, using 1906 to 1983 data. (1981 and 1983 were the most recent years for which the computer model data bases had been updated). The projected average generation for the CVP and CRSP, based on the simulation studies, is shown in Table 1.

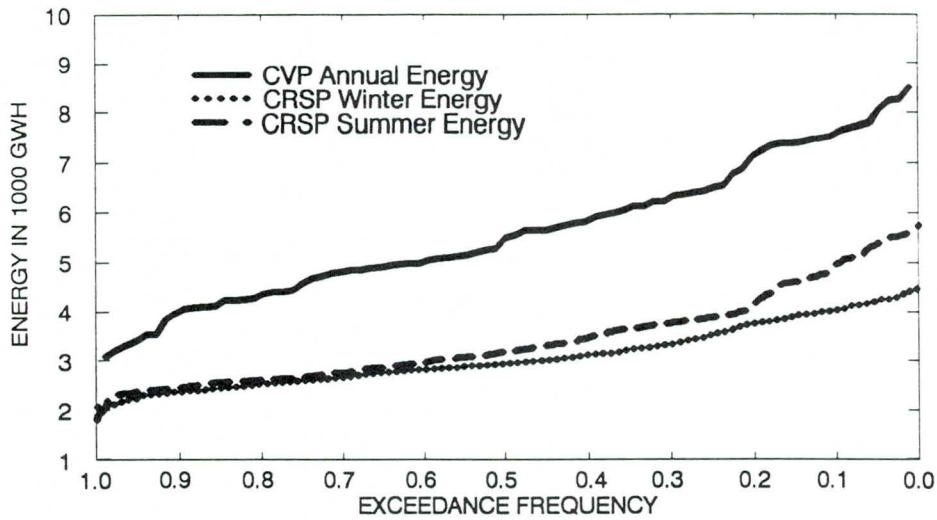

Fig. 2. Expected Frequencies for Energy Generation

Table 1. Computer Model Estimated Generation at Reclamation Hydro Plants (GWh)

Project	Estimated Average Generation		
	Winter	Summer	Annual
Central Valley Project	--	--	5,616
Colorado River Storage Project	3,058	3,424	--

RECENT DROUGHT CONDITIONS

The current drought began in 1987 for the Sacramento River Basin and in 1988 for the Colorado River Basin. The average natural flows prior to the droughts were 18.29 maf (million acre-feet) for the Sacramento River Index (combined estimated flow for four Sacramento River tributaries) and 15.34 maf for the inflow to Lake Powell in the Colorado River basin (Colorado River at Lees Ferry). The estimated natural streamflows during the recent drought years are compared in the following table with historic minimums and averages:

Table 2. Estimated Natural Flows During Recent Drought Years [maf, million acre feet] 1/

Item	Sacramento R. Index		Colorado R. at Lees Ferry	
	(maf)	(Percent of Average)	(maf)	(Percent of Average)
Drought Years:				
Water Year 1987	9.20	50	--	--
Water Year 1988	9.19	50	11.20	73
Water Year 1989	14.79	81	9.14	60
Water Year 1990	9.20	50	8.50	55
Average for Drought Period	10.60	58	9.61	63

Period Prior to Drought:				
Average	18.29	--	15.34	--
Minimum	5.13 (1977)	--	5.02 (1977)	--
Avg.-Low 3-yr period	--	--	9.61 (1988-90)	--
Avg.-Low 4-yr period	9.19 (1931-34)	--	--	--

1. To convert acre feet to cubic meters multiply by 1,233.5

For the Sacramento River Index, the four-year drought of 1987-1990 was the fourth worst of record, with 1931-1934 (9.19 maf average), 1929-1932 (10.28 maf), and 1930-1933 (10.42 maf) having more severe averages. (Note that these droughts all were contained in the 1929-1934 drought period). The 1988-1990 drought in the Colorado River Basin set a new 3-year record. The previously most severe three-year droughts in the Colorado River basin were those of 1953-1955 and 1954-1956 with average annual supplies of 9.79 and 9.89 maf, respectively.

HYDRO GENERATION DURING DROUGHT

The effect of these droughts on hydro generation is summarized in the following table. The energy generated by the CVP and CRSP during the recent drought years is shown in GWh along with the percent of average, based on the computer models' projected averages.

Table 3. Reclamation Project Generation, 1987-1990
[GWh, Gigawatthours]

Year	CVP (Annual)		CRSP (Winter)		CRSP (Summer)	
	GWh	Percent of Average	GWh	Percent of Average	GWh	Percent of Average
1987	4,346	77	--	--	--	--
1988	3,766	67	2,831	93	2,400	70
1989	3,714	66	2,048	67	2,648	77
1990	3,197	57	2,026	66	2,525	74
AVERAGE (for drought period)	3,756	67	2,302	75	2,458	72

These values demonstrate that the generation of electrical energy has been affected substantially by the droughts in the Sacramento and Upper Colorado River Basins. CVP generation has ranged from 57 percent to 77 percent of average during the drought. Exceedance frequencies for the CVP energy, based on Figure 2, range from near 78 percent in 1987, to near 90 percent in 1988 and 1989, and near 99 percent in 1990. CRSP energy has been mostly in the 60 and 70 percent of average range. CRSP winter energy exceedance frequencies, based on CRSP frequency projections, range from near 60 percent in 1988 to near 99 percent in 1989 and 1990. CRSP summer energy figures have all been near the 80th percent exceedance level.

A cursory analysis (using weighted averages) of the effect of the drought-period generation on the long-term average generation is shown in the following table. This analysis suggests some possibly measurable effects on

long-term average generation by the recent droughts. However, caution should be exercised in using such a cursory evaluation, especially because several years in the 1980s prior to the onset of the drought were especially wet. Those years were not incorporated into the computer simulations and would likely have a positive effect on the average generation.

Table 4. Estimated Effect of Drought-Period Generation on Long-Term Average [GWh, Gigawatthours]

	CVP (Annual)	CRSP (Winter)	CRSP (Summer)
Simulation Model Average Generation (GWh)	5,616	3,058	3,424
Number of Years in Simulation (years)	82	78	78
Recent Drought Years Average Generation (GWh)	3,756	2,302	2,458
Number of Recent Drought Years (years)	4	3	3
Weighted Average Generation (GWh)	5,529	3,030	3,388
Difference from Computer Simulation			
in Gigawatthours	-87	-28	-36
in Percent	-1.55	-0.92	-1.05

SUMMARY AND CONCLUSIONS

Generation has been reduced in the CVP and CRSP as a result of the recent droughts. The Sacramento River Basin streamflow has been 58 percent of average for the recent four-year drought period, and the CVP generation has been 67 percent of average for the drought period. The Colorado River Basin streamflow has been 63 percent of average during the recent three-year drought period, and the CRSP generation has been 75 percent of average. Also, for both the CVP and CRSP, exceedance frequencies indicate that some of the generation events are quite rare, with exceedances above 90 percent. The generation is less adverse than streamflow, likely reflecting a benefit of storage.

Examination of the hydrologic record shows events more severe than or nearly approaching the severity of the recent droughts. As a result, recent levels of generation likely fall within the range of expectations considered in the PMAs' risk analyses of marketable resources. However, the duration combined with the magnitude of the droughts may have led to measurable effects on the long-term average generation expected from the projects. Nonetheless, such conclusions are only speculative without incorporation of the wet periods of the 1980s along with the drought periods into computer simulation studies.

With such information, it is unlikely that a reexamination of the hydrologic bases for quantifying marketable resources would be essential at this time. However, with persistence of current drought conditions, such a reexamination may be in order.

REFERENCES CITED

WAPA (Western Area Power Administration), 1989, Quantification and Disposition of Capacity and Energy Available for Marketing -- Final Draft, Division of Power Resources, Golden, Colorado (in-house report).

APPLICATION OF A SIMULATION MODEL FOR WATER–SUPPLY PLANNING IN AN ARID REGION OF CHINA

Zhang Shifa and Wang Jingping

Nanjing Research Institute of Hydrology and Water Resources, Nanjing, China

ABSTRACT

The paper presents a case study analyzing the severe water shortage of Beijing municipality due to inadequate water supply. The factors affecting the drought and water shortage and the long–term trend of drought are also discussed. The paper proposes a simulation model integrated with a mathematical–programming optimization model, and its relevant results are given.

ANALYSIS OF DROUGHT AND WATER SHORTAGE CAUSES

Beijing, located in a temperate zone, is affected by continental climate. Its annual precipitation is 593 mm with extremely uneven seasonal distribution and year–to–year variation; what is more noticeable is the frequent occurrence of consecutive drought years. In addition to the dry climate, the high concentration of its population results in a critical issue of water shortage. Water availability per capita in Beijing is only about $400m^3$ / yr, which is only 1 / 7 of the average for the whole country.

The water–supply system of the city includes the surface water system which is composed of two reservoirs, Guantin and Miyun, as well as the ground water system.

During 1949—1954, dry farming prevailed in the region: less than 3% of the cultivated land was irrigated. Crops were dominated by the maize (corn) and other autumn crops; only a small amount of wheat was grown. Figure 1 shows the water consumption during the growing period, which matches with the precipitation in ordinary cases. It clearly denotes that the water demand could be met by rainfall.

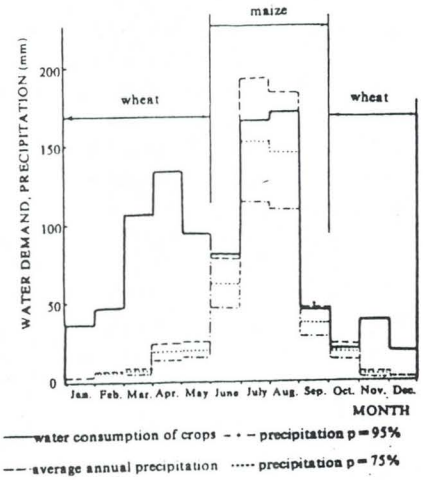

Figure 1. Comparison of water demand and precipitation in Beijing municipality, 1956 – 1984

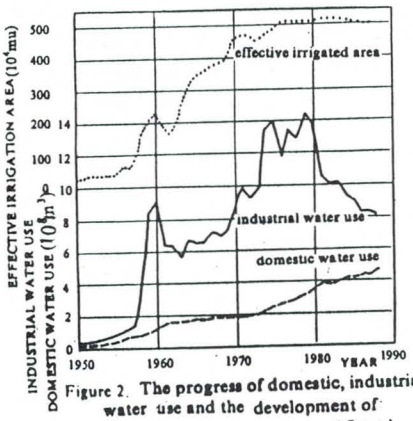

Figure 2. The progress of domestic, industrial water use and the development of irrigation area (1 ha = 15mu)

Since 1956, the irrigated area has increased from 2.7% to 80.6% of the crop land. The area planted in wheat has reached as much as 160,000 ha, being 48% of the total cultivated land. The average precipitation (95.2 mm)of the dry season is far from adequate for meeting the water demand (485 mm).Drought occurs almost every year that irrigation facilities fail to provide sufficient water.Obviously, the structural changes of agriculture and the development of irrigation have substantially raised the agricultural yield as high as 5 times. Figures 2 and 3 illustrate those changes.

As for the industry and domestic water supply, Figure 2 gives a general picture of its development.In suburban areas,the total withdrawal of ground water reaches $850 \times 10^6 m^3$, while the average annual recharge is only $550 \times 10^6 m^3$. The overdraft of ground water has brought about a significant drop of the water table (Fig.4).

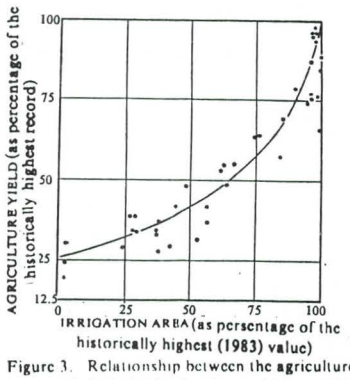

Figure 3. Relationship between the agriculture yield and the irrigation land area, 1949 – 1987

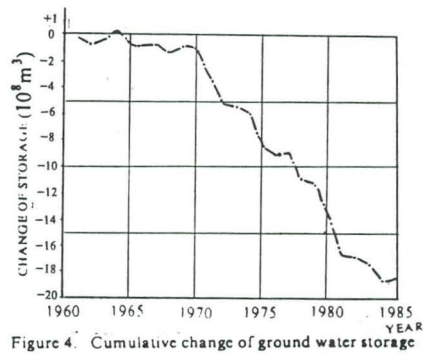

Figure 4. Cumulative change of ground water storage in Beijing suburban area

ANALYSIS OF LONG TERM–TRENDS OF DROUGHT

In accordance with the long term economic development plan of the Beijing Municipality, it is foreseen that, by the end of the century, the agricultural, industrial and domestic water use will be increased considerably while the water flow from adjacent areas will be decreased due to the same reason.

Surface water and ground water

Guantin Reservoir, as the major water supply source of Beijing, has a watershed area of 43,400 km^2. The inflow to the reservoir has been decreasing due to the increasing water use in the adjacent area; for example, the irrigation water amount increased from $300 \times 10^6 m^3$ in 1949 to $825 \times 10^6 m^3$ in 1980. The industrial water use also has changed substantially due to the drastic development in recent ten years. Figure 5 gives the relationship betwen the annual precipitation and the reservoir inflow.The figure shows that the

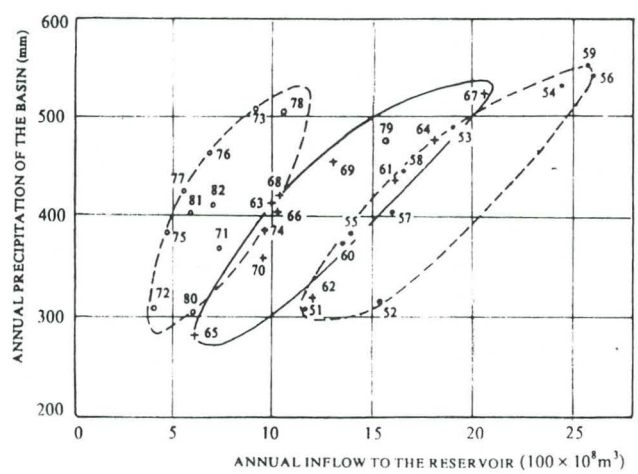

Figure 5 The relationship between annual precipitation and inflow Guantin reservoir, by year of occourrence (e.g., 79 = 1979),1951 to 1982

inflow to the reservoir clearly has declined during the recent 40 years.Predicted frequency curves of annual inflow to Guantin reservoir under various levels of development are given in Fig 6.The reduction of surface water and overdraft of ground water have resulted in dropping down of water table, and the ground water recharge from precipitation and surface water bodies will be affected. The predicted ground water recharge of the study area varies from $1.669 \times 10^9 m^3$(1984) to $1.474 \times 10^9 m^3$(2000).

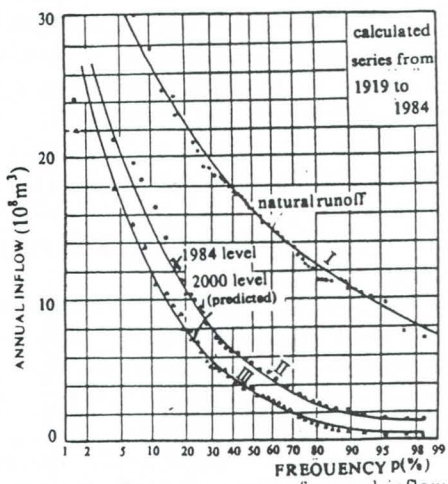

Figure 6. Frequency curve of annual inflow to Guantin reservoir for natural conditions and for development conditions in 1984 and 2000.

Water demand

Irrigation water accounts for 88% of the total water use for rural areas of Beijing, the strategy for coping with this issue is to promote water–saving types of agriculture. Various countermeasures like seepage control of irrigation systems, and improved sprinkling irrigation techniques, as well as agricultural measures were proposed. It is estimated that by year 2000 the water demand for the agricultural sector will be $1.46 \times 10^9 m^3$(p = 50%) and $1.73 \times 10^9 m^3$(p = 75%) respectively.

The evaluation of water use in the industrial sector up to year 2000 is based on the development plan for industry formulated by the Beijing Municipal Government. The following formula is proposed for prediction of industrial water use

$$q_2 = q_1 \ (1 - \eta_2) \ / \ (1 - \eta_1) \tag{1}$$

in which η_1, η_2 are the rates of reuse of industrial water for the initial year and the predicted year; q_1, q_2 are the amounts of water needed for economic output value of 10^4 yuan. The value of η_2 is selected by referring to both local experience and that used abroad taking fully into account the potential water saving measures.

Various factors like total population, number of employees, area of public buildings, area of residence, total salary of the employees, etc, are considered in the prediction of domestic water use up to year 2000.

The quantitative predictions of drought and water shortage under the current water system conditions and predicted inflow and water demand conditions are shown in Fig 7.

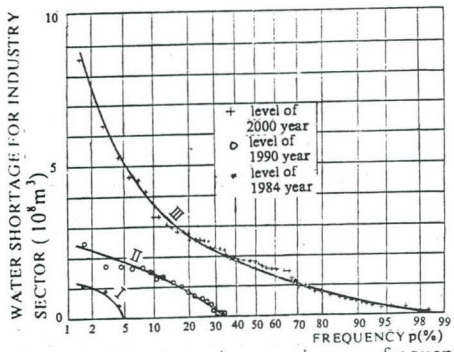

Figure 7. Drought and water shortage frequency curves for levels of development in selected years

WATER SUPPLY PLANNING AND ITS SIMULATION MODEL

The plan has proposed a series of structural and non–structural measures in coping with the water shortage in Beijing for year 2000. Nonstructural measures include the optimal operation of the water resources system, raising the preflood level of the reservoir, the adjustment of overall arrangement for the local industry, etc., while structural measures include various

engineering projects,such as waste–water disposal within the system, joint operation between surface water and ground water systems, and new water sources such as diversion of water from other basins. All those measures have to be considered and integrated into the available water supply system in studying measures for solving the water shortage problems.

The joint operation of the reservoir system and the ground water aquifer deals with quite a number of parameters. The complexity of correlation between inflows from various sources and different areas brings in difficulties in using only mathematical programming methods. This paper proposes an approach which combines a simulation model and a partial mathematical programming model in studying this complicated system.

The simulation process of water supply planning

The process is regarded as a simulation of an integrated system including water–saving measures, the joint operation of reservoirs and the aquifer, different schemes of planned projects, restructuring of industrial and agricultural water use, etc. The model comprises three lines of iterative process: The first line represents the optimal operation of the reservoir systems by means of feedback iteration under given inflow, water–use, and engineering measures; the second line gives the countermeasures to be taken after feedback iteration on the basis of optimal regulation of the reservoir system, provided that dependable water supply is not able to meet the needs of the economy; the third one is the measure for restructuring the industry and agriculture or development of new water–saving measures due to impracticability of the planned projects in view of the constraints in investment, environment, and social factors.

The simulation model

①Objective function

The maximum water use is identified as the objective function of the model under the condition that the domestic, agricultural and industrial water demand for a given dependability are satisfied, i.e,

$$F(Z) = Max \sum_{i=1}^{m} \sum_{j=1}^{N} \{ W_{ui,j} | P_I \geqslant 95\%, \ P_A \geqslant 50\% \} \tag{2}$$

where $W_{ui,j}$—available water amount for sub–area i and time interval j

P_I,P_A—dependability of industrial (including domestic) use and agricultural water use.

m—number of sub–areas (m = 6)

N—total time interval of computation (N = 66 years × 18 time–steps in a year)

②Constraints

The following are considered: conveying capacity for major canals, water demand, aquifer, water quality, policy (for example, order of priority of water supply for different sectors), etc.

③Simulation techniques

The simulation model for the system is composed of a number of blocks having different functions. The blocks consist of an input block; a hydrological block; a prediction block for domestic, industrial and agricultural water use; a multireservoir regulation block; a groundwater regulation block in various areas; a water–supply–allocation block between various areas; a block for joint control of water quality and quantity; a project–planning regulation block; an economic calculation block; a statistical computation block; and an output block, etc. These blocks in association with the compensation effect of different reservoirs are connected on the basis of order of priority for water supply (Fig 8).

After the calibration of the model, it could be used for analysis of design and management for various schemes provided that the required data are available. In order to improve

the adaptability of the model, 15 adjustable variables were developed so as to expedite the performance in dealing with a large number of schemes.

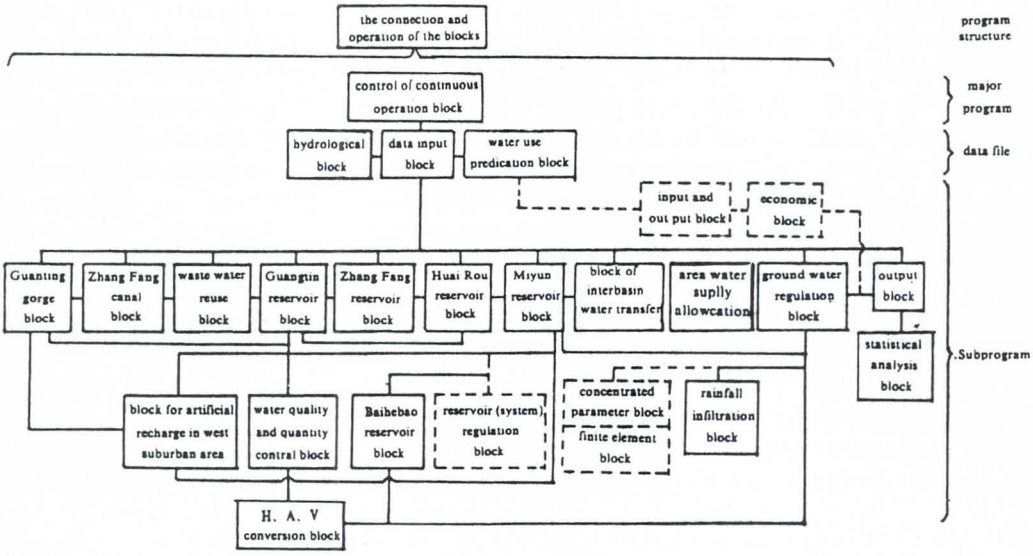

Figure 8 Block diagram of simulation model for water supply planning for Beijing.

Application of simulation technique

①Formulation of joint operation schemes for Guantin and Miyun Reservoir

a、Division of design storage of the reservoirs

The active storages of the two reservoirs are divided into several parts specifically for sectorial use, i.e, industrial and domestic water supply, lower limit of agricultural water supply, normal agricultural water supply, and water supply needed for power generation which could not be used for irrigation. The dead storage refers to the part of a reservoir in which water supply ceases, while the part in excess of the active storage is regarded as spill (Fig 9).

b、Identifying the reservoir operation rule by means of iterative trial–and–error procedure

In performing the iterative computations for a given operation line like AV(t,2), a set of different storage capacities is assumed, while initial values are given for other operation rules AV(t,3), ……,DV(t,4).

The output of the simulation for the whole system is thus obtainable. The value $AV^{(1)}(t,2)$ corresponding to the value of maximum objective function by formula (2) is regarded as the first estimate of the iteration, which can be expressed as

$$W_u\{AV^{(1)}(t,2)\} = Max\ W_u\{AV(t,2)|AV^{(0)}(t,3),AV^{(0)}(t,4),\cdots,DV^{(0)}(t,4)\} \tag{3}$$

The iteration then can be performed for $AV^{(1)}(t,3),AV^{(1)}(t,4),DV^{(1)}(t,2),\cdots,DV^{(1)}(t,4)$,by the same procedure.

The expression of the second iteration is given as

$$W_u\{AV^{(2)}(t,2)\} = Max\ W_u\{AV(t,2)|AV^{(1)}(t,3),AV^{(1)}(t,4),DV^{(1)}(t,2),\cdots,DV^{(1)}(t,4)\} \tag{4}$$

…

A given operation line is determined if the difference between the results of two iterations falls within desired accuracy.

The water shortage situation for various sectors is significantly improved compared with other methods presently widely used.

②Simulation of countermeasures and their quantification

Table 1 gives the results quantifying the simulation of water shortage after various structural and non–structural measures are taken. It shows that, if joint regulation of surface water system (Guantin and Miyun Reservoir) and ground water system is performed, the dependability of the two water supply systems could reach as high as 98.5% and the water supply for a dry year is more reliable (scheme no.4 in Table 1). Scheme no.3 gives an increased release from Guantin Reservoir in considering the requirement of improving the water quality at Sanjiadian, but when compared with scheme no.2 the dependability of water supply drops from 85.5% to 46.3%. Obviously it is impracticable with North China's inadequate water resources to improve the water quality by means of increasing the release from reservoirs.

As an interchangeable water supply capacity in the amount of $400 \times 10^6 m^3$could be attained by joint operation of the surface water and ground water systems, dependability of domestic and industrial water use could reach 95% in the year 2000; therefore,the implementation of a project diverting the water from other basins could be postponed.

Table 1 Simulation results of the plan coping with water shortage in Beijing

scheme no.	level year	Engineering measures							Reservoir operation			Domestic and industry water supply for suburb areas			
		〈1〉	〈2〉	〈3〉	〈4〉	〈5〉	〈6〉	〈7〉	〈8〉	〈9〉	〈10〉	Dependability of surface water supply P_{year}(%)	Dependability of ground water supply P_{year}(%)	Deficit of water supply $100 \times 10^6 m^3$ p = 75%	Deficit of water supply $100 \times 10^6 m^3$ p = 95%
1	present									✓	0	25.4	46.4	3.17	5.80
2		✓							✓		0	95.5	33.0	1.93	2.90
3		✓	Release from Guangtin reservoir should not be less than 28.6m³/s						✓			46.3	43.4	2.49	4.20
4		✓	✓						✓		4.0	98.5	98.5	0	0
5	2000 year	✓							✓		0	0	25.4	3.44	7.31
6		✓	✓	✓		✓	✓		✓		0	89.6	29.9	0.89	2.41
7		✓	✓	✓		✓	✓	1.0~2.5	✓		0	97~98.5	29.9	0.85	1.88
8		✓	✓	✓		✓	✓		✓		2.0	86.6	86.6	0	1.30
9		✓							✓		4.0	61.2	61.2	1.20	4.68
10		✓	✓	✓					✓		4.0	73.1	73.1	0.15	3.52
11		✓	✓	✓		✓	✓		✓		4.0	95.5~98.5	97~98.5	0	0

note: for scheme no.4 and 11, dependability of agriculture water supply reachs P = 50%.

〈1〉 available hydraulic structures
〈2〉 Diversion water from east suburb to west suburb areas
〈3〉 Diversion water from Miyun reservoir to Beijing in winter season
〈4〉 Diversion water from Jumahe river at Zhang Fang
〈5〉 Diversion water from Zhang Fang reservoir
〈6〉 Reuse of waste water
〈7〉 Diversion water from other basins
〈8〉 Optimal operation of the reservoir system
〈9〉 Operation on the basis of annual regulation
〈10〉 Capacity of joint operation of surface and ground water systems $100 \times 10^6 m^3$

If the proposed projects, i.e., Zhangfong reservoir and the project diverting water from other basins, cannot be implemented in 2000, the total amount of water supply will be reduced from $1.21 \times 10^9 m^3$ to $0.93 \times 10^9 m^3$, resulting in the necessity of restructuring the industry and adjusting the indices of economic development.Apparently water resources is a critical issue for the future development of Beijing's economy.

③Benefit analysis for joint operation of surface and ground water systems.The benefit of joint operation of surface–water and ground–water systems relates to the capacity of the

joint operation for all the water–supply facilities; a larger capacity could provide more water in dry years, thus mitigating the water shortage problems (Fig. 10).

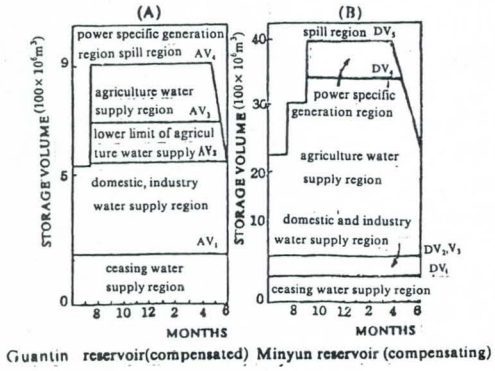

Figure 9. Operation line (rule curves) of Guantin reservoir (A) and Miyun reservoirs (B).

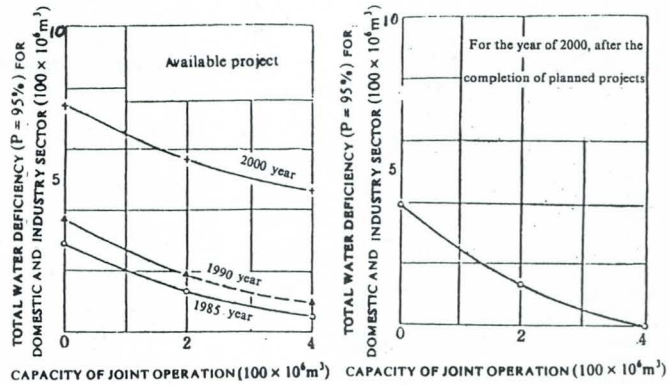

Figure 10. Schematic diagram of the effect of joint operation capacity on the reduction of water deficiency in domestic and industry sector in dry year (P = 95%)

For wet years, surface water should be used as much as possible, while, for dry years, ground water can be exploited to supplement the inadequacy of surface water. As a consequence, the spill of the reservoirs decreases and water supply for dry years increases. The proposed system makes full use of water resources for the study area.

Furthermore, the simulation approach is able to produce a more detailed design value which is conducive to rationally determining various design indices.

CONCLUSION

The study of drought for Beijing Municipality has evolved from the concept of agro–meteo–rological drought to that of "water resources–drought". The latter concept addresses issues of agricultural,industrial and domestic water supply as well as the socio–economic aspects of drought resulting from development.The integrated analysis of various kinds of drought indices enables us to make a comprehensive assessment of drought for a given area.

Potential drought is another subject needing study. It should be pointed out that the current balance between the water supply and demand is at the cost of a deteriorating environment due to overdrafting ground water and using polluted water to irrigate, which is an acute issue needing to be recognized and to be given great importance.

According to the model developed for water supply planning in Beijing, a complicated system is broken down to a number of subsystems by means of integration with a mathematical planning model in order to facilitate the computation and analysis.The model is able to simulate truly a complicated water–supply system, an important merit of which is that simulation could be performed on the basis of assumptions, i.e., to assume a water supply scheme, the response of the system is also one of the alternatives that is comparable with other schemes. The planners and decision makers can exchange their views in order to avoid subjectivity as far as possible, thus enabling the plan to achieve the goal efficiently.

The accuracy of streamflow and water–use data and the reliability of information used for prediction and relevant parameters are one precondition for using the model. In addition to the available data, a large number of field investigations and hydrological surveys were carried out. These are indispensable for obtaining a reliable result.

EFFECTS OF DROUGHT ON PUBLIC-SUPPLIED WATER USE--THREE CASE STUDIES FROM THE CENTRAL UNITED STATES

Richard A. Herbert and David W. Litke

U.S. Geological Survey, Denver, Colorado

ABSTRACT

Because about 82 percent of the people in the United States depend on public water suppliers to provide water for their domestic needs, the effect of drought on these systems is a critical subject. Weather affects both water supply and water demand. Records of daily public-supplied water use were obtained for the Postville Water and Sanitation District, Iowa, for the Johnson County Water District No. 1, Kansas, and for the Denver Water Department, Colorado. The Postville system is relatively unaffected by drought because it has a secure ground-water-supply system, and because it has a small seasonal component to its water use. The demands of a single large industrial user, and unusual water-use rates caused by system maintenance, complicated analysis of water-use data for this system. The Johnson County water-supply system is constrained not by weather factors but by limited treatment-plant capacity. Seasonal demand is a substantial component of water demand in Johnson County. Water use increased appreciably during the dry years of 1987-88, but was restrained by water-use restrictions. The source of water for the Denver system is located in a different climate regime than where the water is used. The seasonal component of water use was isolated by use of a temperature function. Conservation measures apparently were effective in restricting water use.

INTRODUCTION

In 1985, about 82 percent of the people in the United States depended on public water suppliers to provide water for their domestic needs (Solley, 1988). The viability of these supplies during times of drought is therefore of critical concern. Weather affects both water supply and water demand. Changes in water supply due to weather can occur slowly or quickly, depending on the source of the water (ground water or surface water) and on the flexibility of the water storage infrastructure. Changes in water demand due to weather can occur on a daily time scale. Water demand, however, can be managed by use of institutional constraints. Per-capita water use in the United States is more than 70 times as large as that in the African country of Ghana, for example (Maurits la Riviere, 1989); therefore managed decreases in water demand are possible.

This paper describes some of the effects of drought on public water supplies, using data from three different-sized public water suppliers in the central United States. The paper focuses on the effect of weather on water demand and attempts of suppliers to manage that demand, but the effect of weather on water supply is also addressed.

EFFECT OF WEATHER ON WATER DEMAND

Public suppliers deliver water to domestic, commercial, and industrial customers. Generally, domestic customers constitute the largest water-use sector, and weather affects the magnitude of outside water demand made by these domestic customers. In the central United States, supplemental irrigation water is required to maintain lawns and gardens. In the Denver, Colorado, metropolitan area, it has been estimated that almost half of the public-supplied water use consists of lawn watering and other outside uses (U.S. Army Corps of Engineers, 1986). Maidment and others (1985) have determined that this seasonal demand is largely a function of temperature, modified by short-term demand decreases caused by precipitation. In the case studies that follow, the effects of temperature and precipitation on water use are described by analysis of daily water-use-data plots and by isolation of the seasonal component of water use based on calendar months or use of a temperature function.

CASE STUDIES

Drought affected water supplies in parts of the central United States during 1961-67, 1976-77, and 1980-81 (Hanson, 1984). Precipitation was also below normal in localized areas during 1986-88. Data were obtained for 1986-88 for Postville Water and Sanitation District, Iowa (1,475 people served), and for Johnson County Water District No. 1, Kansas (about 240,000 people served). Longer-term data (1965-88) were available from the Denver Water Department, Colorado (about 1 million people served). The locations of these suppliers are shown in figure 1. These three public suppliers were selected for analysis because data sets were readily available, and because they reflect some of the differences in water source, supplier size, and geographic location among public suppliers within the central United States.

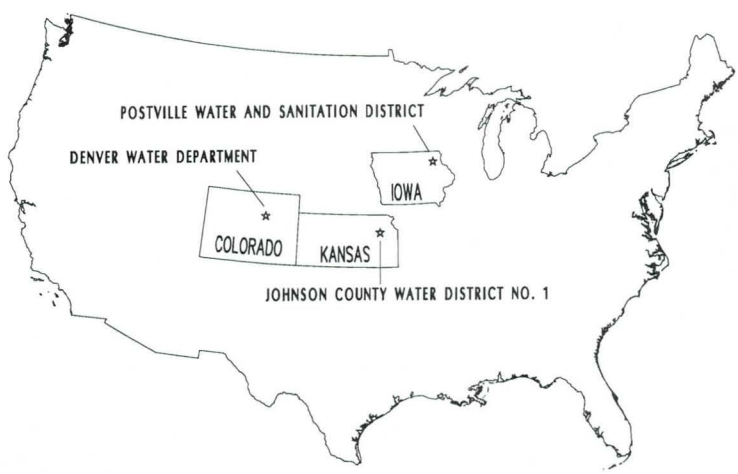

Figure 1.--Location of three public water suppliers.

Postville Water and Sanitation District, Iowa

The Postville Water and Sanitation District pumps water from three deep (about 1,100-foot) wells for delivery to the city of Postville, Iowa, and to a local industry. The population of Postville remained fairly constant at about 1,475

from 1986 to 1988. Because water is obtained from a deep aquifer, which has a large saturated thickness and wide areal extent, short-term droughts have relatively little effect on the water supply.

Summer (April through October) precipitation was about 10 inches above normal in 1986, 2 inches above normal in 1987, and about 9 inches below normal in 1988 (table 1). Average summer water use in the District (table 1) ranged from 366 gallons per capita per day (gcd) to 420 gcd and seems to increase as precipitation decreases. However, a plot of daily water use (figure 2) illustrates the masking effect produced by the large component of industrial water use--water-use rates are large on weekdays when industrial activity is high, but small on weekends, when industrial activity is low. Unusually large use rates also were observed during July and August of 1987. This anomalous use occurred because sustained pumping was required to maintain water pressure at the taps when the District water tower was drained for painting.

Table 1.--Summer (April through October) precipitation and water use, 1986-88.
[gcd: gallons per capita per day; dashes indicate data not available]

Year	Total precipitation (inches)	Average water use (gcd)	Average industrial water use (gcd)	Average domestic and commercial water use (gcd)
POSTVILLE WATER AND SANITATION DISTRICT, IOWA				
1986	36.3	366	232	134
1987	28.6	407	273	134
1988	18.0	420	299	121
Normal	26.6	---	---	---
JOHNSON COUNTY WATER DISTRICT NO. 1, KANSAS				
1986	41.4	179	---	---
1987	23.7	199	---	---
1988	21.1	255	---	---
Normal	29.4	---	---	---
DENVER WATER DEPARTMENT, COLORADO				
1986	9.4	302	---	---
1987	13.9	292	---	---
1988	11.2	304	---	---
Normal	11.5	---	---	---

Domestic and commercial water use can be examined by subtracting the industrial water use from the total water use for the District. A plot of daily domestic and commercial water use (figure 2) indicates that the seasonal component of water use is relatively small in the District. Water use would be expected to increase during droughts but domestic and commercial water use in summer actually decreased during 1988 (table 1). The decrease may have been the result of increased sewer fees imposed in 1986. The sewer fees were based on water use and the increased fees evidently became an effective water-conservation measure.

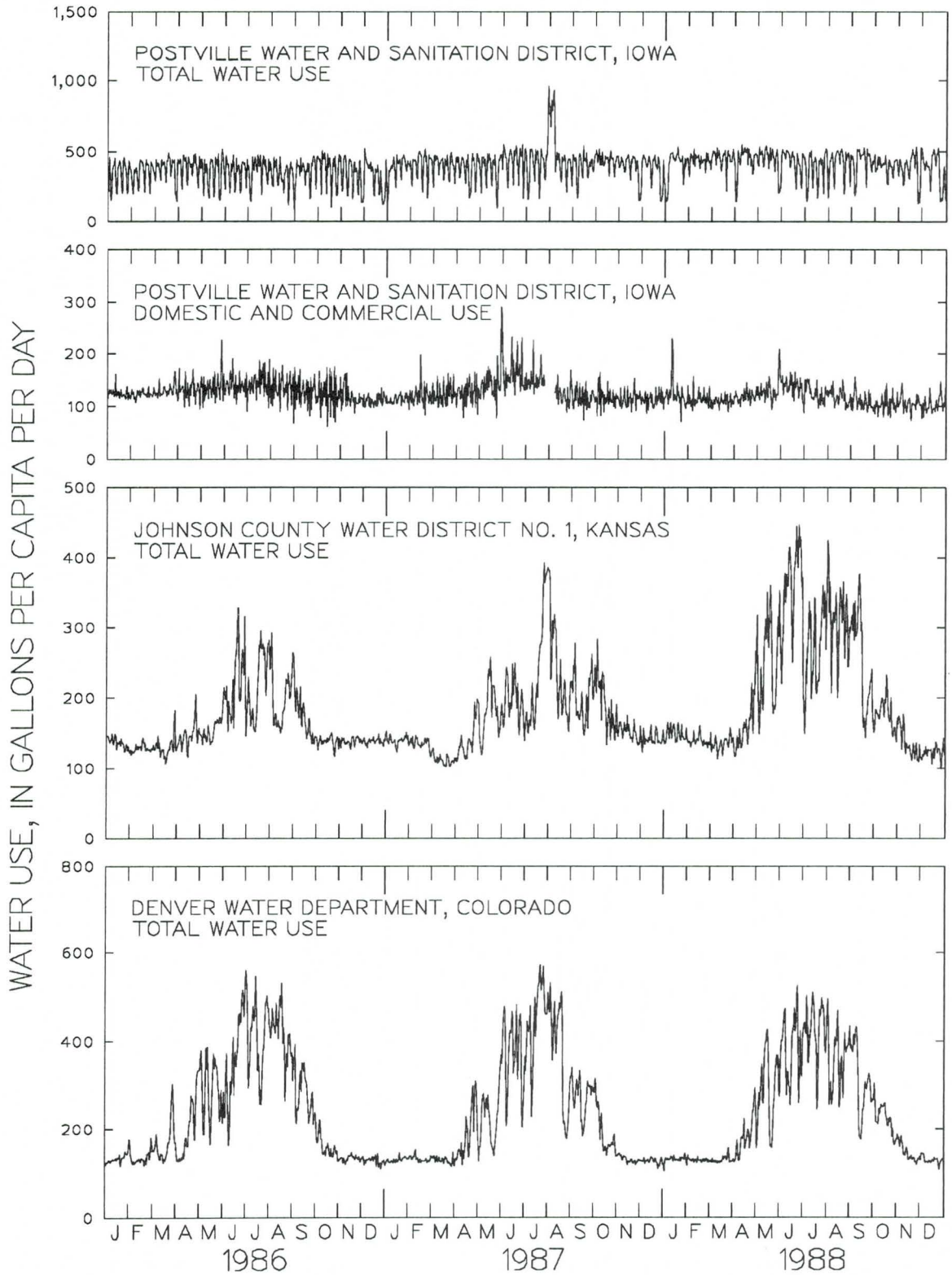

Figure 2.--Daily water use for three public water suppliers, 1986-88.

Johnson County Water District No. 1, Kansas

The Johnson County Water District No. 1 provides water on a retail basis to numerous suburbs that are adjacent to Kansas City, Kansas, and provides water on a wholesale basis to a rural water district and the city of Olathe, Kansas. The population served ranged from about 200,000 in 1986 to about 240,000 in 1988. Water is obtained from three sources: in 1988, about 8 percent was pumped from wells completed in the alluvial aquifer near the Kansas River, about 49 percent came from the Kansas River, and about 43 percent came from the Missouri River. The combined mean annual flow of the Kansas and Missouri Rivers is much larger than the water needs of the District--the controlling factor on supply is the capacity of existing treatment plants to produce finished water. Thus, the supply infrastructure capacity rather than weather considerations limit the Johnson County water supply.

Summer (April through October) precipitation was 12 inches above normal in 1986 (table 1), about 6 inches below normal in 1987, and about 8 inches below normal in 1988. Average summer water use in the District ranged from 179 gcd in 1986 to 255 gcd in 1988. Water use was significantly less in 1986, a non-drought year, than it was in the drought years of 1987 and 1988. A plot of daily water use (figure 2) indicates a fairly large seasonal component, which would be expected to increase during drought. The observed increase in water use may have been even larger if water-use restrictions had not been in effect during 1987 and 1988. The District has dealt with increasing demand by establishing restrictions on water use. During the summers of 1987 and 1988, households that had odd-numbered addresses could use water for lawn and garden irrigation and car washing only on odd-numbered days and households that had even-numbered addresses could use water for these purposes only on even-numbered days. Monitoring consisted of a courtesy patrol to check for non-compliance with watering restrictions. No fines were assessed to offenders, although water could have been shut off for flagrant violators (J.F. Kenney, U.S. Geological Survey, written commun., 1989).

Denver Water Department, Colorado

The Denver Water Department supplies water to about 1 million people in the city and county of Denver, Colorado, and in the surrounding metropolitan area. About 90 percent of the users are residential. Although the service area is located in the Great Plains physiographic region, where annual precipitation ranges from 12 to 16 inches, the water supply for the Denver Water Department is located in the adjacent Southern Rocky Mountain physiographic province where annual precipitation can exceed 60 inches. Drought in the plains area affects water demand, principally because almost half of the water supplied is used to maintain bluegrass lawns; drought in the mountain area affects water supply because the source of water is rainfall-runoff and snowmelt, which is stored in seven reservoirs in the mountains.

The effect of drought in the mountain environment on the Denver water supply system is difficult to analyze because of the complex infrastructure of the system. Department water-supply planners use historical water-discharge records and water-operations modeling to estimate safe yield. Using data for 1947-74, the Denver Water Department has calculated a safe annual yield of 289 gcd. This yield is the annual demand level that could have been sustained throughout the weather conditions observed during this period, which includes the most severe 3-year drought on record (1954-56).

The Denver metropolitan area was not affected by the drought that affected large parts of the central United States in 1986-88. Summer (April through October) precipitation in the Denver metropolitan area was about 2 inches below normal in 1986, about 2 inches above normal in 1987, and about normal in 1988 (table 1). A plot of daily water use for this period (figure 2) indicates that the seasonal component of water use is larger than that observed at the other sites, which is to be expected because precipitation is much less at this site.

In order to determine the effect of weather on seasonal water demand, available daily water-use data that had a longer period of record (1965-88) was examined. Annual water use for this period ranged from 172 to 248 gcd. For the following analysis, daily water-use data were aggregated to the weekly time scale, because previous studies (Maidment and others, 1985; D.W. Litke, unpublished data, 1990) have indicated that lawn-watering behavior is more predictable at this time scale. For each week, the average maximum daily temperature was determined. The relation of average seasonal water use to average maximum daily temperature (figure 3) for each week can then be examined. Below a temperature of about 60 degrees Fahrenheit, water use is insensitive to temperature--this is the base component of water use. Above 60 degrees Fahrenheit, water use increases approximately linearly as temperature increases--the increase is the seasonal component of water use.

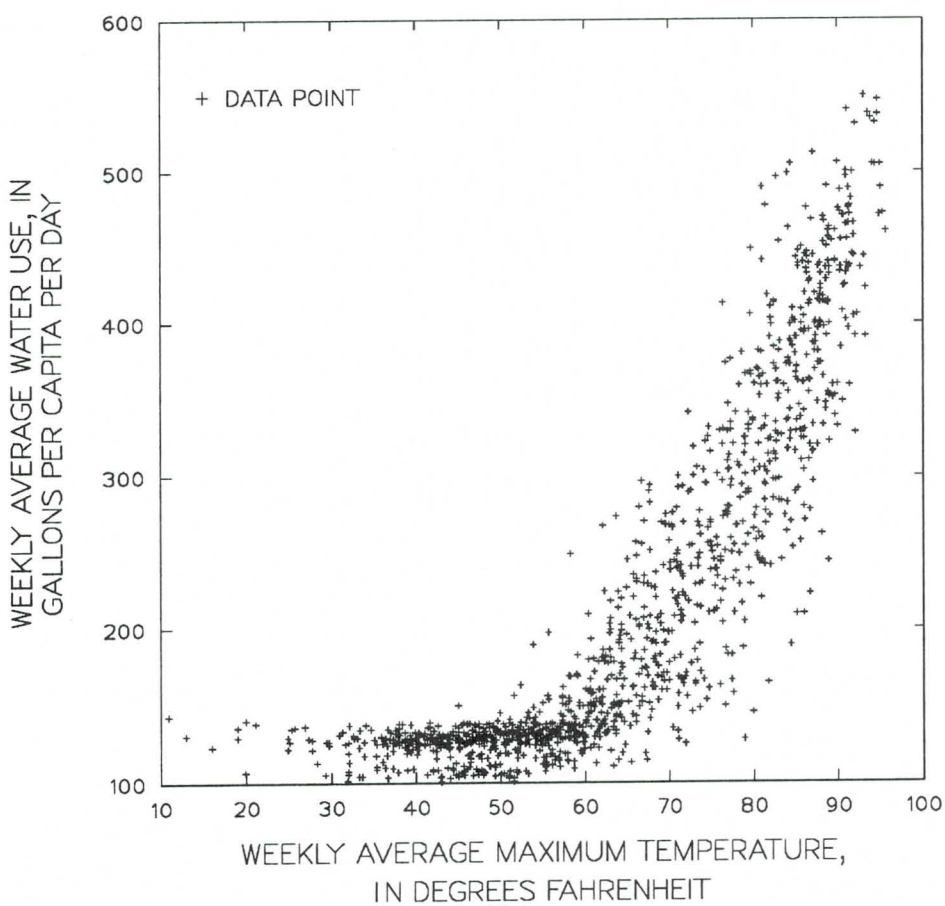

Figure 3.--Relation of average water use to average maximum daily temperature, 1965-88, Denver Water Department service area.

The variability in the relation may be attributed partly to the effect of rainfall, which diminishes water demand, and partly to variability in lawn-watering behavior. Base water use was quantified for each year by taking an average value of water use during weeks when the average maximum temperature was below 60 degrees Fahrenheit. Annual base water use for the 24 years of record ranged from 104 to 135 gcd and had an overall average value of 124 gcd. Seasonal use was quantified for each year by selecting all weeks when the average maximum temperature was above 60 degrees Fahrenheit, subtracting base use from total use for each week, and then computing an average value for the increased uses across the entire year. Annual seasonal water use for the 24 years of record ranged from 63 to 115 gcd and had an overall average value of 93 gcd. Seasonal water use ranged from 37 percent of total use to 48 percent of total use with an overall average value of 42 percent of total use. Because seasonal water use is about half of total use, and because seasonal water use has varied during the 24-year period by a factor of 2, it can be concluded that about 25 percent of the variability in water demand can be attributed to weather.

A theoretical lawn-watering requirement then was examined. Empirical relations of lawn-watering requirement to weather (temperature and precipitation) have been developed for the Denver area based on lysimeter measurements. These relations and historical weather data were used in the modified Blaney-Criddle method to calculate annual lawn-watering requirement for 1965-88. The smallest annual lawn-watering requirement was 19.7 inches, the largest was 35.0 inches, and the average was 26.7 inches.

The relation of annual seasonal water use to annual theoretical lawn-watering requirement was examined (figure 4). The two variables (excluding two outliers) have a linear correlation coefficient of 0.84. The 2 years with the largest theoretical lawn-watering requirement (1977 and 1981) may be considered drought years, although the theoretical lawn-watering requirement gives weight to both temperature and precipitation. Both these years experienced observed seasonal use that was less than expected. This pattern is consistent with the pattern of institutional constraints placed on water use. No water restrictions or conservation practices were in effect from 1971 to 1976. In 1977, mandatory restrictions began with outside watering limited to 3 hours on every third day from June 12th to September 30th. Fines were imposed for violations and enforcement was strict. These restrictions were preceded by less than normal snowfall in the mountains. Public awareness of water problems was increased as a result of well-publicized water shortages in Marin County, California. In 1978, the 3-hour limit was eliminated, but enforcement of watering every third day from June through September remained in effect and continued until 1982. A public-awareness program, which provided news releases of inches of water required by lawns for the next day, was introduced in 1981. In addition, in 1981, xeriscaping (low water-use landscaping) and water conservation were widely publicized. In 1982, when a new water-treatment plant was completed, water-use restrictions became voluntary (M.J. Martin, Denver Water Department, written commun., 1989).

Strict institutional constraints were apparently effective in reducing water use during 1977. An increase in public awareness about water-conservation techniques apparently was effective in reducing water use during 1981. However, these techniques appear to quickly lose their effectiveness in the absence of continued reinforcement, as evidenced by the return of typical seasonal water-use rates in 1978 and 1982 (figure 4).

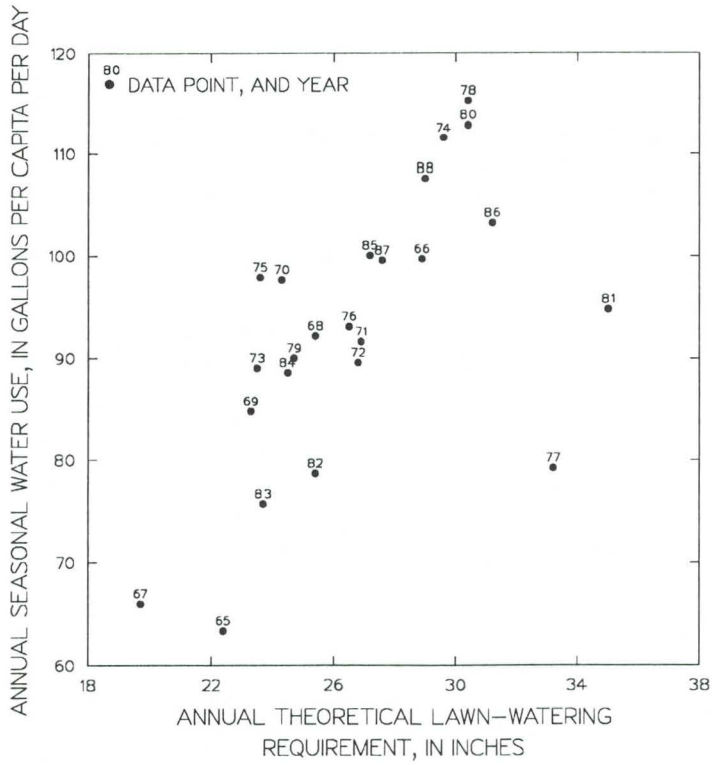

Figure 4.--Relation of seasonal water use to theoretical lawn-watering requirement, 1965-88, Denver Water Department service area.

Because the water-supply and water-demand areas are located in different environments, the probability of simultaneous drought in the mountains and the plains must also be considered when evaluating the effect of drought on the Denver water system. Both environments receive precipitation from several weather systems, and drought apparently affects both environments simultaneously less than one-half the time (Nolan Doeskin, State Climatologist, oral commun., 1991). Drought recurrence probabilities may be similar for both environments, but their quantification and the extent to which they are linked, are still under investigation.

REFERENCES CITED

Hanson, R.L., 1984, Droughts, in Proceedings of the Geologic and Hydrologic Hazards Training Program, March 5-30, 1984, Denver, Colorado, U.S. Geological Survey, Open-File Report 84-760, pp. 773-811.

Maidment, D.R., Miaou, S-P, Nvule, D.N., and Buchberger, S.G., 1985, Analysis of Daily Water Use in Nine Cities: Center for Research in Water Resources, Bureau of Engineering Research, The University of Texas at Austin, Technical Report CRWR 201, 67 p.

Maurits la Riviere, J.W., 1989, Threats to the World's Water: Scientific American, v. 261, no. 3, p. 80-94.

Solly, W.B, Chase, E.B., and Pierce, R.F., 1988, Estimated use of water in the United States in 1985: U.S. Geological Survey Circular 1004, 80 p.

U.S. Army Corps of Engineers, 1986, Future Water Demands, Appendix 2--Metropolitan Denver Water Supply Systemwide Draft Environmental Impact Statement: Omaha, Nebr., 290 p.

EVALUATING DROUGHT RISKS FOR LARGE HIGHLY REGULATED BASINS USING MONTHLY WATER BALANCE MODELING

Gary D. Tasker

U. S. Geological Survey, Reston, Virginia

ABSTRACT

Large basins often have reservoir release and diversion patterns that are complex and nonstationary. Historical records of regulation and diversions often are incomplete or not available in enough detail to adjust observed streamflow records to obtain a long record of natural flows. This makes it difficult to statistically analyze streamflow data to estimate drought risks under present or future regulation and diversion patterns. A monthly water-balance model can be used to obtain a long synthetic record of natural flows. The water-balance model uses observed values of monthly temperature and precipitation to estimate evapotranspiration, change in storage, and natural streamflow. Using these flows as input, present and future regulation and diversion patterns can be simulated with a simple continuity accounting model to keep track of inputs and outputs at key locations in a basin. Such a model allows planners, engineers, and decision makers a means of objectively evaluating the effects of present and possibly modified rules of operation and diversions on drought risks for the basin. The technique is illustrated using a model of the Delaware River basin. The Delaware basin has a complex set of operating rules involving diversions from the basin, reservoir releases to maintain minimum flows, and both groundwater and surface water withdrawals for water supply. Although this basin is in a humid area, it serves to illustrate the principles that can be applied to arid and semi- arid areas. However, it should be noted that the performance in a semi-arid or arid basin may not be as good as in the Delaware River basin.

INTRODUCTION

The Delaware River flows south from the western slopes of the Catskill Mountains in southern New York past Philadelphia, Pennsylvania and enters the Delaware Bay (figure 1). Near Trenton, New Jersey it falls about eight feet over a series of rock ledges and enters the tidal estuary. The drainage area above Trenton is about 6780 square miles. Major diversions from the basin are from three reservoirs in the upper part of the basin for water supply for New York City and from the river near Trenton through the Delaware-Raritan Canal for New Jersey. By agreement, the three reservoirs operated by New York City must release an amount of water to maintain a minimum flow at the Montague gage (drainage area 3480 square miles) and are restricted as to how much water may be diverted. The restrictions vary by months and additional restrictions may be imposed in times of drought. In addition to the diversions from the basin, the river is an important source of water for several municipalities in the basin. Any change in water availability is of interest to water resources planners and managers because the Delaware River is a major source of water for approximately 20 million people in New York, New Jersey, Pennsylvania, and Delaware.

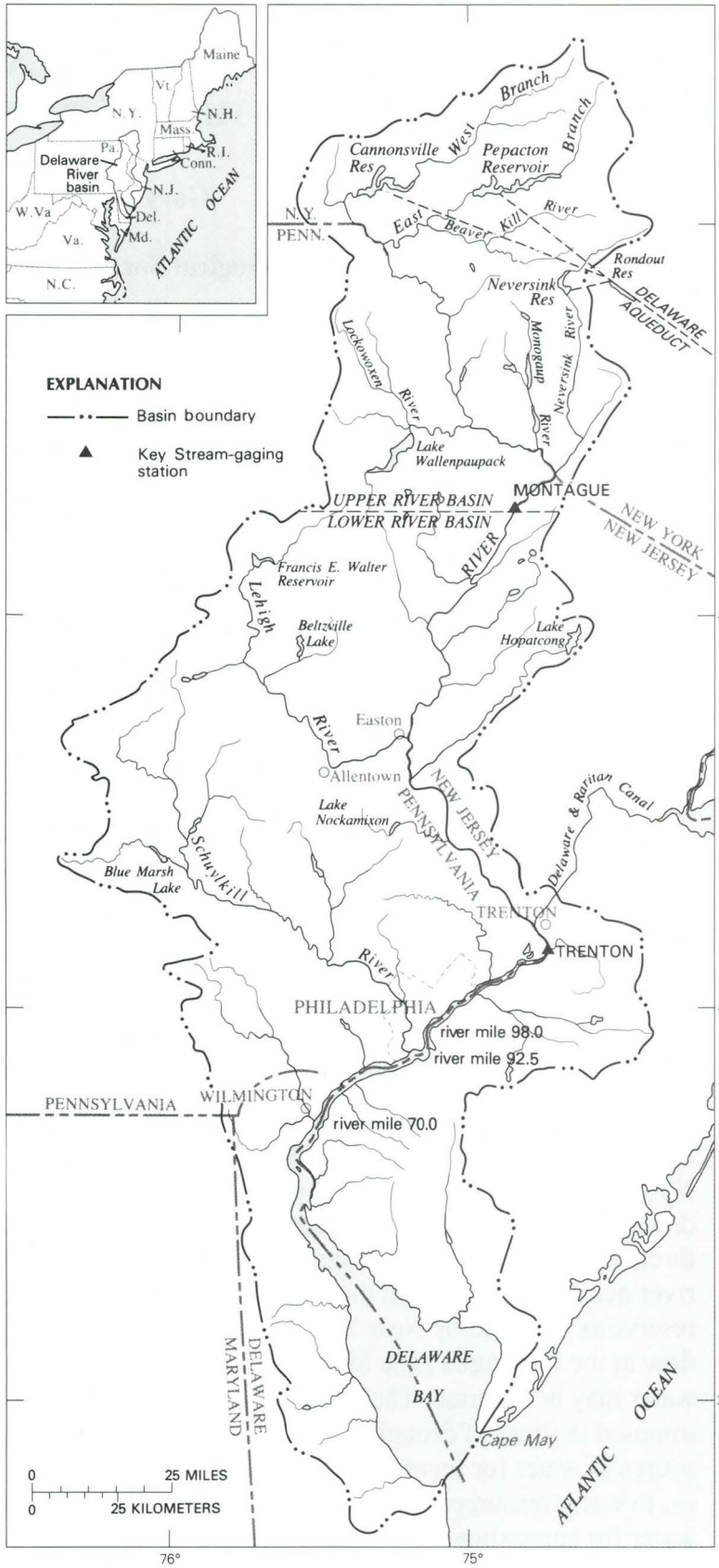

Figure 1. Delaware River basin.

To make a quantitative assessment of drought risks in the basin, computer models are developed to simulate flows in the basin under different rules of operation. The models can be used to evaluate with reasonable confidence the impact of possible mitigation measures such as increasing reservoir capacities and modified operating rules.

WATER-BALANCE MODEL

A monthly time-step water-balance model was developed and calibrated for the basin. The model, a modification of the Thornthwaithe (1948) water budget bookkeeping procedure, accounts for soil moisture, evapotranspiration, water deficit, snowmelt, and surface runoff. The inputs needed are monthly average temperature and precipitation. Agreement between measured and computed monthly runoff can be achieved by adjusting model parameters, such as basin lag and water holding capacity of the basin. The time series of temperature and precipitation values can be an observed historical sequence or can be created by randomly generating serially and cross correlated residuals from long-term monthly mean values. The resulting simulated monthly runoff values are used as input to the basin model described below.

BASIN MODEL

The monthly flows generated by the water-balance model are routed through a basin model that simulates operation of reservoirs, diversion canals, and ground-water wells. The basin model is a mass balance model that accounts for all inflows and outflows at several key nodes in the basin. For example, the flow at the Montague gage in month t would equal the releases from the New York City Reservoirs plus uncontrolled flow for month t minus consumptive uses within the basin above Montague for month t. Releases from the New York City Reservoirs meet minimum instream flow requirements and meet a minimum target flow at Montague. When uncontrolled flow at Montague is not adequate to meet the minimum flow requirement, the New York City Reservoirs release enough water to make up the difference. Other reservoirs in the basin can be operated in a similar manner during low flows to augment flows to meet minimum flow requirements at Trenton.

MODEL VERIFICATION

In order to validate the model a 50-year run was made using observed monthly temperature and precipitation for the period October 1927 through September 1977, and results compared to a daily time-step model. Existing operations were assumed and resulting model discharges determined at the Montague and Trenton gages. In addition, resulting model storage was determined for the combined New York City (NYC) reservoirs. The monthly flows at Montague and Trenton and the monthly NYC reservoir storages were compared to similar variables for the same time period and virtually same operating conditions derived from a model run supplied by the Delaware River Basin Commission (DRBC). The DRBC model is a daily time-step model that uses observed discharges modified by correlation and other means to represent natural flow as inputs. It can model day-to-day operation of the basin.

The purpose of this comparison is to see if the monthly water balance model can reasonably approximate the DRBC model during periods of low flow. Figures 2 and 3 show duration curves for flow at Trenton and storage at the NYC reservoirs based on the 50-year period for both the DRBC model and the water balance model. The two models produced values of flow and storage that are in close agreement below about the 10 percent value of the flow duration curve at Trenton

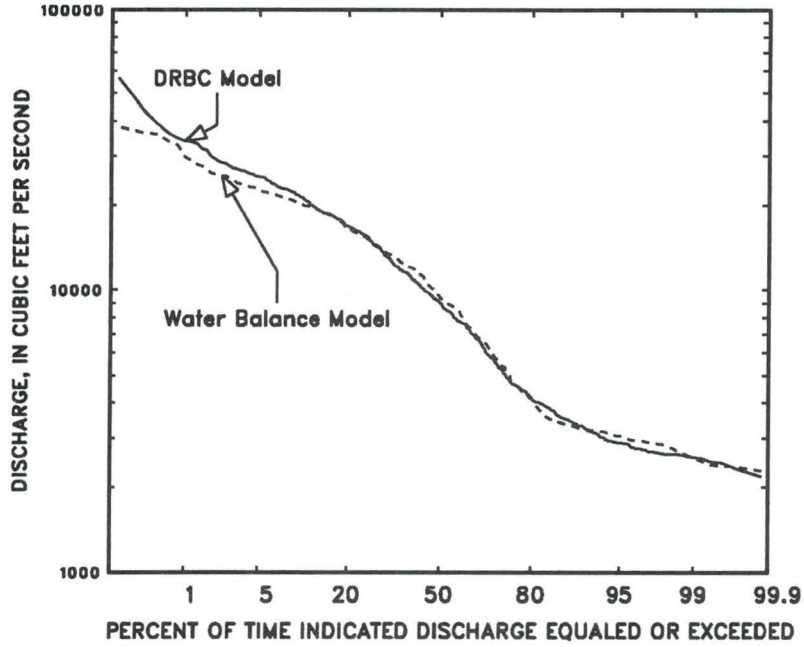

Figure 2. Monthly flow duration curve for water years 1928–77 at Trenton.

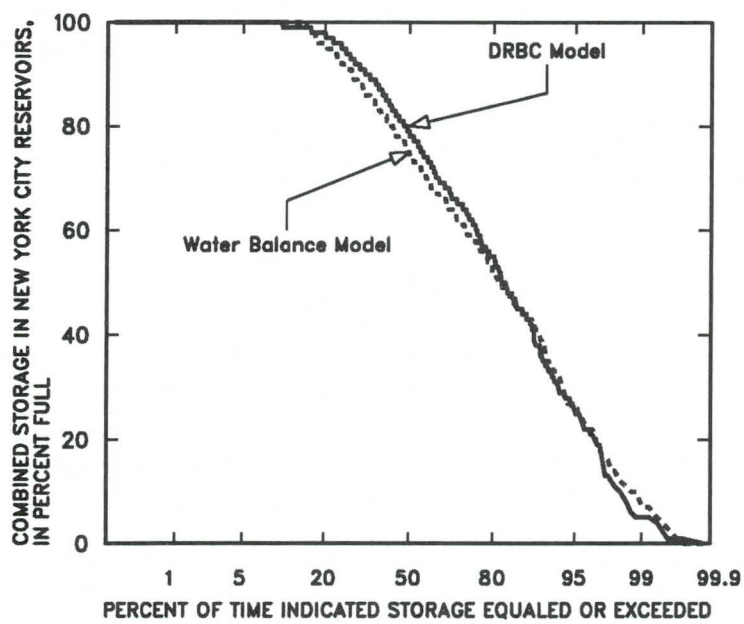

Figure 3. Monthly storage–duration curves for water years 1928–77

(figure 2) and throughout the observed range of storage at the NYC reservoirs (figure 3). These results tend to verify that the monthly water-balance model approach agrees with the DRBC daily time-step model for simulating low flows in a highly regulated basin, although the overall variability of the monthly model is clearly less than the daily model.

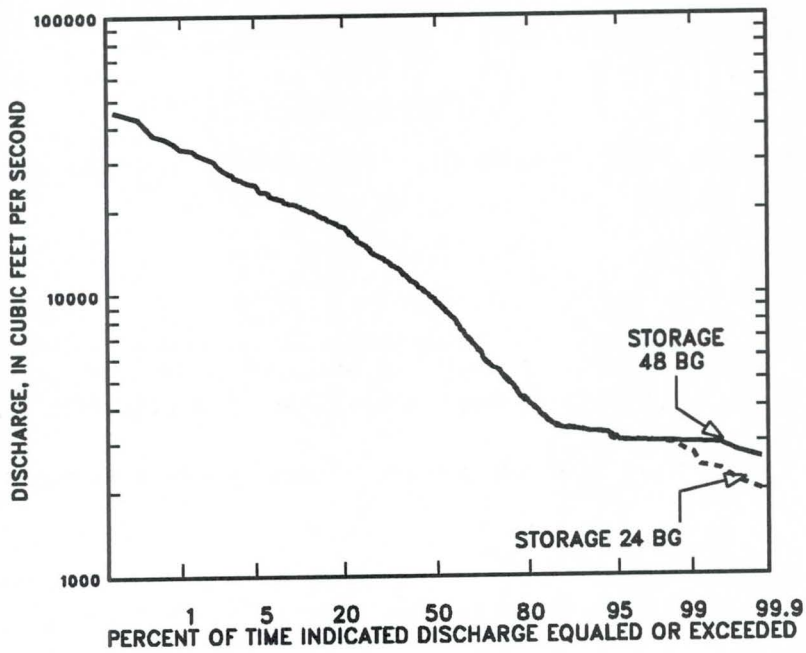

Figure 4. Monthly flow duration curves for 50–years of synthetic flow at Trenton when total storage available for flow augmentation was 24 BG and 48 BG, respectively.

To illustrate one use of the model, suppose one wished to evaluate the effects on low flows at Trenton of increasing the available storage for low-flow augmentation by 24 billion gallons. Figure 4 shows two duration curves generated from 50-years of synthetic flow data under existing operating rules. The lower curve resulted from a run with available storage for flow augmentation set at the present level (approximately 24 billion gallons). The upper curve resulted from a run with available storage increased to approximately 48 billion gallons. The difference between the two curves provides a planner with a quantitative assessment of the effects of increasing storage. This is but one example of how the model could be used to assess effects of changing operating conditions in the basin.

FINAL REMARKS

A monthly water balance model of the Delaware River basin has been shown to simulate monthly low flows in the basin reasonably well by comparison with a more complex and probably more accurate model. One advantage of the monthly water balance model approach is that, because the driving inputs are temperature and precipitation, it can be used to easily assess the effects of changing climate on low flows. This can be done by generating a time series of temperatures and precipitations that are representative of a different climatic state.

REFERENCES CITED

Thornthwaite, C.W., 1948, An approach toward a rational classification of climate: *Geographical Review*, vol. 38, pp 55-94.

A MODEL OF WATER RESOURCES TRANSFORMATION AND ITS RESULTS IN SIMULATING THE URUMQI RIVER BASIN, CHINA

Liu Fengjing and Qu Yaoguang

Lanzhou Institute of Glaciology and Geocryology,
Chinese Academy of Sciences, Lanzhou, Gansu, China

ABSTRACT

This paper uses the Urumqi River basin to demonstrate a case model of water resources transformation in arid lands. In simulation and computation, the condition of balance between supply and demand of water resources is assumed in order to compare with the present situation. By the comparison, the mean annual overexploited amount of the ground water is $1.573X10^8m^3$ in the Urumqi River basin. The relationship between the maximum usage of water (MUW) and the utilization coefficients of the canal system (UCCS) is discussed in detail, and a new concept on development and utilization of water resources is inferred.The concept shows that it is not economical to increase the MUW by means of improving the UCCS in such regions as the Urumqi River basin if the average UCCS exceeds 0.6, and the surface water and ground water have been completely developed and utilized.

INTRODUCTION

Research on water resources transformation (WRT) is crucial to assess total water resources in arid lands. A model of WRT has been constructed in the Urumqi River basin,where the transformation between surface water and ground water is vivid, and information is plentiful. The procedure of the WRT has been deduced, and a new concept on development and utilization of water resources has been obtained by simulating and computing.

DESCRIPTION OF STUDY AREA

The Urumqi River, the mean annual runoff of which is $3.5X10^8m^3$, rises from the northern slope of the Tianshan Mountains. Urumqi City, the capital of Xinjiang Autonomous Region, is located in the center of the Urumqi River basin. The population of Urumqi City is over one million. Although the surface water and ground water have been completely developed in the basin, contradiction between supply and demand of water resources is still sharp.

Based on geological and geographical conditions and characteristics of the WRT,the basin may be divided for computation into four districts(Fig.1), which are connected in series by rivers, canals, and ground water runoff.

Chaiwopu Basin

This district is next to the foot of the Tianshan Mountains and belongs to

the Cenozoic and Mesozoic cavate basin. The Quaternary "egg-and-sand" gravel sediment is up to hundreds of metres thick. Surface water is the main source for water used in the basin. The rest of the water resources coverges on the Ulapo Reservoir, which is closely linked with the next district.

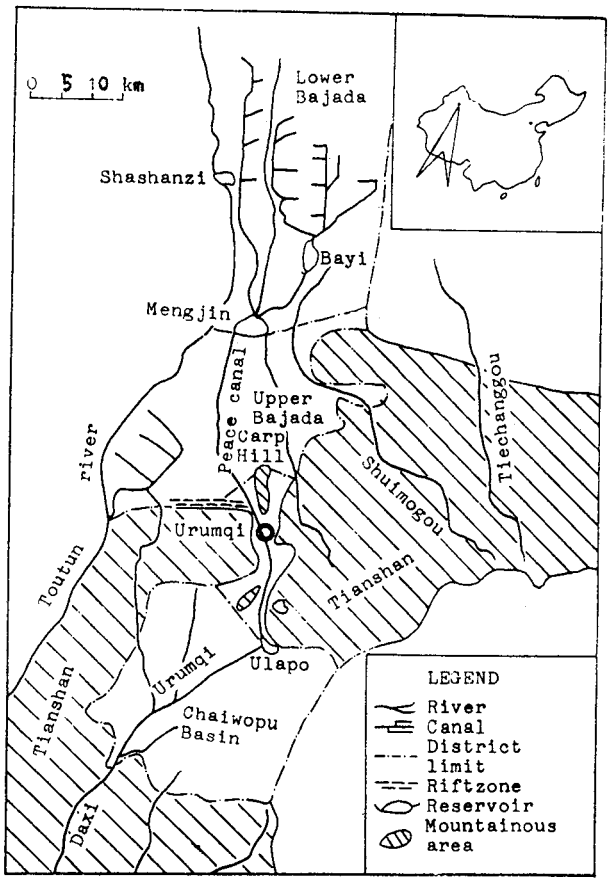

Fig.1 Sketch Map of Urumqi River Basin

Urumqi River Valley

The sediment of"egg-and-sand" gravel, 20 to 30m in thickness,exists in the valley. In general, the depth of phreatic water level is about 10 m. The surface water is regulated by the Ulapo Reservoir, and catchments for ground water are constructed in order to supply municipal,industrial and environmental needs. In fact,the ground water level falls constantly, and the quality becomes worse by degrees in the valley.

Upper Bajada of Urumqi River

This district extends from southern Carp Hill and the rift zone between the Tianshan Mountains and the Bajada to the Gumdy Hill. It is the second natural transformation system of water resources. Surface water is the main source for water used. Spring water and part of the exploited ground water are channelled into Mengjin and Bayi Reservoirs in order to be provided to the next district.In fact,the regional funnel of ground water depression has deepened because of violent overexploitation of ground water.

Lower Bajada of Urumqi River

This district is the last one of development and utilization of water resources. All of the water resources are used in agricultural irrigation.

All components of water resources in every district are listed in table 1. It is worth to specify that these components are mean annual values.

MODEL

Based on the principle of water balance and the procedure of the WRT, the model, which combines simulation with computation and prediction,is composed on certain given conditions in Urumqi River basin.

Given Conditions

It is necessary to end the situation of overexploiting ground water as well

Table 1. Mean annual components of water resources in districts of the Urumqi River basin($10^8 m^3$)

Component*	Chaiwopu Basin	Urumqi Valley	Upper Bajada	Lower Bajada	Total
I	3.286	0.557	1.920	0	5.763
W	0.318	0.196	0.154	0	0.668
Q	1.566	0	0.372	0	1.938
D	0	0.043	0	0.175	0.218
P	0.502	0.035	0.178	0.067	
BI	0.839	0.115	0.344	0	1.297
E	0	0.060	0	0.150	0.210
F	0.069	0	0.050	0.170	0.289
XN	2.322	0.416	2.199	1.064	6.001
XG	0	0.703	0	0	0.703
PN	0.157	0	1.821	0.737	2.714
PG	0	1.022	0.167	0	1.190
SO	0.270	0	0.372	0	
SE	0	0	0.270	0.372	
PO	0	0	0.749	0	

* See text for definition of abbreviations.

as to satisfy the needs of development of cities and industries, and to maintain the stability of the oasis. Therefore, the equilibrium principle on development and utilization of water resources must be assumed in the model. That is,it is assumed that total outflow equals total inflow and that change in storage equals zero. This will result in the following conditions. First, water resources are allocated in this order: urban, industrial and agricultural demands. Next,the ground water level will not fall constantly, and the ground runoff will maintain the present volumes in each district. Similarly, the other components, e.g., spring water, evaporation and leakage of reservoirs, and evaporation of ground water, will maintain their present values in the future based on the equilibrium principle.

Purpose and Function

The model is used to solve the following problems. The first is to account for water withdrawals and usages under present conditions of development and utilization of water resources. The second is to evaluate the maximum withdrawal of water (MWW) and the maximum usage of water (MUW) based on the equilibrium principle.The third is to understand the relationships among the MWW, the MUW, and the utilization coefficients of the canal system(UCCS).The last problem is to compute the overexploited amount of ground water(OAG) and the development and utilization level of water resources.

Model

The model can be described as a block-diagram model,figure 2, and numerical model. The numerical model is composed of transformation formulas, which are derived from equilibrium(water balance) equations of the WRT,and computation formulas, which are constituted by relevant concepts of water resources. All

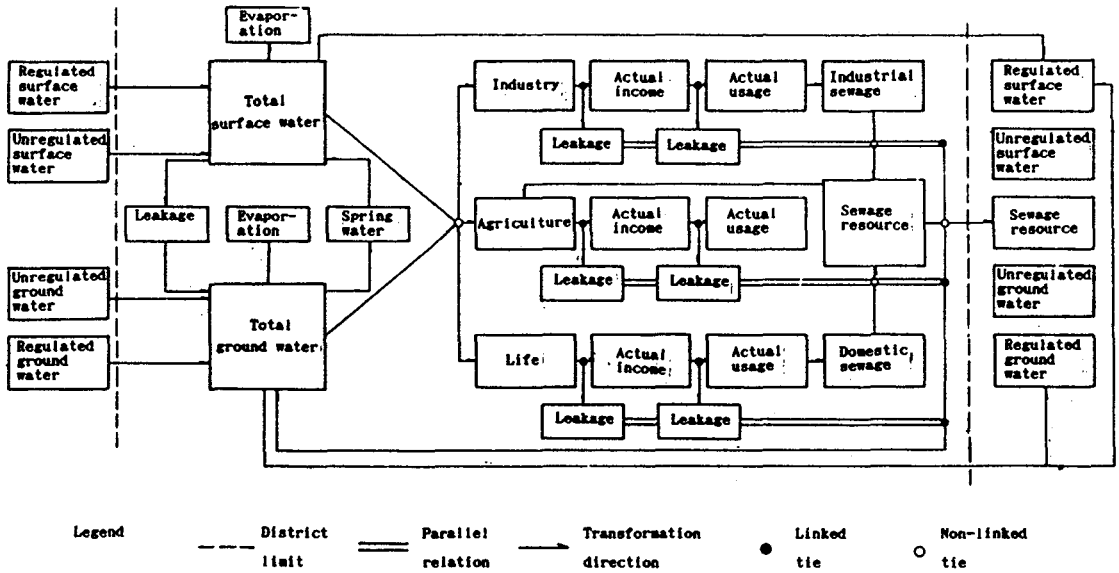

Fig. 2 Block-diagram model of water resources transformation in arid lands

water quantities are expressed as mean annual volumes (m^3).The water balance equations are as follows. For surface water:

$$S(i)=I(i)+Q(i)+S(i-1)+SE(i)-D(i)-E(i)-SO(i)-BI(i)-X(i)$$

and for ground water:

$$P(i)=W(i)+D(i)+P(i-1)+PQ(i)+PF(i)+PJ(i)-Q(i)-F(i)-Y(i)$$

These equations can be solved for X and Y as follows:

$$X(i)=I(i)+Q(i)+S(i-1)+SE(i)-D(i)-E(i)-SO(i)-BI(i)-S(i)$$
$$Y(i)=W(i)+D(i)+P(i-1)+PQ(i)+PF(i)+PJ(i)-Q(i)-F(i)-P(i)$$

In these equations:

S(i)= regulated surface-water outflow from district i to i+1
P(i)= ground-water outflow from district i to i+1
I= unregulated local surface-water inflow
W= unregulated local ground-water inflow
Q= unregulated flow from springs
SE= spring water diversion inflows
SO= spring water diversion outflows
E= evaporation from reservoirs
F= evaporation from ground water
D= leakage from reservoirs
BI= leakage from canal system
PQ= ground-water recharge by leakage from canals
PF= ground-water recharge by field irrigation with surface water
PJ= ground-water recharge by field irrigation with ground water
X= decidable surface-water withdrawal
Y= decidable ground-water withdrawal

Computation formulas used in the water balance are:

$$PQ(i)=0.9[1-A(i)]\cdot XN(i)$$
$$PF(i)=A(i)\cdot C\cdot XN(i)$$
$$PJ(i)=[0.9(1-B)+B\cdot C]\cdot YN(i)$$
$$X(i)=XN(i)+XG(i)$$
$$Y(i)=YN(i)+YG(i)$$

In these equations:

A= utilization coefficient of canal system for surface water

B= utilization coefficient of canal system for ground water

C= recharge coefficient for field irrigation

XN,XG= decidable surface-water withdrawals for agriculture and industry, respectively

YN,YG= decidable ground-water withdrawals for agriculture and industry, respectively

Computation formulas used for totals and measures of performance are:

$$G(i)=W(i)+D(i)+P(i-1)+PQ(i)+PF(i)-P(i)$$
$$T(i)=I(i)+W(i)$$
$$TK(i)=X(i)+Y(i)$$
$$SU(i)=Y(i)-[PN(i)+PG(i)]$$
$$M(i)=A(i)\cdot XN(i)+XG(i)+B\cdot YN(i)+YG(i)$$

$$G=\sum_{i=1}^{n} G(i) \qquad (n=1,2,3,4)$$

$$T=\sum_{i=1}^{n} T(i) \qquad (n=1,2,3,4)$$

$$TK=\sum_{i=1}^{n} TK(i) \qquad (n=1,2,3,4)$$

$$SU=\sum_{i=1}^{n} SU(i) \qquad (n=1,2,3,4)$$

$$M=\sum_{i=1}^{n} M(i) \qquad (n=1,2,3,4)$$

In these equations:

T= total water resources

G= total recharged ground-water volume

TK= total water withdrawal

M= total water usage

SU= total gross amount of overexploited ground water

PN= actual withdrawal of ground water for agriculture

PG= actual withdrawal of ground water for industry

CONCLUSION AND DISCUSSION

Under the equilibrium assumptions on development and utilization of water resources, the MWW and the MUW are $8.477X10^8m^3$ and $5.579X10^8m^3$, respectively. However, the actual withdrawal water amount (AWW) and the actual usage water amount (AUW) are separately $11.337X10^8m^3$ and $7.152X10^8m^3$ under present conditions (Table 2). The fact that the AUW is bigger than the MUW indicates

Table 2. Comparison of actual and maximum annual amounts of water withdrawal and usage under present and alternative future improved conditions of canal utilization coefficient($10^8 m^3$)

	Surface water	Ground water	Total
Present conditions			
Actual withdrawal	6.704	4.633	11.337
Actual usage	3.764	3.388	7.152
Maximum withdrawal	6.169	2.309	8.477
Maximum usage	3.498	2.081	5.579
Improved conditions			
A(1)=0.75			
Maximum withdrawal	5.200	1.632	6.832
Maximum usage	4.133	1.572	5.704
A(1)=0.46			
Maximum withdrawal	5.946	1.606	7.552
Maximum usage	4.086	1.549	5.635

that the situation of overexploitation of ground water exists in the Urumqi River basin. The OAG, which is the difference between the AUW and the MUW, is $1.573X10^8 m^3$ annually.

The future MWW and the future MUW were computed under an assumed increase of the UCCS. If the UCCS in every district are improved from 0.46,0.72,0.62, and 0.63 to 0.75, 0.80, 0.75, and 0.75, respectively, the future MWW and the future MUW are separately $6.832X10^8 m^3$ and $5.704X10^8 m^3$. But if the Chaiwopu Basin is maintained at the present value of UCCS, 0.46, the future MWW and the future MUW are $7.552X10^8 m^3$ and $5.635X10^8 m^3$ (Table 2).Indeed, the MUW is only increased by 1.2 percent. In addition, the Chaiwopu Basin is not only the source of ground water in the basin but also is not suitable to cultivation owing to its light, heat, and soil quality. Therefore, it is suggested that there would be little benefit from increasing the UCCS in the Chaiwopu Basin.

If the Urumqi River basin is considered as an integrated district and given a series of UCCS from 0.1 to 0.9, the chart that expresses the relationships among the MWW, the MUW, and the UCCS may be obtained from the model(Fig. 3). The chart indicates that the increase of UCCS, which marks water conservancy level of the basin,corresponds to decrease of the MWW and increase of the MUW. The MWW uniformly decreases by 7.5 percent as the UCCS is improved by 0.1 for higher values of the UCCS. However, the change of MUW is complicated. Before the UCCS is reached 0.6, the maximum usage of ground water(MUG) is basically constant,but the maximum usage of surface water(MUS) is continuously incremental. Therefore, it is worth to improve the UCCS in order to raise the MUW.After the UCCS is reached 0.6,although the MUW trends to increase,its variation becomes so small that the variation may be ignored. This is because the MUS appears to increase, but the MUG appears to decrease at similar variation rate. This is also demonstrated by table 2. If the UCCS is increased from 0.46, 0.72, 0.62, and 0.63 to 0.46, 0.80, 0.75, and 0.75,

respectively, the MUS increases from $3.498X10^8m^3$ to $4.086X10^8m^3$; the difference is $0.588X10^8m^3$. However, the MUG decreases from $2.081X10^8m^3$ to $1.549X10^8m^3$ and the difference is $0.532X10^8m^3$. In fact, the actual increased amount is only $0.056X10^8m^3$. Consequently, a new concept on development and utilization of water resources is derived from the model. In such regions as Urumqi River basin where the average UCCS has exceeded 0.6 and the surface water and ground water have been completely developed and utilized,it is not economical to increase the MUW by means of improving the UCCS.

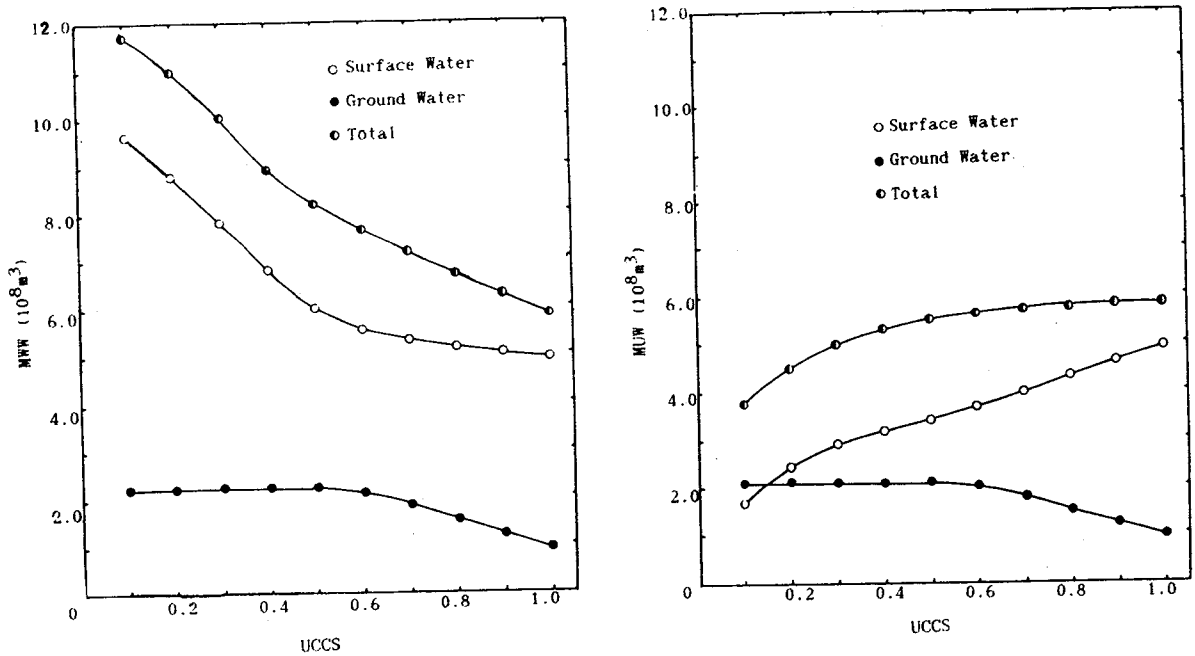

Fig. 3 Responses of maximum withdrawal of water(MWW) and maximum usage of water (MUW) to changes in utilization coefficient of canal system (UCCS)

DROUGHTS IN A STREAM-AQUIFER SYSTEM, SAN SIMEON CREEK, CALIFORNIA

Eugene B. Yates

U.S. Geological Survey, Sacramento, California

ABSTRACT

San Simeon Creek on the central California coast is the principal source of recharge for the small alluvial ground-water basin beneath the creek. The creek dries up in summer, and local water supplies are sustained by storage in the ground-water basin. For water-supply management purposes, three categories of drought were identified: (1) a long summer dry season with excessive ground-water storage depletions, (2) a winter wet season with insufficient stream discharge to recharge the basin fully, and (3) two or more successive winters with incomplete recharge of the ground-water basin. The probability of each type of drought was calculated from the probability distributions of dry-season duration, annual rainfall, annual stream discharge, and tree growth rings. Streamflow records for a gage at the upper end of the basin are short (1971-89) and span a wetter-than-average period. Accurate long-term streamflow distributions were obtained by relating streamflow to rainfall and tree growth rings, which have much longer periods of record. The effects of each type of drought on ground-water conditions were simulated using a transient, finite-element ground-water-flow model. Results demonstrate the feasibility of using a ground-water model to infer the probabilities of selected ground-water conditions from the probability distributions of rainfall and streamflow. Results also indicate that the lack of severe droughts in recent decades might have created a false sense of security regarding water supply.

DROUGHT CONCEPTS

Drought is defined as an extended period of dryness. Quantifying the definition of drought requires selecting thresholds in the frequency or quantity of a hydrologic variable, such as rainfall. The choice of thresholds ultimately is subjective. Rainfall is the source of virtually all terrestrial waters and usually is a good indicator of dryness; however, sometimes other variables might be more appropriate. For example, ground-water budgets in arid areas frequently are more strongly affected by streamflow than by local rainfall. Or for an analysis of water supply, the quantity of water stored in a reservoir or ground-water basin might serve as the best indicator of drought.

Most measures of rainfall, streamflow, or storage have continuous distributions over much of their range; but sometimes, physical limits or thresholds are significant. Examples of thresholds include zero annual rainfall, ground-water levels below well pumps or below sea level, and reservoir levels below the outlet of a dam. Droughts can be defined in terms of these thresholds or in terms of arbitrary ones, such as the tenth percentile of annual rainfall or stream discharge. Associated with each measure of quantity is a probability distribution reflecting frequency of occurrence. These distributions generally are continuous.

CASE STUDY: SAN SIMEON CREEK

Introduction

The purposes of this report are to illustrate these drought concepts as they apply to the stream-aquifer system along San Simeon Creek on the central California coast and to illustrate the coordinated use of surface-water statistics and a ground-water-flow model for quantifying and analyzing droughts. The

distribution of annual rainfall is calculated from measurements of rainfall and tree growth rings. Streamflow is related to rainfall by linear regression. Conditions in the ground-water basin, which is the immediate source of supply for human use, are related to rainfall and streamflow using a digital ground-water-flow model.

Stream-Aquifer System

These drought concepts are illustrated by a case study of water resources along San Simeon Creek on the coast of central California (fig. 1). The lower 3 miles of the creek flow through a narrow valley underlain by a thin ground-water basin. The ground-water basin occupies only 3 percent of the 29-square-mile drainage area of the creek. The basin contains heterogeneous, unconsolidated alluvial deposits. The rest of the drainage area contains relatively impermeable bedrock exposed as steep hills and mountains. Local municipal and agricultural water use is supplied almost entirely by wells tapping the basin. Typically, about 96 percent of annual rainfall in the drainage area of the creek occurs between November and March. Streamflow in the reach overlying the ground-water basin usually ceases for several months during the summer dry season.

A two-dimensional, transient finite-element ground-water-flow model was used to simulate water levels and to estimate selected items in the basinwide ground-water budget. Agricultural pumpage and recharge from rainfall and irrigation-return flow were estimated using a soil-moisture-accounting algorithm. Head-dependent seepage was calculated by the model using a streamflow-routing algorithm. Computational time steps in the model ranged from monthly during the summer dry season to daily during the beginning of the winter streamflow season. Simulated results matched measured ground-water levels and streamflow gains and losses from April 1988 through March 1989. Details of the model will be described in a separate report (E.B. Yates, U.S. Geological Survey, written commun., 1991).

Municipal and agricultural pumpage accounted for 57 percent of ground-water outflow during the 12-month calibration period. Most pumpage during summer is derived from ground-water storage. In 1988, the cumulative dry-season storage deficit was about 500 acre-feet. Recharge from the creek was by far the largest source of inflow. Ground-water levels in most areas are 10 to 30 feet below the creek thalweg at the end of the dry season and recover quickly to the level of the creek as soon as streamflow begins in winter. Additional recharge from the creek is rejected. For example, after 6 months of no flow in

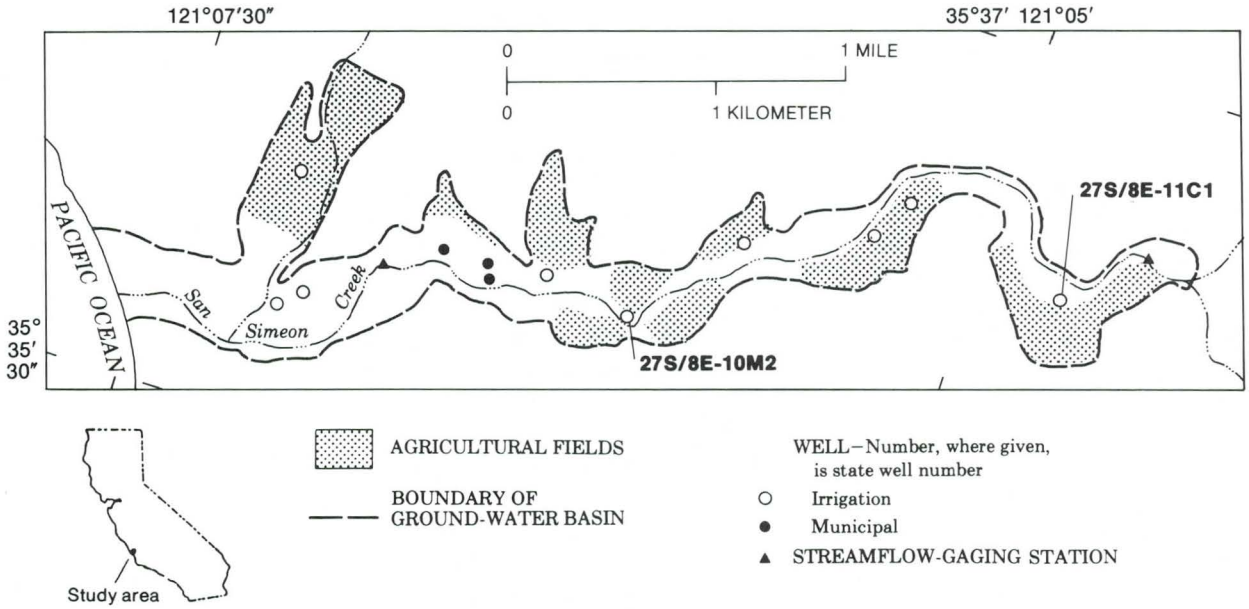

Figure 1. Location and features of San Simeon Creek ground-water basin.

1988, flow in the creek began with a large flood on December 23, 1988. The response of ground-water levels is shown in figure 2. Throughout the basin, water-level recovery during the wet season was about 90 percent complete by the end of the second week of streamflow. Net seepage from the creek accounted for 88 percent of total inflow to the ground-water basin during that period.

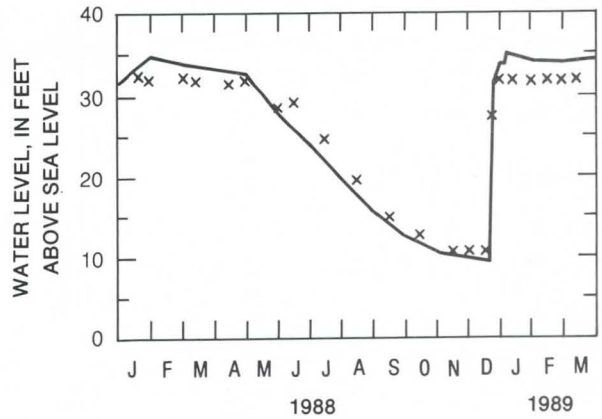

Figure 2. Simulated (—) and measured (x) water level in well 27S/8E-10M2 during 1988-89.

Droughts

For this study, the hydrologic variables selected to define droughts were the duration of the summer dry season and the quantity of annual stream discharge. The dry season is defined as the period without streamflow. Thresholds were selected for these variables that would clearly be associated with adverse effects on water supply. The probability of surpassing these thresholds was calculated from rainfall and streamflow statistics, and overall hydrologic conditions associated with each threshold were simulated using the ground-water-flow model.

Three types of droughts were defined in terms of these two variables: (1) a long summer dry season, (2) a single winter wet season with incomplete recharge, and (3) two consecutive wet seasons with incomplete recharge.

Long Dry Season

The duration of the summer dry season was determined from the 19-year record of daily streamflow data for the gage at the upper end of the ground-water basin (see fig. 1). The distribution of dry-season duration was continuous, and the corresponding minimum dry-season water levels also varied gradationally without apparent thresholds. For convenience, ground-water effects were calculated for monthly increments in dry-season duration.

The measured dry-season durations fit a normal distribution with a mean of 164 days and a standard deviation of 64 days. Normality was verified using the probability plot correlation coefficient test (Looney and Gulledge, 1985). Normal probability tables were used to calculate recurrence intervals of selected dry-season durations (table 1).

These estimates of recurrence intervals are almost certainly too long because the period of record for the stream gage (1971-89) was wetter than average. This is evident in figure 3, which shows the cumulative departure of annual rainfall in San Luis Obispo about 30 miles southeast of the San Simeon basin. Average rainfall during the 120-year record was 21.79 inches, whereas average rainfall during 1971-89 was 24.55 inches. Bianchi and Hanna (1988) developed an empirical equation relating the length of the dry season in San Simeon Creek to monthly rainfall in San Luis Obispo. They estimated that the long-term average length of the dry season is 200 days, or 36 days longer than the estimate obtained directly from streamflow data for San Simeon Creek.

Table 1. Recurrence intervals of selected measured dry-season durations for San Simeon Creek

Recurrence interval (year)	Measured dry-season duration (day)
50	295
20	269
10	245

Simulations of three dry-season durations (235, 266, and 296 days) revealed large effects on ground-water levels at the upper end of the basin because a longer dry season allows more time for ground water to drain down the valley. For example, the minimum

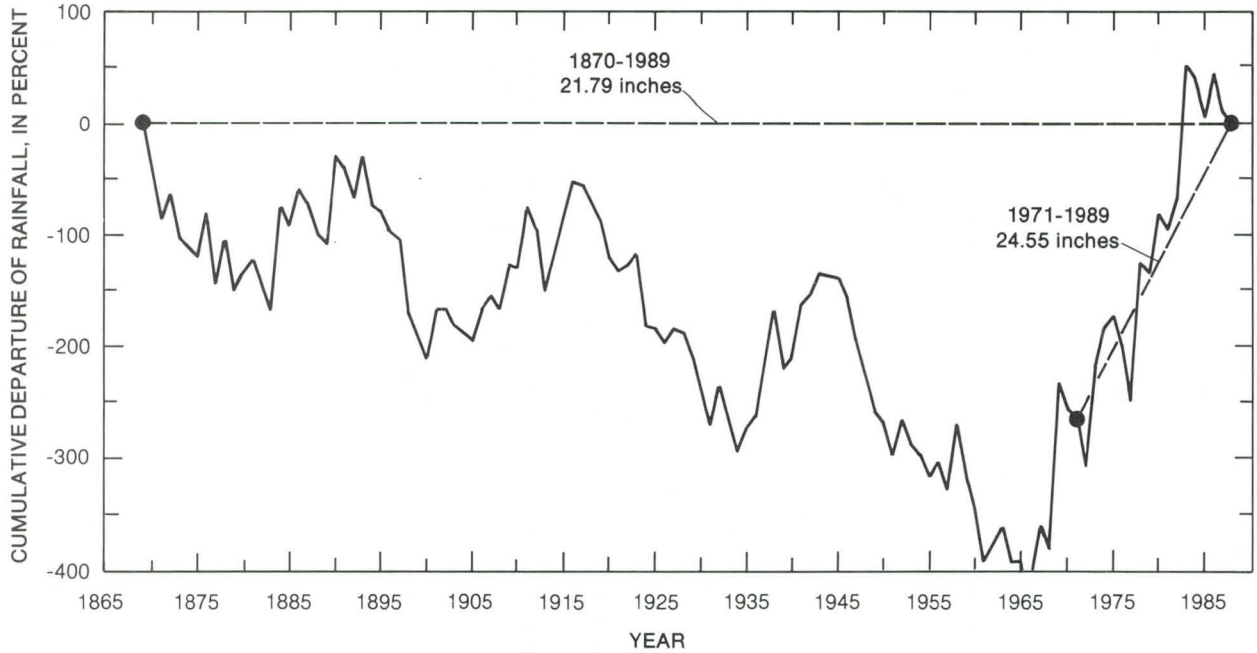

Figure 3. Cumulative departure of annual rainfall in San Luis Obispo, 1870-1989.

seasonal water level at well 27S/8E-11C1 declines 3 to 4 feet for every additional month of dry season (fig. 4). Effects farther down the valley are smaller.

Seawater intrusion was not predicted in any simulation, but wells near the upper end of the valley probably went dry even in the shortest simulated dry season. The ground-water model simulates static water levels and thus cannot accurately determine whether water levels during pumping conditions will decline to the level of the pump intake. However, these results are consistent with conditions in 1988 when the pumping water level in well 27S/8E-11C1 did reach the pump intake.

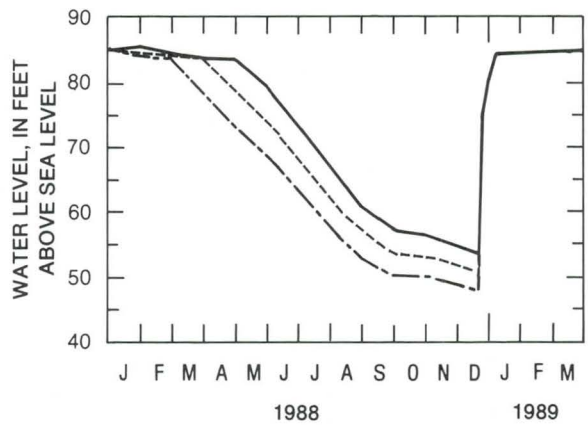

Figure 4. Effect of dry-season duration on simulated water level in well 27S/8E-11C1 during 1988-89. Dry-season duration 235 days (—), 266 days (--), and 296 days (—-—).

Single Wet Season with Incomplete Recharge

Complete recharge of the ground-water basin depends on adequate stream discharge during the winter wet season. Two thresholds of practical significance in this relation are (1) zero stream discharge (worst case) and (2) the minimum quantity of stream discharge needed to replenish the cumulative ground-water storage deficit during the preceding dry season.

Because the relatively wet period of record for streamflow is not representative of long-term conditions, stream discharge was related to the longer record of rainfall in San Luis Obispo. The probability distribution of rainfall in San Luis Obispo for 1870-1989 is shown on a log-normal probability plot in figure 5. The skew of the logarithms is very small (-0.067), so the data form a linear pattern that can be approximated by a log-normal or log-Pearson type III distribution. The mean and standard deviation of the untransformed annual rainfall data are 21.79 and 8.5 inches, respectively.

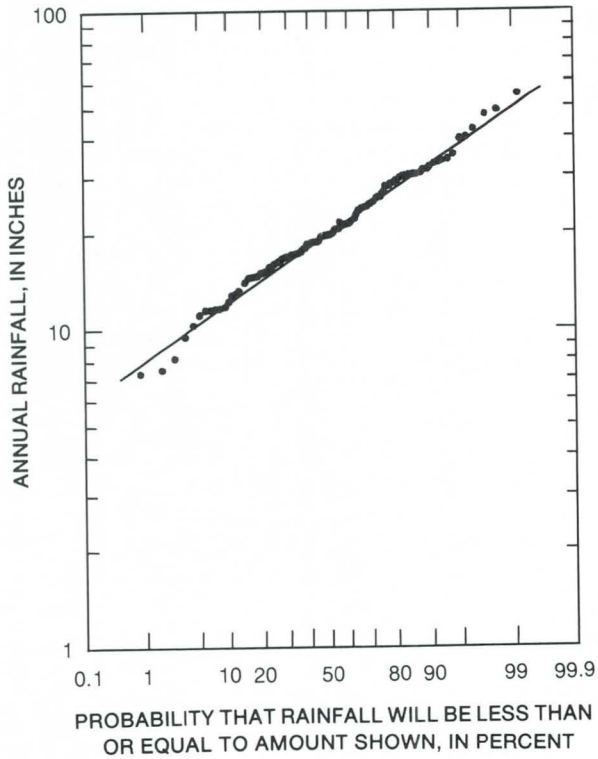

Figure 5. Probability distribution of annual rainfall in San Luis Obispo during 1870-1989.

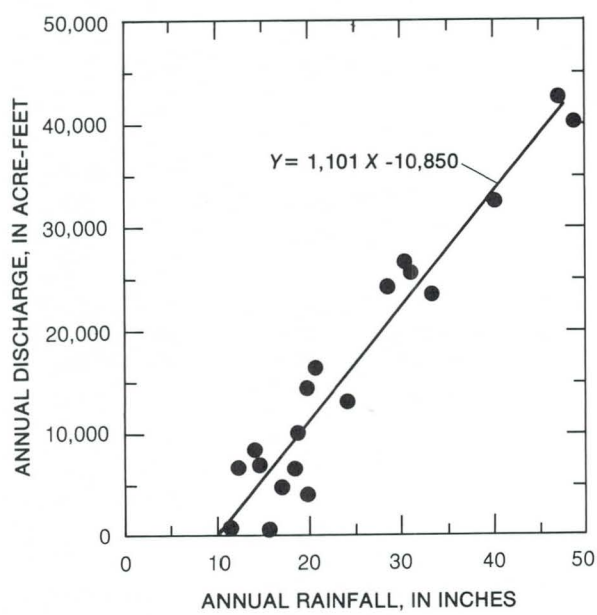

Figure 6. Relation between annual rainfall in San Luis Obispo and annual discharge in San Simeon Creek.

The relation between annual rainfall in San Luis Obispo and annual discharge in San Simeon Creek is reasonably linear (fig. 6). An ordinary least-squares (OLS) regression line fitted to the data has a correlation coefficient of 0.96.

Recurrence intervals of low annual rainfall and corresponding quantities of annual stream discharge are shown in table 2. The rainfall associated with each recurrence interval was calculated for the log-Pearson type III probability distribution by back-transformation using frequency factors (Haan, 1977). The recurrence intervals of zero stream discharge and of the minimum quantity of discharge needed for complete basin recharge are 31 and 25 years, respectively.

The effects of zero stream discharge were simulated using the ground-water-flow model and were compared with results of the calibration simulation, which represents complete basin recovery. Figure 7 shows simulated water levels at well 27S/8E-10M2 resulting from a 2-year simulation with zero stream discharge during the winter wet season between the two dry seasons. There is no water-level recovery during the wet season and water-level declines during the second dry season are almost as large as during the first dry season.

By the end of the second dry season, simulated water levels were below the pump intakes at many wells and about 48 acre-feet of seawater intrusion was predicted.

Successive Wet Seasons with Incomplete Recharge

The likelihood of two successive winters with incomplete recharge would be an important factor in designing water-storage facilities. Annual rainfall and stream discharge were tested for serial correlation to determine whether quantities in 1 year are related to quantities in the following year. The 1-year serial correlation coefficients were both less than 0.07, which is not significant according to a test developed by Anderson (1962). This indicates that the probability of an exceptionally dry year can be assumed to be the same each year, and the probability of 2 successive years of incomplete recharge equals the square of the probability for a single year. The corresponding recurrence interval is about 600 years. The recurrence interval of 2 successive years of zero discharge is about 1,000 years.

A 400-year record of tree growth rings does show a small amount of serial correlation (Michaelson and

Table 2. Recurrence intervals of low annual rainfall at San Luis Obispo and stream discharge in San Simeon Creek

Item	Recurrence interval (years)	Annual rainfall at San Luis Obispo (inches)	Annual discharge in San Simeon Creek (acre-feet)
Minimum quantity likely to occur once in:			
100 years	[1]100	8.20	0
50 years	[1]50	9.15	0
20 years	[1]20	10.80	1,040
10 years	[1]10	12.41	2,810
Zero discharge	31	9.85	[1]0
Minimum discharge for complete basin recharge	25	10.31	[1]500
Minimum recorded discharge	25	10.29	[1]480

[1]These values are given. The remaining entries in each row are calculated from the rainfall-discharge regression equation and the rainfall probability distribution.

others, 1987). Defining an extremely dry year as having a probability of 0.1, the investigators calculated that the probability of two consecutive extremely dry years is 0.017. This probability is 1.7 times greater than if there were no serial correlation. If annual stream discharge exhibited the same degree of serial correlation as extremely dry years in the tree ring record, the recurrence interval of 2 successive years of incomplete recharge would be about 370 years. Analysis of 2-year droughts in the rainfall record indicates that even with dry-season storage deficits as large as the deficit in 1988, complete basin recharge would have occurred in at least 1 year of every 2-year drought since 1870.

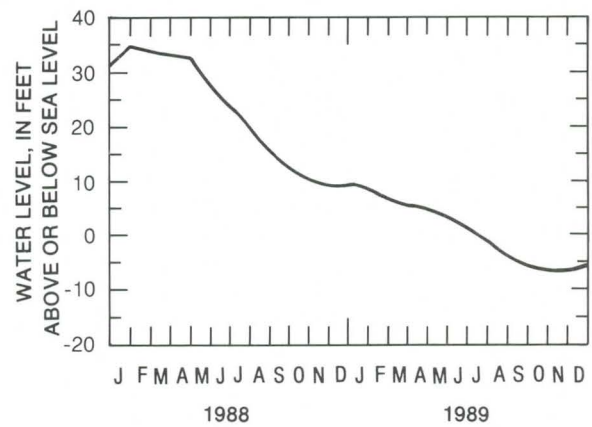

Figure 7. Simulated water level in well 27S/8E-10M2 with zero stream discharge during the winter of 1988-89.

Implications for Planning

The last three decades have been relatively wet. The droughts most clearly remembered by local residents (1976-77 and 1987-90) are only the sixth and seventh driest 2-year and 4-year droughts in the rainfall record, respectively. Most of the present municipal water demand has resulted from rapid population growth during the recent wet period. The lack of severe droughts during that time might have created a false sense of security that could hinder efforts to take remedial action.

REFERENCES CITED

Anderson, R. L., 1962, Distribution of the serial correlation coefficient: Annals of Mathematical Statistics, v. 13, p. 1-13.

Bianchi, W. C., and Hanna, W. C., 1988, Artificial recharge and conjunctive use management, north central coastal basins of California: Paper presented at the American Society of Civil Engineers symposium on Artificial Recharge of Groundwater, Anaheim, California, August 21-28, 1988, 10 p.

Haan, C. T., 1977, Statistical methods in hydrology: Iowa State University Press, Ames, Iowa, 378 p.

Looney, S. W., and Gulledge, T. R., 1985, Use of the correlation coefficient with normal probability plots: The American Statistician, v. 39, p. 75-79.

Michaelson, J., Halston, L. and Davis, F. W., 1987, 400 years of central California precipitation variability reconstructed from tree-rings: Water Resources Bulletin, v. 23, no. 5, p. 809-818.

WATER BALANCE ANALYSIS IN THE MOUNTAIN AREA OF THE URUMQI RIVER BASIN

Zhou Yu-Chao and Zhang Guo-Wei
Xinjiang Hydrological Bureau, Urumqi,Xinjiang

Kang Er-Si
Lanzhou Institute of Glaciology and Geocryology,
Chinese Academy of Sciences,Lanzhou

ABSTRACT

The Urumqi River , which is situated in the arid region in Xinjiang, China, is an experimental basin to study runoff and water resources on the northern slope of The Tianshan Mountains. The basin is also the main water supply source to Urumqi City, the Capital of Xinjiang—Uygur Autonomous Region ; therefore there is a very important social and economical value to study it . This paper tries to evaluate the total amount of water resources and its characteristics, to establish the water balance equation , and to analyze each elemment of the water balance by study of the precipitation, evaporation and runoff in the mountain area . The result is that there is rather high precipitation (526 mm after correction) and relatively abundant water resources in the mountain basin.According to analysis of the parametric features of water balance factors in this basin , the basin can be characterized as having high water yield , strong soil absorption and evaporative capacity, and low water storage within a year .

GENERAL SITUATION OF RIVER BASIN IN MOUNTAIN AREA

The Urumqi River basin , in the central part of the Tianshan Mountains at 86.75-87.93° E and 43.00-44.12° N , trends from southwest to northeast then to north . The river is 214.3 km long and the total area is 4684 km² , 1,070 km² of the river basin lies in the mountain area . This paper mainly analyzes the characteristics of hydrology of the upper river from Yingxongqiao station , which is situated near the outlet of the mountain area and has a drainage area of 924 km² (Fig.1) .

The Urumqi river originates from the Tianger II peak , central part of Eastern Tianshan Mountains , at the elevation of 4,486 m . The elevation of Yingxongqiao Station is 1,920 m and average elevation in mountain area is 3,005 m . In this area , the elevation of the average snowline is 3,780 m . Above the snowline there are 124 glaciers , with an area of 38 km² which takes 4.1% of the drainage area upstream of the Yingxongqiao Station .

In the river head , Glacier No.1 has been observed and studied for several years by the Tianshan Glacial Research station of Chinese Academy of Sciences . Study items include glacier mass balance , glacier physics , glacier hydrology , glacier geomophology , etc . In the mountain area, there are 9 hydrometric stations, 5 meteorologic stations , and 20 raingage stations arranged by the Runoff Experiment Station of Urumqi River of the Xinjiang Water Conservancy Department. Study items include the water balance

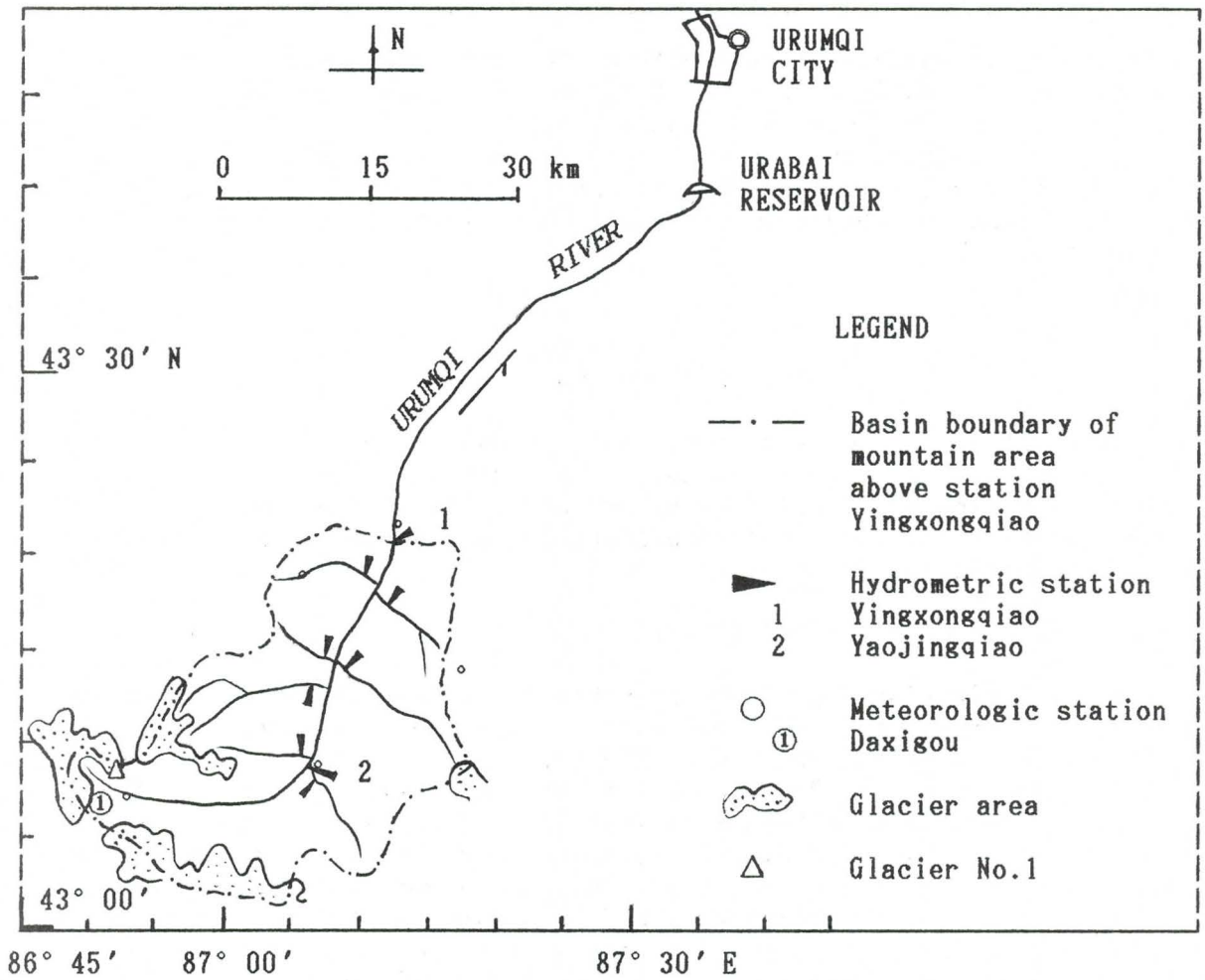

Fig. 1 Map of mountain area of Urumqi River Basin

and runoff component analysis , the relation between precipitation and runoff, and establishment of a mathmatical model of the runoff .

FEATURES OF PRECIPITATION

Precipitation

According to the observed data from 1984 to 1987 in the basin , the average annual precipitation of Urumqi River Basin in the mountain area is 421.7 mm . Based on the study of Yang et al. (1990) on the systematic error of observed precipitation in China, correction has been made to the observed data of the precipitation by 30.9% increase for snowfall in high mountain area due to wind influence, by 13.5% increase for rainfall in middle mountain area due to wet loss of raingauges and by 20.5% increase for rainfall in lower mountain area due to wind influence . The correction factor of observed precipitation is 1.15 for rainfall and 1.3 for snowfall.The corrected value of average precipitation in the mountain area of the Urumqi River is 526 mm, which is 25% more than the observed value .

The snow covered area in the basin and its seasonal translation

The percentage of monthly snow covered area in this basin is 100 % from November to March , and 70 - 85 % in April and October , but even in the hottest months as in July and August , it is still 11 % .

The snow accumulated in November and December translates to snow-melt runoff in the next calendar year , therefore the difference of the snowfall in these two months between this year and last year is the variation of basin snow cover ΔS.

LAND EVAPORATION

In this basin there are observed records of evaporation only from water surface (by small size evaporation gauge , D = 20 cm). The average annual evaporation is estimated at 521.8 mm after correction of the observed data .

The calculating formula for land evaporation E advanced by Prof.Fu Baopu in Nanjing University of China is :

$$E = E_o \left(1 + P/E_o - \left(1 + \left(P/E_o \right)^m \right)^{m^{-1}} \right) \qquad (1)$$

where P is precipitation , E_o is evaporativity which can be replaced by evaporation from the water surface, and m is a feature parameter of the underlying surface (Wu Hekang et al. 1986) .

In the Daxigou station (3539 m a.s.l.) the land evaporation in 1986 is 288.3 mm as calculated with this formula . The Tianshan Glacier Research Station of the Chinese Academy of Sciences made a test of the land evaporation in high mountain area (3640 m a.s.l.) and estimated the land evaporation at 270.3 mm in that year , which is close to the result of this calculation . Therefore, the land evaporation was calculated by this formula from 1984 to 1987 ; the resulting valus were 310.8, 274.6, 311.3, and 323.5 mm, and the average of the four years is 305.0 mm , which is close to the value of land evaporation 293.6 mm resulting from the basin water-balance analysis (Table 2) .

RUNOFF IN HIGH MOUNTAINS AND WATER BALANCE IN THE MOUNTAIN AREA

Glacier runoff in high mountain area

The balance equation of glacial mass is :

$$P' = R' + E' + \Delta B \qquad (2)$$

Where P' , R' , E' are precipitation, meltwater runoff, and glacier surface evaporation in the glacier area , respectively , and ΔB is increase in glacial water storage. The data for the balance can be seen in Table 1 .

The minus ΔB means that , when the temperature in one year is larger than annual average, the glacial meltwater is more than glacier fill.

Table 1 Glacier mass balance in glacier area of Urumqi River basin (mm)

Year	P′	R′	E′	ΔB
1984	500.6	434.9	148.7	- 83.0
1985	369.1	842.4	138.7	-612.0
1986	506.9	952.0	168.9	-614.0
1987	541.0	535.7	203.3	-198.0
Average	479.4	691.3	164.9	-376.8

Equation of water balance in mountain area

The components of the water balance are shown schematically in Fig. 2 (Hydrology Bureau of Water Resources Ministry of China, 1987) .
Equation of water balance in a year is the following :

$$P = R + E + Ug + \Delta V \qquad (3)$$

$$\Delta V = \Delta B + \Delta S + \Delta W \qquad (4)$$

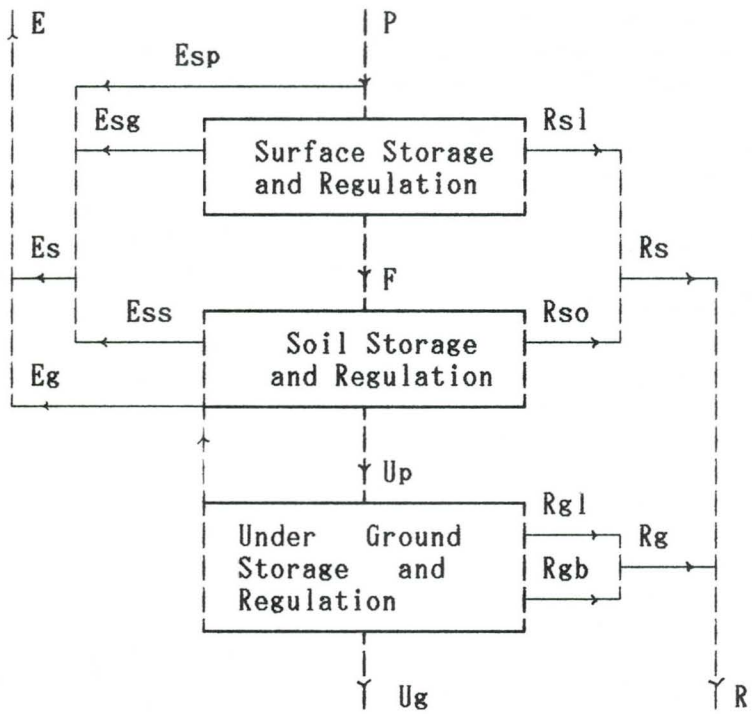

P	Precipitation
F	Total infiltration
Up	Seep into underground water
Ug	Deep percolation
R	Total runoff
Rs	Surface runoff
Rsl	Slope runoff
Rso	Subsurface flow
Rg	Groundwater runoff
Rgl	Shallow groundwater
Rgb	Base flow
E	Total evapotranspiration
Es	Land surface and soil evaporation
Esp	Evaporation of plant interception
Esg	Land evapotranspiration
Ess	Soil evaporation
Eg	Groundwater evaporation

Fig. 2 Schematic diagram of water balance

Where ΔV is difference of basin water storages at the beginning and the end of year ; ΔB is the annual water balance of glacier ; ΔS is the difference between snow accumulations in the November and December in this year and last year;and ΔW is the difference of ground water storages at the beginning and the end of year. For the annual average value of water resources, ΔV = 0. Then P = R + E + Ug .The total amount of water resources in mountain area, W:

$$W = P - Es = R + Ug + Eg \qquad (5)$$

Water balance schedule in the mountain area

Making the basin area upstream of the Yingxongqiao Station as an object of analysis, one tabulates the elements of the water balance as Table 2 .

Table 2 Water balance elements in the mountain area of the Urumqi River Basin (mm)

Year	P	R	Ug	E	ΔV	ΔB	ΔS	ΔW
1984	571.9	261.2	11.0	296.0	3.7	- 3.4	7.3	-0.2
1985	426.2	219.2	9.3	235.8	-38.1	-25.1	-9.3	-3.7
1986	528.2	199.7	8.4	338.5	-18.4	-25.2	5.8	1.0
1987	577.8	265.9	11.2	304.2	- 3.5	- 8.1	0.9	3.7
Average	526.0	236.5	10.0	293.6	-14.1	-15.5	1.2	0.2

In table 2 , Ug, including subsurface flow under the river bed , is measured and calculated from lateral percolation in the foothills of the mountain area ; ΔW is obtained by comparing the flow recession curve of hydrograph in this year with that in last year ; E is calculated via Formula (3) with no observed data available .

Parameter analysis for water balance elements

The water balance formula (3) can be turned to :

$$P = Rsl + Rso + Rgl + Rgb + Ug + E + \Delta V \qquad (6)$$

The total infiltration F is:

$$F = Rso + Rgl + Rgb + Ug + Eg + Ess \qquad (7)$$

Rsl, Rso, Rgl, Rgb , calculated by Zhang Jienggang (1990) and the F are shown as Table 3 .

Table 3 Water balance elements (mm)

Year	R	Rsl	Rso	Rgl	Rgb	F
1984	261.2	156.4	22.2	42.2	40.4	332.8
1985	219.3	130.8	27.4	24.0	37.1	269.6
1986	199.7	111.8	25.7	38.0	24.2	345.2
1987	266.5	160.7	23.8	42.9	39.1	340.2
Average	236.7	139.9	24.8	36.8	35.2	322.0
%	100%	59.1%	10.5%	15.5%	14.9%	

Let the coefficient of water yield in the basin $\alpha_1 = (R + Ug)/P$; this parameter expresses the total amount of surface water and ground water resources produced in the basin . Also coefficient $\alpha_2 = Rs / P$ is for surface runoff; coefficient $\alpha_3 = F/P$ is for soil infiltration ; coefficient $\alpha_4 = (Rg + Ug)/F$ is for ground water recharge; coefficient $\alpha_5 = (Ess + Eg)/F$ is for soil evaporation; coefficient $\alpha_6 = \Delta V / F$ is for storage and regulation in the basin ; coefficient $\alpha_7 = Rg / Rs$ is runoff stability factor. All of these coefficients are shown in Table 4 .

Table 4 The coefficient of water balance element

Year	α_1	α_2	α_3	α_4	α_5	α_6	α_7
1984	0.46	0.31	0.58	0.28	0.65	0.01	0.46
1985	0.54	0.37	0.63	0.26	0.64	-0.14	0.39
1986	0.39	0.26	0.65	0.20	0.72	-0.05	0.45
1987	0.48	0.32	0.59	0.27	0.66	-0.01	0.44
Average	0.47	0.31	0.61	0.25	0.67	-0.05	0.44

The above coefficients indicate that :

(a) α_1 : 47 % precipitation in mountain area can be turned into the utilizable water down stream , so the basin water yield is quite high ;

(b) α_3 : the total infiltration water makes up 61 % which means that the basin surface has quite strong absorbing power ;

(c) α_5 : the surface evaporation takes 67 % of total infiltration, which indicates the most of the infiltration water is lost by evaporation ;

(d) α_6 : the coefficient of basin storage and regulation is very small,only taking 5 % , which shows that most of the precipitation forms runoff or is consumed by evaporation.

ACKNOWLEDGMENTS Many thanks to the Tianshan Glacial Research Station of the Chinese Academy of Sciences and the Runoff Experiment Station of Urumqi River of Water Conservancy Department of Xinjiang—Uygur Autonomous Region, China, for many observed data presented in this paper .

REFERENCES

Yang Daqing, Shi Yafeng, Kang Ersi, Zhang Yinsheng , Shang Sichen, Wang Xinqi , 1990 , Analysis and correction of the systematic errors from precipitation measurement in the Urumqi River Basin : Formation and Estimation of Mountain Water Resources in the Urumqi River Basin, Chinese Science Press , P.14-39 .

Wu Hekang and Zhang Zhiming,1986: Meteorology, Water Resources Press, P.170-171.

Hydrology Bureau of Water Resources Ministry of China,1987 : Water Resources Assessment for China, Water Resources and Electric Power Press, P.134 .

Zhang Jiangang, 1990, Runoff component of the Urumqi River : Formation and Estimation of Mountain water resources in the Urumqi River Basin, Chinese Science Press, P.98 .